

SCIENTIFIC NOTEBOOK

Issued To: Peter Lichtner (PCL) (PL)

Date: Tuesday Nov. 16, 1993 16:24 PM

These are entries pertinent
to the code V-TOUGH. They PCL 4.17.97
were used initially to determine
the development of MULTIFLO, but do not directly input information
to MULTIFLO code.

N. Smith
4/17/97

The Boorum & Pease® Quality Guarantee

The materials and craftsmanship that went into this product are of the finest quality. The pages are thread sewn, meaning they're bound to stay bound. The inks are moisture resistant and will not smear. And the uniform quality of the paper assures consistent rulings, excellent writing surface and erasability. If, at any time during normal use, this product does not perform to your expectations, we will replace it free of charge. Simply write to us:

Boorum & Pease Company

71 Clinton Road, Garden City, NY 11530

Attn: Marketing Services

Any correspondence should include the code number printed at the bottom of this page as well as the book title stamped at the bottom of the spine.

CNWRA
CONTROLLED
COPY 095

Note: Copied from Scientific
Notebook # 095 - Dr. A.
Lichtner used only 4 pages
of this 300 page book before
converting to an electronic
scientific notebook. These pages

One Good Book Deserves Many Others.

Look for the complete line of Boorum & Pease® Columnar, Journal, and Record books. Custom-designed books also available by special order. For more information about our Customized Book Program, contact your office products dealer. See back cover for other books in this series.

Made in U.S.A.
RM201092

ALL being put with
his first
electronic
scientific
notebook.
4/17/97 [Signature]

11.16.93

PCL

Computing Equipment

Desk: Intel Professional Workstation
DX 66 Mhz
OS: NEXTSTEP

Network: rory.cnwra.swri.edu SUNDS IPX
Computers bashful.cnwra.swri.edu SUNDS

Operating system: SUNDS 4.1.2

goliath

SPARC 10
Solaris OS

Consult computerized version of Scientific
Notebook. Formatted in LaTeX.

11.16.93 PCL

V-TOUGH

today

Began work by incorporating changes made to V-TOUGH by consultant Mohan Seth into the .F format using m4. This involved creating the file input.F from Seth's file input.f by adding m4 statements.

The code compiled with no errors and ran successfully. Mohan is to provide original input data file so that results can be compared to the original unmodified version of V-TOUGH.

rec'd

11.18.93

PCL

ACTION PENDING

This work to modify V-TOUGH is an on-going project with IPA and EBS. The basic motivation is to improve the computational efficiency and I/O user friendliness of the code.

Corrosion
Model
Development
<CMD>

Began work to develop a general formulation of corrosion including transport processes, and chemical reactions - aqueous complexing, mineral precip. / diss., redox and electrochemical effects.

This project is part of the EBS ongoing work which was started by John Walton.

The initial phase of work involved becoming familiar with the existing literature on the subject.

11.23.93

A number of errors were found in the V-TOUGH
code as modified by M. Seth. There are:
in file input. f:

COMMON/TIMES/... TIS(200), ...
not 300
COMMON/COMDEBUD/... IDEBUD(100)

Code is still in process of being tested.

Also removed lines beginning with

C-- SPECIAL

C-- SPECIAL ENDS
in file input. f

12.12.93

Code successfully tested at last.

Further entries have been made
in the computerized version of lab
notebook #095. These are printed
out on a quarterly basis & submitted
to Q.A.

N. Fischel
2/24/97

I have reviewed this scientific notebook and find it in compliance with QAP-001. There is sufficient information regarding procedures used for conducting tests, acquiring and analyzing data so that another qualified individual could repeat the activity.

N. Sridhar 2/24/97

Narasi Sridhar
Manager, Engineered Barrier System and Waste Solidification System

308

Q199806260001

Electronic Scientific Notebook No.
095E: Development of the Code MULTIFLO to
Describe Multiphase Reactive Transport
(12/18/1995 through 04/17/1997)

SCIENTIFIC NOTEBOOK

by

Peter C. Lichtner

Printed: December 13, 1994

P. C. Lichtner

SCIENTIFIC NOTEBOOK

INITIALS: PCL

SCIENTIFIC NOTEBOOK

by

Peter C. Lichtner

**Southwest Research Institute
Center for Nuclear Waste Regulatory Analyses
San Antonio, Texas**

P. C. Lichtner

SCIENTIFIC NOTEBOOKINITIALS: PC**INITIAL ENTRIES**

Scientific NoteBook: # 095

Issued to: P. C. Lichtner

Issue Date: Tuesday, November 16, 1993

Computerized Initials: PC

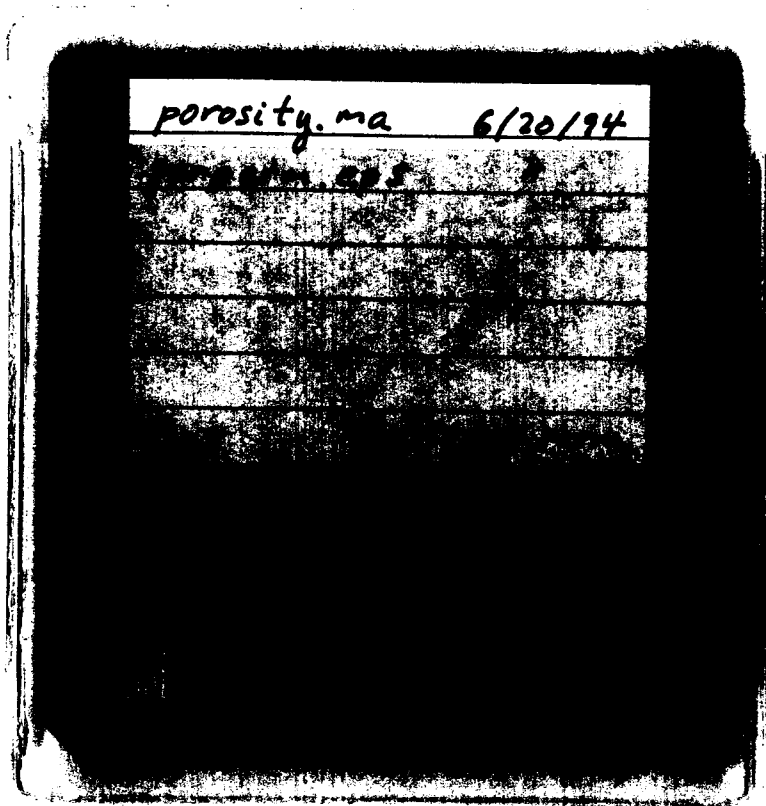
By agreement with the CNWRA QA this NoteBook is to be printed at approximate quarterly intervals. This computerized Scientific NoteBook is intended to address the criteria of CNWRA QAP-001.

Table 0-1: Computing Equipment

Machine Name	Type	OS	Location
gravenstein.cnwra.swri.edu	Intel Professional Workstation	NEXTSTEP	desk Rm A-126
	DX 66 Mhz	Version 3.2	Bldg. 189
rory.cnwra.swri.edu	Sun SPARC 2	SUNOS 4.1.2	network
goliath.cnwra.swri.edu	Sun SPARC 10	SUNOS 4.1.2	network
skippy.cnwra.swri.edu	Sun SPARC 20	SUNOS 4.1.2	network

Table 0-2: File documentation for location of source code and input files used in numerical calculations. All files are stored on a MAC floppy disk, SciNotebook . 94, included with the Scientific Notebook. The source for version 1.0 of the GEM code is contained in the directory: GEM.src.

Code	File Name	Figure
GEM	abc.in, abc.data	Figure 2-1
GEM	cyl.in	Figure 2-3
GEM	ph2to3.in, ph3to2.in, ph5to2.in	Figure 2-4
GEM	nacl.in	Figure 2-5
GEM	ionex.in	Figure 2-6
GEM	pena.in	Figure 2-7
GEM	pena.in	Figure 2-8
Mathematica	power.ma	Figure 3-9
Mathematica	porperm.ma	Figure 3-10



List of Figures

- 2-1 Numerical calculation for conditions approximating local chemical equilibrium in the three component system A-B-C. The results are in excellent agreement with semi-analytical solution for the same problem presented by Lichtner (1991). Calculations are given for an elapsed time of 100 years. 2-6
- 2-2 Coordinates used to define cylindrically and spherically symmetric grids. 2-7
- 2-3 Comparison of GEM(solid curves) with analytical solutions (dots) for cylindrical and spherical geometry. 2-19
- 2-4 Theoretical calculations with GEM for species-dependent diffusion coefficients (solid curves) compared with experiment (dashed curves). Plotted is the crevice pH as a function of time for the bulk (boundary value), mouth (9.5 mm) and tip (0 mm) of the crevice. Zero flux boundary conditions were imposed at the tip. 2-21
- 2-5 Theoretical calculations with GEM for the concentration of Na^+ and Cl^- plotted as a function of distance at the indicated times. 2-24
- 2-6 Flushing of Na^+ and K^+ by a CaCl_2 solution. 2-25
- 2-7 Theoretical calculations with GEM describing oxidation of uraninite in a tuffaceous host rock showing (a) volume fraction profiles, and (b) porosity for an elapsed time of 1000 years. 2-29
- 2-8 Theoretical calculations with GEM describing oxidation of uraninite in a tuffaceous host rock showing (a) Eh and pH, and (b) total uranium and iron aqueous concentrations for an elapsed time of 1000 years. 2-29
- 3-9 Power density in units of Watts MTIHM^{-1} calculated using *Mathematica* to be used in V-TOUGH calculations. 3-3
- 3-10 Best-eye-fit to porosity-permeability data from Yucca Mountain using a power law dependency of porosity on permeability. One point (# 11) is chosen to anchor the lines. 3-4

- 3-11 Liquid saturation plotted as a function of distance for an elapsed time of 50 years
for different vertical slices near the edge of the repository compared to the center. 3-6
- 3-12 Liquid saturation, gas and liquid flux, and evaporation rate plotted as a function of
distance for an elapsed time of 1000 years. 3-7

List of Tables

0-1	Computing Equipment	ii
0-2	File documentation for location of source code and input files used in numerical calculations. All files are stored on a MAC floppy disk, SciNotebook.94 included with the Scientific Notebook. The source for version 1.0 of the GEM code is contained in the directory: GEM_src.	iii
2-3	Volume fractions of the primary mineral assemblage.	2-27
2-4	Compositions of the inlet and initial fluid. Molality units are used with the exception of pH.	2-28

PROJECTS

Contents

INITIAL ENTRIES	ii
FIGURES	v
TABLES	vi
PROJECTS	vii
1 V-TOUGH Modifications	1-1
2 Corrosion Code Development: GEM	2-1
3 IPA: Flow Around the Waste Package	3-1
4 SCCEX Code Analysis	4-1

1 V-TOUGH Modifications

Account Number: 20-5702-523/723

Collaborators: Mohan Seth (Consultant)

Objective: The purpose of this work is to modify V-TOUGH to improve computational efficiency and I/O user friendliness of the code. This is an on-going project with IPA and EBS elements.

11.16.93 Began working today by incorporating changes made to V-TOUGH by consultant Mohan Seth into the .F format using m4. This involved creating the file input.F from Seth's file input.f by adding m4 statements. In the future M. Seth will provide directly the .F files.

The code compiled with no errors and ran successfully.

12.2.93 M. Seth completed work on modifying input to V-TOUGH to free-format.

1.28.94 M. Seth began work to modify V-TOUGH to include print out of evaporation and condensation rates of vapor. In addition he is comparing different conjugant gradient solvers for cpu efficiency.

2.18.94 Questioned the validity of POREFLOW in its treatment of heat flow. POREFLOW uses enthalpy rather than internal energy in the accumulation term in the energy balance equation. This could lead to serious error. The time derivative of the difference in internal energy and enthalpy is noted here to be given by:

$$\frac{\partial}{\partial t} \{ \rho(H - U) \} = \frac{\partial p}{\partial t}, \quad (1-1)$$

recalling that

$$H = U + pV = U + \frac{p}{\rho}. \quad (1-2)$$

5.18.94 An error was discovered in the computation of the evaporation rate. It was found that the evaporation rate was proportional to the volume of an element which it should not be. This problem was corrected. However, a new problem arose when M. Seth attempted an independent calculation based on the vapor transport equations and got different results. This problem has not yet been resolved.

- 6.8.94** As reported by M. Seth (letter to Baca dated June 6, 1994) results with the new solvers from the Austin nspcg solver package were only marginally successful. Work is continuing to find a better conjugate gradient solver to enable faster 2D and make possible 3D calculations.
- 6.10.94** Slight discrepancies were noted between the modified and old version of V-TOUGH. This has been attributed to improving the modified version by using double precision format for constants (e.g. 2.d0 etc.) which can change results very slightly. Results with new version are acceptably close to the old results. The new version will be referred to as **C-TOUGH** from now on.

2 Corrosion Code Development: GEM

Account Number: 20-5702-523

Collaborators: none

Objective: This project is part of the EBS ongoing work which was started by John Walton. The initial phase of work involved becoming familiar with the existing literature on the subject. Main purpose is to upgrade the codes TWITCH and MARIANA developed by Walton to model corrosion.

Date	Entry
11.16.93	Began work to develop a general formulation of corrosion including transport processes and chemical reactions—aqueous complexing, mineral precip./diss., redox and electrochemical effects.
2.2.94	<p>Construction of a general corrosion model was begun. The new code, named GEM, replaces and generalizes the code TWITCH for describing crevice corrosion. Several advantages of GEM compared to TWITCH are:</p> <ul style="list-style-type: none">• GEM uses an equivalent form of the EQ3/6 database, whereas TWITCH required each reaction to be typed into the input file.• GEM employs a self-consistent calculation of the solution current density which provides for accurate charge balance. By contrast, in TWITCH, the error in charge balance incurred during a calculation was redistributed over the aqueous species. This can be a very dangerous procedure—electrical balance <i>must</i> be maintained by the transport equations and therefore can be used as a test of the numerical accuracy of the calculated result rather than forcing it to hold by altering the species concentrations in ways which may be inconsistent with the governing equations.• By using the logarithms of the species concentrations as the independent variables, GEM has no difficulty in accounting for widely spatially varying concentration profiles of a species within a crevice, for example. TWITCH had difficulty in converging under such circumstances.

- GEM is based on a minimal set of primary species to formulate mass balance equations. TWITCH uses separate transport equations for each species in solution.
- TWITCH uses an uncoupled approach for combining local equilibrium reactions with transport. A fully coupled, global implicit finite difference algorithm is employed in GEM to solve the mass transport equations.

Construction of a general corrosion model was begun by adding various new features to an existing finite difference code developed by the author (MCCTM) for chemical transport modeling. These included:

1. Add parameter values for arrays in include file: `params.inc`.
2. Efficient time stepping algorithm.
3. UNIX command line options (`gunits.f`) for specifying file names.
4. Read database.
5. Option for cylindrical or spherical symmetry.
6. Use $\ln C_i$ for independent variables to improve convergence.
7. Add adaptive gridding capability.
8. Plot files as spreadsheet arrays.
9. Separate grids for solids and aqueous and gaseous species.
10. Stationary state calculation.
11. Species dependent diffusion coefficients.
12. Use chemical potential gradient for concentrated solutions.
13. Basis switching.
14. Scaling of Jacobian

It is envisaged that the revised code would eventually be able to handle two-phase fluid transport in partially saturated porous media and multicomponent chemical reactions including electrochemical processes.

2.7.94

Equations were developed for incorporating unequal diffusion coefficients in mass conservation equations. Partial differential equations for constant, but species-dependent,

diffusion coefficients read:

$$\frac{\partial}{\partial t} \phi \Psi_j + \nabla \cdot v \Psi_j - \nabla \cdot \phi \nabla \Psi_j^D = - \sum_r \nu_{jr} I_r, \quad (2-3)$$

where

$$\Psi_j^D = D_j C_j + \sum_i \nu_{ji} D_i C_i. \quad (2-4)$$

It is important to realize, however, that this form does *not* ensure charge conservation.

2.8.94

Equations for determination of the electric potential field in the case of unequal diffusion coefficients were developed. The generalized solute flux Ω_j is given by the expression

$$\Omega_j = -\phi \Psi_j^\epsilon F \frac{\nabla \Phi}{RT} - \phi \nabla \Psi_j^D + v \Psi_j, \quad (2-5)$$

where

$$\Psi_j^\epsilon = z_j D_j C_j + \sum_i \nu_{ji} z_i D_i C_i, \quad (2-6)$$

using the relation of the mobility u_l to the diffusion coefficient given by the expression

$$u_l = \frac{D_l}{RT}. \quad (2-7)$$

The current density is defined by

$$\mathbf{i} = F \sum_j z_j \Omega_j = -\phi F^2 \frac{\nabla \Phi}{RT} \sum_j z_j \Psi_j^\epsilon - \phi F \sum_j z_j \nabla \Psi_j^D. \quad (2-8)$$

It follows that the gradient in the electric potential Φ , or electric field, can be expressed as

$$\nabla \Phi = -RT \frac{\mathbf{i} + \phi F \sum_j z_j \nabla \Psi_j^D}{\phi F^2 \sum_j z_j \Psi_j^\epsilon}. \quad (2-9)$$

Defining Φ_0 by the equation

$$\nabla \Phi_0 = -RT \frac{\sum_j z_j \nabla \Psi_j^D}{F \sum_j z_j \Psi_j^\epsilon}. \quad (2-10)$$

and writing

$$\Phi = \Phi_0 + \delta \Phi, \quad (2-11)$$

yields

$$\nabla \delta \Phi = -RT \frac{\mathbf{i}}{\phi F^2 \sum_j z_j \Psi_j^\epsilon}. \quad (2-12)$$

2.8.94

Scaling. Scaling the Jacobian matrix may offer some advantage in solving the nonlinear partial differential equations representing reactive transport. The Newton-Raphson equations read:

$$\sum_{lm} J_{jn,lm} \Delta x_{lm} = -R_{jn}, \quad (2-13)$$

for unknowns Δx_{lm} , where $J_{jn,lm}$ denotes the Jacobian matrix and R_{jn} denotes the residual. These equations may be scaled by writing

$$\sum_{lm} \frac{J_{jn,lm}}{J_{jn,jn}} \Delta x_{lm} = -\frac{R_{jn}}{J_{jn,jn}}. \quad (2-14)$$

2.9.94

Equations to conserve charge in multicomponent diffusion with unequal diffusion coefficients are developed. Substituting for the gradient of the electric potential in the general form of the solute flux yields the expression for the diffusive component

$$\begin{aligned} \Omega_j^D &= \frac{\Psi_j^\epsilon}{F \sum_l z_l \Psi_l^\epsilon} \mathbf{i} + \phi \Psi_j^\epsilon \frac{\sum_l z_l \nabla \Psi_l}{\sum_{l'} z_{l'} \Psi_{l'}^\epsilon} - \phi \nabla \Psi_j^D, \\ &= \frac{\Psi_j^\epsilon}{F \sum_l z_l \Psi_l^\epsilon} \mathbf{i} + \phi \sum_l \left[\frac{\Psi_j^\epsilon z_l}{\sum_{l'} z_{l'} \Psi_{l'}^\epsilon} - \delta_{jl} \right] \nabla \Psi_l^D. \end{aligned} \quad (2-15)$$

With this expression the generalized flux can be recast in the matrix form

$$\begin{aligned} \Omega_j &= \frac{1}{F} \Gamma_j \mathbf{i} - \phi \sum_l \beta_{jl} \nabla \Psi_l^D + \mathbf{v} \Psi_j, \\ &= \Omega_j^D + \Omega_j^v, \end{aligned} \quad (2-16)$$

where the matrix β_{jl} is defined by

$$\beta_{jl} = \delta_{jl} - \Gamma_j z_l, \quad (2-17)$$

with

$$\Gamma_j = \frac{\Psi_j^\epsilon}{\sum_l z_l \Psi_l^\epsilon}. \quad (2-18)$$

Alternatively, the total flux can be expressed as

$$\Omega_j = \Omega_j^0 + \Omega_j^\Gamma, \quad (2-19)$$

where

$$\Omega_j^0 = -\phi \nabla \Psi_j^D + \Omega_j^v, \quad (2-20)$$

and

$$\Omega_j^\Gamma = \Gamma_j \left[\frac{1}{F} \mathbf{i} + \phi \sum_l z_l \nabla \Psi_l^D \right]. \quad (2-21)$$

Properties of the Matrix β_{jl} . The matrix β_{jl} is a projection operator, i.e. it satisfies the relation

$$\sum_l \beta_{jl} \beta_{lk} = \beta_{jk}, \quad (2-22)$$

or in matrix notation:

$$\beta^2 = \beta. \quad (2-23)$$

Furthermore, it follows that

$$\sum_j z_j \beta_{jk} = 0, \quad (2-24)$$

which is a consequence of the relation

$$\sum_j z_j \Gamma_j = 1, \quad (2-25)$$

according to the definition of Γ_j .

Charge Conservation. It follows from the properties of β_{jl} that, in the absence of an electric current ($\mathbf{i} = 0$), charge is conserved by the mass transport equations. Thus

$$\sum_j z_j \Omega_j^D = -\phi \sum_j z_j \beta_{jl} \nabla \Psi_l^D = 0. \quad (2-26)$$

2.14.94

Code Validation. Code validation was accomplished by comparing results with the semi-analytical solution obtained by Lichtner (Lichtner, P. C. (1991) The quasi-stationary state approximation to fluid-rock reaction: local equilibrium revisited, Ed. Ganguly, *Advances in Physical Geochemistry* 8, 454–562) for the three component system A-B-C.

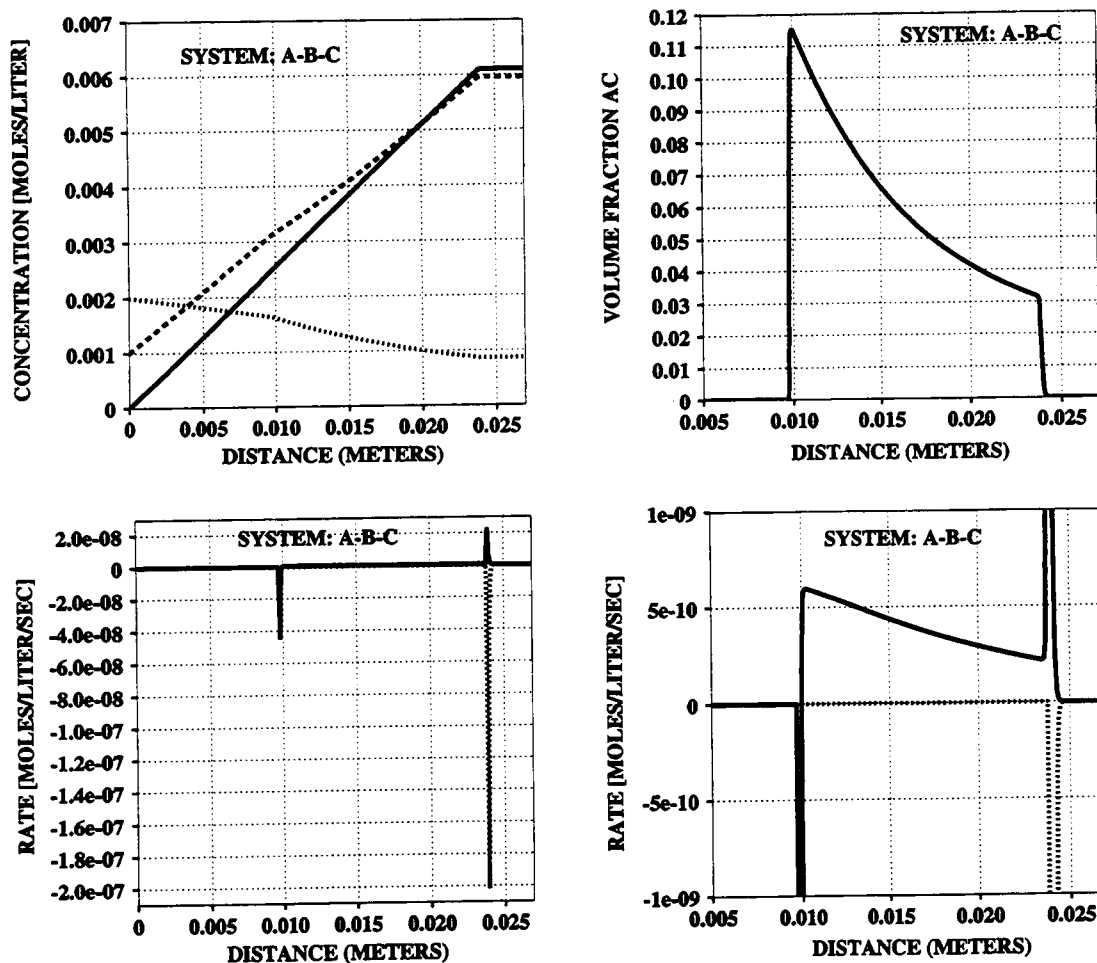


Figure 2-1: Numerical calculation for conditions approximating local chemical equilibrium in the three component system A-B-C. The results are in excellent agreement with semi-analytical solution for the same problem presented by Lichtner (1991). Calculations are given for an elapsed time of 100 years.

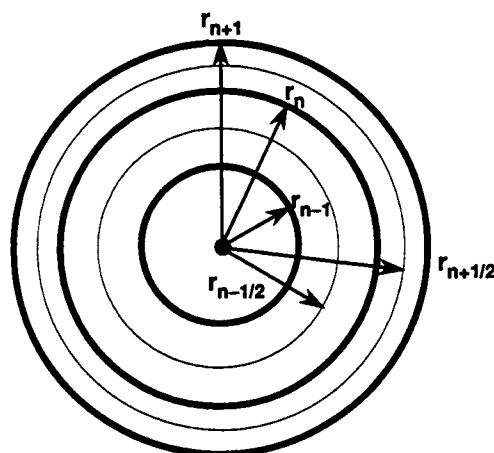


Figure 2-2: Coordinates used to define cylindrically and spherically symmetric grids.

2.18.94 Finite difference equations in cylindrical geometry. For cylindrical coordinates the mass transport equations read

$$\frac{\partial}{\partial t} (\phi C) + \frac{1}{r} \frac{\partial}{\partial r} (r J) = - \sum_m \nu_{jm} I_m, \quad (2-27)$$

with the radial flux given by

$$J = -\phi D \frac{\partial C}{\partial r} + v C. \quad (2-28)$$

Finite difference equations are obtained by integrating over the n th control volume (see Fig. 2-2):

$$\int_{r_{n-1/2}}^{r_{n+1/2}} \phi C 2\pi r dr = \pi (r_{n+1/2}^2 - r_{n-1/2}^2) \phi_n C_n, \quad (2-29)$$

and

$$\int_{r_{n-1/2}}^{r_{n+1/2}} \frac{1}{r} \frac{\partial}{\partial r} (r J) 2\pi r dr = 2\pi (r_{n+1/2} J_{n+1/2} - r_{n-1/2} J_{n-1/2}). \quad (2-30)$$

This procedure yields the finite difference equation given by

$$\phi \frac{\Delta C_n}{\Delta t} V_n + A_{n+1/2} J_{n+1/2} - A_{n-1/2} J_{n-1/2} = -V_n \sum_m \nu_{jm} I_{mn}, \quad (2-31)$$

where the nodal volume is given by

$$V_n = \pi (r_{n+1/2}^2 - r_{n-1/2}^2), \quad (2-32)$$

and the interface surface areas by

$$A_{n+1/2} = 2\pi r_{n+1/2} = \pi (r_{n+1} + r_n), \quad (2-33)$$

$$A_{n-1/2} = 2\pi r_{n-1/2} = \pi (r_n + r_{n-1}). \quad (2-34)$$

In these relations

$$r_{n+1/2} = \frac{1}{2} (r_{n+1} + r_n), \quad (2-35)$$

and

$$r_{n-1/2} = \frac{1}{2} (r_n + r_{n-1}). \quad (2-36)$$

The finite difference form of the diffusive flux is given by

$$J_{n+1/2} = -\phi D_{n+1/2} \frac{C_{n+1} - C_n}{r_{n+1} - r_n}, \quad (2-37)$$

and

$$J_{n-1/2} = -\phi D_{n-1/2} \frac{C_n - C_{n-1}}{r_n - r_{n-1}}. \quad (2-38)$$

The diffusion coefficients evaluated at the interfaces can be calculated either by the harmonic mean:

$$D_{n\pm 1/2} = \frac{2D_{n\pm 1}D_n}{D_{n\pm 1} + D_n}, \quad (2-39)$$

or the arithmetic mean:

$$D_{n\pm 1/2} = \frac{1}{2} (D_{n\pm 1} + D_n). \quad (2-40)$$

For spherical symmetry it follows that

$$\frac{\partial}{\partial t} (\phi C) + \frac{1}{r^2} \frac{\partial}{\partial r} (r^2 J) = - \sum_m \nu_{jm} I_m, \quad (2-41)$$

where the radial flux has the same form as in the cylindrical case but with the coordinate r now referring to the spherical radius. Finite difference equations follow by integrating over a spherical shell as control volume

$$\int_{r_{n-1/2}}^{r_{n+1/2}} \dots 4\pi r^2 dr. \quad (2-42)$$

This gives the nodal volume

$$V_n^{sp} = \frac{4\pi}{3} (r_{n+1/2}^3 - r_{n-1/2}^3), \quad (2-43)$$

and interface areas

$$A_{n+1/2}^{sp} = 4\pi r_{n+1/2}^2 = \pi (r_{n+1} + r_n)^2, \quad (2-44)$$

$$A_{n-1/2}^{sp} = 4\pi r_{n-1/2}^2 = \pi (r_n + r_{n-1})^2. \quad (2-45)$$

In terms of the solute concentration the finite difference equations become

$$\begin{aligned} R_n = & \phi \frac{\Delta C_n}{\Delta t} V_n - \frac{\phi D A_{n+1/2}}{\Delta x_{n+1}} C_{n+1} + \phi D \left(\frac{A_{n+1/2}}{\Delta x_{n+1}} - \frac{A_{n-1/2}}{\Delta x_n} \right) C_n \\ & - \frac{\phi D A_{n-1/2}}{\Delta x_n} C_{n-1} + V_n \sum \nu_{jr} I_{rn} \\ & + \frac{v}{2} A_{n+1/2} C_{n+1} + \frac{v}{2} (A_{n+1/2} - A_{n-1/2}) C_n - \frac{v}{2} A_{n-1/2} C_{n-1}, \end{aligned} \quad (2-46)$$

writing

$$A_{n+1/2} J_{n+1/2} = -\phi D A_{n+1/2} \frac{C_{n+1} - C_n}{\Delta x_{n+1}} + \frac{v}{2} A_{n+1/2} (C_{n+1} + C_n), \quad (2-47)$$

and

$$A_{n-1/2} J_{n-1/2} = -\phi D A_{n-1/2} \frac{C_n - C_{n-1}}{\Delta x_n} + \frac{v}{2} A_{n-1/2} (C_n + C_{n-1}). \quad (2-48)$$

Combining terms yields

$$\begin{aligned} R_n = & \phi \frac{\Delta C_n}{\Delta t} V_n + V_n \sum \nu_{jr} I_{rn} \\ & + \left[\frac{v}{2} - \frac{\phi D}{\Delta x_{n+1}} \right] A_{n+1/2} C_{n+1} \\ & + \left[\frac{v}{2} (A_{n+1/2} - A_{n-1/2}) + \phi D \left(\frac{A_{n+1/2}}{\Delta x_{n+1}} + \frac{A_{n-1/2}}{\Delta x_n} \right) \right] C_n \\ & - \left[\frac{v}{2} + \frac{\phi D}{\Delta x_n} \right] A_{n-1/2} C_{n-1}. \end{aligned} \quad (2-49)$$

By comparison, in one dimension

$$V_n^{1D} = \delta x_n = x_{n+1/2} - x_{n-1/2} = \frac{1}{2} (x_{n+1} - x_{n-1}) = \frac{1}{2} (\Delta x_{n+1} + \Delta x_n), \quad (2-50)$$

and

$$A_{n+1/2}^{1D} = A_{n-1/2}^{1D} = 1, \quad (2-51)$$

where

$$\Delta x_n = x_n - x_{n-1}. \quad (2-52)$$

The finite difference equations simplify to

$$\phi \frac{\Delta C}{\Delta t} \delta x_n + J_{n+1/2} - J_{n-1/2} = -\delta x_n \sum_m \nu_{jm} I_{mn}. \quad (2-53)$$

3.10.94 Zero flux boundary conditions. Zero flux boundary conditions for diffusive transport at the inlet or outlet of the porous column are implemented using a fictitious node point outside the boundary. The boundary is assumed to be located half way between the N th and the $N + 1$ st nodes, and the 0th and 1st nodes. This geometry implies that the node points x_N and x_1 do not correspond to the boundary point. For the N th node point this leads to the condition:

$$\Psi_{j,N+1} = \Psi_{jN}. \quad (2-54)$$

The residual flux term then becomes

$$R_{jN} = (\beta_N + \alpha_N) \Psi_{jN} + \gamma_N \Psi_{j,N-1}. \quad (2-55)$$

For zero flux at the inlet, the condition is

$$\Psi_{j0} = \Psi_{j1}. \quad (2-56)$$

In this case the residual flux term becomes

$$R_{j1} = \beta_1 \Psi_{j2} + (\alpha_1 + \gamma_1) \Psi_{j1}. \quad (2-57)$$

Note that the inlet is assumed to be located midway between the 0th and 1st node points.

3.15.94 Finite difference equations for species dependent diffusion coefficients and constant porosity. The general form of the residuals is given by

$$R_{jn} = R_{jn}^0 + R_{jn}^\Gamma, \quad (2-58)$$

where

$$\begin{aligned} R_{jn}^0 &= \phi \frac{\Psi_{jn}^{t+\Delta t} - \Psi_{jn}^t}{\Delta t} V_n + \sum_r \nu_{jr} I_{rn} V_n \\ &\quad + A_{n+1/2} \Omega_{j,n+1/2} - A_{n-1/2} \Omega_{j,n-1/2}, \\ &= \phi \frac{\Psi_{jn}^{t+\Delta t} - \Psi_{jn}^t}{\Delta t} V_n + \sum_r \nu_{jr} I_{rn} V_n \\ &\quad - \phi \frac{A_{n+1/2}}{\Delta x_{n+1}} \Psi_{j,n+1}^D + \phi \left(\frac{A_{n+1/2}}{\Delta x_{n+1}} + \frac{A_{n-1/2}}{\Delta x_n} \right) \Psi_{jn}^D - \phi \frac{A_{n-1/2}}{\Delta x_n} \Psi_{j,n-1}^D \\ &\quad + \frac{v}{2} \left\{ A_{n+1/2} \Psi_{j,n+1} + (A_{n+1/2} - A_{n-1/2}) \Psi_{jn} - A_{n-1/2} \Psi_{j,n-1} \right\}, \end{aligned} \quad (2-59)$$

and

$$R_{jn}^{\Gamma} = \phi(\Gamma_j)_{n+1/2} A_{n+1/2} \sum_k \frac{\Psi_{k,n+1}^D - \Psi_{kn}^D}{\Delta x_{n+1}} - \phi(\Gamma_j)_{n-1/2} A_{n-1/2} \sum_k \frac{\Psi_{kn}^D - \Psi_{k,n-1}^D}{\Delta x_n}. \quad (2-60)$$

It follows that the residuals can be expressed in the form

$$R_{jn}^0 = \phi \frac{\Psi_{jn}^{t+\Delta t} - \Psi_{jn}^t}{\Delta t} V_n + \sum_r \nu_{jr} I_{rn} V_n + \beta_n \Psi_{jn+1} + \alpha_n \Psi_{jn} + \gamma_n \Psi_{j,n-1} + \beta_n^D \Psi_{j,n+1}^D + \alpha_n^D \Psi_{jn}^D + \gamma_n^D \Psi_{j,n-1}^D, \quad (2-61)$$

and

$$R_{jn}^{\Gamma} = \beta_{jn}^{\Gamma} \sum_k z_k \Psi_{k,n+1}^D + \alpha_{jn}^{\Gamma} \sum_k z_k \Psi_{kn}^D + \gamma_{jn}^{\Gamma} \sum_k z_k \Psi_{k,n-1}^D. \quad (2-62)$$

The various coefficients appearing in these expressions are given by

$$\alpha_n = \frac{v}{2} (A_{n+1/2} - A_{n-1/2}), \quad (2-63)$$

$$\beta_n = \frac{v}{2} A_{n+1/2}, \quad (2-64)$$

$$\gamma_n = -\frac{v}{2} A_{n-1/2}, \quad (2-65)$$

$$\alpha_n^D = \phi \left(\frac{A_{n+1/2}}{\Delta x_{n+1}} + \frac{A_{n-1/2}}{\Delta x_n} \right), \quad (2-66)$$

$$\beta_n^D = -\phi \frac{A_{n+1/2}}{\Delta x_{n+1}}, \quad (2-67)$$

$$\gamma_n^D = -\phi \frac{A_{n-1/2}}{\Delta x_n}, \quad (2-68)$$

$$\alpha_{jn}^{\Gamma} = - \left(\frac{\phi A_{n+1/2}}{\Delta x_{n+1}} (\Gamma_j)_{n+1/2} + \frac{\phi A_{n-1/2}}{\Delta x_n} (\Gamma_j)_{n-1/2} \right), \quad (2-69)$$

$$\beta_{jn}^{\Gamma} = \frac{\phi A_{n+1/2}}{\Delta x_{n+1}} (\Gamma_j)_{n+1/2}, \quad (2-70)$$

$$\gamma_{jn}^{\Gamma} = \frac{\phi A_{n-1/2}}{\Delta x_n} (\Gamma_j)_{n-1/2}. \quad (2-71)$$

3.16.94 Jacobian Matrix. The Jacobian matrix is defined by

$$J_{jn,lm} = \frac{\partial R_{jn}}{\partial \ln C_{lm}}, \\ = \frac{\partial R_{jn}^0}{\partial \ln C_{lm}} + \frac{\partial R_{jn}^{\Gamma}}{\partial \ln C_{lm}}, \quad (2-72)$$

with

$$\begin{aligned} \frac{\partial R_{jn}^0}{\partial \ln C_{lm}} = & \frac{\phi}{\Delta t} \frac{\partial \Psi_{jn}}{\partial \ln C_{lm}} V_n \delta_{mn} + \sum_r \nu_{jr} \frac{\partial I_{rn}}{\partial \ln C_{lm}} V_n \\ & + \beta_n \delta_{m,n+1} \frac{\partial \Psi_{j,n+1}}{\partial \ln C_{lm}} + \alpha_n \delta_{mn} \frac{\partial \Psi_{jn}}{\partial \ln C_{lm}} + \gamma_n \delta_{m,n-1} \frac{\partial \Psi_{j,n-1}}{\partial \ln C_{lm}} \\ & + \beta_n^D \delta_{m,n+1} \frac{\partial \Psi_{j,n+1}^D}{\partial \ln C_{lm}} + \alpha_n^D \delta_{mn} \frac{\partial \Psi_{jn}^D}{\partial \ln C_{lm}} + \gamma_n^D \delta_{m,n-1} \frac{\partial \Psi_{j,n-1}^D}{\partial \ln C_{lm}}, \end{aligned} \quad (2-73)$$

and

$$\begin{aligned} \frac{\partial R_{jn}^\Gamma}{\partial \ln C_{lm}} = & \beta_{jn}^\Gamma \sum_k z_k \frac{\partial \Psi_{k,n+1}^D}{\partial \ln C_{lm}} + \alpha_{jn}^\Gamma \sum_k z_k \frac{\partial \Psi_{kn}^D}{\partial \ln C_{lm}} + \gamma_{jn}^\Gamma \sum_k z_k \frac{\partial \Psi_{k,n-1}^D}{\partial \ln C_{lm}} \\ & + \frac{\partial \beta_{jn}^\Gamma}{\partial \ln C_{lm}} \sum_k z_k \Psi_{k,n+1}^D + \frac{\partial \alpha_{jn}^\Gamma}{\partial \ln C_{lm}} \sum_k z_k \Psi_{kn}^D + \frac{\partial \gamma_{jn}^\Gamma}{\partial \ln C_{lm}} \sum_k z_k \Psi_{k,n-1}^D. \end{aligned} \quad (2-74)$$

3.23.94

Partial derivatives required for computing the Jacobian analytically. To compute the Jacobian analytically the following partial derivatives are required:

$$\frac{\partial \Gamma_j}{\partial \ln C_l} = \frac{\Gamma_j}{\Psi_j^\epsilon} \left\{ \frac{\partial \Psi_j^\epsilon}{\partial \ln C_l} - \Gamma_j \sum_k z_k \frac{\partial \Psi_k^\epsilon}{\partial \ln C_l} \right\}, \quad (2-75)$$

and

$$\frac{\partial R_{jn}^\Gamma}{\partial \ln C_{l,n+1}} = \beta_{jn}^\Gamma \frac{\partial f_{n+1}}{\partial \ln C_{l,n+1}} + \frac{\partial \beta_{jn}^\Gamma}{\partial \ln C_{l,n+1}} f_{n+1} + \frac{\partial \alpha_{jn}^\Gamma}{\partial \ln C_{l,n+1}} f_n, \quad (2-76)$$

$$\frac{\partial R_{jn}^\Gamma}{\partial \ln C_{ln}} = \alpha_{jn}^\Gamma \frac{\partial f_n}{\partial \ln C_{ln}} + \frac{\partial \beta_{jn}^\Gamma}{\partial \ln C_{ln}} f_{n+1} + \frac{\partial \alpha_{jn}^\Gamma}{\partial \ln C_{ln}} f_n + \frac{\partial \gamma_{jn}^\Gamma}{\partial \ln C_{ln}} f_{n-1}, \quad (2-77)$$

$$\frac{\partial R_{jn}^\Gamma}{\partial \ln C_{l,n-1}} = \gamma_{jn}^\Gamma \frac{\partial f_{n-1}}{\partial \ln C_{l,n-1}} + \frac{\partial \alpha_{jn}^\Gamma}{\partial \ln C_{l,n-1}} f_n + \frac{\partial \gamma_{jn}^\Gamma}{\partial \ln C_{l,n-1}} f_{n-1}, \quad (2-78)$$

where

$$f_n = \sum_l z_l \Psi_{ln}^D. \quad (2-79)$$

For the special case of arithmetic mean values of Γ_j at node interfaces the derivatives of the coefficient matrices are given by

$$\frac{\partial \alpha_{jn}^\Gamma}{\partial \ln C_{l,n+1}} = -\frac{\phi}{2} \frac{A_{n+1/2}}{\Delta x_{n+1}} \frac{\partial \Gamma_{j,n+1}}{\partial \ln C_{l,n+1}}, \quad (2-80)$$

$$\frac{\partial \alpha_{jn}^\Gamma}{\partial \ln C_{ln}} = -\frac{\phi}{2} \left(\frac{A_{n+1/2}}{\Delta x_{n+1}} + \frac{A_{n-1/2}}{\Delta x_n} \right) \frac{\partial \Gamma_{jn}}{\partial \ln C_{ln}}, \quad (2-81)$$

$$\frac{\partial \alpha_{jn}^\Gamma}{\partial \ln C_{l,n-1}} = -\frac{\phi}{2} \frac{A_{n-1/2}}{\Delta x_n} \frac{\partial \Gamma_{j,n-1}}{\partial \ln C_{l,n-1}}, \quad (2-82)$$

(2-83)

$$\frac{\partial \beta_{jn}^{\Gamma}}{\partial \ln C_{l,n+1}} = \frac{\phi A_{n+1/2}}{2 \Delta x_{n+1}} \frac{\partial \Gamma_{j,n+1}}{\partial \ln C_{l,n+1}}, \quad (2-84)$$

$$\frac{\partial \beta_{jn}^{\Gamma}}{\partial \ln C_{ln}} = \frac{\phi A_{n+1/2}}{2 \Delta x_{n+1}} \frac{\partial \Gamma_{jn}}{\partial \ln C_{ln}}, \quad (2-85)$$

(2-86)

$$\frac{\partial \gamma_{jn}^{\Gamma}}{\partial \ln C_{ln}} = \frac{\phi A_{n-1/2}}{2 \Delta x_n} \frac{\partial \Gamma_{jn}}{\partial \ln C_{ln}}, \quad (2-87)$$

$$\frac{\partial \gamma_{jn}^{\Gamma}}{\partial \ln C_{l,n-1}} = \frac{\phi A_{n-1/2}}{2 \Delta x_n} \frac{\partial \Gamma_{j,n-1}}{\partial \ln C_{l,n-1}}. \quad (2-88)$$

With these results the Jacobian matrix becomes

$$\frac{\partial R_{jn}^{\Gamma}}{\partial \ln C_{l,n+1}} = \beta_{jn}^{\Gamma} \frac{\partial f_{n+1}}{\partial \ln C_{l,n+1}} + \frac{\phi A_{n+1/2}}{2 \Delta x_{n+1}} (f_{n+1} - f_n) \frac{\partial \Gamma_{j,n+1}}{\partial \ln C_{l,n+1}}, \quad (2-89)$$

$$\frac{\partial R_{jn}^{\Gamma}}{\partial \ln C_{ln}} = \alpha_{jn}^{\Gamma} \frac{\partial f_n}{\partial \ln C_{ln}} + \frac{\phi}{2} \left[\frac{A_{n+1/2}}{\Delta x_{n+1}} (f_{n+1} - f_n) - \frac{A_{n-1/2}}{\Delta x_n} (f_n - f_{n-1}) \right] \frac{\partial \Gamma_{jn}}{\partial \ln C_{ln}}, \quad (2-90)$$

$$\frac{\partial R_{jn}^{\Gamma}}{\partial \ln C_{l,n-1}} = \gamma_{jn}^{\Gamma} \frac{\partial f_{n-1}}{\partial \ln C_{l,n-1}} - \frac{\phi A_{n-1/2}}{2 \Delta x_n} (f_n - f_{n-1}) \frac{\partial \Gamma_{j,n-1}}{\partial \ln C_{l,n-1}}, \quad (2-91)$$

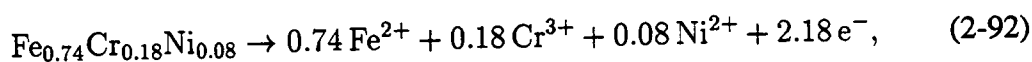
3.30.94 Alavi & Cottis (1987) Experiment

- bulk solution: 0.6 M NaCl, pH 6
- crevice dimensions: 8 cm long, 2.5 cm wide, 0.09 mm gap
- 304 stainless steel alloy: 74% Fe, 18% Cr, 8% Ni
- measurement nodes: 160 nodes with spacing 0.05 cm

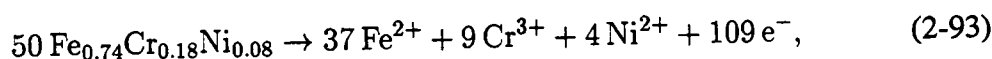
position cm	node #
0.35	7
1.0	20
2.0	40
4.0	80
7.5	150

- measurement times: 2, 18, 24, 43, 90, 116, 164 hours

- anodic current not measured: assumed values: 10^{-5} , 10^{-6} , 10^{-7} A cm $^{-2}$
- stoichiometric dissolution of 304SS can be represented by the reaction:



or, in terms of integer coefficients, by the reaction:



obtained by multiplying the first reaction through by the factor 50.

The crevice volume average dissolution rate of 304SS is related to the current density at the metal surface by the relation

$$I_{304\text{SS}} = -\frac{2}{l_g} i_e^0 \frac{1}{2.18F}, \quad (2-94)$$

noting that $n_e = 2.18$. An effective rate constant can be defined from this relation as

$$k_{eff} = i_e^0 \frac{1}{2.18F}. \quad (2-95)$$

For a crevice gap $l_g = 90 \mu\text{m}$, the specific surface area has the value $2/l_g = 222.222 \text{ cm}^{-1}$. The effective rate constant corresponding to several values of the surface current is given in the accompanying table.

$\log[i_e^0]$ [A cm $^{-2}$]	k_{eff} moles cm $^{-2}$ s $^{-1}$
-5	4.75417×10^{-11}
-6	4.75417×10^{-12}
-7	4.75417×10^{-13}

3.30.94

Electric Potential, Electric Field, Current Densities, Corrosion Reaction Rate, and Current Flux Term. In the absence of an electric current in solution, the electrical potential satisfies the equation

$$\frac{\partial}{\partial x} \Phi_0 = \rho_e^0, \quad (2-96)$$

where the charge density ρ_e^0 is defined by

$$\rho_e^0 = -RT \frac{\sum_j z_j \partial \Psi_j^D / \partial x}{\sum_l z_l \Psi_l^E}. \quad (2-97)$$

Integrating gives

$$\Phi_0(x, t) = \Phi_0^0 + \int_0^x \rho_e^0(x', t) dx'. \quad (2-98)$$

This relation may be expressed in finite difference form as a recursion relation according to

$$\Phi_{0n} = \Phi_{0,n-1} + \rho_{en}^0 \Delta x_n. \quad (2-99)$$

The derivative $\partial \Psi_j^D / \partial x$ is approximated as

$$\left(\frac{\partial \Psi_j^D}{\partial x} \right)_n = \frac{\Psi_{j,n+1}^D - \Psi_{j,n-1}^D}{\Delta x_{n+1} + \Delta x_n}. \quad (2-100)$$

In the presence of an electric current in solution, the electric potential Φ_0 must be augmented by the contribution $\delta \Phi$ involving the solution current density given by

$$\delta \Phi = -RT \frac{i(x, t)}{\phi F^2 \sum_l z_l \Psi_l^\epsilon}, \quad (2-101)$$

where the current density in solution, $i(x, t)$, averaged over the crevice gap is given by

$$i(x, t) = \frac{2}{l_g} \int_0^x i_e(x', t) dx', \quad (2-102)$$

where i_e denotes the total electrochemical current density at the surface of the corroding metal equal to the sum of individual currents

$$i_e = \sum_k i_k. \quad (2-103)$$

The current density i_k is related to the crevice-averaged dissolution rate I_k^{corr} by the expression

$$i_k = \frac{l_g}{2} F n_k I_k^{corr}. \quad (2-104)$$

As a consequence the solution current density can be expressed as

$$i(x, t) = F \sum_k n_k \int_0^x I_k^{corr}(x', t) dx', \quad (2-105)$$

which in finite difference form becomes

$$i_n = F \sum_k n_k \sum_{n'=1}^n I_{kn'}^{corr} \Delta x_{n'}. \quad (2-106)$$

The contribution of the solution current density to the flux is given by

$$\begin{aligned}\Omega_j^e &= \frac{1}{F} \Gamma_j i(x, t), \\ &= \Gamma_j \sum_k n_k \int_0^x I_k^{corr}(x', t) dx', \\ &= \Gamma_j Q(x, t),\end{aligned}\tag{2-107}$$

where

$$Q(x, t) = \sum_k n_k \int_0^x I_k^{corr}(x', t) dx'. \tag{2-108}$$

The contribution to the residual is given by

$$R_{jn}^e = A_{n+1/2} \Omega_{j,n+1/2}^e - A_{n-1/2} \Omega_{j,n-1/2}^e, \tag{2-109}$$

and the Jacobian by

$$J_{jn,lm} = \frac{\partial R_{jn}^e}{\partial \ln C_{lm}} = \frac{\partial \Gamma_{j,n+1/2}}{\partial \ln C_{lm}} Q_{n+1/2} - \frac{\partial \Gamma_{j,n-1/2}}{\partial \ln C_{lm}} Q_{n-1/2}. \tag{2-110}$$

Numerically,

$$Q_n = \sum_k n_k \sum_{n'=1}^n I_{kn'}^{corr} \Delta x_{n'}, \tag{2-111}$$

and

$$Q_{n-1/2} = \frac{1}{2} (Q_n + Q_{n-1}), \tag{2-112}$$

or

$$Q_{n-1/2} = \frac{2Q_n Q_{n-1}}{Q_n + Q_{n-1}}, \tag{2-113}$$

for arithmetic and harmonic means, respectively.

4.5.94

Residual for Electrochemical Current Density and Charge Balance. The solute flux can be expressed in the form:

$$\Omega_j = \Omega_j^0 + \Omega_j^\Gamma + \Omega_j^e, \tag{2-114}$$

where

$$\Omega_j^0 = -\phi \nabla \Psi_j^D + \Omega_j^v, \tag{2-115}$$

$$\Omega_j^\Gamma = \phi \frac{1}{F} \Gamma_j \sum_l z_l \nabla \Psi_l^D, \tag{2-116}$$

and

$$\Omega_j^e = \frac{1}{F} \Gamma_j i. \tag{2-117}$$

The first two terms balance electrical charge identically:

$$\sum_j z_j (\Omega_j^0 + \Omega_j^r) = 0. \quad (2-118)$$

The third term gives the condition

$$F \sum_j z_j \Omega_j^e = i. \quad (2-119)$$

The contribution of the electrochemical term to the residual is given by

$$R_{jn}^e = \frac{1}{F} (A_{n+1/2} \Gamma_{j,n+1/2} i_{n+1/2} - A_{n-1/2} \Gamma_{j,n-1/2} i_{n-1/2}). \quad (2-120)$$

The condition for electroneutrality yields the relation

$$F \sum_j z_j R_{jn} = A_{n+1/2} i_{n+1/2} - A_{n-1/2} i_{n-1/2} + V_n \sum_k i_{kn}, \quad (2-121)$$

where

$$i_k = - \sum_{jk} z_j \nu_{jk} I_k^{corr} = - \sum_k n_k I_k^{corr}. \quad (2-122)$$

This result must be consistent with the differential form

$$\frac{\partial i}{\partial r} = \sum_k i_k, \quad (2-123)$$

which follows directly from the mass conservation equations. The current should be calculated at the node interfaces from the recursion relation

$$i_{n+1/2} = \frac{A_{n-1/2}}{A_{n+1/2}} i_{n-1/2} + \frac{V_n}{A_{n+1/2}} \sum_k i_{kn}, \quad (2-124)$$

which then conserves charge identically.

The Jacobian matrix corresponding to the current density term has the form

$$\begin{aligned} J_{jn,lm}^e &= \frac{\partial R_{jn}^e}{\partial \ln C_{lm}}, \\ &= \frac{1}{F} \left(A_{n+1/2} \frac{\partial \Gamma_{j,n+1/2}}{\partial \ln C_{lm}} i_{n+1/2} - A_{n-1/2} \frac{\partial \Gamma_{j,n-1/2}}{\partial \ln C_{lm}} i_{n-1/2} \right). \end{aligned} \quad (2-125)$$

Non-zero terms are:

$$\frac{\partial R_{jn}^e}{\partial \ln C_{l,n+1}} = \frac{1}{2F} A_{n+1/2} \frac{\partial \Gamma_{j,n+1/2}}{\partial \ln C_{l,n+1}} i_{n+1/2}, \quad (2-126)$$

$$\frac{\partial R_{jn}^e}{\partial \ln C_{ln}} = \frac{1}{2F} [A_{n+1/2} i_{n+1/2} - A_{n-1/2} i_{n-1/2}] \frac{\partial \Gamma_{jn}}{\partial \ln C_{ln}}, \quad (2-127)$$

$$\frac{\partial R_{jn}^e}{\partial \ln C_{l,n-1}} = \frac{1}{2F} A_{n-1/2} \frac{\partial \Gamma_{j,n-1/2}}{\partial \ln C_{l,n-1}} i_{n-1/2}, \quad (2-128)$$

4.11.94 Comparison with Experimental Results by Sridahar and Dunn for Diffusion in an Electrolyte Solution. The computer code **GEM** (General Electrochemical Migration Model) was compared with experimental results of diffusion in a radially symmetric crevice.

- size of apparatus: inner radius = 0 mm, outer radius = 9.5 mm
- electrode positions: inner radius = 0 mm; outer radius = 7.6 mm

Preliminary results showed poor agreement with experiment. Two cases were considered in the experiments. In the first case the outer boundary of the crevice was held at a fixed pH of 2, with the interior of the crevice at a starting pH of 6. In the second case the situation was reversed with an interior pH of 2, and a pH at the outer boundary of 6. A result of the experiments was the much longer time required for the system to reach a steady state in the second case compared to the first case. This could be easily explained as the longer time required to reduce the hydrogen ion concentration to a very low value of 10^{-6} moles liter⁻¹ from an initial value of 10^{-2} moles liter⁻¹ in the second experiment, as compared to the first experiment. However, the theoretical calculations with **GEM** reached a steady-state an order of magnitude in time faster compared to the experimental results (results not shown).

5.10.94 Comparison of GEM with analytical solutions for steady-state counter diffusion. To test the cylindrical and spherical symmetry options in **GEM** comparison is made with steady-state analytical solutions to pure diffusion. These are given by:

$$C(r) = (c_1 \text{Log}[r_2/x] + c_2 \text{Log}[r/r_1]) / \text{Log}[r_2/r_1], \quad (2-129)$$

and

$$C(r) = \frac{(c_2 - c_1)}{(1/r_1 - 1/r_2)} (1/r_1 - 1/r) + c_1, \quad (2-130)$$

for cylindrical and spherical geometry, respectively. The figure shows that there is very close agreement with **GEM**.

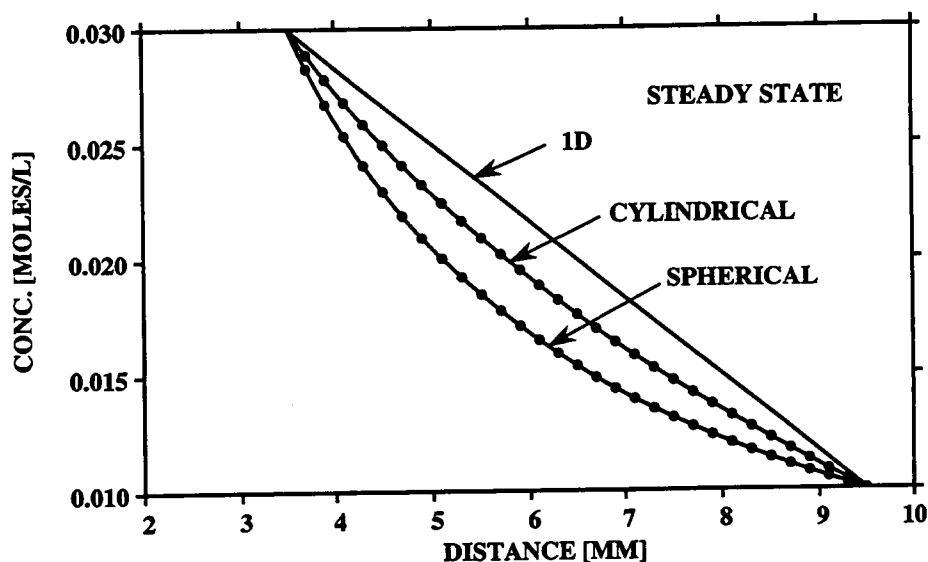
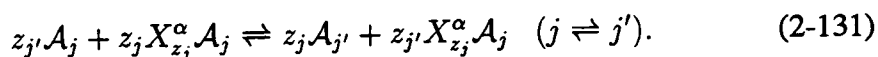


Figure 2-3: Comparison of **GEM**(solid curves) with analytical solutions (dots) for cylindrical and spherical geometry.

6.10.94 Incorporating Ion-Exchange Reactions into GEM The exchange reactions may take place between primary species of the form:



The corresponding mass action equation is given by

$$K_{ij} = \left(\frac{a_j}{\bar{C}_j} \right)^{z_i} \left(\frac{\bar{C}_i}{a_i} \right)^{z_j}. \quad (2-132)$$

Conservation of exchange sites is expressed by

$$Q = \sum_j z_j \bar{C}_j = (1 - \phi) \rho CEC, \quad (2-133)$$

where CEC denotes the cation exchange capacity of the porous medium with the units moles sites/mass solid. The exchange isotherm can be calculated from the mass action equation

$$\bar{C}_j = \frac{k_j a_j}{(k_i a_i)^{z_j/z_i}} \bar{C}_i^{z-j/z_i}, \quad (2-134)$$

for any $i \neq j$. The distribution coefficient K_j^D is defined by

$$K_j^D = \frac{\bar{C}_j}{C_j} = \frac{k_j \gamma_j}{(k_{j_0} a_{j_0})^{z_j/z_{j_0}}} \bar{C}_{j_0}^{z-j/z_{j_0}}. \quad (2-135)$$

Alternatively define

$$\chi_j = \frac{z_j \bar{C}_j}{\sum_i z_i \bar{C}_i} = \frac{z_j \bar{C}_j}{Q}, \quad (2-136)$$

with

$$\sum_j \chi_j = 1. \quad (2-137)$$

Defining

$$K_{ij} = \frac{k_i^{z_j}}{k_j^{z_i}}, \quad (2-138)$$

then

$$k_i = \frac{Q k'_i}{z_i}. \quad (2-139)$$

where

$$K'_{ji} = \left(\frac{a_j}{\chi_j} \right)^{z_i} \left(\frac{\chi_i}{a_i} \right)^{z_j}. \quad (2-140)$$

The exchange isotherm \bar{C}_{j_0} is obtained from the equation

$$1 = \sum z_j \chi_j = z_{j_0} \bar{C}_{j_0} + \sum_{j \neq j_0} \frac{z_j k_j a_j}{(k_{j_0} a_{j_0})^{z_j/z_{j_0}}} \bar{C}_{j_0}^{z_j/z_{j_0}}. \quad (2-141)$$

The derivative of the distribution can be obtained implicitly to give

$$\frac{\partial K_j^D}{\partial C_l} = - \frac{z_j K_j^D (K_j^D \delta_{jl} + K_l^D)}{\sum_i z_i \chi_i}. \quad (2-142)$$

6.12.94 Problem of charge conservation. It is noted that the ion-exchange reactions conserve charge separately in both the aqueous and solid phases. However, this is not true of the surface complexation model which can therefore be expected to violate charge conservation in the aqueous phase. This problem does not seem to have been noted in the literature.

6.17.94 Comparison of GEM with Diffusion Experiments. GEM was compared with diffusion of a NaCl solution in a crevice in the absence of electrochemical reactions. Different initial and bulk pH values of 2, 3 and 5 were used the experiments as shown in the figures below. The agreement was not perfect, but much better than previous results indicating that the experiments are improving with time.

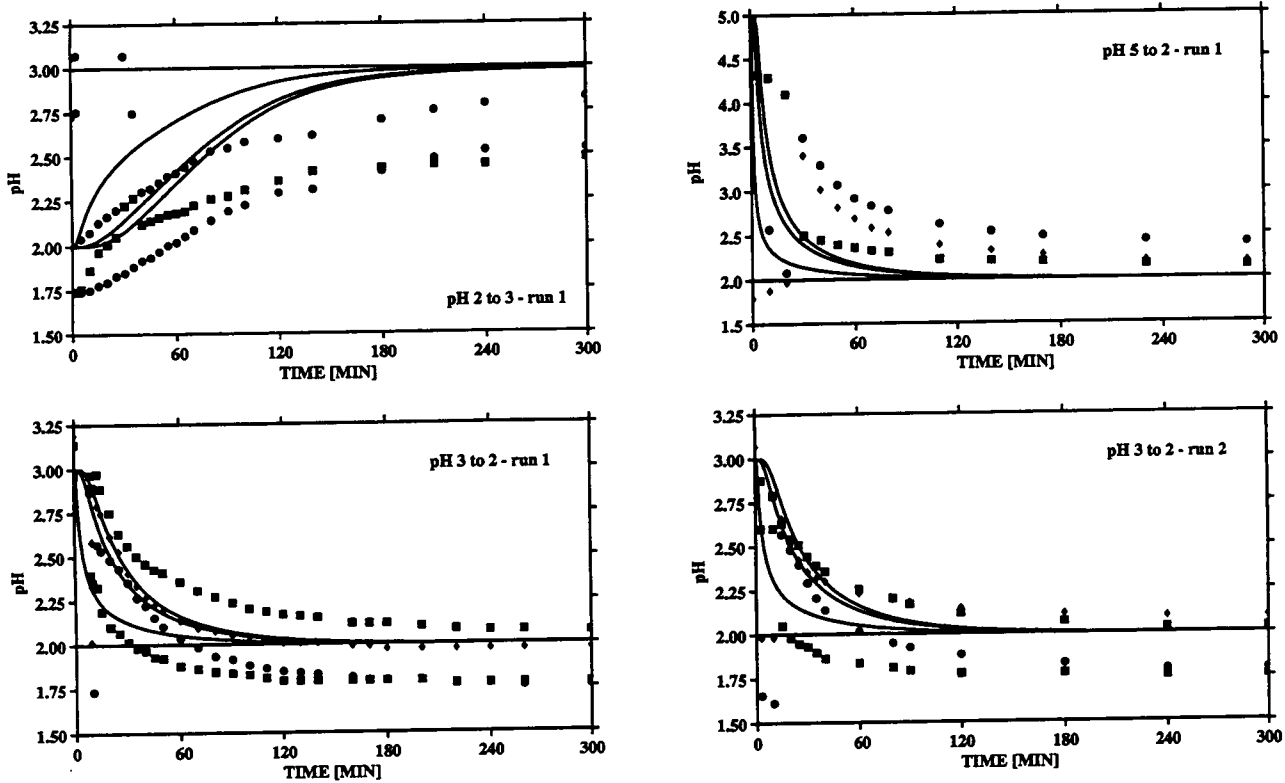


Figure 2-4: Theoretical calculations with GEM for species-dependent diffusion coefficients (solid curves) compared with experiment (dashed curves). Plotted is the crevice pH as a function of time for the bulk (boundary value), mouth (9.5 mm) and tip (0 mm) of the crevice. Zero flux boundary conditions were imposed at the tip.

6.20.94

Corrections to GEM for variable diffusion coefficients. The diffusion coefficients are not constant, but depend on tortuosity which can vary with time and space. Therefore $\nabla \Psi_j^D$ should be replaced by the expression

$$\Psi_j^D = D_j \nabla C_j + \sum_i \nu_{ji} D_i \nabla C_i. \quad (2-143)$$

It might be better here to introduce new notation for $\nabla \Psi_j^D$ and reserve Ψ_j for the expression

$$\Psi_j = C_j + \sum_i \nu_{ji} C_i. \quad (2-144)$$

One possibility is:

$$\Gamma_j^D = D_j \nabla C_j + \sum_i \nu_{ji} D_i \nabla C_i. \quad (2-145)$$

6.24.94 On the Fundamental Difference Between Adsorption and Mineral Precipitation/Dissolution

Reactions. Mineral precipitation/dissolution and adsorption reactions lead to very similar forms of the mass transport equations. Yet there are fundamental differences between the solutions of the transport equations which is explored. The general form of the transport equation valid for both processes is given by

$$\frac{\partial}{\partial t} \phi C + \frac{\partial J}{\partial x} = -I, \quad (2-146)$$

and

$$\frac{\partial \bar{C}}{\partial t} = I, \quad (2-147)$$

where I is the reaction rate corresponding to either adsorption



or mineral precipitation/dissolution



and J denotes the flux

$$J = -\phi D \frac{\partial C}{\partial x} + vC. \quad (2-150)$$

The solute concentration is denoted by C and the adsorbed or solid concentration by \bar{C} . The reaction rate I has two different form depending on the type of reaction. For adsorption it may be written in the form:

$$I = k_f C - k_b \bar{C} = -k_b \bar{C} \left(1 - K \frac{C}{\bar{C}} \right), \quad (2-151)$$

and for precipitation/dissolution as

$$I = k_f C - k_b = -k_b \left(1 - \frac{C}{C_{eq}} \right), \quad (2-152)$$

where

$$K = \frac{k_f}{k_b}, \quad (2-153)$$

and

$$C_{eq} = K^{-1}. \quad (2-154)$$

The form of the reaction rate for precipitation/dissolution arises because the solid has unit activity. This fact gives rise to the very different behavior of the solutions to the transport equations for the two cases.

A dimensionless form for the case of precipitation/dissolution is easily obtained by introducing the dimensionless variables:

$$t' = \frac{t}{\tau}, \quad (2-155)$$

$$x' = \frac{x}{l}, \quad (2-156)$$

$$C' = \frac{C - C_{eq}}{C_{eq}}, \quad (2-157)$$

and

$$\bar{C} = \frac{\bar{C}}{\bar{C}_0}, \quad (2-158)$$

where \bar{C}_0 denotes the initial solid concentration, the characteristic time τ is defined by

$$\tau = \frac{\bar{C}_0}{k_b} = \frac{\bar{C}_0}{k_f C_{eq}}, \quad (2-159)$$

and the characteristic length by

$$l = \frac{v}{k_f}, \quad (2-160)$$

for advection dominated flow, and

$$l = \sqrt{\frac{\phi D}{k_b}}, \quad (2-161)$$

for diffusion dominated transport. With these definitions the transport equations become

$$\frac{C_{eq}}{\bar{C}_0} \frac{\partial}{\partial t'} \phi C' + \frac{1}{k_f l} \frac{\partial J'}{\partial x'} = -C', \quad (2-162)$$

for the solute, and

$$\frac{\partial \bar{C}'}{\partial t'} = C', \quad (2-163)$$

for the solid. Because $\bar{C}_0 \gg C_{eq}$, the term involving the time derivative in the solute transport equation can be neglected compared to the remaining terms to yield the stationary state approximation:

$$\frac{1}{k_f l} \frac{\partial J'}{\partial x'} = -C'. \quad (2-164)$$

For the solid both terms in the equation are of equal magnitude and no further approximation is possible.

This analysis does not apply to the case of adsorption. In the local equilibrium limit the time derivatives of the solute and solid concentrations are proportional to one another

$$\frac{\partial \bar{C}}{\partial t} = K \frac{\partial C}{\partial t}, \quad (2-165)$$

and similarly with t replaced by x , with $K \gg 1$ for strong retardation.

- 6.27.94 The effect of electromigration on a dilute sodium chloride solution.** The effect of species-dependent diffusion coefficients on the migration of ions Na^+ and Cl^- is shown in the figure below. The peak in the sodium ion (and corresponding dip in the chloride concentration) is the effect of the electrical field established to maintain charge balance due to the more rapidly diffusing hydrogen ion compared to the other ions in solution. The effect becomes less pronounced for more concentrated solutions.

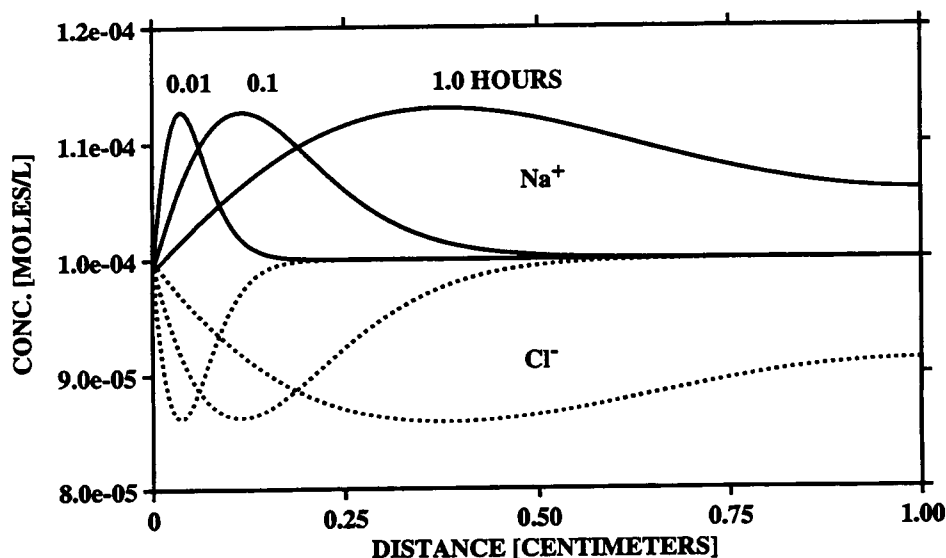


Figure 2-5: Theoretical calculations with GEM for the concentration of Na^+ and Cl^- plotted as a function of distance at the indicated times.

- 8.8.94 Ion-Exchange Reactions.** The GEM code is applied to flushing of Na^+ and K^+ from an ion-exchanger using a CaCl_2 solution. Results are compared with Appelo and Postma (1993), Fig. 10.7, page 432. The initial fluid composition consists of a 10^{-3}M NaNO_3 and $2 \times 10^{-4}\text{M}$ KNO_3 solution at a pH of 5. The eluting fluid is a $6 \times 10^{-4}\text{M}$ CaCl_2 solution also at pH 5. The chloride concentration in the initial and eluting fluid is determined by charge balance. The ion-exchanger initially has equal concentrations of adsorbed Na^+ and K^+ of 0.5 M. The selectivity coefficients used in the calculation

are: $k_{\text{Na}^+} = 1$, $k_{\text{K}^+} = 5$, $k_{\text{Ca}^{2+}} = 1$, and $k_{\text{H}^+} = 0.3$. The exchange capacity of the ion-exchanger is taken as 1.2 M. A fluid flow velocity of 1 m y^{-1} and a diffusion coefficient of $10^{-5} \text{ cm}^2 \text{ s}^{-1}$ is used in the calculation. The resulting profile of the adsorbed ions is shown in Fig. 2-6 for an elapsed time of 1 year.

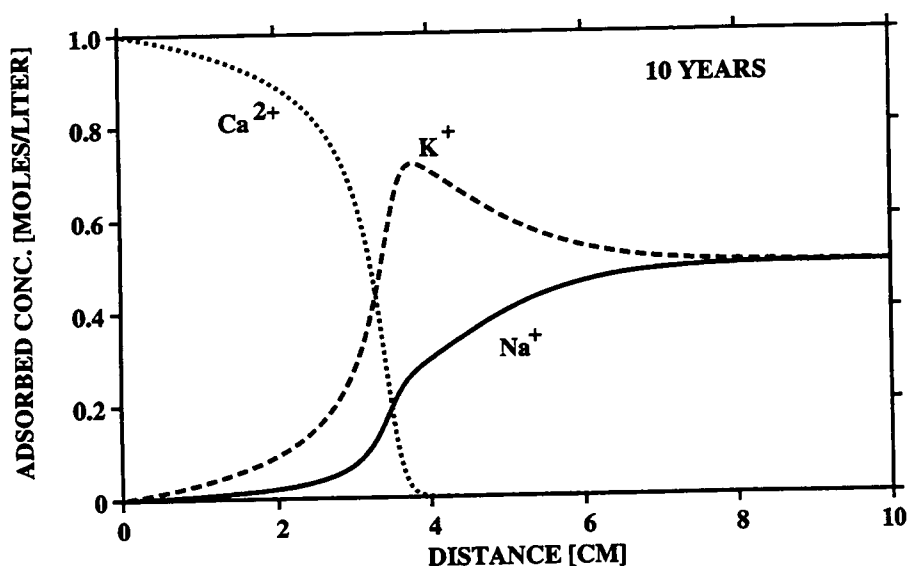
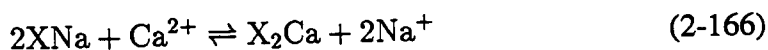


Figure 2-6: Flushing of Na^+ and K^+ by a CaCl_2 solution.

9.10.94 Charge Conservation in General Surface Complexation Models of Sorption. Sorption models which allow for a variable number of unoccupied surface sites do not conserve charge when transport of solute species is taken into account. To demonstrate this exchange of Na^+ with Ca^{2+} is considered. Ion-exchange postulates the reaction



in which charge is conserved separately in both the aqueous and surfaces phases. In this reaction X^- denotes a surface site. Representing the rate of the exchange reaction by I , the following transport equations hold:

$$\mathcal{L}\text{Na} = 2I, \quad (2-167)$$

$$\mathcal{L}\text{Ca} = -I, \quad (2-168)$$

for the aqueous species, where \mathcal{L} denotes the differential operator

$$\mathcal{L} = \phi \frac{\partial}{\partial t} + v \frac{\partial}{\partial x} - \phi D \frac{\partial^2}{\partial x^2}. \quad (2-169)$$

It follows immediately that for the ion-exchange reaction charge is conserved. Defining the total charge as

$$Q = N_{\text{a}} + 2C_{\text{a}}, \quad (2-170)$$

it follows that

$$\mathcal{L}Q = \mathcal{L}N_{\text{a}} + 2\mathcal{L}C_{\text{a}} = 2I - 2I = 0. \quad (2-171)$$

For the sorbed surface concentrations it follows that

$$X\dot{N}_{\text{a}} = -2I, \quad (2-172)$$

and

$$X_2\dot{C}_{\text{a}} = I. \quad (2-173)$$

Hence the total number of sites, defined by

$$\omega_X = XN_{\text{a}} + 2X_2C_{\text{a}}, \quad (2-174)$$

is conserved:

$$\dot{\omega}_X = -2I + 2I = 0. \quad (2-175)$$

For sorption models with a variable number of unoccupied sites, however, charge is not in general conserved. Assume the following reactions occur:



and



with rates $I_{N_{\text{a}}}$ and $I_{C_{\text{a}}}$, respectively. The mass transport equations read:

$$\mathcal{L}N_{\text{a}} = -I_{N_{\text{a}}}, \quad (2-178)$$

and

$$\mathcal{L}C_{\text{a}} = -I_{C_{\text{a}}}. \quad (2-179)$$

For the sorbed species

$$X\dot{N}_{\text{a}} = I_{N_{\text{a}}}, \quad (2-180)$$

$$X\dot{C}_{\text{a}} = I_{C_{\text{a}}}, \quad (2-181)$$

and for unoccupied sites

$$\dot{X} = -I_{N_{\text{a}}} - 2I_{C_{\text{a}}}, \quad (2-182)$$

It follows that the total number of sites, defined by

$$\omega_X = X + X_{Na} + 2X_{Ca}, \quad (2-183)$$

are conserved, as they must:

$$\dot{\omega}_X = \dot{X} + I_{Na} + 2I_{Ca} = 0. \quad (2-184)$$

However, total charge within the aqueous solution is not conserved:

$$\mathcal{L}Q = -I_{Na} - 2I_{Ca} = \dot{X} \neq 0. \quad (2-185)$$

9.15.94

Spent Fuel Oxidation. An important problem in the disposal of HLW is the alteration of spent nuclear fuel under oxidizing and nonoxidizing conditions (Shoesmith and Sunder, 1992). For conditions representative of Yucca Mountain of oxidizing partially saturated porous media and high groundwater silica concentrations, it can be expected that the alteration products of spent fuel may be replacement by minerals soddyite and uranophane. In this section schematic calculations are carried out with the code GEM describing the oxidation of uraninite contained in a tuffaceous host rock representative of the Peña Blanca natural analogue site. The primary mineral assemblage used in the calculation is given in Table 2-3. It is assumed in the calculations that an oxidizing fluid diffusives into a host rock with this composition and oxidizes the uraninite and pyrite producing uranium-bearing secondary minerals and iron oxide.

Table 2-3: Volume fractions of the primary mineral assemblage.

mineral	volume fraction
uraninite	0.3
pyrite	0.02
kaolinite	0.2
amorphous silica	0.45
porosity	0.03

The inlet fluid composition was determined by assuming the oxygen fugacity and CO_2 partial pressure to be in equilibrium with the atmosphere with values of 0.2 and 10^{-3} bars, respectively. The pH was chosen arbitrarily with the value 6. Silica was fixed

Table 2-4: Compositions of the inlet and initial fluid. Molality units are used with the exception of pH.

primary species	inlet fluid	initial fluid
pH	6.0	7.5
Al ³⁺	1.8987E-12	6.0041E-17
Ca ²⁺	2.1587E-05	1.8362E-04
Fe ²⁺	2.0200E-15	8.7977E-04
SO ₄ ²⁻	9.9712E-06	8.5973E-04
SiO ₂	1.8703E-04	1.8703E-04
UO ₂ ²⁺	1.1508E-10	3.9908E-21
HCO ₃ ⁻	1.5360E-05	4.8574E-04
O _{2(aq)}	2.5277E-04	9.4365E-70
Cl ⁻	1.0900E-04	1.0900E-04

by equilibrium with chalcedony, iron was determined by equilibrium with ferrihydrite, and aluminum by equilibrium with kaolinite. Sulfate concentration was taken as 10^{-5} molal. The concentrations of UO_2^{2+} and Ca^{2+} were fixed by equilibrium with soddyite and uranophane. In order to obtain equilibrium with uranophane it was necessary to modify the equilibrium constant given in the EQ3/6 database from 17.29 to 4.0, a change of 13 log units. The value of 4 for the uranophane log K was obtained by adjusting the log K until simultaneous equilibrium could be obtained with uranophane and soddyite and the oxidizing inlet fluid. The initial fluid composition was determined by equilibrium with minerals pyrite, uraninite, kaolinite and chalcedony. The total iron and sulfur concentrations were fixed at 10^{-3} molal. The calcium concentration was fixed by charge conservation and the chloride concentration was assumed to be the same as in the inlet fluid. A pH of 7.5 was assumed. The initial and inlet fluid compositions for the concentrations of primary species used in the calculations are presented in Table 2-4.

The results of the calculation are shown in Figs. 2-7a, b for the mineral volume fractions and porosity plotted as a function of distance corresponding to an elapsed time of 1000 years. As can be seen in the figure, uraninite is converted to soddyite and uranophane, and pyrite to ferrihydrite at an approximately common redox front. In addition enrichment in kaolinite occurs near the inlet. The porosity becomes strongly negative

in the region where soddyite and uranophane form. This can be understood by examining the replacement reactions and the volume changes of reaction. The Eh, pH and total uranium and iron concentration profiles are shown in Figs. 2-8a, b. The aqueous uranium concentration is limited to low values as a result of the low solubilities of the uranium-bearing minerals.

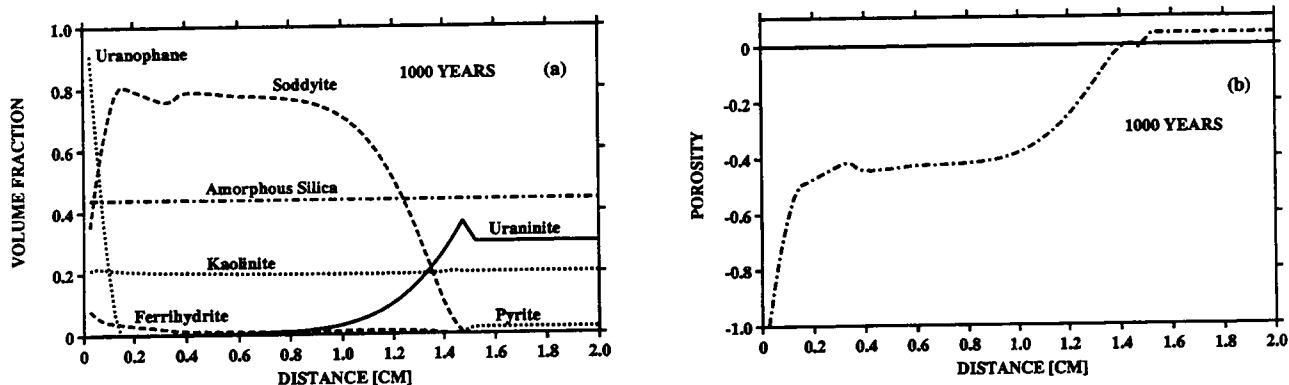


Figure 2-7: Theoretical calculations with GEM describing oxidation of uraninite in a tuffaceous host rock showing (a) volume fraction profiles, and (b) porosity for an elapsed time of 1000 years.

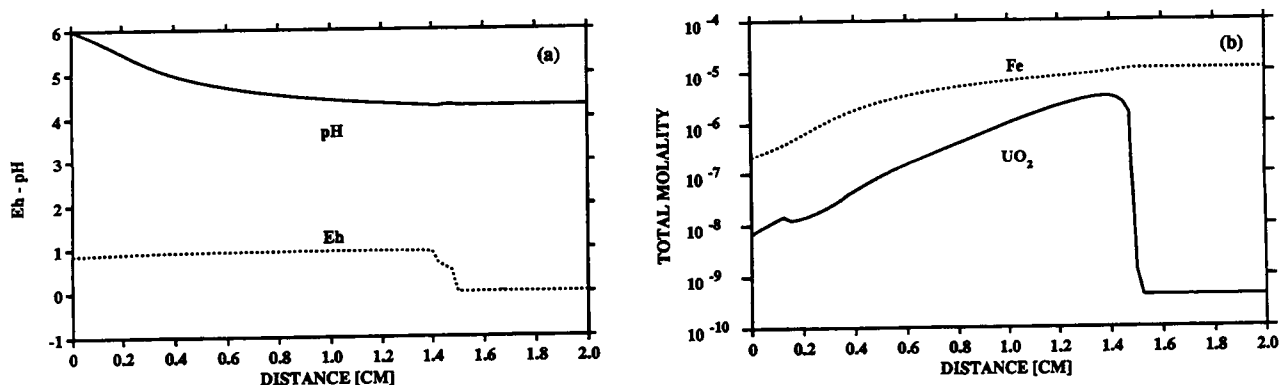
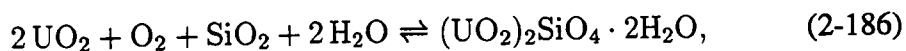


Figure 2-8: Theoretical calculations with GEM describing oxidation of uraninite in a tuffaceous host rock showing (a) Eh and pH, and (b) total uranium and iron aqueous concentrations for an elapsed time of 1000 years.

Replacement of uraninite ($\bar{V}_{uran} = 24.62 \text{ cm}^3 \text{ mole}^{-1}$) by soddyite ($\bar{V}_{sodd} = 131.27 \text{ cm}^3 \text{ mole}^{-1}$) results in the overall reaction of the form

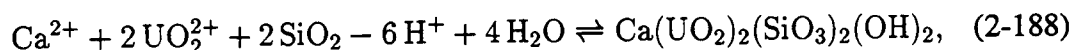


balanced on uranium. The volume change of reaction is given by the ratio

$$\frac{\bar{V}_{uran}}{2\bar{V}_{sodd}} = 2.67, \quad (2-187)$$

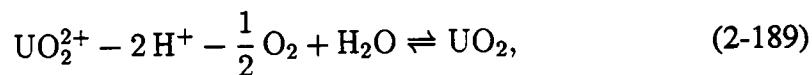
and therefore if the replacement reaction conserves uranium in the solid phases, there must be a volume increase by the factor 2.67, which agrees with the flat portion of the soddyite volume fraction profile shown in Fig. 2-7a. This results in a strong positive volume change of reaction and leads to a negative porosity in the GEM calculations as can be seen in Fig. 2-7b.

Uranophane results in an even larger volume change. The reaction of uranophane is given by

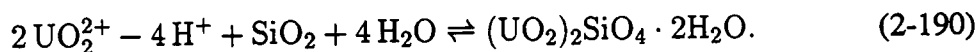


with a molar volume of $224.9 \text{ cm}^3 \text{ mole}^{-1}$. Because of the form of the rate law based on transition state theory, the reactions must approximately conserve uranium in the calculations because of the low solubility of uranophane and soddyite.

However, there are other possibilities for transforming uraninite to soddyite and uranophane. One is conservation of volume, often cited by geologists as a pseudomorphic replacement mechanism in metamorphic environments at high temperatures and pressures. To investigate the more general case consider the individual reactions of uraninite and soddyite written in terms of a common set of primary species. The reaction for uraninite can be written as



and the reaction for soddyite as



The transport equation for dissolved uranium has the form

$$\frac{\partial \phi \Psi_{\text{UO}_2}}{\partial t} + \frac{\partial \Omega_{\text{UO}_2}}{\partial x} = -I_{uran} - 2 I_{sodd}. \quad (2-191)$$

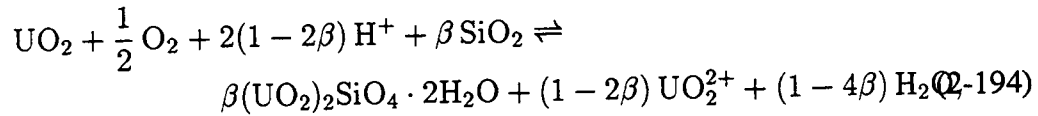
For change in volume fraction of the minerals uraninite and soddyite the mass transfer equations are given, respectively, by

$$\frac{\partial \phi_{uran}}{\partial t} = \bar{V}_{uran} I_{uran}, \quad (2-192)$$

and

$$\frac{\partial \phi_{sodd}}{\partial t} = \bar{V}_{sodd} I_{sodd}. \quad (2-193)$$

Taking a linear combination of the reactions for uraninite and soddyite yields a single overall reaction of the general form



obtained by subtracting the reaction for soddyite multiplied by the coefficient β from the uraninite reaction. The individual reaction rates are related by the expression

$$I_{sodd} = -\beta I_{uran}. \quad (2-195)$$

In this case the transport equation for dissolved uranium has the form

$$\frac{\partial \phi_{\Psi_{\text{UO}_2}}}{\partial t} + \frac{\partial \Omega_{\text{UO}_2}}{\partial x} = (2\beta - 1) I_{uran}, \quad (2-196)$$

and the volume changes satisfy the relation

$$-\frac{\partial \phi_{sodd}/\partial t}{\partial \phi_{uran}/\partial t} = \beta \frac{\bar{V}_{sodd}}{\bar{V}_{uran}}. \quad (2-197)$$

If uranium is conserved in the solid phases and hence also the aqueous phase, then the individual reaction rates of uraninite and soddyite are related by

$$I_{sodd} = -\frac{1}{2} I_{uran}, \quad (2-198)$$

and $\beta = 1/2$, in agreement with the reaction given in Eqn.(2-186). In this case the volume changes satisfy the relation

$$-\frac{\partial \phi_{sodd}/\partial t}{\partial \phi_{uran}/\partial t} = \frac{\bar{V}_{sodd}}{2\bar{V}_{uran}} \simeq 2.67, \quad (2-199)$$

as observed in Fig. 2-7a. If, on the other hand, volume is to remain constant during the replacement reaction, then the volume changes must be equal and

$$-\frac{\partial \phi_{uran}/\partial t}{\partial \phi_{sodd}/\partial t} = 1. \quad (2-200)$$

In this case the reaction rates are related by the equation

$$\bar{V}_{uran} I_{uran} + \bar{V}_{sodd} I_{sodd} = 0, \quad (2-201)$$

or

$$-\frac{I_{sodd}}{I_{uran}} = \frac{\bar{V}_{uran}}{\bar{V}_{sodd}}, \quad (2-202)$$

and

$$\beta = \frac{\bar{V}_{uran}}{\bar{V}_{sodd}} \simeq 0.188. \quad (2-203)$$

To incorporate these constraints into the rate equation, the rate law can be modified to provide a specified precipitation rate far from equilibrium. In the conventional rate law the precipitation rate grows without bound as supersaturation increases, which is somewhat unrealistic given that eventually the rate becomes controlled by transport of solutes. However, by employing the expression

$$I_m = -k_m s_m \frac{1 - K_m Q_m}{1 + \frac{1}{f_m} K_m Q_m}, \quad (2-204)$$

where f_m is a constant, the precipitation rate can be limited to finite values as the fluid composition becomes more and more supersaturated. Far from equilibrium the rate reduces to

$$I_m = \begin{cases} -k_m s_m, & Q_m \rightarrow 0, \text{ (dissolution)} \\ f_m k_m s_m, & Q_m \gg 1, \text{ (precipitation)} \end{cases}, \quad (2-205)$$

for precipitation and dissolution. Taking the constant f_m as the ratio of molar volumes, for example:

$$f_{sodd} = \frac{\bar{V}_{uran}}{\bar{V}_{sodd}}, \quad (2-206)$$

should give a constant volume replacement reaction. However, this form of the rate results in high concentrations of uranium in solution and hence in highly supersaturated conditions for the minerals soddyite and uranophane as well as uraninite. Because of the extremely low solubilities of these minerals, it is unlikely that such large concentrations of uranium in solution could occur. Thus this modification to the rate law does not provide a satisfactory resolution of the problem.

Presumably conservation of volume implies a different reaction mechanism than conservation of uranium. One possibility is that the large pressure increase that would accompany the conservation of uranium mechanism as the pore space became completely occupied leads to a tendency towards conservation of volume. However, the current transition state based rate law used in GEM can only provide the uranium conservation mechanism. These possibilities need to be explored more fully before a definite statement can be made. The Peña Blanca natural analogue site offers a unique possibility to investigate these reactions in the field under insitu stress conditions.

3 IPA: Flow Around the Waste Package

Account Number: 20-5702-723

Collaborators: John Walton (Consultant), Pavitra Praman (Student)

Objective: The purpose of this project is to investigate the flow of liquid water and vapor in the near-field region of a HLW repository.

1.25.94 Letter to J. Walton on the Derivation of the Evaporation Rate using Fick's Law.

Ok John here is an attempt to convince you that there is an analytical solution to the Fick plus Darcy equations. I can't for the life of me see what I could be doing wrong.

I think we now agree that the correct form of the coupled differential equations are:

$$F_1 = -\frac{DP}{RT} \frac{dX_1}{dr} - \frac{k}{\mu} \frac{X_1 P}{RT} \frac{dP}{dr} = \frac{E}{2\pi r}, \quad (3-207)$$

and

$$F_2 = -\frac{DP}{RT} \frac{dX_2}{dr} - \frac{k}{\mu} \frac{X_2 P}{RT} \frac{dP}{dr} = 0, \quad (3-208)$$

for steady-state conditions, the latter equation resulting from the assumption that species 2 is stagnant. By definition:

$$X_1 + X_2 = 1. \quad (3-209)$$

Therefore if we add the two flux equations we get:

$$F_1 + F_2 = -\frac{k}{\mu} \frac{P}{RT} \frac{dP}{dr} = \frac{E}{2\pi r}. \quad (3-210)$$

This equation can be integrated immediately to give

$$P(r) = \sqrt{P_L^2 + \frac{\mu R T E}{\pi k} \ln \left(\frac{r_L}{r} \right)}. \quad (3-211)$$

Next Eqn.(3-207) can be written as

$$F_1 = -\frac{DP}{RT} \frac{dX_1}{dr} + X_1 (F_1 + F_2) = \frac{E}{2\pi r}, \quad (3-212)$$

by making use of Eqn.(3-210). Solving this equation for F_1 noting that $F_2 = 0$, yields

$$F_1 = -\frac{DP}{RT} \frac{1}{1 - X_1} \frac{dX_1}{dr} = \frac{E}{2\pi r}. \quad (3-213)$$

This equation can be likewise immediately integrated if it is assumed that $DP = \text{constant}$, to give:

$$\ln \left[\frac{1 - X_1(r)}{1 - X_1^0} \right] = \frac{RTE}{DP} \ln \left[\frac{r}{r_0} \right]. \quad (3-214)$$

The evaporation rate E is obtained by evaluating this relation at $r = r_L$ to give

$$E = \frac{DP}{RT} \frac{\ln \left[\frac{1 - X_1^L}{1 - X_1^0} \right]}{\ln \left[\frac{r_L}{r_0} \right]} \quad (3-215)$$

John, I sure would like to know what you see is wrong with this! . . . Peter

BTW: Even if $DP \neq \text{constant}$, there still exists an analytical solution.

2.20.94 Fixed Vapor Partial Pressure. One obtains a more complicated result by fixing the vapor partial pressure at the evaporation surface. This is, however, the more realistic case since the partial pressure is fixed by thermodynamic considerations. At the inner boundary the partial pressure of water vapor is fixed to the value:

$$\begin{aligned} P_1^0 &= X_1^0 P_0, \\ &= \left[1 - (1 - X_1^L) \left(\frac{r_0}{r_L} \right)^{RTE/DP} \right] \sqrt{P_L^2 + \frac{\mu RTE}{\pi \kappa} \ln \left[\frac{r_0}{r_L} \right]}. \end{aligned} \quad (3-216)$$

This equation gives a transcendental equation for the evaporation rate E .

4.28.94 Heat Generation Rate in the Global $r - z$ Repository Model.

The input to V-TOUGH for heat generation is in the form of the heat flux $Q(t)$ [$\text{J m}^{-2} \text{s}^{-1}$]. The initial loading of the repository is specified in terms of the APD (Areal Power Density [W m^{-2}]). The APD can be expressed in terms of the total mass of heavy metal M [MTIHM], the repository area \mathcal{A} [m^2], and the initial power per MTIHM P_0 at the time of disposal as

$$APD = \frac{P_0 M_0}{\mathcal{A}}. \quad (3-217)$$

The area of the repository can be estimated as

$$\mathcal{A} = \frac{P_0 M_0}{APD}. \quad (3-218)$$

A typical value assumed for M_0 is 70,000 MTIHM.

Global Disk Model

To compute the initial mass loading M_0 for a given initial APD (Areal Power Density), write

$$Q = M_0 P_0, \quad (3-219)$$

where P_0 denotes the initial power density normalized to one MTIHM, and Q is the total power output of the repository in watts. If the area of the repository is \mathcal{A} , then the total power can also be expressed as

$$Q = \mathcal{A} \times \text{APD}. \quad (3-220)$$

Comparing these expressions gives

$$M_0 = \frac{\mathcal{A} \text{APD}}{P_0}. \quad (3-221)$$

As an example, taking $\mathcal{A} = \pi R^2$, with $R = 1$ km, $\text{APD} = 114 \text{ kW acre}^{-1}$, and $P_0 \simeq 1048.4 \text{ W MTIHM}^{-1}$ for ten year old fuel, yields $M_0 = 84410.1 \text{ MTIHW}$. The power density per unit area Q can be expressed as a function of time as

$$Q(t) = \frac{M_0 P(t)}{\mathcal{A}} = \text{APD} \frac{P(t)}{P_0}. \quad (3-222)$$

The heat generation rate $P(t)$ is calculated using a *Mathematica* program for input into V-TOUGH. The values calculated are shown in the figure below.

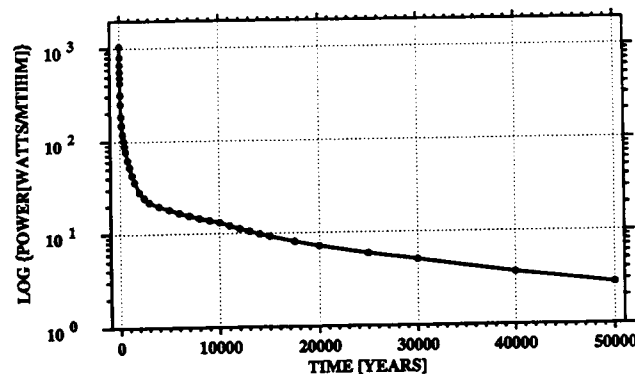


Figure 3-9: Power density in units of Watts MTIHM⁻¹ calculated using *Mathematica* to be used in V-TOUGH calculations.

4.30.94

Porosity-Permeability Relation at Yucca Mountain. A fit was obtained to porosity-permeability data for Yucca, Mountain using *Mathematica*. Data was taken from Intraval Study Phase 2 prepared by Golder Associates reference 913-10024.202, April

29, 1992, Attachment A. The results are given in the form of a *Mathematica* Notebook and included on a floppy disk at end of Scientific Notebook (labeled porosity-perm).

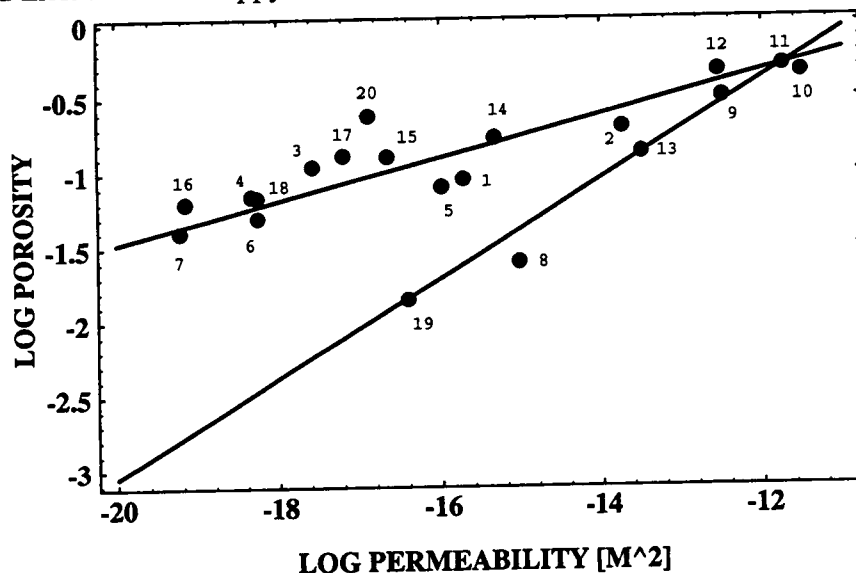


Figure 3-10: Best-eye-fit to porosity-permeability data from Yucca Mountain using a power law dependency of porosity on permeability. One point (# 11) is chosen to anchor the lines.

6.8.94

Heat Generation Rate in the Drift Repository $x - z$ Model.

In the drift model a simple square shaped repository is assumed with the drifts consisting of a series of equally spaced parallel rows, N in number. The spacing d between rows is

$$d = \frac{w}{N-1} \simeq \frac{w}{N}, \quad (3-223)$$

where the latter expression holds for $N \gg 1$, and w denotes the width of the repository.

For a square repository

$$w = \sqrt{A}. \quad (3-224)$$

The total length of the drifts L is determined by the container loading per unit length and the total waste loading. The simplifying assumption is made that containers are stacked end-to-end in the center of the drift. It follows that

$$L = \frac{M_0}{C_L} l_C, \quad (3-225)$$

where C_L is the container loading and l_C the container length. From this relation the number of drifts is obtained as

$$N = \frac{L}{w}. \quad (3-226)$$

It follows that the drift spacing can be expressed as

$$d = \frac{w^2}{L} = \frac{A}{L} = \frac{C_L \mathcal{A}}{M_0 l_C}. \quad (3-227)$$

The linear power density (LPD [W m^{-1}]) is thus given by

$$LPD = dAPD = \frac{PC_L}{l_C}. \quad (3-228)$$

Here two disposable scenarios are considered: a single canister and a multiple purpose container (MPC). The canister length is in both cases 5 m. The loading for a single canister is $l_C = 2.3 \times 10^3$ [kg MTIHM]. For the MPC, the container loading differs depending on the type of fuel. For BWR fuel the MPC contains 40 fuel assemblies with 0.2 MTIHM, or 8×10^3 kg of fuel. For an APD of 57 kW/acre, and 70,000 MTIHM, the area of the repository is 5.2×10^6 m² and the width is 2282.66 m.

	Single canister	MPC
length of drift	152,174 m	43,750 m
number of rows	67	19
spacing	34.76 m	125.65 m

6.9.94

Comparison of 1D & 2D C-TOUGH calculations. It was found that identical results could be obtained from 1D C-TOUGH calculations compared to full 2D calculations in the $r - z$ repository. This includes pressure, temperature, saturation and velocity fields for both liquid and gas. This result has significant implications for more detailed calculations in the near-field which incorporate chemistry and fracture flow, since a 1D calculation is orders of magnitude faster than 2D ones. It could also be useful to IPA-type calculations. This result may not be new, however, as it has also been noted by Buschek and Nitao (private communication Los Alamos exchange meeting, 1994). However these authors do not have appeared to have made any use of this observation.

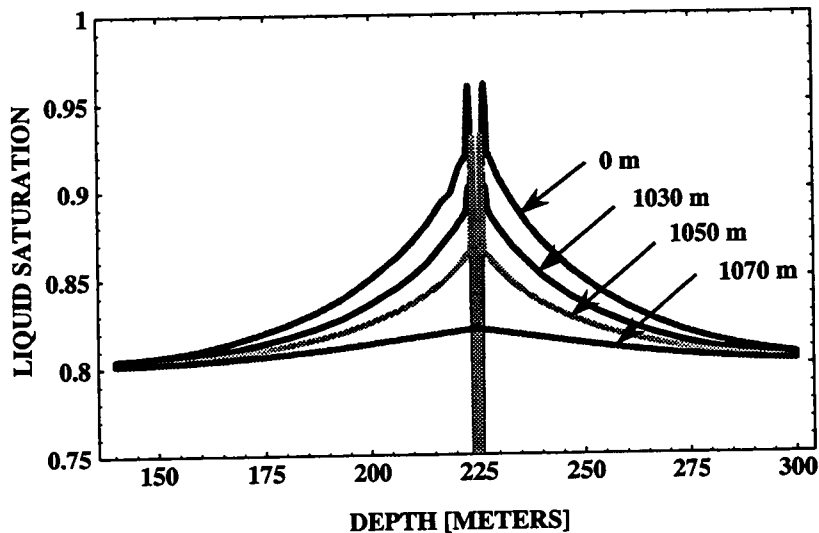


Figure 3-11: Liquid saturation plotted as a function of distance for an elapsed time of 50 years for different vertical slices near the edge of the repository compared to the center.

6.10.94

C-TOUGH calculation on a fine grid. One dimensional calculations were performed using C-TOUGH on a fine grid. Problems were discovered with oscillations with increasing grid refinement. The cause of the oscillations have not yet been resolved.

C-TOUGH RESULTS

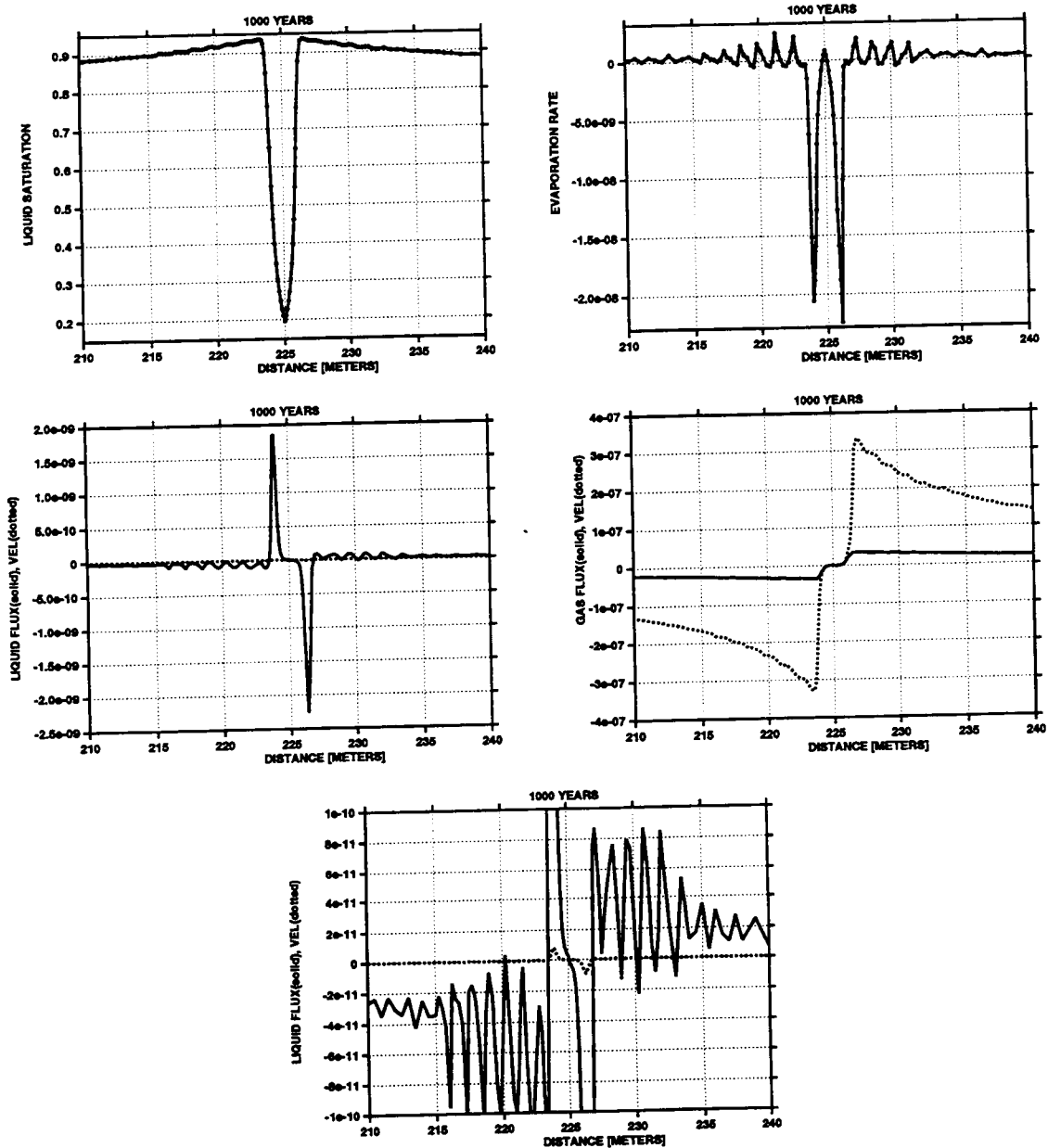


Figure 3-12: Liquid saturation, gas and liquid flux, and evaporation rate plotted as a function of distance for an elapsed time of 1000 years.

7.6.94 New C-TOUGH Solver. Mohan Seth installed a new solver into the two-phase flow code C-TOUGH. Preliminary results indicate that the code is faster and occupies less memory with the new solver. Results of a small size test case are shown below.

New Solver Results:

```
-----
Work Space Required for [A] Array = 210970
Equivalent Minimum Half Band-Width = 10.50
-----
```

CPU SECONDS SPENT IN SUBROUTINES

```
EOS          930.74
BALLA        0.18
MULTI        1917.01
LINEQ        5088.96
CONVER        1.13
OUT(0)       37.40
OUT(1)        0.00
WRIFI        4.03
              0.00
```

TOTAL 7979.46 SECONDS

STEPS = 297 ITES=1613 ELEMENTS= 1036

Old Solver Results:

```
-----
**** HALF BAND WIDTH = 28
-----
```

CPU SECONDS SPENT IN SUBROUTINES

```
EOS          978.80
BALLA        0.15
MULTI        2006.43
LINEQ        13004.97
CONVER        1.35
OUT(0)       39.82
OUT(1)        0.00
WRIFI        3.97
              0.00
```

TOTAL 16035.49 SECONDS

STEPS = 305 ITES=1647 ELEMENTS= 1036

8.25.94 Relative Humidity Calculation Added to CTOUGH

The calculation of relative humidity was added to CTOUGH. It was found necessary to use two different representations of the relative humidity depending on the state of saturation. For completely unsaturated rock ($S_l = 0$) the definition of relative humidity in terms of the gas phase partial pressure was used:

$$h = \frac{P_w^g}{P_{\text{sat}}} = \frac{x_w^g P_g}{P_{\text{sat}}} = \frac{w_w^g M_2^{-1}}{w_w^g M_w^{-1} + w_a^g M_a^{-1}} \frac{P_g}{P_{\text{sat}}} \quad (3-229)$$

For $S_l > 0$, the definition in terms of the Kelvin equation for vapor pressure lowering was used:

$$h = \exp[P_{\text{cap}} M_w / RT \rho]. \quad (3-230)$$

4 SCCEX Code Analysis

Account Number: **20-5702-523**

Collaborators: Tony Torng (SwRI)

Objectives: Prepare users manual for the SCCEX code.

3.22.94 SCCEX code modification. A number of errors were found in the SCCEX code in a table giving the power generation for BWR and PWR fuel. The original code is as follows (found in subroutines.f):

```

      block data b
      implicit real*8 (a-h,o-z)
c
c Data for power generation for BWR and PWR fuel in watts/MTU
c corresponding times are in years
c
c twatt = corresponding time in years
c pwr = watts/mtu for pwr fuel
c bwr = watts/mtu for bwr fuel
c DOE/RW - 184, Volume 2 of 6, 1987
c Table 1C.7
c
      include 'watt.f'
      data twatt/ 5., 6., 7., 8., 9., 10., 16.,
& 18., 20., 25., 30., 40., 50., 60., 70., 80.,
& 90., 100., 200., 300., 400., 500.,1000.,2000.,3000.,
&4000.,5000., 1.e4, 3.e4, 4.e5, 5.e4, 1.e5, 2.e5, 5e5/
      data pwr / 1.8e3,1.53e3,1.37e3,1.27e3,1.2e3,1.14e3,9.49e2,
&9.08e2,8.71e2,7.91e2,7.23e2,6.12e2,5.25e2,4.55e2,3.98e2,3.53e2,
&3.16e2,2.86e2,1.60e2,1.26e2,1.08e2,9.38e1,5.47e1,2.92e1,2.28e1,
&1.88e1,1.35e1,5.19e0,3.71e0,2.9e0,1.05e0,0.618,0.525,0.392/
      data bwr / 1.38e3,1.19e3,1.08e3,1.00e3,9.51e2,9.11e2,7.73e2,
&7.42e2,7.13e2,6.52e2,5.99e2,5.11e2,4.40e2,3.83e2,3.38e2,3.00e2,
&2.70e2,2.45e2,1.42e2,1.14e2,9.72e1,8.50e1,4.99e1,2.68e1,2.10e1,
&1.74e1,1.26e1,4.88e0,3.49e0,2.63e0,0.943, 0.53, 0.458, 0.351/
      end

```

In comparison with the DOE table referenced above a number of discrepancies are apparent. The time of 4,000 years is not present in the DOE table. The time 4.e5 should read 4.e4. The last point should be 1,000,000 years and not 500,000 years as listed in the table. Finally the PWR power at 5.e4 years should read 2.8 and not 2.9. The corrected table appears below.

P. C. Lichtner

SCIENTIFIC NOTEBOOK

INITIALS: PCZ

c correct by pcl 3/22/94

```

include 'watt.h'
data twatt/ 5., 6., 7., 8., 9., 10., 16.,
s 18., 20., 25., 30., 40., 50., 60., 70., 80.,
s 90., 100., 200., 300., 400., 500., 1000., 2000., 3000.,
s 5000., 1.e4, 3.e4, 4.e4, 5.e4, 1.e5, 2.e5, 5.e5, 1.e6/
data pwr / 1.8e3, 1.53e3, 1.37e3, 1.27e3, 1.2e3, 1.14e3, 9.49e2,
s 9.08e2, 8.71e2, 7.91e2, 7.23e2, 6.12e2, 5.25e2, 4.55e2, 3.98e2, 3.53e2,
s 3.16e2, 2.86e2, 1.60e2, 1.26e2, 1.08e2, 9.38e1, 5.47e1, 2.92e1, 2.28e1,
s 1.88e1, 1.35e1, 5.19e0, 3.71e0, 2.8e0, 1.05e0, 0.618, 0.525, 0.392/
data bwr / 1.38e3, 1.19e3, 1.08e3, 1.00e3, 9.51e2, 9.11e2, 7.73e2,
s 7.42e2, 7.13e2, 6.52e2, 5.99e2, 5.11e2, 4.40e2, 3.83e2, 3.38e2, 3.00e2,
s 2.70e2, 2.45e2, 1.42e2, 1.14e2, 9.72e1, 8.50e1, 4.99e1, 2.68e1, 2.10e1,
s 1.74e1, 1.26e1, 4.88e0, 3.49e0, 2.63e0, 0.943, 0.53, 0.458, 0.351/

```

I have reviewed this scientific notebook and find it in compliance with QAP-001. There is sufficient information regarding procedures used for conducting tests, acquiring and analyzing data so that another qualified individual could repeat the activity.

N. Sridhar 4/17/97

Narasi Sridhar
Manager, Engineered Barrier System and Waste Solidification System

ADDITIONAL INFORMATION FOR SCIENTIFIC NOTEBOOK #: 095

Document Date:	12/13/1994
Availability:	Southwest Research Institute® Center for Nuclear Waste Regulatory Analyses 6220 Culebra Road San Antonio, Texas 78228
Contact:	Southwest Research Institute® Center for Nuclear Waste Regulatory Analyses 6220 Culebra Road San Antonio, TX 78228-5166 Attn.: Director of Administration 210.522.5054
Data Sensitivity:	<input checked="" type="checkbox"/> "Non-Sensitive" <input type="checkbox"/> Sensitive <input type="checkbox"/> "Non-Sensitive - Copyright" <input type="checkbox"/> Sensitive - Copyright
Date Generated:	06/20/1994
Operating System: (including version number)	MAC
Application Used: (including version number)	Mathematica
Media Type: (CDs, 3 1/2, 5 1/4 disks, etc.)	(1) 3 1/2 disk
File Types: (.exe, .bat, .zip, etc.)	eps, ma
Remarks: (computer runs, etc.)	Media contains: Source code and input files used in numerical calculations used in the development of the code MULTIFLO.

Electronic Scientific Notebook No.
095E:Development of the Code MULTIFLO to
Describe Multiphase Reactive Transport
(12/18/1995 through 04/17/1997)

SCIENTIFIC NOTEBOOK

Printed: April 6, 1995

P. C. Lichtner

SCIENTIFIC NOTEBOOK

INITIALS:

PC

SCIENTIFIC NOTEBOOK

by

Peter C. Lichtner

Southwest Research Institute
Center for Nuclear Waste Regulatory Analyses
San Antonio, Texas

April 6, 1995

P. C. Lichtner

SCIENTIFIC NOTEBOOKINITIALS: PCZ**INITIAL ENTRIES**

Scientific NoteBook: # 095

Issued to: P. C. Lichtner

Issue Date: Tuesday, November 16, 1993

Computerized Initials: PCZ

By agreement with the CNWRA QA this NoteBook is to be printed at approximate quarterly intervals. This computerized Scientific NoteBook is intended to address the criteria of CNWRA QAP-001.

Table 0-1: Computing Equipment

Machine Name	Type	OS	Location
gravenstein.cnwra.swri.edu	Intel Professional Workstation	NEXTSTEP	desk Rm A-126
	DX 66 Mhz	Version 3.3	Bldg. 189
skippy.cnwra.swri.edu	Sun SPARC 20	SUNOS 4.1.2	network

List of Figures

- 3-1 Numerical calculation for surface reaction using a first order rate law for dissolution of quartz at 25°C. A single component system with species SiO_2 is used. The input file is `surf.in`. Calculations are given for elapsed times of 0.01, 0.1 and 1 years as shown in the legend. 3-5
- 6-2 Temperature plotted as a function of distance from the dike for times of 1 (solid), 10 (dashed) and 100 (dotted) years. 6-6
- 6-3 Liquid saturation plotted as a function of distance from the dike for times of 1 (solid), 10 (dashed), and 100 (dotted) years. 6-7
- 6-4 Comparison of the temperature calculated using CTOUGH (solid curve) with a pure conductive analytical solution (dotted curve) for an elapsed time of 1 year. 6-7
- 6-5 The temperature plotted as a function of time for different distances from the dike at elements: A 25 (solid), A 35 (dashed), A 45 (dotted), and A 50 (dashed-dotted). 6-8

List of Tables

0-1	Computing Equipment	ii
3-2	Thermodynamic data for uranyl silicate minerals and comparison with the EQ3/6 database. The difference values are defined as $\delta = \langle \text{EQ3/6} \rangle - \langle \text{Est.} \rangle$.	3-13
3-3	Aqueous species free energies taken from the EQ3/6 database data0.R16. . .	3-13

PROJECTS

Contents

INITIAL ENTRIES	ii
FIGURES	iii
TABLES	iv
PROJECTS	v
1 V-TOUGH Modifications	1-1
2 Sub-Regional Hydrology Processes: Site-Scale Flow & Transport Model- ing	2-1
3 EBSPAC	3-1
3.1 Reactive Boundary Condition	3-1
3.2 Sorption	3-8
3.3 Thermodynamic Data	3-13
4 IPA: Flow Around the Waste Package	4-1
5 SCCEX Code Analysis	5-1
6 Volcanology Project	6-6

1 V-TOUGH Modifications

Account Number: **20-5702-523/723**

Collaborators: Mohan Seth (Consultant)

Objective: The purpose of this work is to modify V-TOUGH to improve computational efficiency and I/O user friendliness of the code. This is an on-going project within the IPA and EBS elements.

1.1.95 No work currently in progress.

2 Sub-Regional Hydrology Processes: Site-Scale Flow & Transport Modeling

Account Number: **20-5704-176**

Collaborators: Ross Bagtzoglou

Objective: The purpose of this work is to modify the code GEM to include partially saturated porous media.

Date	Entry
------	-------

12.16.94	Work began on modifying the computer code GEM to include flow and transport in partially saturated porous media. The code GEM describes multicomponent transport of solutes in a fully saturated 1D porous medium taking into account aqueous complexing, mineral precipitation/dissolution, and ion-exchange reactions. As an initial approach, the Richards equation was added to GEM using a sequential solution method. Thus at each new time step, first the Richards equation is solved to obtain the saturation and flow field as functions of distance. Second, chemically reacting solutes are transported using the results obtained from solving the Richards equation. As a third step, mineral concentrations are calculated enabling changes in porosity, tortuosity and permeability to be computed which can then alter the flow field. This three-step approach can be justified based on the different time scales of the processes involved. In the future it may prove necessary to fully couple the solvent and solute flow and transport equations for describing extremely dry conditions, in which case these equations become more tightly coupled. The van Genuchten phenomenological equations were used to describe material properties in the Richards equation.
----------	---

3 EBSPAC

Account Number: **20-5702-523**

Collaborators: none

Objective: The purpose of this project is to investigate the near-field environment of a partially saturated HLW repository and to model corrosion of the waste package and spent fuel.

3.1 Reactive Boundary Condition

Date Entry

11.25.94 Non-zero gradient boundary condition. This boundary condition occurs if a chemical reaction is present at the boundary, as for example corrosion at a metal surface. In this case it is necessary to also obtain the value of the concentration at the boundary. Consider a first order kinetic rate law leading to a boundary condition of the form:

$$D \left. \frac{\partial C}{\partial x} \right|_{x=a} = -k (C_a - C_{eq}). \quad (3-1)$$

The left-hand side of this equation represents the diffusive flux away from the surface located at $x = a$ with solute concentration C and diffusion coefficient D . The right-hand side represents the reaction rate at the surface with rate constant k and equilibrium concentration C_{eq} (Murphy et al., 1989). In finite difference form with ghost node designated by x_{N+1} and the boundary located midway between x_N and x_{N+1} , the boundary condition becomes:

$$D \frac{C_{N+1} - C_N}{\Delta x} = -k (C_a - C_{eq}) \quad (3-2)$$

It is necessary to express the concentration at the boundary C_a in terms of the concentration at the node points x_N and x_{N+1} . One way to do this is through the arithmetic mean:

$$C_a = C_{N+1/2} = \frac{1}{2} (C_{N+1} + C_N). \quad (3-3)$$

Introducing

$$C' = C - C_{eq}, \quad (3-4)$$

this leads to the following expression for the concentration at the ghost node:

$$C'_{N+1} = \frac{1 - \frac{k\Delta x}{2D}}{1 + \frac{k\Delta x}{2D}} C'_N. \quad (3-5)$$

However, in the limit $k \rightarrow \infty$ corresponding to local equilibrium this formulation leads to the nonsensical result that

$$\lim_{k \rightarrow \infty} C'_{N+1} = -C'_N < 0, \quad (3-6)$$

that is, the concentration at the ghost node is negative! For this approach to provide physically reasonable results requires that

$$\Delta x \ll \frac{2D}{k}, \quad (3-7)$$

which would lead to an unreasonably small grid spacing.

Fortunately, there is an alternative formulation based on the harmonic mean approximation to the concentration at the boundary. In this case

$$C_{N+1/2} = \frac{2C_{N+1}C_N}{C_{N+1} + C_N}. \quad (3-8)$$

The concentration at the ghost node now becomes

$$\frac{C'_{N+1}}{C'_N} = \sqrt{1 + \left(\frac{k\Delta x}{D}\right)^2} - \frac{k\Delta x}{D}. \quad (3-9)$$

It follows that

$$\frac{C'_{N+1}}{C'_N} = \begin{cases} 1, & k \rightarrow 0 \\ 0, & k \rightarrow \infty \end{cases}. \quad (3-10)$$

Therefore in this case the local equilibrium limit can be retrieved without also requiring that $\Delta x \rightarrow 0$ as in the arithmetic mean approximation.

It should be noted that generally the reaction rate is a highly nonlinear function of the solute concentration, and a simple analytical expression for the concentration at the ghost node is not possible. In such circumstances the ghost node concentration must be obtained numerically.

3.6.95 In spite of the fact that the concentration at the ghost node can become negative, the concentration at the boundary is positive definite as can be seen by the following analysis. Defining

$$\alpha = \frac{k\Delta x}{2D}, \quad (3-11)$$

then

$$\begin{aligned} C_L - C_{eq} &= \frac{1}{2} \left(\frac{1-\alpha}{1+\alpha} + 1 \right) C'_N, \\ &= \frac{1}{2} \frac{1}{1+\alpha} C'_N. \end{aligned} \quad (3-12)$$

In the limit $k \rightarrow \infty$, $C_L \rightarrow C_{eq}$ as is to be expected.

2.16.95 Multicomponent nonlinear flux boundary conditions. The flux boundary condition option is being added to GEM to model corrosion processes at a fixed boundary. The flux boundary condition is of the form

$$\Omega_j = - \sum_m \nu_{jm} \mathcal{R}_m, \quad (3-13)$$

where both sides of this equation are evaluated at the corroding surface. The flux Ω_j is given by

$$\Omega_j = -\phi \left[D_j \frac{\partial C_j}{\partial x} + \sum_i \nu_{ji} D_i \frac{\partial C_i}{\partial x} \right]. \quad (3-14)$$

The rate \mathcal{R}_m is assumed to be given by the Butler-Volmer expression

$$\mathcal{R}_m = \dots \quad (3-15)$$

The finite difference form is equal to

$$-\phi D_j \frac{C_{j1} - C_{j0}}{x_1 - x_0} - \phi \sum_i \nu_{ji} D_i \frac{C_{i1} - C_{i0}}{x_1 - x_0} = - \sum_m \nu_{jm} \mathcal{R}_{m0} (x_1 - x_0), \quad (3-16)$$

where the unknowns are the primary species concentrations.

3.1.95 One-Sided Derivatives.

Better might be to use one-sided derivatives. In this case the boundary condition

$$J = -\phi D \frac{\partial C}{\partial x} = k(C - C_{eq}), \quad (3-17)$$

becomes

$$-\phi D \frac{C_{N+1} - C_N}{x_{N+1} - x_N} = k(C_{N+1} - C_{eq}). \quad (3-18)$$

Solving for C_{N+1} yields

$$C_{N+1} = \frac{C_N + k/(\phi D)(x_{N+1} - x_N)C_{eq}}{1 + k/(\phi D)(x_{N+1} - x_N)}. \quad (3-19)$$

Thus the rate can be expressed as

$$R = k(C_{N+1} - C_{eq}) = k \frac{C_N - C_{eq}}{1 + k/(\phi D)(x_{N+1} - x_N)}. \quad (3-20)$$

Note that C_{N+1} has the correct limiting value in the local equilibrium limit, namely

$$\lim_{k \rightarrow \infty} C_{N+1} = C_{eq}. \quad (3-21)$$

For no reaction ($k = 0$), it follows that $C_{N+1} = C_N$.

3.7.95 One-Sided Derivatives in a Multicomponent System.

In a multicomponent system the surface boundary conditions becomes

$$J_j = -\phi D_j \frac{\partial C_j}{\partial x} = -\sum_m \nu_{jm} I_m(C_1, \dots, C_{N_c}). \quad (3-22)$$

In finite difference form this relation becomes

$$-\phi D \frac{C_{j,N+1} - C_{j,N}}{x_{N+1} - x_N} = -\sum_m \nu_{jm} I_m(C_{1,N+1}, \dots, C_{N_c,N+1}), \quad (3-23)$$

which results in a nonlinear equation for $C_{j,N+1}$.

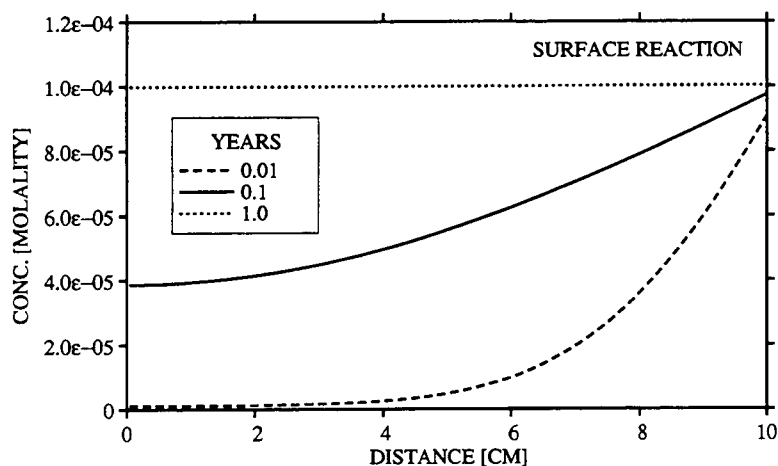
4.4.95 First order linear surface reaction kinetics.

Figure 3-1: Numerical calculation for surface reaction using a first order rate law for dissolution of quartz at 25°C. A single component system with species SiO_2 is used. The input file is `surf.in`. Calculations are given for elapsed times of 0.01, 0.1 and 1 years as shown in the legend.

Input file surf.in for the calculation shown in Figure 3-1 for use with executable GEMSURF.

```
'Quartz dissolution'
'IDATA  ISTART  IPLOT  IFOR   MODES  IFLUX  IACT   IFINDZB LOGLIN'
0       0       1       1       2 2    1       0       0       0

'ITMAX  IHALMAX IVMAX  ID      IMOD   IPRINT  IEXACT  ISCALE  ISTAT'
15      30      6      1       10     -1      0       0       0

'ISTDST ISURF  IJAC   IJACNUM IPOR   ICON   IDIF   NDAMP'
1       1       0     0       0     1      0      0

'CREVICE GAP[METERS]'
10.d-6

'iplot: a s t m si sf v z b in e ex'
      1 1 1 1 0 0 1 0 0 0 0 0

'tol    ttol    tolneg  tolpos  tolexp  dthalf  qkmax    tolstdste'
1.d-12  5.e-2   1.e-3   1.e-2   5.d0    0.5     590.d0   1.e1

'      MCYC  CC C  R SP QK pk rk A1 A2 A3'
'TEST'  0     1  1  1  1  1  1  1  0  0  0

'DO[cm^2/s] VO[m/y] ALPHA PORO PHISUBR W LAMBDA TOLTRF TOLDELT TOLPOR'
1.D-5    0.0    0.0 0.03 1.0  0.5 1.0  0.  1.e3 1.e-3

'flag 1: T(x)  = d x3 + a x2 + b x + c (meters)'
'      2: T(x)  = a + (b-a) exp[-((x-x0)/c)2] + (d - a) x / xlen'
'      3: T(x,t)=a+1/2(b-a)(erf[(x+c-x0)/2sqr(dt)]-erf[(x-c-x0)/2sqr(dt)])'
'p (bars) temp flag  a      b      c      d      x0      xlen'
1.0e0    25.    0     25.d0  300.d0  250.d0  125.d0  1000.d0  2.d3

'INITIAL AND BOUNDARY CONDITIONS: 1-conc., 2-flux, 3-zero gradient'
'inlet outlet nzoneaq'
3       1       3

'SPECIES'
'LABEL ITYPE  GUESS  CTOT  MINERAL'

'sio2(aq)'
'inlet' 1      1.e-6  1.e-6  ' '
'out'   1      1.e-4  1.e-6  'quartz'
'init'  1      1.e-4  1.e-6  'quartz'
'*'      0.

'SPECIES TOLERANCE'
15*1.0

'GRID' 'cm' 0. 1 100 10.d0

'TIME' 'y' 3 0.01 0.1 1. 10. 100. 500. 1.e3 1.e4
```

P. C. Lichtner

SCIENTIFIC NOTEBOOK

INITIALS: PC

```

'TIMESTEP[y]' 2 3.e-11 1.e6
1.e-11          50.    200.

'EXPA' 1 1.E30 1 1.e-6
'PLOT[y]' 3 0.01 0.1 1. 10. 100. 500. 1.e3 1.e4

'BREAK-THROUGH PTS.' 0 93 110 130 150 185

'aqueous complexes      diffusion coef. [cm^2/s]'
'*'                      0.

'ncorr'
0

'minerals'
'quartz'
'*'

'reversible minerals'
'*' 0.

'irreversible mineral nzone itypkin beta fkin delh   rkph rk   tol'
'z1    z2    vol    area'
'*'          1    0    1.0    1.0    0.    0. 0. 0.

'surface mineral itypkin area beta fkin delh   rkph   rk'
'quartz'          0    1.0    1.0    1.    0.    0.    1.e-12
'*'          0    1.0    1.0    1.    0.    0.    0.

'gases'
'*'

'ion-exchange reactions'
0    1.0

```


3.2 Sorption

Date Entry

2.6.95 Charge conservation in sorption reactions. The problem addressed is modeling sorption reactions with transport and the problem of charge conservation in the bulk aqueous solution. A satisfactory model must conserve charge.

The charge density in the electric double layer is given by

$$\rho = F \sum_i z_i C_i, \quad (3-24)$$

where C_i denotes the concentration of the i th species within the double layer. This concentration is presumed to be related to the bulk concentration through the Boltzmann factor

$$C_i = C_i^b e^{-z_i F \Phi(y) / RT}, \quad (3-25)$$

where C_i^b denotes the bulk concentration of the i th species. The electric potential Φ satisfies Poisson's equation

$$\frac{d^2 \Phi}{dy^2} = -\frac{1}{\epsilon_0 D} \rho(y), \quad (3-26)$$

where ϵ_0 denotes the permittivity and D the dielectric constant. The bulk fluid composition is neutral:

$$\sum_i z_i C_i^b = 0, \quad (3-27)$$

where as the charge contained in the double layer cancels the charge adsorbed to the surface. Denoting the double layer surface charge by σ_d , then

$$\sigma_d = - \int_{\delta}^{\infty} \rho(y) dy. \quad (3-28)$$

The surface charge σ_d is related to the electric field \mathcal{E} by the relation

$$\sigma_d = \epsilon \mathcal{E}, \quad (3-29)$$

where $\epsilon = \epsilon_0 D$. The electric field is related to the potential at the surface by Poisson's equation. Writing

$$\frac{d^2 \Phi}{dy^2} = -\frac{d\mathcal{E}}{dy} = -\frac{d\mathcal{E}}{d\Phi} \frac{d\Phi}{dy} = \mathcal{E} \frac{d\mathcal{E}}{d\Phi}, \quad (3-30)$$

it follows that

$$\frac{1}{2}\mathcal{E}^2 = -\frac{1}{\epsilon}\int \rho d\Phi = \frac{RT}{\epsilon}\sum_i C_i^b (e^{-z_i F\Phi/RT} - 1). \quad (3-31)$$

This gives for the surface charge

$$\sigma_d = \epsilon\mathcal{E} = \sqrt{2\epsilon RT \sum_i C_i^b (e^{-z_i F\Phi/RT} - 1)}. \quad (3-32)$$

An alternative expression for the surface density is obtained by integrating the charge density to give

$$\sigma_d = -\sum_i C_i^b \int_{\delta}^{\infty} e^{-z_i F\Phi(y)/RT} dy. \quad (3-33)$$

The Boltzmann factor appearing in Eqn.(3-25) can be understood as the steady-state solution to the diffusive transport equation applied to the double layer. The steady-state concentration satisfies the differential equation

$$\frac{d}{dy} \left(-D_i \frac{dC_i}{dy} - F z_i \frac{D_i C_i}{RT} \frac{d\Phi'}{dy} \right) = 0. \quad (3-34)$$

This equation has as solution the Boltzmann distribution

$$C_i = C_i^b e^{-z_i F\Phi'(y)/RT}. \quad (3-35)$$

The potential Φ' is determined so that the net current in the double layer vanishes:

$$\sum_i z_i \left(D_i \frac{dC_i}{dy} + F z_i \frac{D_i C_i}{RT} \frac{d\Phi'}{dy} \right) = 0. \quad (3-36)$$

This equation leads to the following equation for the electric field

$$\frac{d\Phi'}{dy} = -\frac{RT}{F} \frac{\sum_i z_i D_i dC_i/dy}{\sum_{i'} z_{i'}^2 D_{i'} C_{i'}}. \quad (3-37)$$

It remains to demonstrate that the potentials Φ and Φ' are equivalent.

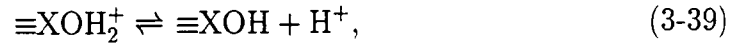
The two-layer model for adsorption may be formulated generally in terms of the following set of surface complexation reactions



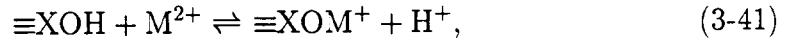
where $\bar{\chi}$ denotes the neutral oxide surface site, $\bar{\nu}_{ji}$ refers to the stoichiometric coefficients involving primary aqueous solute species A_j , and \bar{A}_i^{ad} represents the

i th adsorbed surface species. In what follows an overscore is used to designate quantities referred to the surface of the oxide mineral.

Examples of these reactions for adsorption of a divalent cation M^{2+} on an oxide surface are expressed by



and



where $\equiv\text{XOH}_2^+$ and $\equiv\text{XO}^-$ represent surface hydroxyl groups describing protonation and deprotonation of the surface, $\equiv\text{XOH}$ represents the unoccupied surface sites, and $\equiv\text{XOM}^+$ represents adsorption of the cation M^{2+} .

The mass action equations corresponding to Eqn.(3-38) have the general form

$$\begin{aligned} \bar{C}_i &= \bar{K}_i C_{\bar{x}} \prod_{j=1}^N (\gamma_j C_j P^{z_j})^{\bar{\nu}_{ji}}, \\ &= \bar{K}_i C_{\bar{x}} P^{\bar{z}_i} \prod_{j=1}^N (\gamma_j C_j)^{\bar{\nu}_{ji}}, \end{aligned} \quad (3-42)$$

where C_j denotes the bulk concentration of the j th primary species, and the factor P is given by the Boltzmann distribution

$$P = e^{-F\psi_0/RT}, \quad (3-43)$$

where F denotes the Faraday constant, ψ_0 the electric double layer potential evaluated at the surface, R the gas constant, and T the temperature. The latter expression is obtained noting that the valence associated with the i th adsorbed species \bar{z}_i is related to the valencies of the primary species by the equation

$$\bar{z}_i = \sum_j \bar{\nu}_{ji} z_j. \quad (3-44)$$

Conservation of sites is described by the equation

$$\begin{aligned} \bar{C}_s &= \bar{C}_{\bar{x}} + \sum_i \bar{C}_i, \\ &= \bar{C}_x \left\{ 1 + \sum_i \bar{K}_i P^{\bar{z}_i} \prod_{j=1}^N (\gamma_j C_j)^{\bar{\nu}_{ji}} \right\}. \end{aligned} \quad (3-45)$$

From this relation and the mass action equations, Eqn.(3-42), the sorption isotherms for the concentration of empty sites and adsorbed species are given by

$$\bar{C}_{\bar{x}} = \frac{\bar{C}_s}{1 + \sum \bar{K}_i P^{\bar{z}_i} \prod_{j=1}^N (\gamma_j C_j)^{\bar{\nu}_{ji}}}, \quad (3-46)$$

and

$$\bar{C}_i = \frac{\bar{C}_s \bar{K}_i P^{\bar{z}_i} \prod_{l=1}^N (\gamma_l C_l)^{\bar{\nu}_{li}}}{1 + \sum_{i'} \bar{K}_{i'} P^{\bar{z}_{i'}} \prod_{j=1}^N (\gamma_j C_j)^{\bar{\nu}_{ji'}}}. \quad (3-47)$$

The surface charge σ_0 is balanced by the total charge contained within the double layer according to the expression

$$\begin{aligned} \sigma_0 &= F \sum_i \bar{z}_i \bar{C}_i, \\ &= \alpha \left[\sum_j C_j \left(e^{-z_j F \psi_0 / RT} - 1 \right) + \sum_i C_i \left(e^{-z_i F \psi_0 / RT} - 1 \right) \right], \end{aligned} \quad (3-48)$$

where α is defined by

$$\alpha = \sqrt{2\epsilon D R T}. \quad (3-49)$$

For a z:z electrolyte this equation simplifies to

$$\sigma = \sum_i \bar{z}_i \bar{C}_i = \alpha \sinh \frac{F \psi_0}{RT}. \quad (3-50)$$

Mass transport equations including the effects of adsorption have the form

$$\frac{\partial}{\partial t} \left[\phi \left(C_j + \sum_i \nu_{ji} C_i \right) + \sum_i \bar{\nu}_{ji} \bar{C}_i + \bar{\Psi}_j^\Gamma \right] + \frac{\partial \Omega_j}{\partial x} = 0, \quad (3-51)$$

where Ψ_j and Ω_j denotes the generalized concentration and flux, respectively, defined by

$$\Psi_j = C_j + \sum_i \nu_{ji} C_i, \quad (3-52)$$

$$\bar{\Psi}_j^\Gamma = \Gamma_j C_j + \sum_i \nu_{ji} \Gamma_i C_i, \quad (3-53)$$

and

$$\Omega_j = J_j + \sum_i \nu_{ji} J_i. \quad (3-54)$$

The quantity Γ_j denotes the non-specifically adsorbed contribution to the mass balance defined by

$$\Gamma_j = \int_0^\infty e^{-z_j F \psi(y) / RT} dy, \quad (3-55)$$

where the coordinate y refers to the direction perpendicular to the oxide surface. The accumulation term in the transport equation for bulk solute species is assumed to consist of the sum of contributions from the double layer, the so-called non-specifically adsorbed species, and the bulk solution itself. However, because species in the double layer are not transported in the bulk solution, they give rise to an additional retardation effect beyond that given by the specifically adsorbed species.

With this form of the transport equations charge conservation is guaranteed. Multiplying the transport equation for the j th primary species by the charge z_j and summing over all primary species yields

$$\frac{\partial}{\partial t} \sum_j z_j \left[\phi \Psi_j + \sum_i \bar{\nu}_{ji} \bar{C}_i + \bar{\Psi}_j^\Gamma \right] + \sum_j z_j \frac{\partial \Omega_j}{\partial x} = 0. \quad (3-56)$$

Conservation of charge in the aqueous phase requires that

$$\frac{\partial}{\partial t} \phi \sum_j z_j \Psi_j + \frac{\partial}{\partial x} \sum_j z_j \Omega_j = 0, \quad (3-57)$$

whereas conservation of charge of adsorbed ions and non-specifically adsorbed ions in the double layer requires

$$\frac{\partial}{\partial t} \sum_j z_j \left[\sum_i \bar{\nu}_{ji} \bar{C}_i + \bar{\Psi}_j^\Gamma \right] = 0. \quad (3-58)$$

This latter equation is satisfied by definition of the electric double layer potential ψ in terms of the surface charge σ according to the relation

$$\begin{aligned} \sum_j z_j \sum_i \bar{\nu}_{ji} \bar{C}_i &= - \sum_j z_j \bar{\Psi}_j^\Gamma, \\ &= \sum_i \bar{z}_i \bar{C}_i. \end{aligned} \quad (3-59)$$

Retardation is influenced by the non-specific sorption in the electric double layer as well as specific ion adsorption on the Hemholtz layer. The local distribution coefficient giving the ratio of total concentration of adsorbed species including contributions from both the Hemholtz and Gouy-Chapman layers to the aqueous concentration can be defined as

$$\mathcal{K}_j^D = \frac{\sum_i \bar{\nu}_{ji} \bar{C}_i + \bar{\Psi}_j^\Gamma}{\Psi_j}. \quad (3-60)$$

3.3 Thermodynamic Data

Date Entry

3.13.95 Thermodynamic Data for Uranyl silicate Minerals. Significant discrepancies in the EQ3/6 database were noted for several uranyl silicate minerals of importance for modeling alteration of spent fuel. Recent data is taken from McKenzie¹ (unpublished) based on Nguyen et al. (1991)².

Table 3-2: Thermodynamic data for uranyl silicate minerals and comparison with the EQ3/6 database. The difference values are defined as $\delta = \langle \text{EQ3/6} \rangle - \langle \text{Est.} \rangle$.

Mineral	EQ3/6		New Estimate		Difference	
	ΔG_0 kJ mol ⁻¹	Log K	ΔG_0 kJ mol ⁻¹	Log K	$\delta \Delta G_0$ kJ mol ⁻¹	$\delta \text{Log } K$
uranophane	-4975	17.289	-6213	8.123	1238.22	9.166
soddyite	-3685	0.395	-3706	-3.285	21.	3.80
weeksite	-9043	15.380	-9039	16.081	-4	-0.70

The free energies for aqueous species used in the EQ3/6 log K values and in the new estimates are given in the table below.

Table 3-3: Aqueous species free energies taken from the EQ3/6 database data0.R16.

Species	ΔG_0 kJ mol ⁻¹
UO ₂ ²⁺	-952.556
K ⁺	-282.462
Ca ²⁺	-552.790
SiO ₂	-833.411
H ₂ O	-237.182

¹William F. McKenzie, Gibbs free energies of formation of uranyl silicates at 298°K.

²Son N. Nguyen, Robert J. Silva, Homer C. Weed, John E. Andrews, Jr. (1991) Standard gibbs free energies of formation at 30°C of four uranyl silicates: soddyite, uranophane, sodium boltwoodite and sodium weeksite. LLNL UCRL-JC-106032.

4 IPA: Flow Around the Waste Package

Account Number: **20-5702-723**

Collaborators: John Walton (Consultant)

Objective: The purpose of this project is to investigate the flow of liquid water and vapor in the near-field region of a HLW repository.

1.25.95 Received first draft from J. Walton.

3.30.95 Revised manuscript adding derivation of diffusion-caused-advection. The non-segregative component to the gas flux is described by Darcy's law in the form

$$F_w^g = -\frac{kk_r^g}{\mu_g} \frac{X_w^g P}{RT} \nabla P, \quad (4-61)$$

and

$$F_a^g = -\frac{kk_r^g}{\mu_g} \frac{X_a^g P}{RT} \nabla P, \quad (4-62)$$

for water vapor and air, respectively, where kk_r^g denotes the relative permeability to the gas phase, μ_g refers to the viscosity, and the ideal gas law has been invoked. For steady state conditions the precise form of the non-segregative contribution to the flux is not important. An expression for the total water vapor flux can be derived in which the non-segregative component to the flux does not occur explicitly. It follows that

$$F_g = F_w^g + F_a^g = -\frac{kk_r^g}{\mu_g} \frac{P}{RT} \nabla P. \quad (4-63)$$

Thus, alternatively one can write

$$F_w^g = X_w^g F_g, \quad (4-64)$$

and

$$F_a^g = X_a^g F_g. \quad (4-65)$$

The total gas flux is equal to the sum of the non-segregative components according to the equation

$$N_g = N_w^g + N_a^g = F_w^g + F_a^g, \quad (4-66)$$

as follows from the defining relation for the diffusive flux, which must, by definition, satisfy the condition

$$J_w^g + J_a^g = 0, \quad (4-67)$$

as follows from the definition of mole fraction

$$X_w^g + X_a^g = 1. \quad (4-68)$$

It follows that the total water vapor flux can be expressed alternatively as

$$N_w^g = J_w^g + X_w^g F_g = J_w^g + X_w^g N_g = J_w^g + X_w^g (N_w^g + N_a^g). \quad (4-69)$$

Under the assumption that the system is in a steady-state and assuming that the component of air dissolved in the liquid phase is negligible compared to its concentration in the gas phase, it follows that air is stagnant ($N_a^g = 0$). As a consequence Eq.(4-69) yields

$$N_w^g = \frac{J_w^g}{1 - X_w^g}. \quad (4-70)$$

This form of the flux implicitly includes the effects of a pressure gradient. The flux grows without bound as $X_w^g \rightarrow 1$. This expression for the flux of water vapor is identical to that obtained by Bird et al. (1960), referred to as diffusion-caused-advection.

5 SCCEX Code Analysis

Account Number: **20-5702-523**

Collaborators: Jong Song

Objectives: Prepare users manual for the SCCEX code.

1.19.95 SCCEX code modification.

We (i.e. J. Song) found one bug in the corrosion rate calculation:

cpcl 1.18.95 there appears to be an error in use of rkox
cpcl the temperature dependent factor is missing in tmp2

```

      tmp2 = max(sollay,delta)*rkox/4./F/Dw/taus/spor
      do 100 i = 1, 15
        curhy = -rkhy*exp(Ghy*factor)*
&              exp(-betahy*F/rgas/tk*Ee)
        tmp1 = exp(-betaox*4.*F/rgas/tk*Ee)
c    jcw: 8/18/93
c    Note: Oxygen current must be constrained to be below
c          diffusion limited current
c          curmax is the diffusion limited current,
c    since cathodic current is negative, we take the maximum value
c    to get the lowest absolute value
c
      curmax = -4.*F*Dw*taus*spor*cout/max(sollay,delta)
      curox = -rkox*exp(Gox*factor)*
&          cout*tmp1/(1.0+tmp1*tmp2)
      curox=max(curmax,curox)
      cathod = -(curox+curhy)

```

```

c Estimate corrosion potential by equating oxygen reduction
c plus hydrogen evolution with passive current density
c
  Ee = 0.
  delt = 2.0
  t1=betah*F/(rgas*tk)
  t2=rkox*exp(Gox*factor)*max(sollay,delta)/(4.0*F*Dw*taus*spor)
  t3=betaox*4.0*F/(rgas*tk)
  do 100 i = 1, 15
    curhy=-rkhy*exp(Ghy*factor)*exp(-t1*Ee)
c   jcw: 8/18/93
c   Note: Oxygen current must be constrained to be below
c         diffusion limited current
c         curmax is the diffusion limited current,
c   since cathodic current is negative, we take the maximum value
c   to get the lowest absolute value
c
  curmax = -4.*F*Dw*taus*spor*cout/max(sollay,delta)
  curox = -rkox*exp(Gox*factor)*cout*exp(-t3*Ee)/
&      (1.0+t2*exp(-t3*Ee))

```

```

        curox=max(curmax,curox)
        cathod = -(curox+curhy)
        if(cathod.gt.cpass) then
            Ee=Ee+delt
        else
            Ee=Ee-delt
        endif
        delt=delt/2.0
100 continue
c   jsong: 1/19/95
c
c   To satisfy the condition that the summation of all currents equal to zero,
c   Newton-Raphson method is used as an additional step
c
        do 101 i = 1, 10
            curhy=-rkhy*exp(Ghy*factor)*exp(-t1*Ee)
            curmax = -4.*F*Dw*taus*spor*cout/max(sollay,delta)
            curox = -rkox*exp(Gox*factor)*cout*exp(-t3*Ee)/
&            (1.0+t2*exp(-t3*Ee))
            curox=max(curmax,curox)
            cathod = -(curox+curhy)
            zc=cpass-cathod
            dzc=-t1*curhy-t3*curox/(1+t2*exp(-t3*Ee))
c        write(*,102) i,Ee,curox,curhy,dzc,zc
c 102  format(i3,5(3x,e12.3))
            if(abs(zc).le.1.0e-10) go to 103
            Ee=Ee-zc/dzc
101 continue
        write(*,*) 'The corrosion potential does not converge within 10
&                iterations.'
```

```

c  talt = the time when all waste has been altered
c
      talt = 1./alt + tfail
      if(water.le.1.e-10) water = 1.e-10
      conc = rad(2) / water
      if(time.lt.tfail) then
c  container not failed, only radioactive decay
      drdt(1) = -rlam*rad(1)
      drdt(2) = 0.0
      drdt(3) = 0.0
      else if(time.lt.talt) then
c  can has failed but not all waste form has been altered
c
c  Modified by jsong 1/20/95
c      drdt(1) = -rlam*rad(1) - alt*rad(1)
c      drdt(2) = +alt*rad(1) -Qqout*conc -rlam*rad(2)
c  1st-order eqn
c      drdt(1) = -rlam*rad(1) - alt*exp(-rlam*tfail)
c      drdt(2) = +alt*exp(-rlam*tfail) -Qqout*conc -rlam*rad(2)
c  0th-order eqn
      drdt(1) = -rlam*rad(1) - alt*exp(-rlam*time)
      drdt(2) = +alt*exp(-rlam*time) -Qqout*conc -rlam*rad(2)
c  jcw's model
      else
c  all waste has been altered
      rad(1) = 0.
      drdt(1) = 0.
      drdt(2) = -Qqout*conc - rlam*rad(2)
      endif
      drdt(3) = Qqout*conc
      relrat = drdt(3)

```

```
c  Write to mechanical code
c  i = counter
c  tstop = time
c  tin = canister temperature
c  cthick - penet = remaining canister thickness
c  Vwater/delta = wetted area
c  Qout = effluent flow rate
c
      rthick=cthick-penet(i)
      if(rthick.lt.0.0) rthick=0.0
      write(7,9001) i,tstop, tin, rthick,
& Vwater(i)/delta, Qout
9001 format (1x,i4,1x,7(e10.3,1x))
      ax(jcell,i)=tstop
      bx(jcell,i)=tin
      cc(jcell,i)=cthick-penet(i)
      dqx(jcell,i)=Vwater(i)/delta
      ee(jcell,i)=Qout
```

6 Volcanology Project

Account Number: **20-5704-143**

Collaborators: PI: Charles Connor

Objective: The purpose of this work is to study heat transport from a dike or volcano using CTOUGH. This work has the potential to provide field verification of CTOUGH simulations similar to modeling the heat generated from a HLW repository emplaced in a partially saturated porous medium.

1.18.95 Modified CTOUGH to handle temperatures up to 1200°C. The following parameters were changed in the file `hdr.h`:

```
cpcl parameter(NTABT=248, NTABPL=3, NTABPG=30)
      parameter(NTABT=300, NTABPL=3, NTABPG=30)
cpcl parameter(DTABT=2.0)
      parameter(DTABT=4.0)
```

2.24.95 One-dimensional CTOUGH simulations for a 5m wide dike. The input file used in the calculations is `dikei`. An equivalent continuum model is used to represent the country rock.

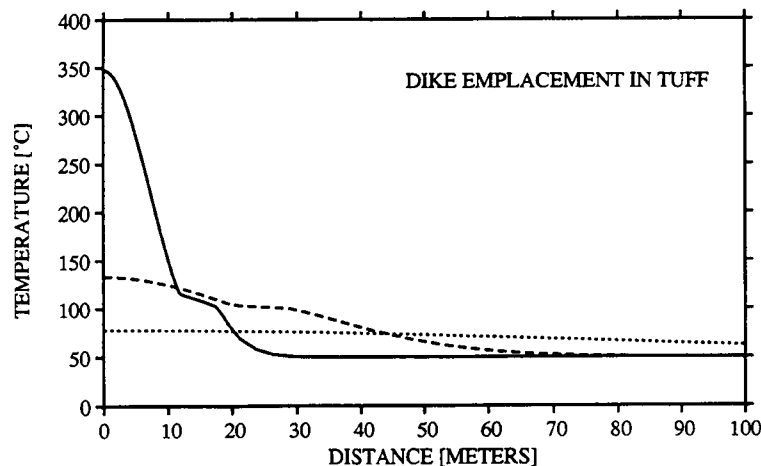


Figure 6-2: Temperature plotted as a function of distance from the dike for times of 1 (solid), 10 (dashed) and 100 (dotted) years.

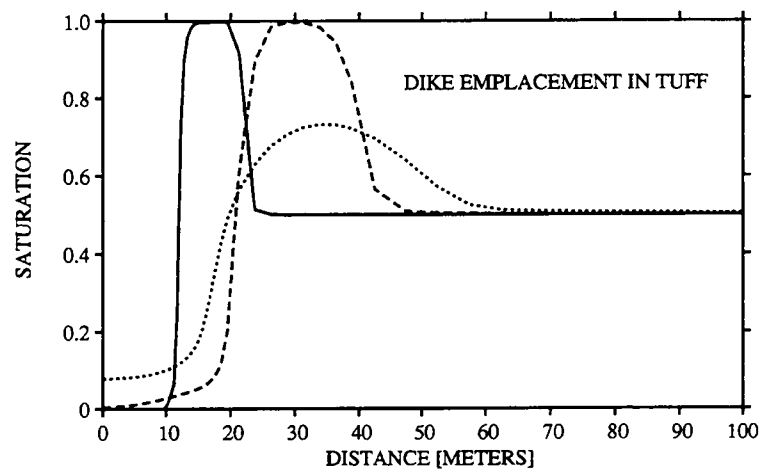


Figure 6-3: Liquid saturation plotted as a function of distance from the dike for times of 1 (solid), 10 (dashed), and 100 (dotted) years.

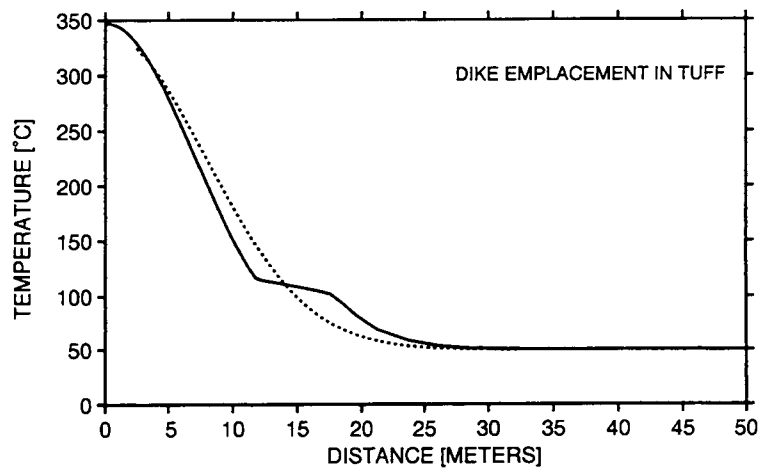


Figure 6-4: Comparison of the temperature calculated using CTOUGH (solid curve) with a pure conductive analytical solution (dotted curve) for an elapsed time of 1 year.

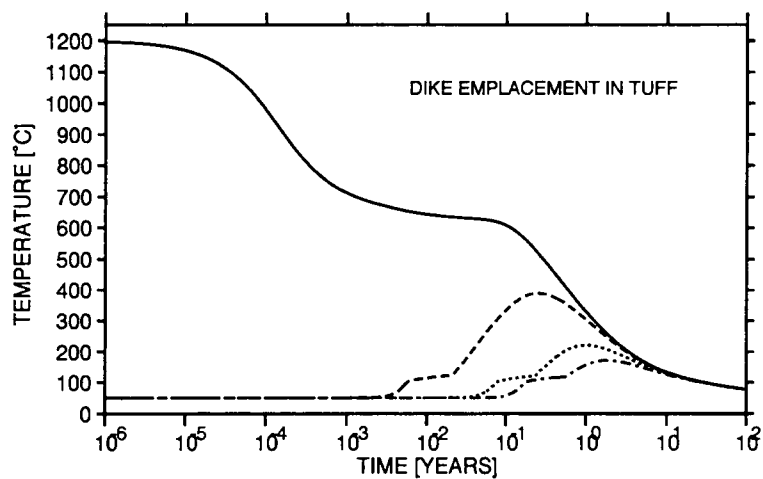


Figure 6-5: The temperature plotted as a function of time for different distances from the dike at elements: A 25 (solid), A 35 (dashed), A 45 (dotted), and A 50 (dashed-dotted).

I have reviewed this scientific notebook and find it in compliance with QAP-001. There is sufficient information regarding procedures used for conducting tests, acquiring and analyzing data so that another qualified individual could repeat the activity.

N. Sridhar 4/17/97

Narasi Sridhar
Manager, Engineered Barrier System and Waste Solidification System

SCIENTIFIC NOTEBOOK

Printed: December 18, 1995

P. C. Lichtner

SCIENTIFIC NOTEBOOK

INITIALS:

PC

SCIENTIFIC NOTEBOOK

by

Peter C. Lichtner

Southwest Research Institute
Center for Nuclear Waste Regulatory Analyses
San Antonio, Texas

December 18, 1995

P. C. Lichtner

SCIENTIFIC NOTEBOOK

INITIALS:

PC

INITIAL ENTRIES

Scientific Notebook: # 095

Issued to: P. C. Lichtner

Issue Date: Tuesday, November 16, 1993

Computerized Initials:

PC

By agreement with the CNWRA QA this Notebook is to be printed at approximate quarterly intervals. This computerized Scientific Notebook is intended to address the criteria of CNWRA QAP-001.

Table 0-1: Computing Equipment

Machine Name	Type	OS	Location
gravenstein.cnwra.swri.edu	Intel Professional Workstation	NEXTSTEP	desk Rm A-126
	DX 66 Mhz	Version 3.3	Bldg. 189
skippy.cnwra.swri.edu	Sun SPARC 20	SUNOS 4.1.2	network

List of Figures

1-1	Liquid saturation for the Hills et al. problem plotted as a function of depth for an elapsed time of 4.32×10^5 seconds.	1-1
1-2	Liquid and vapor fluxes for the 1D repository-scale model with a thermal loading of 114 kW/acre plotted as a function of depth for times of 10, 100, 1,000 and 5,000 years.	1-2
2-3	Sorption of uranium on goethite.	2-4
2-4	Logarithm of the distribution coefficient for sorption of uranium and neptunium on goethite plotted as a function of pH with (dashed curve) and without (solid curve) CO_2 present.	2-9
2-5	Logarithm of the concentration of selected (a) uranium- and (b) neptunium-bearing species plotted as a function of pH.	2-9
5-6	Temperature and liquid saturation for a 5 m dike with an initial temperature of 1200°C and initial saturation of the country rock of 10%.	5-3
6-7	Minimum mole fraction X_{\min} plotted as a function of porosity.	6-5
6-8	Mole fraction X_{SiO_2} plotted as a function of saturation S for porosities 0.1, 0.5 and 0.8.	6-7

List of Tables

0-1	Computing Equipment	ii
1-2	Chemical Constituents	1-6
2-3	Surface complexation reactions for sorption of uranium and neptunium on goethite.	2-7
2-4	Model Conditions	2-8
3-5	Electrochemical data for the listed reactions.	3-3

PROJECTS

Contents

INITIAL ENTRIES ii

FIGURES iii

TABLES iv

PROJECTS v

1 MULTIFLO Development 1-1

2 Sub-Regional Hydrology Processes: Site-Scale Flow & Transport Modeling 2-1

3 EBSPAC 3-1

 3.1 Reactive Surface Boundary Condition 3-1

4 IPA: Flow Around the Waste Package 4-1

5 Volcanology Project 5-2

6 Criticality 6-4

1. MULTIFLO Development

Account Number: **20-5702-523**

Collaborators: Mohan Seth (Consultant)

Objective: The purpose of this work is to develop the code MULTIFLO to describe multiphase reactive transport.

8.4.95 The first test of the two-phase fluid flow engine was made comparing CTOUGH, PORFLO and MULTIFLO for the Hills et al. problem. Excellent agreement is obtained between MULTIFLO and CTOUGH, but PORFLO is somewhat off as shown in Figure 1-1.

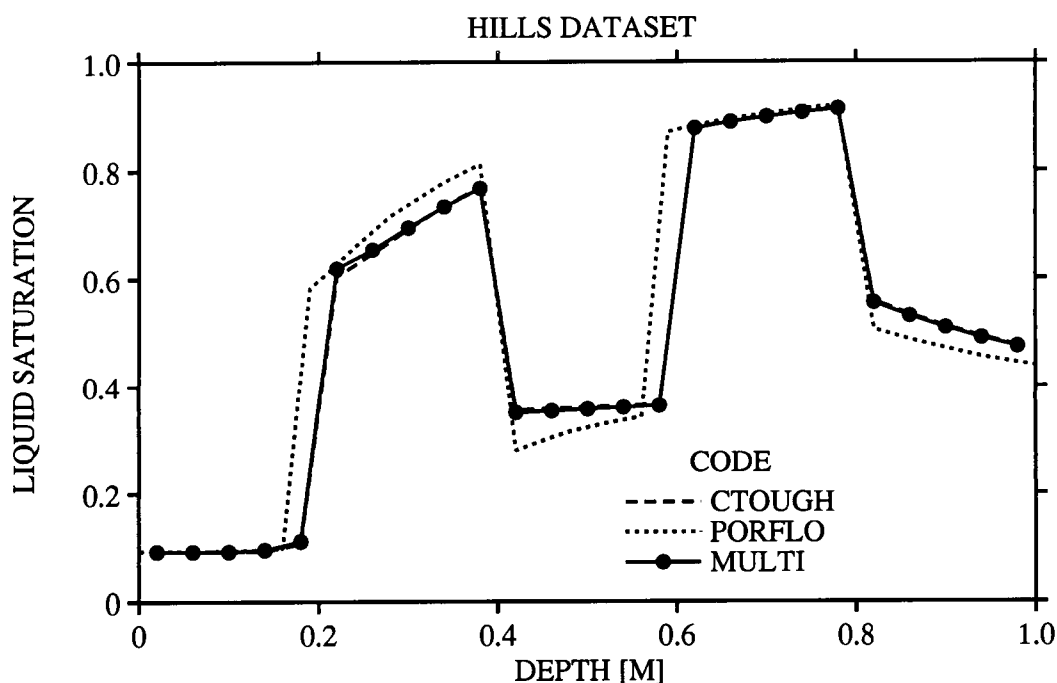


Figure 1-1: Liquid saturation for the Hills et al. problem plotted as a function of depth for an elapsed time of 4.32×10^5 seconds.

9.21.95 Comparison with CTOUGH for the HLW 1D repository-scale model with 114 kW/acre thermal loading. Runs were carried out for the 114 kW/acre thermal loading case out to 100,000 years. CTOUGH took 1101 steps and 615 cpu seconds. MULTIFLO took 270 steps and 289 seconds of cpu time.

Considering that MULTIFLO does not yet use table look up, this is already a substantial improvement of a factor 2 in cpu time.

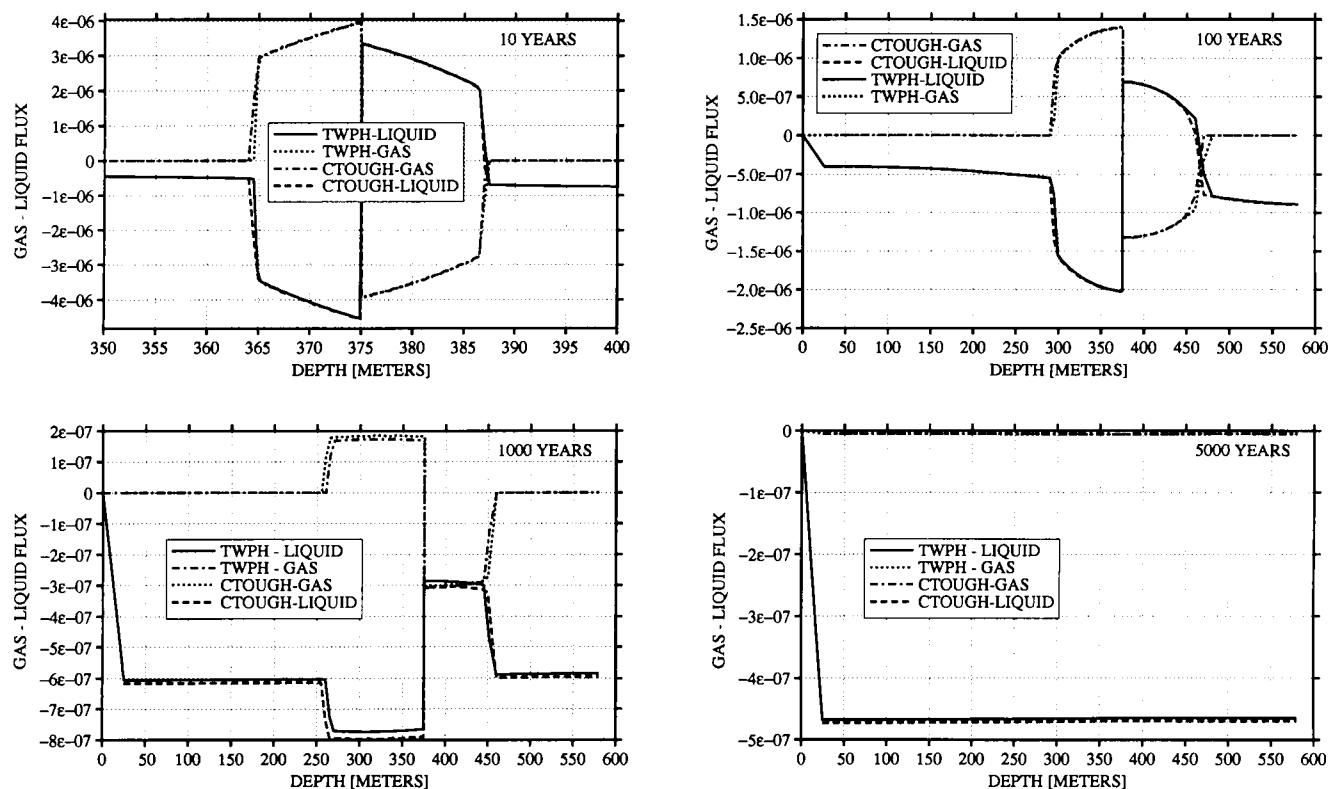


Figure 1-2: Liquid and vapor fluxes for the 1D repository-scale model with a thermal loading of 114 kW/acre plotted as a function of depth for times of 10, 100, 1,000 and 5,000 years.

10.23.95 Differential equations solved by MULTIFLO. The differential equations for water and air solved by MULTIFLO are as follows:

H₂O component:

$$\begin{aligned} \frac{\partial}{\partial t} \phi (\rho_l S_l X_w^l + \rho_g S_g X_w^g) = \nabla \cdot \frac{k k_{rl}}{\mu_l} X_w^l \rho_l \nabla (p - p_c - \gamma_w h) \\ + \nabla \cdot \frac{k k_{rg}}{\mu_g} X_w^g \rho_g \nabla (p - \rho_g g z), \end{aligned} \quad (1-1)$$

air component:

$$\begin{aligned} \frac{\partial}{\partial t} \phi (\rho_l S_l X_a^l + \rho_g S_g X_a^g) = \nabla \cdot \frac{k k_{rl}}{\mu_l} X_a^l \rho_l \nabla (p - p_c - \rho_w g z) \\ + \nabla \cdot \frac{k k_{rg}}{\mu_g} X_a^g \rho_g \nabla (p - \gamma_g h), \end{aligned} \quad (1-2)$$

energy:

$$\begin{aligned} \frac{\partial}{\partial t} \phi (\rho_l S_l U_w^l + \rho_g S_g U_w^g) + \frac{\partial}{\partial t} [(1 - \phi) C_p T] = \nabla \cdot \frac{k k_{rl}}{\mu_l} H_w^l \rho_l \nabla (p - p_c - \gamma_w h) \\ + \nabla \cdot \frac{k k_{rg}}{\mu_g} H_w^g \rho_g \nabla (p - \gamma_g h) \\ + \nabla K \nabla T + Q_{source}, \end{aligned} \quad (1-3)$$

Adding the first two equations gives the total mass balance equation for air and water as:

$$\begin{aligned} \frac{\partial}{\partial t} \phi (\rho_l S_l + \rho_g S_g) = \nabla \cdot \frac{k k_{rl}}{\mu_l} \rho_l \nabla (p - p_c - \rho_w g z) \\ + \nabla \cdot \frac{k k_{rg}}{\mu_g} \rho_g \nabla (p - \rho_g g z). \end{aligned} \quad (1-4)$$

There are three significant differences between CTOUGH and MULTIFLO. These are:

1. MULTIFLO solves Eqns.(1-2)–(1-4), whereas CTOUGH solves Eqns.(1-1)–(1-3).
2. MULTIFLO uses units of moles whereas CTOUGH uses mass units.
3. In the two-phase region CTOUGH uses p , T and S_g as primary variables, whereas MULTIFLO uses p , p_a and S_g .

The results, of course, must be identical.

8.30.95 VAPOR PRESSURE LOWERING–PARTIAL DERIVATIVES FOR

Vapor Pressure Lowering

Kelvin Equation: $p_v = p_s(T) e^{-p_c / \rho_w^o R T}$, $T = T(p_v, s_l)$

Independent Variables: p , p_a , s_l

Density of liquid water: $\rho_l(p, p_a, s_l) = \rho_w^o \{p_s[T(p - p_a, s_l)], T[p - p_a, s_l]\}$

Density of pure liquid water: $\rho_w^\circ(p_v, T)$

Partial Derivatives:

$$\frac{\partial \rho_l}{\partial p} = \frac{\partial \rho_w^\circ}{\partial p_v} \frac{dp_s}{dT} \frac{\partial T}{\partial p_v} + \frac{\partial \rho_w^\circ}{\partial T} \frac{\partial T}{\partial p_v} = \left[\frac{\partial \rho_w^\circ}{\partial p_v} \frac{dp_s}{dT} + \frac{\partial \rho_w^\circ}{\partial T} \right] \frac{\partial T}{\partial p_v}, \quad (1-5)$$

$$\frac{\partial \rho_l}{\partial p_a} = -\frac{\partial \rho_w^\circ}{\partial p_v} \frac{dp_s}{dT} \frac{\partial T}{\partial p_v} - \frac{\partial \rho_w^\circ}{\partial T} \frac{\partial T}{\partial p_v} = -\left[\frac{\partial \rho_w^\circ}{\partial p_v} \frac{dp_s}{dT} + \frac{\partial \rho_w^\circ}{\partial T} \right] \frac{\partial T}{\partial p_v} = -\frac{\partial \rho_l}{\partial p}, \quad (1-6)$$

$$\frac{\partial \rho_l}{\partial s_l} = \frac{\partial \rho_w^\circ}{\partial p_v} \frac{dp_s}{dT} \frac{\partial T}{\partial s_l} + \frac{\partial \rho_w^\circ}{\partial T} \frac{\partial T}{\partial s_l} = \left[\frac{\partial \rho_w^\circ}{\partial p_v} \frac{dp_s}{dT} + \frac{\partial \rho_w^\circ}{\partial T} \right] \frac{\partial T}{\partial s_l}. \quad (1-7)$$

Derivatives $\partial T/\partial p_v$ and $\partial T/\partial s_l$ are obtained by differentiating the Kelvin equation

$$\ln p_v = \ln p_s[T(p_v, s_l)] - \frac{p_c(s_l)}{\rho_w^\circ[p_v, T(p_v, s_l)]RT(p_v, s_l)}, \quad (1-8)$$

implicitly, to give:

$$\frac{\partial T}{\partial p_v} = \frac{\frac{1}{p_v} - \frac{p_c}{(\rho_w^\circ)^2 RT} \frac{\partial \rho_w^\circ}{\partial p}}{\frac{1}{p_s} \frac{dp_s}{dT} + \frac{p_c}{\rho_w^\circ RT^2} + \frac{p_c}{(\rho_w^\circ)^2 RT} \frac{\partial \rho_w^\circ}{\partial T}}, \quad (9a)$$

$$= \frac{\frac{\rho_w^\circ RT}{p_v} - \frac{p_c}{\rho_w^\circ} \frac{\partial \rho_w^\circ}{\partial p}}{\frac{\rho_w^\circ RT}{p_s} \frac{dp_s}{dT} + \frac{p_c}{T} + \frac{p_c}{\rho_w^\circ} \frac{\partial \rho_w^\circ}{\partial T}}, \quad (9b)$$

and

$$\frac{\partial T}{\partial s_l} = \frac{\frac{1}{\rho_w^\circ RT} \frac{dp_c}{ds_l}}{\frac{1}{p_s} \frac{dp_s}{dT} + \frac{p_c}{\rho_w^\circ RT^2} + \frac{p_c}{(\rho_w^\circ)^2 RT} \frac{\partial \rho_w^\circ}{\partial T}}, \quad (10a)$$

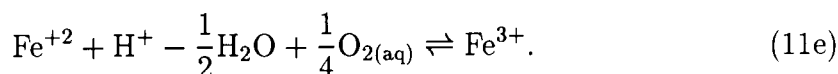
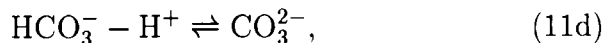
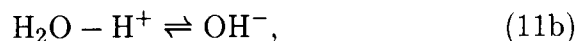
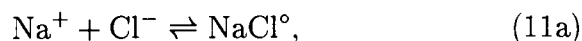
$$= \frac{\frac{dp_c}{ds_l}}{\frac{\rho_w^\circ RT}{p_s} \frac{dp_s}{dT} + \frac{p_c}{T} + \frac{p_c}{\rho_w^\circ} \frac{\partial \rho_w^\circ}{\partial T}}. \quad (10b)$$

10.1.95 Butler-Volmer Reaction Kinetics and Irreversible Homogeneous and Heterogeneous Reactions

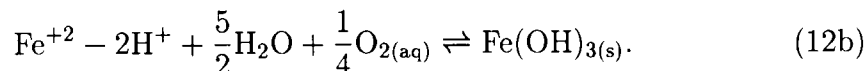
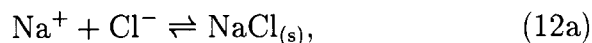
CHEMICAL REACTIONS

Example Problem

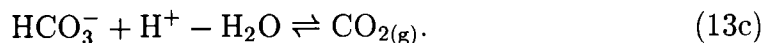
Reversible homogeneous aqueous reactions:



Irreversible heterogeneous secondary product formation reactions:



Reversible heterogeneous gaseous reactions:



Irreversible heterogeneous electrochemical reactions at metal surface:

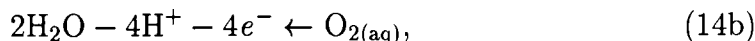


Table 1-2: Chemical Constituents

Primary species:	$\text{Na}^+, \text{Fe}^{2+}, \text{H}^+, \text{HCO}_3^-, \text{O}_{2(\text{aq})}, \text{H}_{2(\text{aq})}, \text{Cl}^-$
Secondary species:	$\text{OH}^-, \text{NaCl}^\circ, \text{CO}_{2(\text{aq})}, \text{CO}_3^{2-}, \text{Fe}^{3+}$
Solids:	$\text{Fe}, \text{NaCl}_{(\text{s})}, \text{Fe}(\text{OH})_{3(\text{s})}$
Gases:	$\text{O}_{2(\text{g})}, \text{H}_{2(\text{g})}, \text{CO}_{2(\text{g})}$

General Case

Notation: primary species: $\{\mathcal{A}_j, \mathcal{A}_r, \mathcal{A}_k^e\}$, secondary species: $\{\mathcal{A}_i\}$, solids: $\{\mathcal{M}_m^e, \mathcal{M}_m\}$, gases: $\{\mathcal{G}_l\}$.

Reversible homogeneous aqueous reactions:

$$I_i^{rev} : \sum_j \nu_{ji}^{rev} \mathcal{A}_j + \sum_k \nu_{ki}^{rev} \mathcal{A}_k^e \rightleftharpoons \mathcal{A}_i. \quad (15)$$

Reversible or irreversible heterogeneous solid reactions:

$$I_m^s : \sum_j \nu_{jm}^s \mathcal{A}_j + \sum_k \nu_{km}^s \mathcal{A}_k^e \rightleftharpoons \mathcal{M}_m. \quad (16)$$

Reversible heterogeneous gaseous reactions:

$$I_l^g : \sum_j \nu_{jl}^g \mathcal{A}_j + \sum_k \nu_{kl}^g \mathcal{A}_k^e \rightleftharpoons \mathcal{G}_l. \quad (17)$$

Irreversible homogeneous aqueous reactions:

$$I_r^{irr} : \sum_j \nu_{jr}^{irr} \mathcal{A}_j + \sum_k \nu_{kr}^{irr} \mathcal{A}_k^e \rightleftharpoons \mathcal{A}_r. \quad (18)$$

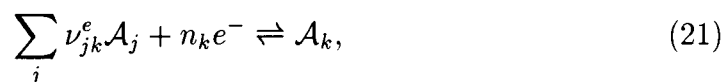
Irreversible heterogeneous half-cell electrochemical reactions:

$$I_k^e : \sum_j \nu_{jk}^e \mathcal{A}_j + n_k e_{(\text{s})}^- \rightleftharpoons \mathcal{A}_k^e, \quad (19)$$

$$I_m^e : \sum_j \nu_{jm}^e \mathcal{A}_j + n_m e_{(\text{s})}^- \rightleftharpoons \mathcal{M}_m^e. \quad (20)$$

Electrochemical Reactions

In electrochemical reactions half-cell reactions involving the electron e^- may take place at spatially distinct sites or they may be balanced locally. In the former case an electric current is produced in the aqueous solution involving the transfer of ionic species to counter the flow of electrons in the solid. A set of simultaneous electrochemical reactions may be expressed generally as



for some species \mathcal{A}_k which may be a solid or aqueous species. The number of electrons n_k participating in the k th electrochemical reaction is related to the valences of the primary species by charge balance

$$z_k = \sum_j z_j \nu_{jk}^e - n_k, \quad (22)$$

or

$$n_k = \sum_j z_j \nu_{jk}^e - z_k. \quad (23)$$

The mass action equation corresponding to reaction (21) is given by

$$\ln K_k = \ln a_k - n_k \ln a_{e^-} - \sum_j \nu_{jk}^e \ln a_j, \quad (24)$$

where K_k denotes the equilibrium constant. Assuming reaction (21) represents an elementary reaction, its rate is equal to

$$I_k^e = k_f \prod_j a_j^{\nu_{jk}^e} e^{\frac{\alpha_k n_k F}{RT} \Phi} - k_b a_k e^{-\frac{(1 - \alpha_k) n_k F}{RT} \Phi}, \quad (25)$$

where k_f and k_b denote the forward and backward rate constants, respectively, Φ represents the electric potential, and α_k refers to the symmetry factor. At equilibrium the rate must vanish leading to the following relation between the equilibrium constant and the rate constants

$$K_k = \frac{k_f}{k_b} = a_k \prod_j a_j^{-\nu_{jk}^e} e^{-\frac{n_k F}{RT} \Phi_k^\circ}. \quad (26)$$

From this expression a relation between the hypothetical electron activity a_{e^-} and the equilibrium potential Φ_k° follows

$$\begin{aligned}\Phi_k^\circ &= \frac{RT}{F} \ln a_{e^-}, \\ &= -\frac{RT}{n_k F} \left\{ \ln K_k - \ln a_k + \sum \nu_{jk}^e \ln a_j \right\},\end{aligned}\quad (27)$$

referred to as the Nernst equation. The rate of reaction Eqn.(21) can be written in the form of the Butler-Volmer equation given by

$$I_k^e = \frac{1}{n_k F} i_k^\circ \left\{ \exp \left[\frac{F}{RT} \alpha_k n_k \eta_k \right] - \exp \left[-\frac{F}{RT} (1 - \alpha_k) n_k \eta_k \right] \right\}, \quad (28)$$

where i_k° denotes the equilibrium exchange current density defined by

$$\begin{aligned}i_k^\circ &= k_f \prod_j a_j^{\nu_{jk}^e} e^{-\frac{\alpha_k n_k F}{RT} \Phi_k^\circ} \\ &= k_b a_k e^{-\frac{(1 - \alpha_k) n_k F}{RT} \Phi_k^\circ}.\end{aligned}\quad (29)$$

The first term in the rate expression represents the anodic and the second term the cathodic current density. The potential η_k refers to the overpotential defined as the difference between the actual potential and the equilibrium potential defined by

$$\eta_k = \Phi - \Phi_k^\circ. \quad (30)$$

For the case when the Butler-Volmer rate law predicts very large rates, the actual rate becomes transport limited determined by transport of solute and gaseous species to or from the reacting surface.

Transport Equations

Aqueous Species:

$$\mathcal{LC}_j = -\sum_k \nu_{jk}^e I_k^e - \sum_m \nu_{jm}^e I_m^e - \sum_m \nu_{jm}^s I_m^s - \sum_r \nu_{jr}^{irr} I_r^{irr} - \sum_i \nu_{ji}^{rev} I_i^{rev}, \quad (31)$$

$$\mathcal{LC}_k = I_k^e - \sum_m \nu_{km}^s I_m^s - \sum_r \nu_{kr}^{irr} I_r^{irr} - \sum_i \nu_{ki}^{rev} I_i^{rev}, \quad (32)$$

$$\mathcal{LC}_i = I_i^{rev}. \quad (33)$$

Here \mathcal{L} denotes the differential operator

$$\mathcal{L} = \frac{\partial}{\partial t} + \nabla \cdot \mathbf{v} - \nabla \cdot \phi D \nabla. \quad (34)$$

Solids:

$$\frac{\partial \phi_m^e}{\partial t} = \bar{V}_m^e I_m^e, \quad (35)$$

$$\frac{\partial \phi_m}{\partial t} = \bar{V}_m I_m^s. \quad (36)$$

Eliminating the reversible rates I_i^{rev} and I_i^{ad} yields the following modified form of the primary species transport equations

$$\begin{aligned} \frac{\partial}{\partial t} \left(\phi \Psi_j + \sum_l \bar{C}_l \right) + \nabla \cdot \Omega_j = & - \sum_k \nu_{jk}^e I_k^e - \sum_m \nu_{jm}^e I_m^e \\ & - \sum_m \nu_{jm}^s I_m^s - \sum_r \nu_{jr}^{irr} I_r^{irr}, \end{aligned} \quad (37)$$

$$\frac{\partial}{\partial t} \left(\phi \Psi_k + \sum_l \bar{C}_l \right) + \nabla \cdot \Omega_k = I_k^e - \sum_m \nu_{km}^s I_m^s - \sum_r \nu_{kr}^{irr} I_r^{irr}, \quad (38)$$

where the generalized concentration Ψ_j and flux Ω_j are defined by

$$\Psi_j = C_j + \sum_i \nu_{ji} C_i, \quad (39)$$

and

$$\Omega_j = J_j + \sum_i \nu_{ji} J_i. \quad (40)$$

The flux \mathbf{J}_i , in general, consists of contributions from advective, diffusive and dispersive transport in addition to an electrochemical migration term. Ignoring dispersion, the flux has the form

$$\mathbf{J}_i = -\tau \phi z_i \frac{D_i C_i}{RT} F \nabla \Phi - \tau \phi D_i (\nabla C_i + C_i \nabla \ln \gamma_i) + \mathbf{q} C_i, \quad (41)$$

where the first term refers to electrochemical migration, the second term to aqueous diffusion, and the last term to advective transport. Here z_i , γ_i and D_i denote the valence, activity coefficient and diffusivity of the i th species, respectively. The quantity Φ represents the electrical potential, F denotes the Faraday constant, τ refers to the tortuosity of the porous medium, and \mathbf{q} denotes

the Darcy fluid velocity. The quantities Ψ_j and Ω_j may be interpreted, generally, as the total concentration and flux of the j th primary species (Lichtner, 1985).

In the presence of electrochemical reactions and with species-dependent diffusion coefficients and activity coefficient corrections, the expression for the generalized flux becomes

$$\Omega_j = -\tau\phi\Psi_j^\epsilon F \frac{\nabla\Phi}{RT} - \tau\phi(\Gamma_j^D + \Gamma_j^\gamma) + \mathbf{q}\Psi_j, \quad (42)$$

obtained by inserting the expression for the flux defined in Eqn.(41) into equation Eqn.(40), where

$$\Psi_j^\epsilon = z_j D_j C_j + \sum_i \nu_{ji} z_i D_i C_i, \quad (43)$$

$$\Gamma_j^D = D_j \nabla C_j + \sum_i \nu_{ji} D_i \nabla C_i, \quad (44)$$

and activity coefficient corrections are accounted for by the term containing Γ_j^γ defined by

$$\Gamma_j^\gamma = D_j C_j \nabla \ln \gamma_j + \sum_i \nu_{ji} D_i C_i \nabla \ln \gamma_i. \quad (45)$$

In the absence of electrochemical effects, assuming that the diffusion coefficients are the same for all species, and neglecting activity coefficient corrections, the generalized flux Ω_j reduces to the expression

$$\Omega_j = (-\tau\phi D \nabla + \mathbf{q}) \Psi_j. \quad (46)$$

In this equation the flux is expressed directly in terms of the generalized concentration Ψ_j . However, in the general case this simplification is not possible.

Charge Conservation

Multiplying the transport equations by the valence of each species and summing over all species yields the result

$$\frac{\partial}{\partial t} \left(\phi \sum_j z_j \Psi_j \right) + \nabla \cdot \sum_j z_j \Omega_j = \sum_k z_k I_k^e - \sum_j z_j \nu_{jk}^e I_k^e. \quad (47)$$

Multiplying through by the Faraday constant, this equation can be expressed as

$$\frac{\partial}{\partial t} (\phi \mathcal{Q}) + \nabla \cdot \mathbf{i} = j_e, \quad (48)$$

where

$$\mathcal{Q} = F \sum z_j \Psi_j, \quad (49)$$

denotes the total charge in solution at a given point and time. The ionic solution current density \mathbf{i} is defined by

$$\mathbf{i} = F \sum_j z_j \Omega_j, \quad (50)$$

and j_e represents the total volume averaged electrochemical current density at the solution-metal interface defined by

$$j_e = F \left[\sum_k z_k I_k^e - \sum_{jk} z_j (\nu_{jk}^e I_k^e + \nu_{jm}^e I_m^e) \right] = -F \left[\sum_k n_k I_k^e + \sum_m n_m I_m^e \right]. \quad (51)$$

The latter equality is obtained by charge balance of the half-reaction Eqn.(21) with z_j and n_k related by the Eqn.(23). For electroneutrality to hold, \mathcal{Q} must vanish requiring that

$$\nabla \cdot \mathbf{i} = j_e. \quad (52)$$

Conversely if Eqn.(52) holds, then electroneutrality in the aqueous solution is maintained.

In the general case of electrochemical reactions, an electric current consisting of ionic species is produced in the aqueous solution to balance the electron current in the solid phase. The total electrochemical current density is proportional to the sum over the individual electrochemical reactions multiplied by the number of electrons involved in each reaction. If the half-cell reactions are balanced locally, the electrochemical reaction rates must satisfy the condition $j_e = 0$, and as a consequence

$$\nabla \cdot \mathbf{i} = 0, \quad (53)$$

from which it follows that $\mathbf{i} = 0$ (*prove!*). In many cases of interest, however, electrons are transported away from the site of reaction through the solid. In this situation half-cell reactions are not balanced locally, and an electric current becomes established in the aqueous solution.

Solution Current Density and the Electric Potential

Eliminating the electric potential from the expression for the solute flux yields the expression:

$$\Omega_j = \frac{1}{F}\omega_j \mathbf{i} - \tau\phi \sum_l \beta_{jl} (\Gamma_l^D + \Gamma_l^\gamma) + \mathbf{q}\Psi_j, \quad (54)$$

where the matrix β_{jl} , a projection operator, is defined by

$$\beta_{jl} = \delta_{jl} - z_l \omega_j, \quad (55)$$

with

$$\omega_j = \frac{\Psi_j^\epsilon}{\sum_l z_l \Psi_l^\epsilon}. \quad (56)$$

This result is obtained by noting that the gradient in the electric potential Φ , equal to the negative of the electric field \mathcal{E} , can be expressed as

$$\mathcal{E} = -\nabla\Phi = \frac{1}{\kappa} \left\{ \mathbf{i} + \tau\phi F \sum_j z_j (\Gamma_j^D + \Gamma_j^\gamma) \right\}, \quad (57)$$

where the quantity κ , defined by the expression

$$\kappa = \frac{\tau\phi F^2}{RT} \sum_j z_j \Psi_j^\epsilon, \quad (58)$$

is referred to as the generalized Debye length. In the form of the flux given by Eqn.(54) the electric current appears rather than the electric potential. In contrast to the expression for the flux with species-independent diffusion coefficients, coupling terms occur between the concentration gradients of the different primary species required to maintain electrical balance of the aqueous solution.

An alternative expression for the generalized flux may be obtained by introducing the flux Ω_j^0 defined by

$$\Omega_j^0 = -\tau\phi (\Gamma_j^D + \Gamma_j^\gamma) + q\Psi_j. \quad (59)$$

The electric current density \mathbf{i}_0 associated with the flux Ω_j^0 is equal to

$$\mathbf{i}_0 = F \sum_j z_j \Omega_j^0. \quad (60)$$

The total flux can be written alternatively as

$$\begin{aligned}
 \Omega_j &= \sum_l \beta_{lj} \Omega_j^0 + \frac{\omega_j}{F} \mathbf{i}, \\
 &= \Omega_j^0 - \omega_j \sum_l z_l \Omega_l^0 + \frac{\omega_j}{F} \mathbf{i}, \\
 &= \Omega_j^0 + \frac{\omega_j}{F} (\mathbf{i} - \mathbf{i}_0).
 \end{aligned} \tag{61}$$

The electric field is related to the current density by the expression

$$\mathcal{E} = -\nabla\Phi = \frac{F}{\kappa} \frac{\Omega_j - \Omega_j^0}{\omega_j} = \frac{\mathbf{i} - \mathbf{i}_0}{\kappa}. \tag{62}$$

It follows that the current can be expressed as a modified form of Ohm's law

$$\mathbf{i} = -\kappa \nabla\Phi + \mathbf{i}_0. \tag{63}$$

FINITE DIFFERENCE EQUATION

In order to solve the electrochemical transport equations numerically an iterative procedure must be used. The current density \mathbf{i} depends on the concentration of the primary species as well as the potential Φ through the Butler-Volmer rate law. Therefore it is necessary to solve Eqns.(52) and (62) simultaneously for given concentrations of the primary species. In this way charge balance is maintained in the aqueous solution.

The residual function is defined by

$$\begin{aligned}
 R_{jn} &= \phi_n \Delta \Psi_{jn} V_n + \Delta t \{ \Omega_{j,n+1} A_{n+1} - \Omega_{jn} A_n \} \\
 &\quad + \Delta t V_n \left\{ \sum \nu_{jk}^e I_{kn}^e + \sum \nu_{jm}^e I_{mn}^e + \sum \nu_{jm}^s I_{mn}^s \right\}.
 \end{aligned} \tag{64}$$

Substituting the expression for the flux

$$\Omega_{jn} = \Omega_{jn}^0 + \frac{\omega_{jn}}{F} (i_n - i_{0n}), \tag{65}$$

and collecting terms yields

$$\begin{aligned}
 R_{jn} &= \phi_n \Delta \Psi_{jn} V_n + \Delta t \{ \Omega_{j,n+1}^0 A_{n+1} - \Omega_{jn}^0 A_n \} \\
 &\quad + \frac{\Delta t}{F} \{ \omega_{j,n+1} (i_{n+1} - i_{0n+1}) A_{n+1} - \omega_{jn} (i_n - i_{0n}) A_n \} \\
 &\quad + \Delta t V_n \left\{ \sum \nu_{jk}^e I_{kn}^e + \sum \nu_{jm}^e I_{mn}^e + \sum \nu_{jm}^s I_{mn}^s \right\}.
 \end{aligned} \tag{66}$$

Multiplying by the charge z_j and summing over all primary species yields

$$\sum z_j R_{jn} = \phi_n V_n \sum z_j \Delta \Psi_{jn} + \frac{\Delta t}{F} \{i_{n+1} A_{n+1} - i_n A_n + j_{en} V_n\}, \quad (67)$$

where

$$\begin{aligned} j_{en} &= F \left(\sum z_j \nu_{jk}^e I_{kn}^e + \sum z_j \nu_{jm}^e I_{mn}^e \right), \\ &= F \left(\sum n_k I_{kn}^e + \sum n_m I_{mn}^e \right). \end{aligned} \quad (68)$$

Charge conservation is ensured by noting that if the current satisfies the finite difference equation

$$i_{n+1} = i_n \frac{A_n}{A_{n+1}} - j_{en} \frac{V_n}{A_{n+1}}, \quad (69)$$

then it follows that

$$\sum z_j \Delta \Psi_{jn} = 0, \quad (70)$$

and therefore if the aqueous solution is initially electrically neutral it must remain so with time.

CODE MODIFICATION

Storage of Variables

primary species
nprim
ncorraq
ncxkin

minerals	
electrochemical	1 ⋮ <i>ncorr</i>
chemical	<i>ncorr</i> + 1 ⋮ <i>nkin</i>

P. C. Lichtner

SCIENTIFIC NOTEBOOK

INITIALS:

PC

aqueous species	
chemical	1 \vdots n_{prim}
electrochemical	$n_{prim} + 1$ \vdots $n_{prim} + n_{corraq}$

2. Sub-Regional Hydrology Processes: Site-Scale Flow & Transport Modeling

Account Number: **20-5704-176**

Collaborators: Ross Bagtzoglou

Objective: The purpose of this work is to modify the code GEM to include partially saturated porous media and sorption processes.

Date **Entry**

4.15.95 **K_D 's: WHAT DO THEY MEAN AND WHEN CAN WE USE THEM?**
Notes on Retardation and Reactive Transport

ABSTRACT

The question of the use of K_D 's is analyzed from the point of view of reactive mass transport. Specifically the question of when a constant retardation factor can be used in modeling is discussed. The question of charge balance is discussed in regard to surface complexation models.

INTRODUCTION

Several difficulties arise when combining batch calculations of distribution coefficients with reactive transport. The batch value corresponds to the local value within a REV. It may or may not be constant.

CONCENTRATION VARIABLES

Concentration variables are defined for a single REV. Each REV is characterized by the pore volume V_p and solid volume V_s with

$$V = V_p + V_s. \quad (2-71)$$

In addition mole numbers for the j th aqueous and adsorbed species, n_j , \bar{n}_j , respectively, define the composition of the aqueous and solid phases. In terms of these quantities the following quantities can be defined:

$$\text{aqueous concentration: } C_j = \frac{n_j}{V_p}, \quad (2-72)$$

$$\text{sorbed concentration: } \bar{C}_j = \frac{\bar{n}_j}{V}, \quad (2-73)$$

$$\text{distribution coefficient: } K_j^D = \frac{\bar{n}_j}{n_j} = \frac{\bar{n}_j}{V} \cdot \frac{V}{V_p} \cdot \frac{V_p}{C_j} = \frac{\bar{C}_j}{\phi C_j}, \quad (2-74)$$

$$\text{cation exchange capacity: } Q_{ex} = \frac{\bar{n}_{ex}}{m_{\text{solid}}} = \frac{\bar{n}_{eq}}{V} \cdot \frac{V}{V_s} \cdot \frac{V_s}{m_{\text{solid}}} = \frac{\bar{\omega}}{\rho_s(1-\phi)}, \quad (2-75)$$

$$\text{bulk density: } \rho_{\text{bulk}} = \frac{m_s}{V} = \frac{m_s}{V_{\text{solid}}} \cdot \frac{V_{\text{solid}}}{V} = \rho_s(1-\phi), \quad (2-76)$$

where the total number of moles of sorbed sites equal to

$$\bar{n}_{ex} = \sum_j z_j \bar{n}_j, \quad (2-77)$$

$$\bar{\omega} = (1-\phi)\rho_s Q_{ex}, \quad (2-78)$$

and

$$\rho_{\text{bulk}} = (1-\phi)\rho_s. \quad (2-79)$$

MONO VALENT EXCHANGE

$$\bar{\mathcal{A}}_i + \mathcal{A}_j \rightleftharpoons \mathcal{A}_i + \bar{\mathcal{A}}_j : I_{ji} \quad (2-80)$$

$$K_{ij} = \frac{C_i}{\bar{C}_i} \cdot \frac{\bar{C}_j}{C_j}. \quad (2-81)$$

$$K_{ij} = \frac{k_j}{k_i}. \quad (2-82)$$

$$\bar{C}_j = \frac{k_j C_j}{k_i C_i} \bar{C}_i. \quad (2-83)$$

$$\sum_j \bar{C}_j = \bar{\omega}. \quad (2-84)$$

$$\bar{C}_j = \frac{\bar{\omega} k_j C_j}{\sum_i k_i C_i}. \quad (2-85)$$

$$K_j^D = \frac{\bar{C}_j}{\phi C_i} = \frac{\bar{\omega} k_j}{\sum_i k_i C_i}. \quad (2-86)$$

MASS TRANSPORT EQUATIONS

$$\frac{\partial}{\partial t} \phi C_j + \frac{\partial J_j}{\partial x} = - \sum_{i \neq j} I_{ji}, \quad (2-87)$$

$$\frac{\partial \bar{C}_j}{\partial t} = \sum_{i \neq j} I_{ji}. \quad (2-88)$$

Alternatively

$$\frac{\partial}{\partial t} [\phi C_j + \bar{C}_j] + \frac{\partial J_j}{\partial x} = 0. \quad (2-89)$$

$$\frac{\partial}{\partial t} [\phi (1 + K_j^D) C_j] + \frac{\partial J_j}{\partial x} = 0. \quad (2-90)$$

$$\frac{\partial}{\partial t} [\phi R_j C_j] + \frac{\partial J_j}{\partial x} = 0, \quad (2-91)$$

where the retardation factor R_j is defined by

$$R_j = 1 + K_j^D. \quad (2-92)$$

An alternative definition of the distribution coefficient is

$$\tilde{K}_j^D = \frac{\bar{n}_j / m_s}{n_j / V_p} = \frac{V_p}{V} \cdot \frac{V}{m_s} \cdot \frac{\bar{n}_j}{n_j} = \frac{\phi}{\rho_{\text{bulk}}} K_j^D. \quad (2-93)$$

With this definition the retardation factor becomes

$$R_j = 1 + \frac{\rho_{\text{bulk}}}{\phi} \tilde{K}_j^D. \quad (2-94)$$

The transport equation may be rewritten in the form

$$\frac{\partial}{\partial t} [\phi C_j] + \frac{\partial J_j^R}{\partial x} + \phi C_j \frac{\partial \ln R_j}{\partial t} + \frac{J_j}{R_j} \frac{\partial \ln R_j}{\partial x} = 0, \quad (2-95)$$

where J_j^R refers to the retarded flux defined as

$$J_j^R = \frac{J_j}{R_j} = -\phi \frac{D}{R_j} \frac{\partial C}{\partial x} + \frac{v}{R_j} C_j. \quad (2-96)$$

5.11.95 Alteration of MINTEQ to printout Kd 's directly.

MINTEQ was altered to directly printout Kd 's, both in dimensionless form and in the standard units of mL/g. The results for uranium sorption on goethite is shown below in Figure 2-3. The calculations were compared with and without carbonate species present.

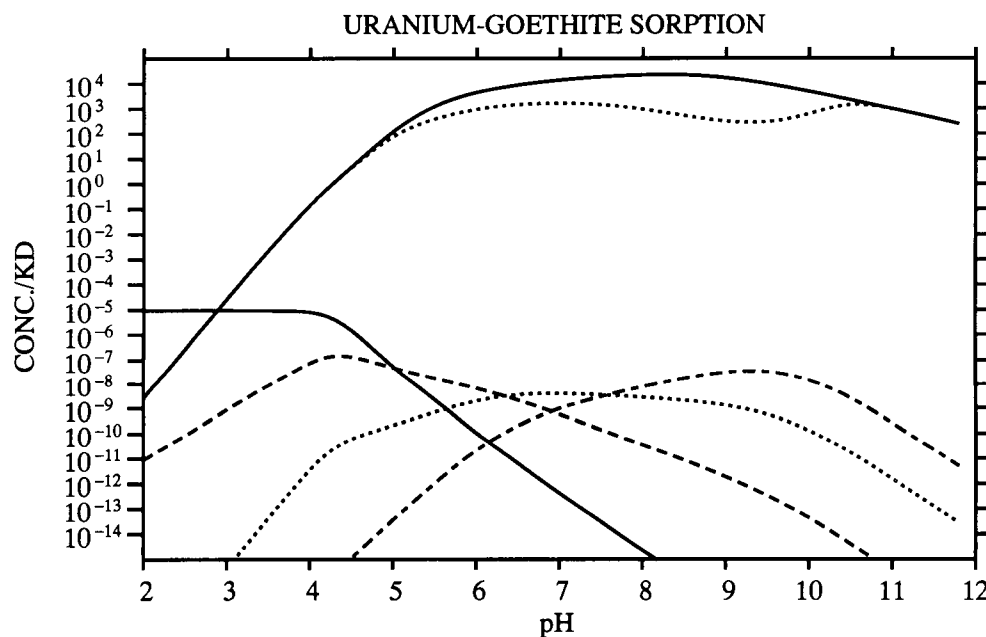


Figure 2-3: Sorption of uranium on goethite.

The upper solid curve corresponds to the retardation without carbonate species present and the upper dashed curve with carbonate species. The lower curves correspond to the concentrations of various uranium-bearing carbonate species.

The input file used in the calculation is listed below which includes carbonate species.

```

U(VI)-Goethite Sorption; Hsi and Langmuir (1985); No CO2; U(VI)=1E-5
DLM; XDUO2(OH)2-; 12/17/92 CNWRA database
25.00 molal 0.000 0.00000e-01
0 0 1 0 0 0 0 0 1 1 1 5 3
activity 330 99
0.1
hsiugood.xyp      893 8931400 8931401 8931402 8931404
4 1 7
1.000E+00 50.00 0.000 0.000 81
330 0.000E-03 -2.00 y /H+1
813 0.000E-01 0.00 y /ADS1PSIo
811 1.918E-04 -3.72 y /ADS1TYP1
140 1.000E-03 -3.72 y /CO3-2
893 1.000E-05 -5.00 y /UO2+2
500 1.000E-01 -1.00 y /Na+1
492 1.000E-01 -1.00 y /NO3-1

3 1
330 2.0000 0.0000 /H+1
6 1
813 0.0000 0.0000 /ADS1PSIo

2 3
8113300 XD- 0.0000 -9.1700 0.000 0.000 0.00 0.00 0.00 0.0000
0.00 3 1.000 811 -1.000 330 -1.000 813 0.000 0 0.000 0 0.000 0
0.000 0 0.000 0 0.000 0 0.000 0 0.000 0 0.000 0
0 0.000 0 0.000 0 0.000 0
8113301 XOH2+ 0.0000 7.3500 0.000 0.000 0.00 0.00 0.00 0.0000
0.00 3 1.000 811 1.000 330 1.000 813 0.000 0 0.000 0 0.000 0
0.000 0 0.000 0 0.000 0 0.000 0 0.000 0 0.000 0
0 0.000 0 0.000 0 0.000 0
8118930 XDUO2(OH)2- 0.0000 -10.1900 0.000 0.000 0.00 0.00 0.00 0.0000
0.00 5 1.000 811 1.000 893 2.000 2 -3.000 330 -1.000 813 0.000 0
0.000 0 0.000 0 0.000 0 0.000 0 0.000 0 0.000 0
0 0.000 0 0.000 0 0.000 0

```

7.8.95

COMBINING SURFACE COMPLEXATION MODELS WITH MASS TRANSPORT

INTRODUCTION

Of fundamental concern to evaluating the suitability of Yucca Mountain, Nevada, as a potential repository for high-level nuclear waste (HLW) is the possibility of release of radionuclides from the waste package and their migration to the accessible environment as dissolved constituents in groundwater. One important

mechanism for retarding radionuclide migration is sorption on mineral surfaces. This contribution discusses some of the complications that result from combining sorption reactions with a time-space description of solute transport by advection, diffusion and dispersion coupled to homogeneous aqueous reactions and heterogeneous mineral precipitation/dissolution reactions.

Several sorption models are currently in use including ion-exchange and surface complexation models. Surface complexation models have been used to model sorption of metal ions and ligands over a wide range of chemical conditions. The more sophisticated formulations of surface complexation models provide for incorporation of the electric double layer. These models are based on the hypothesized formation of surface complexes at the mineral-solution interface analogous to the formation of aqueous complexes. Because of the difficulty in identifying species complexes on mineral surfaces, surface complexes generally serve more as fit parameters than as actual physical species.

A fundamental difficulty which arises when combining surface complexation models with mass transport is maintaining electric neutrality in the aqueous solution. Although in a closed static system electroneutrality is maintained, in an open system involving diffusive and advective transport an aqueous solution that is initially electrically neutral may not remain so as the system evolves in time. This effect of charge imbalance does not occur with ion-exchange models because for each ion sorbed, an equal amount of charge is desorbed and released into solution. Hence the aqueous solution always remains electrically neutral. This need not be the case, however, with surface complexation models. The cause of charge imbalance in these models results from the variable number of occupied surface sites which in general changes with time and distance.

APPLICATION OF SURFACE COMPLEXATION MODELS TO SORPTION OF NP^{5+} AND U^{6+}

The geochemical speciation code MINTEQA2 (Allison et al., 1991) has been developed to implement several different types of surface complexation models. Based on the assumed analogy between reactions at the mineral-water interface and aqueous complexation reactions in the bulk solution, MINTEQA2 uses mass action and mass balance constraints to calculate the distribution of a given con-

taminant between the sorbed and aqueous phases. For the purposes of HLW disposal, the MINTEQA2 thermodynamic database has been modified at CNWRA to include equilibrium constants for actinides and other radionuclides (Turner, 1993). Surface complexation model parameters, determined based on batch sorption experimental data, are also available for a number of radionuclide-mineral systems (Turner, 1995). Output format from MINTEQA2 was modified slightly to directly compute and print sorption in terms of the linear sorption coefficient (K_d in mL/g) that is commonly used in performance assessment transport calculations.

MINTEQA2 was used to calculate sorption of U^{6+} and Np^{5+} on goethite in a batch system over a range in pH. The Diffuse-Layer surface complexation model was used (Allison et al., 1991), and the assumed surface reactions and their binding constants are given in Table 1. Other model conditions are given in Table 2. In this preliminary analysis, the complete groundwater chemistry at Yucca Mountain is not considered, but a relatively dilute system has been assumed, similar to the ionic strength of water from well J-13. The results for the batch distribution coefficients for uranium and neptunium are shown in Figure 1 plotted as a function of pH ranging from 2 to 12. For both actinide-goethite systems, sorption is strongly affected by pH, increasing with increasing pH to a maximum, and then declining slightly at higher pH. For the U^{6+} -goethite system, the sorption maximum is reached at pH 6 to 7, while the calculated sorption maximum for Np^{5+} -goethite is at a higher pH (9 to 10). Over most of the pH range considered, sorption on goethite is typically several orders of magnitude greater for U^{6+} as compared to Np^{5+} . Calculated U^{6+} -goethite sorption is also more strongly affected by pH, with K_d increasing by about 9 orders of magnitude from pH 2 to 7, as compared to a 5 order of magnitude increase in the K_d for Np^{5+} -goethite.

Table 2-3: Surface complexation reactions for sorption of uranium and neptunium on goethite.

reaction			Log K
$>FeOH + H^+$	\rightleftharpoons	$>FeOH_2^+$	9.17
$>FeOH - H^+$	\rightleftharpoons	$>FeO^-$	-7.35
$>FeOH + UO_2^{2+} + 2H_2O - 3H^+$	\rightleftharpoons	$>FeOUO_2(OH)_2^-$	10.19
$>FeOH + NpO_2$	\rightleftharpoons	$>FeOHNpO_2^+$	5.21

Table 2-4: Model Conditions

solid concentration	1 g/L
site density	2.31 sites/nm ²
surface area	50 m ² /g
total site concentration	1.918×10^{-4} moles sites/L
ionic strength	0.001 M NaCl
total U ⁶⁺ , Np ⁵⁺	10 ⁻⁷ M
pH	2–12

The introduction of carbon into a batch system has been shown by experiment to reduce actinide sorption at higher pH (e.g., Hsi and Langmuir, 1985). The current modeling also predicts reduced actinide sorption in the presence of carbonate. The conceptual model used here does not invoke the formation of any actinide-carbonate surface complexes (Table 1), and relies on the formation of aqueous actinide complexes with carbonate over much of the pH range considered to effectively compete with the mineral surface. For the U⁶⁺–goethite system, the formation of strong uranyl-carbonate complexes (Figure 2a) reduces the predicted K_d by about an order of magnitude over much of the pH range (about 4 to 10). As the uranyl carbonate species decrease at higher pH (>10.5) relative to the more hydrolyzed uranyl species UO₂(OH)₃ and UO₂(OH)₄²⁻, the predicted sorption for carbon-free and carbonate systems converge. Calculated sorption for Np⁵⁺–goethite is also reduced in the presence of carbon, but by much less than for the U⁶⁺–goethite system. This is due to the lack of a strong Np⁵⁺–carbonate complex (Figure 2b). For example, the concentration of NpO₂CO₃ does not become significant until a relatively high pH, and only becomes a dominant aqueous species over a relatively narrow pH range (9 to 10). As can be seen from the figures the K_d predicted from the surface complexation model is highly dependent on the solution composition.

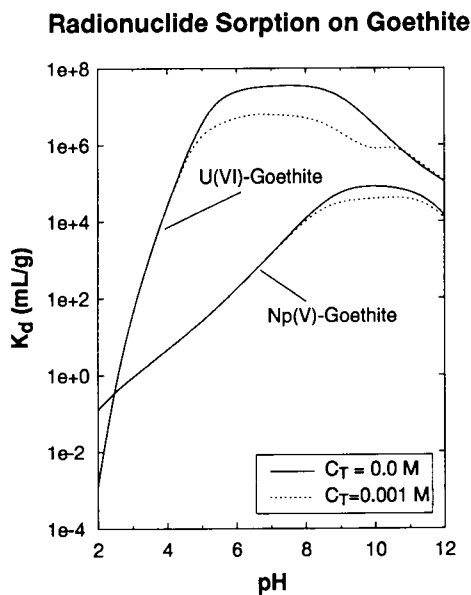


Figure 2-4: Logarithm of the distribution coefficient for sorption of uranium and neptunium on goethite plotted as a function of pH with (dashed curve) and without (solid curve) CO_2 present.

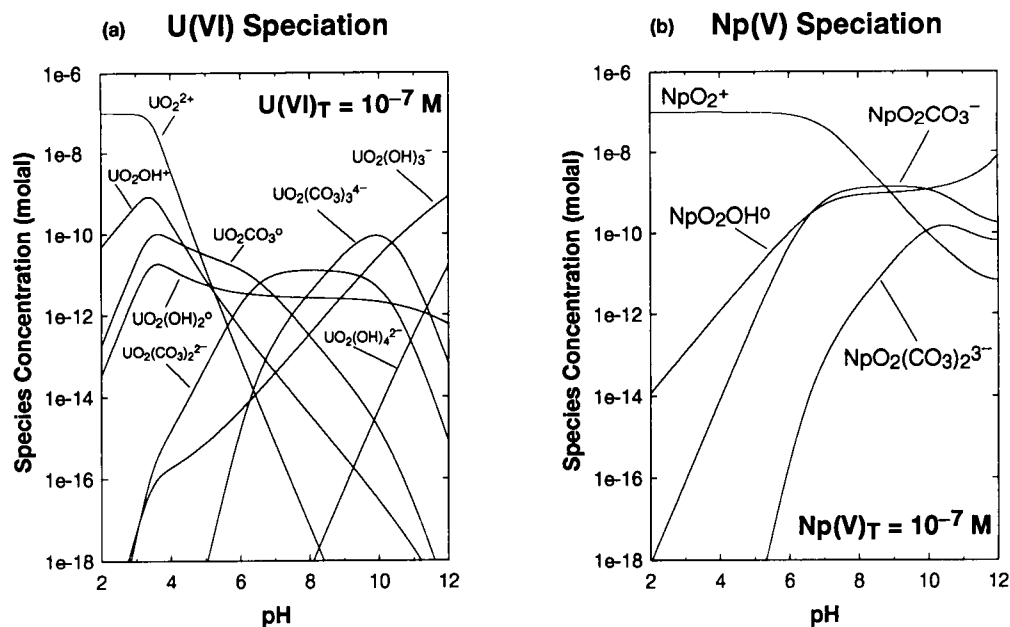


Figure 2-5: Logarithm of the concentration of selected (a) uranium- and (b) neptunium-bearing species plotted as a function of pH.

COMBINING SORPTION REACTIONS WITH MASS TRANSPORT

Incorporating sorption reactions in mass transport equations leads to the spatial separation of different solute species resulting from their relative affinity to the sorbate known as chromatography. Sorption fronts may be self-sharpening or self-broadening depending on the shape of the sorption isotherm. An added complication is caused by the changing number and types of surface sites as minerals dissolve and precipitate. Surface site concentrations are inextricably tied to mineral abundances. An intrinsic surface area, usually expressed in $\text{m}^2 \text{g}^{-1}$ or $\text{m}^2 \text{mol}^{-1}$, can be associated with each mineral. The surface contains a known site density expressed as moles of sites per meter squared. Then knowing the concentration of each mineral the site concentration can be computed. Multisite surface complexation reactions may be formulated as follows

$$\bar{\chi}_m + \sum_{j=1}^N \bar{\nu}_{ji}^m A_j \rightleftharpoons \bar{A}_i^m, \quad (2-97)$$

where $\bar{\chi}_m$ denotes the neutral surface site associated with the m th mineral, $\bar{\nu}_{ji}^m$ refers to the stoichiometric coefficients, and \bar{A}_i^m the i th adsorbed surface species on the m th mineral site. In what follows an overscore is used to designate quantities referred to the mineral surface. Examples of these reactions are presented in Table 2-3 for sorption of uranium and neptunium on goethite with \bar{A}_i^m identified with $\text{>FeOUO}_2(\text{OH})_2^-$ and $\text{>FeOUO}_2(\text{OH})_2^-$, and $\bar{\chi}_m$ with >FeOH .

The number of surface sites corresponding to the m th mineral is given by the equation

$$\bar{C}_s^m = \bar{C}_{\bar{\chi}_m} + \sum_i \bar{C}_i^m. \quad (2-98)$$

The total number of available surface sites is related to intrinsic properties of the particular mineral and proportional to the amount of mineral present. By considering a representative elemental volume (REV) containing n_m moles of the m th mineral with surface area A_m and volume V_m , and \bar{n}_s^m moles of surface sites, it follows that

$$\bar{C}_s^m = \frac{\bar{n}_s^m}{V_{\text{REV}}} = \frac{\bar{n}_s^m}{A_m} \frac{A_m}{n_m} \frac{n_m}{V_m} \frac{V_m}{V_{\text{REV}}} = \frac{\eta_s^m A_m}{V_m} \phi_m, \quad (2-99)$$

where C_s^m denotes the concentration of available sorption sites per unit volume V_{REV} of bulk porous medium, η_m refers to the site density in units of moles of sites m^{-2} , \bar{V}_m represents the molar volume, and \mathcal{A}_m represents the intrinsic surface area in $\text{m}^2 \text{mol}^{-1}$. Note that according to this expression the site concentration is proportional to the instantaneous mineral concentration $\bar{V}_m^{-1} \phi_m$. Thus no allowance is made for covering already occupied sites by a precipitation layer, for example. In addition as a mineral dissolves surface sites are replaced by new ones, it is assumed that the dissolution process is slow to the rate of adsorption and the new sites are instantaneously occupied by sorbing ions. Similar transport equations hold for the multisite case as compared with the single site case formulated above, with an additional sum over the different sites occurring in the primary species transport equations.

If in addition to sorption, mineral precipitation/dissolution reactions take place described by the irreversible reactions



for mineral M_m with stoichiometric coefficients ν_{jm} , the mass transport equations referred to a porous medium with porosity ϕ have the following form (Lichtner, 1985):

$$\frac{\partial}{\partial t} (\phi \Psi_j) + \nabla \cdot \Omega_j = - \sum_m \nu_{jm} I_m - \sum_i \bar{\nu}_{ji} \bar{I}_i, \quad (2-101)$$

for the j th primary species,

$$\frac{\partial \bar{C}_i}{\partial t} = \bar{I}_i, \quad \frac{\partial \bar{C}_{\bar{x}}}{\partial t} = - \sum_i \bar{I}_i, \quad (2-102)$$

for the i th sorbed species and the concentration of empty surface sites. In these equations Ψ_j refers to the total generalized concentration of the j th primary species and Ω_j the generalized flux defined by (Lichtner, 1985)

$$\Psi_j = C_j + \sum_i \nu_{ji} C_i, \quad \Omega_j = J_j + \sum_i \nu_{ji} J_i = (-\phi D \nabla + v) \Psi_j, \quad (2-103)$$

where C_j denotes the concentration of the j th primary species and C_i denotes the concentration of the i th reversible aqueous complex with stoichiometric reaction coefficients ν_{ji} , with J_i the individual species flux, D the diffusion/dispersion

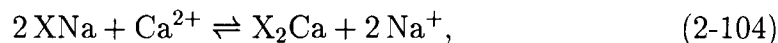
coefficient assumed to be the same for all species, and fluid flow velocity v , \bar{C}_i denotes the concentration of the i th surface complex, $\bar{C}_{\bar{x}}$ denotes the concentration of empty sites, I_m refers to the rate of the m th mineral reaction, and \bar{I}_i refers to the rate of the adsorption reaction. The total number of sorption sites must be conserved by the transport equations.

CHARGE CONSERVATION

To investigate the ability of various sorption models to conserve charge when combined with solute transport, two distinct models are considered: ion-exchange and surface complexation. First a two-component system is considered involving the sorption of Na^+ and Ca^{2+} .

Ion-Exchange

Ion-exchange of Na^+ with Ca^{2+} is described by the reaction



in which charge is conserved separately in both the aqueous and surface phases. In this reaction X^- denotes a surface site. Representing the rate of the exchange reaction by I_{ex} , the following transport equations hold:

$$\mathcal{L}[\text{Na}] = 2 I_{\text{ex}}, \quad \mathcal{L}[\text{Ca}] = -I_{\text{ex}}, \quad (2-105)$$

for the aqueous species Na^+ and Ca^{2+} with their corresponding concentrations denoted by the square brackets $[\dots]$, where \mathcal{L} denotes the differential operator

$$\mathcal{L} = \phi \frac{\partial}{\partial t} + v \frac{\partial}{\partial x} - \phi D \frac{\partial^2}{\partial x^2}. \quad (2-106)$$

In this simple example possible aqueous complexing reactions are omitted. This does not, however, affect the utility of the example regarding charge conservation. It follows immediately that for the ion-exchange reaction charge in the aqueous solution is conserved. The total charge density in solution contributed by cations is equal to

$$Q = [\text{Na}] + 2 [\text{Ca}]. \quad (2-107)$$

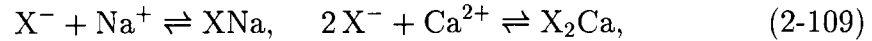
Electroneutrality is achieved by an equal and opposite contribution from anions. Because the anion transport equations are not coupled to the cation transport equations, in order for the solution to remain electrically neutral, both sets of transport equations must conserve charge individually. Therefore only the cations need be explicitly considered in what follows. It follows that

$$\mathcal{L}Q = \mathcal{L}[\text{Na}] + 2\mathcal{L}[\text{Ca}] = 2I_{\text{ex}} - 2I_{\text{ex}} = 0. \quad (2-108)$$

As a consequence of this equation charge is conserved and the aqueous solution will remain electrically neutral with increasing time if it is electrically neutral initially.

Surface Complexation Model

For sorption models with a variable number of unoccupied sites, however, charge is not in general conserved. Consider the following surface complexation reactions:



with rates I_{Na} and I_{Ca} , respectively, where X^- denotes a negatively charge surface site and XNa and X_2Ca represent sorbed species. The mass transport equations read:

$$\mathcal{L}[\text{Na}] = -I_{\text{Na}}, \quad \mathcal{L}[\text{Ca}] = -I_{\text{Ca}}. \quad (2-110)$$

For the sorbed species and unoccupied sites

$$[\dot{\text{XNa}}] = I_{\text{Na}}, \quad [\dot{\text{XCa}}] = I_{\text{Ca}}, \quad [\dot{\text{X}}] = -I_{\text{Na}} - 2I_{\text{Ca}}. \quad (2-111)$$

It follows that the total number of sites is conserved, as they must:

$$\dot{\omega}_{\text{X}} = [\dot{\text{X}}] + I_{\text{Na}} + 2I_{\text{Ca}} = 0, \quad \text{with} \quad \omega_{\text{X}} = [\text{X}] + [\text{XNa}] + 2[\text{X}_2\text{Ca}]. \quad (2-112)$$

However, total charge within the aqueous solution is not conserved:

$$\mathcal{L}Q = -I_{\text{Na}} - 2I_{\text{Ca}} = [\dot{\text{X}}] \neq 0. \quad (2-113)$$

Thus the nonconservation of charge in the surface complexation model is directly related to the rate of change with time of the unoccupied site density.

Multicomponent System

This result can be extended easily to the general case of a multicomponent system. To demonstrate that the transport equations do not necessarily conserve charge, first note that the primary species transport equations Eqn.(2-101) can be simplified by eliminating the sorption reaction rates \bar{I}_i , yielding the equivalent transport equations

$$\frac{\partial}{\partial t} \left(\phi \Psi_j + \sum_i \bar{\nu}_{ji} \bar{C}_i \right) + \nabla \cdot \Omega_j = - \sum_m \nu_{jm} I_m. \quad (2-114)$$

The transport equation for conservation of charge can be derived by multiplying these equations by the valence z_j of the j th primary species and summing over all primary species to give

$$\frac{\partial}{\partial t} \left(\phi Q + \sum_{ij} z_j \bar{\nu}_{ji} \bar{C}_i \right) + \nabla \cdot \Omega_Q = 0, \quad (2-115)$$

where the total charge in solution Q and current density Ω_Q are defined by

$$Q = F \sum_j z_j \Psi_j, \quad \text{and} \quad \Omega_Q = F \sum_j z_j \Omega_j = (-\phi D \nabla + v) Q. \quad (2-116)$$

The right hand side of Eqn.(2-115) vanishes because mineral precipitation/dissolution reactions, as all chemical reactions, conserve charge. The second term in brackets on the left-hand side of Eqn.(2-115) represents the total charge on the surface. Referring to this quantity as \bar{Q} it follows that

$$\bar{Q} = F \sum_{ji} z_j \bar{\nu}_{ji} \bar{C}_i = F \sum_i \bar{z}_i \bar{C}_i. \quad (2-117)$$

With this definition, Eqn.(2-115) can be expressed as

$$\frac{\partial}{\partial t} (\phi Q) + \nabla \cdot \Omega_Q = - \frac{\partial \bar{Q}}{\partial t}. \quad (2-118)$$

Charge is conserved only if the right-hand side of this equation vanishes identically. However, surface charge alone is *not* conserved in surface complexation models as it is in ion-exchange models. For example in the electric double layer model, surface charge plus the charge contained within the diffuse layer is conserved. This suggests that one way to correct for nonconservation of charge is

to include in the mass transport equations the contribution from nonspecific adsorbed ions contained in the diffuse layer. For the simpler surface complexation models which do not explicitly include the double layer, there does appear to be any way to conserve charge when these models are combined with solute transport.

ELECTRIC DOUBLE LAYER MODEL

The deficiency in the surface complexation model to conserve charge when combined with mass transport equations can be rectified by explicitly taking into account in the mass conservation equations the electric double layer and the contribution of nonspecific adsorbed ions in the diffuse layer.

The concentration of ions in the diffuse layer is presumed to be related to the bulk concentration through the Boltzmann factor by the expression

$$C_i^{\text{dl}}(x) = C_i e^{-z_i F \psi(x)/RT}, \quad (2-119)$$

where C_i^{dl} denotes the concentration of the i th species with valence z_i within the diffuse layer, the coordinate x represents the distance from the charged surface, C_i denotes the bulk concentration of the i th species, F denotes the Faraday constant, ψ the electric double layer potential, R the gas constant, and T the temperature. The concentration of adsorbed species is obtained from the mass action equations corresponding to Eqn.(2-97) leading to the expression

$$\bar{C}_i^m = \bar{K}_i^m C_{\bar{x}_m} \prod_{j=1}^N (\gamma_j C_j P_0^{z_j})^{\bar{\nu}_{ji}^m} = \bar{K}_i^m C_{\bar{x}_m} P_0^{\bar{z}_i} \prod_{j=1}^N (\gamma_j C_j)^{\bar{\nu}_{ji}^m}, \quad (2-120)$$

where C_j denotes the bulk concentration of the j th primary species, and the factor P_0 is given by the Boltzmann distribution

$$P_0 = e^{-F\psi_0/RT}, \quad (2-121)$$

where ψ_0 the electric double layer potential evaluated at the surface. The latter expression is obtained noting that the valence associated the the i th adsorbed species \bar{z}_i is related to the valencies of the primary species by the equation

$$\bar{z}_i = \sum_j \bar{\nu}_{ji} z_j. \quad (2-122)$$

From the expression for the total number of surface sites corresponding to the m th mineral given by the equation

$$\bar{C}_s^m = \bar{C}_{\bar{x}_m} + \sum_i \bar{C}_i^m = \bar{C}_{\bar{x}_m} \left\{ 1 + \sum_i \bar{K}_i^m P_0^{\bar{z}_i} \prod_{j=1}^N (\gamma_j C_j)^{\bar{\nu}_{ji}^m} \right\}, \quad (2-123)$$

and the mass action equations, Eqn.(2-120), the sorption isotherms for the concentration of empty sites and adsorbed species are given, respectively, by

$$\bar{C}_{\bar{x}_m} = \frac{\bar{C}_s^m}{1 + \sum_i \bar{K}_i^m P_0^{\bar{z}_i} \prod_{j=1}^N (\gamma_j C_j)^{\bar{\nu}_{ji}^m}}, \quad \text{and} \quad \bar{C}_i^m = \frac{\bar{C}_s^m \bar{K}_i^m P_0^{\bar{z}_i} \prod_{l=1}^N (\gamma_l C_l)^{\bar{\nu}_{li}^m}}{1 + \sum_{i'} \bar{K}_{i'}^m P_0^{\bar{z}_{i'}} \prod_{j=1}^N (\gamma_j C_j)^{\bar{\nu}_{ji'}^m}}. \quad (2-124)$$

SURFACE EXCESS CONCENTRATION

In order to formulate a transport model which has the desirable property of conserving charge, it is necessary to account for the concentration of ions within the diffuse layer. This can be accomplished by introducing the surface excess concentration defined by (Borkovec and Westall, 1983)

$$\Gamma_i^m = \int_{x_d}^{\infty} [C_i^{m,dl}(x) - C_i] dx, \quad (2-125)$$

for the m th mineral surface. The surface excess concentration may be positive or negative. Referring to a REV, the excess concentration in the diffuse layer may be expressed as

$$\delta C_i^{m,dl} = \frac{\delta n_i^m}{V_P} = \frac{\delta n_i^m}{A_m} \frac{A_m}{n_m} \frac{n_m}{V_m} \frac{V_m}{V_{REV}} \frac{V_{REV}}{V_P} = \frac{A_m \phi_m}{\phi \bar{V}_m} \Gamma_i^m, \quad (2-126)$$

where δn_i^m refers to the mole excess contained in the REV. The surface excess concentration in the diffuse layer may be positive or negative.

MASS TRANSPORT EQUATIONS INCLUDING NONSPECIFIC ADSORBED IONS

Mass transport equations including the effects of adsorption and the contribution of nonspecific adsorbed ions in the diffuse layer have the form

$$\frac{\partial}{\partial t} \left[\phi (\Psi_j + \delta \Psi_j^{dl}) + \sum_i \bar{\nu}_{ji} \bar{C}_i \right] + \frac{\partial \Omega_j}{\partial x} = - \sum_m \nu_{jm} I_m, \quad (2-127)$$

where

$$\delta\Psi_j^{\text{dl}} = \sum_m \left[\delta C_j^{m,\text{dl}} + \sum_i \nu_{ji} \delta C_i^{m,\text{dl}} \right]. \quad (2-128)$$

The accumulation term in the transport equation for bulk solute species is assumed to consist of the sum of contributions from the diffuse layer, the so-called nonspecifically adsorbed species, and the bulk solution itself. However, because species in the diffuse layer are not transported in the bulk solution, they give rise to an additional retardation effect beyond that given by the specifically adsorbed species.

With this form of the transport equations charge conservation is guaranteed. Multiplying the transport equation for the j th primary species by the charge z_j and summing over all primary species yields

$$\frac{\partial}{\partial t} (\phi Q) + \nabla \cdot \Omega_Q = \frac{\partial}{\partial t} \left[\bar{Q} + F\phi \sum_j z_j \delta\Psi_j^{\text{dl}} \right]. \quad (2-129)$$

Conservation of charge in the aqueous phase thus follows from conservation of charge of adsorbed and nonspecifically adsorbed species in the diffuse layer which requires that the following relation be satisfied identically

$$\bar{Q} = -F\phi \sum_j z_j \delta\Psi_j^{\text{dl}}. \quad (2-130)$$

This condition is simply the statement that surface charge is balanced by the total charge contained within the diffuse layer.

RETARDATION

Retardation is influenced by the nonspecific sorption in the electric diffuse layer as well as specific ion adsorption on the charged surface. The local distribution coefficient giving the ratio of total concentration of adsorbed species including contributions from both the specific and nonspecific adsorbed species to the aqueous concentration can be defined as

$$\mathcal{K}_j^D = \frac{\sum_i \bar{\nu}_{ji} \bar{C}_i + \delta\Psi_j^{\text{dl}}}{\Psi_j}. \quad (2-131)$$

Without taking the ions in the diffuse layer into account results in the distribution coefficient

$$\kappa_j^{D0} = \frac{\sum_i \bar{\nu}_{ji} \bar{C}_i}{\Psi_j}. \quad (2-132)$$

The ratio of the distribution coefficients with and without the contribution from nonspecific adsorbed ions is thus equal to

$$\frac{\kappa_j^D}{\kappa_j^{D0}} = \frac{\sum_i \bar{\nu}_{ji} \bar{C}_i + \delta \Psi_j^{\text{dl}}}{\sum_i \bar{\nu}_{ji} \bar{C}_i} = 1 + \frac{\delta \Psi_j^{\text{dl}}}{\sum_i \bar{\nu}_{ji} \bar{C}_i}. \quad (2-133)$$

The ratio is close to unity if the contribution from nonspecific adsorbed ions is small compared to the specifically adsorbed ions. However, in general, because $\delta \Psi_j^{\text{dl}}$ may be positive or negative, κ_j^D may become negative or even vanish.

CONCLUSION

Combining sorption reactions with mineral precipitation/dissolution reactions adds new challenges to modeling reactive transport problems. Special attention needs to be given to the resulting transport equations to ensure that electroneutrality is maintained in the aqueous solution as the system evolves with time.

REFERENCES

- Allison, J.D., D.S. Brown, and K.J. Novo-Gradac. 1991. MINTEQA2/PRODEFA2, A Geochemical Assessment Model for Environmental Systems: Version 3.0 User's Manual. EPA/600/3-91/021. Athens, Georgia. Environmental Protection Agency (EPA).
- Borkovec, M., and Westall, J. 1983. Solution of the Poisson-Boltzmann equation for surface excesses of ions in the diffuse layer at the oxide-electrolyte interface. *J. Electroanal. Chem.* 150: 325-337.
- Hsi, C-K.D. and D. Langmuir. 1985. Adsorption of uranyl onto ferric oxyhydroxides: Application of the surface complexation site-binding model. *Geochimica et Cosmochimica Acta* 49:1931-1941.

- Lichtner, P. C. 1985. Continuum model for simultaneous chemical reactions and mass transport in hydrothermal systems. *Geochimica et Cosmochimica Acta*, 49: 779–800.
- Turner, D.R. 1993. Mechanistic Approaches to Radionuclide Sorption Modeling. CNWRA 93-019. CNWRA, San Antonio, Texas.
- Turner, D. R. 1995. A uniform approach to surface complexation modeling of radionuclide sorption. CNWRA 95-001. San Antonio, TX: Center for Nuclear Waste Regulatory Analyses.

3. EBSPAC

Account Number: **20-5702-523**

Collaborators: none

Objective: The purpose of this project is to investigate the near-field environment of a partially saturated HLW repository and to model corrosion of the waste package and spent fuel.

3.1. Reactive Surface Boundary Condition

Date	Entry
------	-------

11.20.95 Butler-Volmer Equation. The Butler-Volmer equation for the current density of the k th electrochemical reaction has the form

$$i_k = i_{k,S}^0 \left[\exp \left(\frac{\alpha_k^a F}{RT} \eta_k \right) - \exp \left(-\frac{\alpha_k^c F}{RT} \eta_k \right) \right], \quad (3-134)$$

where α_k^a and α_k^c refer to the anodic and cathodic transfer coefficients, respectively, the overpotential η_k is defined by

$$\eta_k = V - \Phi_S - U_k^S, \quad (3-135)$$

with V the electrode potential, Φ_S the solution potential adjacent to the electrode surface, and U_k^S the open-circuit potential for the k th reaction evaluated at the surface of the electrode defined by

$$U_k^S = U_k^{\text{ref}} - \frac{RT}{n_k F} \sum_i \nu_{ik} \ln \left[\frac{C_i^S}{C_i^{\text{ref}}} \right], \quad (3-136)$$

with U_k^{ref} the reference potential, C_i^S the solution concentration at the surface of the electrode and C_i^{ref} the reference solution concentration. The exchange current density $i_{k,S}^0$, where the subscript S refers to the surface of the electrode, is defined by

$$i_{k,S}^0 = i_{k,\text{ref}}^0 \prod_i \left(\frac{C_i^S}{C_i^{\text{ref}}} \right)^{\gamma_{ik}}, \quad (3-137)$$

where γ_{ij} is to be determined.

Yan et al. (1993) [Yan, J.-F., Nguyen, T. V., White, R. E., and Griffin, R. B., Mathematical modeling of the formation of calcareous deposits on cathodically protected steel in seawater, *J. Electrochem. Soc.*, **140**, 733–742] propose the following method to determine γ_{ij} . Substituting for the open-circuit potential U_k^S yields the following equivalent expression for the Butler-Volmer equation

$$i_k = i_{k,\text{ref}}^0 \left[\prod_i \left(\frac{C_i^S}{C_i^{\text{ref}}} \right)^{p_{ik}} \exp \left(\frac{\alpha_k^a F}{RT} \tilde{\eta}_k \right) - \prod_i \left(\frac{C_i^S}{C_i^{\text{ref}}} \right)^{q_{ik}} \exp \left(-\frac{\alpha_k^c F}{RT} \tilde{\eta}_k \right) \right], \quad (3-138)$$

where

$$\tilde{\eta}_k = V - \Phi_S - U_k^{\text{ref}}, \quad (3-139)$$

$$p_{ik} = \gamma_{ik} + \frac{\alpha_k^a \nu_{ik}}{n_k}, \quad (3-140)$$

and

$$q_{ik} = \gamma_{ik} - \frac{\alpha_k^c \nu_{ik}}{n_k}, \quad (3-141)$$

For $\nu_{ik} > 0$, $p_{ik} = \nu_{ik}$ and zero otherwise; and for $\nu_{ik} < 0$, $q_{ik} = -\nu_{ik}$ and zero otherwise. Solving for γ_{ik} yields the condition

$$\gamma_{ik} = p_{ik} - \frac{\alpha_k^a \nu_{ik}}{n_k} = q_{ik} + \frac{\alpha_k^c \nu_{ik}}{n_k}. \quad (3-142)$$

This yields the condition:

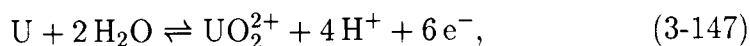
$$\alpha_k^a + \alpha_k^c = n_k, \quad (3-143)$$

which contradicts the convention expression

$$\alpha_k^a + \alpha_k^c = 1. \quad (3-144)$$

Thus it is difficult to understand the results of Yan et al. (1993).

The parameters which enter the Butler-Volmer equation must be tabulated for each reaction of interest. For the reactions



the corresponding thermodynamic and kinetic electrochemical data are presented in Table 3-5.

Table 3-5: Electrochemical data for the listed reactions.

Reaction	α_k^a	α_k^c	n_k	i_k^0 [A m ⁻²]	U_k^\ominus
$\text{Cu} \rightleftharpoons \text{Cu}^+ + \text{e}^-$	1/2	1/2	1	.	0.521
$\text{Fe} \rightleftharpoons \text{Fe}^{2+} + 2 \text{e}^-$			2	.	-0.440
$\text{U} + 2 \text{H}_2\text{O} \rightleftharpoons \text{UO}_2^{2+} + 4 \text{H}^+ + 6 \text{e}^-$			6	.	.
$\text{O}_2 + 4 \text{H}^+ + 4 \text{e}^- \rightleftharpoons 2 \text{H}_2\text{O}$	1	1	-4	1.24×10^{-24}	-1.229
$2 \text{H}^+ + 2 \text{e}^- \rightleftharpoons \text{H}_2$	3	1	-2	2.0×10^{-11}	0.

4. IPA: Flow Around the Waste Package

Account Number: **20-5702-723**

Collaborators: John Walton (Consultant)

Objective: The purpose of this project is to investigate the flow of liquid water and vapor in the very-near-field region of a HLW repository.

6.9.95 Revised manuscript adding discussion of evaporation rate at interfaces. The evaporation rate can be computed from the following equivalent expressions

$$E = -\frac{1}{r} \frac{d}{dr} (rN_w^l) = \frac{1}{r} \frac{d}{dr} (rN_w^g), \quad (4-150)$$

in cylindrical coordinates. At interfaces between two dissimilar materials the evaporation rate has a δ -function singularity. The temperature field $T(r)$ must be continuous across the interface, but because of differing thermal conductivity in the two adjoining media the gradient of the temperature has a jump discontinuity. Consequently the flux has a jump discontinuity and can be represented in terms of the Heaviside function:

$$N = [1 - \theta(r - r_l)] N^{(-)} + \theta(r - r_l) N^{(+)}, \quad (4-151)$$

where $N^{(-)}$ and $N^{(+)}$ denote the flux to the left and right of the interface located at r_l . Differentiating this expression gives

$$\frac{1}{r} \frac{d}{dr} (rN) = \delta(r - r_l)[N] + [1 - \theta(r - r_l)] \frac{1}{r} \frac{d}{dr} (rN^{(-)}) + \theta(r - r_l) \frac{1}{r} \frac{d}{dr} (rN^{(+)}), \quad (4-152)$$

where $[N]$ denotes the jump in the flux across the interface

$$[N] = N^{(+)} - N^{(-)}. \quad (4-153)$$

Introducing the evaporation rate, Eq.(4-152) becomes

$$E = E_\delta \delta(r - r_l) + E^{(-)}[1 - \theta(r - r_l)] + E^{(+)}\theta(r - r_l). \quad (4-154)$$

The first term on the right-hand side of Eq.(4-154) proportional to the Dirac delta function represents the contribution to the evaporation rate at the interface. The second two terms represent the contribution to the left and right of the interface, respectively. Note that the term E_δ has units of moles/m²/s, where $E^{(\pm)}$ has the units moles/m³/s.

P. C. Lichtner

SCIENTIFIC NOTEBOOK

INITIALS: PC

5. Volcanology Project

Account Number: **20-5704-143**

Collaborators: PI: Charles Connor

Objective: The purpose of this work is to study heat transport from a dike or volcano using CTOUGH. This work has the potential to provide field verification of CTOUGH simulations similar to modeling the heat generated from a HLW repository emplaced in a partially saturated porous medium.

12.10.95 Temperature and saturation profiles evolving from an emplaced dike in a tuff country rock.

CTOUGH was used to model the temperature and moisture redistribution around a 5 m wide dike emplaced in a tuff host rock. The equivalent continuum model was used with the following input parameters:

```
dike, icp=9, 12/10/95, dike cooling simulation: 5m
:
:
ROCKS
:
: mat nad  drock  por  permx  permy  permz  cwet  spht
SCOR 2  1.400E+03  0.575  1.5E-10  1.5E-10  1.5E-10  0.23  840.0
:
: comp      expan      cdry      tortx
      0.0      0.0      0.174      0.5
: irp rp(1)  rp(2)      rp(3) rp(4)  rp(5)  rp(6)  rp(7)
  9  1.0E-15  1.315E-4  1.798  0.5    0.001  0.0    0.0
: icp cp(1)  cp(2)      cp(3) cp(4)  cp(5)  cp(6)  cp(7)
  9  1.0E-9  1.315E-4  2.00   0.15  0.001  0.0    0.0
:
: mat nad  drock  por  permx  permy  permz  cwet  spht
DIKE 2  2.800E+03  0.10  1.8E-14  1.8E-14  1.8E-14  2.3    840.0
:
: comp      expan      cdry      tortx
      0.0      0.0      1.74      0.5
: irp rp(1)  rp(2)      rp(3) rp(4)  rp(5)  rp(6)  rp(7)
  9  1.9E-18  5.8E-7  1.798  0.1    0.001  0.0    0.0
: icp cp(1)  cp(2)      cp(3) cp(4)  cp(5)  cp(6)  cp(7)
  9  1.0E-11  1.315E-4  4.23   1.8E-3  0.001  0.0    0.0
```

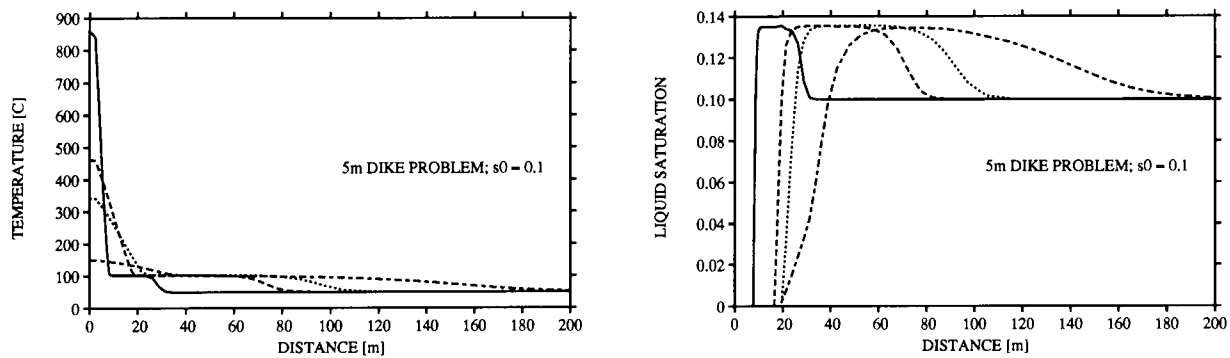


Figure 5-6: Temperature and liquid saturation for a 5 m dike with an initial temperature of 1200°C and initial saturation of the country rock of 10%.

6. Criticality

Account Number: **20-5702-541**

Collaborators: PI: W. M. Murphy (PI), M. Jarzemba, N. Sridhar

Objective: Evaluate the criticality issue brought forth by C. Bowman and F. Venneri.

4.27.95 Developed an expression for X_{\min} . Bowman and Venneri [Underground supercriticality from plutonium and other fissile material, LA-UR 94-4022A, 1995], introduce the mole fraction X defined by

$$X = \frac{n_{\text{SiO}_2}}{n_{\text{SiO}_2} + n_{\text{H}_2\text{O}}}. \quad (6-155)$$

For a rock of given porosity ϕ this quantity must have a minimum value when the pore space is completely filled with liquid water. To determine this value note that the volumes of rock and water are

$$V_{\text{SiO}_2} = \bar{V}_{\text{SiO}_2} n_{\text{SiO}_2}, \quad (6-156)$$

and

$$V_{\text{H}_2\text{O}} = \bar{V}_{\text{H}_2\text{O}} n_{\text{H}_2\text{O}}. \quad (6-157)$$

The porosity ϕ and saturation index S are defined by:

$$\phi = \frac{V_{\text{pore}}}{V} = \frac{V - V_{\text{SiO}_2}}{V} = 1 - \frac{V_{\text{SiO}_2}}{V} = 1 - \phi_{\text{SiO}_2}, \quad (6-158)$$

and

$$S = \frac{V_{\text{H}_2\text{O}}}{V_{\text{pore}}} = \frac{V_{\text{H}_2\text{O}}}{V - V_{\text{SiO}_2}} = \frac{\phi_{\text{H}_2\text{O}}}{1 - \phi_{\text{SiO}_2}}. \quad (6-159)$$

The mole fraction is related to the porosity and saturation by the expression

$$X(S, \phi) = \frac{\bar{V}_{\text{SiO}_2}^{-1} V_{\text{SiO}_2}}{\bar{V}_{\text{SiO}_2}^{-1} V_{\text{SiO}_2} + \bar{V}_{\text{H}_2\text{O}}^{-1} V_{\text{H}_2\text{O}}} = \frac{\bar{V}_{\text{SiO}_2}^{-1} (1 - \phi)}{\bar{V}_{\text{SiO}_2}^{-1} (1 - \phi) + \bar{V}_{\text{H}_2\text{O}}^{-1} S \phi}, \quad (6-160)$$

noting that

$$\frac{V_{\text{H}_2\text{O}}}{V} = \frac{V_{\text{H}_2\text{O}}}{V_{\text{pore}}} \frac{V_{\text{pore}}}{V} = S \phi. \quad (6-161)$$

Thus X_{\min} is given by

$$X_{\min} = X(S = 1, \phi), \quad (6-162)$$

$$= \frac{\bar{V}_{\text{SiO}_2}^{-1} V_{\text{SiO}_2}}{\bar{V}_{\text{SiO}_2}^{-1} V_{\text{SiO}_2} + \bar{V}_{\text{H}_2\text{O}}^{-1} V_{\text{H}_2\text{O}}}, \quad (6-163)$$

$$= \frac{\bar{V}_{\text{SiO}_2}^{-1} (1 - \phi)}{\bar{V}_{\text{SiO}_2}^{-1} (1 - \phi) + \bar{V}_{\text{H}_2\text{O}}^{-1} \phi} = \frac{1}{1 + \frac{\bar{V}_{\text{SiO}_2}}{\bar{V}_{\text{H}_2\text{O}}} \frac{\phi}{1 - \phi}}. \quad (6-164)$$

This analysis neglects the presence of any other solids such as plutonium, for example.

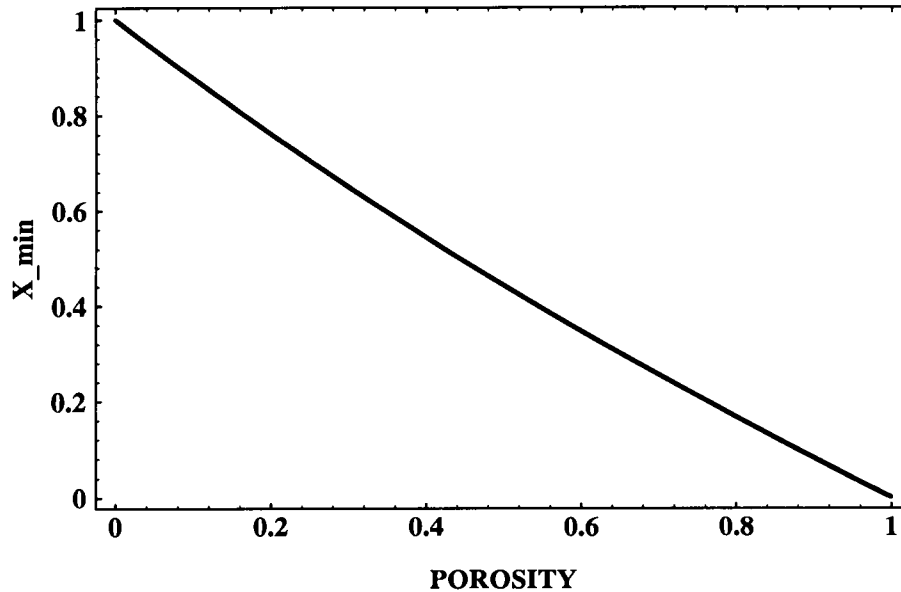


Figure 6-7: Minimum mole fraction X_{\min} plotted as a function of porosity.

According to the figure X_{\min} ranges from 0 to 1. Its maximum value of one occurs for zero porosity in which case the system consists of pure solid and liquid water cannot be present. The other extreme of zero corresponds to unit porosity for which there can be no solid present and the system consists of pure liquid water.

Referring to Figure 1 of Bowman and Venneri (1995) the criticality curves range from a pure liquid water system ($X=0$) to pure solid ($X=1$). Correspondingly the porosity of the rock is not constant but varies from 1 to 0. For the Topopah

Spring unit at Yucca Mountain, the average porosity is 10%. This value would limit X_{\min} to values greater than 0.9 according to Bowman and Venneri's Figure 1, and therefore limit the possibility of autocatalytic behavior to relatively larger volumes of plutonium (i.e. greater than 200 cm radii). Of course, it must be noted that the porosity value of 10% associated with the Topopah Spring unit is an average value and locally the actual porosity could be greater or less than this value.

5.10.95 Dependence of Criticality on Porosity: Air, H₂O and SiO₂. One of the major characteristic features of the proposed repository at Yucca Mountain is its location above the water table. To describe the properties of this system it is essential to consider the ternary system: H₂O–Air–SiO₂. In the work of Bowman and Venneri (1995) a binary system H₂O–SiO₂ was considered without regard to the air component. Their formulation did not take into account the porosity of the partially saturated porous medium on criticality. Although for a rock with a relatively small porosity, the presence of air would not be expected to greatly impact criticality, for porosities close to unity this would not be the case and it can be expected that a significant reduction in criticality would occur requiring significantly greater amounts of Pu. Indeed in the limit $\phi \rightarrow 1$, the system consists of air and Pu only. In this case additional information is required to describe the state of dispersal of Pu.

$$X_w = \frac{N_w}{N_w + N_a + N_s}, \quad (6-165)$$

$$X_a = \frac{N_a}{N_w + N_a + N_s}, \quad (6-166)$$

$$X_s = \frac{N_s}{N_w + N_a + N_s}, \quad (6-167)$$

$$V_{\text{pore}} = V_w + V_a = V - V_s. \quad (6-168)$$

$$\phi = \frac{V_{\text{pore}}}{V} = \frac{V_w + V_a}{V} = 1 - \frac{V_s}{V}, \quad (6-169)$$

$$S = \frac{V_w}{V_{\text{pore}}} = \frac{V_w}{V_w + V_a}. \quad (6-170)$$

$$\frac{V_w}{V} = \frac{V_w}{V_{\text{pore}}} \cdot \frac{V_{\text{pore}}}{V} = S\phi, \quad (6-171)$$

$$\frac{V_a}{V} = \frac{V_a}{V_s} \cdot \frac{V_s}{V} = (1 - S)\phi, \quad (6-172)$$

$$\frac{V_s}{V} = 1 - \phi. \quad (6-173)$$

$$X_w = \frac{\bar{V}_w^{-1} S\phi}{\bar{V}_w^{-1} S\phi + \bar{V}_a^{-1} (1 - S)\phi + \bar{V}_s^{-1} (1 - \phi)}, \quad (6-174)$$

$$X_a = \frac{\bar{V}_a^{-1} (1 - S)\phi}{\bar{V}_w^{-1} S\phi + \bar{V}_a^{-1} (1 - S)\phi + \bar{V}_s^{-1} (1 - \phi)}, \quad (6-175)$$

$$X_s = \frac{\bar{V}_s^{-1} (1 - \phi)}{\bar{V}_w^{-1} S\phi + \bar{V}_a^{-1} (1 - S)\phi + \bar{V}_s^{-1} (1 - \phi)}. \quad (6-176)$$

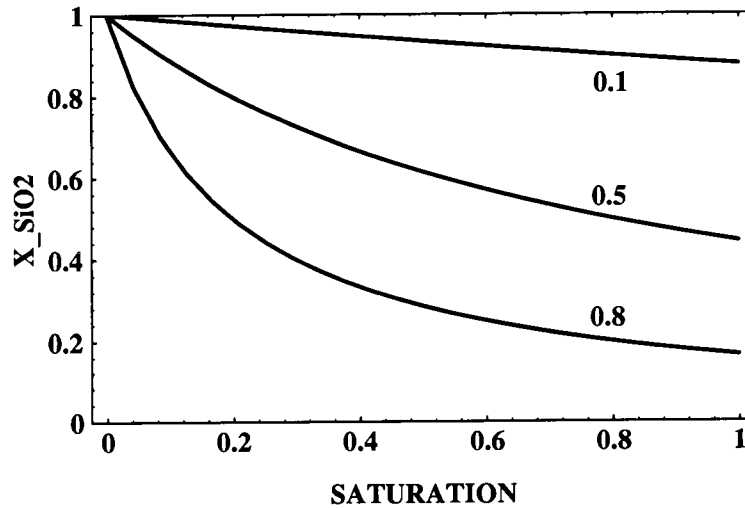


Figure 6-8: Mole fraction X_{SiO_2} plotted as a function of saturation S for porosities 0.1, 0.5 and 0.8.

I have reviewed this scientific notebook and find it in compliance with QAP-001. There is sufficient information regarding procedures used for conducting tests, acquiring and analyzing data so that another qualified individual could repeat the activity.

N. Sridhar 4/17/97

Narasi Sridhar
Manager, Engineered Barrier System and Waste Solidification System

Electronic Scientific Notebook No.
095E:Development of the Code MULTIFLO to
Describe Multiphase Reactive Transport
(12/18/1995 through 04/17/1997)

SCIENTIFIC NOTEBOOK

Printed: March 27, 1996

P. C. Lichtner

SCIENTIFIC NOTEBOOK

INITIALS:

PC

SCIENTIFIC NOTEBOOK

by

Peter C. Lichtner

Southwest Research Institute
Center for Nuclear Waste Regulatory Analyses
San Antonio, Texas

March 27, 1996

P. C. Lichtner

SCIENTIFIC NOTEBOOK

INITIALS:

PC

INITIAL ENTRIES

Scientific NoteBook: # 095

Issued to: P. C. Lichtner

Issue Date: Tuesday, November 16, 1993

Computerized Initials:

PC

By agreement with the CNWRA QA this NoteBook is to be printed at approximate quarterly intervals. This computerized Scientific NoteBook is intended to address the criteria of CNWRA QAP-001.

Table 1: Computing Equipment

Machine Name	Type	OS	Location
gravenstein.cnwra.swri.edu	Pentium Workstation	NEXTSTEP	desk Rm A-126
	133 Mhz	Version 3.3	Bldg. 189
	64 MB RAM		
skippy.cnwra.swri.edu	Sun SPARC 20	SUNOS 4.1.2	network
	96 MB RAM		

List of Figures

1	Comparison of finite difference scheme with the analytical solution.	5
2	Comparison of finite difference schemes with the TVD scheme.	8
3	Comparison of finite difference schemes with the TVD scheme.	8
4	Comparison of MULTIFLO (METRA) with Richards equation.	10

List of Tables

1	Computing Equipment	ii
---	-------------------------------	----

Contents

INITIAL ENTRIES	ii
FIGURES	iii
TABLES	iv
NEAR-FIELD ENVIRONMENT CODE DEVELOPMENT	1

KTI: NEAR-FIELD ENVIRONMENT CODE DEVELOPMENTAccount Number: **20-5708-562**

Collaborators: Dr. M. Seth (Consultant)

Objective: Development of the computer code MULTIFLO, and submodules GEM and METRA.

12.28.95 Finite Difference Equations for the hybrid scheme.

Finite difference equations based on a block-centered stencil with variable grid spacing are developed for the hybrid scheme. The distance between node points is given as

$$\delta x_n = x_n - x_{n-1} = \frac{1}{2} (\Delta x_n + \Delta x_{n-1}). \quad (1)$$

At an interface,

$$C_{n+1/2} = \frac{\Delta x_n C_{n+1} + \Delta x_{n+1} C_n}{\Delta x_{n+1} + \Delta x_n}, \quad (2)$$

and

$$\left. \frac{\partial C}{\partial x} \right|_{n+1/2} = \frac{C_{n+1} - C_n}{x_{n+1} - x_n}. \quad (3)$$

The residual corresponding to the j th primary species and n th node point is defined by

$$R_{jn} = \phi(\Psi_{jn}^{t+\Delta t} - \Psi_{jn}^t) V_n + \Delta t \{ \Omega_{je} A_e - \Omega_{jw} A_w \} + \Delta t V_n \sum_r \nu_{jr} I_{rn}. \quad (4)$$

The fluxes are given by the expressions:

$$A_e \Omega_{je} = -(\phi D A)_e \frac{\Psi_{j,n+1} - \Psi_{jn}}{\delta x_{n+1}} + A_e v_e \Psi_{je}, \quad (5)$$

$$= -T_e (\Psi_{j,n+1} - \Psi_{jn}) + F_e^+ \Psi_{jn} + F_e^- \Psi_{j,n+1}, \quad (6)$$

$$A_w \Omega_{jw} = -(\phi D A)_w \frac{\Psi_{jn} - \Psi_{j,n-1}}{\delta x_n} + A_w v_w \Psi_{je}, \quad (7)$$

$$= -T_e (\Psi_{jn} - \Psi_{j,n-1}) + F_w^+ \Psi_{j,n-1} + F_e^- \Psi_{jn}. \quad (8)$$

The diffusion terms involve the coefficients $T_{w,e}$ defined by

$$T_e = \frac{(\phi DA)_e}{\delta x_{n+1}}, \quad (9)$$

$$T_w = \frac{(\phi DA)_w}{\delta x_n}. \quad (10)$$

The coefficients $F_{w,e}$ are different for central differencing and upwinding. For central differencing one has:

$$F_e^\pm = \frac{\Delta x_n}{\Delta x_{n+1} + \Delta x_n} A_e v_e, \quad (11)$$

$$F_w^\pm = \frac{\Delta x_{n+1}}{\Delta x_{n+1} + \Delta x_n} A_w v_w. \quad (12)$$

For the hybrid scheme one has:

$$F_e^\pm = A_e v_e^\pm, \quad (13)$$

$$F_w^\pm = A_w v_w^\pm, \quad (14)$$

$$v_\alpha^\pm = \frac{1}{2}(v_\alpha \pm |v_\alpha|). \quad (15)$$

With these results the finite difference scheme can be expressed in the general form valid for both difference schemes:

$$R_{jn} = \phi(\Psi_{jn}^{t+\Delta t} - \Psi_{jn}^t) V_n + \Delta t \{E_n \Psi_{j,n+1} + P_n \Psi_{jn} + W_n \Psi_{j,n-1}\} + \Delta t V_n \sum_r \nu_{jr} I_{rn}, \quad (16)$$

where

$$E_n = F_e^- - T_e, \quad (17)$$

$$W_n = -(F_w^+ + T_w), \quad (18)$$

$$\begin{aligned} P_n &= T_e + T_w + F_e^+ - F_w^-, \\ &= F_e - F_w - (E_n + W_n). \end{aligned} \quad (19)$$

It follows that

$$(F_w)_{n+1} = (F_e)_n, \quad (T_w)_{n+1} = (T_e)_n. \quad (20)$$

and

$$W_{n+1} = E_n - (F_e)_n. \quad (21)$$

The jacobian matrix is given by the expression

$$J_{jn,lm} = \frac{\partial R_{jn}}{\partial C_{lm}}, \quad (22)$$

$$= \left(\phi V_n \frac{\partial \Psi_{jn}}{\partial C_{ln}} + \Delta t V_n \sum_r \nu_{jr} \frac{\partial I_{rn}}{\partial C_{ln}} + \Delta t P_n \frac{\partial \Psi_{jn}}{\partial C_{ln}} \right) \delta_{nm} \\ + \Delta t E_n \frac{\partial \Psi_{j,n+1}}{\partial C_{n+1}} \delta_{n+1,m} + \Delta t W_n \frac{\partial \Psi_{j,n-1}}{\partial C_{l,n-1}} \delta_{n-1,m}. \quad (23)$$

Logarithmic Form:

$$J_{jn,lm} = \frac{\partial R_{jn}}{\partial \ln C_{lm}} \quad (24)$$

$$= C_{lm} \frac{\partial R_{jn}}{\partial C_{lm}}. \quad (25)$$

Boundary Conditions:

$$\Psi_{j0} = 2\Psi_j^\circ - \Psi_{j1}, \quad (26)$$

$$\Psi_{j,N+1} = \Psi_{jN}. \quad (27)$$

1.5.96 Test of Gas Transport Algorithm.

Simultaneous transport of two or more phases with chemical reactions taking place between the two phases can lead to retardation or accelerated transport of species within the phases. Consider a two-phase system consisting of a liquid and gas phase in which a single chemical reaction occurs between aqueous and gaseous phases of the form



Assuming local chemical equilibrium between the two phases, the concentrations of aqueous and gaseous species are related by the mass action equation

$$C_g = K C_l. \quad (29)$$

The transport equation is given by

$$\frac{\partial}{\partial t} [\phi (s_l C_l + s_g C_g)] + \nabla \cdot (J_l + J_g) = 0. \quad (30)$$

Substituting for the concentration of the gaseous species in terms of the aqueous species gives for the accumulation term:

$$s_l C_l + s_g C_g = (s_l + K s_g) C_l, \quad (31)$$

and for the flux term:

$$J_l + J_g = -\phi \nabla [(s_l D_l + K s_g D_g) C_l] + (v_l + K v_g) C_l. \quad (32)$$

From these relations it follows that for an isothermal system the concentrations of both species obey the identical transport equation. For constant saturation and porosity, an effective velocity and diffusion coefficient may be introduced resulting in the effective advection-diffusion equation

$$\frac{\partial C}{\partial t} + v_{\text{eff}} \frac{\partial C}{\partial x} - D_{\text{eff}} \frac{\partial^2 C}{\partial x^2} = 0, \quad (33)$$

for one-dimension, where the effective fluid velocity v_{eff} and diffusivity D_{eff} are defined by

$$v_{\text{eff}} = \frac{v_l + K v_g}{\phi [s_l + K(1 - s_l)]}, \quad (34)$$

and

$$D_{\text{eff}} = \frac{s_l D_l + K(1 - s_l) D_g}{s_l + K(1 - s_l)}. \quad (35)$$

For a slightly soluble gas, such as O_2 , $\log K_{\text{O}_2} = 2.898$, and assuming $s_l \simeq s_g$, and $v_l \gg v_g$, $D_g \gg D_l$, it follows that

$$v_{\text{eff}} \simeq \frac{v_l}{\phi K s_g}, \quad (36)$$

and

$$D_{\text{eff}} \simeq D_g. \quad (37)$$

Thus in order to maintain local equilibrium the effective velocity is retarded by the factor $\phi K s_g$ from the aqueous fluid velocity, and the effective diffusivity is equal to the gaseous diffusion coefficient. For binary diffusion of water vapor with a diffusion coefficient of $D_g = 2.15 \times 10^{-5} \text{ m}^2 \text{ s}^{-1}$ at 25 °C compared to $D_l = 10^{-9} \text{ m}^2 \text{ s}^{-1}$, or four orders of magnitude larger, this leads to much more rapid diffusion in the aqueous phase than would be possible in the absence of the

gas phase. A comparison of the finite difference calculation using MULTIFLO with the analytical solution is shown in Fig. 1.

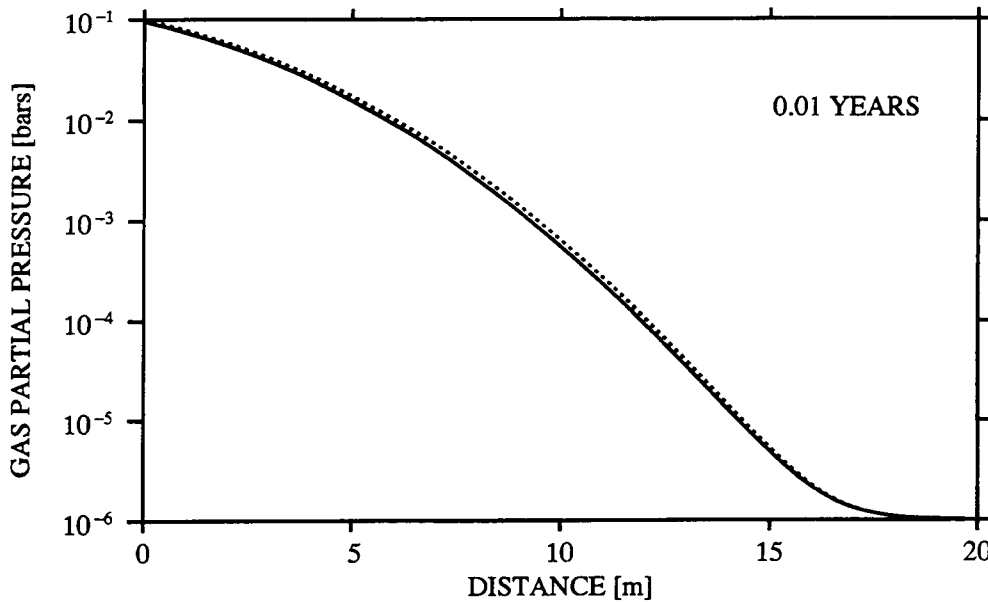
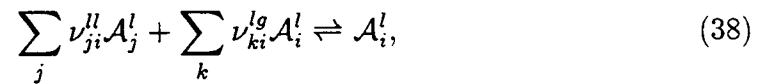
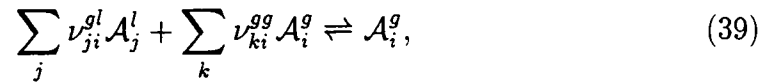


Figure 1: Comparison of finite difference scheme with the analytical solution.

1.15.96 Mixed Phase Primary Species. Consider a set of primary species consisting of gaseous and aqueous species $\{A_j^l, A_k^g\}$. Chemical reactions can be expressed in the form



for aqueous secondary species, and



for gaseous secondary species. The mass transport equations for aqueous and gaseous species have the form

$$\begin{aligned} \frac{\partial}{\partial t} \left\{ \phi \left[s_l \left(C_j^l + \sum_i \nu_{ji}^{ll} C_i^l \right) + s_g \sum_i \nu_{ji}^{lg} C_i^g \right] \right\} \\ + \nabla \cdot \left[\left(J_j^l + \sum_i \nu_{ji}^{ll} J_i^l \right) + \sum_i \nu_{ji}^{lg} J_i^g \right] = 0, \quad (40) \end{aligned}$$

and

$$\begin{aligned} \frac{\partial}{\partial t} \left\{ \phi \left[s_l \sum_i \nu_{ki}^{gl} C_i^l + s_g \left(C_k^g + \sum_i \nu_{ki}^{gg} C_i^g \right) \right] \right\} \\ + \nabla \cdot \left[\left(J_k^g + \sum_i \nu_{ki}^{gg} J_i^g \right) + \sum_i \nu_{ki}^{gl} J_i^l \right] = 0, \end{aligned} \quad (41)$$

respectively. Defining the quantities

$$\Psi_j^l = C_j^l + \sum_i \nu_{ji}^{ll} C_i^l, \quad (42)$$

$$\Psi_k^g = C_k^g + \sum_i \nu_{ki}^{gg} C_i^g, \quad (43)$$

$$\Psi_j^{lg} = \sum_i \nu_{ji}^{lg} C_i^g, \quad (44)$$

$$\Psi_k^{gl} = \sum_i \nu_{ki}^{gl} C_i^l, \quad (45)$$

$$(46)$$

and

$$\Omega_j^l = J_j^l + \sum_i \nu_{ji}^{ll} J_i^l, \quad (47)$$

$$\Omega_k^g = J_k^g + \sum_i \nu_{ki}^{gl} J_i^g, \quad (48)$$

$$\Omega_j^{lg} = \sum_i \nu_{ji}^{lg} J_i^g, \quad (49)$$

$$\Omega_k^{gl} = \sum_i \nu_{ki}^{gl} J_i^l, \quad (50)$$

$$(51)$$

the transport equations become

$$\frac{\partial}{\partial t} \left\{ \phi \left[s_l \Psi_j^l + s_g \Psi_j^{lg} \right] \right\} + \nabla \cdot \left[\Omega_j^l + \Omega_j^{lg} \right] = 0, \quad (52)$$

and

$$\frac{\partial}{\partial t} \left\{ \phi \left[s_l \Psi_k^{gl} + s_g \Psi_k^g \right] \right\} + \nabla \cdot \left[\Omega_k^g + \Omega_k^{gl} \right] = 0. \quad (53)$$

2.9.96 Addition of TVD to GEM. The TVD scheme was added to GEM to compute transport at large grid Péclet numbers.

TVD: Total Variation Diminishing Scheme

$$C_e = \begin{cases} C_{ij} + \frac{1}{2}\zeta(r_{ij}^+) (C_{i+1,j} - C_{ij}), & \text{Pe}_e > 2, \\ \frac{1}{2} (C_{i+1,j} + C_{ij}), & |\text{Pe}_e| \leq 2, \\ C_{i+1,j} + \frac{1}{2}\zeta(r_{ij}^-) (C_{ij} - C_{i+1,j}), & \text{Pe}_e < -2, \end{cases} \quad (54a)$$

$$C_w = \begin{cases} C_{i-1,j} + \frac{1}{2}\zeta(r_{i-1,j}^+) (C_{ij} - C_{i-1,j}), & \text{Pe}_e > 2, \\ \frac{1}{2} (C_{ij} + C_{i-1,j}), & |\text{Pe}_e| \leq 2, \\ C_{ij} + \frac{1}{2}\zeta(r_{i-1,j}^-) (C_{i-1,j} - C_{ij}), & \text{Pe}_e < -2, \end{cases} \quad (54b)$$

$$\zeta(r) = \max[0, \min(2, 2r, \frac{1}{3}(2+r))], \quad (55)$$

$$r_{ij}^+ = \begin{cases} \frac{C_{ij} - C_{i-1,j}}{C_{i+1,j} - C_{ij}}, & |C_{i+1,j} - C_{ij}| > 0, \\ 0, & \text{otherwise,} \end{cases} \quad (56a)$$

$$r_{ij}^- = \begin{cases} \frac{C_{i+1,j} - C_{i+2,j}}{C_{ij} - C_{i+1,j}}, & |C_{ij} - C_{i+1,j}| > 0, \\ 0, & \text{otherwise,} \end{cases} \quad (56b)$$

Explicit Finite Difference

$$C_{ij}^{k+1} = C_{ij}^k - \Delta t \frac{1}{\phi_{ij}} I_{ij} - \frac{\Delta t}{\phi_{ij} V_{ij}} \{v_e C_e A_e - v_w C_w A_w + v_n C_n A_n - v_s C_s A_s \} \quad (57)$$

$$-T_e (C_{i+1,j} - C_{ij}) + T_w (C_{ij} - C_{i-1,j}) - T_n (C_{i,j+1} - C_{ij}) + T_s (C_{ij} - C_{i,j-1}) \}. \quad (58)$$

Comparison with the analytical solution, first-order upwinding and explicit finite difference is shown in the accompanying figures for a Péclet number of 63.42 for an elapsed time of 1 year. The calculations were performed for a grid spacing of 0.05 m, a flow velocity of 10 m/y, and a porosity of 0.5. A rate constant of 10^{-12} moles/cm²/s was employed in the calculation. A solid molar volume of 22.688 cm³/mole and volume fraction of 0.5 were used with a specific surface area of 1/cm.

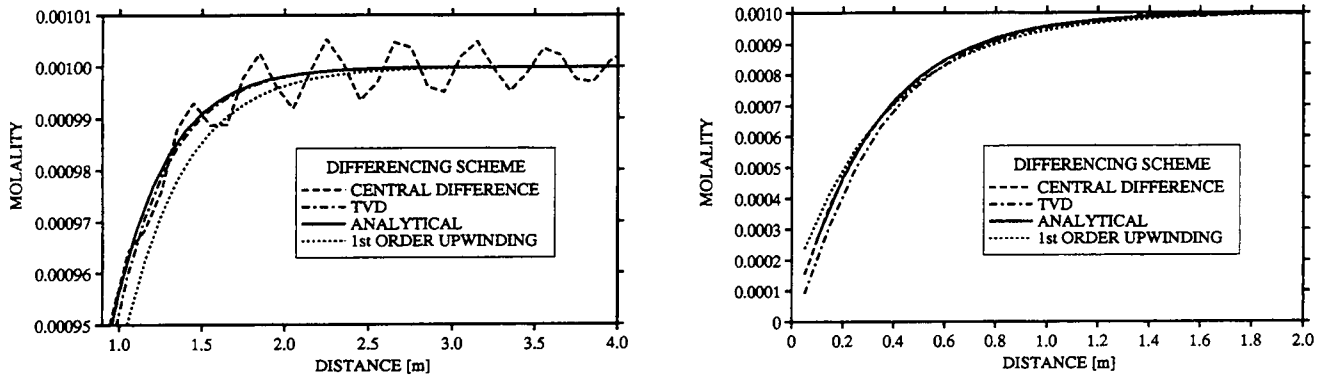


Figure 2: Comparison of finite difference schemes with the TVD scheme.

The next figure shows a comparison of the pH for a Peclet number of 317.

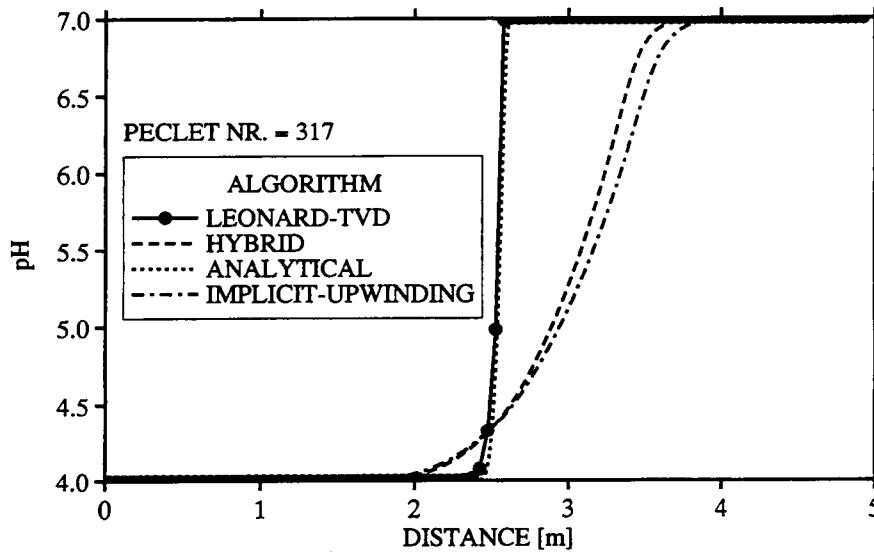


Figure 3: Comparison of finite difference schemes with the TVD scheme.

2.19.95 Steady vertical infiltration with a water table: comparison with Richards equation.

Conservation of mass for an incompressible fluid reads

$$\frac{dv(z)}{dz} = 0, \quad (59)$$

where the fluid flow velocity is given by Darcy's law:

$$v(z) = -\frac{\kappa\kappa_r}{\mu} \left(\frac{dp}{dz} - \rho g \right). \quad (60)$$

Integrating the mass conservation equation once yields

$$\int_0^z \frac{dv(z')}{dz'} dz' = v(z) - v(0). \quad (61)$$

Imposing a constant infiltration rate v_0 at the top implies $v(0) = v_0$. Substituting for Darcy's law yields an ordinary differential equation for the fluid pressure:

$$\frac{dp}{dz} = -\frac{\mu v_0}{\kappa \kappa_r} + \rho g. \quad (62)$$

To solve this equation the relative permeability must be known as a function of pressure. This relation is generally nonlinear and therefore this equation must be integrated numerically. This was accomplished by writing a simple *Mathematica* program:

```
mu = 8.9077 10^-4;
rho = 997.12;
g = 9.8;
v0 = 0.1 / (365 24 60 60);
km = 10^-14;
l = 20;
hycond = rho g km/mu; hycond (365 24 60 60)
pl = 1/2 (rho g - mu v0/km)
pl = 98000.;
hl = pl/(rho g)
mu v0 / km 0.1

am = 2 10^-5 (rho g); bm = 6.66667; lamm = 1-1/bm;
pm = 0.2;

Clear[krel]
krel[h_] := If[h>=0, 1,
(1-(-am h)^(bm-1)(1+(-am h)^bm)^(-(1-1/bm)))^2/
(1+(-am h)^bm)^((1-1/bm)/2)];

Clear[sat]
sat[h_] := If[h>=0, 1, satm[h]];
```

```

Clear[satm]
satm[h_] := (1+(-am h)^bm)^(-1amm);

hz0 = NDSolve[{h'[z]-1==0, h[10]==0},
h, {z, 20, 0}, AccuracyGoal->10, PrecisionGoal->10, WorkingPrecision->10,
MaxSteps->1000]

hz = NDSolve[{h'[z]+v0/hycond/krel[h[z]]-1==0, h[20]==h1},
h, {z, 20, 0}, AccuracyGoal->10, PrecisionGoal->10, WorkingPrecision->10]

```

A comparison of MULTIFLO (METRA) with Richards equation is shown in Fig. 4 for zero and 10 cm/y infiltration rates.

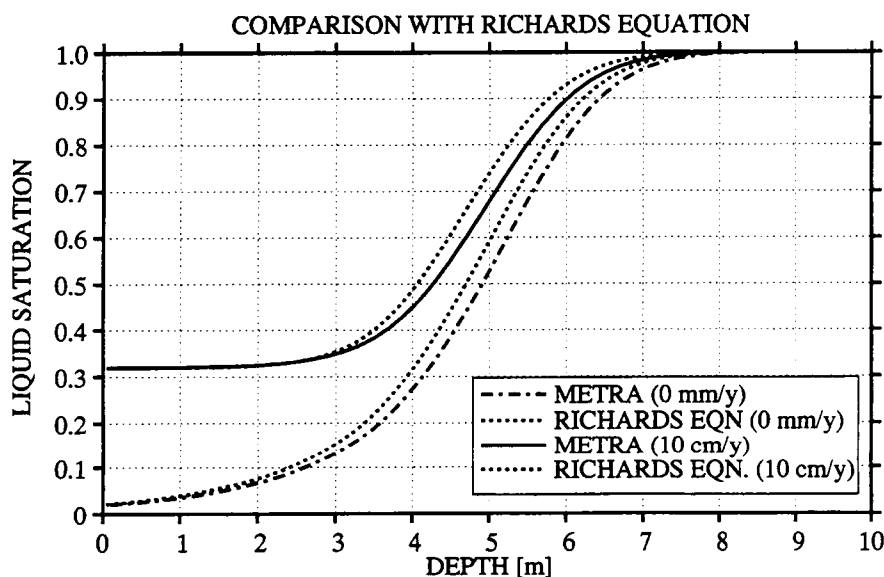


Figure 4: Comparison of MULTIFLO (METRA) with Richards equation.

3.8.96 Implicit Hybrid Scheme. The implicit finite hybrid scheme for non-reactive transport was found to lead to negative concentrations at the inlet. Therefore this approach is being abandoned.

3.15.96 Operator Splitting for Transport of Gas and Liquid Phases

The mass conservation equations for liquid and gas transport coupled to mineral precipitation/dissolution reactions have the form

$$\frac{\partial}{\partial t} [\phi (s_l \Psi_j^l + s_g \Psi_j^g)] + \nabla \cdot [\Omega_j^l + \Omega_j^g] = - \sum_m \nu_{jm} I_m. \quad (63)$$

In operator splitting this equation is solved in three steps:

- (1) The non-reactive transport equations for gaseous and aqueous species are solved independently of each other.

$$\frac{\partial}{\partial t} (\phi s_l \Psi_j^l) + \nabla \cdot \Omega_j^l = 0, \quad (64)$$

and

$$\frac{\partial}{\partial t} (\phi s_g \Psi_j^g) + \nabla \cdot \Omega_j^g = 0. \quad (65)$$

- (2) The total concentration is computed according to

$$\Psi_j = s_l \Psi_j^l + s_g \Psi_j^g, \quad (66)$$

and a speciation calculation is performed to get the individual species concentrations.

- (3) The mineral reaction step is added by solving the reaction path equation over a single time step:

$$\frac{\partial}{\partial t} [\phi (s_l \Psi_j^l + s_g \Psi_j^g)] = - \sum_m \nu_{jm} I_m. \quad (67)$$

This equation is solved implicitly.

An implicit formulation is necessary for the reactive step as can be seen from the analysis of a single component reacting species. Consider the equation

$$\frac{\partial C}{\partial t} = -k(C - C_{eq}). \quad (68)$$

The equation has the solution

$$C(t) = (C_0 - C_{eq})e^{-kt} + C_{eq}. \quad (69)$$

In finite difference form the differential equation becomes for an explicit finite difference scheme

$$C(t + \Delta t) = (1 - k\Delta t)C(t). \quad (70)$$

It is clear that to obtain physically meaningful results the time step Δt must satisfy the inequality

$$\Delta t \leq \frac{1}{k}. \quad (71)$$

For an implicit scheme, however, it follows that

$$C(t + \Delta t) = \frac{C(t)}{1 + k\Delta t}, \quad (72)$$

which is unconditionally stable.

3.22.96 Operator Splitting for Transport of Gas and Liquid Phases—Continued

It was realized that only two steps are necessary for the operator splitting approach to function properly. The middle step to speciate the nonreactive total concentrations is not necessary as these quantities are never used. The operator splitting algorithm is now as follows:

(1) The non-reactive transport equations for gaseous and aqueous species are solved independently of each other to provide the total concentrations $\hat{\Psi}_j^l$ and $\hat{\Psi}_j^g$ where the caret indicates non-reactive transport.

$$\frac{\partial}{\partial t} (\phi s_l \hat{\Psi}_j^l) + \nabla \cdot \hat{\Omega}_j^l = 0, \quad (73)$$

and

$$\frac{\partial}{\partial t} (\phi s_g \hat{\Psi}_j^g) + \nabla \cdot \hat{\Omega}_j^g = 0. \quad (74)$$

(2) The mineral reaction step is added by solving the reaction path equation over a single time step:

$$\frac{\partial}{\partial t} [\phi (s_l \Psi_j^l + s_g \Psi_j^g)] = - \sum_m \nu_{jm} I_m. \quad (75)$$

This equation is solved implicitly. In finite difference form this equation becomes:

$$s_l \Psi_j^l + s_g \Psi_j^g \left(s_l \hat{\Psi}_j^l + s_g \hat{\Psi}_j^g \right) + \frac{\Delta t}{\phi} \sum_m \nu_{jm} I_m = 0. \quad (76)$$

This equation must then be solved for the individual primary species concentrations C_j^l .

I have reviewed this scientific notebook and find it in compliance with QAP-001. There is sufficient information regarding procedures used for conducting tests, acquiring and analyzing data so that another qualified individual could repeat the activity.

N. Sridhar 8/17/97

Narasi Sridhar
Manager, Engineered Barrier System and Waste Solidification System

SCIENTIFIC NOTEBOOK

by

Peter C. Lichtner

SCIENTIFIC NOTEBOOK

by

Peter C. Lichtner

Southwest Research Institute
Center for Nuclear Waste Regulatory Analyses
San Antonio, Texas

June 29, 1996

INITIAL ENTRIES

Scientific NoteBook: # 095

Issued to: P. C. Lichtner

Issue Date: Tuesday, November 16, 1993

Computerized Initials:

PC

By agreement with the CNWRA QA this NoteBook is to be printed at approximate quarterly intervals. This computerized Scientific NoteBook is intended to address the criteria of CNWRA QAP-001.

Table 1: Computing Equipment

Machine Name	Type	OS	Location
gravenstein.cnwra.swri.edu	Pentium Workstation	NEXTSTEP	desk Rm A-126
	133 Mhz	Version 3.3	Bldg. 189
	64 MB RAM		
skippy.cnwra.swri.edu	Sun SPARC 20	SUNOS 4.1.2	network
	96 MB RAM		

PC

Contents

INITIAL ENTRIES	ii
FIGURES	iv
TABLES	v
NEAR-FIELD ENVIRONMENT	1

List of Figures

- 1 The temperature plotted as a function of depth for the indicated times. 21
- 2 The liquid saturation plotted as a function of depth for the indicated times. 21
- 3 Liquid and gas fluxes plotted as a function of depth for the indicated times. 22
- 4 The pH plotted as a function of depth for the indicated times. 22
- 5 The chloride concentration plotted as a function of depth for the indicated times. . . 22

P. C. Lichtner

SCIENTIFIC NOTEBOOK

INITIALS:

PC

List of Tables

1	Computing Equipment	ii
---	-------------------------------	----

KTI: NEAR-FIELD ENVIRONMENTAccount Number: **20-5708-561**

Description: Near-field Environment Technical Assistance

Collaborators: Dr. M. Seth (Consultant)

Objective: Application of the computer code MULTIFLO, and submodules GEM and METRA to the Yucca Mountain HLW Repository.

6.26.96 MULTIPHASE-MULTICOMPONENT NONISOTHERMAL REACTIVE TRANSPORT IN PARTIALLY SATURATED POROUS MEDIA with Application to the Yucca Mountain HLW Repository

The first application of MULTIFLO to the YM HLW repository is based on a simplified representation of the host rock as pure amorphous silica. An outline of the theory and results of preliminary calculations are reported at the International Conference on Deep Geological Disposal of Radioactive Waste to be held by the Canadian Nuclear Society September 16–19, 1996, in Winnipeg, Manitoba, Canada.

The input files for METRA and GEM used in the calculations are archived here. The METRA input file multi.dat contains:

```
Test Data for Multiflo simulator (initial data : 1D, Yucca Mt.)
      April 28, 1995

RSTART 0
:
:   XYZ                      = 1 table look-up,; pref = ref. press.
:   RADIAL                  = 0 correlations;   tref = ref temp.
:   OTHER
:
:grid geometry nx ny  nz ivplwr ipvtab iout   pref tref href
Grid XYZ      1 1 238  1      1      0      0  0
:
:Monitor 135
:debug 1
:0
Pckr                      :relative perm and pc keyword
:  i type-curv swir  rpm(lamda) alpha  swext sgc iecm
:    1 Van-Gen  0.001  0.4438  5.8e-7  0.    0.    1
:
:          swirm rpm(lamda) alpham phim  phif  perm  permf
:          0.001  .7635   1.315e-4  0.10   1.8e-3 1.9e-18 1.e-11
0          :blank line
:
Debug 1
0
Thermal-prop
: no rho      cpr   ckdry cksat   crp crt   tau cdiff  cexp enbd
```

P. C. Lichtner

SCIENTIFIC NOTEBOOK

INITIALS: SC

```

1 2.580e+03 840.0 1.74 2.3 0 0 .5 2.13e-5 1.8 1.
2 2.580e+03 840. 1.74 2.3 0 0 .5 2.13e-5 1.8 1.
0
: igrd rw re
DXYZ 2
: (dx(i),i=1,nx)
3.14
: (dy(j),j=1,ny)
1.
: (dz(k),k=1,nz)
2.5e1 2.5e1 2.5e1 2.5e1 1.75e1 1.0e1 1.0e1 1.0e1 1.0e1 1.0e1
1.0e1 1.0e1 1.0e1 1.0e1 7.5e0 5.0e0 5.0e0 5.0e0 5.0e0 5.0e0
5.0e0 5.0e0 5.0e0 5.0e0 5.0e0 5.0e0 5.0e0 5.0e0 5.0e0 5.0e0
5.0e0 5.0e0 5.0e0 5.0e0 3.5e0 2.0e0 2.0e0 2.0e0 2.0e0 2.0e0
2.0e0 2.0e0 2.0e0 2.0e0 2.0e0 2.0e0 2.0e0 2.0e0 2.0e0 2.0e0
2.0e0 2.0e0 2.0e0 2.0e0 1.5e0 1.0e0 1.0e0 1.0e0 1.0e0 1.0e0
1.0e0 1.0e0 1.0e0 1.0e0 1.0e0 1.0e0 1.0e0 1.0e0 1.0e0 1.0e0
1.0e0 1.0e0 7.5e-1 5.0e-1 5.0e-1 5.0e-1 5.0e-1 5.0e-1 5.0e-1 5.0e-1
5.e-1 5.e-1 5.e-1 5.0e-1 5.0e-1 5.0e-1 3.75e-1 2.5e-1 2.5e-1 2.5e-1
2.5e-1 2.5e-1 2.5e-1 2.5e-1 2.5e-1 2.5e-1 2.5e-1 2.5e-1 2.5e-1 2.5e-1
2.5e-1 2.5e-1 2.5e-1 2.5e-1 2.5e-1 2.5e-1 2.5e-1 2.5e-1 2.5e-1 2.5e-1
2.5e-1 2.5e-1 2.5e-1 2.75e-1 2.5e-1 2.e-1 2.0e-1 2.e-1 2.e-1 2.e-1
2.e-1 2.0e-1 2.0e-1 1.5e-1 1.e-1 1.e-1 1.e-1 1.e-1 1.e-1 1.e-1
1.e-1 1.e-1 1.e-1 1.e-1 1.e-1 1.e-1 1.e-1 1.e-1 1.e-1 1.e-1
1.e-1 1.e-1 1.e-1 1.e-1 1.e-1 1.e-1 1.e-1 1.e-1 1.e-1 1.e-1
1.e-1 1.e-1 1.e-1 1.e-1 1.e-1 1.5e-1 2.e-1 2.0e-1 2.0e-1 2.0e-1
2.e-1 2.e-1 2.0e-1 2.e-1 2.e-1 2.e-1 2.25e-1 2.5e-1 2.5e-1 2.5e-1
2.5e-1 2.5e-1 2.5e-1 2.5e-1 2.5e-1 2.5e-1 2.5e-1 2.5e-1 2.5e-1 2.5e-1
2.5e-1 2.5e-1 2.5e-1 2.5e-1 2.5e-1 2.5e-1 2.5e-1 2.5e-1 2.5e-1 3.75e-1
5.0e-1 5.0e-1 5.0e-1 5.0e-1 5.0e-1 5.0e-1 5.0e-1 5.0e-1 5.0e-1 5.0e-1
5.0e-1 5.0e-1 5.0e-1 5.0e-1 5.0e-1 5.0e-1 7.5e-1 1.0e0 1.0e0 1.0e0
1.0e0 1.0e0 1.5e0 2.0e0 2.0e0 2.0e0 2.0e0 2.0e0 2.0e0 2.0e0
2.0e0 2.0e0 3.5e0 5.0e0 5.0e0 5.0e0 5.0e0 5.0e0 7.5e0 1.0e1
1.0e1 1.0e1 1.0e1 1.5e1 2.0e1 2.0e1 2.0e1 2.0e1
PhiK
: i1 i2 j1 j2 k1 k2 iist ithrm vb por permx permy permz pormm permm
1 1 1 1 1 1 1 2 7.854e7
1 1 1 1 2 237 1 1 0.
1 1 1 1 238 238 1 2 6.2832e7
:
0
Init
: i1 i2 j1 j2 k1 k2 p t sg x2 sgm
: 1 1 1 1 1 238 1.0e5 25.0 0.5 0. .50
1 1 1 1 1 1 .997428E5 .156250E2 .480016E0 .000E0 .480016E0
1 1 1 1 2 2 .100048E6 .162507E2 .477543E0 .000E0 .477543E0
1 1 1 1 3 3 .100353E6 .168771E2 .474387E0 .000E0 .474387E0
1 1 1 1 4 4 .100659E6 .175042E2 .470442E0 .000E0 .470442E0
1 1 1 1 5 5 .100873E6 .179437E2 .467054E0 .000E0 .467054E0
1 1 1 1 6 6 .100995E6 .181949E2 .464834E0 .000E0 .464834E0
1 1 1 1 7 7 .101118E6 .184462E2 .462434E0 .000E0 .462434E0
1 1 1 1 8 8 .101240E6 .186976E2 .459841E0 .000E0 .459841E0
1 1 1 1 9 9 .101363E6 .189490E2 .457046E0 .000E0 .457046E0

```

P. C. Lichtner

SCIENTIFIC NOTEBOOK

INITIALS: PCZ

1 1 1 1	10	10	.101485E6	.192005E2	.454039E0	.000E0	.454039E0
1 1 1 1	11	11	.101608E6	.194519E2	.450809E0	.000E0	.450809E0
1 1 1 1	12	12	.101730E6	.197034E2	.447344E0	.000E0	.447344E0
1 1 1 1	13	13	.101853E6	.199550E2	.443634E0	.000E0	.443634E0
1 1 1 1	14	14	.101975E6	.202065E2	.439666E0	.000E0	.439666E0
1 1 1 1	15	15	.102067E6	.203951E2	.436496E0	.000E0	.436496E0
1 1 1 1	16	16	.102129E6	.205209E2	.434282E0	.000E0	.434282E0
1 1 1 1	17	17	.102190E6	.206466E2	.431997E0	.000E0	.431997E0
1 1 1 1	18	18	.102252E6	.207724E2	.429637E0	.000E0	.429637E0
1 1 1 1	19	19	.102313E6	.208981E2	.427203E0	.000E0	.427203E0
1 1 1 1	20	20	.102374E6	.210238E2	.424692E0	.000E0	.424692E0
1 1 1 1	21	21	.102435E6	.211496E2	.422103E0	.000E0	.422103E0
1 1 1 1	22	22	.102497E6	.212753E2	.419434E0	.000E0	.419434E0
1 1 1 1	23	23	.102558E6	.214009E2	.416683E0	.000E0	.416683E0
1 1 1 1	24	24	.102620E6	.215266E2	.413849E0	.000E0	.413849E0
1 1 1 1	25	25	.102681E6	.216522E2	.410931E0	.000E0	.410931E0
1 1 1 1	26	26	.102742E6	.217779E2	.407926E0	.000E0	.407926E0
1 1 1 1	27	27	.102804E6	.219035E2	.404834E0	.000E0	.404834E0
1 1 1 1	28	28	.102865E6	.220291E2	.401652E0	.000E0	.401652E0
1 1 1 1	29	29	.102927E6	.221546E2	.398378E0	.000E0	.398378E0
1 1 1 1	30	30	.102988E6	.222801E2	.395012E0	.000E0	.395012E0
1 1 1 1	31	31	.103050E6	.224056E2	.391551E0	.000E0	.391551E0
1 1 1 1	32	32	.103111E6	.225311E2	.387994E0	.000E0	.387994E0
1 1 1 1	33	33	.103173E6	.226565E2	.384339E0	.000E0	.384339E0
1 1 1 1	34	34	.103234E6	.227819E2	.380584E0	.000E0	.380584E0
1 1 1 1	35	35	.103277E6	.228697E2	.377891E0	.000E0	.377891E0
1 1 1 1	36	36	.103302E6	.229198E2	.376326E0	.000E0	.376326E0
1 1 1 1	37	37	.103326E6	.229699E2	.374745E0	.000E0	.374745E0
1 1 1 1	38	38	.103351E6	.230201E2	.373148E0	.000E0	.373148E0
1 1 1 1	39	39	.103375E6	.230702E2	.371533E0	.000E0	.371533E0
1 1 1 1	40	40	.103400E6	.231203E2	.369902E0	.000E0	.369902E0
1 1 1 1	41	41	.103425E6	.231704E2	.368254E0	.000E0	.368254E0
1 1 1 1	42	42	.103449E6	.232205E2	.366589E0	.000E0	.366589E0
1 1 1 1	43	43	.103474E6	.232706E2	.364906E0	.000E0	.364906E0
1 1 1 1	44	44	.103498E6	.233207E2	.363207E0	.000E0	.363207E0
1 1 1 1	45	45	.103523E6	.233708E2	.361490E0	.000E0	.361490E0
1 1 1 1	46	46	.103547E6	.234208E2	.359755E0	.000E0	.359755E0
1 1 1 1	47	47	.103572E6	.234709E2	.358003E0	.000E0	.358003E0
1 1 1 1	48	48	.103597E6	.235210E2	.356234E0	.000E0	.356234E0
1 1 1 1	49	49	.103621E6	.235710E2	.354447E0	.000E0	.354447E0
1 1 1 1	50	50	.103646E6	.236211E2	.352641E0	.000E0	.352641E0
1 1 1 1	51	51	.103670E6	.236711E2	.350818E0	.000E0	.350818E0
1 1 1 1	52	52	.103695E6	.237211E2	.348977E0	.000E0	.348977E0
1 1 1 1	53	53	.103720E6	.237711E2	.347118E0	.000E0	.347118E0
1 1 1 1	54	54	.103744E6	.238212E2	.345240E0	.000E0	.345240E0
1 1 1 1	55	55	.103763E6	.238587E2	.343819E0	.000E0	.343819E0
1 1 1 1	56	56	.103775E6	.238837E2	.342866E0	.000E0	.342866E0
1 1 1 1	57	57	.103788E6	.239087E2	.341908E0	.000E0	.341908E0
1 1 1 1	58	58	.103800E6	.239337E2	.340945E0	.000E0	.340945E0
1 1 1 1	59	59	.103812E6	.239586E2	.339978E0	.000E0	.339978E0
1 1 1 1	60	60	.103824E6	.239836E2	.339006E0	.000E0	.339006E0
1 1 1 1	61	61	.103837E6	.240086E2	.338029E0	.000E0	.338029E0
1 1 1 1	62	62	.103849E6	.240336E2	.337048E0	.000E0	.337048E0

P. C. Lichtner

SCIENTIFIC NOTEBOOK

INITIALS:

PC

1 1 1 1	63	63	.103861E6	.240586E2	.336062E0	.000E0	.336062E0
1 1 1 1	64	64	.103874E6	.240836E2	.335071E0	.000E0	.335071E0
1 1 1 1	65	65	.103886E6	.241086E2	.334076E0	.000E0	.334076E0
1 1 1 1	66	66	.103898E6	.241335E2	.333076E0	.000E0	.333076E0
1 1 1 1	67	67	.103911E6	.241585E2	.332071E0	.000E0	.332071E0
1 1 1 1	68	68	.103923E6	.241835E2	.331061E0	.000E0	.331061E0
1 1 1 1	69	69	.103935E6	.242085E2	.330047E0	.000E0	.330047E0
1 1 1 1	70	70	.103947E6	.242334E2	.329028E0	.000E0	.329028E0
1 1 1 1	71	71	.103960E6	.242584E2	.328004E0	.000E0	.328004E0
1 1 1 1	72	72	.103972E6	.242834E2	.326975E0	.000E0	.326975E0
1 1 1 1	73	73	.103981E6	.243021E2	.326200E0	.000E0	.326200E0
1 1 1 1	74	74	.103988E6	.243146E2	.325682E0	.000E0	.325682E0
1 1 1 1	75	75	.103994E6	.243270E2	.325163E0	.000E0	.325163E0
1 1 1 1	76	76	.104000E6	.243395E2	.324642E0	.000E0	.324642E0
1 1 1 1	77	77	.104006E6	.243520E2	.324121E0	.000E0	.324121E0
1 1 1 1	78	78	.104012E6	.243645E2	.323598E0	.000E0	.323598E0
1 1 1 1	79	79	.104018E6	.243770E2	.323074E0	.000E0	.323074E0
1 1 1 1	80	80	.104025E6	.243894E2	.322548E0	.000E0	.322548E0
1 1 1 1	81	81	.104031E6	.244019E2	.322022E0	.000E0	.322022E0
1 1 1 1	82	82	.104037E6	.244144E2	.321494E0	.000E0	.321494E0
1 1 1 1	83	83	.104043E6	.244269E2	.320965E0	.000E0	.320965E0
1 1 1 1	84	84	.104049E6	.244393E2	.320435E0	.000E0	.320435E0
1 1 1 1	85	85	.104055E6	.244518E2	.319903E0	.000E0	.319903E0
1 1 1 1	86	86	.104061E6	.244643E2	.319371E0	.000E0	.319371E0
1 1 1 1	87	87	.104066E6	.244736E2	.318971E0	.000E0	.318971E0
1 1 1 1	88	88	.104069E6	.244799E2	.318703E0	.000E0	.318703E0
1 1 1 1	89	89	.104072E6	.244861E2	.318436E0	.000E0	.318436E0
1 1 1 1	90	90	.104075E6	.244923E2	.318168E0	.000E0	.318168E0
1 1 1 1	91	91	.104078E6	.244986E2	.317900E0	.000E0	.317900E0
1 1 1 1	92	92	.104081E6	.245048E2	.317631E0	.000E0	.317631E0
1 1 1 1	93	93	.104085E6	.245111E2	.317362E0	.000E0	.317362E0
1 1 1 1	94	94	.104088E6	.245173E2	.317093E0	.000E0	.317093E0
1 1 1 1	95	95	.104091E6	.245235E2	.316824E0	.000E0	.316824E0
1 1 1 1	96	96	.104094E6	.245298E2	.316554E0	.000E0	.316554E0
1 1 1 1	97	97	.104097E6	.245360E2	.316284E0	.000E0	.316284E0
1 1 1 1	98	98	.104100E6	.245422E2	.316014E0	.000E0	.316014E0
1 1 1 1	99	99	.104103E6	.245485E2	.315743E0	.000E0	.315743E0
1 1 1 1	100	100	.104106E6	.245547E2	.315472E0	.000E0	.315472E0
1 1 1 1	101	101	.104109E6	.245609E2	.315201E0	.000E0	.315201E0
1 1 1 1	102	102	.104112E6	.245672E2	.314929E0	.000E0	.314929E0
1 1 1 1	103	103	.104115E6	.245734E2	.314658E0	.000E0	.314658E0
1 1 1 1	104	104	.104118E6	.245796E2	.314385E0	.000E0	.314385E0
1 1 1 1	105	105	.104122E6	.245859E2	.314113E0	.000E0	.314113E0
1 1 1 1	106	106	.104124E6	.245921E2	.313840E0	.000E0	.313840E0
1 1 1 1	107	107	.104128E6	.245983E2	.313567E0	.000E0	.313567E0
1 1 1 1	108	108	.104131E6	.246046E2	.313294E0	.000E0	.313294E0
1 1 1 1	109	109	.104134E6	.246108E2	.313020E0	.000E0	.313020E0
1 1 1 1	110	110	.104137E6	.246170E2	.312746E0	.000E0	.312746E0
1 1 1 1	111	111	.104140E6	.246233E2	.312472E0	.000E0	.312472E0
1 1 1 1	112	112	.104143E6	.246295E2	.312197E0	.000E0	.312197E0
1 1 1 1	113	113	.104146E6	.246357E2	.311922E0	.000E0	.311922E0
1 1 1 1	114	114	.104150E6	.246426E2	.311620E0	.000E0	.311620E0
1 1 1 1	115	115	.104153E6	.246488E2	.311344E0	.000E0	.311344E0

P. C. Lichtner

SCIENTIFIC NOTEBOOK

INITIALS: PCZ

1 1 1 1	116	116	.104155E6	.246538E2	.311123E0	.000E0	.311123E0
1 1 1 1	117	117	.104157E6	.246588E2	.310903E0	.000E0	.310903E0
1 1 1 1	118	118	.104160E6	.246638E2	.310682E0	.000E0	.310682E0
1 1 1 1	119	119	.104162E6	.246687E2	.310460E0	.000E0	.310460E0
1 1 1 1	120	120	.104165E6	.246737E2	.310239E0	.000E0	.310239E0
1 1 1 1	121	121	.104167E6	.246787E2	.310017E0	.000E0	.310017E0
1 1 1 1	122	122	.104170E6	.246837E2	.309795E0	.000E0	.309795E0
1 1 1 1	123	123	.104172E6	.246887E2	.309573E0	.000E0	.309573E0
1 1 1 1	124	124	.104174E6	.246924E2	.309406E0	.000E0	.309406E0
1 1 1 1	125	125	.104175E6	.246949E2	.309295E0	.000E0	.309295E0
1 1 1 1	126	126	.104177E6	.246974E2	.309184E0	.000E0	.309184E0
1 1 1 1	127	127	.104178E6	.246999E2	.309073E0	.000E0	.309073E0
1 1 1 1	128	128	.104179E6	.247024E2	.308962E0	.000E0	.308962E0
1 1 1 1	129	129	.104180E6	.247049E2	.308850E0	.000E0	.308850E0
1 1 1 1	130	130	.104181E6	.247074E2	.308739E0	.000E0	.308739E0
1 1 1 1	131	131	.104183E6	.247099E2	.308627E0	.000E0	.308627E0
1 1 1 1	132	132	.104184E6	.247124E2	.308516E0	.000E0	.308516E0
1 1 1 1	133	133	.104185E6	.247149E2	.308404E0	.000E0	.308404E0
1 1 1 1	134	134	.104187E6	.247173E2	.308293E0	.000E0	.308293E0
1 1 1 1	135	135	.104188E6	.247198E2	.308181E0	.000E0	.308181E0
1 1 1 1	136	136	.104189E6	.247223E2	.308069E0	.000E0	.308069E0
1 1 1 1	137	137	.104190E6	.247248E2	.307957E0	.000E0	.307957E0
1 1 1 1	138	138	.104191E6	.247273E2	.307845E0	.000E0	.307845E0
1 1 1 1	139	139	.104193E6	.247298E2	.307734E0	.000E0	.307734E0
1 1 1 1	140	140	.104194E6	.247323E2	.307622E0	.000E0	.307622E0
1 1 1 1	141	141	.104195E6	.247348E2	.307510E0	.000E0	.307510E0
1 1 1 1	142	142	.104196E6	.247373E2	.307398E0	.000E0	.307398E0
1 1 1 1	143	143	.104198E6	.247398E2	.307286E0	.000E0	.307286E0
1 1 1 1	144	144	.104199E6	.247423E2	.307173E0	.000E0	.307173E0
1 1 1 1	145	145	.104200E6	.247448E2	.307061E0	.000E0	.307061E0
1 1 1 1	146	146	.104201E6	.247473E2	.306949E0	.000E0	.306949E0
1 1 1 1	147	147	.104202E6	.247497E2	.306837E0	.000E0	.306837E0
1 1 1 1	148	148	.104204E6	.247522E2	.306725E0	.000E0	.306725E0
1 1 1 1	149	149	.104205E6	.247547E2	.306612E0	.000E0	.306612E0
1 1 1 1	150	150	.104206E6	.247572E2	.306500E0	.000E0	.306500E0
1 1 1 1	151	151	.104207E6	.247597E2	.306387E0	.000E0	.306387E0
1 1 1 1	152	152	.104209E6	.247622E2	.306275E0	.000E0	.306275E0
1 1 1 1	153	153	.104210E6	.247647E2	.306162E0	.000E0	.306162E0
1 1 1 1	154	154	.104211E6	.247672E2	.306050E0	.000E0	.306050E0
1 1 1 1	155	155	.104212E6	.247697E2	.305937E0	.000E0	.305937E0
1 1 1 1	156	156	.104214E6	.247734E2	.305768E0	.000E0	.305768E0
1 1 1 1	157	157	.104217E6	.247784E2	.305542E0	.000E0	.305542E0
1 1 1 1	158	158	.104219E6	.247834E2	.305316E0	.000E0	.305316E0
1 1 1 1	159	159	.104222E6	.247884E2	.305090E0	.000E0	.305090E0
1 1 1 1	160	160	.104224E6	.247933E2	.304864E0	.000E0	.304864E0
1 1 1 1	161	161	.104226E6	.247983E2	.304638E0	.000E0	.304638E0
1 1 1 1	162	162	.104229E6	.248033E2	.304411E0	.000E0	.304411E0
1 1 1 1	163	163	.104231E6	.248083E2	.304184E0	.000E0	.304184E0
1 1 1 1	164	164	.104234E6	.248133E2	.303957E0	.000E0	.303957E0
1 1 1 1	165	165	.104236E6	.248182E2	.303730E0	.000E0	.303730E0
1 1 1 1	166	166	.104239E6	.248232E2	.303503E0	.000E0	.303503E0
1 1 1 1	167	167	.104242E6	.248288E2	.303247E0	.000E0	.303247E0
1 1 1 1	168	168	.104245E6	.248351E2	.302962E0	.000E0	.302962E0

P. C. Lichtner

SCIENTIFIC NOTEBOOK

INITIALS: SCZ

1 1 1 1	169	169	.104248E6	.248413E2	.302677E0	.000E0	.302677E0
1 1 1 1	170	170	.104251E6	.248475E2	.302391E0	.000E0	.302391E0
1 1 1 1	171	171	.104254E6	.248538E2	.302106E0	.000E0	.302106E0
1 1 1 1	172	172	.104257E6	.248600E2	.301820E0	.000E0	.301820E0
1 1 1 1	173	173	.104260E6	.248662E2	.301533E0	.000E0	.301533E0
1 1 1 1	174	174	.104263E6	.248724E2	.301246E0	.000E0	.301246E0
1 1 1 1	175	175	.104266E6	.248787E2	.300960E0	.000E0	.300960E0
1 1 1 1	176	176	.104269E6	.248849E2	.300672E0	.000E0	.300672E0
1 1 1 1	177	177	.104272E6	.248911E2	.300385E0	.000E0	.300385E0
1 1 1 1	178	178	.104276E6	.248973E2	.300097E0	.000E0	.300097E0
1 1 1 1	179	179	.104279E6	.249036E2	.299808E0	.000E0	.299808E0
1 1 1 1	180	180	.104282E6	.249098E2	.299520E0	.000E0	.299520E0
1 1 1 1	181	181	.104285E6	.249160E2	.299231E0	.000E0	.299231E0
1 1 1 1	182	182	.104288E6	.249222E2	.298942E0	.000E0	.298942E0
1 1 1 1	183	183	.104291E6	.249284E2	.298652E0	.000E0	.298652E0
1 1 1 1	184	184	.104294E6	.249347E2	.298363E0	.000E0	.298363E0
1 1 1 1	185	185	.104297E6	.249409E2	.298073E0	.000E0	.298073E0
1 1 1 1	186	186	.104300E6	.249471E2	.297782E0	.000E0	.297782E0
1 1 1 1	187	187	.104303E6	.249533E2	.297492E0	.000E0	.297492E0
1 1 1 1	188	188	.104306E6	.249596E2	.297200E0	.000E0	.297200E0
1 1 1 1	189	189	.104309E6	.249658E2	.296909E0	.000E0	.296909E0
1 1 1 1	190	190	.104314E6	.249751E2	.296471E0	.000E0	.296471E0
1 1 1 1	191	191	.104320E6	.249876E2	.295887E0	.000E0	.295887E0
1 1 1 1	192	192	.104326E6	.250000E2	.295301E0	.000E0	.295301E0
1 1 1 1	193	193	.104333E6	.250125E2	.294714E0	.000E0	.294714E0
1 1 1 1	194	194	.104339E6	.250249E2	.294126E0	.000E0	.294126E0
1 1 1 1	195	195	.104345E6	.250373E2	.293537E0	.000E0	.293537E0
1 1 1 1	196	196	.104351E6	.250498E2	.292946E0	.000E0	.292946E0
1 1 1 1	197	197	.104357E6	.250622E2	.292354E0	.000E0	.292354E0
1 1 1 1	198	198	.104363E6	.250747E2	.291761E0	.000E0	.291761E0
1 1 1 1	199	199	.104370E6	.250871E2	.291166E0	.000E0	.291166E0
1 1 1 1	200	200	.104376E6	.250996E2	.290570E0	.000E0	.290570E0
1 1 1 1	201	201	.104382E6	.251120E2	.289973E0	.000E0	.289973E0
1 1 1 1	202	202	.104388E6	.251244E2	.289375E0	.000E0	.289375E0
1 1 1 1	203	203	.104394E6	.251369E2	.288775E0	.000E0	.288775E0
1 1 1 1	204	204	.104400E6	.251493E2	.288175E0	.000E0	.288175E0
1 1 1 1	205	205	.104407E6	.251617E2	.287573E0	.000E0	.287573E0
1 1 1 1	206	206	.104416E6	.251804E2	.286667E0	.000E0	.286667E0
1 1 1 1	207	207	.104428E6	.252053E2	.285456E0	.000E0	.285456E0
1 1 1 1	208	208	.104440E6	.252301E2	.284239E0	.000E0	.284239E0
1 1 1 1	209	209	.104453E6	.252550E2	.283018E0	.000E0	.283018E0
1 1 1 1	210	210	.104465E6	.252798E2	.281792E0	.000E0	.281792E0
1 1 1 1	211	211	.104477E6	.253047E2	.280560E0	.000E0	.280560E0
1 1 1 1	212	212	.104490E6	.253295E2	.279324E0	.000E0	.279324E0
1 1 1 1	213	213	.104508E6	.253668E2	.277460E0	.000E0	.277460E0
1 1 1 1	214	214	.104533E6	.254165E2	.274958E0	.000E0	.274958E0
1 1 1 1	215	215	.104557E6	.254662E2	.272436E0	.000E0	.272436E0
1 1 1 1	216	216	.104582E6	.255158E2	.269893E0	.000E0	.269893E0
1 1 1 1	217	217	.104607E6	.255655E2	.267331E0	.000E0	.267331E0
1 1 1 1	218	218	.104632E6	.256151E2	.264748E0	.000E0	.264748E0
1 1 1 1	219	219	.104656E6	.256647E2	.262145E0	.000E0	.262145E0
1 1 1 1	220	220	.104681E6	.257143E2	.259523E0	.000E0	.259523E0
1 1 1 1	221	221	.104706E6	.257639E2	.256880E0	.000E0	.256880E0

P. C. Lichtner

SCIENTIFIC NOTEBOOK

INITIALS: SC

```

1 1 1 1 222 222 .104730E6 .258135E2 .254218E0 .000E0 .254218E0
1 1 1 1 223 223 .104774E6 .259002E2 .249514E0 .000E0 .249514E0
1 1 1 1 224 224 .104835E6 .260241E2 .242693E0 .000E0 .242693E0
1 1 1 1 225 225 .104897E6 .261478E2 .235751E0 .000E0 .235751E0
1 1 1 1 226 226 .104959E6 .262715E2 .228690E0 .000E0 .228690E0
1 1 1 1 227 227 .105021E6 .263951E2 .221513E0 .000E0 .221513E0
1 1 1 1 228 228 .105082E6 .265186E2 .214222E0 .000E0 .214222E0
1 1 1 1 229 229 .105175E6 .267036E2 .203090E0 .000E0 .203090E0
1 1 1 1 230 230 .105299E6 .269500E2 .187904E0 .000E0 .187904E0
1 1 1 1 231 231 .105423E6 .271960E2 .172358E0 .000E0 .172358E0
1 1 1 1 232 232 .105547E6 .274417E2 .156519E0 .000E0 .156519E0
1 1 1 1 233 233 .105671E6 .276870E2 .140470E0 .000E0 .140470E0
1 1 1 1 234 234 .105858E6 .280539E2 .116262E0 .000E0 .116262E0
1 1 1 1 235 235 .106108E6 .285422E2 .844672E-01 .000E0 .844672E-01
1 1 1 1 236 236 .106360E6 .290291E2 .546125E-01 .000E0 .546125E-01
1 1 1 1 237 237 .106615E6 .295149E2 .287428E-01 .000E0 .287428E-01
1 1 1 1 238 238 .106881E6 .300000E2 .945630E-02 .000E0 .945630E-02

```

0

Recurrent-data

Output A=1 C=1

: isolv newtnmn newtnmx

Solve 1 2 12

:AUTO-step DPMXE DSMXE DTMPMXE DP2MXe

AUTO-step 1.0E+3 0.03 5.0 1.e3

:

:TOLR TOLP TOLS TOLT TOLP2 TOLM TOLA TOLE

Tolr 10. 1.e-4 1.e-3 1.e+1 1.e-5 1.e-3 1.e-3 0. 0. 0.

:

:Limit dpmx dsmx dtmpmx dp2mx dtmn dtmx icutmx

LIMIT 1.e4 .08 10. 1.e5 1.e-5 1.e4

Plots 1

:Time[y] 1.

:Steady[y] 1.e-4 1.e-3 1.e-5

: ns fach facm (fach and facm are multipliers to
: read-in values of qht and qmt)

Source 1 0.701754386 1.

: is js ks istyp

1 1 135 3

: timeq(sec) T/qht (C/(J/s)) qmt (kg/s)

0.0000E+00 8.8496E+01

6.3115E+07 8.2633E+01

1.2623E+08 7.7981E+01

1.8935E+08 7.4163E+01

2.5246E+08 7.1040E+01

3.1558E+08 6.8186E+01

4.7336E+08 6.2075E+01

6.3115E+08 5.6842E+01

9.4673E+08 4.8249E+01

1.2623E+09 4.1445E+01

1.5779E+09 3.5976E+01

2.3668E+09 2.6482E+01

3.1558E+09 2.1048E+01

4.7336E+09 1.5485E+01

P. C. Lichtner

SCIENTIFIC NOTEBOOK

INITIALS: PCZ

```

6.3115E+09 1.2543E+01
9.4673E+09 1.0050E+01
1.2623E+10 8.6186E+00
1.5779E+10 7.5046E+00
1.8935E+10 6.5329E+00
2.5246E+10 5.2449E+00
3.1558E+10 4.4154E+00
3.9447E+10 3.6166E+00
4.7336E+10 3.0717E+00
6.3115E+10 2.3765E+00
7.8894E+10 2.0768E+00
9.4673E+10 1.8615E+00
1.2623E+11 1.6721E+00
1.5779E+11 1.5382E+00
1.8935E+11 1.4113E+00
2.2090E+11 1.3122E+00
2.5246E+11 1.2319E+00
2.8402E+11 1.1652E+00
3.1558E+11 1.1082E+00
3.4713E+11 1.0203E+00
3.7869E+11 9.4619E-01
4.1025E+11 8.8277E-01
4.4181E+11 8.2784E-01
4.7336E+11 7.7977E-01
5.5226E+11 6.8222E-01
6.3115E+11 6.0763E-01
7.8894E+11 5.0073E-01
9.4673E+11 4.2746E-01
1.2623E+12 3.0564E-01
1.5779E+12 2.3054E-01
1.8935E+12 1.7733E-01
2.2090E+12 1.4204E-01
2.5246E+12 1.1720E-01
2.8402E+12 9.8926E-02
3.1558E+12 8.5011E-02
4.7336E+12 6.1731E-02
0
Output  A=1  C=1
:
SKIP
Bcon  2
1  TOP    1  1  1  1  0.  1.e5  25.0  0.5  0.
1  BOTTOM  1  1  1  1  0.  1.e5  25.0  0.5  0.
NOSKIP
:
:Limit dpmx    dsmx dtmpmx dp2mx dtmn dtmx icutmx
LIMIT 1.e5    .08   10.   1.e5  1.e-5 5.e4
:
:Output  A=1 C=1
:      target dt    dpmx  dsmx  dp2mx  dtmpmx
:
:      print all at every target time
:Skip

```

PLOTS 1 6 7 20 47 70 87 135

Time[y] 10.
 Time[y] 100.
 Time[y] 1000.
 Time[y] 10000.
 Time[y] 50000.
 Time[y] 100000.
 Ends

The GEM input file `gem.in` contains the operator splitting form of MULTIFLO:

'calcite-quartz dissolution'

'idata	istart	iplot	ifor	modes	iflux	iact	ifindzb	loglin'
0	0	1	4	2 2	1	0	0	0

'itmax	ihalmax	ivmax	id	imod	iprint	iexact	iscale	istat'
12	32	4	1	10	-1	0	0	0

'istdst	isurf	ijac	ijacnum	icon	idif	ndamp'
0	0	1	0	1	0	0

'isync	ipor	iperm	perm. fac.'
4	0	0	3.0

'iplot: a	s	t	m	s	i	s	f	v	z	b	i	n	e	e	x	t	i	g	i	t	e	r'
1	1	1	1	0	0	1	0	0	0	0	0	0	0	0	1	1						

'tol	ttol	tolneg	tolpos	tolexp	dthalf	qkmax	tolstdste'
1.d-12	2.	1.e-2	1.e-2	5.d0	0.25	590.d0	1.e-4

'	mcyc	cc	c	r	sp	qk	pk	rk	a1	a2	a3'
'test'	0	1	1	1	1	1	1	1	0	0	0

'por0	phir	sat	w	lambda	toltrf	toldelt	tolpor'
0.1	1.0	0.5	0.5	1.0	0.	1.e3	1.e-3

'vx0	vy0	vz0[m/yr]	alphax	alphay	alphaz	cournr'
10.0	0.0	0.0	0.	0.	0.	0.5

'd0[cm^2/s]	delhaq[kJ/mol]	dgas[cm^2/s]	dgexp	tortaq	tortg'
1.d-5	12.6	2.13d-1	1.8d0	0.5	0.5

'flag 1: T(x) = d x^3 + a x^2 + b x + c (meters)'
 ' 2: T(x) = a + (b-a) exp[-((x-x0)/c)^2] + (d - a) * x / xlen'
 ' 3: T(x,t)=a+1/2(b-a)(erf[(x+c-x0)/2sqr(dt)]-erf[(x-c-x0)/2sqr(dt)])'
 'p (bars) temp flag a b c d x0 xlen'
 1.0e0 30. 0 25.d0 300.d0 250.d0 125.d0 1000.d0 2.d3

'master species'

'h+'

'grid' 'm' 0. 1 50 1.0

```

'nx dx:' 50 50*0.02
'ny dy:' 1 1*0.02
'nz dz:' 1 1*1.0

'igem2d 1-D,2,3 isat isotherm iread'
      3      0      1      0

'level north nitmax idetail isolve rmaxtol rtwotol smaxtol'
      1      1     100      0      3  1.e-25 1.e-25 1.e-12

'initial and boundary conditions: 1-conc., 2-flux, 3-zero gradient'
'inlet outlet nzoneaq'
      1      3      3

'init'
'species      itype  guess  ctot   mineral diffusion coeff.'
'ca+2'        1      2.9e-4 2.9e-4 ' '      0.8e-5
'na+'         1      2.e-3  2.e-3  ' '      0.8e-5
'k+'          1      1.4e-4 1.e-4  ' '      0.8e-5
'h+'          8      1.e-7  6.9   ' '      9.6e-5
'hco3-'       7      2.7e-3 2.7e-3 ' '      2.0e-5
'sio2(aq)'    1      1.1e-3 1.1e-3 ' '      1.4e-5
'cl-'         1      1.8e-4 1.8e-4 ' '      1.4e-5
'*'           0      0.     0.    ' '      0.

'boundary conditions: inlet' 1 3
'species      itype  guess  ctot   mineral'
'ca+2'        1      2.9e-4 2.9e-4 ' '      0.8e-5
'na+'         1      2.e-3  2.e-3  ' '      0.8e-5
'k+'          1      1.4e-4 1.e-4  ' '      0.8e-5
'h+'          8      1.e-7  6.9   ' '      9.6e-5
'hco3-'       7      2.7e-3 2.7e-3 ' '      2.0e-5
'sio2(aq)'    1      1.1e-3 1.1e-3 ' '      1.4e-5
'cl-'         1      1.8e-4 1.8e-4 ' '      1.4e-5

'boundary conditions: outlet' 2 3
'species      itype  guess  ctot   mineral'
'ca+2'        1      2.9e-4 2.9e-4 ' '      0.8e-5
'na+'         1      2.e-3  2.e-3  ' '      0.8e-5
'k+'          1      1.4e-4 1.e-4  ' '      0.8e-5
'h+'          8      1.e-7  6.9   ' '      9.6e-5
'hco3-'       7      2.7e-3 2.7e-3 ' '      2.0e-5
'sio2(aq)'    1      1.1e-3 1.1e-3 ' '      1.4e-5
'cl-'         1      1.8e-4 1.8e-4 ' '      1.4e-5

'end of data' 0 0

'irreversible species diffusion coef. [cm^2/s]      ncorraq ncxkin'
'label itype guess ctot mineral'                  0      0
'*'      0.

'species tolerance'
8*1.e-0

```

'aqueous complexes'

```
'oh-'          5.5e-5
'co2(aq)'      2.5e-5
'co3-2'        2.5e-5
'caco3(aq)'
'cahco3+'
'caoh+'
'cacl+'
'cacl2(aq)'
'nahco3(aq)'
'nacl(aq)'
'naoh(aq)'
'kcl(aq)'
'h3sio4-'
'h2sio4-2'
'*' 0.
```

'minerals'

```
'quartz'
'calcite'
'halite'
'natron'
'natrosilite' <na2si2o5>
'na2sio3'
'na4sio4'
'nahcolite'
'na2co3'
'*
```

'gases'

```
'co2(g)'
'*
```

'irr mineral	itypkin	beta	fkin	delh	rkph	rk	tau'
'z1 z2	vol	area'					
'quartz'	0	1.0	1.0	75.	0.	1.e-17	1.e-3
1 238 1 1 1 1	0.9	1.					
0 1 1 1 1 1	0.	0.					
'calcite'	0	1.0	1.0	35.	0.	1.e-10	1.e-3
1 238 1 1 1 1	0.	1.					
0 1 1 1 1 1	0.	0.					
'halite'	0	1.0	1.0	30.	0.	1.e-12	1.e-3
1 238 1 1 1 1	0.	1.					
0 1 1 1 1 1	0.	0.					
'nahcolite'	0	1.0	1.0	30.	0.	1.e-12	1.e-3
1 238 1 1 1 1	0.	1.					
0 1 1 1 1 1	0.	0.					
'natrosilite'	0	1.0	1.0	30.	0.	1.e-12	1.e-3
1 238 1 1 1 1	0.	1.					
0 1 1 1 1 1	0.	0.					
'*'	0	1.0	1.0	0.	0.	3.16e-16	1.e-2

'surface mineral itypkin area beta fkin delh rkph rk'


```

'*'          0      1.0      1.0      1.      0.      0.      0.

'corrsion solids      i0      acorr      bcorr      epot0 [V]'
'*'                  0.      0.      0.      0.

'crevice gap[meters]      potential [v]'
90.d-6                  -0.2

'electrochemical aqueous species      i0      acorr      bcorr      epot0[v] tol'
'*'                                0.      0.      0.      0.      1.e-8

'irreversible aqueous species aq cmplx: beta      fkin      delh      rkf'
'*'          1.      1.0      0.      0.

'ion-exchange reactions'
0      1.0

'time' 'y' 12 10. 25. 50. 100. 500. 1000. 5000. 10000. 25000. 50000. 75000. 100000.

'timestep[y]' 1 3.e-9
1.e-9      100.

'break-through pts.' 0
93 110 130 150 185

```

ABSTRACT

A numerical model MULTIFLO is developed for describing reactive transport in a multiphase-multicomponent, nonisothermal, partially saturated porous medium. The model includes chemical reactions between aqueous, gaseous and solid phases. Reactions involving minerals are considered to be irreversible and described through appropriate kinetic rate laws. Homogeneous reactions within the aqueous phase and heterogeneous reactions between aqueous and gaseous phases are assumed to be reversible, their reaction rates controlled by transport and local equilibrium mass action relations. Flow of aqueous and gaseous phases is described by Darcy's law in a partially saturated porous medium. Solute transport includes contributions from advection, diffusion and dispersion. Enhanced binary diffusion of water vapor for transport in a two-phase system is taken into account. A sequentially coupled scheme is used to couple transport of water, air and heat to solute and minor gas components, and solids. Changes in porosity and permeability caused by chemical reactions are coupled to the flow field. Several options are available for solving numerically the transport equations including fully implicit, explicit and operator splitting methods. A Leonard-TVD scheme is used for describing high Peclet number flows. Mineral mass transfer equations are solved explicitly using the quasi-stationary state approximation. The coupled flow and transport model is applied to the proposed high-level

nuclear waste storage facility located in unsaturated rock at Yucca Mountain, Nevada. A repository-scale model is used to calculate the redistribution of moisture, heat, and various chemical constituents caused by the thermal perturbation produced by the waste.

INTRODUCTION

Of potentially fundamental importance to the longevity of a waste canister in a high-level waste (HLW) repository is the chemical composition of groundwater in the near-field region which could potentially come in contact with the container. This includes environmental variables defining the oxidation state, pH, chloride concentration, and other compositional variables of ingressing fluid which may impact the waste container and waste form. Depending on the composition of this fluid, the rate of corrosion and leaching of spent fuel could be greatly accelerated or inhibited.

A number of authors have presented model calculations of the redistribution of moisture resulting from the emplacement of nuclear waste at the proposed Yucca Mountain (YM) HLW site in Nevada (Buscheck and Nitao, 1993; Pruess and Tsang, 1993). These calculations indicate that heat produced from the waste creates a dryout zone surrounding the repository with enhanced zones of saturation above and below the repository horizon caused by condensation of water vapor. The degree of dryness and time to rewet the repository depends on the heat load of the radioactive waste.

Unique to an unsaturated repository design concept is the possible increase in salinity of liquid water in the near-field region caused by continuous evaporation of water resulting from heat produced by the waste canisters. The amount of water that can be evaporated depends not only on the initial saturation of the pore spaces in the rock adjacent to the canisters, but also on the flow of water towards the waste packages resulting from capillary forces and gravity driven flow. Salts could form both on the waste package and in the near field as a result of evaporation (Walton, 1993). Degradation of cement could result in the formation of hyperalkaline fluids which would react strongly with the silicate host rock producing calcium silicate hydrates and affect the sorption characteristics of the near field.

The purpose of this work is two-fold. The first is to present a general formulation of multicomponent-multiphase nonisothermal reactive transport model applicable to partially saturated porous media. The second is to apply the model to the proposed high-level nuclear waste storage facility at YM, Nevada.

REACTIVE MASS AND HEAT TRANSPORT IN HYDROTHERMAL SYSTEMS

In this section equations are developed to describe flow and transport in a nonisothermal, multiphase-multicomponent system. Darcy's law is used to describe flow of liquid

and gas phases in a partially saturated porous medium. Chemically reacting species may be present in the aqueous, gaseous or solid phases. The transport equations for solute and gaseous species include advection and diffusion/dispersion. Mineral reactions are assumed to be irreversible, described through a kinetic rate law. Homogeneous reactions within the aqueous phase and heterogeneous reactions between the aqueous and gaseous phases are assumed to obey conditions of local chemical equilibrium. Note that contrary to statements by White (1995) the rates of reactions in local equilibrium do not vanish, but are governed by solute transport and appropriate mass action equations.

Chemical reactions taking place in the system consisting of N species are written in terms of a basic set of N_c independent species, or components, referred to as primary species denoted by the set $\{B_j; j = 1, \dots, N_c\}$. The remaining $N - N_c$ species are referred to as secondary species. The primary species may be aqueous or gaseous species depending on the phases present. For a general geochemical system consisting of N_l aqueous and N_g gaseous secondary species, and N_m minerals, the chemical reactions can be expressed in the canonical form (Lichtner, 1985):

$$\sum_{j=1}^{N_c} \nu_{ji}^l B_j \rightleftharpoons \mathcal{A}_i^l; \quad (i = 1, \dots, N_l), \quad (1)$$

for aqueous species \mathcal{A}_i^l :

$$\sum_{j=1}^{N_c} \nu_{ji}^g B_j \rightleftharpoons \mathcal{A}_i^g; \quad (i = 1, \dots, N_g), \quad (2)$$

for gaseous species \mathcal{A}_i^g , and for minerals \mathcal{M}_m :

$$\sum_{j=1}^{N_c} \nu_{jm} B_j \rightleftharpoons \mathcal{M}_m; \quad (i = 1, \dots, N_m). \quad (3)$$

The matrices ν_{ji}^l , ν_{ji}^g , and ν_{jm} denote the stoichiometric reaction coefficients giving the number of moles of the j th primary species in one mole of the i th secondary species corresponding to aqueous, gaseous and mineral species, respectively. Each reaction is associated with a single secondary species with unit stoichiometric coefficient. A species is distinguished by its chemical formula and the phase to which it belongs. Reactions (1) and (2) are considered to be reversible representing conditions of local equilibrium.

A special role is played by the solvent species H_2O , which is generally in much greater abundance than all other species (with notable exceptions). For the gas phase, both

nitrogen (referred to here simply as air) and water vapor are considered to be the dominant gas species. Reactions involving water vapor and nitrogen are



representing a phase change of water from liquid to gas describing evaporation, condensation and boiling, and partitioning of air between the aqueous and gas phases:



The species water in the aqueous or gaseous phase ($\text{H}_2\text{O}_{(l,g)}$) is always chosen as a primary species. The remaining primary species may be any independent set of species which conveniently characterize the chemical properties of the system under investigation. In what follows they are chosen to be a subset of the aqueous or gaseous species. Minerals are not used as primary species because any given mineral may not be present over the entire computational domain. Aqueous primary species are used for pure liquid and two-phase systems, and gaseous primary species for pure gas phase systems. For systems in which both single and two-phase regions are possible, basis switching is necessary at the boundary of a pure liquid or two-phase region and a pure gas phase region.

Multiphase-Multicomponent Mass Transport Equations

Taking into account chemical reactions in the form represented by Eqns.(1), (2) and (3), the mass and energy transport equations have the following form for the H_2O component (w)

$$\begin{aligned} \frac{\partial}{\partial t} \left[\phi \left(s_l n_l X_w^l + s_g n_g X_w^g \right) \right] + \nabla \cdot \left(\mathbf{q}_l n_l X_w^l + \mathbf{q}_g n_g X_w^g - D_g^{\text{eff}} n_g \nabla X_w^g \right) = \\ - \sum_{m=1}^{N_m} \nu_{wm} I_m + Q_w, \end{aligned} \quad (6)$$

for the air component (a):

$$\begin{aligned} \frac{\partial}{\partial t} \left[\phi \left(s_l n_l X_a^l + s_g n_g X_a^g \right) \right] + \nabla \cdot \left(\mathbf{q}_l n_l X_a^l + \mathbf{q}_g n_g X_a^g - D_g^{\text{eff}} n_g \nabla X_a^g \right) = \\ - \sum_{m=1}^{N_m} \nu_{am} I_m + Q_a, \end{aligned} \quad (7)$$

and for the energy balance equation:

$$\begin{aligned} \frac{\partial}{\partial t} \left[\phi \left(s_l n_l U_l + s_g n_g U_g \right) \right] + \nabla \cdot \left(\mathbf{q}_l n_l H_l + \mathbf{q}_g n_g H_g \right) \\ + \frac{\partial}{\partial t} \left[(1 - \phi) C_p^{\text{rock}} \rho_{\text{rock}} T \right] - \nabla \cdot \kappa \nabla T = Q_e. \end{aligned} \quad (8)$$

In these equations $n_{l,g}$ denotes the density of liquid and gas phases, on a molar basis, and $X_{w,a}^{l,g}$ the mole fraction of water and air in the liquid and gas phases, respectively. The quantities $Q_{w,a}$, and Q_e added to the right hand sides of the transport equations represent source terms in addition to the chemical reaction terms. Diffusion of water in the aqueous phase is neglected. The liquid (l) and gas (g) phases occupy fractions s_l and s_g , respectively, with

$$s_l + s_g = 1. \quad (9)$$

The velocity of phase π , \mathbf{q}_π , is determined by Darcy's law:

$$\mathbf{q}_\pi = -\frac{kk_{r\pi}}{\mu_\pi} \nabla (p_\pi - \rho_\pi g z), \quad (10)$$

where k refers to the saturated permeability of the porous medium, $k_{r\pi}$ represents the relative permeability and μ_π the viscosity of phase π , g denotes the acceleration of gravity, and z the vertical height. The temperature is denoted by T , U_π represents the total internal energy and H_π the total enthalpy of the π th fluid phase, C_p the heat capacity, and κ the thermal conductivity. Heat produced by chemical reactions is ignored. The effective binary gas diffusion coefficient is defined in terms of temperature, pressure and material properties by

$$D_g^{\text{eff}} = \omega \tau \phi s_g D_g^0 \frac{p_0}{p} \left[\frac{T + T_0}{T_0} \right]^\theta, \quad (11)$$

where T_0 , p_0 denote reference temperature and pressure, θ is an empirical constant, and ω is an enhancement factor (Walton and Lichtner, 1995). The enhancement factor is inversely proportional to the gas saturation s_g which thus cancels from the expression for the effective gas diffusion coefficient.

The transport equations for aqueous and gaseous primary species, taking into account local equilibrium of homogeneous reactions within the aqueous and gaseous phases and heterogeneous reactions between these phases, have the form

$$\frac{\partial}{\partial t} (\phi \Psi_j) + \nabla \cdot \mathbf{\Omega}_j = - \sum_{m=1}^{N_m} \nu_{jm} I_m, \quad (12)$$

where the generalized concentration Ψ_j and flux $\mathbf{\Omega}_j$ are defined by

$$\Psi_j = s_l \Psi_j^l + s_g \Psi_j^g, \quad (13)$$

and

$$\mathbf{\Omega}_j = \mathbf{\Omega}_j^l + \mathbf{\Omega}_j^g, \quad (14)$$

with

$$\Psi_j^l = \delta_{\pi_j l} C_j^l + \sum_{i=1}^{N_c^l} \nu_{ji}^l C_i^l, \quad \Psi_j^g = \delta_{\pi_j g} C_j^g + \sum_{i=1}^{N_c^g} \nu_{ji}^g C_i^g, \quad (15)$$

and

$$\Omega_j^l = \delta_{\pi_j l} \mathbf{J}_j^l + \sum_{i=1}^{N_c^l} \nu_{ji}^l \mathbf{J}_i^l, \quad \Omega_j^g = \delta_{\pi_j g} \mathbf{J}_j^g + \sum_{i=1}^{N_c^g} \nu_{ji}^g \mathbf{J}_i^g, \quad (16)$$

where $\pi_j = l, g$ depending on whether the j th primary species belongs to the liquid or gas phase. The kronecker delta function appears in Eqns.(15) and (16) because any particular primary species can belong to only one phase. Here C_i^π and \mathbf{J}_i^π denote the concentration and flux of the i th species in the π th phase, ϕ_m and \bar{V}_m denote the volume fraction and molar volume, respectively, of the m th mineral, and the reaction rates of the various reactions taking place in the system appear as source/sink terms on the right hand side. The liquid flux \mathbf{J}_j^l appearing in these equations is defined by

$$\mathbf{J}_i^l = -\phi \tau s_l D_l \nabla C_i^l + \mathbf{q}_l C_i^l, \quad (17)$$

and the gas flux by the equation

$$\mathbf{J}_i^g = -\phi \tau s_g D_g \nabla C_i^g + \mathbf{q}_g C_i^g, \quad (18)$$

where D_π denotes the diffusion coefficient in phase π . For species-independent diffusion coefficients the solute flux Ω_j^π simplifies to the expression

$$\Omega_j^\pi = (-\tau \phi s_\pi D_\pi \nabla + \mathbf{q}_\pi) \Psi_j^\pi, \quad (19)$$

involving directly the generalized concentration Ψ_j^π .

The mineral mass transfer equations are given by

$$\frac{\partial \phi_m}{\partial t} = \bar{V}_m I_m, \quad (20)$$

written in terms of the mineral volume fraction ϕ_m , where \bar{V}_m denotes the mineral molar volume.

These equations are completely general and include both the solvent and solute species, and gases. Solving the solute and gas mass conservation equations provides not only the concentrations of both primary and secondary species, but also the mineral reaction rates. Combined with mineral mass transfer equations, an energy balance equation, constitutive relations for rock properties, kinetic rate laws and mass action

relations, and finally initial and boundary conditions, they completely describe the system.

Constitutive Relations

Rock Properties. Capillary pressure and relative permeability are related to saturation by the van Genuchten relations (van Genuchten, 1980). Vapor pressure lowering may raise the temperature at which liquid water is stable considerably above 100°C. The equivalent continuum model is used to account for highly fractured rock such as characterizes Yucca Mountain tuff (Klavetter and Peters, 1988).

By relating permeability to porosity, it is possible to couple changes in porosity resulting from mineral precipitation and dissolution to the flow field and transport of solutes. One possibility is to assume permeability is coupled to porosity through a power law relation of the form

$$k = k_0 \left(\frac{\phi}{\phi_0} \right)^n. \quad (21)$$

Porosity and mineral volume fractions in turn are related by an equation of the form

$$\phi = 1 - \sum_{m=1}^{N_m} \phi_m. \quad (22)$$

However, this expression is not completely general and may be deceptively simple because no distinction is made between connected and total porosity.

Mass Action Equations. Constitutive relations in the form of mass action equations are required for aqueous and gaseous species. The concentration of aqueous and gaseous secondary species are related to the concentrations of primary species by the equation

$$C_i^\pi = \rho_\pi^{\alpha_\pi} (\gamma_i^\pi)^{-1} K_i^\pi \prod_{j=1}^{N_c} (\gamma_j^\pi C_j^\pi)^{\nu_{ji}^\pi}, \quad (23)$$

where γ_i^π denotes the activity coefficient, K_i^π the equilibrium constant. The quantity α_π accounts for the difference between molality to molarity units, and is defined by

$$\alpha_\pi = \rho_\pi^{\sum_{ji} \nu_{ji}^\pi} - \delta_{\pi l}. \quad (24)$$

The equilibrium constants K_i^π are in general functions of temperature and pressure.

Kinetic Rate Law. Mineral reactions are assumed to be irreversible, their reaction rates described through a kinetic rate law. For simplicity and because of lack of knowledge of detailed reaction mechanisms, mineral reactions are represented by an overall reaction between the solid and aqueous solution. The form of the reaction rate

is based on transition state theory. Precipitation or dissolution may occur depending on the sign of the affinity \mathbf{A}_m of the reaction, defined by

$$\mathbf{A}_m = -RT \ln K_m Q_m, \quad (25)$$

with equilibrium constant K_m , gas constant R , and Q_m the ion activity product defined by

$$Q_m = \prod_{j=1}^{N_c} (\gamma_j C_j)^{\nu_{jm}}. \quad (26)$$

The reaction rate has the form

$$I_m = \begin{cases} -k_m s_m \left[\prod_i a_i^{n_i} \right] (1 - e^{-\mathbf{A}_m/RT}), & \text{if } \phi_m > 0, \text{ or if } \phi_m = 0 \text{ and } \mathbf{A}_m < 0, \\ 0, & \text{otherwise,} \end{cases} \quad (27)$$

where k_m denotes the kinetic rate constant, s_m denotes the mineral surface area participating in the reaction, a_i represents the activity of the i th species, and n_i is a constant. This form of the rate takes into account the moving boundary nature of the transport-reaction problem. The rate has units of moles per unit time per unit volume of bulk porous medium and is taken as positive for precipitation and negative for dissolution. Thus it represents the average rate taken over a REV. The rate law given by Eqn.(27) should really be referred to as a pseudo-kinetic rate law. Because it refers to the overall mineral precipitation/dissolution reaction, it generally does not describe the actual kinetic mechanism by which the mineral reacts. Nevertheless, it provides a useful form to describe departures from equilibrium. Close to equilibrium the rate becomes proportional to the chemical affinity. The temperature dependence of the kinetic rate constants may be calculated from the expression:

$$k_m(T) = \frac{T k_m^0}{T_0} \exp \left[- \left(\frac{1}{T} - \frac{1}{T_0} \right) \frac{\Delta H_m^\dagger}{R} \right], \quad (28)$$

where k_m^0 denotes the rate constant at T_0 and ΔH_m^\dagger denotes the enthalpy of activation. For a typical activation energy of 35 kJ mole⁻¹ corresponding to the kinetic rate constant for feldspar, a 100°C increase in temperature implies an increase in the rate constant by more than one and a half orders of magnitude from its value at 25°C.

SEQUENTIALLY COUPLED TWO-PHASE FLOW AND TRANSPORT

A sequentially coupled methodology is used to solve the multidimensional, multiphase, multicomponent fluid and solute flow and transport equations in a partially saturated

porous medium. In this approach, heat, air-water vapor, and solvent mass conservation equations are solved separately from solute mass conservation equations. Thus at each new time step, first the heat and mass flow equations are solved simultaneously to obtain the temperature, pressure, saturation and flow field as functions of distance. Second, chemically reacting solutes are transported using the results obtained from solving the heat and solvent mass conservation equations. As a third step, mineral concentrations are calculated enabling changes in porosity, tortuosity and permeability to be computed which can then alter the flow field. This three-step approach can be justified based on the different time scales of the processes involved. Thus alteration of rock properties through chemical reactions proceeds much more slowly compared to changes in the aqueous solution composition and flow and temperature fields caused by decay of the radioactive waste form. Another way to put it, the system adjusts quasi-statically to chemical alteration of the host rock (Lichtner, 1988, 1992). The sequentially coupled approach is expected to be a good approximation for sufficiently dilute solutions in which density corrections are not important. To carry out this scheme, the code MULTIFLO was developed. MULTIFLO consists of two modules METRA and GEM. METRA is similar to other two-phase codes such as TOUGH (Pruess, 1987). The code GEM (Lichtner, 1995) consists of the reactive transport part of the MULTIFLO code.

The code METRA uses a fully implicit finite difference scheme with upstream weighting. The jacobian is computed analytically. Several solution schemes are possible including a D4 ordered direct solver and the WATSOLV conjugate gradient solver (VanderKwaak et al., 1995). The time-stepping algorithm used in GEM involves different strategies depending on the dimensionality of the problem. For 1D systems a fully implicit time-stepping algorithm with dynamically computed adaptive time steps. For 2D and 3D problems an operator splitting algorithm is employed in which flow and transport time steps are decoupled from the chemical algorithm. Several different solver options are available for inverting the sparse jacobian matrix. For 1D problems a block tridiagonal solver is used, and for 2D and 3D problems the conjugate gradient solver WATSOLV is used.

APPLICATION TO THE PROPOSED NUCLEAR WASTE REPOSITORY AT YUCCA MOUNTAIN, NEVADA

In this section the two-phase reactive transport equations are applied the proposed Yucca Mountain repository. A moderate heat loading of 80 kW acre^{-1} is assumed in the calculations. With this heat load a liquid phase is always present and complete dryout does not occur following emplacement of the waste. The Yucca Mountain host

rock is modeled in these preliminary calculations as pure amorphous silica with 10% porosity. This assumption is considered reasonable for the purposes of the calculations presented here which are to estimate the change in salinity caused by evaporation and condensation process.

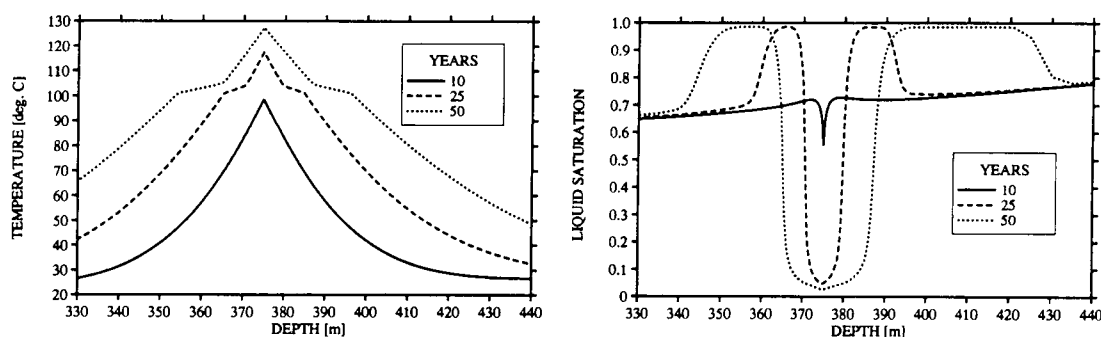


Figure 1: The temperature plotted as a function of depth for the indicated times. Figure 2: The liquid saturation plotted as a function of depth for the indicated times.

Results

Preliminary results of a 1D calculation using the computer code MULTIFLO along the vertical through the centerline of the repository are shown in Figs. 1–5. Near the center of the repository a 1D calculation has been demonstrated to accurately represent the behavior of the system. Only near the edges of the disk representing the repository is a 2D simulation necessary. The temperature profile plotted as a function of depth below the ground surface is shown in Fig. 1 for times of 10, 25, and 50 years. The maximum temperature obtained for this heat load is approximately 130°C which occurs after an elapsed time of about 50 years. The liquid saturation profile is shown in Fig. 2. Above and below the repository horizon the pore spaces become almost fully saturated during the dryout period. This saturation state is a dynamic condition caused by continuous evaporation of liquid drawn toward the repository by capillary forces and condensation further away in cooler regions as shown in Fig. 3. The resulting pH profile is shown in Fig. 4 and the chloride concentration in Fig. 5. In the region in which evaporation occurs, the pH dramatically increases as CO₂ degasses from the liquid phase. Likewise the chloride concentration increases by approximately a factor of 4. By contrast in the condensation zones, the pH and chloride concentration decrease from their ambient values. This is to be expected since the condensing liquid is devoid of dissolved salts.

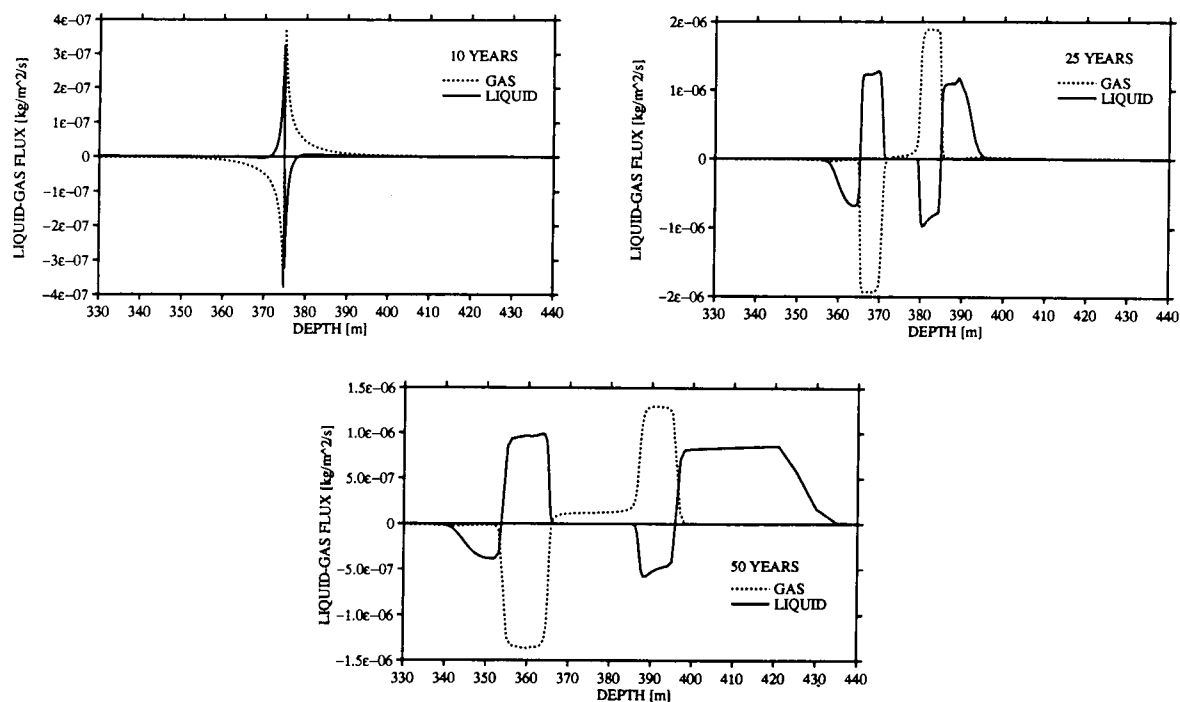


Figure 3: Liquid and gas fluxes plotted as a function of depth for the indicated times.

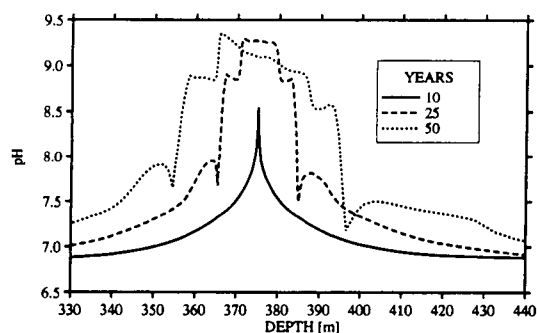


Figure 4: The pH plotted as a function of depth for the indicated times.

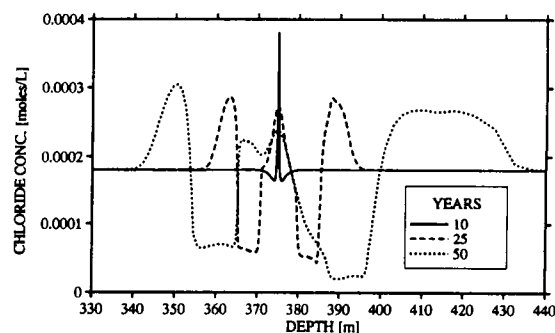


Figure 5: The chloride concentration plotted as a function of depth for the indicated times.

CONCLUSION

This work investigated the effects of liquid evaporation and condensation on the possibility of brine formation in the near-field region of a HLW repository located in a partially saturated host rock. This work provided the conceptual and mathematical framework for such an endeavor. Such calculations involve two-phase fluid transport coupled to multicomponent solute and gas transport and fluid/rock interaction. Results showed that significant changes in pH and salinity could occur with moderate

thermal loading of the repository.

REFERENCES

- [1] Buscheck, T. A. and Nitao, J. J. (1993) The analysis of repository-heat-driven hydrothermal flow at Yucca Mountain. *Proceedings of the Fourth Annual International Conference Las Vegas, Nevada, April 26-30*, vol. **1**, 847–867.
- [2] Klavetter E. A. and Peters, R. R. (1988) A continuum model for water movement in an unsaturated fractured rock mass. *Water Resources Research*, **24**, 416–430.
- [3] Lichtner P. C. (1985) Continuum model for simultaneous chemical reactions and mass transport in hydrothermal systems. *Geochimica et Cosmochimica Acta*, **49**, 779–800.
- [4] Lichtner, P. C. (1988) The quasi-stationary state approximation to coupled mass transport and fluid-rock interaction in a porous media. *Geochimica et Cosmochimica Acta*, **52**, 143–165.
- [5] Lichtner, P. C. (1992) Time-space continuum description of fluid/rock interaction in permeable media. *Water Resources Research*, **28**, 3135–3155.
Lichtner, P. C. (1995) Principles and practice of reactive transport modeling. *Mat. Res. Soc. Symp. Proc.*, Kyoto, Japan, **353**, 117–130.
- [6] Pruess, K. (1987) TOUGH user's guide. Lawrence Berkeley Laboratory Report, LBL-20700.
- [7] Pruess, K. and Tsang, Y. (1993) Modeling of strongly heat-driven flow processes at a potential high-level nuclear waste repository at Yucca Mountain, Nevada. *Proceedings of the Fourth Annual International Conference Las Vegas, Nevada, April 26-30*, vol. **1**, 568–575.
- [8] Rimstidt, J. D. and Barnes, H. L. (1980) The kinetics of silica-water reactions. *Geochimica et Cosmochimica Acta*, **44**, 1683–1699.
- [9] van Genuchten, M. (1980) A closed form equation for predicting the hydraulic conductivity of unsaturated soils: *Soil Science Society of America Journal* **44**: 892–898.
- [10] VanderKwaak, J. E., Forsyth, P. A., MacQuarrie, K. T. B., and Sudicky, E. A. (1995) WATSOLV Sparse matrix iterative solver package user's guide, 23 pp.
- [11] Walton, J. C. (1993) Effects of evaporation and solute concentration on presence and composition of water in and around the waste package at Yucca Mountain. *Waste Management*. In press.

- [12] White, S. P. (1995) Multiphase nonisothermal transport of systems of reacting chemicals. *Water Resources Research*, **31**, 1761-1772.

Account Number: **20-5708-562**

Description: Near-field Environment Code Development – MULTIFLO

Collaborators: Dr. M. Seth (Consultant)

Objective: Development of the computer code MULTIFLO, and submodules GEM and METRA.

4.8.96 **ARRAY STORAGE**

Field variables defined at nodes:

Concentration:

$$C_n = C(1 : nxyz) = C(i + (j - 1) * nx), \quad n = i + (j - 1) * nx. \quad (29)$$

Field variables defined at interfaces:

Velocity:

$$\begin{aligned} v_x &= v_x(1 : nx + 1; 1 : ny; 1 : nz) \\ &= v_x(i + (j - 1) * nxp1 + (k - 1) * nxp1 * ny), \\ &= v_x(n + i + j - 1 + (k - 1) * ny), \end{aligned} \quad (30a)$$

$$\begin{aligned} v_y &= v_y(1 : nx; 1 : ny + 1; 1 : nz) \\ &= v_y(i + (j - 1) * nx + (k - 1) * nx * nyp1), \\ &= v_y(n + (k - 1) * nx), \end{aligned} \quad (30b)$$

$$\begin{aligned} v_z &= v_z(1 : nx; 1 : ny; 1 : nz + 1) \\ &= v_z(i + (j - 1) * nx + (k - 1) * nx * ny), \\ &= v_z(n). \end{aligned} \quad (30c)$$

Flux:

$$\begin{aligned} q_n^x &= q^x(1 : nx + 1; 1 : ny; 1 : nz), \\ &= q^x(j, i + (j - 1) * nxp1 + (k - 1) * nxp1 * ny), \end{aligned} \quad (31a)$$

$$\begin{aligned} q_n^y &= q^y(1 : nx; 1 : ny + 1; 1 : nz), \\ &= q^y(j, i + (j - 1) * nx + (k - 1) * nx * nyp1), \end{aligned} \quad (31b)$$

$$\begin{aligned} q_n^z &= q^z(1 : nx; 1 : ny; 1 : nz + 1), \\ &= q^z(i + (j - 1) * nx + (k - 1) * nx * ny). \end{aligned} \quad (31c)$$

Porosity & Permeability:

$$\begin{aligned}\phi_n &= \phi(0 : nx + 1; 0 : ny + 1; 0 : nz + 1), \\ &= \phi(i + j * nxp2 + k * nxp2 * nyp2),\end{aligned}\tag{32a}$$

$$\begin{aligned}\kappa_n &= \kappa(0 : nx + 1; 0 : ny + 1; 0 : nz + 1), \\ &= \kappa(i + j * nxp2 + k * nxp2 * nyp2).\end{aligned}\tag{32b}$$

Interior nodes:

$$n = i + (j - 1)nx + (k - 1)nxy, \quad nx > 1, ny > 1, nz > 1, \tag{33a}$$

$$n = i + (j - 1)nx, \quad nx > 1, ny > 1, nz = 1, \tag{33b}$$

$$n = i + (k - 1)nx, \quad nx > 1, ny = 1, nz > 1, \tag{33c}$$

$$n = i, \quad nx > 1, ny = 1, nz = 1, \tag{33d}$$

$$n = k, \quad nx = 1, ny = 1, nz > 1. \tag{33e}$$

Single layer of ghost nodes:

$$n = i + j(nx + 2) + k(nx + 2)(ny + 2), \quad nx > 1, ny > 1, nz > 1, \tag{34a}$$

$$n = i + j(nx + 2), \quad nx > 1, ny > 1, nz = 1, \tag{34b}$$

$$n = i + k(nx + 2), \quad nx > 1, ny = 1, nz > 1, \tag{34c}$$

$$n = i, \quad nx > 1, ny = 1, nz = 1, \tag{34d}$$

$$n = k, \quad nx = 1, ny = 1, nz > 1, (nxp2 = -1, nxyp2 = 1). \tag{34e}$$

Double layer of ghost nodes for implementing TVD:

$$n = i + j(nx + 4) + k(nx + 4)(ny + 4), \quad nx > 1, ny > 1, nz > 1, \tag{35a}$$

$$n = i + j(nx + 4), \quad nx > 1, ny > 1, nz = 1, \tag{35b}$$

$$n = i + k(nx + 4), \quad nx > 1, ny = 1, nz > 1, \tag{35c}$$

$$n = i, \quad nx > 1, ny = 1, nz = 1, \tag{35d}$$

$$n = k, \quad nx = 1, ny = 1, nz > 1. \tag{35e}$$

Velocity:

$$n = i + (j - 1)(nx + 1) + (k - 1)(nx + 1)ny, \quad nx > 1, ny > 1, nz > 1, \tag{36a}$$

$$n = i + (j - 1)(nx + 1), \quad nx > 1, ny > 1, nz = 1, \tag{36b}$$

$$v_x : \quad n = i + (k - 1)(nx + 1), \quad nx > 1, ny = 1, nz > 1, \tag{36c}$$

$$n = i, \quad nx > 1, ny = 1, nz = 1, \tag{36d}$$

$$n = k, \quad nx = 1, ny = 1, nz > 1. \tag{36e}$$

$$n = i + (j - 1)nx + (k - 1)nx(ny + 1), \quad nx > 1, ny > 1, nz > 1, \quad (37a)$$

$$n = i + (j - 1)nx, \quad nx > 1, ny > 1, nz = 1, \quad (37b)$$

$$v_y : \quad n = i + (k - 1)nx, \quad nx > 1, ny = 1, nz > 1, \quad (37c)$$

$$n = i, \quad nx > 1, ny = 1, nz = 1, \quad (37d)$$

$$n = k, \quad nx = 1, ny = 1, nz > 1. \quad (37e)$$

$$n = i + (j - 1)nx + (k - 1)nxny, \quad nx > 1, ny > 1, nz > 1, \quad (38a)$$

$$n = i + (j - 1)nx, \quad nx > 1, ny > 1, nz = 1, \quad (38b)$$

$$v_z : \quad n = i + (k - 1)nx, \quad nx > 1, ny = 1, nz > 1, \quad (38c)$$

$$n = i, \quad nx > 1, ny = 1, nz = 1, \quad (38d)$$

$$n = k, \quad nx = 1, ny = 1, nz > 1. \quad (38e)$$

4.16.96 Modification of GEM Input File. A free-format input file capability was added to GEM as part of the MULTIFLO code development. The new input file enables a consistent interface between METRA and GEM. Keywords

```
data keywords/'OPT1','OPT2','OPT3','COUP','PLTF','TOLR','DEBU',
*           'MISC','FLOW','DIFF','PINI','MAST','DXYZ','CXYZ',
*           'ISYS','SOLV','COMP','BCON','CMIR','STOL','AQCX',
*           'MNRL','GASE','MNIR','SMIR','CORR','ECAQ','AQIR',
*           'IONX','BRKP','TIME','DTST','ENDS',' ',' ' /
```

were introduced for each data block. Comment lines begin with a colon (:), and the skip--noskip option to skip portions of the input file is available. An example file kfeld.in is listed below.

```
quartz dissolution
Testing with free format and dynamic memory
:      nx ny nz idif igem2d
Grid   100 1 1 0 2
:
:  idata istart mode iplot imod iprint iexact
Opt1  0 0 2 1 50 -1 0
:
:  itmax ihalmax ivmax ndamp
Opt2  30 20 3 5
:
:  isurf iact loglin icon id iops ifor
Opt3  1 0 0 1 1 1 5
:
:isync ipor iperm perm. fac.
Coup  0 0 0 3.
```



```

:
:iplot: a s t m si sf v z b in
Pltf 1 0 1 1 0 0 1
: e exti gitex
0 0 0 0 0
:
: tol ttol tolneg tolpos tolexp dthalf qkmax tolstdste
Tolr 1.d-10 2. 1.e0 1.e-2 5.d0 .5 590. 1.e-6
:
: mcyc cc c flx r sp qk pk rk a1 a2 a3
Debug 0 1 1 0 1 1 1 1 1
:
: por0 phir sat w lambda toltrf toldelt tolpor
Misc .1 1. 1. .5 1. 0. 1.e3 1.e-3
:
: vx0 vy0 vz0[m/yr] alphax alphay alphaz cournr
Flow 1. 0. 0. 0. 0. 0. .1
:
:d0[cm^2/s] delhaq[kJ/mol] dgas[cm^2/s] dgexp tortaq tortg
Diff 1.d-5 12.6 2.13d-1 1.8 .5d0 .5d0
:
:flag 1: T(x) = d x^3 + a x^2 + b x + c (meters)
: 2: T(x) = a + (b-a) exp[-((x-x0)/c)^2] + (d - a) * x / xlen
: 3: T(x,t)=a+1/2(b-a)(erf[(x+c-x0)/2sqr(dt)]-erf[(x-c-x0)/2sqr(dt)])
:p (bars) temp flag a b c d x0 xlen
Pinit 1.0 25 0 25 300 250 125 1000. 2.d3
:
:master species for controlling time stepping
Master h+
:
:grid 'm' 0. 1 200 200.
:
Dxyz
0.01 0.01 0.01 0.01 0.01 0.01 0.01 0.01 0.01 0.01
0.01 0.01 0.01 0.01 0.01 0.01 0.01 0.01 0.01 0.01
0.01 0.01 0.01 0.01 0.01 0.01 0.01 0.01 0.01 0.01
0.01 0.01 0.01 0.01 0.01 0.01 0.01 0.01 0.01 0.01
0.01 0.01 0.01 0.01 0.01 0.01 0.01 0.01 0.01 0.01
0.02 0.02 0.02 0.02 0.02 0.02 0.02 0.02 0.02 0.02
0.02 0.02 0.02 0.02 0.02 0.02 0.02 0.02 0.02 0.02
0.02 0.02 0.02 0.02 0.02 0.02 0.02 0.02 0.02 0.02
0.02 0.02 0.02 0.02 0.02 0.02 0.02 0.02 0.02 0.02
0.02 0.02 0.02 0.02 0.02 0.02 0.02 0.02 0.02 0.02
1.
1.
:
: isat isotherm iread
Isys -1 0 0
:
: level north nitmax idetail isolv rmaxtol rtwotol smaxtol
Solv 1 1 100 0 3 1.e-20 1.e-20 1.e-12
:
:initial and boundary conditions: 1-conc., 2-flux, 3-zero gradient

```

```

:inlet outlet nzoneaq
Comp 1 3 3
:
:species      itype  guess  ctot  mineral diffusion
k+            3      1.e-4  1.e-4  k-feldspar
al+3          3      1.e-15  1.e-4  muscovite
h+            8      1.e-7   7.0    dummy
sio2(aq)      3      1.e-4  1.e-3  quartz
                                :blank
:
Bcon
  1 1
:species      itype  guess  ctot  mineral
k+            1      1.e-6  1.e-6  dummy
al+3          1      1.e-8  1.e-8  dummy
h+            8      1.e-4  4.0    dummy
sio2(aq)      1      1.e-6  1.e-6  dummy
:
  2 3
:species      itype  guess  ctot  mineral
k+            3      1.e-4  1.e-4  k-feldspar
al+3          3      1.e-15  1.e-4  muscovite
h+            8      1.e-7   7.0    dummy
sio2(aq)      3      1.e-4  1.e-3  quartz
:
skip
  5 3
:species      itype  guess  ctot  mineral
sio2(aq)      3      1.e-4  1.e-3  quartz
  6 3
:species      itype  guess  ctot  mineral
sio2(aq)      3      1.e-4  1.e-3  quartz
noskip
  0 0
:
Cmir 0 0
      :blank
:
Stol 1. 1. 1. 1. 1.
:
Aqcx
oh-          5.5e-5
aloh+2       1.0e-5
al(oh)2+     1.0e-5
al(oh)3(aq)  1.0e-5
al(oh)4-     1.0e-5
h3sio4-      1.0e-5
h2sio4-2     1.0e-5
              :blank
:
Mnrl
quartz
kaolinite

```

P. C. Lichtner

SCIENTIFIC NOTEBOOK

INITIALS:

SC

```

k-feldspar
muscovite
gibbsite
:blank
Gases
:blank
:
:irr mineral   itypkin beta   fkin   delh   rkph   rk   tau
:i1 i2 j1 j2 k1 k2   vol   area
Mnir
k-feldspar     0       1.0    1.0    0.  2.24e-13  3.02e-16  1.e-2
1 100 1 1 1 1  0.2    12.
0
gibbsite       0       1.0    1.0    0.   0.   1.00e-14  1.e-2
1 100 1 1 1 1  0.     1.
0
kaolinite      0       1.0    1.0    0.   0.   1.00e-14  1.e-2
1 100 1 1 1 1  0.     1.
0
muscovite      0       1.0    1.0    0.   0.   1.00e-14  1.e-2
1 100 1 1 1 1  0.     1.
0
quartz         0       1.0    1.0    1.   0.   3.16e-18  1.e-2
1 100 1 1 1 1  0.7    40.
0
:blank
:
:surface mineral itypkin area beta   fkin   delh   rkph   rk
:           0       1.0    1.0    1.   0.   0.   0.
:
:corrosion solids   i0     acorr   bcorr   curlim
:           0.     0.     0.     0.
:
:crevice gap[meters] potential [v]
Ecaq      90.d-6      -.2
:blank
:
:electrochemical aqueous species i0     acorr   bcorr   curlim
:           0.     0.     0.     0.
:
Aqir
:blank
:
:ion-exchange reactions
Ionx  0      1.0
:
:Brkp  5
:93  110  130  150  185
:
Time[y]  1 1.e4 4 2.5e4 5.e4 1.e5 2.e5
:
Dtstep[y]  1 3.e-8
1.e-8      1.e2

```

P. C. Lichtner

SCIENTIFIC NOTEBOOK

INITIALS:

PCZ

:
Ends

I have reviewed this scientific notebook and find it in compliance with QAP-001. There is sufficient information regarding procedures used for conducting tests, acquiring and analyzing data so that another qualified individual could repeat the activity.

N. Sridhar 4/17/97

Narasi Sridhar
Manager, Engineered Barrier System and Waste Solidification System

SCIENTIFIC NOTEBOOK

by

Peter C. Lichtner

SCIENTIFIC NOTEBOOK

by

Peter C. Lichtner

Southwest Research Institute
Center for Nuclear Waste Regulatory Analyses
San Antonio, Texas

October 2, 1996

INITIAL ENTRIES

Scientific NoteBook: # 095

Issued to: P. C. Lichtner

Issue Date: Tuesday, November 16, 1993

Computerized Initials: SCZ

By agreement with the CNWRA QA this NoteBook is to be printed at approximate quarterly intervals. This computerized Scientific NoteBook is intended to address the criteria of CNWRA QAP-001.

Table 1: Computing Equipment

Machine Name	Type	OS	Location
gravenstein.cnwra.swri.edu	Pentium Workstation	NEXTSTEP	desk Rm A-126
	133 Mhz	Version 3.3	Bldg. 189
	64 MB RAM		
skippy.cnwra.swri.edu	Sun SPARC 20	SUNOS 4.1.2	network
	96 MB RAM		

Contents

INITIAL ENTRIES	ii
FIGURES	v
TABLES	vi
NEAR-FIELD ENVIRONMENT	1
1 MATHEMATICAL MODEL	5
1.1 Basic Governing Equations	5
1.2 Auxiliary Relationships	7
1.2.1 Van Genuchten Relations	8
1.2.2 Kelvin's Equation for Vapor Pressure Lowering	8
1.3 Initial and Boundary Conditions	9
1.4 Selection of Primary Variables	10
1.5 Assumptions and Limitations	11
1.6 Special Cases	11
2 FINITE-DIFFERENCE REPRESENTATION	13
2.1 Gridding and Discretization	14
2.2 Gridding in Cylindrical Coordinates	15
2.3 Finite Difference Representation	17
2.4 Newton-Raphson Linearization and Solution	19
3 CONSTRUCTION OF JACOBIAN MATRIX AND RESIDUAL VECTOR	22
3.1 Representation of Intrinsic Properties and Their Derivatives in Terms of Primary Variables	22

3.1.1	Single Liquid Phase	22
3.1.2	Single Gas Phase	23
3.1.3	Two-Phase System: Vapor Pressure Lowering Absent	25
3.1.4	Two-Phase System: Vapor Pressure Lowering Present	28
3.2	Expansion of Accumulation Terms	29
3.2.1	Single Liquid Phase	30
3.2.2	Single Gas Phase	31
3.2.3	Two-Phase System: Vapor Pressure Lowering Absent	32
3.2.4	Two-Phase System: Vapor Pressure Lowering Present	33
3.3	Expansion of Flux Terms	33
3.3.1	Liquid Flux	36
3.3.2	Convective Gas Flux	42
3.3.3	Binary Gas Diffusion	44
3.3.4	Heat Conduction Flux	46
4	Boundary Conditions	47
4.1	Dirichlet Condition	48
4.2	Neumann Condition	49
4.3	Sources and Sinks	49
4.4	Consolidation of Equations in Matrix Form for Solution	49
4.5	Phase Transition and Updating	50
5	NOMENCLATURE	51

List of Figures

- 1 Representative volume element of size b with grain size d and film thickness δ . 3

List of Tables

1	Computing Equipment	ii
2	Choice of primary variables.	11
3	Table showing the difference between arithmetic and logarithmic means ($r_i =$ 1).	16
4	Possible combinations of phases in neighboring blocks.	35
5	Possible combinations with different phases in neighboring blocks.	36

KTI: NEAR-FIELD ENVIRONMENTAccount Number: **20-5708-561**

Description: Near-field Environment Technical Assistance

Collaborators: Dr. M. Seth (Consultant)

Objective: Application of the computer code MULTIFLO, and submodules GEM and METRA to the Yucca Mountain HLW Repository to provide estimates of the near-field environment.

8.16.96 Estimate of Bounding Chloride Concentration

A simple upper bound on the chloride concentration may be derived by assuming equilibrium with e.g. halite. As evaporation takes place the sodium and chloride concentrations must remain approximately proportional to one another

$$a_{\text{Na}^+} = \alpha a_{\text{Cl}^-}. \quad (0.1)$$

Equilibrium with halite implies

$$K = \frac{1}{a_{\text{Na}^+} a_{\text{Cl}^-}} = \frac{1}{\alpha a_{\text{Cl}^-}^2}. \quad (0.2)$$

Therefore

$$a_{\text{Cl}^-} = \frac{1}{\sqrt{\alpha K}} \quad (0.3)$$

The log K for halite at 100°C is equal to 1.578. Taking $\alpha = 11.11$, derived from J-13 well-water ($a_{\text{Na}^+} = 2 \times 10^{-3}$, $a_{\text{Cl}^-} = 1.8 \times 10^{-4}$), it follows that $a_{\text{Cl}^-} \simeq 0.05$ moles/kg-H₂O.

The maximum silica concentration estimated from equilibrium with quartz, chalcedony and cristobalite gives, respectively, $a_{\text{SiO}_2} = 0.000835$, 0.00137, and 0.00218 molal. By contrast J-13 well-water has a silica concentration of 0.0011 molal.

Bounds on the pH are more difficult to obtain. Likewise calcium and carbonate have no obvious upper bounds since their concentrations will depend on the pH.

The following are the contents of Mathematica Notebook `chloride.ma`.

BOUNDING CALCULATION FOR CHLORIDE CONCENTRATION

'halite' 27.015 2 1.0 'cl-' 1.0 'na+'
1.4920 1.5855 1.6176 1.5780
1.4499 1.2422 0.9364 0.4683'quartz' 22.688 1 1.0 'sio2(aq)'
-4.6319 -3.9993 -3.4734 -3.0782
-2.7191 -2.4378 -2.2057 -2.0168'chalcedony' 22.688 1 1.0 'sio2(aq)'
-4.3359 -3.7281 -3.2307 -2.8615
-2.5280 -2.2669 -2.0512 -1.8760'cristobalite' 25.740 1 1.0 'sio2(aq)'
-4.0213 -3.4488 -2.9921 -2.6605
-2.3644 -2.1326 -1.9402 -1.7832'calcite' 36.934 3 -1.0 'h+' 1.0 'ca+2' 1.0 'hco3-'
2.2257 1.8487 1.3330 0.7743
0.0999 -0.5838 -1.3262 -2.2154

J-13

ca+2	1	2.9e-4	2.9e-4	blank	0.8e-5
na+	1	2.e-3	2.e-3	blank	0.8e-5
k+	1	1.4e-4	1.e-4	blank	0.8e-5
h+	8	1.e-7	6.9	blank	9.6e-5
hco3-	7	2.7e-3	2.7e-3	blank	2.0e-5
sio2(aq)	1	1.1e-3	1.1e-3	blank	1.4e-5
cl-	1	1.8e-4	1.8e-4	blank	1.4e-5

J-13 sio2

In[109]:=

10^{-3.0782,-2.8615,-2.6605}

```
Out[109]=
{0.000835218, 0.00137562, 0.00218524}
```

```
halite saturation: na+ - cl-
```

```
In[105]:=
alpha = 2 10^-3/(1.8 10^-4)
logk = 1.578
acl = 1/Sqrt[alpha 10^logk]
```

```
Out[105]=
11.1111
```

```
Out[106]=
1.578
```

```
Out[107]=
0.0487665
```

9.9.96 Water Film Thickness. An expression is derived for the thickness of the water film corresponding to a given liquid saturation.

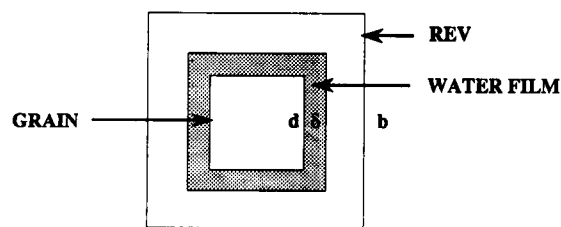


Figure 1: Representative volume element of size b with grain size d and film thickness δ .

The total REV volume is divided up into gas, liquid and solid volumes:

$$V = V_g + V_l + V_s. \quad (0.4)$$

The liquid volume can be represented as

$$V_l = \phi_s V, \quad (0.5)$$

for liquid saturation s_l and porosity ϕ . According to the geometry defined in Figure 1, the liquid volume is related to the film thickness δ by the expression

$$V_l = (d + 2\delta)^3 - d^3 = d^3 \left[\left(1 + \frac{2\delta}{d} \right)^3 - 1 \right]. \quad (0.6)$$

The porosity is related to grain size by the equation

$$\phi = \frac{V_p}{V} = \frac{V - V_s}{V} = 1 - \left(\frac{d}{b} \right)^3. \quad (0.7)$$

As a result the liquid volume can be expressed as

$$V_l = \frac{\phi s_l d^3}{1 - \phi}. \quad (0.8)$$

Equating Eqns.(0.6) and (0.8) yields for the film thickness

$$\delta = \frac{d}{2} \left[\left(1 + \frac{\phi s_l}{1 - \phi} \right)^{1/3} - 1 \right]. \quad (0.9)$$

For $s_l \ll 1$, it follows that

$$\delta \simeq \frac{\phi s_l d}{6(1 - \phi)}. \quad (0.10)$$

For a porosity of 10% and liquid saturation of 2% with 1 mm grain size, the film thickness is approximately $\delta \simeq 3.7 \times 10^{-7}$ m.

Account Number: **20-5708-562**

Description: Near-field Environment Code Development – MULTIFLO

Collaborators: Dr. M. Seth (Consultant)

Objective: Development of the computer code MULTIFLO, and submodules GEM and METRA.

7.15.96 **Technical notes on the computer code METRA.** The following describes the equations constituting the model, the underlying assumptions and limitations, and the special cases for simulation of single phase liquid and pure heat conduction flows, that are incorporated into the code *METRA* (Seth and Lichtner, 1996).

1. MATHEMATICAL MODEL

Remark on Notation. In the following, sub- and superscripts w and a refer to species H_2O and air, and l and g to liquid and gas phases, respectively. Furthermore, to simplify the notation, water vapor is denoted by the subscript v as e.g. water vapor partial pressure $p_v = p_w^g$. The subscript a refers to air in the gas phase if a phase designation is not present, as e.g. the air partial pressure $p_a = p_a^g$. Properties referring to a pure phase are marked by the superscript o , as e.g. the densities of pure liquid water ρ_w^o and water vapor ρ_v^o . Occasionally pressure is denoted simply by p without a subscript, in which case its meaning must be taken from the context in which it occurs. A complete definition of all symbols is given in the nomenclature section.

1.1. Basic Governing Equations

The governing equations for flow of H_2O , air, and energy are simply the statements of conservation of mass and energy, and may be stated succinctly as:

$$\text{Rate of Accumulation} = \text{Net Flux} + \text{Generation Rate (source/sink)}. \quad (1.1)$$

Mathematically, the governing equations are expressed as:

$$\frac{\partial m_a}{\partial t} = -\nabla \cdot (\rho_l X_a^l \mathbf{v}_l + \rho_g X_a^g \mathbf{v}_g + \rho_g \mathbf{v}_a^D) + q_{m_a}^G, \quad (1.2)$$

$$\frac{\partial m}{\partial t} = -\nabla \cdot (\rho_l \mathbf{v}_l + \rho_g \mathbf{v}_g) + q_m^G, \quad (1.3)$$

$$\frac{\partial e}{\partial t} = -\nabla \cdot (\rho_l H_l \mathbf{v}_l + \rho_g H_g \mathbf{v}_g - \kappa_{\text{eff}} \nabla T) + q_H^G, \quad (1.4)$$

for number of moles air m_a , total number of moles m , and the total energy e , respectively, per unit bulk volume of rock. In these equations the following definitions are used: the total number of moles in the liquid and gas phases m is defined by

$$m = \phi(s_l \rho_l + s_g \rho_g), \quad (1.5)$$

where ϕ denotes the porosity of the porous medium, ρ_l , ρ_g denote the molar density, and s_l , s_g the saturation of the liquid and gas phases, respectively. The quantity m_a refers to the total number of moles of air in the liquid and gas phases, defined by the expression

$$m_a = \phi(s_l \rho_l X_a^l + s_g \rho_g X_a^g), \quad (1.6)$$

where X_a^l , X_a^g denote the air mole fraction in the liquid and gas phases, respectively. The quantity e denotes the total energy (joules m^{-3}), defined by

$$e = \phi[\rho_l s_l U_l + \rho_g s_g U_g + (1 - \phi) C_p^{\text{rock}} \rho_{\text{rock}} T], \quad (1.7)$$

where U_l , U_g refer to the internal energy of the liquid and gas phases, and C_p^{rock} denotes the heat capacity of the rock. The Darcy velocity of the π th phase is equal to

$$\mathbf{v}_\pi = -\frac{k k_{r\pi}}{\mu_\pi} \nabla(p_\pi - \gamma_\pi h), \quad (1.8)$$

where h represents the height, k denotes the saturated permeability, $k_{r\pi}$ the relative permeability, μ_π the viscosity, p_π the pressure of the π th fluid phase, and

$$\gamma_\pi = W_\pi^{-1} \rho_\pi g, \quad (1.9)$$

with W_π the gram formula weight of the π th phase and g the acceleration of gravity. The air diffusive velocity (m/sec), is defined by

$$v_a^D = -\tau\phi D_{va}^0 \left(\frac{T}{T_K} \right)^\theta \frac{p_0}{p_g} s_g \nabla X_a^g, \quad (1.10)$$

with $T_K = 273.15$ °K, and p_0 represents a reference pressure. Nomenclature for other variables is provided in Section 5.

In the above, mole balances are chosen as opposed to mass balances for reasons of simplicity in treating the properties of gas mixtures using the ideal gas law. Similar considerations and somewhat improved computational efficiency appealed to us in describing the above conservation equations in terms of the air mole balance, total mole balance, and the total energy balance. The simplification results from cancellation of the terms arising from the diffusive fluxes of water-vapor and air in the total mole balance equation. Alternative equivalent formulations include: (a) mole or mass balance of H_2O , mole or mass balance of air, and the total energy balance, and (b) mole or mass balance of H_2O , total mass or mole balance, and the total energy balance. TOUGH and its derivative codes employ the mass balance formulation consisting of equations corresponding to set (a).

1.2. Auxiliary Relationships

In addition to the flow equations, the following constraint and constitutive relationships are assumed to hold:

$$s_l + s_g = 1, \quad (1.11)$$

$$p_g - p_l = p_c, \quad (1.12)$$

$$\frac{p_v}{p_g} = X_w^g, \quad \frac{p_a}{p_g} = X_a^g, \quad (1.13)$$

$$p_v + p_a = p_g, \quad X_w^g + X_a^g = 1, \quad (1.14)$$

$$X_w^l + X_a^l = 1, \quad (1.15)$$

$$X_a^g = K_H X_a^l, \quad (1.16)$$

and

$$p_v = p_s(T), \quad (1.17)$$

where $p_s(T)$ denotes the saturation pressure for pure water. In Eqn. (1.13) the ideal gas law, and in Eqn. (1.16) Henry's ideal solution behavior is assumed. Equations (1.2–1.17) completely define the mathematical model providing an equal number of equations as unknowns.

1.2.1. Van Genuchten Relations

Capillary pressure is related to saturation by various phenomenological relations one of which is the van Genuchten relation given by

$$s_l^{\text{eff}}(p_c) = \left[1 + (\alpha|p_c|)^\beta\right]^{-\lambda}, \quad (1.18)$$

where p_c represents the capillary pressure, and s_l^{eff} is defined by

$$s_l^{\text{eff}} = \frac{s_l - s_l^r}{s_l^0 - s_l^r}, \quad (1.19)$$

where s_l^r denotes the residual saturation, and s_l^0 denotes the maximum saturation. The quantity β is related to λ by the expression

$$\lambda = 1 - \frac{1}{\beta}, \quad \beta = \frac{1}{1 - \lambda}. \quad (1.20)$$

Relative permeability for the liquid phase is given by the expression

$$k_{rl} = \sqrt{s_l^{\text{eff}}} \left[1 - (1 - (s_l^{\text{eff}})^{1/\lambda})^\lambda\right]^2, \quad (1.21)$$

and for the gas phase by

$$k_{rg} = 1 - k_{rl}. \quad (1.22)$$

1.2.2. Kelvin's Equation for Vapor Pressure Lowering

Vapor pressure lowering resulting from capillary suction is described by Kelvin's equation given by

$$p_v = p_{\text{sat}}(T)e^{p_c/\rho_l RT}, \quad (1.23)$$

where p_v represents the vapor pressure, p_{sat} the saturation pressure of pure water, p_c capillary pressure, ρ_l liquid mole density, and T denotes the temperature and R the gas constant.

1.3. Initial and Boundary Conditions

The initial conditions considered are:

$$p_g = p_g(x, y, z, t = 0) = \text{an arbitrary assigned function,} \quad (1.24)$$

$$p_l = p_l(x, y, z, t = 0) = \text{an arbitrary assigned function,} \quad (1.25)$$

$$s_g = s_g(x, y, z, t = 0) = \text{an arbitrary assigned function,} \quad (1.26)$$

$$T = T(x, y, z, t = 0) = \text{an arbitrary assigned function,} \quad (1.27)$$

$$\begin{aligned} X_a^g &= X_a^g(x, y, z, t = 0) = \text{function of } T \text{ in two-phase region,} \\ &= \text{arbitrary assigned function in a single gas phase region,} \end{aligned} \quad (1.28)$$

$$\begin{aligned} X_a^l &= X_a^l(x, y, z, t = 0) = \text{function of } T \text{ in two-phase region,} \\ &= \text{arbitrary assigned function in a single liquid phase region.} \end{aligned} \quad (1.29)$$

In a two-phase system only three of the above six conditions are mutually independent. Thus, for a two-phase system, conditions given by Eqns. (1.24), (1.26) and (1.28) are imposed. For a single liquid phase system conditions Eqn. (1.25), (1.28), and (1.29), and for a single gas phase system, (1.24), (1.28), and (1.29) are invoked. For the case of a two-phase system, X_a^g and X_a^l are internally computed from the given temperature distribution according to the expression

$$X_a^g = 1 - \frac{p_s(T)}{p_g}, \quad (1.30)$$

and

$$X_a^l = K_H^{-1} X_a^g. \quad (1.31)$$

If $p_g = p_s(T)$, the air component must be zero. Thus, a two-phase steam-water system (such as a typical geothermal reservoir) can be simulated by setting the total gas pressure equal to the saturation pressure.

The boundary conditions considered are:

(a) Neumann condition, \mathbf{n} normal to the boundary:

$$\frac{\partial p}{\partial n} = f(t), \quad \frac{\partial T}{\partial n} = g(t), \quad (1.32)$$

$$v_n = -\frac{k}{\mu} \left(\frac{\partial p}{\partial n} - W_l^{-1} \rho_l \mathbf{z} \cdot \mathbf{n} \right). \quad (1.33)$$

(b) Dirichlet condition:

$$\begin{aligned} p(x, y, z, t) &= g_1, \\ T(x, y, z, t) &= g_2, \\ s(x, y, z, t) &= g_3, \end{aligned} \quad (1.34)$$

(c) Any combination of Neumann and Dirichlet conditions.

Note that, all the above conditions may be varied dynamically and spatially. A more detailed numerical treatment of the boundary conditions is given in the Section 4.

1.4. Selection of Primary Variables

For a two-phase system Eqns. (1.2–1.17) involve eleven unknowns, namely, p_l , p_v , p_g , p_a , s_l , s_g , T , X_w^l , X_w^g , X_a^l , and X_a^g . There are, however, eight relations among them leaving three independent variables. For a single phase system not all of the constitutive relations apply; however, there are also only three independent variables possible. For a single liquid phase system, ($s_g = 0$, and $s_l = 1$), these unknowns are p_l , T , and X_a^l (or X_w^l); and for a single gas phase system, they are p_g , T , X_a^g or p_a (or X_w^g or p_v). Thus, for a single phase system, the choice of selecting the primary variables is limited to the above. Note that for a two-phase system, if the capillary pressure vanishes then $p_g = p_l = p$ (say).

For a two-phase system, the choice of primary variables should include one of the phase pressures (p_g or p_l), one of the saturations (s_g or s_l), and one from the list of the remaining unknowns (T , p_a). Pruess (1991) observed that selection of set (p_g , s_g , T) as primary variables results in convergence difficulties during the phase transition from a single phase system to a two-phase system and vice-versa, and suggested the use of set (p_g , p_a , s_g) as the dependent variables. This is the choice used in *METRA*. In summary, the possible primary variables depending on the state of the fluid are listed in Table 2.

Table 2: Choice of primary variables.

Thermodynamic State of Fluid	Primary Variables		
	1	2	3
Liquid	p_l	T	X_a^l
Gas	p_g	p_a	T
Two-Phase	p_g	p_a	s_g
	p_g	T	s_g

1.5. Assumptions and Limitations

Inherent in the above equations are certain key assumptions. They are:

1. Darcy's law for multiphase flow is valid in the flow regime of interest. Darcy's law is generally not valid for non-laminar flow characteristic of high velocity flow fields.
2. The phases attain instantaneous thermodynamic equilibrium.
3. The gas phase obeys the Ideal Gas Law. At higher temperature and pressure, the gas deviates from such behavior.
4. The solubility of gas in the liquid phase is governed by Henry's Law for ideal solutions. This law is valid for dilute solutions only. Air has a very low solubility in water, and as such, its behavior conforms to an ideal solution; however, if the air is replaced by a gas with much higher solubility such as CO_2 , ideal solution theory may not be applicable over the full range of pressure and temperature.
5. Although not imposed on the above equations, treatment of the liquid properties assumes that the solubility of gas in water has negligible effect on water properties, and as such the liquid properties are taken to be the same as that of pure water.
6. Chemical reaction between the rock and fluids is not considered.
7. Diffusion in the liquid phase is neglected.

1.6. Special Cases

In *METRA*, two special cases are treated which are of some interest. These are:

1. Isothermal flow of slightly compressible single phase liquid.
2. Heat flow due to pure conduction.

While *METRA* can treat both of the above cases in multiphase mode, simplicity in coding them as special modules, and the gain realized in the computing speed in excess of an order of magnitude justified their inclusion in *METRA*. In multiphase mode, *METRA* solves three nonlinear equations per grid-block, whereas the special modules solve only one linear equation per grid-block. The flow equations for the above cases reduce to:

$$\phi \frac{\partial \rho_l}{\partial t} = -\nabla \cdot (\rho_l \mathbf{v}_l) + q_l^G, \text{ for single liquid phase,} \quad (1.35)$$

and

$$(1 - \phi) C_p^{\text{rock}} \rho_{\text{rock}} \frac{\partial T}{\partial t} = -\kappa_{\text{eff}} \nabla T + q_H^G, \text{ for pure conduction.} \quad (1.36)$$

The liquid compressibility is given as

$$c_l = \frac{1}{\rho_l} \frac{d\rho_l}{dp}, \quad (1.37)$$

and for a slightly compressible liquid the accumulation term is replaced by

$$\phi \frac{\partial \rho_l}{\partial t} = \phi \frac{d\rho_l}{dp} \frac{\partial p}{\partial t} = \phi \rho_l c_l \frac{\partial p}{\partial t}. \quad (1.38)$$

2. FINITE-DIFFERENCE REPRESENTATION

Since the basic governing partial differential equations (PDEs), Eqns. (1.2), (1.3) and (1.4), are highly nonlinear they are not amenable to analytical techniques and must be solved numerically. All numerical methods, in essence, replace the original problem by an another one which is easier to solve and whose solution (hopefully) is a close approximation to the original one. The original PDEs are approximated by a set of nonlinear algebraic equations employing the well established implicit finite difference procedure. All terms are treated fully implicitly in order to ensure a high degree of numerical stability, albeit, at the expense of substantially increased computational work per time step and a more laborious coding task. Furthermore, a higher degree of implicitness introduces a larger truncation error with larger time-steps. These shortcomings are, however, more than offset the virtue of being able to take much larger time steps and being able to control the step-size within the acceptable truncation error.

In passing, it should be pointed out that although a semi-implicit formulation with a somewhat reduced level of implicitness can dramatically reduce the computing time per time-step, it may introduce a limitation in the size of the time step resulting from stability considerations. Such a formulation would be adequate and, in fact, is desirable for simple problems with low flux rates. Ideally, an adaptive implicit formulation where the degree of implicitness can be altered dynamically and spatially would retain the desired degree of stability and yet the computing time per time step would be several fold lesser than the fully implicit formulation. The coding task for such a formulation, however, is more demanding and complex. The fully implicit formulation is chosen in view of its reliability and robustness for simpler as well as difficult problems, and at the same time, the coding task is not overly penalizing.

In the following, the choices of gridding and discretization in cartesian and cylindrical geometries are described, the accumulation and flux terms are expressed in the finite-difference forms, the procedure for construction of Jacobian matrix is outlined, and an overall linearization and solution procedure is presented. A more detailed discussion and derivation of the Jacobian and its coefficients are given in the next section.

2.1. Gridding and Discretization

A finite-difference procedure entails discretizing the solution domain into a finite number of sub-domains commonly referred to as “grid-blocks” or “elements”. In cartesian geometry, these elements are in the form of rectangular (2-D) or parallelepiped (3-D) regions, while in the cylindrical geometry, they are concentric cylinders, or segments of concentric cylinders, (see Figures 1-2 below).

There are generally two types of grids used in the discretization:

1. Block Centered Grid, and
2. Interface Centered Grid.

In a block centered grid, the block interfaces are first defined and the centers are then placed mid-way between the interfaces, while in an interface centered grid, the block centers are first defined and the block interfaces are placed half-way between the two consecutive block centers. Figures 3-4 show the examples of such grids. Note that in an interface centered grid: (a) the block centers are not at the center of the grid block (except if the block sizes are equal, i.e. the centers are placed at equal intervals), and (b) there is one less node compared to a corresponding block centered grid.

Block Centered Grid

Interface Centered Grid

For equal size grid blocks, the two systems of grids are identical except for the boundary points. For flux or no flow boundary condition (Neumann condition), the block centered grid is the most convenient, while the condition of a constant field variable at the boundary, the interface grid is more natural. In practical applications, however, both types of boundary conditions are frequently needed simultaneously.

It may be remarked that the discretization error is of 2nd order for equal size grid blocks and the error increases as the ratio of size of the two consecutive blocks in any direction departs from unity. For a cylindrical system, the logarithm of the radius of the block centers must be at equal intervals for minimum spatial truncation error. That is, the geometric ratio of two consecutive block widths must be essentially constant.

Block centered grids are being widely used with satisfactory results, however, the interface centered grid may have a more sound theoretical basis. This stems in part from the fact that the differential equation is approximated at the grid points and not at the grid interfaces, and therefore, the boundaries should be half way between the grid points (unlike the block centered grids). Nevertheless, the two approaches are expected to give equivalent results.

2.2. Gridding in Cylindrical Coordinates

METRA has an option to invoke cartesian or cylindrical coordinate systems. This section outlines briefly the procedure for constructing such grids. There are two points which should be borne in mind with respect to cylindrical grids:

1. The block boundaries between two radial points ($i, i+1$) should be at the log mean radius and *not* at the arithmetic mean radius as is sometime done.
2. The block centers should be spaced at essentially equal logarithmic increments in the r direction to minimize the space truncation error to 2nd order.

The rationale for placing the boundaries at the mean log radius can be understood heuristically as follows. Consider a 1-D radial grid with the grid centers located at i , and $i+1$ with corresponding radii at r_i and r_{i+1} , respectively. The interface between these points is denoted by $r_{i+1/2}$, which is located somewhere between these points. Proceeding somewhat heuristically, the flux q_r at any point r is given by:

$$q_r = -\frac{2\pi k}{\mu} r \frac{dp}{dr}. \quad (2.1)$$

Integrating the above between the limits r_i and r_{i+1} , with $q_r = \text{constant}$, it follows that

$$q_r = -\frac{2\pi k}{\mu} \frac{p_{i+1} - p_i}{\ln \left(\frac{r_{i+1}}{r_i} \right)}. \quad (2.2)$$

Note that Eqn. (2.2) is an exact expression for the flux. Now the finite-difference representation of Eqn. (2.1) is:

$$q_r = -\frac{2\pi k}{\mu} r_{i+1/2} \frac{p_{i+1} - p_i}{r_{i+1} - r_i}. \quad (2.3)$$

It is required that Eqns. (2.2) and (2.1) be identical. Comparing the two expressions suggests that the following identity must be satisfied:

$$r_{i+1/2} = \frac{r_{i+1} - r_i}{\ln \left(\frac{r_{i+1}}{r_i} \right)} \quad (2.4)$$

= log mean radius between r_i and r_{i+1} .

Table 3 suggests that: (a) the log mean radii is always smaller than the corresponding arithmetic mean, and (b) the difference between the log mean and the arithmetic mean is small if (r_{i+1}/r_i) is small and grows with an increase in this ratio.

Table 3: Table showing the difference between arithmetic and logarithmic means ($r_i = 1$).

r_{i+1}/r_i	arithmetic mean	logarithmic mean
2.	1.5	1.44
3.	2.0	1.82
4.	2.5	2.16
5.	3.0	2.48
7.	3.5	3.08
10.	5.5	3.91
20.	10.5	6.34

Next the procedure for calculating the block center radii is discussed for equally spacing the centers logarithmically for two cases.

1. Centers for any two of the blocks given. Let r_j and r_k be the given centers for any two radial blocks. It is required that

$$\ln \left(\frac{r_2}{r_1} \right) = \ln \left(\frac{r_3}{r_2} \right) = \dots = \ln \left(\frac{r_{n+1}}{r_n} \right), \quad (2.5)$$

or

$$\frac{r_2}{r_1} = \frac{r_3}{r_2} = \dots = \frac{r_{n+1}}{r_n} = c \text{ (a constant)}. \quad (2.6)$$

Then,

$$r_k = c^{k-j} r_j, \quad (k > j). \quad (2.7)$$

Also,

$$r_i = r_1 c^{i-1}. \quad (2.8)$$

Knowing r_j and r_k , c can be calculated from Eqn. (2.5). Once c is known, r_i for rest of the blocks can be calculated using equations of the same form.

2. Centers for the first block (r_1) and the exterior radius (r_L) given. This represents a more typical case in many practical applications. The calculation of the block centers for this case is not so straightforward. Placing boundaries at log mean radii, the positions of the block interfaces are given by

$$r_{i+1/2} = \frac{r_{i+1} - r_i}{\ln \left(\frac{r_{i+1}}{r_i} \right)}. \quad (2.9)$$

Using Eqn. (2.9), it follows that

$$r_L = r_{n+1/2} = \frac{r_1 c^{n-1} (c - 1)}{\ln c}. \quad (2.10)$$

The constant c can be calculated numerically from Eqn. (2.10) using a Newton-Raphson procedure. Once c is known, the other radii of the remaining block centers can be readily calculated using Eqn. (2.8).

In *METRA*, an option is provided to calculate block boundaries as arithmetic average or logmean value. The former is provided primarily to compare the results of *METRA* with other codes which may use such averaging. *METRA* also has the facility to explicitly read all the block centers, however, if they are read for the first i blocks ($i < n$), then the rest from $i + 1$ to the last n th centers are computed internally.

2.3. Finite Difference Representation

In this section, the PDEs given by Eqns. (1.2), (1.3) and (1.4) are expressed in finite difference form. Consider a block centered grid of unequal grid spacing where Δx_i is the size of the i th block and the grid points are located at the

mid-point from the block boundaries. The partial differential equations are integrated over a block with volume V_B ($= \Delta x \Delta y \Delta z$ in cartesian coordinates). The quantities $M_a = m_a V_B$, $M = m V_B$, and $E = e V_B$, moles or energy in place. The total mole accumulation term is expressed in the backward first order time difference form for the i th grid block as

$$\frac{dM_i}{dt} = \Delta_t M_i = \frac{M_i^{n+1} - M_i^n}{\Delta t}, \quad (2.11)$$

where, the subscript i refers to the i th grid block, the superscripts n and $n+1$ designate the time level t_n and t_{n+1} respectively, and $\Delta t = t_{n+1} - t_n$. Since the quantity M_i denotes the moles in place in the grid-block, the difference equation, Eqn. (2.11) defines the change in number of moles in unit time, or simply the rate of change of mole accumulation.

The total mole flux terms in central difference form for flow in the x -direction may be written for the i th block as:

$$\begin{aligned} \int_{V_B} \nabla \cdot (\rho_l \mathbf{v}_l + \rho_g \mathbf{v}_g) dV &= \int_{\partial V_B} (\rho_l \mathbf{v}_l + \rho_g \mathbf{v}_g) \cdot d\mathbf{S} \\ &= \left[(\rho_l v_l + \rho_g v_g)_{i+1/2}^{n+1} A_{i+1/2} - (\rho_l v_l + \rho_g v_g)_{i-1/2}^{n+1} A_{i-1/2} \right], \\ &= A_{x_i} \left[(\rho_l v_l + \rho_g v_g)_{i+1/2}^{n+1} - (\rho_l v_l + \rho_g v_g)_{i-1/2}^{n+1} \right], \end{aligned} \quad (2.12)$$

where the cross-sectional area for flow in the i -direction is designated as

$$A_{x_i} = \Delta y_i \Delta z_i, \quad (2.13)$$

valid for a cartesian coordinate system. The former expression is valid for a curvilinear coordinate system with appropriately chosen interface areas.

For brevity and simplification in presentation, the following notation is introduced. For flux in the x -direction define

$$\Delta_x q_x = \Delta_x (q_{lx} + q_{gx}) = A_{x_i} \left[(\rho_l v_l + \rho_g v_g)_{i+1/2}^{n+1} - (\rho_l v_l + \rho_g v_g)_{i-1/2}^{n+1} \right]. \quad (14a)$$

Similarly, in y and z directions,

$$\Delta_y q_y = \Delta_y (q_{ly} + q_{gy}) = A_{y_i} \left[(\rho_l v_l + \rho_g v_g)_{i+1/2}^{n+1} - (\rho_l v_l + \rho_g v_g)_{i-1/2}^{n+1} \right], \quad (14b)$$

$$\Delta_z q_z = \Delta_z (q_{lz} + q_{gz}) = A_{z_i} \left[(\rho_l v_l + \rho_g v_g)_{i+1/2}^{n+1} - (\rho_l v_l + \rho_g v_g)_{i-1/2}^{n+1} \right]. \quad (14c)$$

Finally,

$$\Delta_x q_x + \Delta_y q_y + \Delta_z q_z = \Delta q, \quad (14d)$$

with

$$A_{y_j} = \Delta x_i \Delta z_k, \text{ and } A_{z_k} = \Delta x_i \Delta y_j. \quad (15)$$

Note that the finite difference operator Δ corresponds to the differential operator $\nabla \cdot$, the divergence. With this notation, Eqns. (1.2), (1.3) and (1.4) can be represented in finite-difference form for a general 3-D system as:

$$\Delta_t M_a = \Delta q_{m_a} + Q_{m_a}^G, \quad (16a)$$

$$\Delta_t M = \Delta q_m + Q_m^G, \quad (16b)$$

$$\Delta_t E = \Delta q_H + Q_H^G, \quad (16c)$$

where

$$q_{m_a} = \rho_l X_a^l v_l + \rho_g X_a^g v_g + \rho_g v_a^D, \quad (17a)$$

$$q_m = \rho_l v_l + \rho_g v_g, \quad (17b)$$

$$q_H = \rho_l H_l v_l + \rho_g H_g v_g + q_C, \quad (17c)$$

and

$$Q_{m_a}^G = V_B q_{m_a}^G, \text{ moles/sec}, \quad (18a)$$

$$Q_m^G = V_B q_m^G, \text{ moles/sec}, \quad (18b)$$

$$Q_H^G = V_B q_H^G, \text{ Joules/sec.} \quad (18c)$$

Equations (16a), (16b), and (16c) are written for each grid block such that for a N_B block system, there are a total of $3N_B$ equations with an equal number of unknowns.

2.4. Newton-Raphson Linearization and Solution

Since the algebraic set of Eqns. (16a), (16b), and (16c) are nonlinear, they must be solved iteratively using the Newton-Raphson (N-R) procedure. The N-R procedure entails three steps: (a) first order linearization of the equations, (b) solving the linearized set of equations, and (c) iteratively updating the solution

until the convergence is reached within the desired limit of tolerances. To couch these equations for N-R treatment, write:

$$f^{n+1}(x_1, x_2, x_3) = \Delta_t M_a - \Delta q_{m_a} - Q_{m_a}^G = 0, \quad (19a)$$

$$g^{n+1}(x_1, x_2, x_3) = \Delta_t M - \Delta q_m - Q_m^G = 0, \quad (19b)$$

$$h^{n+1}(x_1, x_2, x_3) = \Delta_t E - \Delta q_H - Q_H^G = 0, \quad (19c)$$

for the $n + 1$ st time step. It is tacitly assumed that the quantities M_a , M , E , q , and Q have already been expressed in terms of the desired primary variables. As pointed out earlier, these variables in general vary with the state of the fluid and as such they are replaced appropriately for each grid block following the "variable substitution" approach. The independent variables are designated as x_1 , x_2 , and x_3 where

$$x_1 = p \text{ for all systems,} \quad (20a)$$

$$x_2 = p_a \text{ for two-phase and single gas phase system,} \quad (20b)$$

$$x_3 = s_g \text{ for two-phase, and } T \text{ for single phase systems,} \quad (20c)$$

with $p = p_l$ for single liquid phase system, and $p = p_g$ for both two-phase and single gas phase systems. Expanding the functions f , g , and h at the k th Newtonian iteration, it follows that

$$f^{k+1} = f^k + f_{x_1}^k \delta x_1 + f_{x_2}^k \delta x_2 + f_{x_3}^k \delta x_3 = 0, \quad (21a)$$

$$g^{k+1} = g^k + g_{x_1}^k \delta x_1 + g_{x_2}^k \delta x_2 + g_{x_3}^k \delta x_3 = 0, \quad (21b)$$

$$h^{k+1} = h^k + h_{x_1}^k \delta x_1 + h_{x_2}^k \delta x_2 + h_{x_3}^k \delta x_3 = 0, \quad (21c)$$

where $f_{x_i}^k$, $g_{x_i}^k$, and $h_{x_i}^k$, are the derivatives of the functions with respect to unknown x_i , ($i = 1, 2, 3$), and

$$\delta x_i = x_i^{k+1} - x_i^k. \quad (22)$$

Equations (21a) can be expressed in a matrix form as:

$$\begin{bmatrix} f_{x_1}^k & f_{x_2}^k & f_{x_3}^k \\ g_{x_1}^k & g_{x_2}^k & g_{x_3}^k \\ h_{x_1}^k & h_{x_2}^k & h_{x_3}^k \end{bmatrix} \cdot \begin{bmatrix} \delta x_1 \\ \delta x_2 \\ \delta x_3 \end{bmatrix} = - \begin{bmatrix} f^k \\ g^k \\ h^k \end{bmatrix}, \quad (23)$$

or

$$\mathbf{A} \cdot \delta \mathbf{x} = \mathbf{r}. \quad (24)$$

The matrix \mathbf{A} of coefficients is referred to as the Jacobian matrix, and the right hand side, \mathbf{r} , as the residual vector.

The solution proceeds such that for the first Newtonian iteration ($k = 1$), the functions f , g , h , and their derivatives are evaluated at the beginning of a time step corresponding to the time t , and subsequently they are reevaluated at each iteration until the solution has converged. Upon convergence, the variables x_i as well as the quantities which are functions of x_i are updated to the next time level $t + \Delta t$. The process is repeated for each time step until the desired simulation time is reached. Convergence is achieved when one of the following two criteria, or both, are satisfied.

$$(a) \quad |f^k|_{\max} < \epsilon_{m_a}, \quad |g^k|_{\max} < \epsilon_m, \quad \text{and} \quad |h^k|_{\max} < \epsilon_H, \quad (25a)$$

where ϵ_i are the tolerances for convergence, and

$$(b) \quad |\delta x_i| < \epsilon_{x_i}, \quad \text{for } i = 1, 2, 3. \quad (25b)$$

3. CONSTRUCTION OF JACOBIAN MATRIX AND RESIDUAL VECTOR

Because the construction of the Jacobian matrix and the residual vector constitute the core of any numerical simulation model of this type, the derivation of these quantities are developed in detail. It may be noted that an inadequate treatment of these quantities or explicit representation of some of them may impair the rate of convergence and the numerical stability controlling the maximum time step size.

Since the intrinsic quantities, the density, the enthalpy, and their derivatives (with respect to the primary variables) are required in calculating the Jacobian coefficients arising from both the accumulation and the flux terms, it is convenient to first express these quantities in terms of the desired primary variables. First the accumulation terms are treated followed by the fluxes.

3.1. Representation of Intrinsic Properties and Their Derivatives in Terms of Primary Variables

These quantities are treated separately depending on the thermodynamic state of the fluid.

3.1.1. Single Liquid Phase

The intrinsic properties of the liquid phase are taken to be independent of the dissolved air content as well as other dissolved constituents, and are assigned the values of pure water. That is, the liquid density, with $p = p_l$ is approximated by

$$\rho_l \simeq \rho_w^\circ(p, T), \quad (1)$$

where ρ_w° refers to the density of pure liquid water. The derivative of the density can be expressed as

$$\delta \rho_l = \rho_{wp}^\circ \delta p + \rho_{wT}^\circ \delta T, \quad (2)$$

where ρ_{wp}° and ρ_{wT}° are the partial derivatives of ρ_w° with respect to pressure and temperature, respectively.

Similarly the liquid internal energy is approximated as

$$U_l \simeq U_w^\circ(p, T) = H_w^\circ - \frac{p}{\rho_w^\circ}, \quad (3)$$

where H_w° and U_w° refer to the enthalpy and internal energy of pure liquid water, and

$$\begin{aligned} \delta U_l &= \left(H_{wp}^\circ + \frac{p}{\rho_w^\circ} \rho_{wp}^\circ - \frac{1}{\rho_w^\circ} \right) \delta p + \left(H_{wT}^\circ + \frac{p}{\rho_w^\circ} \rho_{wT}^\circ \right) \delta T, \\ &= U_{lp} \delta p + U_{lT} \delta T, \end{aligned} \quad (4)$$

where H_{wp}° , and H_{wT}° are the partial derivatives of H_w° with respect to pressure and temperature, and U_{lp} , and U_{lT} are the corresponding derivatives of the total internal energy of the liquid with respect to pressure and temperature, respectively.

The functional relation of porosity to pore compressibility c_{rp} and expansibility c_{rT} is assumed to have the form

$$\phi = \phi_{\text{ref}} [1 + c_{rp}(p - p_{\text{ref}}) + c_{rT}(T - T_{\text{ref}})], \quad (6)$$

and

$$\begin{aligned} \delta \phi &= \phi_{\text{ref}} c_{rp} \delta p + \phi_{\text{ref}} c_{rT} \delta T, \\ &= \phi_p \delta p + \phi_T \delta T, \end{aligned} \quad (7)$$

where ϕ_p and ϕ_T are derivatives with respect to pressure and temperature, respectively.

3.1.2. Single Gas Phase

Employing the ideal gas law for air, the molar density of air is given by

$$\rho_a^g = \frac{p_a}{RT}. \quad (8)$$

The density of a mixture of water vapor and air, with $p = p_g$, is assumed to be given by the sum of the water vapor and air molar densities

$$\rho_g \simeq \rho_v^\circ(p_v, T) + \frac{p_a}{RT} = \rho_g(p, p_a, T), \quad (9)$$

where the water vapor density ρ_v° and air density are evaluated at their respective partial pressures. The water vapor partial pressure p_v is a function of the primary variables p and p_a . It follows that

$$\delta p_v = \delta p - \delta p_a. \quad (10)$$

Then

$$\begin{aligned} \delta \rho_g &= \frac{\partial \rho_v^\circ}{\partial p_v} (\delta p - \delta p_a) + \frac{\partial \rho_v^\circ}{\partial T} \delta T + \frac{1}{R} \left[\frac{\delta p_a}{T} - \frac{p_a}{T^2} \delta T \right], \\ &= \frac{\partial \rho_v^\circ}{\partial p_v} \delta p + \frac{\partial \rho_v^\circ}{\partial T} \delta T + \left[\frac{1}{RT} - \frac{\partial \rho_v^\circ}{\partial p_v} \right] \delta p_a - \frac{p_a}{RT^2} \delta T, \\ &= \rho_{gp} \delta p + \rho_{gp_a} \delta p_a + \rho_{gT} \delta T. \end{aligned} \quad (11)$$

The enthalpy of the gas mixture is weighted by the mole fraction of air and water vapor according to the expression

$$H_g \simeq X_w^g H_v^\circ(p_v, T) + X_a^g C_{va} T = H_g(p, p_a, T), \quad (12)$$

where C_{va} denotes the heat capacity of air. The derivative is given by

$$\begin{aligned} \delta H_g &= X_w^g \left[\frac{\partial H_v^\circ}{\partial p_v} (\delta p - \delta p_a) + \frac{\partial H_v^\circ}{\partial T} \delta T \right] \\ &\quad + H_v^\circ \delta X_w^g + X_a^g C_{va} \delta T + C_{va} T \delta X_a^g. \end{aligned} \quad (13)$$

Making use of the relations

$$\begin{aligned} \delta X_w^g &= -\delta X_a^g = \frac{p_a}{p^2} \delta p - \frac{\delta p_a}{p}, \\ &= \frac{1}{p} (X_a^g \delta p - \delta p_a), \end{aligned} \quad (14)$$

it follows that

$$\delta H_g = H_{gp} \delta p + H_{gp_a} \delta p_a + H_{gT} \delta T, \quad (15)$$

where

$$H_{gp} = X_w^g \frac{\partial H_v^\circ}{\partial p_v} + (H_v^\circ - C_{va} T) \frac{X_a^g}{p}, \quad (16a)$$

$$H_{gp_a} = -X_w^g \frac{\partial H_v^\circ}{\partial p_v} - (H_v^\circ - C_{va} T) \frac{1}{p}, \quad (16b)$$

$$H_{gT} = X_w^g \frac{\partial H_v^\circ}{\partial T} + X_a^g C_{va}. \quad (16c)$$

The variation of porosity as a function of pressure and temperature is the same as given by Eqn. (7).

3.1.3. Two-Phase System: Vapor Pressure Lowering Absent

For a two-phase system the independent variables are $p = p_g$, p_a and s_g . In the absence of vapor pressure lowering temperature is represented as a function of vapor pressure: $T = T(p_v)$.

Gas Properties Proceeding from Eqn. (9) and recognizing that the vapor pressure $p_v = p - p_a$, the gas density can be written as:

$$\rho_g \simeq \rho_v^\circ(p_v, T(p_v)) + \frac{p_a}{RT(p_v)} = \rho_g(p, p_a). \quad (17)$$

Its derivative is given by

$$\begin{aligned} \delta \rho_g &= \left[\frac{\partial \rho_v^\circ}{\partial p_v} + \frac{\partial \rho_v^\circ}{\partial T} \frac{dT}{dp_v} \right] (\delta p - \delta p_a) + \frac{\delta p_a}{RT} - \frac{p_a}{RT^2} T_{p_v} (\delta p - \delta p_a), \\ &= \rho_{gp} \delta p + \rho_{gp_a} \delta p_a, \end{aligned} \quad (18)$$

where

$$\rho_{gp} = \frac{\partial \rho_v^\circ}{\partial p_v} + \left(\frac{\partial \rho_v^\circ}{\partial T} - \frac{p_a}{RT^2} \right) T_{p_v}, \quad (19a)$$

and

$$\rho_{gp_a} = - \left(\frac{\partial \rho_v^\circ}{\partial p_v} + \frac{\partial \rho_v^\circ}{\partial T} T_{p_v} \right) + \frac{1}{RT} \left(1 + \frac{p_a}{T} T_{p_v} \right), \quad (19b)$$

with

$$T_{p_v} = \frac{dT}{dp_v}. \quad (20)$$

The enthalpy of a saturated gas mixture is given by:

$$H_g \simeq X_w^g H_v^\circ + X_a^g C_{va} T = H_g(p, p_a). \quad (21)$$

After some algebraic manipulations and recognizing that $X_a^g = p_a/p$, and $X_w^g = 1 - X_a^g$, the gas enthalpy derivative can be expressed as,

$$\delta H_g = H_{gp} \delta p + H_{gp_a} \delta p_a, \quad (22)$$

where

$$H_{gp} = X_w^g \left(\frac{\partial H_v^\circ}{\partial p_v} + \frac{\partial H_v^\circ}{\partial T} T_{p_v} \right) + \frac{X_a^g}{p} (H_v^\circ - C_{va} T) + X_a^g C_{va} T_{p_v}, \quad (23a)$$

and

$$H_{gp_a} = -X_w^g \left(\frac{\partial H_v^\circ}{\partial p_v} + \frac{\partial H_v^\circ}{\partial T} T_{p_v} \right) - \frac{1}{p} (H_v^\circ - C_{va} T) - X_a^g C_{va} T_{p_v}. \quad (23b)$$

Liquid Properties For the saturated liquid density there are two cases to consider: the absence and presence of capillary forces.

Capillary Forces Absent. First consider the case in which capillary forces are absent. In this case $p_l = p_v$. The saturated liquid density is approximated by the pure liquid water density as:

$$\rho_l \simeq \rho_w^\circ(p_l, T) = \rho_l(p, p_a), \quad (24)$$

a function of the two primary variables $p = p_g$ and p_a , since along the saturation curve of pure water $p_l = p_v = p - p_a$. It follows that the derivative of ρ_l is given by

$$\begin{aligned} \delta \rho_l &= \frac{\partial \rho_w^\circ}{\partial p_l} (\delta p - \delta p_a) + \frac{\partial \rho_w^\circ}{\partial T} T_{p_v} (\delta p - \delta p_a), \\ &= \rho_{lp} \delta p + \rho_{lp_a} \delta p_a, \end{aligned} \quad (25)$$

where

$$\rho_{lp} = \frac{\partial \rho_w^\circ}{\partial p_l} + \frac{\partial \rho_w^\circ}{\partial T} T_{p_v}, \quad (26a)$$

$$\rho_{lp_a} = - \left(\frac{\partial \rho_w^\circ}{\partial p_l} + \frac{\partial \rho_w^\circ}{\partial T} T_{p_v} \right). \quad (26b)$$

The liquid internal energy is approximated by pure liquid water internal energy:

$$U_l \simeq U_w^\circ(p_v, T(p_v)), \quad (27)$$

and

$$\begin{aligned} \delta U_l &= \frac{\partial U_w^\circ}{\partial p_l} (\delta p - \delta p_a) + \frac{\partial U_w^\circ}{\partial T} T_{p_v} (\delta p - \delta p_a), \\ &= U_{lp} \delta p + U_{lp_a} \delta p_a, \end{aligned} \quad (28)$$

where U_{lp} , and U_{lp_a} are the derivatives with respect to total gas pressure and air partial pressure, respectively, defined by

$$U_{lp} = \frac{\partial U_w^\circ}{\partial p_l} + \frac{\partial U_w^\circ}{\partial T} T_{p_v}, \quad (29a)$$

$$U_{lp_a} = - \left(\frac{\partial U_w^\circ}{\partial p_l} + \frac{\partial U_w^\circ}{\partial T} T_{p_v} \right). \quad (29b)$$

Capillary Forces Present. In the presence of capillary forces $p_l = p - p_c(s_g) = p_l(p, s_g)$, where p_c represents the capillary pressure a function of saturation. In this case the liquid density is a function of all three primary variables

$$\rho_l \simeq \rho_w^\circ(p_l, T) = \rho_l(p, p_a, s_g). \quad (30)$$

It follows that the derivative of ρ_l is given by

$$\begin{aligned} \delta \rho_l &= \frac{\partial \rho_w^\circ}{\partial p_l} \left(\delta p - \frac{\partial p_c}{\partial s_g} \delta s_g \right) + \frac{\partial \rho_w^\circ}{\partial T} T_{p_v} (\delta p - \delta p_a), \\ &= \rho_{lp} \delta p + \rho_{lp_a} \delta p_a + \rho_{ls_g} \delta s_g, \end{aligned} \quad (31)$$

where

$$\rho_{lp} = \frac{\partial \rho_w^\circ}{\partial p_l} + \frac{\partial \rho_w^\circ}{\partial T} T_{p_v}, \quad (32a)$$

$$\rho_{lp_a} = -\frac{\partial \rho_w^\circ}{\partial T} T_{p_v}, \quad (32b)$$

$$\rho_{ls_g} = -\frac{\partial \rho_w^\circ}{\partial p_l} \frac{\partial p_c}{\partial s_g}. \quad (32c)$$

The liquid internal energy has the form

$$U_l \simeq U_w^\circ(p_l, T(p_v)), \quad (33)$$

and

$$\begin{aligned} \delta U_l &= \frac{\partial U_w^\circ}{\partial p_l} \left(\delta p - \frac{\partial p_c}{\partial s_g} \delta s_g \right) + \frac{\partial U_w^\circ}{\partial T} T_{p_v} (\delta p - \delta p_a), \\ &= U_{lp} \delta p + U_{lp_a} \delta p_a + U_{ls_g} \delta s_g, \end{aligned} \quad (34)$$

where U_{lp} , U_{lp_a} , and U_{ls_g} are the derivatives with respect to total gas pressure, air partial pressure and saturation, respectively, defined by

$$U_{lp} = \frac{\partial U_w^\circ}{\partial p_l} + \frac{\partial U_w^\circ}{\partial T} T_{p_v}, \quad (35a)$$

$$U_{lp_a} = -\frac{\partial U_w^\circ}{\partial T} T_{p_v}, \quad (35b)$$

$$U_{ls_g} = -\frac{\partial U_w^\circ}{\partial p_l} \frac{\partial p_c}{\partial s_g}. \quad (35c)$$

3.1.4. Two-Phase System: Vapor Pressure Lowering Present

In the presence of vapor pressure lowering $T = T(p_v, s_g)$ as follows from the Kelvin equation

$$p_v = p_s(T) e^{-p_c(s_g)/\rho_l RT}, \quad (36)$$

where p_c denotes the capillary pressure. The density of liquid water has the functional form:

$$\rho_l(p, p_a, s_g) = \rho_w^\circ \{p_s[T(p - p_a, s_g)], T[p - p_a, s_l]\}, \quad (37)$$

where the density of pure liquid water is denoted by $\rho_w^\circ(p_v, T)$.

In this case the total derivative of the liquid density becomes

$$\delta \rho_l = \rho_{lp} \delta p + \rho_{lp_a} \delta p_a + \rho_{ls_g} \delta s_g, \quad (38)$$

where

$$\rho_{lp} = \frac{\partial \rho_l}{\partial p} = \left[\frac{\partial \rho_w^\circ}{\partial p_v} \frac{dp_s}{dT} + \frac{\partial \rho_w^\circ}{\partial T} \right] \frac{\partial T}{\partial p_v}, \quad (39a)$$

$$\rho_{lp_a} = \frac{\partial \rho_l}{\partial p_a} = - \left[\frac{\partial \rho_w^\circ}{\partial p_v} \frac{dp_s}{dT} + \frac{\partial \rho_w^\circ}{\partial T} \right] \frac{\partial T}{\partial p_v} = - \frac{\partial \rho_l}{\partial p}, \quad (39b)$$

$$\rho_{ls_g} = \frac{\partial \rho_l}{\partial s_g} = \left[\frac{\partial \rho_w^\circ}{\partial p_v} \frac{dp_s}{dT} + \frac{\partial \rho_w^\circ}{\partial T} \right] \frac{\partial T}{\partial s_g}. \quad (39c)$$

Likewise the internal energy has the functional form

$$U_l(p, p_a, s_g) = U_w^\circ \{p_s[T(p - p_a, s_g)], T[p - p_a, s_l]\}, \quad (40)$$

with the derivative

$$\delta U_l = U_{lp} \delta p + U_{lp_a} \delta p_a + U_{ls_g} \delta s_g, \quad (41)$$

where U_{lp} , U_{lp_a} , and U_{ls_g} are the derivatives with respect to total gas pressure, air partial pressure and saturation, respectively, defined by

$$U_{lp} = \frac{\partial U_l}{\partial p} = \left[\frac{\partial U_w^\circ}{\partial p_v} \frac{dp_s}{dT} + \frac{\partial U_w^\circ}{\partial T} \right] \frac{\partial T}{\partial p_v}, \quad (42a)$$

$$U_{lp_a} = \frac{\partial U_l}{\partial p_a} = - \left[\frac{\partial U_w^\circ}{\partial p_v} \frac{dp_s}{dT} + \frac{\partial U_w^\circ}{\partial T} \right] \frac{\partial T}{\partial p_v} = - \frac{\partial U_w^\circ}{\partial p}, \quad (42b)$$

$$U_{ls_g} = \frac{\partial U_l}{\partial s_g} = \left[\frac{\partial U_w^\circ}{\partial p_v} \frac{dp_s}{dT} + \frac{\partial U_w^\circ}{\partial T} \right] \frac{\partial T}{\partial s_g}. \quad (42c)$$

Derivatives $\partial T/\partial p_v$ and $\partial T/\partial s_g$ are obtained by explicitly differentiating the logarithmic form of the Kelvin equation

$$\ln p_v = \ln p_s[T(p_v, s_g)] - \frac{p_c(s_g)}{\rho_w^\circ[p_v, T(p_v, s_g)]RT(p_v, s_g)}, \quad (43)$$

to give:

$$\frac{\partial T}{\partial p_v} = \frac{\frac{\rho_w^\circ RT}{p_v} - \frac{p_c}{\rho_w^\circ} \frac{\partial \rho_w^\circ}{\partial p}}{\frac{\rho_w^\circ RT}{p_s} \frac{dp_s}{dT} + \frac{p_c}{T} + \frac{p_c}{\rho_w^\circ} \frac{\partial \rho_w^\circ}{\partial T}}, \quad (44)$$

and

$$\frac{\partial T}{\partial s_g} = \frac{\frac{dp_c}{ds_g}}{\frac{\rho_w^\circ RT}{p_s} \frac{dp_s}{dT} + \frac{p_c}{T} + \frac{p_c}{\rho_w^\circ} \frac{\partial \rho_w^\circ}{\partial T}}. \quad (45)$$

The variation of porosity with temperature and pressure given by Eqn. (7) must be expressed in terms of δp and δp_a . From Eqn. (7)

$$\begin{aligned} \delta \phi &= \phi_p \delta p + \phi_T T_{p_v} (\delta p - \delta p_a), \\ &= (\phi_p + \phi_T T_{p_v}) \delta p - \phi_T T_{p_v} \delta p_a, \\ &= \phi_p \delta p + \phi_{p_a} \delta p_a, \end{aligned} \quad (46)$$

where

$$\phi_p = \phi_p + \phi_T T_{p_v}, \quad (47)$$

and

$$\phi_{p_a} = -\phi_T T_{p_v} \delta p_a. \quad (48)$$

3.2. Expansion of Accumulation Terms

As before, the accumulation terms are expanded for a single liquid phase, single gas phase, and finally a two-phase system. For each case, first the accumulation terms corresponding to the air component are treated, then the total moles, and

then the energy terms. From Eqns. (21a), the expansion of these terms may be expressed as:

$$\Delta_t M_a = \frac{1}{\Delta t} \left[M_a^k + \frac{\partial M_a^k}{\partial x_1} \delta x_1 + \frac{\partial M_a^k}{\partial x_2} \delta x_2 + \frac{\partial M_a^k}{\partial x_3} \delta x_3 - M_a^n \right], \quad (49a)$$

and

$$\Delta_t M = \frac{1}{\Delta t} \left[M^k + \frac{\partial M^k}{\partial x_1} \delta x_1 + \frac{\partial M^k}{\partial x_2} \delta x_2 + \frac{\partial M^k}{\partial x_3} \delta x_3 - M^n \right], \quad (49b)$$

$$\Delta_t E = \frac{1}{\Delta t} \left[E^k + \frac{\partial E^k}{\partial x_1} \delta x_1 + \frac{\partial E^k}{\partial x_2} \delta x_2 + \frac{\partial E^k}{\partial x_3} \delta x_3 - E^n \right], \quad (49c)$$

where x_i are the primary variables. The derivatives of M_a , M , and E are presented explicitly below for each case.

3.2.1. Single Liquid Phase

With zero gas saturation ($s_g = 0$, and $s_l = 1$), the primary variables for this case are $p = p_l$, X_a^l , and T .

Air Accumulation Terms:

$$M_a = V_B \phi \rho_l X_a^l, \quad (50a)$$

$$\frac{\partial M_a}{\partial p} = V_B [\phi \rho_{lp} + \phi_p \rho_l] X_a^l, \quad (50b)$$

$$\frac{\partial M_a}{\partial T} = V_B [\phi \rho_{lT} + \rho_l \phi_T] X_a^l, \quad (50c)$$

$$\frac{\partial M_a}{\partial X_a^l} = V_B \phi \rho_l. \quad (50d)$$

Total Moles Accumulation Terms:

$$M = V_B \phi \rho_l. \quad (51a)$$

By setting $X_a^l = 1$, and its associated derivatives to zero in the above equations, the coefficients can be directly written as:

$$\frac{\partial M}{\partial p} = V_B [\phi \rho_{lp} + \rho_l \phi_p], \quad (51b)$$

$$\frac{\partial M}{\partial T} = V_B [\phi \rho_{lT} + \rho_l \phi_T], \quad (51c)$$

$$\frac{\partial M}{\partial X_a^l} = 0. \quad (51d)$$

Total Energy Accumulation Terms:

$$E = V_B [\phi \rho_l U_l + (1 - \phi) \rho_{\text{rock}} C_p^{\text{rock}} T], \quad (52a)$$

$$\frac{\partial E}{\partial p} = V_B [\phi \rho_l U_{lp} + (\phi \rho_{lp} + \phi_p \rho_l) U_l], \quad (52b)$$

$$\frac{\partial E}{\partial T} = V_B [\phi \rho_l U_{lT} + (\phi \rho_{lT} + \phi_T \rho_l) U_l + (1 - \phi) \rho_{\text{rock}} C_p^{\text{rock}} T], \quad (52c)$$

$$\frac{\partial E}{\partial X_a^l} = 0. \quad (52d)$$

3.2.2. Single Gas Phase

With zero liquid saturation ($s_l = 0$, and $s_g = 1$), the primary unknowns for this case are $p = p_g$, p_a , and T .

Air Accumulation Terms:

$$M_a = V_B \phi \rho_g X_a^g, \quad (53a)$$

$$\frac{\partial M_a}{\partial p} = V_B [\phi \rho_{gp} + \rho_g \phi_p] X_a^g, \quad (53b)$$

$$\frac{\partial M_a}{\partial T} = V_B [\phi \rho_{gT} + \rho_g \phi_T] X_a^g, \quad (53c)$$

$$\frac{\partial M_a}{\partial X_a^g} = V_B \phi \rho_g. \quad (53d)$$

Total Moles Accumulation Terms:

$$M = V_B \phi \rho_l. \quad (54a)$$

By letting $X_a^g = 1$, and setting its associated derivatives to zero in the above relations, it is possible to directly write the coefficients as:

$$\frac{\partial M}{\partial p} = V_B [\phi \rho_{gp} + \rho_g \phi_p], \quad (54b)$$

$$\frac{\partial M}{\partial T} = V_B [\phi \rho_{gT} + \rho_g \phi_T], \quad (54c)$$

$$\frac{\partial M}{\partial X_a^g} = 0. \quad (54d)$$

Total Energy Accumulation Terms:

$$E = V_B [\phi \rho_l U_l + (1 - \phi) \rho_{\text{rock}} C_p^{\text{rock}} T], \quad (55a)$$

$$\frac{\partial E}{\partial p} = V_B [\phi \rho_l U_{lp} + (\phi \rho_{lp} + \phi_p \rho_l) U_l], \quad (55b)$$

$$\frac{\partial E}{\partial T} = V_B [\phi \rho_l U_{lT} + (\phi \rho_{lT} + \phi_T \rho_l) U_l + (1 - \phi) \rho_{\text{rock}} C_p^{\text{rock}}], \quad (55c)$$

$$\frac{\partial E}{\partial X_a^l} = 0. \quad (55d)$$

3.2.3. Two-Phase System: Vapor Pressure Lowering Absent

The chosen independent variables for this case are $p = p_g$, p_a , and s_g . We, therefore, expand M_a , M and E in terms of these variables.

Air Accumulation Terms:

$$M_a = V_B [\phi \rho_l s_l X_a^l + \phi \rho_g s_g X_a^g] = V_B \phi \left[\frac{\rho_l s_l}{K_H} + \rho_g s_g \right] X_a^g, \quad (56a)$$

$$\frac{\partial M_a}{\partial p} = V_B \left[X_a^g \phi \left(\frac{\rho_{wp} s_l}{K_H} + \rho_{gp} s_g \right) + \left(\frac{\rho_l s_l}{K_H} + \rho_g s_g \right) \left(\phi_p - \frac{1}{p} \right) X_a^g \right], \quad (56b)$$

$$\frac{\partial M_a}{\partial p_a} = V_B \left[X_a^g \phi \left(-\frac{\rho_{wp} s_l}{K_H} + \rho_{gp_a} s_g \right) + \left(\frac{\rho_l s_l}{K_H} + \rho_g s_g \right) \left(X_a^g \phi_p + \frac{1}{p} \right) X_a^g \right], \quad (56c)$$

$$\frac{\partial M}{\partial s_g} = V_B \phi X_a^g (\rho_g - \rho_l). \quad (56d)$$

In the above the identity $\delta s_l = -\delta s_g$, and the Henry's law for solubility of air in pure water is used.

Total Mole Accumulation Terms:

$$M = V_B \phi [\rho_l s_l + \rho_g s_g]. \quad (57a)$$

As before, set $X_a^g = 1$, and the corresponding derivatives to zero in the above equations, and write directly the desired terms as:

$$\frac{\partial M}{\partial p} = V_B [\phi (s_l \rho_{wp} + s_g \rho_{gp}) + \phi_p (\rho_l s_l + \rho_g s_g)], \quad (57b)$$

$$\frac{\partial M}{\partial p_a} = V_B [(-s_l \rho_{wp} + s_g \rho_{gp_a})] \phi, \quad (57c)$$

$$\frac{\partial M}{\partial s_g} = V_B \phi [\rho_g - \rho_l]. \quad (57d)$$

Total Energy Accumulation Terms: The energy term is given by

$$E = V_B [(\rho_l s_l U_l + \rho_g s_g U_g) \phi + (1 - \phi) C_p^{\text{rock}} \rho_{\text{rock}} T]. \quad (58)$$

In order to avoid the storage and computation of the internal energy, the above equation is expressed in terms of enthalpy. Substituting the internal energy in terms of enthalpy ($U = H - p/\rho$), yields:

$$E = V_B [(\rho_l s_l H_l + \rho_g s_g H_g - p) \phi + (1 - \phi) C_p^{\text{rock}} \rho_{\text{rock}} T], \quad (59a)$$

$$\frac{\partial E}{\partial p} = V_B \{ [s_l (\rho_l H_{wp} + H_w \rho_{wp}) + s_g (\rho_g H_{gp} + H_g \rho_{gp}) - 1] \phi + (1 - \phi) C_p^{\text{rock}} \rho_{\text{rock}} T_{sp} \}, \quad (59b)$$

$$\frac{\partial E}{\partial p_a} = V_B \{ [-s_l (\rho_l H_{wp} + H_w \rho_{wp}) + s_g (\rho_g H_{gp_a} + H_g \rho_{gp_a}) - 1] \phi + (1 - \phi) C_p^{\text{rock}} \rho_{\text{rock}} T_{sp} \}, \quad (59c)$$

$$\frac{\partial E}{\partial s_g} = V_B \phi [\rho_g H_g - \rho_l H_l]. \quad (59d)$$

3.2.4. Two-Phase System: Vapor Pressure Lowering Present

The above completes the accumulation coefficients which contribute to the make-up of the main diagonal of the Jacobian matrix. Additional contribution to the diagonal will arise from the flux derivatives discussed in the following section.

3.3. Expansion of Flux Terms

The finite difference representation of flux terms was derived in Eqn. (2.12) and Eqn. (16a), (16b) and (16c) for general 3-D systems. Rewriting the net flux in the x -direction it follows that,

$$q_{x,i+1/2} - q_{x,i-1/2} = A_{x_i} \left[(\rho_l U_l + \rho_g U_g)_{i+1/2}^{n+1} - (\rho_l U_l + \rho_g U_g)_{i-1/2}^{n+1} \right], \quad (60)$$

at the $n + 1$ st time step. Note that the fluxes $q_{i\pm 1/2}$ must be evaluated at the block interface located at $(i - 1/2)$ between the i th and $i - 1$ st blocks, and thus the flux is controlled by the thermodynamic state of the fluid and the rock properties of the grid blocks on either side of the interface. In order to better

understand the processes involved, first the liquid flux across the interface at $(i - 1/2)$ is considered.

Assuming cartesian coordinates, the liquid flux is given by

$$q_{x,i-1/2}^l = (k\lambda_l\rho_l)_{i-1/2}\Delta y_j\Delta z_k\Delta\Phi_l, \quad (61)$$

where

$$\begin{aligned} \Delta\Phi_l &= \text{potential difference between the blocks,} \\ &= p_{l,i} - p_{l,i-1} - \bar{\gamma}_{l,i-1/2}\Delta h, \end{aligned} \quad (62)$$

with

$$\lambda_l = \frac{k_{rl}}{\mu_l} = \text{mobility.} \quad (63)$$

In the above equation, the absolute rock permeability k , the mobility (k_{rl}/μ_l) , and the liquid density (ρ_l) must be evaluated at the interface. A different averaging scheme is employed for each of the above quantities as discussed below.

The absolute rock permeability is calculated as the harmonic average of k_{i-1} and k_i , (similar to resistances in parallel), the density is taken as the arithmetic average, and the mobility is averaged based on a weighing factor applied to the upstream block. Thus

$$k_{i-1/2} = \frac{2k_i k_{i-1}}{\Delta x_i k_{i-1} + \Delta x_{i-1} k_i}, \quad (64)$$

$$\rho_{l,i-1/2} = \frac{\rho_{l,i} + \rho_{l,i-1}}{2}, \quad (65)$$

and

$$\lambda_{l,i-1/2} = \omega\lambda_{lu} + (1 - \omega)\lambda_{ld}, \quad (66)$$

where ω = weighing factor, and the subscripts u and d refer to the upstream and downstream blocks, respectively. A value of $\omega = 1/2$ results in an arithmetic value for the mobility. Substituting the averages as defined above, the flux at the interface is given by

$$q_{x,i-1/2}^l = \Upsilon_{x,i-1/2}\rho_{l,i-1/2}\lambda_{lu}\Delta\Phi_l, \quad (67)$$

where the transmissibility is defined by

$$\Upsilon_{x,i-1/2} = \frac{2k_i k_{i-1}}{\Delta x_i k_{i-1} + \Delta x_{i-1} k_i} \Delta y_j \Delta z_k, \quad (68)$$

and $\omega = 1$. Note that for $i = 1$, the transmissibility Υ_x is set to zero, as it is at $n_x + 1$, the outermost interface. This in essence sets the boundary condition of zero flux at the boundary of the system. If the permeability is constant with time, Υ_x remains unchanged. The gas flux can be written analogously as:

$$q_{x,i-1/2}^g = \Upsilon_{x,i-1/2} \rho_{g,i-1/2} \lambda_{gu} \Delta \Phi_g, \quad (69)$$

where

$$\Delta \Phi_g = p_{g,i} - p_{g,i-1} - \bar{\gamma}_g \Delta h. \quad (70)$$

Table 4: Possible combinations of phases in neighboring blocks.

Liquid Flux		Gas Flux	
upstream block	downstream block	upstream block	downstream block
liquid	liquid two-phase gas	gas	liquid two-phase gas
two-phase	liquid two-phase gas	two-phase	liquid two-phase gas

Fluxes in y - and z -directions follow the identical logic. Since the primary independent variables change with the thermodynamic state of the fluid, the expansion of the flux must be expressed in terms of these variables. Depending on the upstream block and its state, there are twelve possible scenarios for such expansion as given in Table 4. For those scenarios for which different phases are present in adjacent blocks, there are additional sub-scenarios depending on whether the i th or $(i - 1)$ st block is the upstream block as indicated in Table 5.

In the following the liquid flux is treated first under the above described scenarios, followed by the gas flux. For each case, the expansion of the associated air and the energy fluxes is also presented.

Table 5: Possible combinations with different phases in neighboring blocks.

upstream block	downstream block
gas	liquid two-phase
liquid	gas two-phase
two-phase	gas liquid

3.3.1. Liquid Flux

From Eqn. (67) and suppressing the subscript x , it follows that

$$q_{l,i-1/2}^{k+1} = q_{l,i-1/2}^k + \delta q_{l,i-1/2}, \quad (71)$$

where

$$\delta q_{l,i-1/2} = \Upsilon_{i-1/2} \left[\Delta \Phi_l \rho_{l,i-1/2} \delta \lambda_{lu} + \rho_{l,i-1/2} \lambda_{lu} \Delta p_c - \rho_{l,i-1/2} \lambda_{lu} \Delta \delta p_c + 2\alpha \delta \rho_{l,i-1/2} \right], \quad (72)$$

and

$$\delta \lambda_l = \frac{d\lambda_l}{ds_g} ds_g, \quad (73)$$

$$\Delta p_c = p_{c,i} - p_{c,i-1}, \quad (74)$$

$$\delta p_c = \frac{dp_c}{ds_g} ds_g, \quad (75)$$

$$\alpha = \frac{1}{2} \lambda_l (\Delta \Phi_l - \rho_{l,i-1/2} c_f), \quad (76)$$

with

$$c_f = W_w \frac{\Delta h}{g}. \quad (77)$$

The associate air flux is given by

$$q_{a,i-1/2}^{k+1} = (X_a^l q_l)_{i-1/2}^k + (\delta X_a^l q_l)_{i-1/2}, \quad (78)$$

where

$$(\delta X_a^l q_l)_{i-1/2} = X_{au}^l \delta q_{l,i-1/2} + q_{l,i-1/2} \delta X_{au}^l. \quad (79)$$

Upstream weighing is used for the air mole fraction X_a^l .

The convective energy flux associated with the liquid phase is given by

$$q_l H_l|_{i-1/2}^{k+1} = q_l H_l|_{i-1/2}^k + (\delta q_l H_l)_{i-1/2}, \quad (80)$$

and

$$\delta q_l H_l = q_l \delta H_l + H_l \delta q_l, \quad (81)$$

where

$$\delta H_{l,i-1/2} = \frac{1}{2} (\delta H_{li} + \delta H_{l,i-1}). \quad (82)$$

The enthalpy at the interface is evaluated as the arithmetic average of the adjacent values in blocks i and $i-1$.

Eqns. (72–81) are general expressions for fluxes which can be applied to each of the different scenarios mentioned above. The quantities $\delta \rho_l$, δX_a^l , and δH_l in these equations must be expressed in terms of their primary variables during the expansion. For example, liquid density must be expressed as a function of p , and T for all liquid case, and as a function of p and p_a for saturated liquid.

Single Liquid Phase Present in Upstream and Downstream Blocks.

For this case

$$p_c = \delta \lambda_{lu} = 0, \quad (83)$$

and

$$\delta \rho_{l,i-1/2} = \frac{1}{2} (\rho_l p_l \delta p_l + \rho_{lT,i} \delta T_i + \rho_{lp,i-1} \delta p_{i-1} + \rho_{lT,i-1} \delta p_{i-1}). \quad (84)$$

Substituting Eqns. (83) and (84) into Eqn. (72) and collecting coefficients, yields for the total mole flux:

$$q_{l,i-1}^{k+1} = q_{l,i-1/2}^k \delta q_{l,i-1/2}, \quad (85)$$

and

$$\begin{aligned}\delta q_{l,i-1/2} = & \delta p_i [T_{i-1/2} \rho_{l,i-1/2} \lambda_{lu} + \alpha \rho_{lp,i}] \\ & + \delta p_{i-1} [-T_{i-1/2} \rho_{l,i-1/2} \lambda_{lu} + \alpha \rho_{lp,i}] \\ & + \delta T_i [-\alpha \rho_{lT}] + \delta T_{i-1} [\alpha \rho_{lT,i-1}].\end{aligned}\quad (86)$$

For the air flux in liquid:

$$\begin{aligned}\delta X_a^l q_l|_{i-1/2} = & X_{ai}^l \delta q_{l,i-1/2} + q_{l,i-1/2} X_{ai}^l, \quad \text{if } i\text{th block upstream,} \\ = & X_{a,i-1}^l \delta q_{l,i-1/2} + X_{a,i-1}^g q_{l,i-1/2}, \quad \text{if } (i-1)\text{st block upstream,}\end{aligned}\quad (87)$$

and the convective energy flux with liquid:

$$\begin{aligned}\delta q_l H_l|_{i-1/2} = & \frac{1}{2} q_{l,i-1/2} (H_{lp,i} \delta p_i + H_{lT} \delta T_i + H_{lp,i-1} \delta p_{i-1} + H_{lT} \delta T_{i-1}) \\ & + H_{l,i-1/2} \delta q_{l,i-1/2}.\end{aligned}\quad (88)$$

Liquid Phase Upstream and Two-Phase Downstream. Since, by assumption, the upstream block is all liquid, it follows that

$$\delta p_{cu} = \delta \lambda_{lu} = 0, \text{ and } p_c \neq 0, \quad (89)$$

and

$$\delta \rho_{l,i-1/2} = \frac{1}{2} \left[\rho_{lp,u} \delta p_u + \frac{d\rho_l}{dp_s} (\delta p - \delta p_a) + \rho_{lT,u} \delta T_u \right]. \quad (90)$$

Substituting Eqns. (89) and (90) into Eqn. (72) yields:

$$\begin{aligned}\delta q_{l,i-1/2} = & T_{i-1/2} [\rho_{l,i-1/2} \lambda_{lu} (\delta p_i - \delta p_{i-1} - \delta p_{c,i} + \delta p_{c,i-1}) \\ & + \alpha \rho_{lp} \delta p + \frac{d\rho_l}{dp_s} (\delta p - \delta p_a) - \rho_{lT,u} \delta T_u].\end{aligned}\quad (91)$$

There are two sub-scenarios in this case as described below.

1. *i*th block upstream (*i* - 1st two-phase). From Eqn. (90), and collecting the coefficients, the expansion can be directly written as:

$$\begin{aligned}\delta q_{l,i-1/2} = & \delta p_i [T_{i-1/2} \rho_{l,i-1/2} \lambda_{li} + \alpha \rho_{lp,i}] \\ & + \delta p_{i-1} \left[-T_{i-1/2} \rho_{l,i-1/2} \lambda_{li} + \alpha \left(\frac{d\rho_l}{dp_s} \right)_{i-1} \right] \\ & + \delta s_{g,i-1} [T_{i-1/2} \lambda_{li} \rho_{l,i-1/2} p_{cp,i-1}] \\ & + \delta p_{a,i-1} \left[-\alpha \left(\frac{d\rho_l}{dp_s} \right)_{i-1} \right] + \delta T_i \alpha \rho_{lT,i},\end{aligned}\quad (92)$$

The air flux is given by:

$$\delta q_l X_a^l|_{i-1/2} = X_a^l \delta q_{l,i-1/2} + q_{l,i-1/2} \delta X_{a,i}^l. \quad (93)$$

The convective liquid energy flux is:

$$\delta q_l H_l|_{i-1/2} = q_{l,i-1/2} \delta H_{l,i-1/2} + H_l \delta q_{l,i-1/2}, \quad (94)$$

where

$$\delta H_{l,i-1/2} = \frac{1}{2} \left[H_l p_i \delta p_i + H_{lT_i} \delta T_i + \frac{d\rho_l}{dp_s} (\delta p - \delta p_a)_{i-1} \right]. \quad (95)$$

2. i th block downstream (two-phase), and $(i-1)$ st block all liquid:

$$\begin{aligned} \delta q_{l,i-1/2} = & \delta p_i \left[T_{i-1/2} \rho_{l,i-1/2} \lambda_{lu} + \alpha \left(\frac{d\rho_l}{dp_s} \right)_i \right] \\ & + \delta p_{i-1} \left[-T_{i-1/2} \rho_{l,i-1/2} \lambda_{lu} + \alpha \rho_{lp,i} \right] \\ & + \delta s_{g,i} \left[T_{i-1/2} \lambda_{lu} \rho_{l,i-1/2} p_{cp,i} \right] \\ & + \delta p_{a,i} \left[-\alpha \left(\frac{d\rho_l}{dp_s} \right)_i \right] + \delta T_{i-1} \alpha \rho_{lT,i-1}, \end{aligned} \quad (96)$$

The air flux:

$$\delta q_l X_a^l|_{i-1/2} = X_{a,i-1}^l \delta q_{l,i-1/2} + q_{l,i-1/2} \delta X_{a,i-1}^l. \quad (97)$$

The convective liquid energy flux:

$$\delta q_l H_l|_{i-1/2} = q_{l,i-1/2} \delta H_{l,i-1/2} + H_{l,i-1/2} \delta q_{l,i-1/2}, \quad (98)$$

where

$$\delta H_{l,i-1/2} = \frac{1}{2} \left[\frac{dH_l}{dp_s} (\delta p - \delta p_a)_{i-1} + H_l p_i \delta p_i + H_{lT_i} \delta T_i \right]. \quad (99)$$

Upstream Block Single Liquid Phase and Downstream Block Single Gas Phase. For this case, the density and enthalpy of the upstream block is assigned to the downstream block. In other words, instead of assigning the arithmetically averaged values for these quantities, the properties of the upstream block are used.

1. The i th block upstream with all liquid:

$$\delta q_{i-1/2} = T_{i-1/2} [\rho_{lu}(\delta p_i - \delta p_{i-1}) + 2\alpha(\rho_{lp,i}\delta p_i + \rho_{lT,i}\delta T_i)]. \quad (100)$$

The air flux in liquid:

$$\delta q_l X_{a,i-1/2}^l = q_{l,i-1/2} \delta X_{a,i}^l + X_{a,i}^l \delta q_{l,i-1/2}. \quad (101)$$

Convective liquid energy flux:

$$\delta q_l H_l|_{i-1/2} = q_{l,i-1/2} (H_{lp,i}\delta p_i + H_{lT,i}\delta T_i) + H_{li}\delta q_{l,i-1/2}. \quad (102)$$

2. The i th block downstream with all gas:

$$\delta q_{l,i-1/2} = T_{i-1/2} [\rho_{li,i-1}(\delta p_i - \delta p_{i-1}) + 2\alpha(\rho_{lp,i-1}\delta p_{i-1} + \rho_{lT,i-1}\delta T_{i-1})]. \quad (103)$$

The air flux in liquid:

$$\delta q_l X_a^l|_{i-1/2} = q_{l,i-1/2} \delta X_{a,i-1}^l + X_{a,i-1}^l \delta q_{l,i-1/2}. \quad (104)$$

Convective liquid energy flux:

$$\delta q_l H_l|_{i-1/2} = q_{l,i-1/2} (H_{lp,i-1}\delta p_{i-1} + H_{lT,i-1}\delta T_{i-1}) + H_{li-1}\delta q_{l,i-1/2}. \quad (105)$$

Upstream Block Two-Phase and Downstream Block Single Liquid Phase. For this case, $p_{c,i} = 0$, and $p_{c,i-1} = 0$. Depending on the i th ($i-1$)st block upstream there are the following two expansions.

1. The i th block two-phase and ($i-1$)st all liquid:

$$\begin{aligned} \delta q_{l,i-1/2} = T_{i-1/2} \left\{ \Delta P h_{li} \rho_{l,i-1/2} \lambda_{lp,i} \delta s_{g,i} + \rho_{l,i-1/2} \lambda_{li,i} \Delta \delta p - \rho_{l,i-1/2} \lambda_{li,i} p_{cp,i} \delta s_{g,i} \right. \\ \left. + \alpha \left[\left(\frac{d\rho_l}{dp_s} (p - p_a) \right)_i + (\rho_{lT} \delta T + \rho_{lp} \delta p)_{i-1} \right] \right\}. \end{aligned} \quad (106)$$

The air flux with liquid:

$$\delta q_l X_a^l|_{i-1/2} = X_{ai}^l \delta q_{l,i-1/2} + q_{l,i-1/2} \left(\frac{\delta p_a}{p} - \frac{X_a^l}{p} \delta p \right)_i. \quad (107)$$

Convective liquid energy flux:

$$\delta q_l H_l|_{i-1/2} = H_l \delta q_{l,i-1/2} + \frac{1}{2} q_{l,i-1/2} \left[\left(\frac{dH_l}{dp_s} (\delta p - \delta p_a) \right)_i + H_{lp,i} \delta p_i + H_{lT,i} \delta T_i \right]. \quad (108)$$

2. The $(i-1)$ st block upstream (two-phase) and i th block all liquid:

$$\begin{aligned} \delta q_{l,i-1/2} = T_{i-1/2} \{ & \Delta \Phi_l \rho_{l,i-1/2} \lambda_{lp,i-1} \delta s_{g,i} + \rho_{l,i-1/2} \lambda_{li} \Delta \delta p \\ & + \rho_{l,i-1/2} \lambda_{li-1} p_{cp,i-1} \delta s_{g,i-1} \\ & + \alpha \left[\left(\frac{d\rho_l}{dp_s} (p - p_a) \right)_{i-1} + (\rho_{lT} \delta T + \rho_{lp} \delta p)_i \right] \}. \end{aligned} \quad (109)$$

The air flux with liquid:

$$\delta q_l X_a^l|_{i-1/2} = X_{a,i-1}^l \delta q_{l,i-1/2} + q_{l,i-1/2} \delta X_{a,i-1}^l, \quad (110)$$

and

$$\delta X_{a,i-1}^l = \delta \left(\frac{p_a}{p} \right)_{i-1} = \frac{\delta p_{a,i-1}}{p_{i-1}} - \frac{X_{a,i-1}}{p_{i-1}} \delta p_{i-1}. \quad (111)$$

Convective liquid energy flux:

$$\delta q_l H_l|_{i-1/2} = H_{l,i-1/2} \delta q_{l,i-1/2} + q_{l,i-1/2} \delta H_{l,i-1/2}, \quad (112)$$

where

$$\delta H_{l,i-1/2} = \frac{1}{2} \left[H_{lp,i} \delta p_l + H_{lT,i} \delta T_i + \left(\frac{dH_p}{dp_s} \right)_{i-1} (\delta p_{i-1} - \delta p_a)_{i-1} \right]. \quad (113)$$

Both Blocks Two-Phase.

$$\begin{aligned} \delta q_{l,i-1/2} = T_{i-1/2} \{ & \Delta \Phi_{li} \rho_{l,i-1/2} \lambda_{lp,i} \delta s_{g,u} + \rho_{l,i-1/2} \lambda_{lu} \Delta p_c \\ & + \rho_{l,i} \lambda_{lu} (p_{cp,i} \delta s_{g,i} - p_{cp,i-1} \delta s_{g,i-1}) \\ & + \alpha \left[\frac{d\rho_g}{dp_s} (\delta p - \delta p_a)_i + \left(\frac{d\rho_l}{dp_s} \right)_{i-1} (\delta p - \delta p_a)_{i-1} \right] \}. \end{aligned} \quad (114)$$

The air flux with liquid:

$$\delta q_l X_a^l|_{i-1/2} = q_{l,i-1/2} \delta X_{au}^l + X_{au}^l \delta q_{l,i-1/2}, \quad (115)$$

where

$$\delta X_{au}^l = \frac{\delta p_{au}}{p_u} - \frac{X_{au}^l}{p_u} \delta p_u. \quad (116)$$

Convective liquid energy flux:

$$\delta q_l H_l|_{i-1/2} = q_{l,i-1/2} \delta H_{l,i-1/2} + H_{l,i-1/2} \delta q_{l,i-1/2}, \quad (117)$$

where

$$\delta H_{l,i-1/2} = \frac{1}{2} \left[\left(\frac{dH_l}{dp_s} (\delta p - \delta p_a) \right)_i + \left(\frac{dH_l}{dp_s} (\delta p - \delta p_a) \right)_{i-1} \right]. \quad (118)$$

Upstream Block Two-Phase and Downstream Block Single Gas Phase.

For this case the liquid properties of upstream block are assigned to the downstream block. Thus if the i th block is upstream

$$\begin{aligned} \delta q_{l,i-1/2} = T_{i-1/2} [& \Delta \Phi_l \rho_{l,i-1/2} \lambda_{lp,i} \delta s_{g,i} + \rho_{l,i-1/2} \lambda_{li,i} \Delta \delta p \\ & - \rho_{l,i-1/2} \lambda_{li,i} p_{cp,i} \delta s_{g,i} + \alpha \delta p_{li}], \end{aligned} \quad (119)$$

where

$$\delta \rho_{l,i-1/2} = \left[\frac{d\rho_l}{dp_s} (\delta p - \delta p_s) \right]_i. \quad (120)$$

If the $(i-1)$ st block is upstream then

$$\begin{aligned} \delta q_{l,i-1/2} = T_{i-1/2} [& \Delta \Phi_l \rho_{l,i-1/2} \lambda_{lp,i-1} \delta s_{g,i-1} + \rho_{l,i-1/2} \lambda_{li,i-1} \Delta \delta p \\ & + \rho_{l,i-1/2} \lambda_{li,i-1} p_{cp,i-1} \delta s_{g,i-1} + \alpha \delta \rho_{li,i-1}] \end{aligned} \quad (121)$$

where

$$\delta \rho_{l,i-1/2} = \left[\frac{d\rho_l}{dp_s} (\delta p - \delta p_s) \right]_{i-1}. \quad (122)$$

Air and convective liquid energy fluxes are computed as before.

3.3.2. Convective Gas Flux

From Eqn. (69) and suppressing the subscript x , the general expansion for gas flux can be written as:

$$q_{g,i-1/2}^{k+1} = q_{g,i-1/2}^k + \delta q_{g,i-1/2}, \quad (123)$$

with

$$\delta q_{g,i-1/2} = T_{i-1/2} [\lambda_{gu} \rho_{g,i-1/2} (p_i - p_{i-1} - 2c_f \rho_{g,i-1/2})], \quad (124)$$

where

$$c_f = \frac{W_g \Delta h}{2}, \quad (125)$$

or

$$\begin{aligned} \delta q_{g,i-1/2} = T_{i-1/2} [& \rho_{g,i-1/2} \lambda_{gu} (\delta p_i - \delta p_{i-1}) + \rho_{g,i-1/2} \lambda_{gp_u} \Delta \Phi_g \delta s_{gu} \\ & + \alpha (\delta \rho_{gu} + \delta \rho_{gd})], \end{aligned} \quad (126)$$

where

$$\alpha = \gamma_{gu} \left(\frac{1}{2} \Delta \Phi_g - c_f \rho_{g,i-1} \right), \quad (127)$$

Eqns. (124) and (126) are general expansions for the gas flux where $T_{i-1/2}$ must be evaluated in terms of the primary variables. For the gas density, consider different scenarios are considered as before, and these expansions are substituted for the density in the general expansions.

Upstream Block Two-Phase. For this case, it follows that

$$\delta \rho_{gu} = \left[\frac{d\rho_g}{dp_s} (\delta p - \delta p_a) \right]_u. \quad (128)$$

Eqn. (128) is used for all gas flux expansions when the upstream block contains two-phases.

The expansion of the density of gas in the downstream block depends on the state of the fluid in the block. If the downstream block is all liquid, then

$$\delta \rho_{gd} = \delta \rho_{gu}, \quad (129)$$

where the properties of the upstream block are substituted if the downstream block is all liquid.

If the downstream block has two-phases, Eqn. (128) evaluated at the downstream conditions is used. That is,

$$\rho_{gd} = \left[\frac{d\rho_g}{dp_s} (\delta p - \delta p_a) \right]_d. \quad (130)$$

If the downstream block is a single gas phase, then

$$\rho_{gd} = [\rho_{gp} \delta p + \rho_{gT} \delta T + \rho_{gp_a} \delta p_a]_d. \quad (131)$$

Upstream Block Single Gas Phase. For all cases, the density is given by Eqn. (131) evaluated at the upstream block as,

$$\delta\rho_{gu} = [\rho_{gp}\delta p + \rho_{gT}\delta T + \rho_{gp_a}\delta p_a]_u. \quad (132)$$

For the downstream blocks, the expansions are the same as above for each case of all liquid, all gas, and two-phase conditions.

The associated air flux in the gas phase is given by:

$$\begin{aligned} q_g X_a^g|_{i-1/2}^{k+1} &= q_g X_a^g|_{i-1/2}^k + \delta q_g X_a^g|_{i-1/2}, \\ &= q_g X_a^g|_{i-1/2}^k + X_{au}^g \delta q_g + q_g \delta X_{au}^g. \end{aligned} \quad (133)$$

If the upstream block is a single phase gas or two-phase system, then

$$\delta X_{au}^g = \delta \left(\frac{p_a}{p} \right)_u = \left(\frac{\delta p}{p} - \frac{X_a^g}{p} \right)_u. \quad (134)$$

If the upstream block is all liquid, then the air flux is set to zero.

The convective energy flux with the gas phase is given by,

$$\delta q_g H_g|_{i-1/2}^{k+1} = q_g H_g|_{i-1/2}^k + H_{g,i-1/2} \delta q_{g,i-1/2} + q_{g,i-1/2} \delta H_{g,i-1/2}, \quad (135)$$

with

$$\delta H_{g,i-1/2} = \frac{1}{2}(\delta H_{gu} + \delta H_{gd}). \quad (136)$$

Expansion of δH_g as given by the Eqns. (15) and (22) for single and two-phase conditions are used. These relations are applied after establishing the upstream and the downstream blocks in terms of the grid indices i or $i - 1$.

3.3.3. Binary Gas Diffusion

The diffusive transport of the gas component is controlled by the mole fraction gradients of air and water vapor in the gas phase. The diffusion process is governed by the well known Fick's Law which is modified for the porous media through the concept of tortuosity. The gas diffusive flux is expressed in the finite difference form at i th block interface located at $(i - 1/2)$ as

$$\begin{aligned} q_{g,i-1/2}^D &= \frac{2A_x}{(\Delta x_i + \Delta x_{i-1})} \left[\tau \phi D_{va}^0 \left(\frac{T}{T_K} \right)^\theta \frac{p_g^0}{p_g} \rho_g s_g \right]_{i-1/2} \Delta X_a^g, \\ &= \frac{2A_x}{(\Delta x_i + \Delta x_{i-1})} \left[\tau \phi \frac{D_{va}^0}{RT} \left(\frac{T}{T_K} \right)^\theta s_g \right]_{i-1/2} \Delta X_a^g. \end{aligned} \quad (137)$$

where the ideal gas law $\rho_g = p_g/RT$ is used. Defining the diffusive transmissibility as

$$\Upsilon_{i-1/2}^D = \frac{2A_x}{(\Delta x_i + \Delta x_{i-1})} \left[\bar{\tau} \bar{\phi} \frac{D_{va}^0}{RT_K} \right]_{i-1/2}, \quad (138)$$

it follows that

$$q_{u,i-1/2}^D = \Upsilon_{i-1/2}^D \bar{s}_g \bar{T}^{\theta-1} \Delta X_a^g, \quad (139)$$

where $\bar{\tau}$, $\bar{\phi}$, and \bar{s}_g are defined as their geometric mean values and $\bar{T}^{\theta-1}$ as the arithmetic mean of the i th and $(i-1)$ st blocks. These quantities are defined as:

$$\bar{s}_{g,i-1/2} = \sqrt{s_{g,i} s_{g,i-1}}, \quad (140)$$

$$\bar{\tau}_{i-1/2} = \sqrt{\tau_i \tau_{i-1}}, \quad (141)$$

$$\bar{\phi}_{i-1/2} = \sqrt{\phi_i \phi_{i-1}}, \quad (142)$$

$$\bar{T}^{\theta-1} = \frac{1}{2} (T_i^{\theta-1} + T_{i-1}^{\theta-1}). \quad (143)$$

Note that the diffusive flux is nonzero, only if the gas saturation on either side of an interface is nonzero. Employing Eqn. (139) the derivatives of the diffusive flux for different scenarios are computed as follows.

Both Blocks Two-phase.

$$\frac{\partial q_a^D}{\partial p_i} = \Upsilon_{i-1/2}^D \bar{s}_{g,i-1/2} \left[(\theta - 1) T_i^{\theta-2} T_{p_i} \Delta X_a^g - \frac{1}{p_i} \bar{T}^{\theta-1} X_{a,i}^g \right], \quad (144)$$

$$\frac{\partial q_a^D}{\partial p_{i-1}} = \Upsilon_{i-1/2}^D \bar{s}_{g,i-1/2} \left[(\theta - 1) T_{i-1}^{\theta-2} T_{p_{i-1}} \Delta X_a^g - \frac{1}{p_{i-1}} \bar{T}^{\theta-1} X_{a,i-1}^g \right], \quad (145)$$

$$\frac{\partial q_a^D}{\partial s_{g,i}} = \frac{1}{2s_{g,i}} q_{a,i-1/2}^D, \quad (146)$$

$$\frac{\partial q_a^D}{\partial s_{g,i-1}} = \frac{1}{2s_{g,i-1}} q_{a,i-1/2}^D, \quad (147)$$

$$\frac{\partial q_a^D}{\partial p_{a,i}} = \Upsilon_{i-1/2}^D \bar{s}_{g,i-1/2} \left[(\theta - 1) T_i^{\theta-2} T_{p_i} \Delta X_a^g - \frac{1}{p_i} \bar{T}^{\theta-1} X_{a,i}^g \right], \quad (148)$$

$$\frac{\partial q_a^D}{\partial p_{a,i-1}} = \Upsilon_{i-1/2}^D \bar{s}_{g,i-1/2} \left[(\theta - 1) T_{i-1}^{\theta-2} T_{p_{i-1}} \Delta X_a^g - \frac{1}{p_{i-1}} \bar{T}^{\theta-1} X_{a,i-1}^g \right]. \quad (149)$$

The i th Block Two-Phase and $(i - 1)$ st Block Single Gas Phase. In this case, the temperature in place of gas saturation for the $(i - 1)$ st block is the unknown, and hence, the derivatives are written as:

$$\frac{\partial q_a^D}{\partial p_i} = \Upsilon_{i-1/2}^D \bar{s}_{g,i-1/2} \left[(\theta - 1) T_i^{\theta-2} T_{p_i} \Delta X_a^g - \frac{1}{p_i} \bar{T}^{\theta-1} X_{a,i}^g \right], \quad (150)$$

$$\frac{\partial q_a^D}{\partial p_{i-1}} = \Upsilon_{i-1/2}^D \bar{s}_{g,i-1/2} \bar{T}_{i-1}^{\theta-1} X_{a,i-1}^g \frac{1}{p_{i-1}}, \quad (151)$$

$$\frac{\partial q_a^D}{\partial s_{g,i}} = \frac{1}{2s_{g,i}} q_{a,i-1/2}^D, \quad (152)$$

$$\frac{\partial q_a^D}{\partial T_{i-1}} = \Upsilon_{i-1/2}^D \bar{s}_{g,i-1} (\theta - 1) \Delta X_a^g, \quad (153)$$

$$\frac{\partial q_a^D}{\partial p_{a,i}} = \Upsilon_{i-1/2}^D \bar{s}_{g,i-1/2} \left[(\theta - 1) T_i^{\theta-2} T_{p_i} \Delta X_a^g - \frac{1}{p_i} \bar{T}^{\theta-1} X_{a,i}^g \right], \quad (154)$$

$$\frac{\partial q_a^D}{\partial p_{a,i-1}} = -\Upsilon_{x d} \bar{s}_{g,i-1/2} T_{i-1}^{\theta-1} \frac{1}{p_{i-1}}. \quad (155)$$

Derivatives for other cases are derived similarly and all the terms may be directly written from the above.

Enhanced Binary Diffusion. The enhanced binary diffusion is defined by Eqn. (137) by setting gas saturation to unity. Thus, enhanced diffusion plays a role only in case of two-phase region. The derivatives for this case can be written directly by letting the terms containing derivative of gas saturations to zero, and setting $s_g = 1$ in the above expansion.

3.3.4. Heat Conduction Flux

Energy transport by conduction is given by the last term within the parenthesis of the energy balance Eqn. (1.4), and may be expressed in finite difference form as:

$$q_{e,i-1/2}^{k+1} = \frac{2A_x}{\Delta x_i + \Delta x_{i-1}} \bar{\kappa}_{\text{eff}} \Delta T \quad (156)$$

where the effective thermal conductivity $\bar{\kappa}_{\text{eff}}$ is calculated as the harmonic average value between blocks i and $(i - 1)$. The quantity $\bar{\kappa}_{\text{eff}}$ is treated as a linear function of liquid saturation as

$$\kappa_{\text{eff}} = s_l \kappa_{\text{eff}}^{s_l=1} - \kappa_{\text{eff}}^{s_l=0}, \quad (157)$$

and

$$\bar{\kappa}_{\text{eff},i-1/2} = \frac{2\kappa_{\text{eff},i}\kappa_{\text{eff},i-1}}{\Delta x_i\kappa_{\text{eff},i-1} + \Delta x_{i-1}\kappa_{\text{eff},i}}. \quad (158)$$

Defining

$$\Upsilon_{C,i-1/2} = \frac{2\bar{\kappa}_{\text{eff}}}{\Delta x_i + \Delta x_{i-1}} A_x, \quad (159)$$

the conduction flux is expressed as,

$$q_{C,i-1/2} = \Upsilon_{C,i-1/2}(T_i - T_{i-1}), \quad (160)$$

and

$$\delta q_{C,i-1/2} = \Upsilon_{C,i-1/2}(\delta T_i - \delta T_{i-1}). \quad (161)$$

For a two-phase system, temperature is not one of the primary variables. Therefore, it is necessary to express the temperature in terms of p and p_a , which in the absence of vapor pressure lowering is given by

$$\delta T = T_{p_v}(\delta p - \delta p_a). \quad (162)$$

With vapor pressure lowering, temperature also becomes a function of saturation and one has

$$\delta T = T_{p_v}(\delta p - \delta p_a) + T_{s_g}\delta s_g. \quad (163)$$

Note that while the thermal conductivity is iteratively updated based on the liquid saturation at the previous iteration, it is not allowed to vary during a Newtonian iteration. Such treatment is believed to be adequate in view of typically a small change in the saturation over an iteration, not excessive difference in the conductivities of the dry and saturated rocks, and the fact that conduction is generally a slow process.

4. Boundary Conditions

In this section, the treatment of both the Dirichlet and Neumann boundary conditions is discussed as implemented in *METRA*.

4.1. Dirichlet Condition

Under this condition, the field variables (p , s_g , T , X_a^g , etc.) are kept fixed over a specified time interval. To satisfy this condition, fluxes are imposed through the boundary surface such that they result in exactly the desired conditions at the boundary.

Consider an arbitrary i th boundary block with the boundary located at a distance $\Delta x_i/2$ from the grid block center. The boundary air flux is given by:

$$q_{ma}^{bc} = -\frac{2A}{\Delta x_i} [X_{au}^l \lambda_{lu} \bar{\rho}_l (p_i - p_{c,i} - p^{bc} + p_c^{bc}) + X_{au}^g \lambda_{gu} \bar{\rho}_g (p_i - p^{bc})], \quad (1)$$

$$\text{where } i = \text{first or the last point, if the boundary in } i\text{-direction,} \quad (2)$$

$$= \text{first or the last point, if the boundary in } j\text{-direction,} \quad (3)$$

$$= \text{first or the last point, if the boundary in } k\text{-direction,} \quad (4)$$

and A is the boundary surface area perpendicular to the direction of flow. The superscript bc refers to the boundary where the designated field variables are fixed. The total mole flux at the boundary is:

$$\begin{aligned} q_m^{bc} &= q_{ml}^{bc} + q_{mg}^{bc}, \\ &= -\frac{2A}{\Delta x_i} [\lambda_{lu} \bar{\rho}_l (p_i - p_{c,i} - p^{bc} + p_c^{bc}) + \lambda_{gu} \bar{\rho}_g (p_i - p^{bc})]. \end{aligned} \quad (5)$$

The energy flux is:

$$q_H^{bc} = q_{ml}^{bc} H_{wu} + q_{mg}^{bc} H_{gu} - 2\bar{\kappa}_{\text{eff}} A (\Upsilon_i - \Upsilon^{bc}). \quad (6)$$

It is required that the total fluxes at the boundaries satisfy Eqns. (1), (5) and (6). The expression for the boundary fluxes are identical to interblock fluxes discussed above, except for one important distinction. The primary variables designated with the superscript bc are fixed, and as such all derivatives with respect to these quantities vanish. Thus, by setting all derivatives with respect to $(i-1)$ st block in the preceding derivatives to zero, and letting the corresponding primary variables as constants (p , s_g , T , etc.) the desired expansions are obtained. Note that the fluxes are multiplied by a factor of two to account for half Δx distance between the boundary and the block center. The general expansions for such boundary conditions may be expressed for air, total moles and energy as,

$$(q_\eta^{bc})^{k+1} = (q_\eta^{bc})^k + \frac{\partial q_\eta^{bc}}{\partial x_1} \delta x_1 + \frac{\partial q_\eta^{bc}}{\partial x_2} \delta x_2 + \frac{\partial q_\eta^{bc}}{\partial x_3} \delta x_3, \quad (7)$$

where subscript $\eta = m_a, m$, or H respectively. These derivatives contribute directly to the diagonal coefficients of the jacobian, and the fluxes to the residuals.

4.2. Neumann Condition

These boundary conditions are simply treated as sources and sinks as discussed in the next section. It is often more convenient to specify the “specific flux” (flux/area) in practical applications in which case the given specific flux must be multiplied by the block area perpendicular to the direction of flow.

A more useful variation of this flux condition is to designate a maximum flux rate subject to the constraint of a limiting boundary surface pressure. For example, at a high discharge rate, not all water may infiltrate into the ground due to the limiting atmospheric pressure at the surface. In this case, the excess discharge will constitute the runoff or overflow. These conditions are, however, not treated in *METRA*.

4.3. Sources and Sinks

These quantities are simply added to the residuals and does not warrant any mathematical treatment. However, if they are functions of the field variables, they must be expanded and expressed in terms of the primary variables, and then added to the Jacobian and the residuals.

METRA treats the sources and sinks as a given function of time. They are evaluated at time $t + \Delta t$ and simply added to the residuals. In our treatment, the sources are positive quantities and sinks are negative.

4.4. Consolidation of Equations in Matrix Form for Solution

The expansions of accumulation, flux, boundary conditions, and sources/sinks as detailed in the preceding sections are substituted in the finite-difference Eqs. (5.19-21), and then the coefficients are rearranged and collected in terms of the primary variables. The resulting set of equations for a typical grid block (i, j, k) in 3-D grid geometry takes the form

$$F_x \delta x + F_{x_{i-1}} \delta x_{i-1} + F_{x_{i+1}} \delta x_{i+1} + F_{x_{j-1}} \delta x_{j-1} + F_{x_{j+1}} \delta x_{j+1} + F_{x_{k-1}} \delta x_{k-1} + F_{x_{k+1}} \delta x_{k+1}, \quad (8)$$

where F_{x_i} is a 3×3 block sub-matrix of the form:

$$F_x = \begin{bmatrix} \frac{\partial f}{\partial g} & \frac{\partial f}{\partial g} & \frac{\partial f}{\partial g} \\ \frac{\partial x_1}{\partial g} & \frac{\partial x_2}{\partial g} & \frac{\partial x_3}{\partial g} \\ \frac{\partial x_1}{\partial h} & \frac{\partial x_2}{\partial h} & \frac{\partial x_3}{\partial h} \\ \frac{\partial x_1}{\partial x_1} & \frac{\partial x_2}{\partial x_2} & \frac{\partial x_3}{\partial x_3} \end{bmatrix}, \quad \text{and} \quad \delta x = \begin{bmatrix} \delta x_1 \\ \delta x_2 \\ \delta x_3 \end{bmatrix}. \quad (9)$$

The derivatives $\partial f/\partial x$, $\partial g/\partial x$, and $\partial h/\partial x$, arise respectively from the expansion of air, total mole, and the energy balances. The set given by Eqn. (8) is solved for δx either using direct or iterative methods as discussed below. The solution is iteratively refined employing the N-R procedure outlined in section 2.4.

4.5. Phase Transition and Updating

Depending on the thermodynamic state, any grid block may undergo a phase change from single phase to two-phase or vice-versa. During such transition, the primary variables must be reset as defined earlier for each phase condition.

If the calculated gas saturation s_g for a two-phase block at the $(k+1)$ st iteration is greater than 1, the block has crossed the phase boundary to the superheated state. In this case, set $s_g = 1$, $p = (1 - \epsilon)p_s(T^k)$, and choose the primary variables as p , p_a , and T for the next iteration, where ϵ is an arbitrarily small positive number of the order of 10^{-6} .

If the calculated gas saturation s_g for the block is negative, the block has crossed the phase boundary into the subcooled or all liquid state region. In this case, set $s_g = 0$, $p = (1 + \epsilon)p_s(T^k)$, and choose the primary variables as p , T , and X_a^l .

If a single phase liquid crosses into the two-phase region, the calculated T at k th Newtonian iteration will exceed the saturation temperature, and pressure will exceed the saturation pressure. In this case, the gas saturation is set equal to $s_g = \epsilon$, and temperature to lie on the saturation curve $p = p_s(T^k)$. The primary variables are reset to their values at the beginning of the time step.

Likewise, if a single phase gas block crosses into two-phase region, the calculated temperature will be below the saturation temperature. In this case, the saturation is set equal to $s_g = 1 - \epsilon$, and the pressure to $p = p_s(T^k)$.

At each iteration, the primary variables and corresponding dependent variables are updated. An oscillatory behavior occurred in the primary variables (albeit,

small) and the velocities when the temperature was updated using the following relation for a two-phase block:

$$T^{k+1} = T^k + \frac{dT}{dp_s}(\delta p - \delta p_s). \quad (10)$$

It was later discovered that calculating T^{k+1} directly from the known saturation pressure results in essentially eliminating or largely damping the oscillations.

5. NOMENCLATURE

Roman Symbols		
Symbol	units	Description
$A_{x,r}$	m^2	area in x or r direction
A_y	m^2	area in y
A_z	m^2	area in z direction
A	—	Jacobian Coefficient Matrix
C_a	joules/mole/C	specific heat of air
C_p^{rock}	joules/kgm/C	Specific heat of rock
D_{va}	m^2/s	Binary diffusion coefficients
E	joules	Energy accumulation term
g	m^2/s	acceleration of gravity
h	meter	depth measured positive downward
H_l	joules/mole	liquid enthalpy
H_g	joules/mole	gas enthalpy
H_w°	joules/mole	water vapor enthalpy
k	m^2	Intrinsic absolute rock permeability
k_{rl}	—	Relative permeability to liquid
k_{Rg}	—	Relative permeability to gas
K		Effective rock thermal conductivity
M	moles	total moles
M_a	moles	total air moles
q_m	moles/s/ m^3	Total mass generation rate
q_{m_a}	moles/s/ m^3	Air mass generation rate
q_e	joules/s/ m^3	Energy generation rate
Q	moles/s	Total mole influx rate

Symbol	units	Description
Q_{m_a}	moles/s	Total air mole influx rate
Q_e	moles/s	Total energy influx rate
p_g	pascals	Gas Phase Pressure
p_l	pascals	Liquid Phase Pressure
p_v	pascals	Partial pressure of water vapor
p_a	pascals	Partial pressure of air
p_c	pascals	gas-liquid capillary pressure
r	meter	radius from the axis in cylindrical co-ordinates
r_L	meter	outer radius of cylinder
s_l	—	Liquid Saturation
s_g	—	Gas Saturation
t	s	Time
T	°C	Temperature
T	°K	Absolute temperature = $T + 273.15$
U_l	joules/mole	liquid internal energy
U_g	joules/mole	gas internal energy
U_w°	joules/mole	water vapor internal energy
v_l	meter/s	liquid velocity
v_g	meter/s	gas velocity
v	joules/s	conductive heat flux per unit area
v^D	meter/s	Binary diffusive velocity
V_B	m ³	block volume
X_a^l	—	mole fraction of air in liquid
X_a^g	—	mole fraction of air in gas
X_w^l	—	mole fraction of water in liquid
X_w^g	—	mole fraction of water in gas
x, y, z	meter	cartesian coordinates

Greek Symbols

∇		divergence operator
Δ		difference operator
Δ_t		time difference operator
μ_a	Pa·s	air viscosity
μ_g	Pa·s	gas viscosity

Symbol	units	Description
μ_l	Pa·s	liquid viscosity
μ_w	Pa·s	water viscosity
ρ_a	moles/m ³	air molar density
ρ_g	moles/m ³	gas molar density
ρ_l	moles/m ³	liquid molar density
ρ_w°	moles/m ³	water molar density
ϕ	fraction	porosity
θ		angular coordinate
τ		tortuosity
Subscripts		
a		air phase
g		gas phase
i, j, k		grid indices
l		liquid phase
s		saturation pressure
Superscripts		
a		air
k		Newtonian iteratin level
$n, n + 1$		time level in FD
w		water

I have reviewed this scientific notebook and find it in compliance with QAP-001. There is sufficient information regarding procedures used for conducting tests, acquiring and analyzing data so that another qualified individual could repeat the activity.

N. Sridhar 4/17/97

Narasi Sridhar
Manager, Engineered Barrier System and Waste Solidification System

SCIENTIFIC NOTEBOOK

by

Peter C. Lichtner

Printed: April 30, 1997

P. C. Lichtner

SCIENTIFIC NOTEBOOK

INITIALS:

PC

SCIENTIFIC NOTEBOOK

by

Peter C. Lichtner

**Southwest Research Institute
Center for Nuclear Waste Regulatory Analyses
San Antonio, Texas**

For Period: First Quarter

January 1, 1997 — March 30, 1997

Printed April 30, 1997

INITIAL ENTRIES

Scientific NoteBook: # 095

Issued to: P. C. Lichtner

Issue Date: Tuesday, November 16, 1993

Computerized Initials: PC

By agreement with the CNWRA QA this NoteBook is to be printed at approximate quarterly intervals. This computerized Scientific NoteBook is intended to address the criteria of CNWRA QAP-001.

Table 1: Computing Equipment

Machine Name	Type	OS	Location
gravenstein.cnwra.swri.edu	Pentium Workstation	NEXTSTEP	desk Rm A-126
	133 Mhz	Version 3.3	Bldg. 189
	64 MB RAM		
skippy.cnwra.swri.edu	Sun SPARC 20	SUNOS 4.1.2	network
	96 MB RAM		

Contents

INITIAL ENTRIES	ii
FIGURES	iv
TABLES	v
NEAR-FIELD ENVIRONMENT	1
1 REFERENCES	27

List of Figures

- 1 Increase in chloride concentration as water is evaporated from a container initially filled with 1 kg of water as described by Eqn.(1). To convert to molality note that 1000 mg/liter chloride is equivalent to 0.0282 molal. 2
- 2 Enrichment factor for chloride at 100 years plotted as a function of depth computed using MULTIFLO with a residual saturation of 0.08 (solid curve) and 0.01 (dashed curve) compared with the simple evaporation model (dotted curve $s_l^r = 0.08$, dash-dotted curve $s_l^r = 0.01$) 13
- 3 Enrichment factor for chloride at the repository horizon plotted as a function of time computed using MULTIFLO with residual saturations of 0.08 (solid curve) and 0.01 (dashed curve) compared with the simple evaporation model (dotted curve $s_l^r = 0.08$, dash-dotted curve $s_l^r = 0.01$). 14
- 4 Log permeability enhancement factor plotted as a function of the exponent n in Eqn.(12) for the alteration of cristobalite to quartz. The solid line is for an initial cristobalite volume fraction of 0.14, and the dashed line 0.39 used by Johnson and Glassley. 16
- 5 Volume fractions for cristobalite (dotted curve) and quartz (dashed curve) depicted as a function of depth for an elapsed time of 1000 years. Also shown is the porosity (solid curve). Calculations were performed using MULTIFLO based on the repository-scale model. 17
- 6 Repository-scale model. 19
- 7 Temperature at the repository horizon plotted as a function of time. 20
- 8 The liquid saturation at the repository horizon plotted as a function of time. 20
- 9 The pH plotted as a function of time.) 21
- 10 Molality of dissolved oxygen plotted as a function of time. 22
- 11 Molality of total calcium (solid), sulfate (dash-dotted), magnesium (dotted) and chloride (dashed) plotted as a function of time. 22

List of Tables

1	Computing Equipment	ii
2	Initial fluid composition for major species corresponding to J-13 well water (Harrar et al., 1990).	4
3	Fluid composition for major species corresponding to UZ4-TP-3 (91.4 m) (Yang and Turner, 1988), and J-13 well water (Ogard and Kerrisk, 1984).	18

KTI: NEAR-FIELD ENVIRONMENTAccount Number: **20-5708-561**

Description: Near-field Environment Technical Assistance

Collaborators: Dr. M. Seth (Consultant)

Objective: Application of the computer code MULTIFLO, and submodules GEM and METRA to the Yucca Mountain HLW Repository.

1.30.96 *xz*-Repository Scale Calculation—Bounding Calculations

To derive bounds on some quantity it must first be determined how tight the bounds need to be, to be useful. Reasonable bounds are usually much more difficult to obtain than absolute bounds which are often overly conservative to be of much use. In the analysis which follows, pure evaporation, in which solute flux is assumed to be negligible, is analyzed.

Pure Evaporation The increase in concentration due to evaporation of water for a nonvolatile and nonreactive species such as chloride, assuming the aqueous solution remains undersaturated with respect to chloride-bearing minerals such as halite, can be easily calculated from the equation

$$m_i = \frac{n_i^0}{M_w^0 - n_w W_w}, \quad (1)$$

where m_i refers to the molality of the species in question, n_i^0 denotes the initial number of moles of that species in a given mass of water $M_w^0 = n_w^0 W_w$, n_w represents the number of moles of water evaporated, and $W_w = 0.018$ kg/mole- H_2O is the molecular weight of water. There are 55.51 moles of water in 1 kg. This relation is valid for a system which is closed with respect to the flux of liquid water into or out of the system. In particular, this same assumption applies to EQ6-type calculations. Shown in Figure 1 is a plot of Eqn.(1) for an initial mass of 1 kg water and an initial chloride concentration of 8 mg/kg- H_2O [compare with Figure 3.4-6 in the DOE report (Wilder, 1996) computed using EQ6].

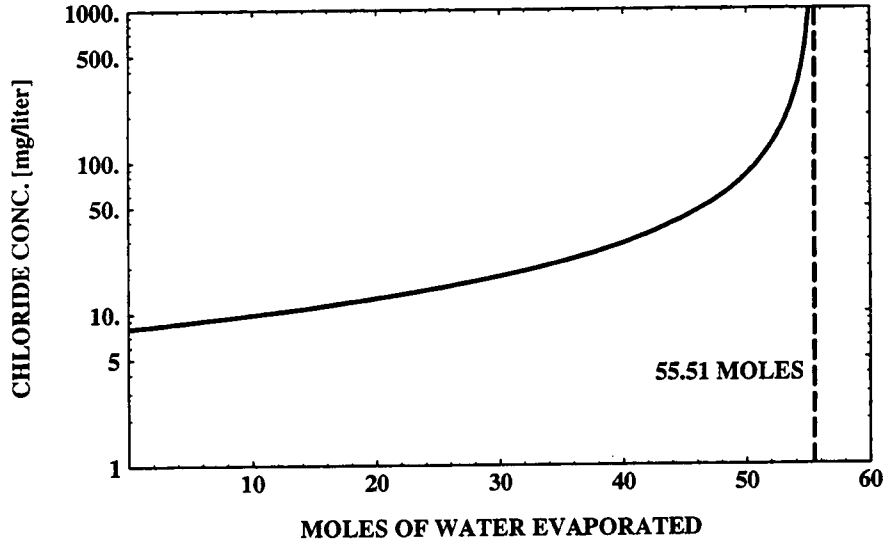


Figure 1: Increase in chloride concentration as water is evaporated from a container initially filled with 1 kg of water as described by Eqn.(1). To convert to molality note that 1000 mg/liter chloride is equivalent to 0.0282 molal.

To relate Eqn.(1) to the change in solute concentration in the near-field region of the repository, it is necessary to relate the number of moles of liquid water evaporated to the local value of the liquid saturation of the host rock. Provided the change in liquid saturation is caused by evaporation only, and not by the flux of liquid into or out of the control volume, liquid saturation s_l is related to the number of moles of water evaporated according to the equation

$$1 - \frac{s_l}{s_l^0} = \frac{n_w}{n_w^0}, \quad (2)$$

where the quantity n_w^0 represents the initial moles of water in a given volume of bulk rock, and s_l^0 refers to the initial liquid saturation. To obtain this equation note that liquid saturation is defined as the ratio of volume of liquid V_w to pore volume V_p

$$s_l = \frac{V_w}{V_p}, \quad (3)$$

and the liquid volume is related to the number of moles of water evaporated by the expression

$$V_w = (n_w^0 - n_w) \bar{V}_w, \quad (4)$$

with the initial volume of liquid given by $V_w^0 = n_w^0 \bar{V}_w$, and where \bar{V}_w denotes the molar volume of pure water. It follows that the molality is inversely proportional to

the liquid saturation

$$m_i = M_i^0 \frac{s_l^0}{s_i}. \quad (5)$$

It is useful to define the enrichment factor η_i as the ratio of the concentration of some solute species at time t and location r , to the initial concentration at the same location. For a simple evaporative process, η_i is equal to the ratio of the initial saturation to the actual saturation

$$\eta_i = \frac{m_i}{M_i^0} = \frac{s_l^0}{s_i} = \frac{n_w^0}{n_w^0 - n_w}. \quad (6)$$

According to this relation, the enrichment of some solute species due to pure evaporation is inversely proportional to the amount of water remaining in the control volume. If 90% of the water is evaporated, the enrichment factor for chloride is approximately 10 (Figure 1). As complete evaporation is achieved, the enrichment factor tends towards infinity. Clearly, at some point along the evaporation path when the aqueous solution reaches saturation with solid phases (salts), this relation must break down and the concentration becomes solubility limited.

2.7.97 Solubility Limit

A solubility-based estimate for the increase in chloride concentration resulting from evaporation may be derived by assuming the aqueous solution comes to equilibrium with a salt, e.g. halite. As evaporation proceeds, it is assumed that the sodium and chloride concentrations remain proportional to one another

$$a_{\text{Na}^+} = \alpha a_{\text{Cl}^-}, \quad (7)$$

with proportionality constant $\alpha \simeq 10$, as derived from J-13 well water (see Table 2). This is only correct if reaction with the solid phase does not remove sodium from solution. Equilibrium with halite implies the mass action equation

$$K = a_{\text{Na}^+} a_{\text{Cl}^-} = \alpha a_{\text{Cl}^-}^2. \quad (8)$$

Therefore

$$a_{\text{Cl}^-} = \sqrt{\frac{K}{\alpha}}. \quad (9)$$

The $\log K$ for halite at 100°C is equal to 1.578, according to the EQ3/6 database (Wolery, 1992). (Note that because of vapor pressure lowering caused by capillary forces,

the boiling point of water can be raised significantly above 96°C corresponding to the elevation of YM.) It follows that at this temperature the equilibrium activities for chloride and sodium are equal to $a_{\text{Cl}^-} = 1.945$ and $a_{\text{Na}^+} = 19.45$. This leads to an enrichment factor of roughly

$$\eta_{\text{Cl}^-} = \frac{C_{\text{Cl}^-}}{C_{\text{Cl}^-}^0} = \frac{1}{a_{\text{Cl}^-}^0} \sqrt{\frac{K}{\alpha}} \sim 10^4. \quad (10)$$

To obtain the actual concentrations, activity coefficient corrections must be applied. However, this result requires only that $\gamma_{\text{Na}^+} \simeq \gamma_{\text{Cl}^-}$.

Table 2: Initial fluid composition for major species corresponding to J-13 well water (Harrar et al., 1990).

pH	6.8–8.3
Species	Molality $\times 10^3$
Ca ²⁺	0.290 – 0.370
Na ⁺	1.830 – 2.170
K ⁺	0.100 – 0.140
HCO ₃ ⁻	0.193 – 0.234
SiO ₂ (aq)	0.950 – 1.140
Cl ⁻	0.178 – 0.237

The chloride concentration in equilibrium with halite could be substantially increased if the sodium concentration is lowered by precipitation of other sodium-bearing solids such as feldspars. Thus this estimate could underestimate the chloride concentration. However, if halite saturation is never reached the predicted enrichment factor could be orders of magnitude larger than that which actually occurs in the repository. Equal concentrations of sodium and chloride in equilibrium with halite at 100°C implies roughly 6 M concentration of each species. Clearly, it is difficult to find a bound within reasonable limits even for a nonvolatile species such as chloride.

An estimate of the pH is more difficult to obtain and may depend on reactions with the host rock minerals as well as properties of the gas phase. Likewise, calcium and carbonate have no obvious bounds since their concentrations will be pH-dependent and will depend on reaction with calcite, for example.

2.21.97 Estimate of Chloride Concentration Based on MULTIFLO Calculations

The computer code MULTIFLO (Lichtner, 1966; Lichtner and Seth, 1996b; Seth and Lichtner, 1996) provides a fully coupled, quantitative, description of two-phase fluid flow and reactive transport of aqueous and gaseous species. Heat flow is also accounted for in the code. The same complexity in chemistry is employed in MULTIFLO as in EQ6. The thermodynamic databases used by the two codes are equivalent.

Fully coupled calculations using MULTIFLO are presented for the change in chloride concentration based on a repository-scale model. The repository is represented as a circular disk with a heat load of 83.4 MTU/acre. An initial saturation of approximately 80 percent throughout most of the unsaturated zone, becoming fully saturated at the water table, is assumed. For this case complete dryout does not occur. A single spatial dimension along the vertical through the center of the repository is considered. The repository horizon is located at a depth of 375 m from the surface.

The input files for GEM and METRA for use with versions 1.0 that are used in the calculations are listed below.

GEM:

Test Data for Multiflo Simulator (Yucca Mt., 1D, 83.4 AML)
March 10, 1997

```

:
:      geometry nx  ny  nz    mode  iprint
GRID    XYZ      1   1 121     2      0
:
OPTS
:  idata istart imod  iexact
:    0      0      10      0
:
:  itmax ihalmax ivmax ndamp
:    16     16      0      5
:
:  method iops  ifor  isurf iact  loglin  icon
:    1      0     3     1     1      0     1
:
:      isync ipor iperm perm-fac.
COUPLE  0     -1     0      3.
:
PLTFiles
:iplot  a  s  t  m si sf  v  z  b in  e ex ti  g itex
:    1    1  1  1  1  0  0  1  0  2  0  0  0  0  1  0
:
:      tol  ttol  tolneg  tolpos  tolexp  dthalf  qkmax  tolstdst
TOLR  1.d-10  2.e-3  1.e0  1.e-2  5.d0     .5      590.    1.e-12
:
:      mcyc  cc  c   flx r  sp  qk  pk  rk  a1  a2  a3

```

P. C. Lichtner

SCIENTIFIC NOTEBOOK

INITIALS: PCZ

```

DEBUg    0      1 1 0 1 1 1 1 1
:
:      isat isotherm iread por0 phir sat w lambda toldelt tolpor
ISYSstem 0      1      0      .11 1. 0.5 .5 1. 1.e-3 1.e-3
:
:      vx0  vy0  vz0[m/yr]  alphax  alphay  alphaz  cournr
FLOW      0.    0.    1.      0.    0.    0.    1.
:
:      d0[cm^2/s]  delhaq[kJ/mol]  dgas[cm^2/s]  dgexp  tortaq  tortg  idif
DIFF      1.d-5    12.6            2.13d-1      1.8  1.d0  1.d0  0
:
:flag 1: T(x)  = d x^3 + a x^2 + b x + c (meters)
:      2: T(x)  = a + (b-a) exp[-((x-x0)/c)^2] + (d - a) * x / xlen
:      3:T(x,t)=a+1/2(b-a) (erf[(x+c-x0)/2sqr(dt)]-erf[(x-c-x0)/2sqr(dt)])
:      p (bars) temp flag a      b      c      d      x0  xlen
PTINit 1.0      25.  0  25  300  250  125  1000.  2.d3
:
:master species for controlling time stepping
MASTER h+
:
:grid m 0. 1 200 200.
:
DXYZ
      1.
      1.
      121*1.
:
:      isolv level north nitmax idetail rmaxtol rtwotol smaxtol
SOLV      3  1      1      100      0      1.e-20 1.e-20 1.e-12
:
:initial and boundary conditions: 1-conc., 2-flux, 3-zero gradient
:inlet outlet nzoneaq
COMP      1  3  3
:
:species itype guess ctot mineral diffusion
ca+2      1      4.e-4 4.e-4 blank 0.8e-5
na+      1      2.e-3 2.e-3 blank 0.8e-5
h+      8      1.e-8 8.0 blank 9.6e-5
hco3-     4      2.7e-3 -2.99 co2(g)
sio2(aq)  1      2.e-3 2.e-3 blank 0.8e-5
cl-      -1      2.e-3 2.e-3 blank 0.8e-5
:blank
:
BCON
      3 3
:species itype guess ctot mineral
ca+2      1      4.e-4 4.e-4 blank
na+      1      2.e-3 2.e-3 blank
h+      8      1.e-8 8.0 blank
hco3-     4      2.7e-3 -2.99 co2(g)
sio2(aq)  1      2.e-3 2.e-3 blank
cl-      -1      2.e-3 2.e-3 blank
:

```

```

4 3
:species itype guess ctot mineral
ca+2      1    4.e-4  4.e-4  blank
na+       1    2.e-3  2.e-3  blank
h+        8    1.e-8  8.0    blank
hco3-     4    2.7e-3 -2.99   co2(g)
sio2(aq)   1    2.e-3  2.e-3  blank
cl-       -1    2.e-3  2.e-3  blank
:
0 0
:
CMIR      0    0
          :blank
:
STOL      1. 1. 1. 1. 1. 1. 1. 1.
:
AQCX
oh-
co2(aq)
co3-2
caco3(aq)
cahco3+
caoh+
cac1+
cac12(aq)
nahco3(aq)
nacl(aq)
naoh(aq)
h3sio4-
h2sio4-2
          :blank
:
MNRL
cristobalite
quartz
chalcedony
calcite
tobermorite-14a
halite
          :blank
:
GASEs
co2(g)
          :blank
:
MNIR
:mineral itypkin fkin delh beta rka    betb rkb rk    tau
:i1 i2 j1 j2 k1 k2 vol area
cristobalite 0 1.0 75. 1.0 0.    1.0 0. -16.34 1.e-3
1 1 1 1 1 121 0.14 1.e1
0
quartz        0 1.0 75. 1.0 0.    1.0 0. -17.39 1.e-3
1 1 1 1 1 121 0.14 1.e1

```

P. C. Lichtner

SCIENTIFIC NOTEBOOK

INITIALS: PCZ

```

0
chalcedony  0  1.0  75.  1.0  0.  1.0  0. -30.39  1.e-3
1 1 1 1 1 121  0.61  0.e1
0
calcite      0  1.0  35.  1.0  0.  1.0  0. -10.00  1.e-4
1 1 1 1 1 121  0.  1.
0
tobermorite-14a 0 1.0  30.  1.0  0.  1.0  0. -12.00  1.e-4
1 1 1 1 1 121  0.  10.
0
halite       0  1.0  30.  1.0  0.  1.0  0. -12.00  1.e-3
1 1 1 1 1 121  0.  10.
0
:blank

:
:surface mineral itypkin area beta fkin delh rkph rk
:  0  1.0  1.0  1.  0.  0.  0.
:
:corrosion solids i0 acorr bcorr curlim
:  0.  0.  0.  0.
:
:crevice gap[meters] potential [v]
ECAQ      90.d-6      -.2
:blank

:
:electrochemical aqueous species i0 acorr bcorr curlim
:  0.  0.  0.  0.
:
AQIR
:blank

:
:ion-exchange reactions
Ionx  0  1.0
:
BRKP  1
72
:
DTStep[y]  1 3.e-8
1.e-8      100.d0
:
TIME[y] 8 10. 50. 100. 500. 1000. 5000. 10000. 1.e5
:
ENDS

```

METRA:

Data for Multiflo simulator (initial data : 2D, 83.4 AML, Yucca Mt.)
Dec. 27, 1996

RSTART 0

```

:
: XYZ = 1 table look-up, pref = ref. press.
: RADIAL = 0 correlations, tref = ref temp.

```



```

:      OTHER
:grid geometry nx ny nz ivplwr ipvcal iout gravity pref tref href
Grid XYZ      1  1 121  1      0      3  0      0  0  0
:
Pckr                      :relative perm and pc keyword
:  i type-curv swirm rpmm(lamda) alpham swext sgc iecm
:                      swirf rpmf(lamda) alphaf phim phif permu permf
:Topopah Spring (150-475 m)
:  1 Van-Gen 0.08  0.4400  5.8e-7  0.  0.  1
:                      0.04  0.7636  1.305e-5 0.11  1.8e-3 1.9e-18 3.9e-12
:  1 Van-Gen 0.001 0.4400  5.8e-7  0.  0.  1
:                      0.001 0.7636  1.305e-5 0.11  1.8e-3 1.9e-18 3.9e-12
:blank line
:
Thermal-prop
: no rho      cpr  ckdry cksat  crp crt  tau cdiff  cexp enbd
  1 2.580e+3 840.  2.10  2.10    0    0   .5 2.13e-5 1.8 0.
0
:  igrid  rw      re
DXYZ  0      0.    1.
: (dx(i),i=1,nx)
1.
:
: (dy(j),j=1,ny)
1.
:
: (dz(k),k=1,nz)
10. 10. 10. 10. 10. 10. 10. 10. 10. 10.
10. 10. 10. 10. 10. 10. 10. 10. 10. 10.
10. 10. 10. 10.  5.  5.  5.  5.  5.  5.
  5.  5.  5.  5.  5.  5.  5.  5.  5.  5.
  2.  2.  2.  2.  2.  2.  2.  2.  2.  2.
  2.  2.  2.  2.  2.  2.  2.  2.  2.  2.
  2.  2.  2.  1.5 1.  1.  1.  1.  1.  1.
  1.  1.  1.  1.  1.  1.  1.  1.  1.  1.5
  2.  2.  2.  2.  2.  2.  2.  2.  2.  2.
  2.  2.  2.  2.  2.  2.  2.  2.  5.  5.
  5.  5.  5.  5.  5.  5.  5.  5. 10. 10.
10. 10. 10. 10. 10. 10. 10. 10. 10. 10.
10.
PhiK
: i1 i2 j1 j2 k1 k2 iist ithrm vb porm permx permy permz
  1 1 1 1 1 121 1 1 0.
0
Init init
: i1 i2 j1 j2 k1 k2 pm tm sgm x2m
: 1 1 1 1 1 121 1.e5 25.0 0.5 0.
: 0
:
:EQUIL 587.50 1.e5 30. 0.0255319 0.0 -1
:EQUIL 5.0 1.e5 25. 0. 0.2 1
:EQUIL 595.0 1.065627E+05 25. 0.0 0.0 -1
:

```

```

Recurrent-data
Bcon 2
:itype iface i1 i2 j1 j2
1 TOP 1 1 1 1
:time qbc pbc tbc sgbc xabc
0. 0. 8.55e4 15.0 0.2 0.
0
1 BOTTOM 1 1 1 1
0. 0. 9.05e4 30.0 0.0 0.
0
:
Rstart 1 0
Output A=1 C=1 B=1 S=-50
: isolve newtnmn newtnmx north nitmx level
Solve 2 1 7 4 100 1
:
:AUTO-step DPMXE DSMXE DTMPMXE DP2MXE TACCEL IAUTODT FAC1
AUTO-step 1.0E+3 0.03 5.0 1.e3 1.e-3 0 0
:
:TOLR TOLP TOLS TOLT TOLP2 TOLM TOLA TOLE rtwotol rmxtol smxtol
Tolr 10. 1.e-4 1.e-3 1.e+1 1.e-5 1.e-3 1.e-3 1.e-20 1.e-20 1.e-20
:
:Limit dpmx dsmtx dtmpmx dp2mx dtmn dtmx icutmx
LIMIT 1.e4 .08 10. 1.e5 1.e-6 1.e3
Plots 1
:Steady[y] 1.e-8 1.e-6 1.e-1
:Ends
: ns fach facm (fach and facm are multipliers to
: read-in values of qht and qmt)
:Source 1 1.32494 1. !110.5 AML
:Source 1 1.19904 1. !100 AML
:Source 1 1.13909 1. ! 95 AML
:Source 1 1.07914 1. ! 90 AML
:Source 1 1.04916 1. ! 87.5 AML
:Source 1 1.01918 1. ! 85 AML
Source 1 1. 1. ! 83.4 AML
:Source 1 3.14159 1. !radial 83.4 AML
: is js ks istyp
1 1 1 1 72 72 31
: 1 1 1 1 72 72 33
: timeq(sec) T/qht (C/(J/s)) qmt (kg/s)
0.00000E+00 1.87730E+01
6.30720E+07 1.81217E+01
1.26144E+08 1.75357E+01
1.89216E+08 1.68897E+01
2.52288E+08 1.63046E+01
3.15360E+08 1.57715E+01
4.73040E+08 1.45818E+01
6.30720E+08 1.34618E+01
7.88400E+08 1.25071E+01
9.46080E+08 1.16163E+01
1.26144E+09 1.02515E+01
1.57680E+09 8.99586E+00

```

P. C. Lichtner

SCIENTIFIC NOTEBOOK

INITIALS: PC

```

2.36520E+09 6.82702E+00
3.15360E+09 5.65219E+00
4.73040E+09 4.24896E+00
6.30720E+09 3.53303E+00
9.46080E+09 2.82589E+00
1.26144E+10 2.40733E+00
1.57680E+10 2.08456E+00
1.89216E+10 1.81067E+00
2.52288E+10 1.44680E+00
3.15360E+10 1.20944E+00
3.94200E+10 9.81818E-01
4.73040E+10 8.27487E-01
6.30720E+10 6.33691E-01
7.88400E+10 5.48998E-01
9.46080E+10 4.89297E-01
1.26144E+11 4.38708E-01
1.57680E+11 4.02873E-01
1.89216E+11 3.70297E-01
2.20752E+11 3.44801E-01
2.52288E+11 3.24128E-01
2.83824E+11 3.06917E-01
3.15360E+11 2.92001E-01
3.46896E+11 2.69319E-01
3.78432E+11 2.50151E-01
4.09968E+11 2.33722E-01
4.41504E+11 2.19473E-01
4.73040E+11 2.06987E-01
5.51880E+11 1.81593E-01
6.30720E+11 1.62125E-01
7.88400E+11 1.34131E-01
9.46080E+11 1.14855E-01
1.26144E+12 8.27996E-02
1.57680E+12 6.29212E-02
1.89216E+12 4.90735E-02
2.20752E+12 3.97719E-02
2.52288E+12 3.31523E-02
2.83824E+12 2.82343E-02
3.15360E+12 2.44608E-02
4.73040E+12 1.84539E-02
0
Output  A=1  C=1 S=-50
:
:RSTArt 0 1
:
:  isolv newtnmn newtnmx
Solve 3      2      7
:
:AUTO-step  DPMXE    DSMXE DTMPMXE DP2MXe TACCEL IAUTO
AUTO-step  5.E+4    0.025  3.0    1.e4    1.e-2  0
:
:TOLR TOLP TOLS TOLT TOLP2 TOLM TOLA TOLE
Tolr  1.e+1 1.e-4 1.e-2 5.e+1 1.e-5 1.e-6 1.e-3 1.e-20 1.e-20 1.e-12
:

```

```

:Limit dpmx dsmx dtmpmx dp2mx dtmn dtmx icutmx
LIMIT 1.e4 .05 5. 1.e5 1.e-6 1.e4 5
Plots 1 1 72
:Time[y] 5.
Time[y] 10.
:Time[y] 15.
:Time[y] 20.
:Time[y] 25.
Time[y] 50.
Time[y] 100.
Time[y] 500.
Time[y] 1000.
Time[y] 5000.
Time[y] 10000.
Time[y] 1.e5
:Time[y] 1.5e5
Ends

```

The enrichment factor for chloride predicted by MULTIFLO is compared to the ratio of the initial liquid saturation to the liquid saturation at the same time and location, as given in Eqn.(6). The latter corresponds to the enrichment that would be obtained if only pure evaporation is taken into account, equivalent to results obtained using the computer code EQ6. Two different residual saturations s_r^* of 0.08 and 0.01 are considered. The residual saturation occurs as a parameter in the van Genuchten relations for saturation and relative permeability in terms of capillary suction (van Genuchten, 1980). Physically the residual saturation, also referred to as the irreducible or equilibrium saturation, represents the threshold liquid saturation at which the liquid phase becomes disconnected, breaking up into isolated islands of liquid water. At and below the residual saturation, the liquid relative permeability becomes zero and flow is not possible. The liquid saturation may be reduced below the residual value by evaporation with water carried away in the vapor phase.

In Figure 2 the enrichment factor for chloride is displayed as a function of depth for an elapsed time of 100 years, and in Figure 3 as a function of time at the repository horizon. Generally, a lower residual saturation results in a higher enrichment factor. As can be seen from the figures, the pure evaporative enrichment factor overestimates the MULTIFLO calculated value by as much as a factor of two for the lower residual saturation in the vicinity of the repository horizon. For the higher residual saturation (0.08), the two results are of comparable magnitude. In the regions of condensation above and below the repository where the aqueous solution becomes more dilute, the pure evaporation enrichment factor exceeds the MULTIFLO calculated value. This difference in behavior can be attributed to the added contribution of the flux of solute

species driven by capillary forces to the total inventory. This factor is not accounted for in the pure evaporation calculation. At early times the flux adds solute species to the control volume, whereas at later times, because the refluxing fluid is more dilute than the ambient groundwater concentration, a reduction in the enrichment factor ensues.

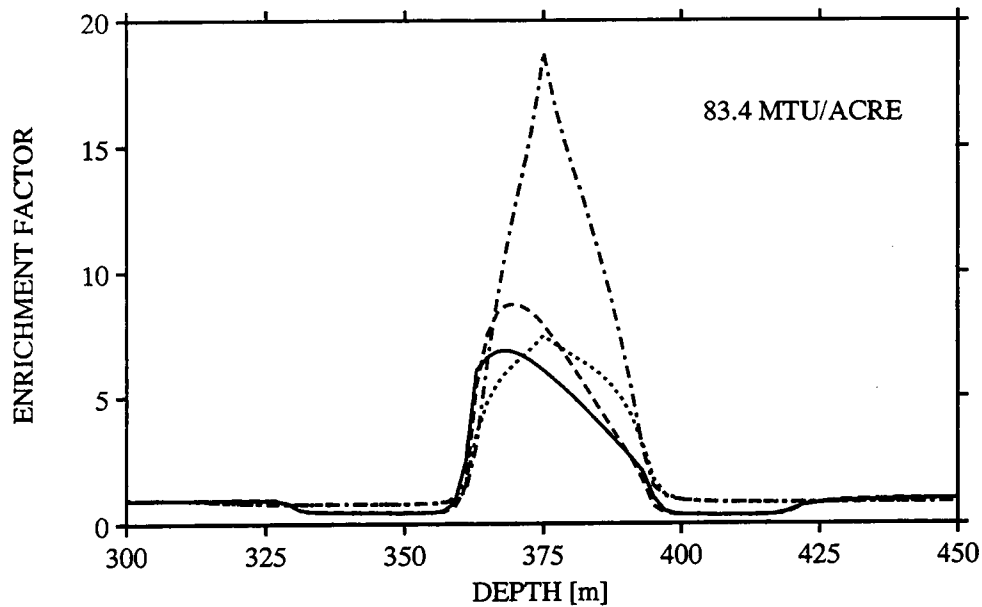


Figure 2: Enrichment factor for chloride at 100 years plotted as a function of depth computed using MULTIFLO with a residual saturation of 0.08 (solid curve) and 0.01 (dashed curve) compared with the simple evaporation model (dotted curve $s_l^r = 0.08$, dash-dotted curve $s_l^r = 0.01$)

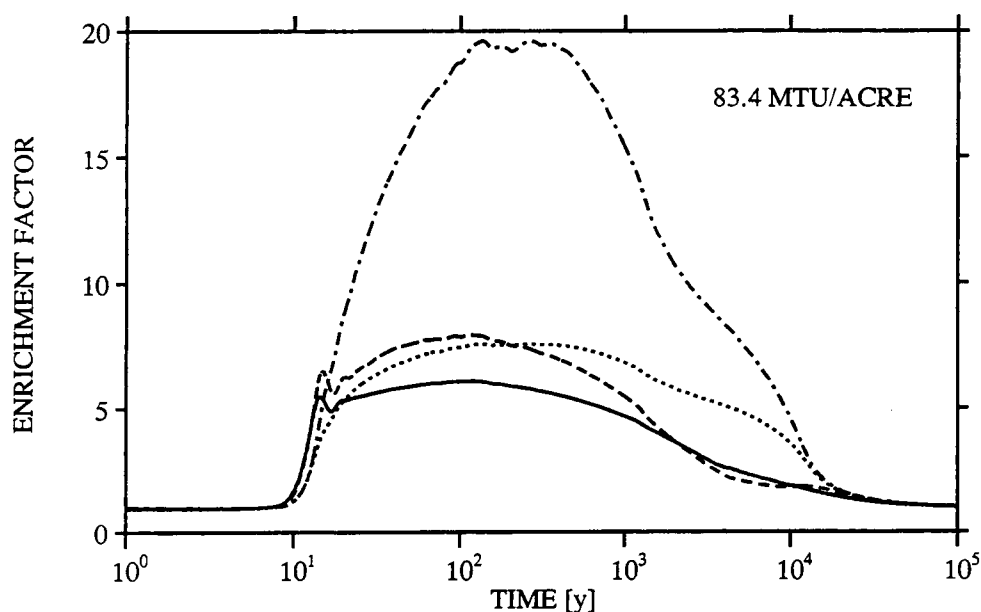


Figure 3: Enrichment factor for chloride at the repository horizon plotted as a function of time computed using MULTIFLO with residual saturations of 0.08 (solid curve) and 0.01 (dashed curve) compared with the simple evaporation model (dotted curve $s_r^* = 0.08$, dash-dotted curve $s_r^* = 0.01$).

It is apparent that EQ6 calculations alone are insufficient and relatively limited in their ability to bound the aqueous and gaseous phase compositions that would result from extended boiling and evaporation of liquid water in the near-field region of the repository. Mechanisms responsible for determining how the solute concentration changes with changing temperature and moisture content include both boiling and evaporative effects and reflux of liquid water. There are two cases to consider: the first case corresponds to a heat load for which complete dryout does not occur; and the second case to a heat load for which complete dryout does occur. In the first case, the enrichment factor for a nonreactive species such as chloride is roughly equal to the amount of water evaporated. Saturation of chloride with halite or other chloride-bearing minerals is presumed not to occur and, therefore, in this case a simple evaporation model may be used. What is needed is a TH calculation providing the liquid saturation, which determines the amount of water evaporated. As evaporation proceeds, the liquid saturation will eventually fall below the residual saturation for the medium assuming there is sufficient heat supplied by the spent nuclear fuel. For saturations at or below the residual saturation the aqueous phase consists of isolated islands of liquid and as a result the liquid flux becomes vanishingly small because of the small liquid relative

permeability. Thus under these circumstances, regions of extreme dryout which are below the residual saturation act as closed systems with respect to flow of liquid. The vapor phase, however, is free to move throughout these regions.

The second case, however, is more complicated. In this case all dissolved species completely precipitate out as salts during complete dryout, and then redissolve as the rewetting phase takes place. In this case the solution concentration is determined by the amount of water present during the rewetting phase—not on the amount of water evaporated. Thus it is the reflux of water into the dryout zone which is important. This quantity lies outside the scope of EQ6 calculations. Because the rate of rewetting proceeds much more slowly compared to dryout, much larger concentrations can be expected during the rewetting phase. Thus for this case, EQ6-type calculations which consider evaporation only and predict the stable mineral assemblage at complete dryout, provide *no* information whatsoever regarding the solution composition during the rewetting phase. Knowing the extent of resaturation it may be possible to run EQ6 calculations in reverse and obtain the solution composition resulting from adding liquid water to the mineral precipitate obtained during dryout. However, this has not yet been done to the authors' knowledge. In essence this is what the computer code MULTIFLO accomplishes by combining a reactive transport calculation with a thermal-hydrologic calculation to determine the temperature, liquid saturation, aqueous and gaseous compositions, and mineral deposition profiles with time. Such calculations are currently in progress for the complete dryout case.

3.14.97 Porosity-Permeability Variations in the Near Field

The transformation of cristobalite to quartz creates porosity as a result of the larger cristobalite molar volume compared to quartz. The increase in porosity is proportional to the cristobalite volume fraction as given by the expression

$$\Delta\phi = \phi - \phi_0 = \left(1 - \frac{\bar{V}_{\text{qtz}}}{\bar{V}_{\text{cris}}}\right) \phi_{\text{cris}}^0 \quad (11)$$

Here ϕ_0 represent the initial porosity before transformation, and ϕ_{cris}^0 denotes the initial volume fraction of cristobalite. The quantities $\bar{V}_{\text{qtz}} = 22.688 \text{ cm}^3/\text{mole}$ and $\bar{V}_{\text{cris}} = 25.75 \text{ cm}^3/\text{mole}$ denote the molar volumes of quartz and α -cristobalite, respectively.

Porosity-Permeability The transformation of cristobalite to quartz and alteration of other silicate minerals may lead to changes in porosity and hence permeability of

the YM tuff. Several phenomenological expressions exist for relating porosity and permeability (Oelkers, 1996). One relation is the power law expression

$$\kappa = \kappa_0 \left[\frac{\phi}{\phi_0} \right]^n, \quad (12)$$

where κ_0 and ϕ_0 refer to the initial permeability and porosity, respectively, and n is a constant. Shown in Figure 4 is a comparison of the resulting change in permeability for complete alteration of cristobalite to quartz for the initial volume fraction for cristobalite of 0.39, and the value 0.14, plotted as a function of the exponent n .

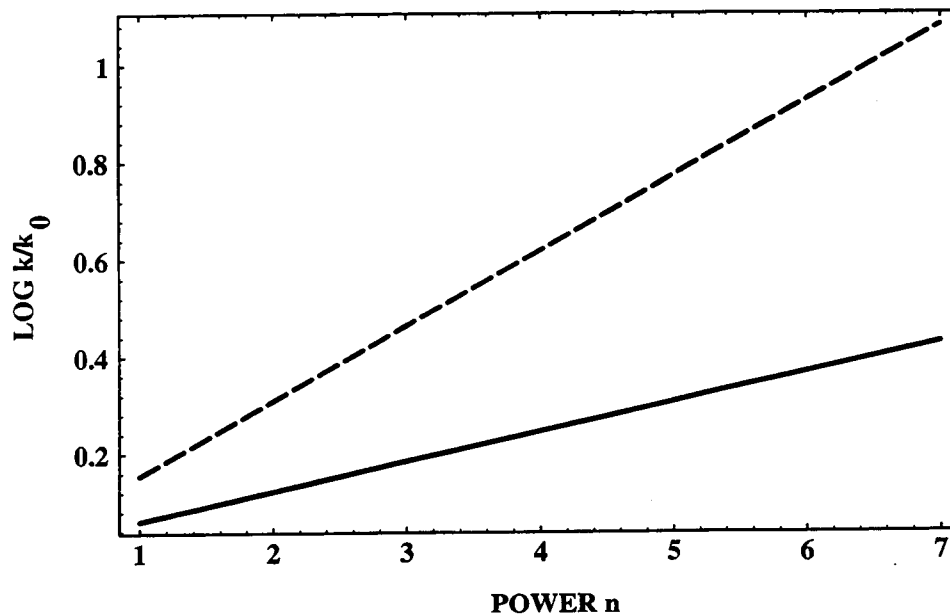


Figure 4: Log permeability enhancement factor plotted as a function of the exponent n in Eqn.(12) for the alteration of cristobalite to quartz. The solid line is for an initial cristobalite volume fraction of 0.14, and the dashed line 0.39 used by Johnson and Glassley.

MULTIFLO calculations are performed for the repository-scale model with a simplistic representation of the YM host rock consisting of equal amounts of quartz and cristobalite with initial volume fractions set at 0.14, and with an initial porosity of 0.11. Input data to the calculations require specifying: (1) initial and boundary fluid compositions, (2) initial composition of host rock in terms of mineral volume fractions, (3) porosity, (4) possible secondary alteration products, (5) flow velocity (constant), (6) temperature profile (constant), and (7) kinetic rate constants and surface areas of all reacting minerals. Shown in Figure 5 are the volume fractions for cristobalite and quartz and the porosity depicted as a function of depth for an elapsed time

of 1000 years. As can be seen from the figure, a slight increase in porosity occurs in the vicinity of the repository as cristobalite is transformed into quartz over a depth of several hundred meters. Rate constants for cristobalite and quartz were taken as $\log k [\text{moles cm}^{-2} \text{s}^{-1}] = -16.34$ and -17.39 , respectively, with equal specific surface areas of 10 cm^{-1} . The activation enthalpy was assumed to be the same for both minerals and equal to 75 kJ mole^{-1} (Dove, 1995).

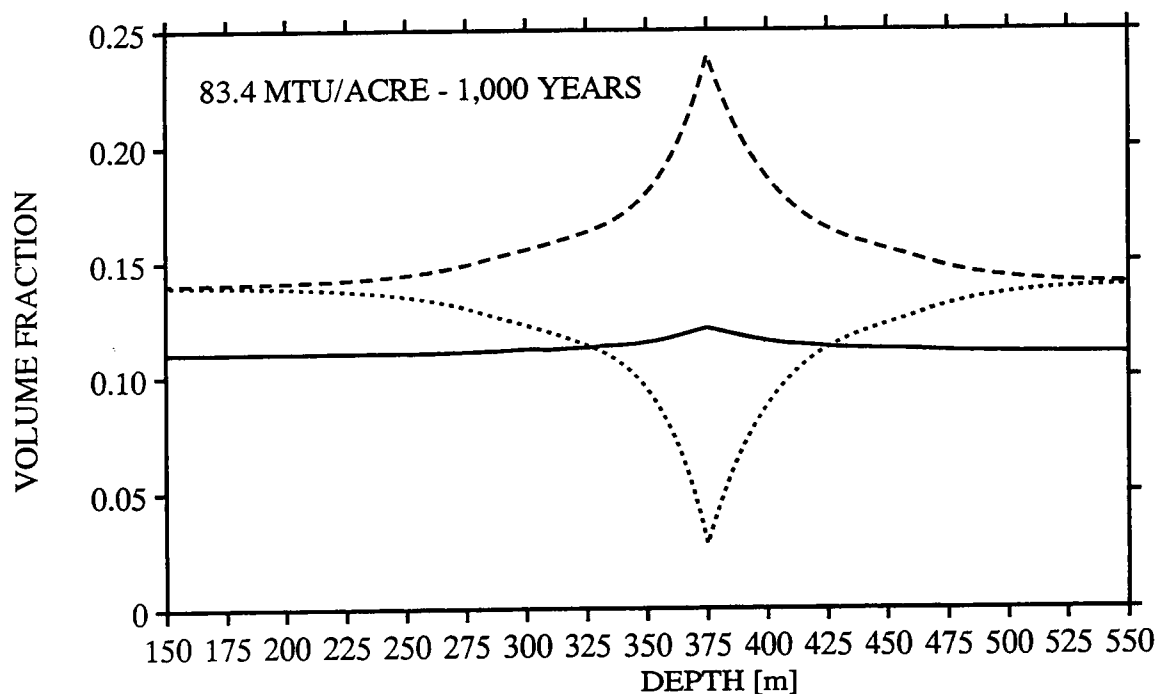


Figure 5: Volume fractions for cristobalite (dotted curve) and quartz (dashed curve) depicted as a function of depth for an elapsed time of 1000 years. Also shown is the porosity (solid curve). Calculations were performed using MULTIFLO based on the repository-scale model.

3.25.97 THC Model Calculations

Changes in the near-field chemistry are predicted by coupled thermal-hydrologic-chemical (THC) model calculations using the computer code MULTIFLO (Lichtner, 1996; Lichtner and Seth, 1996a).

The repository is represented as a circular disk with a heat load of 83.4 MTU/acre. An initial saturation of approximately 80 percent throughout most of the unsaturated zone, becoming fully saturated at the water table, is assumed. For this case complete dryout does not occur. A single spatial dimension along the vertical through the center

of the repository is considered (see Figure 6). The repository horizon is located at a depth of 375 m from the surface.

The initial fluid composition is taken from unsaturated zone water measured in borehole UZ-TP (table 3). The fluid composition at the top of the mountain is assumed the same as the initial fluid composition, and at the bottom is taken as J-13 well water (table 3). The host rock is assumed to consist of the single mineral quartz with a porosity of 11 percent. Calcite is allowed to precipitate as a secondary alteration product.

Table 3: Fluid composition for major species corresponding to UZ4-TP-3 (91.4 m) (Yang and Turner, 1988), and J-13 well water (Ogard and Kerrisk, 1984).

Species	Molality $\times 10^4$	
	UZ4	J-13
Ca^{2+}	2.50	0.29
Mg^{2+}	0.78	0.072
Na^+	3.00	1.96
K^+	0.36	0.136
HCO_3^-	0.99	0
$\text{SiO}_2(\text{aq})$	1.50	1.07
Cl^-	2.80	0.18
SO_4^{2-}	1.70	0.19
pH	8.2	6.9
pCO ₂	-2.0	-2.0

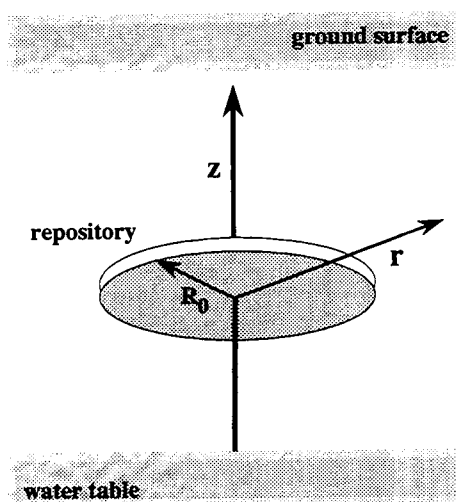


Figure 6: Repository-scale model.

Results. The effect of evaporation on the near-field chemistry is shown in the following figures. Calculations are based on the equivalent continuum formulation of two-phase fluid flow through fractured porous media. Matrix permeability of $1.9 \times 10^{-18} \text{ m}^2$ and fracture permeability $1 \times 10^{-11} \text{ m}^2$ are used in the calculation. Van Genuchten parameters of $\alpha_m = 5 \times 10^{-7} \text{ Pa}^{-1}$, $\beta_m = 0.44$, and residual saturation $s_m^r = 0.001$ are employed for the matrix, and $\alpha_f = 1.305 \times 10^{-5} \text{ Pa}^{-1}$, $\beta_f = 0.7636$, and residual saturation $s_f^r = 0.001$ for the fracture network. Boundary conditions of 15°C at the surface and 30°C at the water table are imposed. The initial saturation is obtained by equilibrating the system with unit saturation at the water table and 80 percent saturation at the surface.

The temperature and liquid saturation fields at the repository horizon as functions of time are shown in figures 7 and 8. A maximum temperature of approximately 125°C is reached over a time interval of 50–500 years. After 500 years the repository begins to cool. Although the temperature rises above the nominal boiling point, because of the effect of vapor pressure lowering on the boiling point, liquid water remains present at all times as can be seen in figure 8. During the early time behavior the saturation increases slightly and then decreases dropping to a minimum value of approximately 0.02.

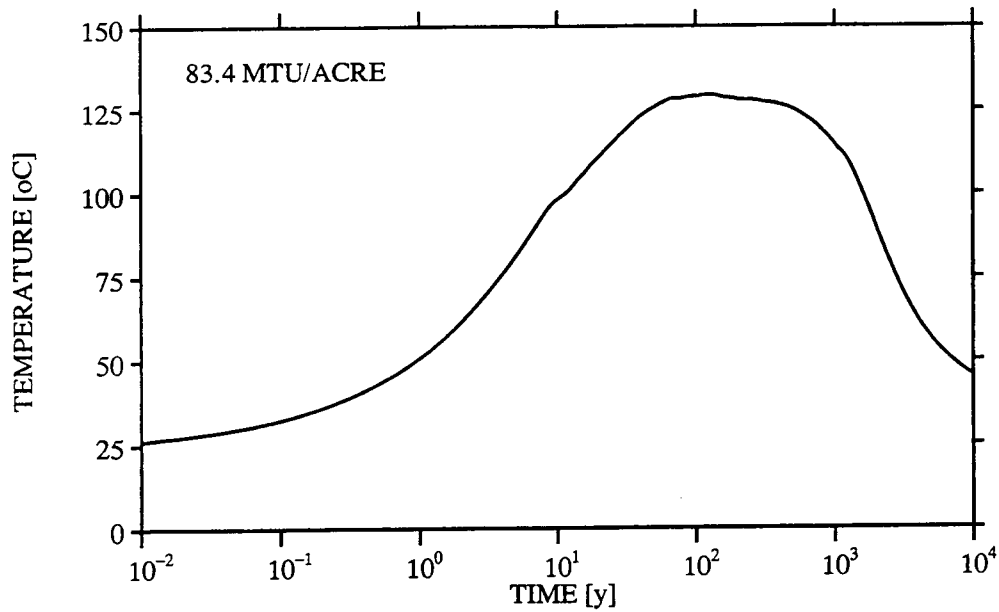


Figure 7: Temperature at the repository horizon plotted as a function of time.

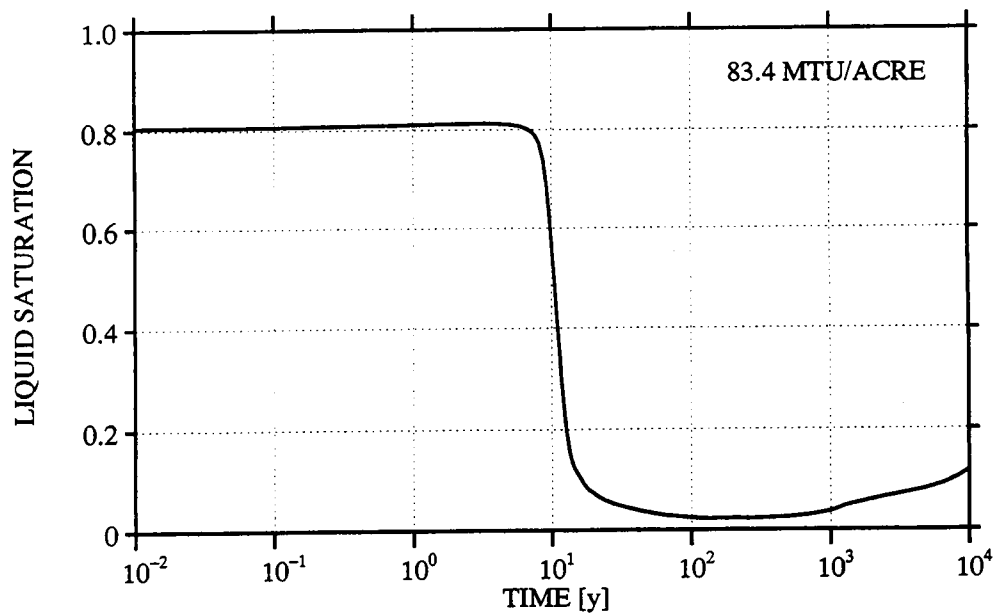
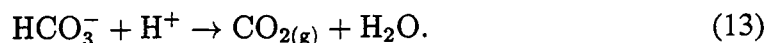


Figure 8: The liquid saturation at the repository horizon plotted as a function of time.

Results for the pH at the repository horizon are shown in figure 9 depicted as a function of time. A strong increase in pH occurs near the repository horizon as a result of

degassing of CO_2 caused by the increase in temperature as heat is released from the repository according to the reaction:



The change in pH is sensitive to the initial CO_2 concentration in the groundwater.

In figure 10 the concentration of dissolved oxygen at the repository is shown as a function of time. For a time period of approximately 1,000 years the oxygen concentration drops to very low values, presumably caused by boiling resulting in an upward flow of water vapor purging the near field. This result is consistent with the calculated rise in pH as CO_2 is degassed from the near field. It is important to note, however, that effects of radiolysis on generation of oxygen within the waste package are not considered here. Neither is the consumption of oxygen by oxidation of the iron container. Thus the actual oxygen concentration at the waste package is likely to be different from that predicted in these calculations.

Shown in figure 11 are the total calcium, sulfate, magnesium and chloride concentrations. The sharp drop in the calcium concentration at approximately 1,000 years coincides with the drop in pH. At this time the rewetting phase of the repository begins.

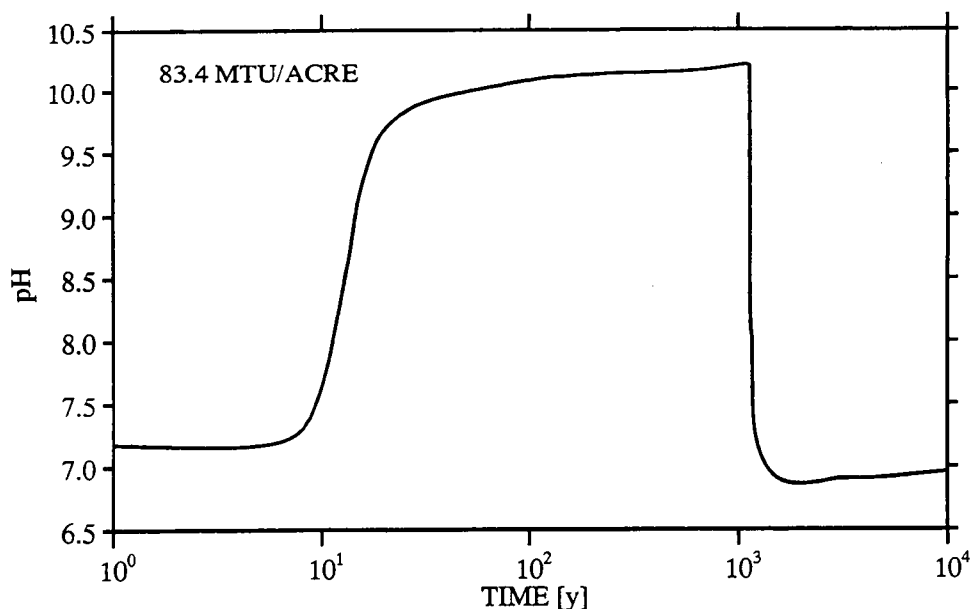


Figure 9: The pH plotted as a function of time.)

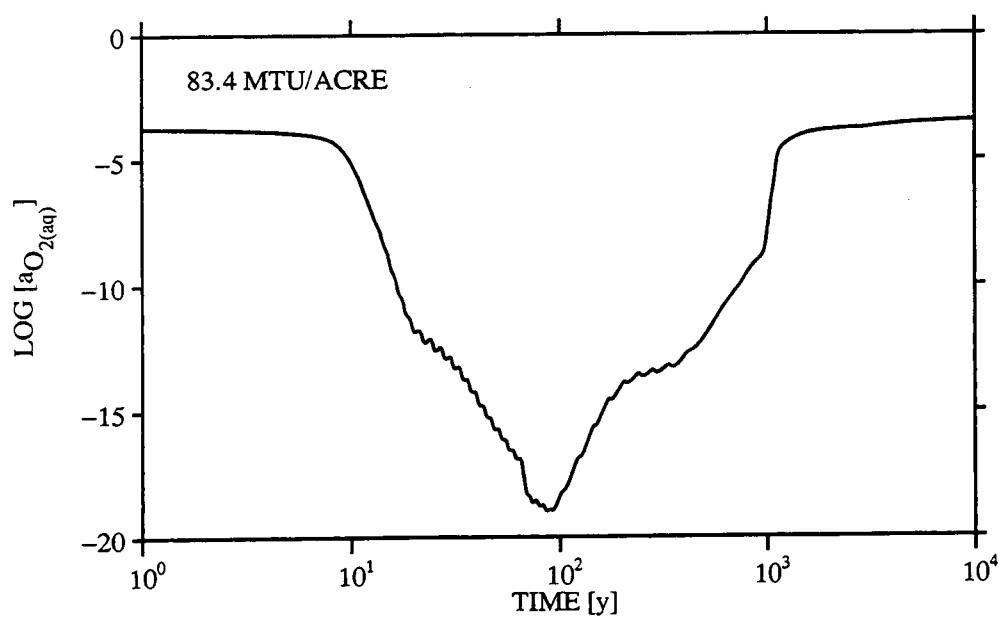


Figure 10: Molality of dissolved oxygen plotted as a function of time.

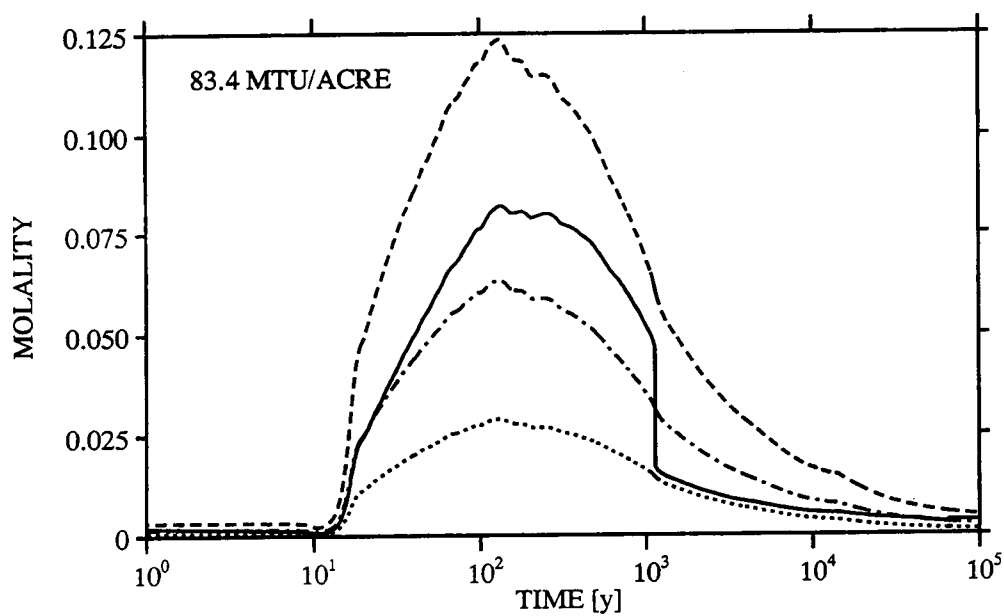


Figure 11: Molality of total calcium (solid), sulfate (dash-dotted), magnesium (dotted) and chloride (dashed) plotted as a function of time.

Remarks. There are several caveats to keep in mind when applying the calculations presented in this report to the very near-field of the repository defined as the waste package environment. First, the calculations were based on a repository-scale model which does not account for the detailed geometry of emplacement of the waste. Temperatures are likely to be higher at the waste package than that predicted by the repository-scale model. Second, the calculations were based on the equivalent continuum model which does not properly account for infiltration. Significant infiltration would be expected to have a dilution effect of the near-field solution chemistry. Third, simplifications were made in describing the composition of the host rock which could affect the near-field chemistry. Finally, the effect of the waste form and container on the near-field chemistry was not taken into account.

Account Number: **20-5708-562**

Description: Near-field Environment Code Development – MULTIFLO

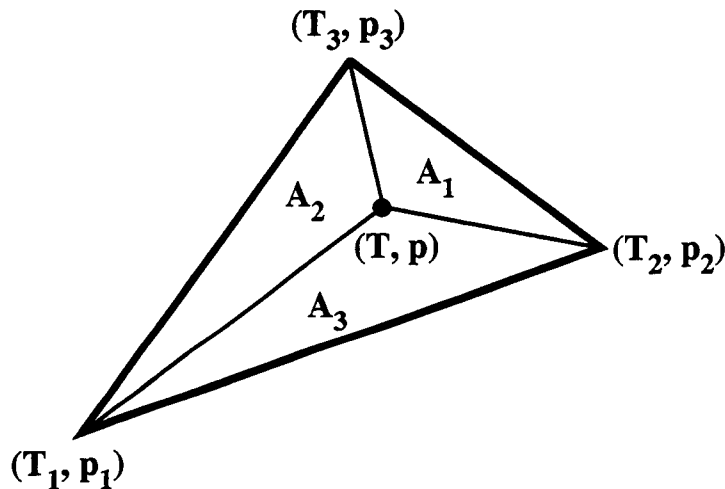
Collaborators: Dr. M. Seth (Consultant)

Objective: Development of the computer code MULTIFLO, and submodules GEM and METRA.

1.15.97 Interpolation on an unstructured grid.

Equations were developed for incorporation into MULTIFLO for interpolation on a unstructured grid made up of quadrilaterals and triangles. This change was necessary due to a bug found in the present interpolation scheme used in MULTIFLO for water material properties.

Triangle



For some physical property $\psi(T, p)$ defined at the vertices of an arbitrarily shaped triangle, its value at some point (T, p) within the triangular region is given by

$$\psi(T, p) = \sum_{i=1}^3 \psi_i \phi_i(T, p), \quad (14)$$

where basis functions ϕ_i are defined by

$$\phi_i = \frac{A_i}{A}. \quad (15)$$

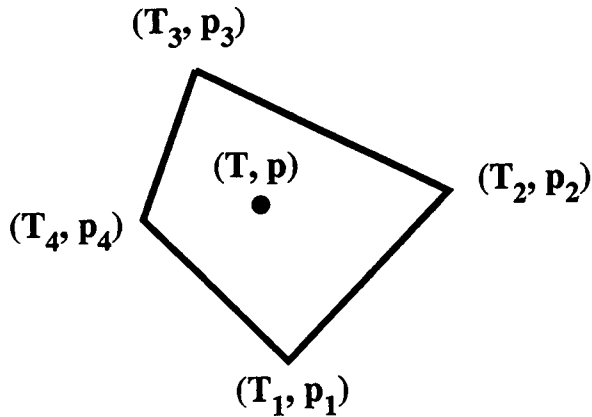
$$A = \sum_{i=1}^3 A_i. \quad (16)$$

$$\phi_1(T, p) = \frac{1}{2A} \{T_2 p_3 - T_3 p_2 + T(p_2 - p_3) + p(T_3 - T_2)\}, \quad (17)$$

$$\phi_2(T, p) = \frac{1}{2A} \{T_3 p_1 - T_1 p_3 + T(p_3 - p_1) + p(T_1 - T_3)\}, \quad (18)$$

$$\phi_3(T, p) = \frac{1}{2A} \{T_1 p_2 - T_2 p_1 + T(p_1 - p_2) + p(T_2 - T_1)\}, \quad (19)$$

$$2A = T_2 p_3 - T_3 p_2 + T_3 p_1 - T_1 p_3 + T_1 p_2 - T_2 p_1. \quad (20)$$

Quadrilateral

$$\psi(T, p) = \sum_{i=1}^4 \psi_i \phi_i(\xi(T, p), \eta(T, p)). \quad (21)$$

$$\phi_1(\xi, \eta) = (1 - \xi)(1 - \eta), \quad (22)$$

$$\phi_2(\xi, \eta) = \xi(1 - \eta), \quad (23)$$

$$\phi_3(\xi, \eta) = \xi\eta, \quad (24)$$

$$\phi_4(\xi, \eta) = (1 - \xi)\eta, \quad (25)$$

The basis function coordinates, (ξ, η) , are defined implicitly in terms of (T, p) through the equations

$$T = \sum_{i=1}^4 T_i \phi_i(\xi, \eta), \quad (26)$$

$$p = \sum_{i=1}^4 p_i \phi_i(\xi, \eta). \quad (27)$$

For the special case of parallel sides ($T_1 = T_4$, $T_2 = T_3$) the following solution is obtained:

$$\xi(T) = \frac{T - T_1}{T_2 - T_1}, \quad (28)$$

$$\eta(T, p) = \frac{p - p_1 - (p_2 - p_1) \xi(T)}{p_4 - p_1 + (p_1 - p_2 + p_3 - p_4) \xi(T)}. \quad (29)$$

1. REFERENCES

- Aagaard P., and H.C. Helgeson. 1982. Thermodynamic and kinetic constraints on reaction rates among minerals and aqueous solutions. I. Theoretical considerations. *American Journal of Science*, 282:237–285.
- Archie 1952. Introduction to petrophysics of reservoir rocks. *American Association Petrology Geological Bulletin* 34:943–961.
- Blum, A.E., and L.L. Stillings. 1995. Feldspar dissolution kinetics. In *Chemical Weathering Rates of Silicate Minerals*, (eds. White, A.F. and Brantley, S.L.), Chapter 7, *Reviews in Mineralogy* Volume 31:291–342.
- Buscheck, T.A., and J.J. Nitao. 1993. The analysis of repository-heat-driven hydrothermal flow at Yucca Mountain, *Proceedings of the Fourth Annual International Conference Las Vegas, Nevada*, April 26-30, 1:847–867.
- Dove, P. 1995. Controls on silica reactivity in weathering environments. In *Chemical Weathering Rates of Silicate Minerals*, (eds. White, A.F. and Brantley, S.L.), Chapter 6, *Reviews in Mineralogy* Volume 31:235–290.
- Harrar, J.E. (Chairman), J.F. Carley, W.F. Isherwood, and E. Raber. 1990. *Report of the committee to Review the Use of J-13 Well Water in Nevada Nuclear Waste Storage Investigations*. UCID-21867. Livermore, CA: Lawrence Livermore National Laboratory.
- Helgeson, H.C., W.M. Murphy, and P. Aagaard. 1984. Thermodynamic and kinetic constraints on reaction rates among minerals and aqueous solutions. II. Rate constants, effective surface area, and the hydrolysis of feldspar. *Geochimica et Cosmochimica Acta* 51:3137–3153.
- Lichtner, P.C. 1996. Continuum formulation of multicomponent-multiphase reactive transport. In *Reactive Transport in Porous Media*, (eds. Lichtner, P.C., Steefel, C.I., and Oelkers, E.H.), Chapter 1, *Reviews in Mineralogy* Volume 34:1–81.
- Lichtner, P.C., and M.S. Seth. 1996a. Multiphase-multicomponent reactive transport nonisothermal reactive transport in partially saturated porous media. Presented at the International Conference on Deep Geological Disposal of Radioactive Waste, Canadian Nuclear Society. September 16-19, Winnipeg, Manitoba, Canada.
- Lichtner, P.C., and M.S. Seth. 1996b. User's manual for MULTIFLO: Part II MULTIFLO 1.0 and GEM 1.0, Multicomponent-multiphase reactive transport model. CNWRA 96-010. San Antonio, Texas: Center for Nuclear Regulatory Analyses.
- Lichtner, P.C. and J.C. Walton. 1994. Near-field liquid-vapor transport in a partially saturated high-level nuclear waste repository. CNWRA 94-022. San Antonio, Texas: Center for Nuclear Regulatory Analyses.
- Lichtner, P.C. and J.C. Walton. 1994. Near-field liquid-vapor transport in a partially saturated high-level nuclear waste repository. CNWRA 94-022. San Antonio, Texas: Center for Nuclear Regulatory Analyses.
- Murphy, W.M., and R.T. Pabalan. 1994. Geochemical investigations related to the Yucca Mountain environment and potential nuclear waste repository. NUREG/CR-6288.
- Murphy, W.M., E.H. Oelkers, and, P.C. Lichtner. 1989. Surface reaction versus diffusion control of mineral dissolution and growth rates in geochemical processes. *Chemical Geology* 78:357–380.
- Nitao, J.J. 1996. Reference Manual for the NUFT Flow and Transport Code, Version 1.0. UCRL-ID-113520, Lawrence Livermore National Laboratory.
- Norton, D. and R. Knapp. 1977. Transport phenomena in hydrothermal systems: The nature of porosity. *American Journal of Science* 277:913–936.
- Oelkers, E.H., J. Schott, J.L. Devidal. 1994. The effect of aluminum, pH, and chemical affinity on the rates of aluminosilicate dissolution reactions. *Geochim. Cosmochim. Acta* 58:2011–2024.

- Oelkers, E.H. 1996. Physical and chemical properties of rocks and fluids for chemical mass transport calculations. In *Reactive Transport in Porous Media*, (eds. Lichtner, P.C., Steefel, C.I., and Oelkers, E.H.), Chapter 1, *Reviews in Mineralogy Volume 34*:131–191.
- Ogard, A.E., and J.F. Kerrisk. 1984. Groundwater chemistry along flow paths between a proposed repository site and the accessible environment. LA10188-MS, Los Alamos National Laboratory.
- Pruess, K. 1991. TOUGH2—A general purpose numerical simulator for multiphase fluid and heat flow. LBL-29400. Berkeley, CA, University of California, Lawrence Berkeley Laboratory.
- Pruess, K. and Y. Tsang. 1994. Thermal Modeling for a Potential High-Level Nuclear Waste Repository at Yucca Mountain, Nevada. LBL-35381, UC-600. Berkeley, CA: Lawrence Berkeley Laboratory.
- Robinson 1995. LANL.
- Seth, M.S., and P.C. Lichtner. 1996. User's manual for MULTIFLO: Part I Metra 1.0 β , Two-phase nonisothermal flow simulator. CNWRA 96-005. San Antonio, Texas: Center for Nuclear Regulatory Analyses.
- Steefel, C.I. and S.B. Yabusaki. 1995. OS3D/GIMRT: Software for modeling multicomponent-multidimensional reactive transport. User's manual and programmer's guide, Version 1.0, 58 p.
- van Genuchten, M. 1980. A closed form equation for predicting the hydraulic conductivity of unsaturated soils. *Soil Science Society of American Journal* 44:892–898.
- Vaniman, D.T., D.L. Bish, S.J. Chipera, B.A. Carlos, and G.D. Guthrie. 1996. Summary and Synthesis Report on Mineralogy and Petrology Studies for the Yucca Mountain Site Characterization Project. Volume 1. Chemistry and Mineralogy of the Transport Environment at Yucca Mountain. Milestone 3665. U.S. Department of Energy, Earth and Environmental Sciences, Los Alamos National Laboratory: Los Alamos, NM.
- Walton, J.C. 1993. Effects of evaporation and solute concentration on presence and composition of water in and around the waste package at Yucca Mountain, *Waste Management*, 13:293–301.
- White, S.P. 1995. Multiphase nonisothermal transport of systems of reacting chemicals. *Wat. Res. Res.* 31:1761–1772.
- Wilder, D.G. 1996. Editor Volume II: Near-field and altered-zone environment report. DOE, August.
- Wolery, T.W. 1992. EQ3/6, a software package for geochemical modeling of aqueous systems. Package overview and installation guide (Version 7.0). Lawrence Livermore National Laboratory, Livermore, CA, UCRL-MA-110662, 66 p.
- Zyvoloski, G., Z. Dash, and, S. Kelkar. 1992. FEHMN 1.0: Finite element heat and mass transfer code. LA-12062-MS, Rev 1. Los Alamos, NM, Los Alamos National Laboratory.

SCIENTIFIC NOTEBOOK

by

Peter C. Lichtner

Printed: February 3, 1997

P. C. Lichtner

SCIENTIFIC NOTEBOOK

INITIALS:

PC

SCIENTIFIC NOTEBOOK

by

Peter C. Lichtner

**Southwest Research Institute
Center for Nuclear Waste Regulatory Analyses
San Antonio, Texas**

February 3, 1997

Period: October–December, 1996, 4th Quarter

P. C. Lichtner

SCIENTIFIC NOTEBOOKINITIALS: PCL**INITIAL ENTRIES**

Scientific NoteBook: # 095

Issued to: P. C. Lichtner

Issue Date: Tuesday, November 16, 1993

Computerized Initials: PCL

By agreement with the CNWRA QA this NoteBook is to be printed at approximate quarterly intervals. This computerized Scientific NoteBook is intended to address the criteria of CNWRA QAP-001.

Table 1: Computing Equipment

Machine Name	Type	OS	Location
gravenstein.cnwra.swri.edu	Pentium Workstation	NEXTSTEP	desk Rm A-126
	133 Mhz	Version 3.3	Bldg. 189
	64 MB RAM		
skippy.cnwra.swri.edu	Sun SPARC 20	SUNOS 4.1.2	network
	96 MB RAM		

Contents

INITIAL ENTRIES ii

FIGURES iv

TABLES v

NEAR-FIELD ENVIRONMENT 1

BHP COPPER PROJECT 8

List of Figures

- 1 Comparison of MPATH and MULTFLO. 2
- 2 The pH-dependence of the albite rate constant. The blue and green lines refer to
the acidic and basic rate constants, and the brown line to the neutral rate constant.
The red curve is the sum of the different regions. 11

List of Tables

1 Computing Equipment ii

2 Ion-exchange selectivity coefficients for half-reactions. Data taken from Parkhurst (1995). 10

P. C. Lichtner

SCIENTIFIC NOTEBOOK

INITIALS: SC

KTI: NEAR-FIELD ENVIRONMENT

Account Number: **20-5708-561**

Description: Near-field Environment Technical Assistance

Collaborators: Dr. M. Seth (Consultant)

No activity.

Account Number: **20-5708-562**

Description: Near-field Environment Code Development – MULTIFLO

Collaborators: Dr. M. Seth (Consultant)

Objective: Development of the computer code MULTIFLO, and submodules GEM and METRA.

10.16.96 Validation Comparison of MULTIFLO with MPATH.

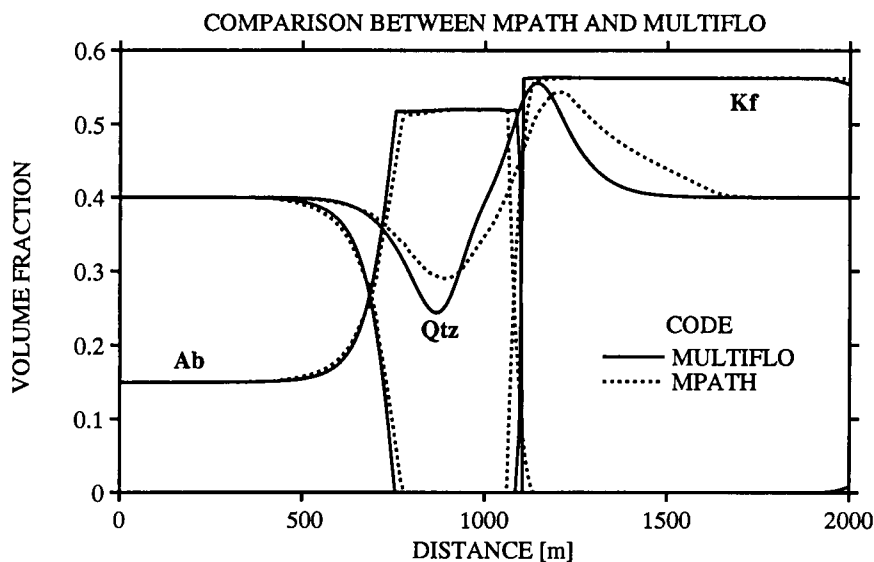


Figure 1: Comparison of MPATH and MULTIFLO.

To validate MULTIFLO for nonisothermal systems, a comparison was made with previously published results using the code MPATH describing reactive flow and transport in a hydrothermal system (Lichtner, 1992, Time-space continuum description of fluid/rock interaction in permeable media, Water Resources Research, v. 28, 3135–3155). In this example a gaussian heat source is centered at 1,000 m from the origin with a maximum temperature of 300°C. For more details refer to Lichtner (1992). The comparison is shown in Figure 1 for an elapsed time of 200,000 years. The agreement for minerals K-feldspar and albite is excellent, whereas for quartz the agreement is not as good. The two codes use very different algorithms: MPATH is based on the multiple reaction path approach, whereas MULTIFLO uses an implicit finite difference scheme with first order upwinding.

The multiflo input file used in the calculation is listed below:

Test Data for Multiflo Simulator (Yucca Mt., 1D, 80 kW/acre)

July 22, 1996

```

:
:      geometry nx  ny  nz      mode  iprint
GRID    XYZ      200  1   1      2      0
:
OPTS
: idata istart imod  iexact
  0      0      10      0
:
: itmax ihalmax ivmax ndamp
  10      10      0      5
:
: method iops  ifor   isurf iact  loglin  icon
      1      0      3      1      1      0      1
:
:      isync ipor iperm perm-fac.
COUPle  0      0      0      3.
:
PLTFiles
: iplot  a  s  t  m si sf  v  z  b in  e ex ti  g itex
      1  1  1  1  1  0  0  1  0  0  0  0  0  0  0
:
:      tol  ttol  tolneg  tolpos  tolexp  dthalf  qkmax  tolstdst
TOLR  1.d-10  2.e-3  1.e0  1.e-2  5.d0    .25    590.    1.e-6
:
:      mcyc  cc  c  flx r  sp  qk  pk  rk  coef
DEBUg  0      1  1  0  1  1  1  1  1  0
:
:      isat isothrm iread  por0  phir  sat  w  lambda toldelt  tolpor
ISYSstem -1      1      0      0.05  1.  1.0  .5  1.    1.e-3  1.e-3
:
:      vx0  vy0  vz0[m/yr]  alphax  alphay  alphaz  cournr
FLOW  1.    0.    0.        0.        0.        0.        1.
:
:      d0[cm^2/s]  delhaq[kJ/mol]  dgas[cm^2/s]  dgexp  tortaq  tortg  idif
DIFF  1.d-5      12.6              2.13d-1      1.8  1.d0  1.d0  0
:
: flag 1: T(x)  = d x^3 + a x^2 + b x + c (meters)
:      2: T(x)  = a + (b-a) exp[-((x-x0)/c)^2] + (d - a) * x / xlen

```

P. C. Lichtner

SCIENTIFIC NOTEBOOK

INITIALS: PC

```

: 3:T(x,t)=a+1/2(b-a) (erf[(x+c-x0)/2sqr(dt)]-erf[(x-c-x0)/2sqr(dt)])
: p (bars) temp flag a b c d x0 xlen
PTINit 100.0 25. 2 25.d0 300.d0-250.d0 25.d0 1.d3 1.d3
:
:master species for controlling time stepping
MASTer h+
:
:grid m 0. 1 200 200.
:
DXYZ
200*10.
1.
1.
:
: isolv level north nitmax idetail rmaxtol rtwotol smaxtol
SOLV 3 1 1 100 0 1.e-20 1.e-20 1.e-12
:
:initial and boundary conditions: 1-conc., 2-flux, 3-zero gradient
:inlet outlet nzoneaq
COMP 1 3 3
:
:species itype guess ctot mineral diffusion
k+ 3 8.e-5 1.e-2 k-feldspar 2.5e-5
na+ 3 8.e-2 1.e-5 albite 2.5e-5
al+3 3 1.e-21 1.e-4 muscovite 2.5e-5
h+ 8 1.e-9 9.0 none 9.6e-5
sio2(aq) 3 1.e-4 1.e-4 quartz 2.0e-5
cl- -1 8.e-2 1.e-4 none 1.e-5
:blank
:
BCON
1 1
:species itype guess ctot mineral diffusion
k+ 3 8.e-5 1.e-2 k-feldspar
na+ 3 8.e-2 1.e-5 albite
al+3 3 1.e-21 1.e-4 muscovite
h+ 8 1.e-9 9.0 none
sio2(aq) 3 1.e-4 1.e-4 quartz
cl- -1 8.e-2 1.e-4 none
:
2 3
:species itype guess ctot mineral

```

P. C. Lichtner

SCIENTIFIC NOTEBOOK

INITIALS: SC

```

k+      3      8.e-5      1.e-2      k-feldspar
na+      3      8.e-2      1.e-5      albite
al+3     3      1.e-21     1.e-4     muscovite
h+       8      1.e-9      9.0       none
sio2(aq) 3      1.e-4      1.e-4     quartz
cl-      -1     8.e-2      1.e-4     none
:
  0 0
:
CMIR    0  0
        :blank
:
STOL   1.  1.  1.  1.  1.  1.  1.  1.  1.  1.  1.  1.
:
AQCX
oh-          5.5e-5
aloh+2       1.0e-5
al(oh)2+     1.0e-5
al(oh)3(aq)  1.0e-5
al(oh)4-     1.0e-5
h3sio4-
naoh(aq)
:koh(aq)
        :blank
:
MNRL
quartz
sio2(am)
kaolinite
gibbsite
k-feldspar
albite
muscovite
        :blank
:
GASEs
        :blank
:
MNIR
:irr mineral itypkin beta fkin delh rkph rk tau
:i1 i2 j1 j2 k1 k2 vol area
quartz      0      1.0      1.0      75.      0.      1.e-16      1.e-2

```

P. C. Lichtner

SCIENTIFIC NOTEBOOK

INITIALS: SC

```

1 200 1 1 1 1    0.4    16.
0
k-feldspar      0    1.0    1.0    35.    0.    3.00e-16    1.e-2
1 200 1 1 1 1    0.4    16.
0
albite          0    1.0    1.0    35.    0.    3.00e-16    1.e-2
1 200 1 1 1 1    0.15    8.
0
muscovite       0    1.0    1.0    35.    0.    1.00e-16    1.e-2
1 200 1 1 1 1    0.0    10.
0

      :blank

:
:surface mineral itypkin area  beta    fkin    delh    rkph    rk
:    0  1.0  1.0    1.  0.    0.    0.
:
:corrosion solids i0  acorr  bcorr  curlim
:    0.  0.  0.  0.
:
:crevice gap[meters]  potential [v]
ECAQ      90.d-6      -.2
      :blank

:
:electrochemical aqueous species i0    acorr  bcorr  curlim
:    0.  0.  0.  0.
:
AQIR
      :blank

:
:ion-exchange reactions
Ionx  0    1.0
:
:BRKP  5
:93  110  130  150  185
:
Dtstep[y]    1 3.e-8
1.e-8        50.0
:
Time  4 2.5e4 5.e4 1.e5 2.e5
:
ENDS

```


11.1.96 Bug fix in METRA.

A bug was discovered in the subroutine `updtvpk.f`. The variable `u1` was not defined. The code was changed as follows:

in `updtvpk`, change:

```
arg = -upcwk/(udwk*rgas*tkabs)
```

to 2 lines as below:

```
u1 = -upcwk/(udwk*rgas)
```

```
arg = u1/tkabs
```

End of changes.

BHP COPPER PROJECTAccount Number: **20-8519-001**

Description: Near-field Environment Technical Assistance

Collaborators: G. Wittmeyer, D. Turner

Date Due: Final Report December 22, 1996

Objective: Application of the computer code MULTIFLO to determine how the BHP Copper Florence pilot leaching facility must be designed and operated in order to maximize copper recovery.

11.1.96 Modifications to MULTIFLO.

Several modifications to MULTIFLO were necessary to make it order to address the BHP project. These were primarily: (i) adding an option to inject and withdraw fluid at a single or group of nodes in the GEM algorithm, and (ii) activating the ion-exchange algorithm in GEM, and (iii) modifying the kinetic rate law used in GEM to include pH-dependent rate constants.

Source Term. A source term was added to the transport equations in GEM to describe injection and extraction of fluid at a specified flow rate. The transport equations have the form for fully saturated conditions

$$\frac{\partial}{\partial t} (\phi \Psi_j) + \nabla \cdot \Omega_j = Q_j \delta(\mathbf{r}) - \sum_m \nu_{jm} I_m, \quad (1)$$

with source strength Q_j with units moles s^{-1} defined by

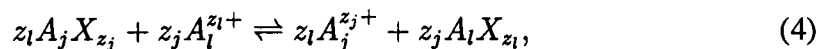
$$Q_j = q \Psi_j, \quad (2)$$

where q represents the volumetric flow rate [$\text{cm}^3 \text{s}^{-1}$] and Ψ_j is the total concentration of the j th primary species evaluated at the source. In terms of a mass flow rate q_m [kg s^{-1}]:

$$q = \frac{q_m}{\rho}, \quad (3)$$

where ρ represents the fluid density.

Ion-Exchange. Ion-exchange is described using the Vanislov formulation in terms of mole fraction. For the exchange reaction



the mass action equation reads

$$K_{jl} = \left(\frac{\chi_l}{a_l} \right)^{z_j} \left(\frac{a_j}{\chi_j} \right)^{z_l} \quad (5)$$

with selectivity coefficient K_{jl} and mole fraction χ_j defined by

$$\chi_j = \frac{z_j \bar{C}_j}{\sum_l z_l \bar{C}_l}. \quad (6)$$

The solid concentration \bar{C}_j is related to the number of surface exchange sites per bulk volume ω by the expression

$$\omega = \sum_l z_l \bar{C}_l. \quad (7)$$

It is convenient to write the exchange reaction in terms of half-reactions:



with mass action equation

$$k_j = \frac{\chi_j}{a_j a_{X^-}^{z_j}}. \quad (9)$$

The selectivity coefficients K_{jl} are related to k_j by the expression

$$K_{jl} = \frac{k_l^{z_j}}{k_j^{z_l}}, \quad (10)$$

or

$$\log K_{jl} = z_j \log k_l - z_l \log k_j. \quad (11)$$

The coefficients k_j are tabulated in Table 2, valid for low ionic strength groundwater compositions.

Table 2: Ion-exchange selectivity coefficients for half-reactions. Data taken from Parkhurst (1995).

Half Reaction	$\log K$	K
$\text{Na}^+ + \text{X}^- \rightleftharpoons \text{NaX}$	0.0	1.0
$\text{K}^+ + \text{X}^- \rightleftharpoons \text{KX}$	0.7	5.0119
$\text{H}^+ + \text{X}^- \rightleftharpoons \text{HX}$	1.0	10.0
$\text{Ca}^{2+} + 2 \text{X}^- \rightleftharpoons \text{CaX}_2$	0.8	6.3096
$\text{Mg}^{2+} + 2 \text{X}^- \rightleftharpoons \text{MgX}_2$	0.6	3.9811
$\text{Fe}^{2+} + 2 \text{X}^- \rightleftharpoons \text{FeX}_2$	0.44	2.7542
$\text{Cu}^{2+} + 2 \text{X}^- \rightleftharpoons \text{CuX}_2$	0.6	3.9811
$\text{Al}^{3+} + 3 \text{X}^- \rightleftharpoons \text{AlX}_3$	0.67	4.6774

The cation exchange capacity (CEC) must be transformed from the usual units of meq/100g solid, to units of moles dm^{-3} according to the relation

$$\omega = \frac{\bar{N}}{V} = \sum_s \frac{\bar{N}}{M_s} \frac{M_s}{V_s} \frac{V_s}{V} = 10^3 \sum_m \frac{\text{CEC}_m}{100} \rho_m \phi_m, \quad (12)$$

for density ρ_m [g cm^{-3}] and volume fraction ϕ_m of the m th mineral.

Rate Law. An option for a pH-dependent rate constant of the form:

$$k = k_0 + k_a a_{\text{H}^+}^{n_a} + k_b a_{\text{H}^+}^{n_b}, \quad (13)$$

was added to GEM. Here k_a and k_b refer to the acidic and basic pH regions, and k_0 refers to the neutral pH region. The pH-dependence of the albite rate constant is illustrated in Figure 2 for $\log k_0 = -16$, $\log k_a = -13.875$ and $\log k_b = -18.475$, and $n_a = 0.5$ and $n_b = -0.3$.

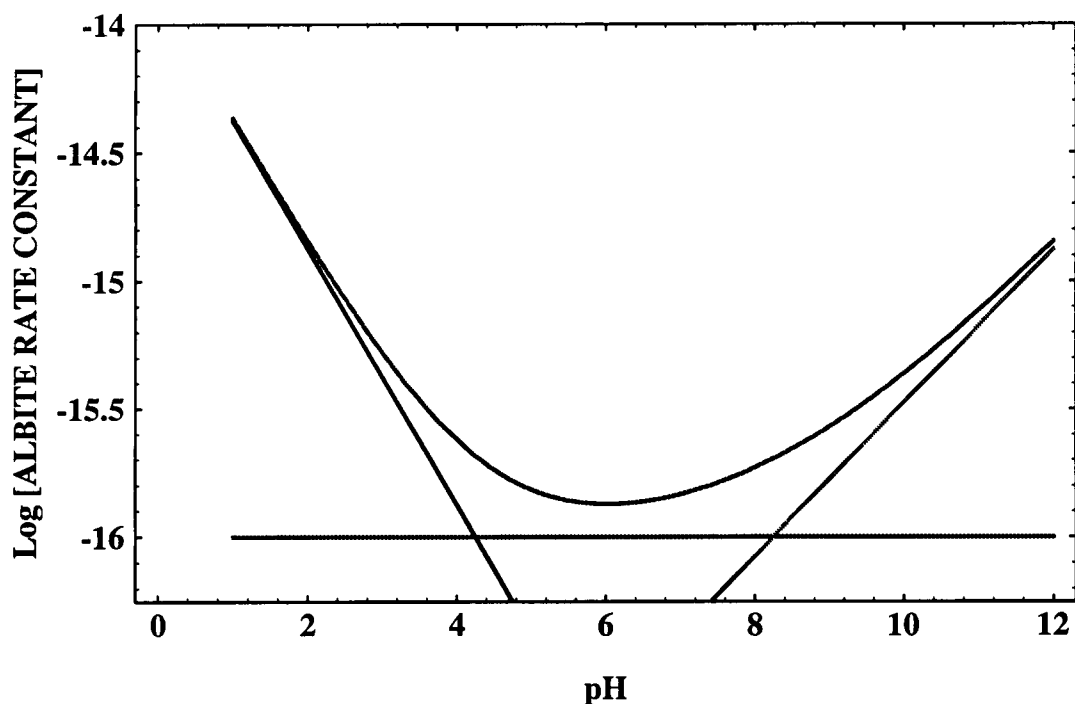


Figure 2: The pH-dependence of the albite rate constant. The blue and green lines refer to the acidic and basic rate constants, and the brown line to the neutral rate constant. The red curve is the sum of the different regions.

11.13.96 Issued Preliminary Report.

11.21.96 Issued Interim Report.

12.19.96 Issued Final Report.

12.19.96 Contents of Mathematica Notebooks used in the BHP Project

```
\include{mathematica/magmacopper}
\include{mathematica/conversion}
\include{mathematica/cec}
\include{mathematica/rates}
\include{mathematica/leq}
```

file: magmacopper.nb

INITIALIZATION

```
$Version
NeXTStep486 2.2 (January 27, 1994)
```

```
Off[General::spell]
```

```
Off[General::spell1]
```

```
Needs["Graphics'Graphics'"]
```

```
Needs["Graphics'Legend'"]
```

```
Needs["Graphics'Colors'"]
```

```
Needs["Graphics'Graphics3D'"]
```

copper concentration

```
1.5/63.55
0.0236035
```

```
t = 3 da / (365. da/y)
```

```
len = 25 m/y t/.15
```

```
1.2 m/t .15
```

```
1.2/25 365 0.15
```

```
0.00821918 y
```

```
1.36986 m
```

```
21.9 m
```

```
-----
```

```
y
```

```
2.628
```

```
4 ft 12 in/ft (2.54 cm/in)
```

```
121.92 cm
```

```
p = 0.15; v = 1.3333 f/da 0.3048 m/f 365. da/y p
```

```
22.2498 m
```

```
-----
```

```
y
```

```
dx = 4. f .3048 m/f /100
```

```
pe = v / (365 24 60 60 s/y) dx / (p 10^-9 m^2/s)
```

0.012192 m
57.3461

a = Pi (6. in 2.54 cm/in /2)^ 2 10^-4 m^2/cm^2//N

gallit = 3.785 gal/liter;

gft3 = 0.001 gal/min /gallit 10^-3 m^3/liter 365 24 60 min/y /a

2
0.0182415 m
7.61254

y

l = 4 f .3048 m/f; volp = l a 0.15; l
1.2192 m

volp /(3 da) (365 da/y)/a
22.2504 m

y

k = 1. 10^-8 moles/cm^2/h 1/3600 h/s;

surf = 250 m^2/g 2.4 g cm^-3 10^4 cm^2/m^2

rate = k surf
6
6. 10

0.0000166667 moles

3
cm s

SOLUBILITY OF CHRYSOCOLLA

7.6560 - 2.7136
4.9424

chrysocollla 73.19

3 1.000 cu+2 -2.000 h+ 1.000 sio2(aq)

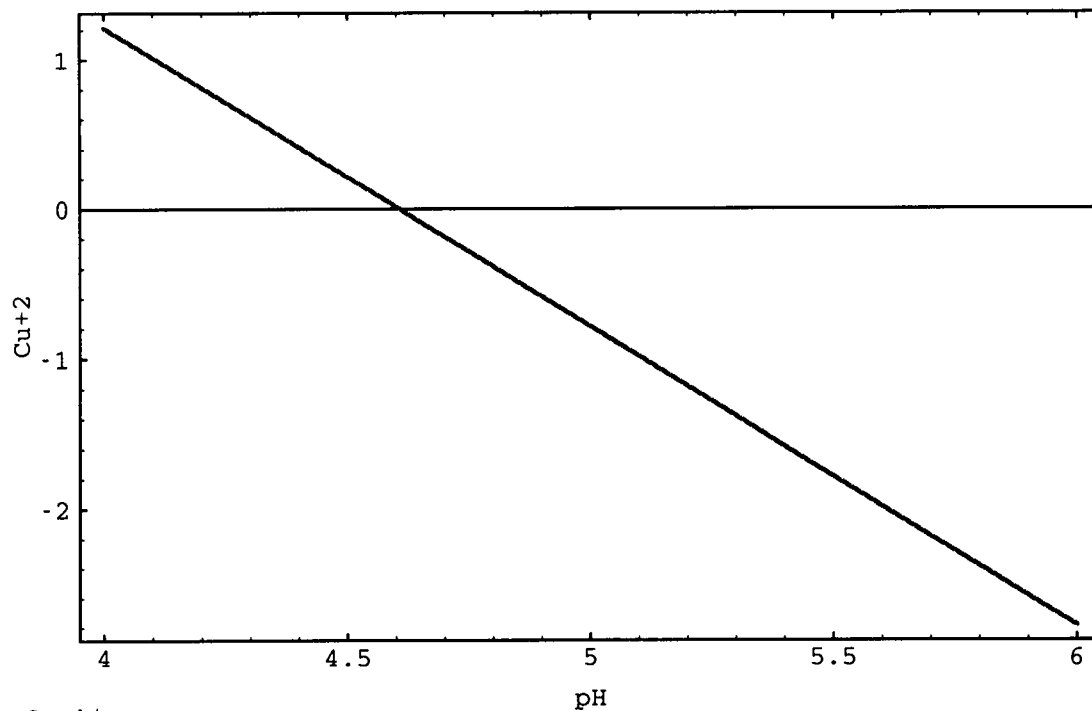
6.214

logkchy = 6.214; logsio2 = -3;

logcu[ph.] := logkchy - 2 ph - logsio2;

Plot[logcu[ph], {ph, 4, 6}, PlotRange->All,

PlotStyle->{Red}, Frame->True, FrameLabel->{"pH", "Cu+2"}]



-Graphics-

5 0.025/0.073
1.71233

BHP COPPERFLORENCE PROJECT

```
hycond = {0.1, 2, 10} ft/d 12 in/ft 2.54 cm/in 1/(24 h/d 60 m/h 60 s/m)
0.0000352778 cm 0.000705556 cm 0.00352778 cm
{-----, -----, -----}
      s           s           s
```

```
rho = 10^ 3 kg/m^ 3; mu = 10^ -3 kg/(m s); g = 980 m/s^ 2;
```

```
perm = mu/(rho g) hycond 10^ -2 m/cm
      -16 2      -15 2      -14 2
{3.59977 10 m , 7.19955 10 m , 3.59977 10 m }
```


file: conversion.nb**BHP**

```
$Version
NeXTStep486 2.2 (January 27, 1994)
```

```
Off[General::spell]
```

```
Off[General::spell1]
```

units: ft -> meter

```
mft = 2.54 cm/in 12 in /ft m/(100 cm)
0.3048 m
-----
ft
```

units: gal -> m³

```
cbmgal = 231 in^3/gal (ft/(12 in))^3 mft^3

1 ft^3 /(7.48 gal) (mft)^3
0.00378541 m^3
-----
gal
0.00378567 m^3
-----
gal
```

copper formula weight

```
cu = 63.54600;
```

metra

```
*LIQUid      Liquid Density (kgms/m3)      = 0.9971E+03
              Liquid Viscosity              = 0.8908E-03
              Liquid Compressibiity (1/pa) = 0.4499E-09
```

```
vis = 0.8908 10^-3 kg/(m s);
```

```
rho = 0.9971 10^3 kg/m^3;
```

well spacing

len = {4, 50, 75, 100} ft mft
 {1.2192 m, 15.24 m, 22.86 m, 30.48 m}

well spacing revised /11.25.96/

len = {4, 25, 37.5, 50} ft mft

 dx = len/25
 {1.2192 m, 7.62 m, 11.43 m, 15.24 m}
 {0.048768 m, 0.3048 m, 0.4572 m, 0.6096 m}

flow rate

10 gal/min cbmgal min/(60 s)

$$\frac{0.000630902 \text{ m}^3}{\text{s}}$$

column test

H₂SO₄: grams per mole
 98.0734

0.075 liter 10⁻³/(60)
 1.25 liter

len = 4 ft mft

len/100
 0.012192 m

q = 1. ml/min 1 min/(60 s) cm³/ml

$$\frac{0.0166667 \text{ cm}^3}{\text{s}}$$

dia = 6 in;

dia = dia 2.54 cm/in

area = N[Pi] (dia/2)²
 15.24 cm²
 182.415 cm²

P. C. Lichtner

SCIENTIFIC NOTEBOOK

INITIALS: PC

$$vcol = q/area \ 0.01 \ m/cm \ 60 \ 60 \ 24 \ 365 \ s/y$$

28.8135 m

y

0.075 /cu

0.00118025

0.142/cu

0.0022346

1.66/cu

0.0261228

1.8/cu

0.0283259

.028/.017

1.64706

permeability

$$0.5 \ ft/d \ mft \ vis \ / \ (\rho 9.8 \ m/s^2) \ d/(24 \ 60 \ 60 \ s)$$

$$1.608 \ 10^{-13} \ m^2$$
grid spacing

len/64

{0.238125 m, 0.357187 m, 0.47625 m}

injection rate scale factor

thickness = 400. ft mft

121.92 m

1/thickness

0.0082021

m

NOTES**Reaction Rates****calcite**

$$v_{cc} = 36.934 \text{ cm}^3/\text{mole};$$

$$r_{cc} = 10^{-4} \text{ mole/cm}^2/\text{hr} \cdot 1./ (60. \cdot 60. \text{ s/hr});$$

$$a_{cc} = 3.7 \cdot 10^{-3} \text{ cm}^2/\text{mole} / v_{cc};$$

$$\{r_{cc}, a_{cc}, r_{cc} a_{cc}\}$$

$$\left\{ \frac{2.77778 \cdot 10^{-8} \text{ mole}}{\text{cm}^2 \text{ s}}, \frac{100.179}{\text{cm}}, \frac{2.78274 \cdot 10^{-6} \text{ mole}}{\text{cm}^3 \text{ s}} \right\}$$

chrysocolla

$$v_{chry} = 73.190 \text{ cm}^3/\text{mole};$$

$$r_{chry} = 5.3 \cdot 10^{-7} \text{ mole/cm}^2/\text{hr} \cdot 1./ (60. \cdot 60. \text{ s/hr});$$

$$a_{chry} = 7.3 \cdot 10^{-3} \text{ cm}^2/\text{mole} / v_{chry};$$

$$\{r_{chry}, a_{chry}, r_{chry} a_{chry}\}$$

$$\left\{ \frac{1.47222 \cdot 10^{-10} \text{ mole}}{\text{cm}^2 \text{ s}}, \frac{99.7404}{\text{cm}}, \frac{1.4684 \cdot 10^{-8} \text{ mole}}{\text{cm}^3 \text{ s}} \right\}$$

kaolinite

$$v_{kln} = 100 \text{ cm}^3/\text{mole};$$

$$r_{kln} = 4. \cdot 10^{-15} \text{ mole/cm}^2/\text{hr} \cdot 1./ (60. \cdot 60. \text{ s/hr});$$

$$a_{kln} = 1.4 \cdot 10^{-4} \text{ cm}^2/\text{mole} / v_{kln};$$

$$\{r_{kln}, a_{kln}, r_{kln} a_{kln}\}$$

$$\left\{ \frac{1.11111 \cdot 10^{-18} \text{ mole}}{\text{cm}^2 \text{ s}}, \frac{140.}{\text{cm}}, \frac{1.55556 \cdot 10^{-16} \text{ mole}}{\text{cm}^3 \text{ s}} \right\}$$

$$.9/60$$

$$0.015$$

$$\text{diff} = 2.13 \cdot 10^{-5} \cdot ((150+273.15+25)/(25+273.15))^{1.8}$$

$$t_0 = 7 \cdot 24 \cdot 60 \cdot 60$$

$$\text{Sqrt}[\text{diff} \cdot t_0]$$

$$\frac{0.0000443567}{5.17947}$$

$$0.02/0.025$$

$$0.8$$

$$(0.02/0.025)^{(2/3)}$$

$$0.861774$$

$$((69-53)/69.)^{(2/3)}$$

$$0.377439$$

$$1./9.$$

$$0.111111$$

$$1 - (0.025 + 0.245 + 0.2 + 0.1 + 0.1 + 0.05)$$

$$0.28$$

$$0.425 - 0.18$$

$$0.245$$

VOLUME FRACTIONS

chrysocolla

$$2.68/(175.66/73.190) \cdot 0.007$$

$$0.00781649$$

goethite

$$2.68/(88.854/20.82) \cdot 0.02$$

$$0.0125594$$

calcite

$$2.68/(100.087/36.934) \cdot 0.0025$$

$$0.00247243$$

kaolinite

$$2.68 / (258.16 / 99.52) \cdot 0.07$$

$$0.0723193$$

$$\text{tot} = 0.00782 + 0.0126 + 0.00247 + 0.0723 + 0.03 + 0.01$$

$$0.13519$$

$$\text{qtz} = 1 - 0.28 - \text{tot}$$

$$0.58481$$

$$.6 / 40$$

$$0.015$$

rate constants

$$\text{mg} = 24.30500;$$

$$\text{dc} = (350 - 120) / \text{mg} \cdot 10^{-3} \cdot 10^{-3}$$

$$\text{dt} = 60. \cdot 24 \cdot 60 \cdot 60$$

$$\text{dc} / \text{dt} / 3$$

$$9.46307 \cdot 10^{-6}$$

$$5.184 \cdot 10^{-13}$$

$$6.0848 \cdot 10^{-13}$$

$$k = 39.09830;$$

$$\text{dc} = (175 - 50) / k \cdot 10^{-3} \cdot 10^{-3}$$

$$\text{dc} / \text{dt}$$

$$3.19707 \cdot 10^{-6}$$

$$6.16719 \cdot 10^{-13}$$

$$(350 - 150) / (185 - 60) // N$$

$$1.6$$

$$350. / \text{mg} \cdot 10^{-3}$$

$$0.0144003$$

$$150. / k \cdot 10^{-3}$$

$$0.00383648$$

chrysocolla rate constant

$$ah = 10^{-1.16};$$

$$k = 10^{-5.3} ah^{0.72} 10^{-4}$$

$$k_0 = 2 \cdot 10^{-10};$$

$$por = 0.28;$$

$$s = k_0/k$$

$$b = 6/s/(1+por)$$

$$6/s (1+por)$$

$$\begin{array}{r} 7.32487 \cdot 10^{-11} \\ 2.73042 \\ 1.71877 \\ 1.58217 \end{array}$$

$$28./68.6$$

$$0.408163$$

$$.0015/ (.0015+.006)$$

$$0.2$$

$$.0025/.0075$$

$$0.333333$$

$$53.22/68.67$$

$$0.775011$$

mass balance check

$$molcu = (0.028 \cdot 30./2 + 27 \cdot 0.004 + 3 \cdot 0.004/2) \text{ mole/liter da } 1.44 \text{ liter/da}$$

$$0.76896 \text{ mole}$$

$$masscu = molcu \text{ cu g/mole}$$

$$48.8643 \text{ g}$$

$$dia = 6 \text{ in};$$

$$dia = dia \cdot 2.54 \text{ cm/in};$$

$$area = N[Pi] (dia/2)^2;$$

$$len = 4 \text{ ft } 12 \text{ in/ft } 2.54 \text{ cm/in};$$

$$vol = area \text{ len}$$

22240. ³cm

molechrys = .0025 vol/(73.19 cm³/mole)
0.759667 mole

masscul = molechrys cu g/mole
48.2738 g

fracture chrysocolla

molechrysf = .0015 vol/(73.19 cm³/mole)
0.4558 mole

matrix chrysocolla

matchry = molechrys - molechrysf
0.303867 mole

matchry 175.66 cm³/mole /vol
0.00240005

vchry = (55 da 0.004 mole/liter) 1.44 liter/da 73.19 cm³/mole

vchry/vol
³
23.1866 cm
0.00104256

chrysocolla

2.68/(175.66 /73.190) 0.007
0.00781649

porosity

1- (0.0015 + 0.005 + 0.0126 + 0.0723 + 0.03 + 0.01 + 0.485 + 0.1)
0.2836

fluid residence time [days]

$$0.29 \cdot 1.2 / (28.8 / 365)$$

$$4.41042$$

$$(10^{-1})^{.72} / (10^{-4})^{.72}$$

$$144.544$$

$$kchry = 10^{-4.35}; (*kchry = 10^{-6.2};*)$$

$$kten = 10^{-7.6560};$$

$$acu = 10^{-3};$$

$$asio2 = 10^{-3};$$

$$pH = -\text{Log}[10, \text{Sqrt}[acu \cdot asio2 / kchry]]$$

$$5.175$$

$$25 \cdot 25$$

$$625$$

$$len = 15 \cdot \text{Sqrt}[2.]$$

$$21.2132$$

$$22 / .2$$

$$110.$$

$$0.02 \cdot 22 \text{ m} / (8. \text{ d}) \cdot (365. \text{ d/y})$$

$$20.075 \text{ m}$$

$$\text{-----}$$

$$y$$

retardation of front

$$2 \cdot y / (22 \text{ m} / (20 \text{ m/y} / .28))$$

$$6.49351$$

$$1 - (0.0015 + 0.006 + 0.0126 + 0.0723 + 0.03 + 0.5876)$$

$$0.29$$

DISSOLUTION TIMES

```
pcf = 0.0015;

pcm = 0.006;

pgoe = 0.0126;

pkln = 0.0723;

pmont = 0.03;

por = 0.02;

pqtz = 1 - (pcf+pcm+pgoe+pkln+pmont+por)

por = 0.05;

pqtz = 1 - (pcf+pcm+pgoe+pkln+pmont+por)

por = 0.29;

pqtz = 1 - (pcf+pcm+pgoe+pkln+pmont+por)

vc = 73.19;

vgoe = 20.82;

vkn1 = 99.52;

vmont = 133.264;

vqtz = 22.688;

rcf = 2 10^ -11;

rcm = 10^ -12;

rgoe = 10^ -10;

rkln = 10^ -13;

rmont = 10^ -13;

rqtz = 10^ -14;

phi = {pcf,pcm,pgoe,pkln,pmont,pqtz};
```

```

v = {vc,vc,vgoe,vknl,vmont,vqtz};

rate = {rcf,rcm,rgoe,rkln,rmont,rqtz};

tau = 3 phi/(v rate)/(365 24 60 60)

rkln = 5 10-13;

rmont = 5 10-13;

rate = {rcf,rcm,rgoe,rkln,rmont,rqtz};

tau = 3 phi/(v rate)/(365 24 60 60)

rkln = 3 10-12;

rmont = 3 10-12;

rate = {rcf,rcm,rgoe,rkln,rmont,rqtz};

tau = 3 phi/(v rate)/(365 24 60 60)
0.8576
0.8276
0.5876
{0.0974819, 7.79856, 0.575711, 691.103, 214.152, 246377.}
{0.0974819, 7.79856, 0.575711, 138.221, 42.8305, 246377.}
{0.0974819, 7.79856, 0.575711, 23.0368, 7.13842, 246377.}

```

file: cec.nb

\$Version

NeXTStep486 2.2 (January 27, 1994)

Off[General::spell]

Off[General::spell1]

Appelo Constants [Parkhurst (1995)]

```
{na,k,ca,mg,h,fe,cu,al} = 10^ {0, 0.7, 0.8, 0.6, 1.0, 0.44, 0.6, 0.67}
{1, 5.01187, 6.30957, 3.98107, 10., 2.75423, 3.98107, 4.67735}
```

Montmorillonite

CEC: 80-120 meq/100 g

phis = 0.03;

cec = 1.2 meq/g;

vs = 133.264 cm³/mol;

ws = 366.117 g/mol;

omeg = phis ws / vs cec 10³ cm³/dm³ 10⁻³ eq/meq
 0.098903 eq

 3
 dm

phis = 0.03;

cec = 0.25 meq/g;

vs = 133.264 cm³/mol;

ws = 366.117 g/mol;

omeg = ws / vs phis cec 10³ cm³/dm³ 10⁻³ eq/meq
 0.0206048 eq

 3
 dm

1./ .30103

3.32193

0.6 25
15.

apatite - gypsum

'hydroxylapatite' 159.600 4 -4.0 'h+' 1.0 'h2o' 3.0 'hpo4-2' 5.0 'ca+2' -3.0746

'gypsum' 74.690 3 1.0 'ca+2' 1.0 'so4-2' 2.0 'h2o' -4.4823

5 74.69- 159.6
213.85

5 74.69/159.6
2.33991

BHP COLUMN DATA

0.5 wt% Ca in rock

0.1 wt% P

BULK CEC

por = 0.02;

cec = 0.05 meq/g;

rho = 2.65 g/cm³;

omeg = (1-por) rho cec 10⁻³ cm³/dm³ 10⁻³ eq/meq
0.12985 eq

3
dm

sorbed concentration

sorbed = {sna,sk,sca,smg} = {1.5, 1., 3.5, 1.2} meq/(100 g) 10⁻³ eq/meq;

z = {1,1,2,2};

cec = z.sorbed (1-por) rho 10⁻³ cm³/dm³

0.309043 eq

³
 dm

cbar = sorbed (1-por) rho 10⁻³ cm³/dm³

0.038955 eq 0.02597 eq 0.090895 eq 0.031164 eq
 {-----, -----, -----, -----}
³ ³ ³ ³
 dm dm dm dm

chi = cbar {1,1,2,2} / cec

{0.12605, 0.0840336, 0.588235, 0.201681}

{sna,sk,sca,smg} = chi

{0.12605, 0.0840336, 0.588235, 0.201681}

Apply[Plus,chi]

1.

solution composition

cna = 6.83 10⁻⁰³;

ck = 3.9011 10⁻⁰⁵;

cca = 1.5404 10⁻⁰³;

cmg = 9.8453 10⁻⁰⁵;

knak = sna/cna ck/sk

0.00856757

knaca = (sna/cna)² cca/sca

0.891928

knamg = (sna/cna)² cmg/smg

0.166269

{1, 1/knak, 1/knaca, 1/knamg}

{1, 116.719, 1.12117, 6.01434}

anorthite - accounts for 0.2 wt% Ca

0.002 2.65 g/cm³ 10⁻³ cm³/dm³ / (40.08 g/mol) (100.790 cm³/mol 10⁻³ dm³/cm³)
 0.013328

STUMM AND MORGAN p. 646**Dakota mont. - river water**

cec = 54.3;

montmorillonite

chi = {sna,smg,sca,sk,sh} = {0.03,0.28,0.66,0.002,0.028}
 {0.03, 0.28, 0.66, 0.002, 0.028}

illite

chi = {sna,smg,sca,sk,sh} = {0.01,0.01,0.74,0.15,0.09}
 {0.01, 0.01, 0.74, 0.15, 0.09}

Apply[Plus,chi]

1.

{cna,cmg,cca,ck,ch} = {10^{-3.6},10^{-3.8},10^{-3.4},10^{-4.2},10^{-7.}};

knamg = (sna/cna)² cmg/smg
 25.1189

knaca = (sna/cna)² cca/sca
 0.852645

knak = sna/cna ck/sk
 0.0167459

knah = sna/cna ch/sh
 0.0000442341

kcamg = (sca/cca)² (cmg/smg)²
 867.888

Dakota mont. - seawater

cec = 54.3;

montmorillonite

```
chi = {sna,smg,sca,sk,sh} = {0.5,0.22,0.26,0.02,0.}
{0.5, 0.22, 0.26, 0.02, 0.}
```

illite

```
chi = {sna,smg,sca,sk,sh} = {0.47,0.24,0.11,0.17,0.01}
{0.47, 0.24, 0.11, 0.17, 0.01}
```

```
Apply[Plus,chi]
```

```
1.
```

```
{cna,cmg,cca,ck,ch} = {0.7 10^-0.3, 0.3 10^-1.3, 0.3 10^-2., 0.7 10^-2.,10^-7.};
```

```
knamg = (sna/cna)^2 cmg/smg
0.112437
```

```
knaca = (sna/cna)^2 cca/sca
0.0489472
```

```
knak = sna/cna ck/sk
0.0551631
```

```
knah = sna/cna ch/sh
0.0000133968
```

```
kcamg = (sca/cca)^2 (cmg/smg)^2
5.27671
```

'hydroxylapatite' 159.600 4 -4.0 'h+' 1.0 'h2o' 3.0 'hpo4-2' 5.0 'ca+2' -3.0746

```
papatite= 0.4 10^-2 2.65 g/cm^3 /w mol/g 159.6 cm^3/mol
0.0119185
```

```
w = 2 p + 5 o
141.945
```

Barium chloride solution

```
ck = 6.4 10^-3 g/liter/k mol/g
0.00016369 mol
-----
liter
```



```

cna = 9.8 10-3 g/liter/na mol/g
0.000426277 mol
-----
liter

cca = 29. 10-3 g/liter/ca mol/g
0.000723553 mol
-----
liter

cmg = 6.5 10-3 g/liter/mg mol/g
0.000267435 mol
-----
liter

z={1,1,2,2}
{1, 1, 2, 2}

chi = {sk,sna,sca,smg} = z {2.8,6.5,14.2/2,4.1/2} 10-2 mol/g
0.028 mol  0.065 mol  0.142 mol  0.041 mol
{-----, -----, -----, -----}
   g           g           g           g

tot=Apply[Plus,chi]
0.276 mol
-----
g

chinew = {sk,sna,sca,smg} = {sk,sna,sca,smg}/tot
{0.101449, 0.235507, 0.514493, 0.148551}

Apply[Plus,chinew]
1.

knak = cna/sna sk/ck
1.1218

knaca = (cna/sna)2 sca/cca
0.00232961 mol
-----
liter

knamg = (cna/sna)2 smg/cmg
0.00181983 mol
-----
liter

0.03 0.98 .274 2.65
0.0213473

```

```

chrysf = 0.0015;

chrysm = 0.006;

goethite = 0.0126;

kaolinite = 0.0723;

apatite = 0.012;

(*quartz = 0.6276;*)

montmor = 0.0133;

por = 0.02;

quartz = 1-(chrysf +

chrysm +

goethite +

kaolinite +

apatite +

montmor +

por)
0.8623

```

```

15 m Sqrt[2.]/(8. da) 365 da/y
967.852 m
-----
y

```

```

15 m Sqrt[2.]
21.2132 m

```

total CEC:

```

2.65 g/cm^3 (0.03 27.4 + 0.0723 7.1) meq/g 10^-2 10^3 cm^3/dm^3 10^-3 mole/meq
0.0353862 mole
-----
3
dm

```

permeability factor

$$(0.001/0.02)^{-4}$$

$$6.25 \cdot 10^{-6}$$

Phreeqc - Appelo

$$10^{-0.08}$$

$$1.20226$$

$$10^{-.7}$$

$$0.199526$$

$$10^{-.3}$$

$$0.501187$$

$$10^{-.4}$$

$$0.398107$$

$$\text{Log}[10, .4]$$

$$-0.39794$$

$$7.6560 - 3.9993$$

$$3.6567$$

porosity

$$1 - (0.0015 + 0.006 + 0.0126 + 0.02)$$

$$0.9599$$

$$92000./60/60$$

$$25.5556$$

$$\text{Log}[10, 1.933 \cdot 10^{-3}]$$

$$-2.71377$$

```
Clear[h, m, d];
```

```
len = 22. m;
```

```
v0 = 20 m/y / 0.02;
```

```
t = len/v0 365 d/y
```

```
r = 3.14 10-2;
```

```
t / r / (365 d/y)
```

```
8.03 d  
0.700637 y
```

file: rates.nb

```
$Version
NeXTStep486 2.2 (January 27, 1994)
```

```
Off[General::spell]
```

```
Off[General::spell1]
```

```
$DefaultFont={"Times-Bold",14}
{Times-Bold, 14}
```

```
Needs["Graphics'Legend'"]
```

```
Needs["Graphics'Colors'"]
```

```
Needs["Graphics'Graphics3D'"]
```

ALBITE (Blum and Stillings)

```
ratek[pH_] := Log[10, k1 (10^-pH)^ 0.5 + k2 (10^-pH)^ -0.3 + k0]
```

```
k0 = 10^-16;
```

```
k1 = 10^-16.75 (10^-5.75)^ -0.5
1.33352 10^-14
```

```
Log[10,k1]
-13.875
```

```
k11 = Log[10,k1 (10^-1)^ 0.5]
-14.375
```

```
k2 = 10^-16.75 (10^-5.75)^ 0.3
3.34965 10^-19
```

```
Log[10,k2]
-18.475
```

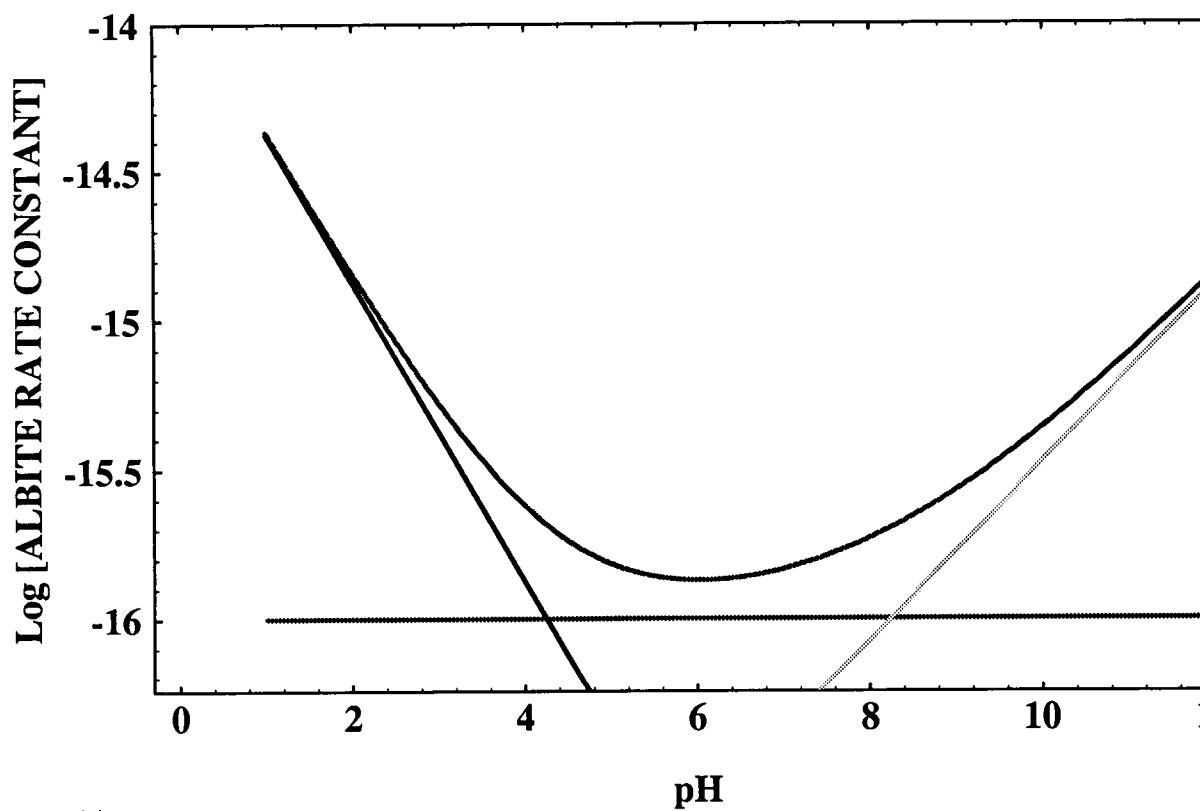
```
ratek[1]//N
-14.3648
```

```
Log[10, 2 10^-16.75]
-16.449
```

```

Plot[{ratek[pH],Log[10,k0],Log[10,k1 (10^-pH)^0.5],
Log[10, k2 (10^-pH)^-0.3]},{pH,1,12},
PlotRange->{-14,-16.25},Frame->True, PlotStyle->{Red,Brown,Blue,Green},
FrameLabel->{pH,"Log [ALBITE RATE CONSTANT]"},
AxesOrigin->{0,0}]

```



-Graphics-

AMORPHOUS SILICA [Rimstidt and Barnes (1980)]

$\log k = -15.6$; $k_0 = 10^{-\log k}$

2.51189×10^{-16}

$\text{surfarea} = 5 \times 10^{-12}/k_0$

19905.4

$6.8299015554135 \times 10^{-6}$ 365 24 60 60

215.388

LOCAL EQUILIBRIUM DISSOLUTION OF CHRYSOCOLLA**file: leq.nb**

```

$Version
NeXTStep486 2.2 (January 27, 1994)

Off[General::spell]

Off[General::spell1]

'chrysocolla' 73.190

4 -2.0 'h+' 1.0 'cu+2' 1.0 'sio2(aq)' 3.0 'h2o'

3.9279, 6.2142

'antlerite' 90.960

4 -4.0 'h+' 1.0 'so4-2' 3.0 'cu+2' 4.0 'h2o'

8.7302

'sio2(am)' 29.0 1 1.0 'sio2(aq)' -2.7136

vchry = 73.190 10-3;

vsio2 = 29. 10-3;

pchry0 = 0.0015;

por0 = 0.02;

psio2 = vsio2/vchry pchry0
0.000594343

gh = 1.0; gcu = 1.0;

gh = 0.8480; gcu = 0.4524;

kchry = 10-3.9279; ksio2 = 10-2.7136;

ch0 = 10-1.5;

cu0 = 10-8; csio20 = 0.; cso40 = ch0/2;

```

```

Clear[ch];

eqn = kchry/ksio2 (gh ch)^ 2 + ch/2 - (cu0+ch0/2) == 0;

ch = ch /. FindRoot[eqn, {ch,ch0/100}];

pH = -Log[10,ch]

ch
4.22168
0.0000600237

cu = cu0 - (ch-ch0)/2
0.0157814

dcu = cu-cu0
0.0157814

dh = ch-ch0
-0.0315628

v2 = por0 (cu-cu0)/(por0 (cu-cu0) + pchry0/vchry)
0.0151669

v2 = por0 (cu-cu0)/(pchry0/vchry)
0.0154005

v2 = por0 (ch-ch0)/(por0 (ch-ch0) - 2 pchry0/vchry)
0.0151669

r=1/v2

v0 = 20/por0 m/y;

t1 = 22 m/v0 r

t1 365 d/y
65.9329
1.45052 y
529.441 d

ret = 1+pchry0/vchry/(por0 (cu-cu0))
65.9329

ret por0
1.31866

```


retardation using asymptot $1./0.0266$

37.594

 $1./0.0314$

31.8471

 $1 - (0.0015 + 0.006 + 0.0126 + 0.0723 + 0.03 + 0.29)$

0.5876

 $1 - (0.0015 + 0.006 + 0.0126 + 0.0723 + 0.03 + 0.012 + 0.02)$

0.8456

 $0.0015/.0075$

0.2

I have reviewed this scientific notebook and find it in compliance with QAP-001. There is sufficient information regarding procedures used for conducting tests, acquiring and analyzing data so that another qualified individual could repeat the activity.

N. Sridhar 4/17/97

Narasi Sridhar
Manager, Engineered Barrier System and Waste Solidification System

SOE Electronic Scientific Notebook No.
Ne: 095E:Development of the Code MULTIFLO to
Tec Describe Multiphase Reactive Transport
(12/18/1995 through 04/17/1997)

SCIENTIFIC NOTEBOOK

by

Peter C. Lichtner

No. 095

Printed: July 7, 1997

P. C. Lichtner

SCIENTIFIC NOTEBOOK

INITIALS:

PC

SCIENTIFIC NOTEBOOK

by

Peter C. Lichtner

No. 095

Southwest Research Institute
Center for Nuclear Waste Regulatory Analyses
San Antonio, Texas

July 7, 1997

INITIAL ENTRIES

Scientific NoteBook: # 095

Issued to: P. C. Lichtner

Issue Date: Tuesday, November 16, 1993

Computerized Initials: PC

By agreement with the CNWRA QA this NoteBook is to be printed at approximate quarterly intervals. This computerized Scientific NoteBook is intended to address the criteria of CNWRA QAP-001.

Table 1: Computing Equipment

Machine Name	Type	OS	Location
gravenstein.cnwra.swri.edu	Pentium Workstation	NEXTSTEP	desk Rm A-126
	133 Mhz	Version 3.3	Bldg. 189
	64 MB RAM		
skippy.cnwra.swri.edu	Sun SPARC 20	SUNOS 4.1.2	network
	96 MB RAM		

Contents

INITIAL ENTRIES	ii
FIGURES	iv
TABLES	v
NEAR-FIELD ENVIRONMENT	1
BHP COPPER PROJECT	1

Printed: July 7, 1997

P. C. Lichtner

SCIENTIFIC NOTEBOOK

INITIALS: PCL

List of Figures

.

List of Tables

1	Computing Equipment	ii
2	Definition of variables nprim and ncpri.	42

KTI: NEAR-FIELD ENVIRONMENTAccount Number: **20-5708-561**

Description: Near-field Environment Technical Assistance

Collaborators: Dr. R. Pabalan

Collaborators: Dr. C. I. Steefel (Consultant)

Collaborators: Dr. M. Seth (Consultant)

Objective: Application of the computer code MULTIFLO, and submodules GEM and METRA to the Yucca Mountain HLW Repository.

5.5.97 *xz*-Repository Scale Calculation. An *xz*-repository scale calculation was performed using a random heterogeneous porous medium to investigate the stability of the evaporation front. It is thought that an unstable front could explain the phenomena of wetting of heaters observed in various heater tests even when the temperature is above boiling. The calculation appears to be very time consuming and only results for 10 years have been obtained. The heterogeneous medium results in very small time steps on the order of 10^{-2} years. Just to run the simulation to 100 years will require 10,000 steps! 1,000 steps takes about a day. The grid used in the calculation is 30×121 . This may have to be made smaller to get results in a reasonable time period.

5.9.97 Adding Hydration-Dehydration Reactions to MULTIFLO. There appear to be two possible approaches to incorporate hydration-dehydration reactions into MULTIFLO, depending on how the METRA flow equations are interpreted. The general coupled system of flow and transport equations have the form:

$$\frac{\partial}{\partial t} (\phi \Psi_j) + \nabla \cdot \Omega_j = - \sum_m \nu_{jm} I_m. \quad (1)$$

The subscript j refers to dissolved constituents such as Na^+ , Cl^- etc., and H_2O . In this equation ϕ denotes the porosity, Ψ_j denotes the total concentration defined by

$$\Psi_j = c_j + \sum_i \nu_{ji} c_i, \quad (2)$$

for primary species concentrations c_j and secondary species c_i , and the total flux Ω_j is given by

$$\Omega_j = J_j + \sum_i \nu_{ji} J_i, \quad (3)$$

for individual solute fluxes J_l . The reaction rate of the m th mineral I_m is defined to be positive for precipitation and negative for dissolution. The stoichiometric coefficients are denoted by ν_{jm} . Conservation of mass and charge for the m th mineral reaction implies

$$\sum_j W_j \nu_{jm} = W_m, \quad (4)$$

and

$$\sum_j z_j \nu_{jm} = 0, \quad (5)$$

where W_l denotes the formula weight of the l th species. Multiplying the transport equations by W_j and summing over all primary species yields the total mass conservation equation

$$\frac{\partial}{\partial t} \left(\phi \sum_j W_j \Psi_j \right) + \nabla \cdot \left(\sum_j W_j \Omega_j \right) = - \sum_m W_m I_m. \quad (6)$$

The fluid density ρ_l is defined by

$$\rho_l = \sum_j W_j \Psi_j = \sum_j W_j c_j + \sum_i W_i c_i, \quad (7)$$

and the flux is given by

$$\sum_j W_j \Omega_j = v \rho_l. \quad (8)$$

It is assumed that the diffusion terms cancel out in the summed total mass conservation equation. In terms of the fluid density the total mass transport equation becomes

$$\frac{\partial}{\partial t} (\phi \rho_l) + v \rho_l = - \sum_m W_m I_m. \quad (9)$$

Using a mole number basis rather than mass, summing the primary species transport equations gives the total mole conservation equation

$$\frac{\partial}{\partial t} \left(\phi \sum_j \Psi_j \right) + \nabla \cdot \left(\sum_j \Omega_j \right) = - \sum_{jm} \nu_{jm} I_m. \quad (10)$$

The mole number liquid density is given by

$$n_l = \sum_j \Psi_j, \quad (11)$$

and the flux is given by

$$\sum_j \Omega_j = v n_l. \quad (12)$$

In terms of the fluid density the total mole transport equation becomes

$$\frac{\partial}{\partial t} (\phi n_l) + \nabla \cdot v n_l = - \sum_{jm} \nu_{jm} I_m. \quad (13)$$

Alternate Form. Alternatively, the mass transport equation for H₂O has the form

$$\frac{\partial}{\partial t} (\phi \Psi_w) + \nabla \cdot \Omega_w = - \sum_m \nu_{wm} I_m. \quad (14)$$

In this equation, a reaction contributes to the H₂O mass balance only if $\nu_{wm} \neq 0$.

One clear advantage of the first form [Eqn.(9) or (13)] compared to the second [Eqn.(14)], is that the diffusion terms cancel out. However, because the rates summed over all primary species appears on the right hand side rather than just the contribution from H₂O, it is necessary to properly calculate the correction to the density due to the dissolved constituents in solution whenever this term is sufficiently large (when compared to the density of pure water).

5.12.97 Parallel Dependent Kinetic Reactions. In some cases it may be necessary to consider linearly dependent reactions to account for different kinetic reaction mechanisms. Consider the set of linearly independent reactions which are heterogeneous

$$\sum_j \nu_{jm} \mathcal{A}_j \rightleftharpoons \mathcal{M}_m, \quad (15)$$

and homogeneous

$$\sum_j \nu_{ji} \mathcal{A}_j \rightleftharpoons \mathcal{A}_i. \quad (16)$$

Then a set of linear dependent reactions to these reactions may be written as

$$\sum_j \nu_{jm}^r \mathcal{A}_j + \sum_i \nu_{im}^r \mathcal{A}_i \rightleftharpoons \mathcal{M}_m. \quad (17)$$

There must exist coefficients c_{im}^r not all zero such that

$$\sum_j \nu_{jm} \mathcal{A}_j + \sum_i c_{im}^r \left(\mathcal{A}_i - \sum_j \nu_{ji} \mathcal{A}_j \right) \rightleftharpoons \mathcal{M}_m, \quad (18)$$

which can be regrouped as

$$\sum_j \left(\nu_{jm} - \sum_i c_{im}^\tau \nu_{ji} \right) \mathcal{A}_j + \sum_i c_{im}^\tau \mathcal{A}_i \rightleftharpoons \mathcal{M}_m. \quad (19)$$

Comparing coefficients implies the identities

$$\nu_{jm}^\tau = \nu_{jm} - \sum_i c_{im}^\tau \nu_{ji}, \quad (20)$$

and

$$\nu_{im}^\tau = c_{im}^\tau. \quad (21)$$

The mass transport equations including the contribution from the linear dependent reactions have the form

$$\frac{\partial}{\partial t} \phi C_j + \nabla \cdot J_j = - \sum_m \nu_{jm} I_m - \sum_i \nu_{ji} I_i - \sum_{m\tau} \nu_{jm}^\tau I_m^\tau, \quad (22)$$

for primary species, and

$$\frac{\partial}{\partial t} \phi C_i + \nabla \cdot J_i = I_i - \sum_{m\tau} \nu_{im}^\tau I_m^\tau, \quad (23)$$

for secondary species, and

$$\frac{\partial}{\partial t} \phi_m = \bar{V}_m \left(I_m + \sum_\tau I_m^\tau \right), \quad (24)$$

for minerals. Eliminating the reaction rates I_i for secondary species from the primary species transport equations leads to

$$\frac{\partial}{\partial t} \phi \Psi_j + \nabla \cdot \Omega_j = - \sum_m \nu_{jm} \left(I_m + \sum_\tau I_m^\tau \right), \quad (25)$$

which only involves the sum of the linear independent and dependent reaction rates.

The reaction rates for the linear dependent reactions have the form

$$I_m^\tau = -k_m^\tau s_m [1 - K_m^\tau Q_m^\tau], \quad (26)$$

where

$$Q_m^\tau = \prod_j (\gamma_j C_j)^{\nu_{jm}^\tau} \prod_i (\gamma_i C_i)^{\nu_{im}^\tau} = K_i^{\nu_{im}^\tau} \prod_j (\gamma_j C_j)^{\nu_{jm}^\tau + \sum_i \nu_{ji} \nu_{im}^\tau}. \quad (27)$$

The equilibrium constants for the linearly dependent reactions are related to the independent equilibrium constants by

$$K_m^\tau = K_m \prod_i K_i^{-c_{im}^\tau}. \quad (28)$$

It follows that

$$K_m^\tau Q_m^\tau = K_m Q_m. \quad (29)$$

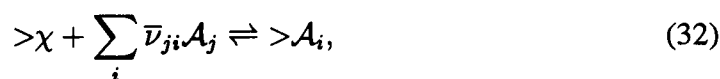
$$R_j = - \sum_m \nu_{jm} \left(I_m + \sum_\tau I_m^\tau \right), \quad (30)$$

$$= - \sum_m \nu_{jm} \left(k_m + \sum_\tau k_m^\tau \right) s_m [1 - K_m Q_m]. \quad (31)$$

The quantities k_m , k_m^τ , are effective rate “constants” which may depend on pH, f_{O_2} , and other solution variables.

5.22.97 Sorption Described by Surface Complexation. The cement–tuff interaction task in the near-field KTI requires computing the interaction of radionuclides with cement pore water as it interacts with the tuff host rock at Yucca Mountain. Important points to consider are the speciation of the radionuclides in the high pH fluid and sorption onto CSH phases formed by reaction of the hyperalkaline plume with the tuff host rock.

First a simple surface complexation model is considered without taking into account double layer effects. The sorption reactions have the form



where the symbol ‘>’ designates sorbed species. The species $>\chi$ refers to a neutral unoccupied site. The total site density is equal to

$$\bar{C}_s = \bar{C}_\chi + \sum_i \bar{C}_i. \quad (33)$$

Mass action equations corresponding to Eqn.(32) are given by

$$\bar{C}_i = \bar{K}_i \bar{C}_\chi \prod_j (\gamma_j C_j)^{\bar{\nu}_{ji}}. \quad (34)$$

The free site density concentration is given by

$$\bar{C}_x = \frac{\bar{C}_s}{1 + \sum_i \bar{K}_i \prod_j (\gamma_j C_j)^{\bar{\nu}_{ji}}}. \quad (35)$$

The primary species mass transport equations have the form:

$$\frac{\partial}{\partial t} \phi C_j + \nabla \cdot J_j = - \sum_i \bar{\nu}_{ji} \bar{I}_i - \sum_m \nu_{jm} I_m, \quad (36)$$

sorbed complexes:

$$\frac{\partial \bar{C}_i}{\partial t} = \bar{I}_i, \quad (37)$$

and free sites:

$$\frac{\partial \bar{C}_x}{\partial t} = - \sum_i \bar{I}_i. \quad (38)$$

Eliminating \bar{I}_i yields

$$\frac{\partial}{\partial t} \left[\phi C_j + \sum_i \bar{\nu}_{ji} \bar{C}_i \right] + \nabla \cdot J_j = - \sum_m \nu_{jm} I_m. \quad (39)$$

Combining Eqns.(38) and (37) leads to the conservation of sites equation

$$\frac{\partial \bar{C}_s}{\partial t} = 0. \quad (40)$$

However, in this model charge is not conserved within the aqueous solution. Consider

$$\frac{\partial \bar{Q}}{\partial t} = \frac{\partial}{\partial t} \sum_i \bar{z}_i \bar{C}_i = \sum_i \bar{z}_i \bar{I}_i. \quad (41)$$

The right hand side does not, in general, vanish. The charge conservation equation has the form

$$\frac{\partial}{\partial t} (\phi Q + \bar{Q}) + \nabla \cdot Q = 0, \quad (42)$$

in which \bar{Q} acts as a source/sink of charge.

Jacobian. The jacobian matrix requires the derivatives:

$$\frac{\partial \bar{C}_i}{\partial C_l}, \quad \frac{\partial \bar{C}_x}{\partial C_l}. \quad (43)$$

It follows that:

$$\frac{\partial \bar{C}_i}{\partial C_l} = \left(\frac{1}{\bar{C}_x} \frac{\partial \bar{C}_x}{\partial C_l} + \frac{\bar{\nu}_{li}}{C_l} \right) \bar{C}_i, \quad (44)$$

and

$$\frac{\partial \bar{C}_x}{\partial C_l} = \frac{1}{C_l} \left[\frac{1}{1 + \sum_i \bar{K}_i \prod_j (\gamma_j C_j)^{\bar{\nu}_{ji}}} \right] \sum_i \bar{\nu}_{li} \bar{C}_i. \quad (45)$$

6.2.97 Equilibration of UZ-TP-3 Pore Water. UZ-TP-3 pore water was equilibrated using the code GEM. It was found that charge of the solution was positive indicating that a higher anion concentration was needed to balance the charge, and that the mineral sepiolite was highly (6 orders of magnitude) supersaturated. The calculation suggests that magnesium was not measured correctly. The results of the speciation calculation are given below.

```

=====
initial conditions: region 2: 51 100 1 1 1 1
=====
iter = 2      ionic strength = 1.4134E-02
pH = 8.200
species      molality      psi      act. coef.  act. ratio/H+  constraint
ca+2         2.6876E-03    3.0000E-03  0.6362      13.74         1 total
mg+2         7.4850E-04    8.8200E-04  0.6536      13.19         1 total
na+          2.7546E-03    2.7800E-03  0.8872      5.596         1 total
k+           4.0734E-04    4.1000E-04  0.8834      4.766         1 total
h+           6.9887E-09    2.8851E-03  0.9028      0.            8 pH
co3-2        2.9774E-05    3.0256E-03  0.6220     -20.84        4 co2(g)
cl-          2.7371E-03    2.7400E-03  0.8834     -10.72        1 total
so4-2        1.3852E-03    1.7000E-03  0.6170     -19.17        1 total
al+3         4.8966E-22    1.8499E-12  0.3943      3.157         3 ortho55-45
sio2(aq)     3.2126E-03    3.2800E-03  1.000      -2.493        1 total

complex      molality      act. coef.  act/H+
oh-          1.81052E-06  0.88531     -13.898
hso4-        5.79268E-10  0.88716     -17.393
h2so4(aq)    3.24251E-21  1.0000      -20.489
hcl(aq)      3.26172E-12  1.0000      -11.487
hco3-        2.80801E-03  0.88716     -10.707
co2(aq)      3.47616E-05  1.0000      -4.4589
nacl(aq)     9.87436E-07  1.0000      -6.0055

```

kcl(aq)	2.78594E-08	1.0000	-7.5550
koh(aq)	1.97754E-10	1.0000	-9.7039
kso4-	2.62726E-06	0.88716	-13.736
aloh+2	5.43030E-19	0.62196	-1.9540
al(oh)2+	1.39055E-16	0.88716	-7.7012
al(oh)3(aq)	5.34549E-14	1.0000	-13.272
al(oh)4-	1.79633E-12	0.88716	-19.901
al(so4)2-	1.26255E-23	0.88716	-31.054
also4+	1.90312E-22	0.88716	-13.565
caoh+	4.31464E-08	0.88716	0.79055
cahco3+	5.34620E-05	0.88716	3.8836
caco3(aq)	6.72429E-05	1.0000	-4.1724
caso4(aq)	1.88724E-04	1.0000	-3.7242
cacl+	9.39273E-07	0.88716	2.1284
cacl2(aq)	2.27112E-09	1.0000	-8.6438
cah2sio4(aq)	3.78623E-08	1.0000	-7.4218
cah3sio4+	1.58564E-06	0.88716	2.3558
ca(h3sio4)2(3.92164E-07	1.0000	-6.4065
mgco3(aq)	8.63005E-06	1.0000	-5.0640
mgghco3+	1.49146E-05	0.88716	3.3292
mgso4(aq)	1.07893E-04	1.0000	-3.9670
mgcl+	9.77369E-07	0.88716	2.1457
mggh2sio4(aq)	1.30249E-07	1.0000	-6.8852
mggh3sio4+	8.06811E-07	0.88716	2.0624
mgoh+	1.43355E-07	0.88716	1.3120
nahco3(aq)	8.68084E-06	1.0000	-5.0614
naco3-	1.66748E-07	0.88716	-14.934
naoh(aq)	6.21244E-10	1.0000	-9.2067
naso4-	1.55540E-05	0.88716	-12.964
h2sio4-2	1.43414E-09	0.61698	-25.155
h3sio4-	6.40263E-05	0.88716	-12.349

mineral saturation indices			
mineral	log S.I.	mineral	log S.I.
calcite	0.9806	katoite	-32.27
dolomite	2.602	foshagite	-18.87
chalcedony	1.235	tobermorite-14a	-10.64
ortho55-45	-1.7157E-10	portlandite	-8.922
montmor-na	-1.474	friedel-salt	-31.46
quartz	1.506	tobermorite(AU)	-11.14
crystalite(alpha	0.9557	CSH(0.8)	-2.667
tridymite	1.335	CSH(1.1)	-4.217
sio2(am)	0.2205	CSH(1.8)	-10.55
kaolinite	-6.025	hydrogarnet(AU)	-31.99
albite	-1.770	Ca3Al2Si0.5O7-5H2O	-28.70
gibbsite	-4.870	Si-hydrogarnet	-25.19
k-feldspar	0.4377	gehlenite-hydrate	-19.13
muscovite	-7.652	Ca2Al2O5-8H2O	-26.47
gypsum	-1.353	monocarboaluminate	-30.69
natrolite	-9.052	hemicarboaluminate	-36.59
laumontite	-4.235	tricarboaluminate	-27.43
analcime	-3.091	monochloroaluminat	-33.37
sepiolite	6.955	hemichloroaluminat	-38.33

brucite	-3.208	trichloroaluminate	-34.17
ettringite(AU)	-26.06	3CaO.CaCl ₂ ·15H ₂ O	-35.80
ettringite	-33.37	oxychlorat	-35.85
hillebrandite	-12.05	monosulfate	-30.53
hydrotalcite	-17.31		

gas	log partial pressure	pressure
co ₂ (g)	-2.990	1.0233E-03

charge balance - q = 1.6478E-03

solution density = 1.0011 g/cm³

6.6.97 Cement Alteration. A problem was discovered in attempting to model cement alteration. Calcification of the cement resulted in the porosity going to zero. This lead to a reduction in the time step because the reaction rates are calculated on a REV basis. To circumvent this problem the mineral surface area was multiplied by the ratio of the current porosity to the initial porosity raised to the two-thirds power (to account for the surface to volume ratio):

$$S = S_0 \left[\frac{\phi}{\phi_0} \right]^{2/3} . \quad (46)$$

With this factor the surface goes to zero with the porosity and the time step remains sufficiently large.

6.9.97 Cement-Tuff, Tuff-Cement, and Cement-Tuff Contact Input Files. The three input files used in the cement task are listed for cement-tuff, tuff-cement, and cement-tuff contact. The initial fluid composition of the pore water in equilibrium with the tuff is generated by assuming a pH of 8.2 and equilibrating the fluid with the minerals orthoclase with the composition of 55% potassium and 45% sodium, calcite, dolomite, muscovite, and K-feldspar. Chloride was set by charge balance. Total sulfate was fixed at 0.177 mmol/L corresponding to J-13 well water and the logarithm of the CO₂ partial pressure was assumed to be -2.99. The cement pore fluid was generated by equilibration with minerals portlandite, calcite, brucite, friedel-salt, ettringite, CSH(1.8), and tricarboaluminate. Alkalies K⁺ and Na⁺ were fixed at total concentrations of 4.1 and 27.8 mmol/L, respectively, which is an order of magnitude larger than UZ-TP-3 pore water. The alkali concentration strongly affects the pH, determined by charge balance.

Infiltration of cement pore fluid into tuff.

June 9, 1997

```

:
:      geometry nx ny nz mode iprint idebug
GRID   XYZ      100  1  1  2      1    0
:
:
OPTS
:   idata istart imod iexact iscale ihrmc
:     0      0      10    0      0      1
:
:   itmax ihalmax ivmax ndamp
:    32     60      0      0
:
:   method iops ifor   isurf iact loglin icon  cournr
:     1      0      1      1      1      0      1      5.
:
:   isync ipor iperm perm-fac. por-fac.
COUPLE 0      1      0      3.      0.
:
:
PLTFiles
:iplot a s t m si sf v z b in e ex ti g itex
:     1  1  1  1  1  0  0  1  0  2  0  0  0  0  0  0
:
:   tol  ttol  tolneg tolpos  tolexp dthalf qkmax  tolstdst tolc
TOLR 1.d-8  1.e-1  1.e0  1.e-2  4.d0    .5      590.  1.e-6  1.e-12
:
:   mcyc cc c flx r sp qk pk rk a1 a2 a3
DEBUg  0      1  1  0  1  1  1  1  1  1
:
:   isat isothrm iread por0 phir sat w lambda toldelt  tolpor
ISYSstem -1    0      0      0.1  1.  1.0  0.5  1.0  1.e-3  1.e-10
:
:   vx0 vy0 vz0 vgx vgy vgz[m/yr]  alphax  alphay  alphaz[m]
FLOW  0.    0.    0.    0.    0.    0.      0.      0.      0.
:
:   d0[cm^2/s] delhaq[kJ/mol] dgas[cm^2/s] dgexp tortaq tortg idif
DIFF  1.d-5    12.6          2.13d-1      1.8  0.5d0  1.d0    0
:
:flag 1: T(x)  = d x^3 + a x^2 + b x + c (meters)
:   2: T(x)  = a + (b-a) exp[-((x-x0)/c)^2] + (d - a) * x / xlen
:   3:T(x,t)=a+1/2(b-a) (erf[(x+c-x0)/2sqr(dt)]-erf[(x-c-x0)/2sqr(dt)])
:   p(bars) temp flag a b c d x0 xlen
PTINit 1.e5  25.  0  25  300  250  125  1000.  2.d3
:
:master species for controlling time stepping
MASTER ALL
:
:grid m 0. 1 200 200.
:
:
DXYZ
1.e-4 1.09604e-4 1.20129e-4 1.31666e-4 1.44311e-4 1.5817e-4 1.7336e-4
1.90009e-4 2.08256e-4 2.28256e-4 2.50177e-4 2.74203e-4 3.00537e-4
3.29399e-4 3.61033e-4 3.95705e-4 4.33707e-4 4.75359e-4 5.2101e-4
5.71046e-4 6.25887e-4 6.85994e-4 7.51875e-4 8.24081e-4 9.03223e-4

```

```

9.89965e-4 1.08504e-3 1.18924e-3 1.30345e-3 1.42863e-3 1.56583e-3
1.7162e-3 1.88102e-3 2.06166e-3 2.25966e-3 2.47667e-3 2.71452e-3
2.97521e-3 3.26093e-3 3.5741e-3 3.91734e-3 4.29355e-3 4.70588e-3
5.15782e-3 5.65315e-3 6.19606e-3 6.7911e-3 7.44329e-3 8.15812e-3
8.94159e-3 9.8003e-3 1.07415e-2 1.17731e-2 1.29037e-2 1.41429e-2
1.55011e-2 1.69898e-2 1.86214e-2 2.04098e-2 2.23698e-2 2.45181e-2
2.68728e-2 2.94535e-2 3.22821e-2 3.53823e-2 3.87803e-2 4.25046e-2
4.65866e-2 5.10606e-2 5.59642e-2 6.13388e-2 6.72295e-2 7.3686e-2
8.07625e-2 8.85186e-2 9.70195e-2 1.06337e-1 1.16549e-1 1.27742e-1
1.4001e-1 1.53456e-1 1.68193e-1 1.84346e-1 2.02049e-1 2.21453e-1
2.42721e-1 2.66031e-1 2.91579e-1 3.19581e-1 3.50273e-1 3.83911e-1
4.20781e-1 4.61191e-1 5.05482e-1 5.54026e-1 6.07232e-1 6.65549e-1
7.29465e-1 7.9952e-1 8.76303e-1

```

```
1*1.
```

```
1.
```

```

:
:  isolv level north nitmax idetail rmaxtol rtwotol smaxtol
SOLV  1  1  1  100  0  1.e-20 1.e-20 1.e-12
:
:initial and boundary conditions: 1-conc., 2-flux, 3-zero gradient
:  inlet  outlet  nzoneaq
COMP  -1  3  3
:
:i1 i2 j1 j2 k1 k2
  1 100 1 1 1 1
:
:species  ctot      units  itype  mineral
ca+2      1.82e-03  mol    3      calcite
mg+2      1.00e-04  mol    3      dolomite
na+       1.76e-02  mol    3      ortho55-45
k+        5.11e-05  mol    3      k-feldspar
h+        8.2       mol    8      none
co3-2     -2.99     mol    4      co2(g)
cl-       2.74e-03  mol   -1      none
so4-2     1.77e-04  mol    1      none
al+3      1.00e-12  mol    3      muscovite
sio2(aq)  3.28e-03  mol    3      chalcedony

```

```
:blank
```

```
0
```

```
:
```

```
BCON
```

```
:bndk
```

```
1
```

```

:ibndtyp i1 i2 j1 j2 k1 k2 tmpbc
  1 1 1 1 1 1 1 25.

```

```

:species  ctot      units  itype  mineral
ca+2      1.000e+00  mol    3      portlandite
mg+2      1.000e-04  mol    3      brucite
na+       2.78e-02  mol    1      none
k+        4.1e-03   mol    1      none
h+       1.245e+01  mol   -1      none
co3-2     5.000e-07  mol    3      calcite
cl-       1.025e-03  mol    3      friedel-salt

```

P. C. Lichtner

SCIENTIFIC NOTEBOOK

INITIALS: PCZ

```

so4-2      1.000e-02    mol    3      ettringite(AU)
al+3       1.000e-12    mol    3      tricarboaluminate
sio2(aq)    1.000e-08    mol    3      hillebrandite
:
0
:
:bndk
  2
:
:ibndtyp i1 i2 j1 j2 k1 k2 tmpbc
      3 100 100 1 1 1 1 25.
:species  ctot      units  itype    mineral
ca+2      1.82e-03    mol    3      calcite
mg+2      1.00e-04    mol    3      dolomite
na+       1.76e-02    mol    3      ortho55-45
k+        5.11e-05    mol    3      k-feldspar
h+        8.2         mol    8      none
co3-2     -2.99       mol    4      co2(g)
cl-       2.74e-03    mol    -1     none
so4-2     1.77e-04    mol    1      none
al+3      1.00e-12    mol    3      muscovite
sio2(aq)   3.28e-03    mol    3      chalcedony
:
0
:
0 0
:
STOL  1. 1. 1. 1. 1. 1. 1. 1. 1. 1.
:
AQCX
:h+
oh-      5.5e-5
hso4-
h2so4(aq)
hcl(aq)
hco3-
:co3-2
co2(aq)
nacl(aq)
kcl(aq)
koh(aq)
kso4-
:al+3
aloh+2    1.0e-5
al(oh)2+  1.0e-5
al(oh)3(aq) 1.0e-5
al(oh)4-  1.0e-5
al(so4)2-
also4+
caoh+
cahco3+
caco3(aq)
caso4(aq)

```

cacl+
cacl2(aq)
cah2sio4(aq)
cah3sio4+
ca(h3sio4)2(aq)
mgco3(aq)
mghco3+
mgso4(aq)
mgcl+
mgh2sio4(aq)
mgh3sio4+
mgoh+
nahco3(aq)
naco3-
naoh(aq)
naso4-
h2sio4-2
h3sio4-
:blank
:
MNRL
calcite
dolomite
chalcedony
ortho55-45
montmor-na
quartz
cristobalite(alpha)
tridymite
sio2(am)
kaolinite
albite
gibbsite
k-feldspar
muscovite
gypsum
natrolite
laumontite
analcime
sepiolite
brucite
ettringite(AU)
ettringite
hillebrandite
katoite
foshagite
tobermorite-14a
portlandite
friedel-salt
tobermorite(AU)
CSH(0.8)
CSH(1.1)
CSH(1.8)

```

hydrogarnet (AU)
Ca3Al2Si0.5O7-5H2O
Si-hydrogarnet
gehlenite-hydrate
Ca2Al2O5-8H2O
monocarboaluminate
hemicarboaluminate
tricarboaluminate
monochloroaluminate
hemichloroaluminate
trichloroaluminate
3CaO.CaCl2-15H2O
oxychlorat
monosulfate
hydrotalcite
      :blank
:
GASEs
co2(g)
      :blank
:
MNIR
:mineral itypkin npar fkin delh beta rka betb rkb rk0 tau
:i1 i2 j1 j2 k1 k2 vol area
quartz      3  0  1.0  75.  1.0  0.  -0.3 -17.5 -17.39 1.e-3
1 100 1  1  1  1  0.15  1.e2
0
cristobalite(alpha) 3  0  1.0  75.  1.0  0.  -0.3 -17.5 -16.34 1.e-3
1 100 1  1  1  1  0.10  1.e2
0
tridymite    3  0  1.0  75.  1.0  0.  -0.3 -17.5 -17.39 1.e-3
1 100 1  1  1  1  0.05  1.e2
0
ortho55-45    3  0  1.0  35.  0.5 -13.875 -0.3 -18.475 -16.50 1.e-3
1 100 1  1  1  1  0.60  1.e2
0
muscovite     0  0  1.0  35.  1.0  0.   1.0  0. -16.50 1.e-3
1 100 1  1  1  1  0.0   1.e0
0
calcite        0  0  1.0  0.   1.  0.   1.  0. -11.  1.e-2
1 100 1  1  1  1   0.0  1.
0
dolomite       0  0  1.0  0.   1.  0.   1.  0. -13.  1.e-2
1 100 1  1  1  1   0.0  1.
0
kaolinite      0  0  1.0  0.   1.  0.   1.  0. -16.  1.e-2
1 100 1  1  1  1   0.0  1.
0
albite         0  0  1.0  0.   1.  0.   1.  0. -15.  1.e-2
1 100 1  1  1  1   0.0  1.
0
chalcedony     0  0  1.0  0.   1.  0.   1.  0. -15.  1.e-2
1 100 1  1  1  1   0.   1.

```

```

0
k-feldspar      0  0  1.0  0.  1.  0.      1.  0. -15.  1.e-2
1 100 1  1  1  1      0.  1.
0
gibbsite        0  0  1.0  0.  1.  0.      1.  0. -14.  1.e-2
1 100 1  1  1  1      0.  1.
0
natrolite       0  0  1.0  0.  1.  0.      1.  0. -14.  1.e-2
1 100 1  1  1  1      0.  1.
0
laumontite      0  0  1.0  0.  1.  0.      1.  0. -14.  1.e-2
1 100 1  1  1  1      0.  1.
0
analcime        0  0  1.0  0.  1.  0.      1.  0. -14.  1.e-2
1 100 1  1  1  1      0.  1.
0
sepiolite       0  0  1.0  0.  1.  0.      1.  0. -14.  1.e-2
1 100 1  1  1  1      0.  1.
0
brucite         0  0  1.0  0.  1.  0.      1.  0. -12.  1.e-2
1 100 1  1  1  1      0.  1.
0
ettringite(AU)  0  0  1.0  0.  1.  0.      1.  0. -12.  1.e-2
1 100 1  1  1  1      0.  1.
0
hydrogarnet(AU) 0  0  1.0  0.  1.  0.      1.  0. -12.  1.e-2
1 100 1  1  1  1      0.  1.
0
CSH(0.8)        0  0  1.0  0.  1.  0.      1.  0. -11.  1.e-2
1 100 1  1  1  1      0.  1.
0
CSH(1.1)        0  0  1.0  0.  1.  0.      1.  0. -11.  1.e-2
1 100 1  1  1  1      0.  1.
0
CSH(1.8)        0  0  1.0  0.  1.  0.      1.  0. -11.  1.e-2
1 100 1  1  1  1      0.  1.
0
tobermorite(AU) 0  0  1.0  0.  1.  0.      1.  0. -11.  1.e-2
1 100 1  1  1  1      0.  1.
0
portlandite     0  0  1.0  0.  1.  0.      1.  0. -12.  1.e-2
1 100 1  1  1  1      0.  1.
0
gypsum          0  0  1.0  0.  1.  0.      1.  0. -11.  1.e-2
1 100 1  1  1  1      0.  1.
0
Ca3Al2Si0.5O7-5H2O 0  0  1.0  0.  1.  0.  1.  0. -11.  1.e-2
1 100 1  1  1  1      0.  1.
0
Si-hydrogarnet  0  0  1.0  0.  1.  0.      1.  0. -11.  1.e-2
1 100 1  1  1  1      0.  1.
0
gehlenite-hydrate 0  0  1.0  0.  1.  0.  1.  0. -11.  1.e-2

```

```

1 100 1 1 1 1 0. 1.
0
Ca2Al2O5-8H2O 0 0 1.0 0. 1. 0. 1. 0. -11. 1.e-2
1 100 1 1 1 1 0. 1.
0
monocarboaluminate 0 0 1.0 0. 1. 0. 1. 0. -11. 1.e-2
1 100 1 1 1 1 0. 1.
0
hemicarboaluminate 0 0 1.0 0. 1. 0. 1. 0. -11. 1.e-2
1 100 1 1 1 1 0. 1.
0
tricarboaluminate 0 0 1.0 0. 1. 0. 1. 0. -11. 1.e-2
1 100 1 1 1 1 0. 1.
0
monochloroaluminate 0 0 1.0 0. 1. 0. 1. 0. -11. 1.e-2
1 100 1 1 1 1 0. 1.
0
hemichloroaluminate 0 0 1.0 0. 1. 0. 1. 0. -11. 1.e-2
1 100 1 1 1 1 0. 1.
0
trichloroaluminate 0 0 1.0 0. 1. 0. 1. 0. -11. 1.e-2
1 100 1 1 1 1 0. 1.
0
3CaO.CaCl2-15H2O 0 0 1.0 0. 1. 0. 1. 0. -11. 1.e-2
1 100 1 1 1 1 0. 1.
0
oxychlorat 0 0 1.0 0. 1. 0. 1. 0. -11. 1.e-2
1 100 1 1 1 1 0. 1.
0
monosulfate 0 0 1.0 0. 1. 0. 1. 0. -11. 1.e-2
1 100 1 1 1 1 0. 1.
0
hydrotalcite 0 0 1.0 0. 1. 0. 1. 0. -11. 1.e-2
1 100 1 1 1 1 0. 1.
0
friedel-salt 0 0 1.0 0. 1. 0. 1. 0. -11. 1.e-2
1 100 1 1 1 1 0. 1.
0
:blank
:
:ion-exchange reactions
:Ionx 0 1.0
:
:BRKP 1
:100
:
Dtstep[y] 1 3.e-9
1.e-9 10.0
:
Time 15 0.5 1. 5. 10. 15. 20. 25. 30. 35.
40. 50. 100. 250. 500. 1000.
:
ENDS

```


Tuff-Cement Input File.

Infiltration of cement pore fluid into a tuff host rock.

June 9, 1997

```

:
:      geometry nx ny nz mode iprint idebug
GRID   XYZ      100 1 1 2      1 0
:
:
OPTS
:   idata istart imod iexact iscale ihrmc
:       0      0      10 0      0      1
:
:
:   itmax ihalmax ivmax ndamp
:       32      60      0      0
:
:
:   method iops ifor isurf iact loglin icon cournr
:       1      0      1      1      1      0      1      5.
:
:
:   isync ipor iperm perm-fac. por-fac.
COUPLE 0      1      0      3.      0.
:
:
PLTFiles
:iplot a s t m si sf v z b in e ex ti g itex
:       1 1 1 1 1 0 0 1 0 2 0 0 0 0 0 0
:
:
:   tol ttol tolneg tolpos tolexp dthalf qkmax tolstdst tolc
TOLR 1.d-12 1.e-2 1.e0 1.e-2 4.d0 .5 590. 1.e-6 1.e-12
:
:
:   mcyc cc c flx r sp qk pk rk a1 a2 a3
DEBUg 0 1 1 0 1 1 1 1 1
:
:
:   isat isothrm iread por0 phir sat w lambda toldelt tolpor
ISYSstem -1 0 0 0.3 1. 1.0 0.5 1.0 1.e-3 1.e-10
:
:
:   vx0 vy0 vz0 vgx vgy vgz[m/yr] alphax alphay alphaz[m]
FLOW 0. 0. 0. 0. 0. 0. 0. 0. 0. 0.
:
:
:   d0[cm^2/s] delhaq[kJ/mol] dgas[cm^2/s] dgexp tortaq tortg idif
DIFF 1.d-5 12.6 2.13d-1 1.8 0.5d0 1.d0 0
:
:flag 1: T(x) = d x^3 + a x^2 + b x + c (meters)
:   2: T(x) = a + (b-a) exp[-((x-x0)/c)^2] + (d - a) * x / xlen
:   3: T(x,t)=a+1/2(b-a)(erf[(x+c-x0)/2sqr(dt)]-erf[(x-c-x0)/2sqr(dt)])
:   p(bars) temp flag a b c d x0 xlen
PTINit 1.e5 25. 0 25 300 250 125 1000. 2.d3
:
:master species for controlling time stepping
MASTer ALL
:
:grid m 0. 1 200 200.
:
:
DXYZ
1.e-4 1.0673e-4 1.13913e-4 1.21579e-4 1.29762e-4 1.38495e-4 1.47815e-4

```

```

1.57763e-4 1.68381e-4 1.79713e-4 1.91808e-4 2.04716e-4 2.18494e-4
2.33199e-4 2.48893e-4 2.65644e-4 2.83521e-4 3.02602e-4 3.22968e-4
3.44704e-4 3.67902e-4 3.92662e-4 4.19088e-4 4.47293e-4 4.77396e-4
5.09525e-4 5.43816e-4 5.80415e-4 6.19477e-4 6.61168e-4 7.05665e-4
7.53156e-4 8.03844e-4 8.57943e-4 9.15683e-4 9.77308e-4 1.04308e-3
1.11328e-3 1.18821e-3 1.26817e-3 1.35352e-3 1.44461e-3 1.54183e-3
1.6456e-3 1.75635e-3 1.87455e-3 2.00071e-3 2.13536e-3 2.27907e-3
2.43245e-3 2.59616e-3 2.77088e-3 2.95736e-3 3.15639e-3 3.36882e-3
3.59554e-3 3.83752e-3 4.09578e-3 4.37143e-3 4.66563e-3 4.97963e-3
5.31476e-3 5.67244e-3 6.0542e-3 6.46165e-3 6.89652e-3 7.36066e-3
7.85603e-3 8.38475e-3 8.94904e-3 9.55131e-3 1.01941e-2 1.08802e-2
1.16124e-2 1.23939e-2 1.32281e-2 1.41183e-2 1.50685e-2 1.60826e-2
1.7165e-2 1.83202e-2 1.95531e-2 2.0869e-2 2.22735e-2 2.37725e-2
2.53724e-2 2.708e-2 2.89025e-2 3.08477e-2 3.29237e-2 3.51395e-2
3.75044e-2 4.00284e-2 4.27224e-2 4.55976e-2 4.86663e-2 5.19416e-2
5.54373e-2 5.91682e-2 6.31502e-2

```

```
1*1.
```

```
1.
```

```

:
:  isolv level north nitmax idetail rmaxtol rtwotol smaxtol
SOLV  1  1  1  100  0  1.e-20 1.e-20 1.e-12
:
:initial and boundary conditions: 1-conc., 2-flux, 3-zero gradient
:  inlet  outlet  nzoneaq
COMP  -1  3  3
:
:i1 i2 j1 j2 k1 k2
  1 100 1  1  1  1
:
:species  ctot      units  itype  mineral
ca+2      1.000e+00  mol    3      portlandite
mg+2      1.000e-04  mol    3      brucite
na+       2.78e-02   mol    1      none
k+        4.1e-03    mol    1      none
h+        1.245e+01  mol   -1     none
co3-2     5.000e-07  mol    3      calcite
cl-       1.025e-03  mol    3      friedel-salt
so4-2     1.000e-02  mol    3      ettringite(AU)
al+3      1.000e-12  mol    3      tricarboaluminate
sio2(aq)  1.000e-08  mol    3      hillebrandite

```

```
:blank
```

```
0
```

```
:
```

```
BCON
```

```
:bndk
```

```
1
```

```

:ibndtyp i1 i2 j1 j2 k1 k2 tmpbc
  1  1  1  1  1  1  1  25.

```

```

:species  ctot      units  itype  mineral
ca+2      1.82e-03  mol    3      calcite
mg+2      1.00e-04  mol    3      dolomite
na+       1.76e-02  mol    3      ortho55-45
k+        5.11e-05  mol    3      k-feldspar

```

P. C. Lichtner

SCIENTIFIC NOTEBOOK

INITIALS: JCL

```

h+      8.2      mol      8      none
co3-2   -2.99    mol      4      co2(g)
cl-     2.74e-03 mol     -1      none
so4-2   1.77e-04 mol      1      none
al+3    1.00e-12 mol      3      muscovite
sio2(aq) 3.28e-03 mol      3      chalcedony
:
0
:
:bndk
  2
:
:ibndtyp i1 i2 j1 j2 k1 k2 tmpbc
      3 100 100 1 1 1 1 25.
:species  ctot      units      itype      mineral
ca+2      1.000e+00    mol      3      portlandite
mg+2      1.000e-04    mol      3      brucite
na+       2.78e-02     mol      1      none
k+        4.1e-03      mol      1      none
h+        1.245e+01    mol     -1      none
co3-2     5.000e-07    mol      3      calcite
cl-       1.025e-03    mol      3      friedel-salt
so4-2     1.000e-02    mol      3      ettringite(AU)
al+3      1.000e-12    mol      3      tricarboaluminate
sio2(aq)  1.000e-08    mol      3      hillebrandite
:
0
:
0 0
:
STOL  1. 1. 1. 1. 1. 1. 1. 1. 1. 1.
:
AQCX
:h+
oh-      5.5e-5
hso4-
h2so4(aq)
hcl(aq)
hco3-
:co3-2
co2(aq)
nacl(aq)
kcl(aq)
koh(aq)
kso4-
:al+3
aloh+2    1.0e-5
al(oh)2+  1.0e-5
al(oh)3(aq) 1.0e-5
al(oh)4-  1.0e-5
al(so4)2-
also4+
caoh+

```

cahco3+
caco3(aq)
caso4(aq)
cac1+
cac12(aq)
cah2sio4(aq)
cah3sio4+
ca(h3sio4)2(aq)
mgco3(aq)
mghco3+
mgso4(aq)
mgcl+
mgh2sio4(aq)
mgh3sio4+
mgoh+
nahco3(aq)
naco3-
naoh(aq)
naso4-
h2sio4-2
h3sio4-
:blank
:
MNRL
calcite
dolomite
chalcedony
ortho55-45
montmor-na
quartz
cristobalite(alpha)
tridymite
sio2(am)
kaolinite
albite
gibbsite
k-feldspar
muscovite
gypsum
natrolite
laumontite
analcime
sepiolite
brucite
ettringite(AU)
ettringite
hillebrandite
katoite
foshagite
tobermorite-14a
portlandite
friedel-salt
tobermorite(AU)

```

CSH(0.8)
CSH(1.1)
CSH(1.8)
hydrogarnet(AU)
Ca3Al2Si0.5O7-5H2O
Si-hydrogarnet
gehlenite-hydrate
Ca2Al2O5-8H2O
monocarboaluminate
hemicarboaluminate
tricarboaluminate
monochloroaluminate
hemichloroaluminate
trichloroaluminate
3CaO.CaCl2-15H2O
oxychlorat
monosulfate
hydrotalcite
    :blank
:
GASEs
co2(g)
    :blank
:
MNIR
:mineral itypkin npar fkin delh beta rka betb rkb rk0 tau
:i1 i2 j1 j2 k1 k2 vol area
quartz      3  0  1.0  75.  1.0  0.   -0.3 -17.5 -17.39 1.e-3
1 100 1  1  1  1  0.   1.e2
0
cristobalite(alpha) 3  0  1.0  75.  1.0  0.  -0.3 -17.5 -16.34 1.e-3
1 100 1  1  1  1  0.   1.e2
0
tridymite    3  0  1.0  75.  1.0  0.   -0.3 -17.5 -17.39 1.e-3
1 100 1  1  1  1  0.   1.e2
0
ortho55-45    3  0  1.0  35.  0.5 -13.875 -0.3 -18.475 -16.50 1.e-3
1 100 1  1  1  1  0.   1.e2
0
muscovite     0  0  1.0  35.  1.0  0.    1.0  0. -16.50 1.e-3
1 100 1  1  1  1  0.   1.e0
0
calcite        0  0  1.0  0.   1.  0.    1.  0. -11.  1.e-2
1 100 1  1  1  1  0.   1.
0
dolomite       0  0  1.0  0.   1.  0.    1.  0. -13.  1.e-2
1 100 1  1  1  1  0.   1.
0
kaolinite      0  0  1.0  0.   1.  0.    1.  0. -16.  1.e-2
1 100 1  1  1  1  0.   1.
0
albite         0  0  1.0  0.   1.  0.    1.  0. -15.  1.e-2
1 100 1  1  1  1  0.   1.

```

```

0
chalcedony      0  0  1.0  0.  1.  0.      1.  0.  -15.  1.e-2
1 100 1  1  1  1      0.  1.
0
k-feldspar      0  0  1.0  0.  1.  0.      1.  0.  -15.  1.e-2
1 100 1  1  1  1      0.  1.
0
gibbsite        0  0  1.0  0.  1.  0.      1.  0.  -14.  1.e-2
1 100 1  1  1  1      0.  1.
0
natrolite       0  0  1.0  0.  1.  0.      1.  0.  -14.  1.e-2
1 100 1  1  1  1      0.  1.
0
laumontite      0  0  1.0  0.  1.  0.      1.  0.  -14.  1.e-2
1 100 1  1  1  1      0.  1.
0
analcime        0  0  1.0  0.  1.  0.      1.  0.  -14.  1.e-2
1 100 1  1  1  1      0.  1.
0
sepiolite       0  0  1.0  0.  1.  0.      1.  0.  -14.  1.e-2
1 100 1  1  1  1      0.  1.
0
brucite         0  0  1.0  0.  1.  0.      1.  0.  -12.  1.e-2
1 100 1  1  1  1      0.  1.
0
ettringite(AU)  0  0  1.0  0.  1.  0.      1.  0.  -12.  1.e-2
1 100 1  1  1  1      0.065 1.
0
hydrogarnet(AU) 0  0  1.0  0.  1.  0.      1.  0.  -12.  1.e-2
1 100 1  1  1  1      0.075 1.
0
CSH(0.8)        0  0  1.0  0.  1.  0.      1.  0.  -11.  1.e-2
1 100 1  1  1  1      0.  1.
0
CSH(1.1)        0  0  1.0  0.  1.  0.      1.  0.  -11.  1.e-2
1 100 1  1  1  1      0.  1.
0
CSH(1.8)        0  0  1.0  0.  1.  0.      1.  0.  -11.  1.e-2
1 100 1  1  1  1      0.42  1.
0
tobermorite(AU) 0  0  1.0  0.  1.  0.      1.  0.  -11.  1.e-2
1 100 1  1  1  1      0.  1.
0
portlandite     0  0  1.0  0.  1.  0.      1.  0.  -12.  1.e-2
1 100 1  1  1  1      0.1  1.
0
gypsum          0  0  1.0  0.  1.  0.      1.  0.  -11.  1.e-2
1 100 1  1  1  1      0.  1.
0
Ca3Al2Si0.5O7-5H2O 0  0  1.0  0.  1.  0.  1.  0.  -11.  1.e-2
1 100 1  1  1  1      0.  1.
0
Si-hydrogarnet  0  0  1.0  0.  1.  0.      1.  0.  -11.  1.e-2

```

```

1 100 1 1 1 1 0. 1.
0
gehlenite-hydrate 0 0 1.0 0. 1. 0. 1. 0. -11. 1.e-2
1 100 1 1 1 1 0. 1.
0
Ca2Al2O5-8H2O 0 0 1.0 0. 1. 0. 1. 0. -11. 1.e-2
1 100 1 1 1 1 0. 1.
0
monocarboaluminate 0 0 1.0 0. 1. 0. 1. 0. -11. 1.e-2
1 100 1 1 1 1 0. 1.
0
hemicarboaluminate 0 0 1.0 0. 1. 0. 1. 0. -11. 1.e-2
1 100 1 1 1 1 0. 1.
0
tricarboaluminate 0 0 1.0 0. 1. 0. 1. 0. -11. 1.e-2
1 100 1 1 1 1 0. 1.
0
monochloroaluminate 0 0 1.0 0. 1. 0. 1. 0. -11. 1.e-2
1 100 1 1 1 1 0. 1.
0
hemichloroaluminate 0 0 1.0 0. 1. 0. 1. 0. -11. 1.e-2
1 100 1 1 1 1 0. 1.
0
trichloroaluminate 0 0 1.0 0. 1. 0. 1. 0. -11. 1.e-2
1 100 1 1 1 1 0. 1.
0
3CaO.CaCl2-15H2O 0 0 1.0 0. 1. 0. 1. 0. -11. 1.e-2
1 100 1 1 1 1 0. 1.
0
oxychlorat 0 0 1.0 0. 1. 0. 1. 0. -11. 1.e-2
1 100 1 1 1 1 0. 1.
0
monosulfate 0 0 1.0 0. 1. 0. 1. 0. -11. 1.e-2
1 100 1 1 1 1 0. 1.
0
hydrotalcite 0 0 1.0 0. 1. 0. 1. 0. -11. 1.e-2
1 100 1 1 1 1 0.04 1.
0
friedel-salt 0 0 1.0 0. 1. 0. 1. 0. -11. 1.e-2
1 100 1 1 1 1 0. 1.
0
:blank
:
:ion-exchange reactions
:Ionx 0 1.0
:
:BRKP 1
:100
:
Dtstep[y] 1 3.e-9
1.e-9 10.0
:
Time 15 0.5 1. 5. 10. 15. 20. 25. 30. 35.

```

40. 50. 100. 250. 500. 1000.

:

ENDS

Cement-Tuff Contact Input File.

Cement-tuff contact.

June 9, 1997

```

:
:      geometry nx ny nz mode iprint idebug
GRID   XYZ      100 1 1 2      1 0
:
: OPTS
:   idata istart imod iexact iscale ihrmc
:     0      0      10 0      0      1
:
:
:   itmax ihalmax ivmax ndamp
:     32     60      0      0
:
:
:   method iops ifor isurf iact loglin icon  counr
:     1      0      1      1      1      0      1      5.
:
:
:   isync ipor iperm perm-fac. por-fac.
COUPLE 0      1      0      3.      0.
:
: PLTFiles
: iplot a s t m si sf v z b in e ex ti g itex
:     1 1 1 1 1 0 0 1 0 2 0 0 0 0 0 0
:
:   tol  ttol  tolneg tolpos  tolexp dthalf qkmax  tolstdst tolc
TOLR 1.d-8 1.e-1 1.e0 1.e-2 4.d0 .5 590. 1.e-6 1.e-12
:
:   mcyc cc c flx r sp qk pk rk a1 a2 a3
DEBUG 0 1 1 0 1 1 1 1 1
:
:   isat isothrm iread por0 phir sat w lambda toldelt tolpor
ISYSem -1 0 0 0.1 1. 1.0 0.5 1.0 1.e-3 1.e-10
:
:   vx0 vy0 vz0 vgx vgy vgz[m/yr] alphax alphay alphaz[m]
FLOW 0. 0. 0. 0. 0. 0. 0. 0. 0. 0.
:
:   d0[cm^2/s] delhaq[kJ/mol] dgas[cm^2/s] dgexp tortaq tortg idif
DIFF 1.d-5 12.6 2.13d-1 1.8 0.5d0 1.d0 0
:
: flag 1: T(x) = d x^3 + a x^2 + b x + c (meters)
:   2: T(x) = a + (b-a) exp[-((x-x0)/c)^2] + (d - a) * x / xlen
:   3: T(x,t)=a+1/2(b-a)(erf[(x+c-x0)/2sqr(dt)]-erf[(x-c-x0)/2sqr(dt)])
:   p(bars) temp flag a b c d x0 xlen
PTINit 1.e5 25. 0 25 300 250 125 1000. 2.d3
:
: master species for controlling time stepping
MASTER ALL
:

```



```

:grid m 0. 1 200 200.
:
DXYZ
1.37157e-1 1.18357e-1 1.02134e-1 8.81341e-2 7.60535e-2 6.56288e-2
5.6633e-2 4.88702e-2 4.21715e-2 3.63911e-2 3.14029e-2 2.70985e-2
2.33841e-2 2.01788e-2 1.74129e-2 1.50261e-2 1.29664e-2 1.11891e-2
9.65541e-3 8.33194e-3 7.18987e-3 6.20435e-3 5.35391e-3 4.62005e-3
3.98677e-3 3.4403e-3 2.96874e-3 2.56181e-3 2.21066e-3 1.90764e-3
1.64616e-3 1.42052e-3 1.22581e-3 1.05779e-3 9.12794e-4 7.87677e-4
6.79709e-4 5.86541e-4 5.06143e-4 4.36766e-4 3.76898e-4 3.25236e-4
2.80656e-4 2.42186e-4 2.08989e-4 1.80343e-4 1.55623e-4 1.34292e-4
1.15884e-4 1.e-4 1.e-4 1.21865e-4 1.48512e-4 1.80984e-4 2.20557e-4
2.68783e-4 3.27554e-4 3.99175e-4 4.86456e-4 5.92822e-4 7.22444e-4
8.8041e-4 1.07291e-3 1.30751e-3 1.59341e-3 1.94181e-3 2.36639e-3
2.88382e-3 3.51437e-3 4.28281e-3 5.21926e-3 6.36047e-3 7.75121e-3
9.44605e-3 1.15115e-2 1.40285e-2 1.70959e-2 2.0834e-2 2.53894e-2
3.09409e-2 3.77062e-2 4.59509e-2 5.59982e-2 6.82425e-2 8.31639e-2
1.01348e-1 1.23508e-1 1.50514e-1 1.83424e-1 2.23531e-1 2.72407e-1
3.31969e-1 4.04556e-1 4.93014e-1 6.00813e-1 7.32183e-1 8.92278e-1
1.08738 1.32514 1.61489
1*1.
1.
:
:  isolv level north nitmax idetail rmaxtol rtwotol smaxtol
SOLV 1 1 1 100 0 1.e-20 1.e-20 1.e-12
:
:initial and boundary conditions: 1-conc., 2-flux, 3-zero gradient
:  inlet outlet nzoneaq
COMP -1 3 3
:
:i1 i2 j1 j2 k1 k2
1 50 1 1 1 1
:
:species ctot units itype mineral
ca+2 1.000e+00 mol 3 portlandite
mg+2 1.000e-04 mol 3 brucite
na+ 2.78e-02 mol 1 none
k+ 4.1e-03 mol 1 none
h+ 1.245e+01 mol -1 none
co3-2 5.000e-07 mol 3 calcite
cl- 1.025e-03 mol 3 friedel-salt
so4-2 1.000e-02 mol 3 ettringite(AU)
al+3 1.000e-12 mol 3 tricarboaluminate
sio2(aq) 1.000e-08 mol 3 hillebrandite
:
:blank
:
:i1 i2 j1 j2 k1 k2
51 100 1 1 1 1
:
:species ctot units itype mineral
ca+2 1.82e-03 mol 3 calcite
mg+2 1.00e-04 mol 3 dolomite

```

P. C. Lichtner

SCIENTIFIC NOTEBOOK

INITIALS: PCZ

```

na+      1.76e-02    mol    3      ortho55-45
k+       5.11e-05    mol    3      k-feldspar
h+       8.2         mol    8      none
co3-2    -2.99      mol    4      co2(g)
cl-      2.74e-03    mol   -1      none
so4-2    1.77e-04    mol    1      none
al+3     1.00e-12    mol    3      muscovite
sio2(aq) 3.28e-03    mol    3      chalcedony
      :blank
0
:
BCON
:bndk
1
:ibndtyp i1 i2 j1 j2 k1 k2 tmpbc
      3   1   1   1   1   1   1   25.
:species  ctot      units      itype      mineral
ca+2      1.000e+00    mol      3      portlandite
mg+2      1.000e-04    mol      3      brucite
na+       2.78e-02     mol      1      none
k+        4.1e-03      mol      1      none
h+        1.245e+01    mol     -1      none
co3-2     5.000e-07    mol      3      calcite
cl-       1.025e-03    mol      3      friedel-salt
so4-2     1.000e-02    mol      3      ettringite(AU)
al+3      1.000e-12    mol      3      tricarboaluminate
sio2(aq)   1.000e-08    mol      3      hillebrandite
:
0
:
:bndk
2
:
:ibndtyp i1 i2 j1 j2 k1 k2 tmpbc
      3  100 100   1   1   1   1   25.
:species  ctot      units      itype      mineral
ca+2      1.82e-03     mol      3      calcite
mg+2      1.00e-04     mol      3      dolomite
na+       1.76e-02     mol      3      ortho55-45
k+        5.11e-05     mol      3      k-feldspar
h+        8.2         mol      8      none
co3-2     -2.99      mol      4      co2(g)
cl-       2.74e-03     mol     -1      none
so4-2     1.77e-04     mol      1      none
al+3      1.00e-12     mol      3      muscovite
sio2(aq)   3.28e-03     mol      3      chalcedony
:
0
:
0 0
:
STOL  1. 1. 1. 1. 1. 1. 1. 1. 1. 1.
:

```

AQCX
 :h+
 oh- 5.5e-5
 hso4-
 h2so4(aq)
 hcl(aq)
 hco3-
 :co3-2
 co2(aq)
 nacl(aq)
 kcl(aq)
 koh(aq)
 kso4-
 :al+3
 aloh+2 1.0e-5
 al(oh)2+ 1.0e-5
 al(oh)3(aq) 1.0e-5
 al(oh)4- 1.0e-5
 al(so4)2-
 also4+
 caoh+
 cahco3+
 caco3(aq)
 caso4(aq)
 cac1+
 cac12(aq)
 cah2sio4(aq)
 cah3sio4+
 ca(h3sio4)2(aq)
 mgco3(aq)
 mghco3+
 mgso4(aq)
 mgcl+
 mgh2sio4(aq)
 mgh3sio4+
 mgoh+
 nahco3(aq)
 naco3-
 naoh(aq)
 naso4-
 h2sio4-2
 h3sio4-
 :blank
 :
 MNRL
 calcite
 dolomite
 chalcedony
 ortho55-45
 montmor-na
 quartz
 cristobalite(alpha)
 tridymite

```

sio2(am)
kaolinite
albite
gibbsite
k-feldspar
muscovite
gypsum
natrolite
laumontite
analcime
sepiolite
brucite
ettringite(AU)
ettringite
hillebrandite
katoite
foshagite
tobermorite-14a
portlandite
friedel-salt
tobermorite(AU)
CSH(0.8)
CSH(1.1)
CSH(1.8)
hydrogarnet(AU)
Ca3Al2Si0.5O7-5H2O
Si-hydrogarnet
gehlenite-hydrate
Ca2Al2O5-8H2O
monocarboaluminate
hemicarboaluminate
tricarboaluminate
monochloroaluminate
hemichloroaluminate
trichloroaluminate
3CaO.CaCl2-15H2O
oxychlorat
monosulfate
hydrotalcite
      :blank
:
GASEs
co2(g)
      :blank
:
MNIR
:mineral itypkin npar fkin delh beta rka betb rkb rk0 tau
:i1 i2 j1 j2 k1 k2 vol area
quartz      3  0  1.0  75.  1.0  0.  -0.3  -17.5 -17.39 1.e-3
  1  50 1  1  1  1  0.  1.e2
51 100 1  1  1  1  0.15 1.e2
0
crystalite(alpha) 3 0 1.0 75.  1.0  0.  -0.3  -17.5 -16.34 1.e-3

```

P. C. Lichtner

SCIENTIFIC NOTEBOOK

INITIALS: PC

```

1  50 1 1 1 1 0. 1.e2
51 100 1 1 1 1 0.10 1.e2
0
tridymite 3 0 1.0 75. 1.0 0. -0.3 -17.5 -17.39 1.e-3
1  50 1 1 1 1 0. 1.e2
51 100 1 1 1 1 0.05 1.e2
0
ortho55-45 3 0 1.0 35. 0.5 -13.875 -0.3 -18.475 -16.50 1.e-3
1  50 1 1 1 1 0. 1.e2
51 100 1 1 1 1 0.60 1.e2
0
muscovite 0 0 1.0 35. 1.0 0. 1.0 0. -16.50 1.e-3
1  100 1 1 1 1 0.0 1.e0
0
calcite 0 0 1.0 0. 1. 0. 1. 0. -11. 1.e-2
1  100 1 1 1 1 0.0 1.
0
dolomite 0 0 1.0 0. 1. 0. 1. 0. -13. 1.e-2
1  100 1 1 1 1 0.0 1.
0
kaolinite 0 0 1.0 0. 1. 0. 1. 0. -16. 1.e-2
1  100 1 1 1 1 0.0 1.
0
albite 0 0 1.0 0. 1. 0. 1. 0. -15. 1.e-2
1  100 1 1 1 1 0.0 1.
0
chalcedony 0 0 1.0 0. 1. 0. 1. 0. -15. 1.e-2
1  100 1 1 1 1 0. 1.
0
k-feldspar 0 0 1.0 0. 1. 0. 1. 0. -15. 1.e-2
1  100 1 1 1 1 0. 1.
0
gibbsite 0 0 1.0 0. 1. 0. 1. 0. -14. 1.e-2
1  100 1 1 1 1 0. 1.
0
natrolite 0 0 1.0 0. 1. 0. 1. 0. -14. 1.e-2
1  100 1 1 1 1 0. 1.
0
laumontite 0 0 1.0 0. 1. 0. 1. 0. -14. 1.e-2
1  100 1 1 1 1 0. 1.
0
analcime 0 0 1.0 0. 1. 0. 1. 0. -14. 1.e-2
1  100 1 1 1 1 0. 1.
0
sepiolite 0 0 1.0 0. 1. 0. 1. 0. -14. 1.e-2
1  100 1 1 1 1 0. 1.
0
brucite 0 0 1.0 0. 1. 0. 1. 0. -12. 1.e-2
1  100 1 1 1 1 0. 1.
0
ettringite(AU) 0 0 1.0 0. 1. 0. 1. 0. -12. 1.e-2
1  50 1 1 1 1 0.065 1.
51 100 1 1 1 1 0. 1.

```

```

0
hydrogarnet(AU) 0 0 1.0 0. 1. 0. 1. 0. -12. 1.e-2
 1 50 1 1 1 1 0.075 1.
51 100 1 1 1 1 0. 1.
0
CSH(0.8) 0 0 1.0 0. 1. 0. 1. 0. -11. 1.e-2
 1 100 1 1 1 1 0. 1.
0
CSH(1.1) 0 0 1.0 0. 1. 0. 1. 0. -11. 1.e-2
 1 100 1 1 1 1 0. 1.
0
CSH(1.8) 0 0 1.0 0. 1. 0. 1. 0. -11. 1.e-2
 1 50 1 1 1 1 0.42 1.
51 100 1 1 1 1 0. 1.
0
tobermorite(AU) 0 0 1.0 0. 1. 0. 1. 0. -11. 1.e-2
 1 100 1 1 1 1 0. 1.
0
portlandite 0 0 1.0 0. 1. 0. 1. 0. -12. 1.e-2
 1 50 1 1 1 1 0.1 1.
51 100 1 1 1 1 0. 1.
0
gypsum 0 0 1.0 0. 1. 0. 1. 0. -11. 1.e-2
 1 100 1 1 1 1 0. 1.
0
Ca3Al2Si0.5O7-5H2O 0 0 1.0 0. 1. 0. 1. 0. -11. 1.e-2
 1 100 1 1 1 1 0. 1.
0
Si-hydrogarnet 0 0 1.0 0. 1. 0. 1. 0. -11. 1.e-2
 1 100 1 1 1 1 0. 1.
0
gehlenite-hydrate 0 0 1.0 0. 1. 0. 1. 0. -11. 1.e-2
 1 100 1 1 1 1 0. 1.
0
Ca2Al2O5-8H2O 0 0 1.0 0. 1. 0. 1. 0. -11. 1.e-2
 1 100 1 1 1 1 0. 1.
0
monocarboaluminate 0 0 1.0 0. 1. 0. 1. 0. -11. 1.e-2
 1 100 1 1 1 1 0. 1.
0
hemicarboaluminate 0 0 1.0 0. 1. 0. 1. 0. -11. 1.e-2
 1 100 1 1 1 1 0. 1.
0
tricarboaluminate 0 0 1.0 0. 1. 0. 1. 0. -11. 1.e-2
 1 100 1 1 1 1 0. 1.
0
monochloroaluminate 0 0 1.0 0. 1. 0. 1. 0. -11. 1.e-2
 1 100 1 1 1 1 0. 1.
0
hemichloroaluminate 0 0 1.0 0. 1. 0. 1. 0. -11. 1.e-2
 1 100 1 1 1 1 0. 1.
0
trichloroaluminate 0 0 1.0 0. 1. 0. 1. 0. -11. 1.e-2

```

```

1 100 1 1 1 1 0. 1.
0
3CaO.CaCl2-15H2O 0 0 1.0 0. 1. 0. 1. 0. -11. 1.e-2
1 100 1 1 1 1 0. 1.
0
oxychlorat 0 0 1.0 0. 1. 0. 1. 0. -11. 1.e-2
1 100 1 1 1 1 0. 1.
0
monosulfate 0 0 1.0 0. 1. 0. 1. 0. -11. 1.e-2
1 100 1 1 1 1 0. 1.
0
hydrotalcite 0 0 1.0 0. 1. 0. 1. 0. -11. 1.e-2
1 50 1 1 1 1 0.04 1.
51 100 1 1 1 1 0. 1.
0
friedel-salt 0 0 1.0 0. 1. 0. 1. 0. -11. 1.e-2
1 100 1 1 1 1 0. 1.
0
:blank
:
:ion-exchange reactions
:Ionx 0 1.0
:
:BRKP 1
:100
:
Dtstep[y] 1 3.e-10
1.e-10 10.0
:
Time 15 0.5 1. 5. 10. 15. 20. 25. 30. 35.
40. 50. 100. 250. 500. 1000.
:
ENDS

```

Account Number: **20-5708-562**

Description: Near-field Environment Code Development – MULTIFLO

Collaborators: Dr. M. Seth (Consultant)

Objective: Development of the computer code MULTIFLO, and submodules GEM and METRA.

4.2.97 FOR_STUDY Test of MULTIFLO.

The FORTRAN Static Analyzer was run on MULTIFLO to check for bugs. The default options described in the FOR_STUDY manual were used in the test. Two serious errors were found: one in METRA and one GEM. In the METRA subroutine `slvliq.f`, the call to `trans.f` was changed from:

```

      if(ipor.gt.0) then
        call trans (tx,ty,tz,aa(itdx),aa(itdy),aa(itdz),
*               permx,permy,permz,aa(iprmr))

```

to:

```

      if(ipor.gt.0) then
        call trans (tx,ty,tz,aa(itdx),aa(itdy),aa(itdz),
*               permx,permy,permz,aa(iprmr),aa)

```

4.7.97 FOR_STUDY Test of MULTIFLO.

A minor error was discovered in subroutine `inpmetra.f`:

```

> Error #171 inpmetra.f,1189: Local name IFMT
> was referenced but never set
>
> 100  format(10f10.0)
>      ifmt = 2                !<--line added
>      if(ioutpt.ge.2)
>      * call prints (h,h,time,nx,ny,nzz,ifmt,10,
>      * 'Depth to Top of Layer(s)          ', 'Meters  ')
>

```


In GEM, the call to bndcond.f was modified from:

```
c-----set boundary conditions for gas phase
      call bndcond (ng,ppsig,ppsig,psigbnd,j,j,1)
```

to:

```
c-----set boundary conditions for gas phase
      call bndcond (nc,ppsig,ppsig,psigbnd,j,j,1)
```

4.3.97 QA Installation Test of MULTIFLO.

To meet QA TOP-018 requirements an Installation Test of MULTIFLO was performed. The code was compiled and run on the machine hornet.cnwra.swri.edu, an ultra-sparc machine. The results were compared with those obtained from running the code on skippy.cnwra.swri.edu, a sparc 20 machine. Slight differences are expected due to the different machine types. The input files used in the test are listed below for metra and gem:

```
METRA Data for Multiflo simulator (initial data:1D, 83.4 AML, Yucca Mt.)
      Apr. 3, 1997

RSTART  0
:
:      XYZ              = 1 table look-up, pref = ref. press.
:      RADIAL          = 0 correlations,   tref = ref temp.
:      OTHER
:grid geometry nx ny nz ivplwr ipvcal iout gravity pref tref href
Grid XYZ      1  1 121  1  0  3  0  0  0  0  0
:
Pckr                      :relative perm and pc keyword
:  i type-curv swirm rpmm(lamda) alpham swext sgc iecm
:      swirf rpmf(lamda) alphaf phim phif permm permf
:Topopah Spring (150-475 m)
:  1 Van-Gen  0.08  0.4400  5.8e-7  0.  0.  1
:      0.04  0.7636  1.305e-5 0.11  1.8e-3 1.9e-18 3.9e-12
:  1 Van-Gen  0.001 0.4400  5.8e-7  0.  0.  1
:      0.001 0.7636  1.305e-5 0.11  1.8e-3 1.9e-18 3.9e-12
:      1 Van-Gen  0.001 0.4400  5.8e-7  0.  0.  1
:      0.001 0.7636  1.305e-5 0.11  1.8e-3 1.9e-18 1.0e-11
:blank line
:
Thermal-prop
: no rho      cpr  ckdry  cksat  crp crt  tau cdiff  cexp  enbd
:  1  2.580e+3 840.  2.10  2.10  0  0  .5  2.13e-5 1.8  0.
0
:  igrid  rw  re
```

```

DXYZ  0      0.      1.
: (dx(i),i=1,nx)
1.
:
: (dy(j),j=1,ny)
1.
:
: (dz(k),k=1,nz)
10. 10. 10. 10. 10. 10. 10. 10. 10. 10.
10. 10. 10. 10. 10. 10. 10. 10. 10. 10.
10. 10. 10. 10.  5.  5.  5.  5.  5.  5.
 5.  5.  5.  5.  5.  5.  5.  5.  5.  5.
 2.  2.  2.  2.  2.  2.  2.  2.  2.  2.
 2.  2.  2.  2.  2.  2.  2.  2.  2.  2.
 2.  2.  2.  1.5 1.  1.  1.  1.  1.  1.
 1.  1.  1.  1.  1.  1.  1.  1.  1.  1.5
 2.  2.  2.  2.  2.  2.  2.  2.  2.  2.
 2.  2.  2.  2.  2.  2.  2.  2.  5.  5.
 5.  5.  5.  5.  5.  5.  5.  5. 10. 10.
10. 10. 10. 10. 10. 10. 10. 10. 10. 10.
10.
PhiK
: i1 i2 j1 j2 k1 k2 iist ithrm vb porm permx permy permz
  1  1  1  1  1 121  1  1  0.
  0
Init  init
: i1 i2 j1 j2 k1 k2  pm  tm  sgm  x2m
:  1  1  1  1  1 121 1.e5 25.0 0.5  0.
:  0
:
:EQUIL 587.50 1.e5 30. 0.0255319 0.0 -1
:EQUIL 5.0 1.e5 25. 0.0 0.2 1
:EQUIL 595.0 1.065627E+05 25. 0.0 0.0 -1
:
Recurrent-data
Bcon 2
:itype iface i1 i2 j1 j2
1 TOP 1 1 1 1
:time qbc pbc tbc sgbc xabc
 0. 0. 8.55e4 15.0 0.2 0.
0
1 BOTTOM 1 1 1 1
 0. 0. 9.05e4 30.0 0.0 0.
0
:
Rstart 1 0
Output A=1 C=1 B=1 S=-1
:  isolve newtnmn newtnmx north nitmx level
Solve 2 1 7 4 100 1
:
:AUTO-step DPMXE DSMXE DTMPMXE DP2MXe TACCEL IAUTODT FAC1
AUTO-step 1.0E+3 0.03 5.0 1.e3 1.e-3 0 0
:

```

```

:TOLR TOLP TOLS TOLT TOLP2 TOLM TOLA TOLE rtwotol rmxtol smxtol
Tolr 10. 1.e-4 1.e-3 1.e+1 1.e-5 1.e-3 1.e-3 1.e-20 1.e-20 1.e-20
:
:Limit dpmx dsmx dtmpmx dp2mx dtmn dtmx icutmx
LIMIT 1.e4 .08 10. 1.e5 1.e-6 1.e3
Plots 1
:Steady[y] 1.e-8 1.e-6 1.e-1
:Ends
: ns fach facm (fach and facm are multipliers to
: read-in values of qht and qmt)
:Source 1 1.32494 1. !110.5 AML
:Source 1 1.19904 1. !100 AML
:Source 1 1.13909 1. ! 95 AML
:Source 1 1.07914 1. ! 90 AML
:Source 1 1.04916 1. ! 87.5 AML
:Source 1 1.01918 1. ! 85 AML
Source 1 1. 1. ! 83.4 AML
:Source 1 3.14159 1. !radial 83.4 AML
: is js ks istyp
1 1 1 1 72 72 31
: 1 1 1 1 72 72 33
: timeq(sec) T/qht (C/(J/s)) qmt (kg/s)
0.00000E+00 1.87730E+01
6.30720E+07 1.81217E+01
1.26144E+08 1.75357E+01
1.89216E+08 1.68897E+01
2.52288E+08 1.63046E+01
3.15360E+08 1.57715E+01
4.73040E+08 1.45818E+01
6.30720E+08 1.34618E+01
7.88400E+08 1.25071E+01
9.46080E+08 1.16163E+01
1.26144E+09 1.02515E+01
1.57680E+09 8.99586E+00
2.36520E+09 6.82702E+00
3.15360E+09 5.65219E+00
4.73040E+09 4.24896E+00
6.30720E+09 3.53303E+00
9.46080E+09 2.82589E+00
1.26144E+10 2.40733E+00
1.57680E+10 2.08456E+00
1.89216E+10 1.81067E+00
2.52288E+10 1.44680E+00
3.15360E+10 1.20944E+00
3.94200E+10 9.81818E-01
4.73040E+10 8.27487E-01
6.30720E+10 6.33691E-01
7.88400E+10 5.48998E-01
9.46080E+10 4.89297E-01
1.26144E+11 4.38708E-01
1.57680E+11 4.02873E-01
1.89216E+11 3.70297E-01
2.20752E+11 3.44801E-01

```

```

2.52288E+11 3.24128E-01
2.83824E+11 3.06917E-01
3.15360E+11 2.92001E-01
3.46896E+11 2.69319E-01
3.78432E+11 2.50151E-01
4.09968E+11 2.33722E-01
4.41504E+11 2.19473E-01
4.73040E+11 2.06987E-01
5.51880E+11 1.81593E-01
6.30720E+11 1.62125E-01
7.88400E+11 1.34131E-01
9.46080E+11 1.14855E-01
1.26144E+12 8.27996E-02
1.57680E+12 6.29212E-02
1.89216E+12 4.90735E-02
2.20752E+12 3.97719E-02
2.52288E+12 3.31523E-02
2.83824E+12 2.82343E-02
3.15360E+12 2.44608E-02
4.73040E+12 1.84539E-02
0
Output  A=1  C=1 S=-1
:
:RSTArt 0 1
:
:  isolv  newtnmn  newtnmx
Solve 3      2      7
:
:AUTO-step  DPMXE  DSMXE  DTMPMXE  DP2MXe  TACCEL  IAUTO
AUTO-step  5.E+4  0.025  3.0  1.e4  1.e-2  0
:
:TOLR TOLP TOLS TOLT TOLP2 TOLM TOLA TOLE
Tolr 1.e+1 1.e-4 1.e-2 5.e+1 1.e-5 1.e-6 1.e-3 1.e-20 1.e-20 1.e-12
:
:Limit dpmx dsmx dtmpmx dp2mx dtmn dtmx icutmx
LIMIT 1.e4 .05 5. 1.e5 1.e-6 1.e4 5
Plots 1 1 1
72
Time[y] 10.
Time[y] 50.
Time[y] 100.
Time[y] 500.
Time[y] 1000.
Time[y] 5000.
Time[y] 10000.
Time[y] 1.e5
:Time[y] 1.5e5
Ends

GEM Test Data for Multiflo Simulator (Yucca Mt., 1D, 83.4 AML)
Apr. 3, 1997
:
: geometry nx ny nz mode iprint idebug

```

```

GRID      XYZ      1  1 121      2      0      0
:
OPTS
:  idata istart imod iexact iscale
:    0      0      1      0      0
:
:  itmax ihalmax ivmax ndamp
:    16     16      0      5
:
:  method iops ifor isurf iact loglin icon  counr
:    1      0      2      1      1      0      1      1.
:
:  isync ipor iperm perm-fac.
COUPLE 0      -1      0      3.
:
PLTFiles
:iplot  a  s  t  m  si  sf  v  z  b  in  e  ex  ti  g  itex
:    1  1  1  1  1  0  0  1  0  2  0  0  0  0  1  0
:
:  tol  ttol  tolneg  tolpos  tolexp  dthalf  qkmax  tolstdste  tolc
TOLR 1.d-10 2.e-3 1.e0 1.e-2 5.d0 .5 590. 1.e-12 1.e-10
:
:  mcyc cc c flx c sp qk pk rk a1 a2 a3
DEBUG 0      1  1  0  1  1  1  1  1
:
:  isat isotherm iread por0 phir sat w lambda toldelt  tolpor
ISYSem 0  1      0      .11 1. 0.5 .5 1. 1.e-3 1.e-3
:
:  vx0 vy0 vz0 vgx0 vgy0 vgz0[m/yr] alphax alphay alphaz[m]
FLOW 0. 0. 1. 0. 0. 0. 0. 0. 0. 0.
:
:  d0[cm^2/s] delhaq[kJ/mol] dgas[cm^2/s] dgexp tortaq tortg idif
DIFF 1.d-5 12.6 2.13d-1 1.8 1.d0 1.d0 0
:
:flag 1: T(x) = d x^3 + a x^2 + b x + c (meters)
:  2: T(x) = a + (b-a) exp[-((x-x0)/c)^2] + (d - a) * x / xlen
:  3:T(x,t)=a+1/2(b-a)(erf[(x+c-x0)/2sqr(dt)]-erf[(x-c-x0)/2sqr(dt)])
:  p (bars) temp flag a b c d x0 xlen
PTINit 1.e5 25. 0 25 300 250 125 1000. 2.d3
:
:master species for controlling time stepping
MASTer h+
:
:grid m 0. 1 200 200.
:
DXYZ
:  1.
:  1.
: 121*1.
:
:  isolv level north nitmax idetail rmaxtol rtwtol smaxtol
SOLV 3 1 1 100 0 1.e-20 1.e-20 1.e-12
:

```

```

:initial and boundary conditions: 1-conc., 2-flux, 3-zero gradient
:inlet outlet nzoneaq
COMP 1 3 3
:
:species itype guess ctot mineral diffusion
ca+2 1 4.e-4 2.5e-3 blank
mg+2 1 1.e-4 7.8e-4 blank
na+ 1 2.e-3 3.0e-3 blank
k+ 1 2.e-4 3.6e-4 blank
h+ 3 1.e-8 8.2 calcite
hco3- 4 2.7e-3 -2.00 co2(g)
sio2(aq) 1 1.e-3 1.5e-3 blank
cl- -1 2.e-3 2.8e-3 blank
so4-2 1 3.e-4 1.7e-3 blank
:o2(aq) 4 1.e-3 0.2 o2(g)
:blank
:
BCON
3 1
:species itype guess ctot mineral
ca+2 1 4.e-4 2.5e-3 blank
mg+2 1 1.e-4 7.8e-4 blank
na+ 1 2.e-3 3.0e-3 blank
k+ 1 2.e-4 3.6e-4 blank
h+ 3 1.e-8 8.2 calcite
hco3- 4 2.7e-3 -2.00 co2(g)
sio2(aq) 1 1.e-3 1.5e-3 blank
cl- -1 2.e-3 2.8e-3 blank
so4-2 1 3.e-4 1.7e-3 blank
:o2(aq) 4 1.e-3 0.2 o2(g)
:
4 1
:species itype guess ctot mineral
ca+2 1 4.e-4 2.5e-4 blank
mg+2 1 1.e-4 7.2e-5 blank
na+ 1 2.e-3 1.96e-3 blank
k+ 1 2.e-4 1.36e-4 blank
h+ 8 1.e-7 6.9 calcite
hco3- -1 2.3e-3 -2.00 co2(g)
sio2(aq) 1 1.e-3 1.07e-3 blank
cl- 1 2.e-4 1.8e-4 blank
so4-2 1 3.e-4 1.9e-4 blank
:o2(aq) 7 1.e-4 1.74e-4 blank
:
0 0
:
CMIR 0 0
:blank
:
: 9 entries per line
STOL 1. 1. 1. 1. 1. 1. 1. 1. 1. 1.
:
AQCX

```

```

oh-
hso4-
hcl(aq)
co2(aq)
co3-2
caco3(aq)
cahco3+
caoh+
cac1+
cac12(aq)
caso4(aq)
mgoh+
mgco3(aq)
mgcl+
mghco3+
mgso4(aq)
nahco3(aq)
nacl(aq)
naoh(aq)
naso4-
kcl(aq)
khso4(aq)
kso4-
h3sio4-
h2sio4-2
      :blank
:
MNRL
quartz
calcite
tobermorite-14a
      :blank
:
GASES
co2(g)
:o2(g)
      :blank
:
MNIR
:mineral itypkin fkin delh beta rka betb rkb rk tau
:i1 i2 j1 j2 k1 k2 vol area
quartz      0  1.0  75.  1.0  0.    1.0  0. -17.39 1.e-3
1 1 1 1 1 121 0.89 1.e1
0
calcite      0  1.0  35.  1.0  0.    1.0  0. -10.00 1.e-4
1 1 1 1 1 121 0.    1.
0
      :blank
:
:surface mineral itypkin area beta fkin delh rkph rk
:    0  1.0  1.0    1.  0.    0.    0.
:
:corrosion solids i0 acorr bcorr curlim

```

```

:      0.  0.  0.  0.
:
:crevice gap[meters]  potential [v]
ECAQ      90.d-6      -.2
:blank

:
:electrochemical aqueous species i0      acorr      bcorr      curlim
:      0.  0.  0.  0.
:
AQIR
:blank

:
:ion-exchange reactions
Ionx      0      1.0
:
BRKP      1
72
:
DTSTep[y]      1 3.e-8
1.e-8      100.d0
:
TIME[y] 1 10. 50. 100. 500. 1000. 5000. 10000. 1.e5
:
ENDS

```

Only slight differences (4th decimal place) were found in the masout file. No differences were found in the plot files. The Installation Test was deemed successful.

4.10.97 Modifications to Final April Release of MULTIFLO 1.0

- **GEM:** The following routines were altered in GEM:

readat.f	startup.f
speciate.f	eqlib.f
eqres.f	eqjac.f
output2.f	solprdt.f
updtgem.f	maingem.f
gunits.f	initgem.f
modbnd.f	bndcond.f
hybrid.f	

One new routine cflimit.f was added to GEM.

- **MULTIFLO:** The routine gem.f was altered in MULTIFLO.

In addition to several bug fixes, two essential new features were added to the code. The first allows the user to specify different initial and boundary conditions in different regions of space and also, for nonisothermal systems, equilibrate the initial fluid composition at each node. The second alteration enables a Courant number limitation to be imposed on the time step size for the fully implicit time stepping algorithm. Previously this was only imposed for the explicit and operator splitting algorithms.

Bug Fixes

Subroutine: `../metra/inpmetra.f`

One bug in `../metra/inpmetra.f` was fixed. The variable `ifmt` was undefined in the statement:

```

      if(ioutpt.ge.2)
*   call prints (h,h,time,nx,ny,nzz,ifmt,10,
*   'Depth to Top of Layer(s) ', 'Meters ')

      go to 500

```

Added `ifmt = 2` before call prints.

Subroutine: `../gem/startup.f`

```

c      initialize variables

      do j=1,ncomp
        psi0(j)   = psi0(j)*rho(1)
        psibc0(j) = psibc0(j)*rho(1)
        psibcl(j) = psibcl(j)*rho(1)
        omeg0(j)  = omeg0(j)*rho(1)
        fluxint(j) = zero
        do k = 1, nbndcon
          psibnd(j,k) = psibnd(j,k)*rho(1)
        enddo
      enddo

```

Added `ibnd(k)` in place of `k` in `psibnd(j,k)`.

Subroutine: `../gem/startup.f`

Activity coefficients for the initial aqueous solution were not properly stored. Stored initial activity coefficients in `gemloc` and `gemxloc` for primary and aqueous complexes.

Subroutine: `../gem/readat.f`

Definition of variables `nxp4` and `nxyp4` was corrected.

5.12.97 **Subroutine difoft.f.** The subroutine `difoft.f` computes aqueous and gaseous diffusion coefficients as a function of temperature at node centers. The subroutine was modified to account for the dependence of tortuosity on porosity for aqueous diffusion according to a phenomenological relation of the form

$$\tau = \tau_0 \left(\frac{\phi}{\phi_0} \right)^n. \quad (47)$$

The diffusive flux has the form

$$J_i^D = -s_l \tau_l \phi D \nabla C_i, \quad (48)$$

in a partially saturated porous medium.

5.9.13 MULTIFLO Code Implementation of Hydration-Dehydration Reactions.

Two new variables `ncpri` and `nprim` are introduced. They have the definition given in Table 2. Water is not included in the transport equations in GEM as it is already accounted for in METRA. The variable `ncpri` was introduced to read in all species in a reaction including water from `database.f`.

Table 2: Definition of variables `nprim` and `ncpri`.

	w/H ₂ O	wo/H ₂ O
<code>ncomp</code>	# of primary species including water	# of primary species
<code>nprim</code>	<code>ncomp-1</code>	<code>ncomp</code>
<code>ncpri</code>	<code>ncomp</code>	<code>ncomp+1</code>

The total reaction rate is calculated in `updtgem.f` at the end of each GEM timestep. The result is stored in the variable `rtot`, which is located in `metragem.h` so it can be used by METRA.

The following code was added to METRA in subroutine `source.f`:

```
c add dehydration rate (positive for release of H2O)
  if(icode.eq.3) then
    do m = 1,nb
      uqh = hwk(m)*rtot(m)
      r(1,m) = r(1,m) - rtot(m)
```

```

      r(3,m) = r(3,m) - uqh
      sume = sume + uqh
      sumw = sumw + rtot(m)
    end do
  end if

```

5.9.16 MULTIFLO Code Implementation of Hydration-Dehydration Reactions [Continued].

The approach to distinguish the number of mass action equations from the number of mass conservation relations through the variable `nprim` was abandoned. Instead `ncomp` is defined always to be the number of primary species minus water if present, and thus is always equal to the number of mass conservation equations. To include the activity of water in mass action equations a new statement will be added of the form:

```

    if (jh2o .gt. 0) then
      prod = prod + shom(jh2o,i) * ah2o(n)
    endif

```

following the calculation of secondary species concentrations wherever it appears in the code. A similar statement is needed for calculation of ion activity products in `kinrxn.f`. The activity of water is presently set to unity, but in the future will be calculated.

5.19.97 Modified METRA to Properly Compute Relative Humidity The routines `updtpsk`, `updtpvk`, and `plots` in METRA were modified to properly compute the relative humidity for the case of a pure gas phase, and for the pure liquid case for which the relative humidity is defined as one—in this case relative humidity is not really defined and could be greater than one. The problem was discovered by Jim Winterle for the pure gas case where he found relative humidities greater than one. For the pure gas case the relative humidity was coming out greater than one because the saturation pressure was not being stored and the value used in `plots` was bogus. This situation was corrected by storing `psat` in `updtpsk` and `updtpvk` as follows:

```

    upsk = psk(tk(m))
    psatk(m) = upsk <---new line

```

```

      if (upsk.le.pk(m) - pak(m) .and.sg(m) .ge.one) then
c          phase change from all gas to 2-ph

```

This change had no effect on the computation other than the value of relative humidity computed in plots. In plots.f the relative humidity is now computed according to

```

      if (one - sg(m) .lt.one) then
        rh = (p(m) - pa(m)) / psatk(m)
      else
        rh = one
      endif

```

The new release of METRA is referred to Version 1.0, May, 1997.

5.20.97 Handling Complete Dry-Out in MULTIFLO. A basic problem encountered with high heat loading of the repository, and for drift scale problems for which complete dry-out can be expected over some limited region surrounding the waste container, is the formation of a pure gas phase region. Presently MULTIFLO requires some aqueous phase to always be present, and it is not possible in the current version to have only a pure gas phase present. This is because the chemical system is defined through primary species which are required to belong to the aqueous phase. However, even if this limitation were not present there would still be the formidable task of describing highly concentrated solutions as they approach complete evaporation of liquid water. To circumvent these difficulties it is proposed to introduce a saturation cutoff to remove control volumes from the set of active nodes in the GEM module. METRA by itself can handle pure liquid or gas regions as well as two-phase regions. The aqueous and solid inventories are stored and removed from active computation until the saturation returns to a value above the cutoff value. Pseudo code for introducing a saturation cutoff is presented below.

```

c-----initialization (assume entire system is initially wet)
      do n = 1, nb
        idry(n) = 1
      enddo

      do n = 1, nb

```

```

c-----saturation cutoff
      if (sat(n) .lt. satcut) then
        idry(n) = 0

c-----store aqueous inventory (note a 2D array is too
c      wasteful of memory--correct this!)
      do j = 1, ncomp
        psistore(j,n) = sat(n)*psi(j,nnn)
      enddo
    endif

      enddo

      do n = 1, nb

c-----check for rewetting
      if (idry(n).eq.0 .and. sat(n).gt.satcut) then
        idry(n) = 1

c-----reload aqueous inventory
      do j = 1, ncomp
        psi(j,nnn) = psistore(j,n)/sat(n)
      enddo
    endif

      enddo

c-----zero residual and set diagonal coefficients to unity in
c      dryout zone in subroutine coefgem.
      if (idry(n) .eq. 0) then
        r(j,n) = zero
        cdl(j,j,n) = one
      endif

c-----shutoff reaction in kanrxn.f and coefrxn.f
      if (idry(n) .eq. 1) then
        ...
      endif

```

5.28.97 Modifications to the MULTIFLO USER's MANUAL.

INITIALIZATION DATA

The Initialization Data constitute the bulk of data file which are specified by the following keywords. The data can be entered in any order except the 'GRID' data should be the first, as it is used to define the memory requirement dynamically (yet to be done!).

The keyword used are:

CONN <--added
CMP2

LIQUID

DEBUg	MONItor
DEPTH	PCKR
DXYZ	PHIK
ENDS	RECUrrent-data
GRID	SOURce
INIT	THERmal

Since the code uses only the first four characters, the rest of the characters in a key word (shown in small case) are used only for a more descriptive identification of the keyword.

The presentation below is in alphabetical order except the GRID keyword which must be the first, as it specifies the problem size to be used for dimensioning purposes.

GRID Keyword
(Required for all Initial Runs)

It defines the grid geometry (radial or cartesian), the size, and other optional parameters.

Read: GRID GEOMTRY NX NY NZ IVPLWR IVPTAB IDIR PREF TREF HREF

GRID = GRID

GEOMTRY = RADIAL for cylindrical geometry.
= XYZ for cartesian geometry.
= UNSTRUCTURED grid for integral finite-volume difference (IFVD)

NX = Number of grid blocks in x or r direction.

NY = Number of grid blocks in y or theta direction.

NZ = Number of grid blocks in z direction.

The variables NX, NY, and NZ are ignored for IFVD grid.
.....

IVPLWR = 1, Lower vapor-pressure of H2O due to capillarity.
= 0, Do not lower the vapor-pressure

IPVTAB = Index for calculating water pvt properties.

= 0, Use correlations for water properties.
= 1, Construct tables using correlations and
then use tables for saturated water, (Recommended).

IPVTAB = 1 not yet available if IVPLWR = 1.

IDIR = 0 D4 ordered direct method will not be used.
 = 1 The direct method may be used. IDIR allocates memory
 for D4-method and must be set to 1 if this method is
 to be used at any time during a run. Declaration of
 IDIR > 0 does not require that this method be used.
 Specification for the solver is specified by SOLVE
 keyword in the recurrent-data.

PREF = Reference pressure for pore compressibility,
 pascals. (default = initial pressure of block (1,1,1)).

TREF = Reference temperature for pore compressibility,
 deg C. (default = initial temperature of block (1,1,1)).

HREF = Reference depth of grid block (1,1,1). That is, specify
 the depth of the first block (top). Other blocks
 depths are computed internally with reference to this
 depth. Note that the depth increases (positive)
 downwards.

=====

CONN Keyword
 (Required for IFVD formulation)

CONN keyword assigns connections between nodes, nodal distances, areas,
and dip-angle between the connecting nodes.

Read: CONN

Read: M1 M2 INC IPRM1 IPRM2 DIST1 DIST2 AREA DIP

CONN = Keyword for reading nodal connection data.

M1,M2 = Begining and ending connected node numbers in increments
of INC. The above read connects the nodes as under:

Node M1 is connected to node M1 + INC, and M1+INC is
connected to node M1+2*INC, and so on. That is, in gneral,
node M1+k*INC is connected to M1+(k+1)*INC. The node-
connection sequence is continued till M1+(k+1)*INC
is greater or equal to M2. Default INC = 1.

IPRM1, = Permeability directions for a pair of connecting nodes.
 IPRM2 The permeability direction is 1, 2, and 3 corresponding
 to x,y, and z-direction permeabilities. The permeability
 values in x,y, and z directions are read by [PHIK]
 keyword.

DIST1, = Distances of nodes to the interface between them. (m)
 DIST2

AREA = Interface area. (m2)

DIP = Angle of line joining the node centers with respect to horizontal.

Example:

```

~ ~ ~ ~ ~ ~ ~
~ ~ ~ ~ ~ ~ ~

```

=====

DEBU Keyword
(Optional)

This keyword prints-out intermediate variables for designated region or grid blocks for debugging or examination purposes. This option should not be used for routine production runs.

Read: DEBU IBUG

if IFVD formulation,

Read: I1 I2 J1 J2 K1 K2

```

. . . . .
. . . . .

```

0

if not IFVD formulation:

read: M1 M2 Inc

```

. . .
. . .

```

0

DEBU = Keyword for printing intermediate variables.

IDBUG = Index designating the level or extent of output.

= 0, turn-off the previously set debug output
 = 1, print minimum amount of debug output.
 = 2, print intermediate level of debug output.
 = 3, print full debug output.

I1,I2 = Indices bounding the region in x (r), y (theta) and
 J1,J2 z-directions for which the requested output will be
 K1,K2 printed.

M1,M2 = Beginning and ending node numbers. Debug output
 and INC will be printed for nodes M1 through M2 in increments
 of INC. Default value of INC = 1. These indices are
 used in the same sense as a conventional 'do loop'
 of Fortran.

Read one region per line and terminate the read-sequence by reading a blank line or a line with one or more zeros.

Since debug can generate a large amount of output, it is desirable to limit this option for a small number of grid blocks and for a limited number of time steps.

Once activated, debug can be deactivated by reading another DEBUG keyword in a Recurrent data set with IBUG = 0, and no other data.

~ ~ ~ ~ ~
~ ~ ~ ~ ~

=====

DXYZ Keyword

(Required for all Initial Runs but not for IFVD)

This keyword designates the sized of grid-blocks in x (r), y (theta), and z directions. It also specifies the choice of grid as to the block-centered (default) or point-distributed.

Read: DXYZ IGRID RW RE

Read: (DX(I), I = 1, NX)

Read: (DY(J), J = 1, NY)

Read: (DZ(K), K = 1, NZ)

~ ~ ~ ~ ~
~ ~ ~ ~ ~

=====

INIT Keyword

INIT keyword read initial pressure, saturation, temperature and mole fractions of component 2 (air). For two-phase region, temperature is used to calculate partial pressure of air-phase which is used as a primary variable for solution.

Read: INIT

if IFVD formulation,

Read: M1 M2 INC P T SG XA SGM

otherwise,

read: I1 I2 J1 J2 K1 K2 P T SG XA SGM

INIT = Keyword for reading initial condition.

I1, I2 = First and last index in x (r) direction

J1, J2 = First and Last index in y (theta) direction

K1, K2 = First and last index in z-direction

M1,M2 = Beginning and ending node numbers. Read P, T, etc.
 and INC for nodes M1 through M2 in increments of INC. Default
 value of INC = 1. These indices are used in the same
 sense as a conventional 'do loop' of Fortran.

These indices define a region for which the
 properties are constant.

P = pressure for the defined region, Pa.

T = Temperature for the defined region, Deg. C.

SG = Gas phase saturation for the defined region, fraction.

XA = Mole fraction of air in the defined region.

SGM = Matrix gas phase saturation for the defined region, fraction.
 This is ignored for a non-ecm system.

~ ~ ~ ~ ~
 ~ ~ ~ ~ ~

=====

PHIK Keyword
 (Required for all Initial Runs)

This keyword assigns rock porosity, permeability, depth, and the
 associated type relative permeability capillary pressure characteristics.

Read: PHIK

if IFVD formulation,

Read: M1 M2 INC IST ITHRM VB POR PERMX PERMY PERMZ PORM PERMM

Otherwise,

Read: I1 I2 J1 J2 K1 K2 IST ITHRM VB POR PERMX PERMY PERMZ PORM PERMM

PHIK = Keyword for reading porosity/permeability data

I1,I2 = First and the last index of a region in x (r) direction.

J1,J2 = First and the last index of a region in y (theta) dir.

K1,K2 = First and the last index of a region in z direction.

M1,M2 = Beginning and ending node numbers. Read the properties
 and INC for nodes M1 through M2 in increments of INC. Default
 value of INC = 1. These indices are used in the same
 sense as a conventional 'do loop' of Fortran.

These indices define a region for which the

The properties of a region bounded by the above indices are defined to be constant.

IST = Characteristic Curve number for relative permeability and capillary pressure. The curve numbers are identified by the sequential numbers read in PCKR data.

ITHRM = Thermal properties data set number read-in by the keyword THERmal. The sequential number of rock thermal properties must be assigned.

~ ~ ~ ~ ~
~ ~ ~ ~ ~

=====

RECURRENT DATA BEGINS

=====

BCONdition Keyword
(Conditional)

BCONdition

This keyword assigns boundary conditions which can be changed at subsequent time interval. The boundary condition include both the Dirichilet and Neumann types.

Read: BCON NBC

if IFVD formulation,

Read: ITYPE M1 M2 INC IPERBC DISTBC AREABC
read: TIMEBC QBC PBC TBC SGBC XABC EMSIVT

otherwise,

Read: ITYPE IFACE I1 I2 J1 J2
read: TIMEBC QBC PBC TBC SGBC XABC EMSIVT

BCON = Keyword for assigning boundary conditions.

NBC = Number of boundary conditions.

ITYPE = Type of Boundary condition.
= 1 Dirichilet (constant field variables)
= 2 Neumann (constant flux)
= 3
= 4

M1,M2 = Begining and ending node numbers. Read the Boundary condition nodes connected to nodes M1 through M2 in increments of INC. Default value of INC = 1. These

indices are used in the same sense as a conventional
'do loop' of Fortran.

IPERBC = Permeability direction (1 <= IPERMBC <= 3).

DISTBC = Distance of nodes from the boundary (m). DISTBC > 0.

AREABC = Flow area between the boundary node and the interior
node M1 through M2 in increments of INC.

IFACE = Surface at which the boundary condition is imposed.

= RIGHT, right face, that is at I = 1 (x = r = 0.)

= LEFT, left face, that is at I = NX.

= TOP, top surface, that is at K = 1.

= BOTTOM, bottom surface, that is at K = NZ.

= FRONT, front surface of the block at J = 1.

= BACK, Back surface of the block at J = NY.

I1,I2 = These indices define the region on the designated
J1,J2 face where the conditions are imposed.

QBC = Flux rate (kg/s/m2), if ITYPE = 2.
= not used if ITYPE = 1.

PBC = Pressure at the designated surface, pa with reference
to the adjacent block center.

~ ~ ~ ~ ~
~ ~ ~ ~ ~

=====

DEBUg Keyword
(Optional)

DEBUg

This keyword prints-out intermediate variables for designated region or
grid blocks for debugging or examination purposes. This option should not
be used for routine production runs.

Read: DEBUg IBUG

If IFVD formulation,

Read: M1 M2 INC

. . .
. . .
0

otherwise,

Read: I1 I2 J1 J2 K1 K2

 0

DEBUg = Keyword for printing intermediate variables.

IDBUG = Index designating the level or extent of output.

= 0, turn-off the debug output

= 1, print minimum amount of debug output.

= 2, print intermediate level of debug output.

= 3, print full debug output.

= 4, special customized output.

M1,M2 = Begining and ending node numbers. Print debug output
 and INC for nodes M1 through M2 in increments of INC. Default
 value of INC = 1. These indices are used in the same
 sense as a conventional 'do loop' of Fortran.

I1,I2 = Indices bounding the region in x (r), y (theta) and
 J1,J2 z-directions for which the requested output will be
 K1,K2 printed.

~ ~ ~ ~ ~
 ~ ~ ~ ~ ~

=====

SOURce Keyword
 (Optional)

This keyword assigns a set of tables for sources and sinks as a function
 of time. These data may be also specified or modified through the
 Recurrent data set which has the identical data format as given below.

Read: SOURce NS SCALH SCALM

If IFVD formulation,

Read: M1 M2 INC ISTYP

otherwise,

Read: IS1 IS2 JS1 JS2 KS1 KS2 ISTYPE

Read: TIMEQ QHT QMT

. . .
 . . .
 0

SOURce = Keyword for assigning source/sink table

NS = Total number of sources and sinks
 SCALH = Scale factor or multiplier to read-in values of QHT
 SCALM = Scale factor or multiplier to read-in values of QMT

IS1,IS2, = Region of the source/sink in the grid
 JS1,JS2,
 KS1,KS2

M1,M2 = Beginning and ending node numbers. Location of Sources/Sinks
 and INC in nodes M1 through M2 in increments of INC. Default
 value of INC = 1. These indices are used in the same
 sense as a conventional 'do loop' of Fortran.

~ ~ ~ ~ ~
 ~ ~ ~ ~ ~

=====
 Mods/additions end.

Sample data for a 10x1x68 grid

=====
 Data for Multiflo simulator (initial data : 2D, 83.4 AML, Yucca Mt.)
 Dec. 27, 1996

RSTART 0

```

:
:   XYZ           = 1 table look-up, pref = ref. press.
:   RADIAL        = 0 correlations,   tref = ref temp.
:   OTHER
:grid geometry   nx ny  nz ivplwr ipvtab iout gravity pref tref href
Grid unstruc     0 0   0 0    1    3    0    0    0    0
:
Pckr                                :relative perm and pc keyword
:  i  type-curv swirm  rpmn(lamda)  alpham  swext  sgc  iecm
:      swirf  rpmf(lamda)  alphaf  phim  phif  permm  permf
:Tiva Canyon (0-100 m)
  1 Van-Gen  0.04   0.3600   8.4e-7    0.    0.    1
              0.04   0.7636   1.305e-5 0.087 1.8e-3 9.7e-19 3.9e-12
:Paintbrush (100-150 m)
  2 Van-Gen  0.10   0.8500   1.53e-6    0.    0.    1
              0.04   0.7636   1.305e-5 0.421 1.8e-3 3.9e-14 3.9e-13
:Topopah Spring (150-475 m)
  3 Van-Gen  0.08   0.4400   5.8e-7    0.    0.    1
              0.04   0.7636   1.305e-5 0.139 1.8e-3 1.9e-18 3.9e-12
:Calico Hills (475-600 m)
  4 Van-Gen  0.11   0.3800   3.13e-7    0.    0.    1
              0.04   0.7636   1.305e-5 0.306 1.8e-3 2.0e-18 3.9e-12
:blank line
:
Thermal-prop
: no rho      cpr  ckdry  cksat   crp  crt   tau  cdiff  cexp  enbd
  1 2.580e+3 728.   1.69  1.69    0    0    .5  2.13e-5 1.8  0.
  2 2.580e+3 422.   0.61  0.61    0    0    .5  2.13e-5 1.8  0.

```

```

3 2.580e+3 840. 2.10 2.10 0 0 .5 2.13e-5 1.8 0.
4 2.580e+3 526. 1.42 1.42 0 0 .5 2.13e-5 1.8 0.
0
PhiK
: m1 m2 inc iist ithrm vb porm permx permy permz
1 680 1 1 1 1.e4
0
Init !init
: m1 m2 inc pm tm sgm x2m
1 680 1 1.e5 25.0 0.5 0.
0
Connections
: m1 m2 inc iperm1 iperm1 d1 d2 area dip
1 10 1 1 1 5. 5. 1000. 0.
11 20 1 1 1 5. 5. 1000. 0.
21 30 1 1 1 5. 5. 1000. 0.
31 40 1 1 1 5. 5. 1000. 0.
41 50 1 1 1 5. 5. 1000. 0.
51 60 1 1 1 5. 5. 1000. 0.
61 70 1 1 1 5. 5. 1000. 0.
71 80 1 1 1 5. 5. 1000. 0.
81 90 1 1 1 5. 5. 1000. 0.
91 100 1 1 1 5. 5. 1000. 0.
101 110 1 1 1 5. 5. 1000. 0.
111 120 1 1 1 5. 5. 1000. 0.
121 130 1 1 1 5. 5. 1000. 0.
131 140 1 1 1 5. 5. 1000. 0.
141 150 1 1 1 5. 5. 1000. 0.
151 160 1 1 1 5. 5. 1000. 0.
161 170 1 1 1 5. 5. 1000. 0.
171 180 1 1 1 5. 5. 1000. 0.
181 190 1 1 1 5. 5. 1000. 0.
191 200 1 1 1 5. 5. 1000. 0.
201 210 1 1 1 5. 5. 1000. 0.
211 220 1 1 1 5. 5. 1000. 0.
221 230 1 1 1 5. 5. 1000. 0.
231 240 1 1 1 5. 5. 1000. 0.
241 250 1 1 1 5. 5. 1000. 0.
251 260 1 1 1 5. 5. 1000. 0.
261 270 1 1 1 5. 5. 1000. 0.
271 280 1 1 1 5. 5. 1000. 0.
281 290 1 1 1 5. 5. 1000. 0.
291 200 1 1 1 5. 5. 1000. 0.
301 310 1 1 1 5. 5. 1000. 0.
311 320 1 1 1 5. 5. 1000. 0.
321 330 1 1 1 5. 5. 1000. 0.
331 340 1 1 1 5. 5. 1000. 0.
341 350 1 1 1 5. 5. 1000. 0.
351 360 1 1 1 5. 5. 1000. 0.
361 370 1 1 1 5. 5. 1000. 0.
371 380 1 1 1 5. 5. 1000. 0.
381 390 1 1 1 5. 5. 1000. 0.
391 400 1 1 1 5. 5. 1000. 0.

```

```

401 410 1 1 1 5. 5. 1000. 0.
411 420 1 1 1 5. 5. 1000. 0.
421 430 1 1 1 5. 5. 1000. 0.
431 440 1 1 1 5. 5. 1000. 0.
441 450 1 1 1 5. 5. 1000. 0.
451 460 1 1 1 5. 5. 1000. 0.
461 470 1 1 1 5. 5. 1000. 0.
471 480 1 1 1 5. 5. 1000. 0.
481 490 1 1 1 5. 5. 1000. 0.
491 500 1 1 1 5. 5. 1000. 0.
501 510 1 1 1 5. 5. 1000. 0.
511 520 1 1 1 5. 5. 1000. 0.
521 530 1 1 1 5. 5. 1000. 0.
531 540 1 1 1 5. 5. 1000. 0.
541 550 1 1 1 5. 5. 1000. 0.
551 560 1 1 1 5. 5. 1000. 0.
561 570 1 1 1 5. 5. 1000. 0.
571 580 1 1 1 5. 5. 1000. 0.
581 590 1 1 1 5. 5. 1000. 0.
591 600 1 1 1 5. 5. 1000. 0.
601 610 1 1 1 5. 5. 1000. 0.
611 620 1 1 1 5. 5. 1000. 0.
621 630 1 1 1 5. 5. 1000. 0.
631 640 1 1 1 5. 5. 1000. 0.
641 650 1 1 1 5. 5. 1000. 0.
651 660 1 1 1 5. 5. 1000. 0.
661 670 1 1 1 5. 5. 1000. 0.
671 680 1 1 1 5. 5. 1000. 0.
: m1 m2 inc iperm1 iperm1 d1 d2 area dip
1 680 10 3 3 20.0 20.0 250. 90.
2 680 10 3 3 20.0 20.0 250. 90.
3 680 10 3 3 20.0 20.0 250. 90.
4 680 10 3 3 20.0 20.0 250. 90.
5 680 10 3 3 20.0 20.0 250. 90.
6 680 10 3 3 20.0 20.0 250. 90.
7 680 10 3 3 20.0 20.0 250. 90.
8 680 10 3 3 20.0 20.0 250. 90.
9 680 10 3 3 20.0 20.0 250. 90.
10 680 10 3 3 20.0 20.0 250. 90.
0
:
:EQUIL 587.50 1.e5 30. 0.0255319 0.0 -1
:
Recurrent-data
:
Skip
Bcon 2
:itype iface i1 i2 j1 j2
1 TOP 1 10 1 1
:time qbc pbc tbc sgbc xabc
0. 0. 8.55e4 15.0 0.2 0.
0
1 BOTTOM 1 10 1 1

```



```

0. 0. 9.05e4 30.0 0.0 0.
0
Noskip
:
:Rstart 1 0
Output C=-1 B=-1 Q=-1
:
:AUTO-step DPMXE DSMXE DTMPMXE DP2MXe TACCEL IAUTODT FAC1
AUTO-step 5.0E+3 0.03 5.0 5.e3 1.e-3 0 0
:
:TOLR TOLP TOLS TOLT TOLP2 TOLM TOLA TOLE rtwtol rmxtol smxtol
Tolr 10. 1.e-4 1.e-3 1.e+1 1.e-5 1.e-3 1.e-3 1.e-20 1.e-20 1.e-20
:
:Limit dpmx dsmx dtmpmx dp2mx dtmn dtmx icutmx
LIMIT 1.e4 .08 10. 1.e5 1.e-6 1.e3
:Plots 1
:Steady[y] 1.e-8 1.e-6 1.e-3
:Ends
: ns fach facm (fach and facm are multipliers to
: read-in values of qht and qmt)
Source 1 .5 1.
: is js ks istyp
: 1 10 1 1 40 40 32
391 400 1 31
: timeq(sec) T/qht (C/(J/s)) qmt (kg/s)
0.00000E+00 1.d4
0
:
:RSTArt 0 1
:
: solve newtnmn newtnmx north nitmx level
Solve 4 1 7 4 100 1
:
:AUTO-step DPMXE DSMXE DTMPMXE DP2MXe TACCEL IAUTO
AUTO-step 1.E+4 0.025 3.0 1.e4 1.e-2 0
:
:TOLR TOLP TOLS TOLT TOLP2 TOLM TOLA TOLE
Tolr 10.e+0 1.e-4 1.e-2 5.e+1 1.e-5 1.e-6 1.e-3 1.e-20 1.e-20 1.e-12
:
:Limit dpmx dsmx dtmpmx dp2mx dtmn dtmx icutmx
LIMIT 5.e4 .05 5. 1.e5 1.e-6 1.e4 5
Plots 1 1 1
380
Time[y] 1.e-8 1.e-8
Time[y] 1.
Ends
Time[y] 10.
Time[y] 100.
Time[y] 500.
Time[y] 1000.
Time[y] 5000.
Time[y] 10000.
Ends

```

BHP COPPER PROJECT

Account Number: **20-8519-001**

Description: Near-field Environment Technical Assistance

Collaborators: G. Wittmeyer

Date Due: Final Report December 22, 1996

Objective: Application of the computer code MULTIFLO to determine how the BHP Copper Florence pilot leaching facility must be designed and operated in order to maximize copper recovery.

No action.

Electronic Scientific Notebook No.
095E:Development of the Code MULTIFLO to
Describe Multiphase Reactive Transport
(12/18/1995 through 04/17/1997)

SCIENTIFIC NOTEBOOK

by

Peter C. Lichtner

Printed: September 22, 1997

1/40

P. C. Lichtner

SCIENTIFIC NOTEBOOK

INITIALS: PCZ

SCIENTIFIC NOTEBOOK

by

Peter C. Lichtner

Southwest Research Institute
Center for Nuclear Waste Regulatory Analyses
San Antonio, Texas

September 22, 1997

2/40

Printed: September 22, 1997

P. C. Lichtner

SCIENTIFIC NOTEBOOK

INITIALS: PC

INITIAL ENTRIES

Scientific NoteBook: # 095

Issued to: P. C. Lichtner

Issue Date: Tuesday, November 16, 1993

Computerized Initials: PC

By agreement with the CNWRA QA this NoteBook is to be printed at approximate quarterly intervals. This computerized Scientific NoteBook is intended to address the criteria of CNWRA QAP-001.

Table 1: Computing Equipment

Machine Name	Type	OS	Location
gravenstein.cnwra.swri.edu	Pentium Workstation	NEXTSTEP	desk Rm A-126
	133 Mhz	Version 3.3	Bldg. 189
	128 MB RAM		
skippy.cnwra.swri.edu	Sun SPARC 20	SOLARIS 5.5	network
	128 MB RAM		

3/40

Contents

INITIAL ENTRIES ii

FIGURES iv

TABLES v

NEAR-FIELD ENVIRONMENT 1

BHP COPPER PROJECT 1

BHP COPPER PROJECT 1

List of Figures

1	Geometry and definition of coordinate system used in the fracture-matrix interaction problem. . .	5
2	Chloride concentration near the waste package for 83 MTU/Acre heat loading.	11
3	The pH near the waste package for 83 MTU/Acre heat loading.	12
4	Comparison of $\text{CO}_{2(g)}$ concentrations for the operator splitting and implicit finite difference algorithms in MULTIFLO after elapsed times of 10, 50 and 100 years. The solid curves refer to operator splitting and the dotted curves to implicit finite difference algorithm.	25
5	Comparison of the pH for the operator splitting and implicit finite difference algorithms in MULTIFLO after elapsed times of 10, 50 and 100 years. The solid curves refer to operator splitting and the dotted curves to implicit finite difference algorithm.	25
6	Comparison of $\text{CO}_{2(g)}$ concentrations for the operator splitting and implicit finite difference algorithms in MULTIFLO. The solid, long-short-dash, and dash-dotted curves refer to the operator splitting algorithm at 10, 50 and 100 years. The dotted curves refer to the implicit finite difference algorithm at the same times.	28
7	Comparison of the pH at 100 years for the operator splitting and implicit finite difference algorithms in MULTIFLO. The solid curve refers to the operator splitting algorithm and the dotted curve to the implicit finite difference algorithm.	28
8	Comparison of the concentration of Na^+ at 100 years for the operator splitting and implicit finite difference algorithms in MULTIFLO. The solid curve refers to the operator splitting algorithm and the dotted curve to the implicit finite difference algorithm.	29
9	The $\text{CO}_{2(g)}$ concentration for operator splitting and implicit finite difference algorithms in MULTIFLO for the case of zero flux at 100 years.	31
10	TPA code results for Run 3.	3
11	Chloride concentration for a recent drift-scale calculation (dotted curve) and that plotted from the file nearfld.res used in the TPA code (solid curve).	3

5/40

Printed: September 22, 1997

P. C. Lichtner

SCIENTIFIC NOTEBOOK

INITIALS:

SCZ

List of Tables

1 Computing Equipment ii

KTI: NEAR-FIELD ENVIRONMENTAccount Number: **20-5708-561**

Description: Near-field Environment Technical Assistance

Collaborators: Dr. R. Pabalan

Collaborators: Dr. C. I. Steefel (Consultant)

Collaborators: Dr. M. Seth (Consultant)

Objective: Application of the computer code MULTIFLO, and submodules GEM and METRA to the Yucca Mountain HLW Repository.

7.2.97 Conversion of mole % to volume fraction using Mathematica. Pabalan provided cement composition in terms of mole % which for use in MULTIFLO must be converted to volume fraction. An assumed porosity of the cement of 30% was used in the conversion.

Mole Percent -> Volume Fraction

Mole percent stored in list w:

wpdt = 41.63;

wcsh=46.84;

whygnt=7.;

whtalct=2.87;

wett=1.65;

w={wpdt,wcsh,whygnt,whtalct, wett} 10⁻²

Check sum to one:

Apply[Plus,w]

{0.4163, 0.4684, 0.07, 0.0287, 0.0165}

0.9999

Molar volume:

vpdt = 33.056;

vcsh=124.10;

```

vhygnt=149.520;
vhytalct=207.57;
vett=569.89;
v={vpdt,vcsh,vhygnt,vhytalct, vett}
{33.056, 124.1, 149.52, 207.57, 569.89}

```

Compute volume fraction (stored in list phi):

```

p = 0.3
nv=(1-p)/(w.v)
0.00716358

```

```

phi=w v nv
{0.0985796, 0.416408, 0.0749769, 0.0426753, 0.0673605}

```

```

Apply[Plus,phi]
0.7

```

```

ans = {0.0986, 0.4164, 0.075, 0.0426, 0.0674};

```

```

Apply[Plus,ans]
0.7

```

Rounded off values:

```

ans = {0.1, 0.42, 0.075, 0.040, 0.065};

```

```

Apply[Plus,ans]
0.7

```

7.4.97 Evaporation from a closed system. The equation describing evaporation from a closed system is simply

$$\frac{d}{dt}(\phi s(t)C(t)) = 0, \quad (1)$$

where ϕ denotes the porosity, $s(t)$ the liquid saturation, and $C(t)$ the solute concentration. The liquid saturation is presumed to be some prescribed function of time. The

solution to this differential equation for constant porosity is given by

$$s(t)C(t) = s_0C_0, \quad (2)$$

with s_0 and C_0 the initial saturation and concentration, respectively. Therefore the change in solute concentration with saturation is equal to

$$C(t) = \frac{s_0}{s(t)}C_0. \quad (3)$$

Thus the concentration enrichment depends only on the initial and final saturation states. With, e.g. $s(t)$ of the form

$$s(t) = s_1 + (s_0 - s_1)e^{-t}, \quad (4)$$

then

$$C(t) = C_0 \frac{s_0}{s_1 + (s_0 - s_1)e^{-t}}. \quad (5)$$

In the limit $t \rightarrow \infty$,

$$\lim_{t \rightarrow \infty} C(t) \rightarrow C_0 \frac{s_0}{s_1}. \quad (6)$$

7.10.97 Drift-scale simulations. A problem with drift scale simulations is accounting for the air gap between the waste package and the drift wall. Heat is transport through the gap by radiation and conduction and possibly convection through the intervening gas phase. However, it is not possible to model convection using Darcy's law without the presence of a solid phase to define the gas permeability.

7.14.97 Fracture-Matrix Interaction. Many circumstances involving fluid flow and transport in natural systems involve flow through fractures accompanied by diffusion into the surrounding rock matrix. This is especially true of Yucca Mountain which consists of highly fractured volcanic tuff. Of interest is the extent to which the rock matrix and fracture fluids are altered by their mutual interaction. As a result of this interaction, mineral products are formed in the matrix and as fracture fillings, possibly causing sealing or opening of the matrix and fractures to further transport of solute species. This situation recently has been investigated by Steefel and Lichtner (1997) for the situation of infiltration of a hyperalkaline fluid emanating from a cementitious barrier into a fracture.

For the geometry shown in Figure 1, flow through a single fracture with simultaneous diffusion into the adjacent rock matrix can be represented by the coupled partial differential equations

$$\frac{\partial C_f}{\partial t} + v_f \frac{\partial C_f}{\partial z} - s_f \phi D \frac{\partial C_m}{\partial x} \bigg|_{x=\delta} = -k s_f (C_f - C_{eq}), \quad (7a)$$

for the fracture, and

$$\frac{\partial}{\partial t} (\phi C_m) - \phi D \frac{\partial^2 C_m}{\partial x^2} = -k s_m (C_m - C_{eq}), \quad (7b)$$

for the matrix, where

- z coordinate along the fracture [L],
- x coordinate perpendicular to fracture [L],
- t time [T],
- v_f groundwater velocity in the fracture [L/T],
- C_f solute concentration in fracture [mole/L³],
- C_m solute concentration in rock matrix [mole/L³],
- ϕ rock matrix porosity [dimensionless],
- k mineral kinetic rate constant [L/T],
- D effective matrix diffusion coefficient [L²/T],
- s_f fracture surface area per unit fracture volume [1/L],
- s_m matrix surface area per unit bulk matrix volume [1/L],

A linear kinetic rate expression is used for the fracture and matrix. The fracture surface area per unit fracture volume is equal to the reciprocal of half the fracture aperture 2δ

$$s_f = \frac{1}{\delta}. \quad (8)$$

The third term on the left-hand side of Eqn.(7a) represents the flux from the matrix into the fracture coupling the fracture and matrix equations. The matrix transport equation is coupled to the fracture equation by the boundary condition

$$C_m(0, t; z) = C_f(z, t), \quad (9)$$

equating the matrix concentration at the wall rock to the concentration in fracture along the entire length of the fracture. For simplicity, pure advective transport is assumed for the fracture equation, and diffusion in the matrix is required to take place

in the direction perpendicular to the fracture. Steefel and Lichtner (1997) consider the general case by solving the transport equations numerically for a multicomponent system.

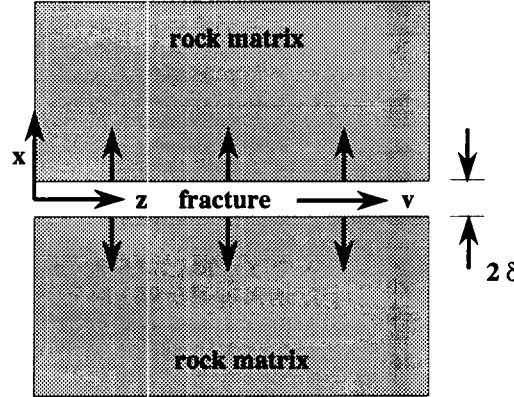


Figure 1: Geometry and definition of coordinate system used in the fracture-matrix interaction problem.

To solve the fracture and matrix transport equations the initial fluid concentrations in the fracture and matrix, and the initial mineral concentration in the matrix must be specified. In addition boundary conditions must be specified at the inlet and outlet to the fracture and at the boundary of the matrix, normally taken as zero concentration gradient at the symmetry plane between two fractures. These conditions can be represented by the equations

$$C_f(z, 0) = C_f^\infty, \quad (10a)$$

$$C_m(x, 0; z) = C_m^\infty, \quad (10b)$$

$$C_f(0, t) = C_f^0, \quad (10c)$$

$$\frac{\partial C_f}{\partial z}(\infty, t) = 0, \quad (10d)$$

$$\frac{\partial C_m}{\partial x}(d/2, t) = 0, \quad (10e)$$

where d denotes the fracture spacing. With these initial and boundary conditions an analytical solution exists to the transient transport equations (Tang, 1981; Steefel and Lichtner, 1997).

To study the qualitative nature of the solution to these equations it is instructive to consider the stationary state solution. To this end the transport equations are first

written in terms of dimensionless independent variables consisting of distances x' and z' and time t' defined as

$$x' = \frac{x}{\delta}, \quad z' = \frac{z}{\delta}, \quad \text{and } t' = \frac{Dt}{\delta^2}. \quad (11)$$

New concentration variables are defined as

$$C'_f = C_f - C_{eq}, \quad (12a)$$

and

$$C'_m = C_m - C_{eq}. \quad (12b)$$

With these new variables the transport equations become

$$\frac{\partial C'_f}{\partial t'} + \text{Pe} \frac{\partial C'_f}{\partial z'} - \frac{\partial C'_m}{\partial x'} \bigg|_{x'=1} = -\text{Da}_f C'_f, \quad (13a)$$

for the fracture, and

$$\frac{\partial C'_m}{\partial t'} - \frac{\partial^2 C'_m}{\partial x'^2} = -\text{Da}_m C'_m, \quad (13b)$$

for the matrix. Dimensionless constants, the Peclet number Pe , and Damköhler numbers Da_f and Da_m , have been introduced defined by

$$\text{Pe} = \frac{v_f \delta}{\phi D}, \quad (14)$$

and

$$\text{Da}_f = \frac{k \delta}{\phi D}, \quad (15a)$$

$$\text{Da}_m = \frac{k s_m \delta^2}{\phi D}. \quad (15b)$$

The two Damköhler numbers are related by the ratio of the matrix and fracture surface areas

$$\text{Da}_m = \frac{s_m}{s_f} \text{Da}_f. \quad (16)$$

The Peclet number and fracture Damköhler number are related by the expression

$$\text{Pe} = \frac{v_f}{k} \text{Da}_f. \quad (17)$$

The stationary state solution, obtained by ignoring the time derivative terms in the transport equations, is given by

$$C'_f(z') = (C_0 - C_{eq}) e^{-z'/\lambda'_f}, \quad (18a)$$

and

$$\begin{aligned} C'_m(x', z') &= C'_f(z') \exp \left[-\frac{x' - 1}{\lambda'_m} \right], \\ &= (C_0 - C_{eq}) \exp \left[-\left(\frac{-z'}{\lambda'_f} + \frac{x' - 1}{\lambda'_m} \right) \right]. \end{aligned} \quad (18b)$$

The boundary conditions are satisfied for both of these expressions provided the fracture spacing is infinite $d \rightarrow \infty$, i.e. only a single fracture is considered. The case of finite fracture spacing is considered in more detail below. The quantities λ'_f and λ'_m refer to dimensionless equilibration lengths in the fracture and rock matrix, respectively. The matrix equilibration length is defined as

$$\lambda'_m = \frac{1}{\sqrt{Da_m}}. \quad (19)$$

The fracture equilibration length also involves λ'_m according to the expression

$$\lambda'_f = \frac{1}{\frac{1}{\lambda_f^{0'}} + \frac{1}{Pe\lambda'_m}}, \quad (20)$$

where $\lambda_f^{0'}$ refers to the fracture equilibration length in the absence of interaction with the matrix

$$\lambda_f^{0'} = \frac{v_f}{k}. \quad (21)$$

As might have been anticipated, a wedge-shaped concentration profile in the matrix is obtained. Remarkable is that the slope of equal concentration contours are given by the simple form as the ratio of the equilibration lengths in the matrix and fracture

$$\text{slope} = \frac{dx}{dz} = \frac{\lambda_m}{\lambda_f}. \quad (22)$$

The slope can be expressed in terms of the dimensionless Peclet and matrix Damköhler numbers as (Steefel and Lichtner, 1997)

$$\frac{dx}{dz} = \frac{1}{Pe} \left(1 + \frac{1}{s_m \delta} \sqrt{Da_m} \right). \quad (23)$$

Even more remarkable is the result that this ratio is independent of the rate constants and surface areas for surface controlled reaction—just the situation for which one might have expected the ratio to depend on the rate constants and surface areas. For the reverse case of transport controlled reaction, the ratio does depend on the rate constants and surface areas. As discussed by Steefel and Lichtner (1997) for a sufficiently large value of the Peclet number the slope becomes zero and the equiconcentration contour lines are parallel to the fracture. This situation is indicative of weak interaction between the fracture and matrix. In the opposite case for $Da_m \gg 1$, the slope approaches a very large number and the equiconcentration contour lines become perpendicular to the fracture. In this case strong coupling exists between the fracture and matrix. In this latter case the dual porosity system consisting of fracture and matrix may be replaced by a single porosity system greatly simplifying the problem.

Finite Fracture Spacing. For finite fracture spacing it is necessary to take into account the no flow boundary condition at the symmetry plane between fractures given by Eqn.(10e). This leads to the following stationary state solution for the matrix

$$C'_m(x', z') = C'_f(z') \frac{\cosh \left[\frac{x' - d/2\delta}{\lambda'_m} \right]}{\cosh \left[\frac{1 - d/2\delta}{\lambda'_m} \right]}, \quad (24)$$

where \cosh denotes the hyperbolic cosine function defined by $\cosh(x) = (e^x + e^{-x})/2$. The fracture coupling term evaluates to

$$\left. \frac{dC'_m}{dx'} \right|_{x'=1} = \frac{1}{\lambda'_m} \tanh \left[\frac{1 - d/2\delta}{\lambda'_m} \right] C'_f(z'), \quad (25)$$

defined in terms of the hyperbolic tangent $\tanh(x) = (e^x - e^{-x})/(e^x + e^{-x})$. For the situation when the matrix equilibration length is much larger than the fracture spacing ($\lambda_m \gg d$), the coupling term reduces to

$$\begin{aligned} \left. \frac{dC'_m}{dx'} \right|_{x'=1} &= \frac{1}{\lambda'_m{}^2} \left(1 - \frac{d}{2\delta} \right) C'_f(z'), \\ &= - \left(\frac{1 - \phi_f}{\phi_f} \right) Da_m C'_f(z'), \end{aligned} \quad (26)$$

where the fracture porosity ϕ_f is defined by

$$\phi_f = \frac{V_f}{V_{REV}} = \frac{2\delta}{d}. \quad (27)$$

Substituting this result into the stationary state fracture transport equation and multiplying through by ϕ_f gives

$$\phi_f v_f \frac{\partial C'_f}{\partial z'} = - [\phi_f Da_f + (1 - \phi_f) Da_m] C'_f, \quad (28)$$

The term in square brackets on the right-hand side will be recognized as the surface area per unit bulk volume of an equivalent porous medium made up of the fracture network and rock matrix. To see this consider a REV of the fracture-matrix equivalent continuum. The total surface area s_{ec} consisting of fracture and matrix surface area can be expressed as

$$\begin{aligned} s_{ec} &= \frac{A_f + A_m}{V_{REV}}, \\ &= \frac{A_f}{V_f} \frac{V_f}{V_{REV}} + \frac{A_m}{V_m} \frac{V_m}{V_{REV}}, \\ &= \phi_f s_f + (1 - \phi_f) s_m, \end{aligned} \quad (29)$$

noting that

$$\begin{aligned} \frac{V_m}{V_{REV}} &= \frac{V_{REV} - V_f}{V_{REV}}, \\ &= 1 - \phi_f. \end{aligned} \quad (30)$$

The flow velocity appearing on the left-hand side of Eqn.(28) will be recognized as the Darcy velocity in the equivalent continuum medium. Thus in the limit when the matrix equilibration length is much larger than the fracture spacing, a description based on the dual fracture-matrix continuum can be replaced by a single continuum in which the mineral surface area is averaged over the fracture and matrix continua. This simplification can also be shown to apply to the transient transport equations in which the porosity in the single continuum transport equation is taken as the average porosity of the fracture network and matrix defined as

$$\phi_{ec} = \phi_f + (1 - \phi_f) \phi_m, \quad (31)$$

with ϕ_m representing the matrix porosity.

7.16.97 Density corrections. It may be necessary to incorporate density corrections into MULTIFLO in the case where large concentrations are produced by evaporation. The density of the fluid can be expressed as

$$\rho = \frac{M}{V}, \quad (32)$$

where the total mass and volume of the fluid are equal to

$$M = M_w + \sum_i M_i, \quad (33)$$

and

$$V = V_w + \sum_i V_i. \quad (34)$$

Writing the density as

$$\rho = \rho_w + \left(\frac{M_w + \sum_i M_i}{V_w + \sum_i V_i} - \rho_w \right), \quad (35)$$

and noting that the quantity in brackets can be written as

$$\left(\frac{M_w + \sum_i M_i}{V_w + \sum_i V_i} - \rho_w \right) = -\rho_w \frac{1}{V} \sum_i V_i, \quad (36)$$

the expression for the density becomes

$$\rho = \rho_w + \sum_i C_i W_i \left(1 - \frac{\rho_w}{\rho_i} \right), \quad (37)$$

where

$$\rho_i = \frac{M_i}{V_i}, \quad (38)$$

and

$$C_i = \frac{M_i W_i^{-1}}{V}. \quad (39)$$

Also note that V_i is calculated from the partial molar volume as

$$V_i = n_i \frac{\partial V}{\partial n_i} = n_i \bar{V}_i. \quad (40)$$

The expression for the density may be simplified for the case when $\rho_i \gg \rho_w$, in which case

$$\rho = \rho_w + \sum_i C_i W_i, \quad (41)$$

$$= \rho_w + \sum_j \Psi_j W_j, \quad (42)$$

where Ψ_j refers to the total component concentration.

7.17.97 Drift scale calculations with MULTIFLO. Shown in Figure 2 is the first drift scale calculation for the chloride concentration and in Figure 3 for the pH. The waste package extends over the region 339.1 m to 340.9 m in the vertical, and from 0 m to 1.9 m horizontally. The drift in which the waste package is placed occupies the region 337.5 m to 342.5 m and 0 m to 2.5 m. The maximum concentration in chloride is located at the top of the drift directly above the waste package.

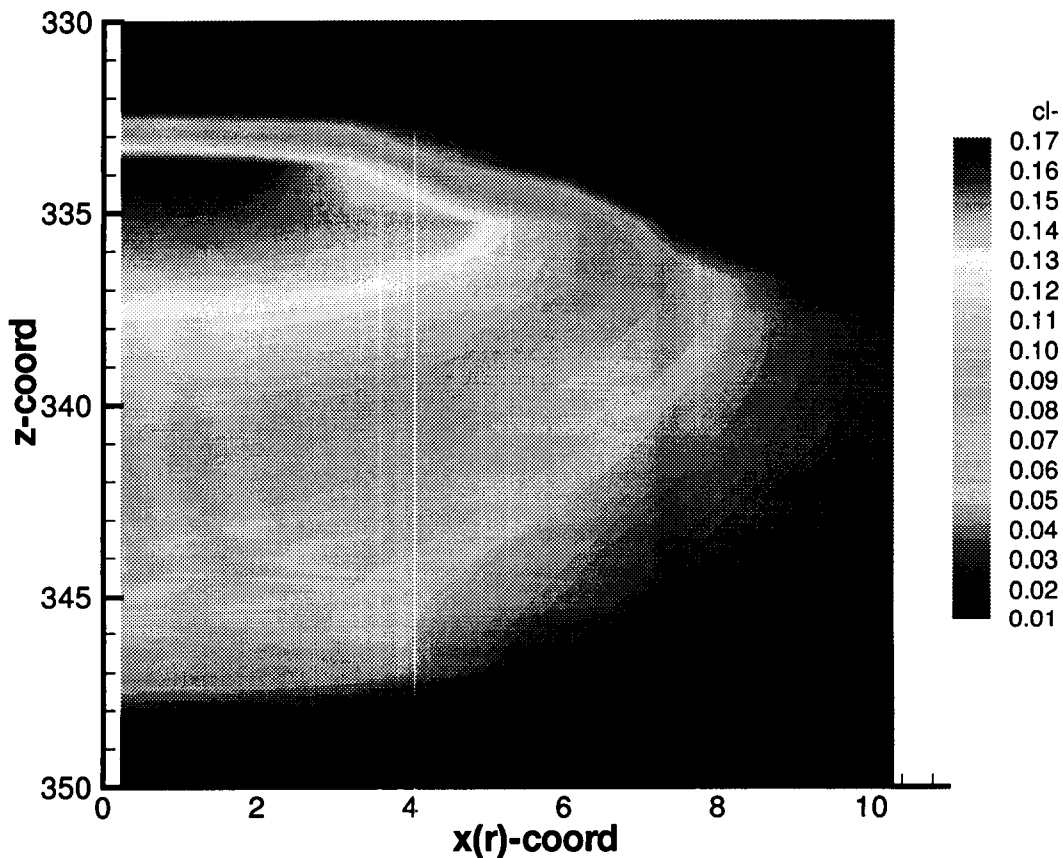


Figure 2: Chloride concentration near the waste package for 83 MTU/Acre heat loading.

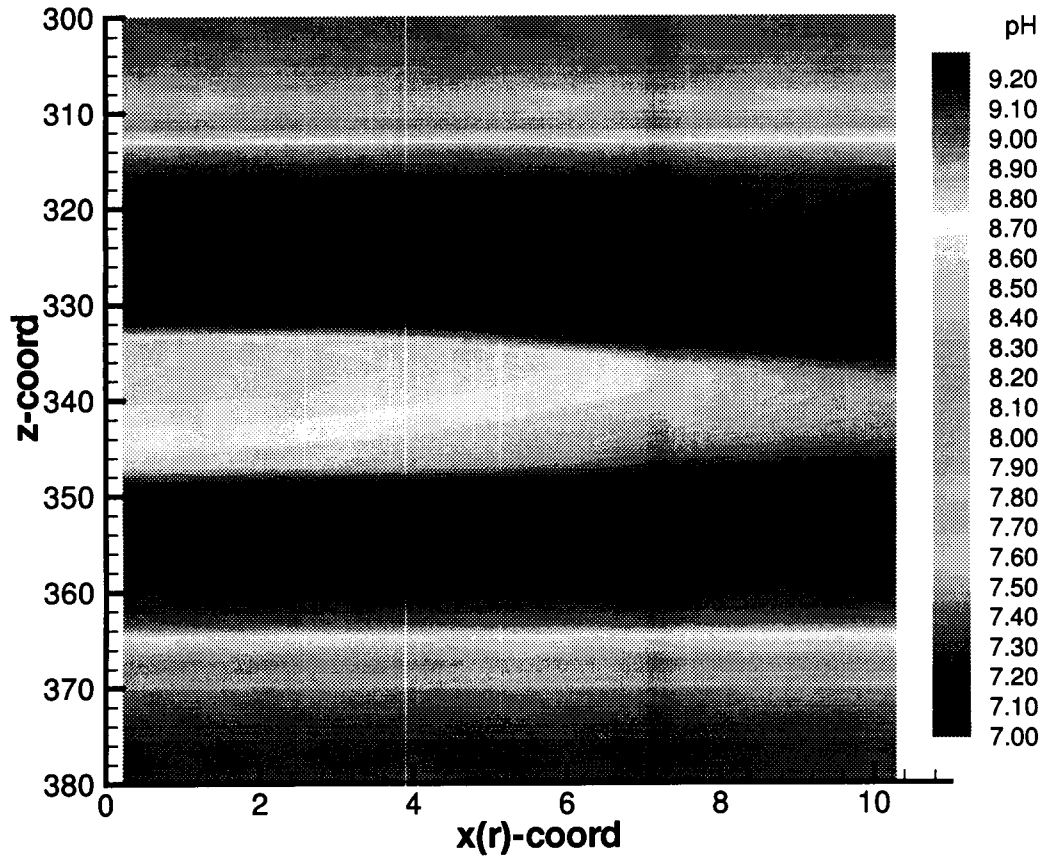


Figure 3: The pH near the waste package for 83 MTU/Acre heat loading.

The input files for gem and metra used in the calculation are as listed below:

Test Data for Multiflo Simulator (Yucca Mt., 1D, 80 kW/acre)

July 22, 1996

```

:
:      geometry nx  ny  nz  mode  iprint idebug
GRID  XYZ      11  1  74    2    0    0
:
OPTS
:  idata istart imod  iexact  iscale  ihrmc
:    0    0    10    0    0    0
:
:  itmax ihalmax ivmax ndamp
:   16    8    0    5
:
:  method iops  ifor  isurf iact  loglin  icon  counr
:    1    0    2    1    1    0    1  1.e3
:
:  isync ipor iperm permfac porfac

```

```

COUPle  0      -1      0      3.      0.
:
PLTFiles
:iplot   a  s  t  m  si  sf  v  z  b  in  e  ex  ti  g  itex
      1  1  1  1  1  0  0  1  0  2  0  0  0  1  0
:
:      tol  ttol  tolneg  tolpos  tolexp  dthalf  qkmax  tolstdst  tolc
TOLR  1.d-10  2.e-3  1.e0  1.e-2  5.d0  .5  590.  1.e-6  1.e-16
:
:      mcyc  cc  c  flx  r  sp  qk  pk  rk  a1  a2  a3
DEBUg  0      1  1  0  1  1  1  1  1
:
:      isat  isothrm  iread  por0  phir  sat  w  lambda  toldelt  tolpor
ISYSem 0      1      0      .10162  1.  0.5  .5  1.  1.e-3  1.e-3
:
:      vx0  vy0  vz0  vgx0  vgy0  vgz0[m/yr]  alphax  alphay  alphaz[m]
FLOW  0.  0.  0.  0.  0.  0.  0.  0.  0.
:
:      d0[cm^2/s]  delhaq[kJ/mol]  dgas[cm^2/s]  dgexp  tortaq  tortg  idif
DIFF  1.d-5  12.6  2.13d-1  1.8  1.d0  1.d0  0
:
:flag 1: T(x)  = d x^3 + a x^2 + b x + c (meters)
:      2: T(x)  = a + (b-a) exp[-((x-x0)/c)^2] + (d - a) * x / xlen
:      3:T(x,t)=a+1/2(b-a)(erf[(x+c-x0)/2sqr(dt)]-erf[(x-c-x0)/2sqr(dt)])
:      p (bars) temp flag  a  b  c  d  x0  xlen
PTINit 1.e5  25.  0  25  300  250  125  1000.  2.d3
:
:master species for controlling time stepping
MASTer h+
:
:grid m 0. 1 200 200.
:
DXYZ
  11*1.
  1.
  74*1.
:
:  isolv level north nitmax idetail rmaxtol rtwotol smaxtol
SOLV  3  1  1  100  0  1.e-20  1.e-20  1.e-12
:
:initial and boundary conditions: 1-conc., 2-flux, 3-zero gradient
:inlet  outlet  nzoneaq
COMP  1  3  3
:
:i1  i2  j1  j2  k1  k2
  1  11  1  1  1  74
:
:species itype guess ctot mineral diffusion
ca+2      1  mol  2.5e-3 blank
na+      1  mol  3.e-3 blank
h+       8  mol  8.0 blank
hco3-    4  mol  -2.99 co2(g)
sio2(aq) 1  mol  1.5e-3 blank

```

```

cl-      -1    mol    2.8e-3  blank
      :blank
0
:
BCON
:bndk
  1
:ibndtyp i1 i2 j1 j2 k1 k2 tmpbc
      3    1    1    1    1    1    74    15.
:species itype guess ctot mineral
ca+2      1    mol    2.5e-3  blank
na+       1    mol    3.e-3    blank
h+        8    mol    8.0      blank
hco3-     4    mol    -2.99    co2(g)
sio2(aq)   1    mol    1.5e-3  blank
cl-      -1    mol    2.8e-3  blank
0
:
:bndk
  2
:ibndtyp i1 i2 j1 j2 k1 k2 tmpbc
      3    1    1    1    1    1    74    15.
:species itype guess ctot mineral
ca+2      1    mol    2.5e-3  blank
na+       1    mol    3.e-3    blank
h+        8    mol    8.0      blank
hco3-     4    mol    -2.99    co2(g)
sio2(aq)   1    mol    1.5e-3  blank
cl-      -1    mol    2.8e-3  blank
0
:
:bndk
  3
:ibndtyp i1 i2 j1 j2 k1 k2 tmpbc
      1    1  11    1    1    1    1    15.
:species itype guess ctot mineral
ca+2      1    mol    2.5e-3  blank
na+       1    mol    3.e-3    blank
h+        8    mol    8.0      blank
hco3-     4    mol    -2.99    co2(g)
sio2(aq)   1    mol    1.5e-3  blank
cl-      -1    mol    2.8e-3  blank
0
:
:bndk
  4
:ibndtyp i1 i2 j1 j2 k1 k2 tmpbc
      1    1  11    1    1    1    1    30.
:species itype guess ctot mineral
ca+2      1    mol    2.5e-3  blank
na+       1    mol    3.e-3    blank
h+        8    mol    8.0      blank
hco3-     4    mol    -2.99    co2(g)

```

P. C. Lichtner

SCIENTIFIC NOTEBOOK

INITIALS: SCZ

```

sio2(aq)  1  mol  1.5e-3  blank
cl-      -1  mol  2.8e-3  blank
0
:
  0 0
:
STOL  1. 1. 1. 1. 1. 1. 1.
:
AQCX
oh-
co2(aq)
co3-2
caco3(aq)
cahco3+
caoh+
cac1+
cac12(aq)
nahco3(aq)
nacl(aq)
naoh(aq)
h3sio4-
h2sio4-2
      :blank
:
MNRL
cristobalite(alpha)
quartz
calcite
tobermorite-14a
chalcedony
halite
      :blank
:
GASEs
co2(g)
      :blank
:
MNIR
:mineral itypkin  npar fkin delh  beta  rka  betb  rkb  rk  tau
:i1 i2 j1 j2 k1 k2  vol  area
cristobalite(alpha) 0 0 1.0  75.  1.0  0.  1.0  0. -16.34 1.e-3
  1 11 1 1 1 74 0.14 1.e1
0
quartz              0 0  1.0  75.  1.0  0.  1.0  0. -17.39 1.e-3
  1 11 1 1 1 74 0.14 1.e1
0
chalcedony          0 0  1.0  75.  1.0  0.  1.0  0. -30.39 1.e-3
  1 11 1 1 1 74 0.61 0.e1
0
calcite             0 0  1.0  35.  1.0  0.  1.0  0. -10.00 1.e-3
  1 11 1 1 1 74 0.  1.
0
tobermorite-14a 0 0  1.0  30.  1.0  0.  1.0  0. -12.00 1.e-3

```

P. C. Lichtner

SCIENTIFIC NOTEBOOK

INITIALS: SCZ

```

1 11 1 1 1 74 0. 10.
0
      :blank
:
:ion-exchange reactions
Ionx  0      1.0
:
BRKP  1
1 1 37
:
DTStep[y]      1 3.e-8
1.e-8          1.e2
:
TIME[y]  7 10. 50. 100. 500. 1000. 5000. 10000.
:
ENDS

Simulation of Yucca Mountain
Drift Scale
:
:
RSTART  0
:
:      XYZ                      = 1 table look-up;; pref = ref. press.
:      RADIAL                  = 0 correlations;   tref = ref temp.
:      OTHER
:
:grid geometry nx ny nz ivplwr ipvtab iout      pref tref href
Grid XYZ      11 1 74 1      0      3      0      0
:
:Monitor 81
:
: *****
:
Pckr                      :relative perm and pc keyword
:  i  type-curve swirm rpmm(lamda) alpham swext sgc      iecm
:      swirf rpmpf(lamda) alphaf phim phif permm permf
: (TCw)
1 Van-Gen 0.021 0.3830 7.907e-7      0.0      0.0      1
          0.040 0.764 1.23e-3 0.087 .0018 2.083e-18 3.9e-12
: (PTn)
2 Van-Gen 0.154 0.578 5.559e-5      0.0      0.0      1
          0.040 0.764 1.40e-3 0.421 .0018 3.879e-14 3.9e-13
: (TSw)
3 Van-Gen 0.045 0.444 1.355e-6      0.0      0.0      1
          0.040 0.764 1.22e-3 0.139 .0018 2.131e-18 3.9e-12
: (TSv)
4 Van-Gen 0.118 0.551 2.193e-7      0.0      0.0      1
          0.040 0.764 1.31e-3 0.065 .0018 9.967e-19 3.9e-12
: (CHnv)
5 Van-Gen 0.097 0.593 2.786e-6      0.0      0.0      1
          0.040 0.764 1.22e-3 0.331 .0018 1.118e-16 3.9e-13
: (CHnz)

```


P. C. Lichtner

SCIENTIFIC NOTEBOOK

INITIALS: PC

```

      6 Van-Gen  0.121  0.414  5.943e-7      0.0      0.0      1
                0.040  0.764  7.30e-4  0.306  .0018  1.617e-18  3.9e-12
:
: *****
: Metal Waste Package
: *****
:      8 Van-Gen  0.0001 0.4400 5.80e-7      0.0      0.0      0
:                0.0001 0.764  1.305e-5  0.0      0.0  0.0e-99  0.0e-99
:
: *****
: Backfill material
: *****
:      7 Van-Gen  0.01   0.700  1.106e-5  0.0      0.0      1
:                0.04   0.764  1.305e-5  0.50   1.8e-3  3.9e-14  3.9e-12
:
: *****
: Air
: *****
:      9 Van-Gen  0.0001  0.4400      1.355e-6      0.0      0.0      1
:                0.0001 0.764  1.22e-3  0.139  .0018  2.131e-18  3.9e-12
:
: *****
: Fracture
: *****
:      10 Van-Gen  0.080  0.4400      5.8e-7      0.0      0.0      1
:                 0.040  0.764  1.305e-5  0.139  1.8e-3  1.0e-12  1.0e-12
:
0      : blank line to end pckr data
:
: *****
: Debug options
: *****
:Debug  1
:0
:
: *****
: Thermal properties
: *****
:
Thermal-prop
: no rho      cpr      ckdry  cksat      crp  crt      tau  cdiff  cexp  enbd
1  2.580e+03 728.      1.69   2.23      0    0      .5  2.13e-5  1.8  0.
2  2.580e+03 422.      0.61   0.81      0    0      .5  2.13e-5  1.8  0.
3  2.580e+03 840.      2.10   2.78      0    0      .5  2.13e-5  1.8  0.
4  2.580e+03 948.      1.28   1.69      0    0      .5  2.13e-5  1.8  0.
5  2.580e+03 488.      0.84   1.11      0    0      .5  2.13e-5  1.8  0.
6  2.580e+03 526.      1.42   1.88      0    0      .5  2.13e-5  1.8  0.
7  2.580e+03 1.e+6    1.69   2.23      0    0      .5  2.13e-5  1.8  0.
:
: *****
: Air
: *****
:

```

P. C. Lichtner

SCIENTIFIC NOTEBOOK

INITIALS: SCZ

```

      8 1.2      57.4      20.0 20.0      0      0      .5 2.13e-5 1.8 0.
:
: *****
: Metal Waste Package
: *****
:
: 9 7.800e+03 450.0      50.0 50.0      0      0      .5 2.13e-5 1.8 0.
:
: *****
: Backfill material
: *****
:
: 8 2.580e+03 840.0      0.25 0.49      0      0      .5 2.13e-5 1.8 0.
:
: *****
: Fracture
: *****
:
: 11 2.580e+03 840.0      2.10 2.78      0      0      .5 2.13e-5 1.8 0.
:
0
: *****
: Define size of grid-blocks
: *****
:
: COND
:
:      igrd      rw      re
DXYZ      0
: (dx(i),i=1,nx)
0.4500 0.4500 0.5333 0.5333 0.5333 1.417 1.417 1.417 1.417 1.417
1.417
: (dy(j),j=1,ny)
1.
: (dz(k),k=1,nz)
23.75 23.75 23.75 23.75 13.25 13.25 13.25 13.25 15.00 15.00
15.00 15.00 15.00 15.00 15.00 15.00 6.667 6.667 6.667 6.667
6.667 6.667 3.667 3.667 3.667 3.667 3.667 3.667 1.500 1.500
1.500 1.500 1.500 0.5333 0.5333 0.5333 0.9000 0.9000 0.5333 0.5333
0.5333 1.000 1.000 1.000 1.000 1.000 2.500 2.500 2.500 2.500
2.500 6.800 6.800 6.800 6.800 6.800 10.00 10.00 10.00 10.00
10.00 10.00 10.00 10.00 4.000 4.000 20.25 20.25 20.25 20.25
30.25 30.25 30.25 30.25
:
PhiK
: i1 i2 j1 j2 k1 k2 iist ithrm vb por permx permy permz pormm permm
1 11 1 1 1 1 1 7 0. : TCw
1 11 1 1 2 4 1 1 0. : TCw
1 11 1 1 5 8 2 2 0. : PTn
1 11 1 1 9 64 3 3 0. : TSw
1 11 1 1 65 66 4 4 0. : TSv
1 11 1 1 67 70 5 5 0. : CHnv
1 11 1 1 71 74 6 6 0. : CHnz

```

P. C. Lichtner

SCIENTIFIC NOTEBOOK

INITIALS: SCZ

```

:
: NOTE: Drift, Waste, & Backfill have the rock properties (iist)
:       of TSw (3) but their own thermal properties. Residual saturation
:       of drift reduced so it can dry out.
:
: 1  5  1  1  8 14 9 10 0.      : Drift
: 1  2  1  1 10 13 3  9 0. 0. 0. 0. 0. : Waste Package
: 1  5  1  1 14 14 3  8 0.      : Backfill/Pedestal/Floor
: 1  8  1  1 23 23 6  6 1.e12     : Sink for water
:
: 1  5  1  1 33 40 3  8 0.      : Drift
: 1  2  1  1 36 37 3  9 0.      : WP
0
:
Init  init
: i1 i2 j1 j2 k1 k2 pm tm sgm x2m
: 1 11 1 1 1 74 1.e5 25.0 0.5 0.
: 0
:
:       depth pdepth tdepth tgrad param iequil
: Equil 684. 101325. 20. 0. 0. -1
:
Recurrent
:
Bcon 2
: itype iface i1 i2 j1 j2
3      TOP 1 11 1 1
: time qbc pbc tbc sgbc xabc
: 0. 0.0003 8.55e4 15.0 0.2 0.
0
: itype iface i1 i2 j1 j2
1      BOTTOM 1 11 1 1
: 0. 0. 9.05e4 30.0 0.001 0.
0
:
: SKIP
: Source 1 0.0208 1.
Source 1 0.016443 1.
: is1 is2 js1 js2 ks1 ks2 istyp
: 1 11 1 1 1 1 12
: NOTE - infiltration rate calculated as kg/(s-m^3) -
: per unit pore volume.
: timeq(sec) T/qht (C/(J/s)) qmt (kg/s)
: 0 13.05 4.5966e-9 !2.91E-9
: 1.e40 13.05 4.5966e-9 !2.91E-9
: 0
: Power decay data from Randy Manteufel, 4/25/96
: is js ks istyp
: 1 2 1 1 36 37 32
: timeq(sec) T/qht (C/(J/s)) qmt (kg/s)
: 0.3156E+06 0.8469E+04
: 0.9467E+07 0.8423E+04
: 0.1578E+08 0.8391E+04

```

0.3156E+08	0.8314E+04
0.3541E+08	0.8296E+04
0.3973E+08	0.8276E+04
0.4458E+08	0.8253E+04
0.5002E+08	0.8228E+04
0.5612E+08	0.8199E+04
0.6297E+08	0.8168E+04
0.7065E+08	0.8131E+04
0.7927E+08	0.8089E+04
0.8894E+08	0.8043E+04
0.9979E+08	0.7993E+04
0.1120E+09	0.7937E+04
0.1256E+09	0.7876E+04
0.1410E+09	0.7810E+04
0.1582E+09	0.7737E+04
0.1775E+09	0.7658E+04
0.1991E+09	0.7572E+04
0.2234E+09	0.7477E+04
0.2507E+09	0.7355E+04
0.2813E+09	0.7224E+04
0.3156E+09	0.7084E+04
0.3541E+09	0.6936E+04
0.3973E+09	0.6780E+04
0.4458E+09	0.6615E+04
0.5002E+09	0.6443E+04
0.5612E+09	0.6250E+04
0.6297E+09	0.6029E+04
0.7065E+09	0.5802E+04
0.7927E+09	0.5571E+04
0.8894E+09	0.5326E+04
0.9979E+09	0.5059E+04
0.1120E+10	0.4793E+04
0.1256E+10	0.4541E+04
0.1410E+10	0.4298E+04
0.1582E+10	0.4002E+04
0.1775E+10	0.3675E+04
0.1991E+10	0.3393E+04
0.2234E+10	0.3126E+04
0.2507E+10	0.2880E+04
0.2813E+10	0.2666E+04
0.3156E+10	0.2464E+04
0.3541E+10	0.2273E+04
0.3973E+10	0.2093E+04
0.4458E+10	0.1925E+04
0.5002E+10	0.1767E+04
0.5612E+10	0.1623E+04
0.6297E+10	0.1523E+04
0.7065E+10	0.1429E+04
0.7927E+10	0.1339E+04
0.8894E+10	0.1255E+04
0.9979E+10	0.1179E+04
0.1120E+11	0.1107E+04
0.1256E+11	0.1036E+04

P. C. Lichtner

SCIENTIFIC NOTEBOOK

INITIALS: SCZ

```

0.1410E+11  0.9655E+03
0.1582E+11  0.8926E+03
0.1775E+11  0.8164E+03
0.1991E+11  0.7463E+03
0.2234E+11  0.6821E+03
0.2507E+11  0.6231E+03
0.2813E+11  0.5691E+03
0.3156E+11  0.5179E+03
0.3541E+11  0.4650E+03
0.3973E+11  0.4174E+03
0.4458E+11  0.3746E+03
0.5002E+11  0.3361E+03
0.5612E+11  0.3016E+03
0.6297E+11  0.2713E+03
0.7065E+11  0.2519E+03
0.7927E+11  0.2339E+03
0.8894E+11  0.2172E+03
0.9979E+11  0.2049E+03
0.1120E+12  0.1961E+03
0.1256E+12  0.1877E+03
0.1410E+12  0.1797E+03
0.1582E+12  0.1719E+03
0.1775E+12  0.1630E+03
0.1991E+12  0.1545E+03
0.2234E+12  0.1465E+03
0.2507E+12  0.1389E+03
0.2813E+12  0.1317E+03
0.3156E+12  0.1247E+03
0
:
:NOSKIP
:
Output  A=1  C=1
:
:  isolv  newtnmn  newtnmx
Solve 2      2      7      2
:
:          DPMXE    DSMXE  DTMPMXE  DP2MXE
AUTO-step  5.e+3    0.025   5.0      1.e4    1.e-2    0
:
:          TOLP  TOLS  TOLT  TOLP2  TOLM  TOLA  TOLE
Tolr  1.e+1  1.e-4  1.e-2  5.e+1  1.e-5  1.e-6  1.e-3  1.e-20  1.e-20  1.e-12
:
:          dpmx    dsmx  dtmpmx  dp2mx  dtmn  dtmx  icutmx
LIMIT  1.e4    .05    10.    5.e4  1.e-7  1.e5
:
:          target  dt    dpmx    dsmx    dp2mx    dtmpmx
:
:          print all at every target time
PLOTS 1 1 1
397
rstart 1 0
:skip

```

```

:Time[y] 1.e-5
:Time[y] 1.0
Time[y] 10.0
Time[y] 50.0
Time[y] 100.0
Time[y] 500.0
Time[y] 1.e3
Time[y] 5.e3
Time[y] 1.e4
:noskip
:
:STEADY[y] 1.e-6 1.e-4 1.e-4
Ends

```

9.22.97 **Scaling relations to determine sensitivity to kinetic rate constants and dispersivity.** To investigate the sensitivity of the results to changes in the kinetic rate constants, surface area and tortuosity or diffusivity, consider a general scale transformation of the time and space coordinates of the form

$$t' = at, \quad (43)$$

and

$$x' = bx. \quad (44)$$

A field variable \mathcal{F} may be shown to obey the transformation law

$$\mathcal{F}(x, t; \frac{b^2}{a}D, \frac{1}{a}k) = \mathcal{F}(\frac{x}{b}, \frac{t}{a}; D, k), \quad (45)$$

where \mathcal{F} stands for the solute concentration or porosity. This relation holds provided the initial and boundary conditions remain invariant under the scale transformation. The transformation results in scaled diffusivity and rate constants, D' and k' , related to the constants a and b by

$$D' = \frac{b^2}{a}D, \quad (46)$$

and

$$k' = \frac{1}{a}k. \quad (47)$$

It follows that, conversely, the scale factors a and b may be expressed in terms of the old and new diffusivity and rate constants by the equations

$$a = \frac{k}{k'}, \quad (48)$$

and

$$b = \sqrt{\frac{D' k}{D k'}}. \quad (49)$$

If τ_0 represents the time for the porosity to become zero at distance ξ_0 with diffusivity D and rate constant k , then for scaled diffusivity D' and rate constant k' , sealing takes place at time τ'_0 and distance ξ'_0 related to τ_0 and ξ_0 by

$$\tau'_0 = \frac{k}{k'} \tau_0, \quad (50)$$

and

$$\xi'_0 = \sqrt{\frac{D' k}{D k'}} \xi_0. \quad (51)$$

The significance of these results is that varying the diffusivity does not affect the time, but only distance. Varying the kinetic rate constant affects both time and distance. According to these relations, for example, reducing the diffusivity and kinetic rate constants each by a factor of 100, requires a 100 times longer time span for sealing to occur, but the distance where sealing occurs remains the same.

Account Number: **20-5708-562**

Description: Near-field Environment Code Development – MULTIFLO

Collaborators: Dr. M. Seth (Consultant)

Objective: Development of the computer code MULTIFLO, and submodules GEM and ME-TRA.

7.9.97 Bugs in massbal.f corrected. Two bugs in the subroutine massbal.f were corrected. These changes did not affect any of the results of MULTIFLO except for the total mass in place. The corrections involved changing the order of the nodal do-loops and multiplying by the factor 1.d3 to correct for $\text{dm}^3 \rightarrow \text{m}^3$ conversion. The corrected code segment is as follows:

```

do kz=1,nz
  do jy=1,ny
    do ix=1,nx
      n = n + 1
      nnn = ix+jghst(jy)+kghst(kz)
      suma = suma+por(n)*sat(n)*psi(j,nnn)*voln(n)*1.d3
      sumg = sumg+por(n)*(one-sat(n))*psig(j,nnn)*voln(n)*1.d3
      if (j.le.nex) sumx = sumx+cec*xex(j,n)/z(j)*voln(n)*1.d3
    enddo
  enddo
enddo

```

8.1.97 Comparison of Operator Splitting and Implicit Finite Difference Algorithms. A discrepancy was found between the operator splitting and implicit finite difference algorithms applied to the repository scale model for Yucca Mountain. At present the reason for this discrepancy is not known. The comparison is shown in Figure 4 for $\text{CO}_{2(g)}$ and Figure 5 for the pH. There is considerable discrepancy between the two algorithms.

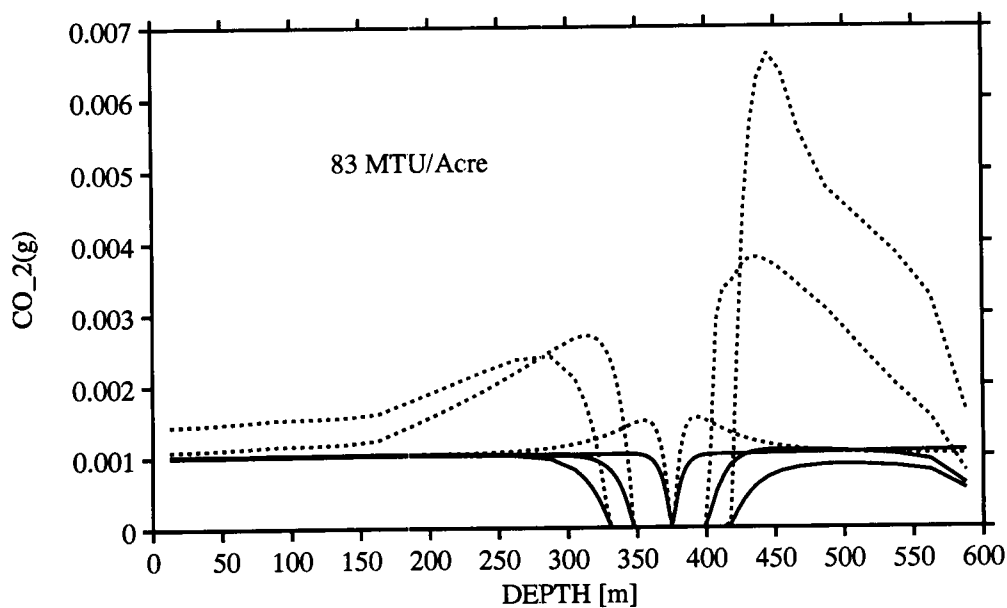


Figure 4: Comparison of $\text{CO}_2(g)$ concentrations for the operator splitting and implicit finite difference algorithms in MULTIFLO after elapsed times of 10, 50 and 100 years. The solid curves refer to operator splitting and the dotted curves to implicit finite difference algorithm.

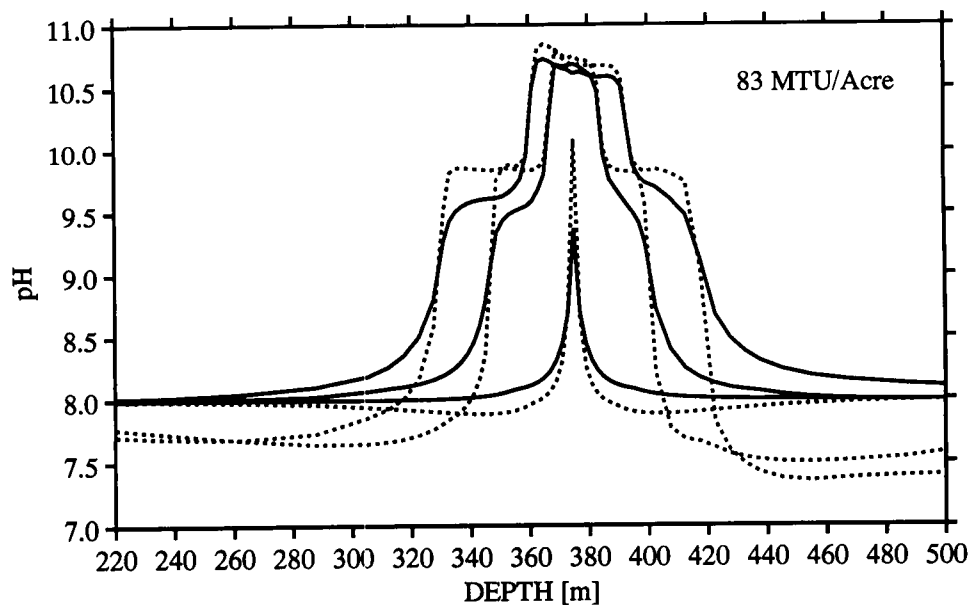


Figure 5: Comparison of the pH for the operator splitting and implicit finite difference algorithms in MULTIFLO after elapsed times of 10, 50 and 100 years. The solid curves refer to operator splitting and the dotted curves to implicit finite difference algorithm.

For the simple case of a single component system with the reaction



the finite difference equations may be solved analytically in the absence of transport. In this case

$$\frac{d}{dt} [\phi (s_l C_l + s_g C_g)] = 0. \quad (53)$$

Gas and liquid concentrations are related by a temperature-dependent constant

$$C_g = K(T) C_l. \quad (54)$$

In finite difference form for constant porosity the differential equation becomes

$$s_l^{t+\Delta t} C_l^{t+\Delta t} + s_g^{t+\Delta t} C_g^{t+\Delta t} = s_l^t C_l^t + s_g^t C_g^t. \quad (55)$$

This yields

$$C_l^{t+\Delta t} = \frac{s_l^t C_l^t + s_g^t C_g^t}{s_l^{t+\Delta t} + K(T_{t+\Delta t}) s_g^{t+\Delta t}}. \quad (56)$$

The gas concentration is then given by

$$C_g^{t+\Delta t} = K(T_{t+\Delta t}) C_l^{t+\Delta t}. \quad (57)$$

8.4.97

Flux boundary conditions. Flux boundary conditions were added to GEM to allow simulation of infiltration. The flux is specified in the input file through the flow rate v_0 . The flux at the boundary is then set equal to

$$J = -\phi s D \frac{\partial C}{\partial x} + v_0 C = v_0 C_0, \quad (58)$$

where C_0 is the computed inlet concentration. In finite difference form this equation becomes

$$-\phi s D \frac{C_1 - C_{-1}}{\Delta x} + v_0 C_b = v_0 C_0, \quad (59)$$

where C_b is the unknown boundary concentration. Alternatively,

$$-\phi s D \frac{C_1 - C_b}{\Delta x/2} + v_0 C_b = v_0 C_0. \quad (60)$$

Equating these expressions leads to ghost node concentration C_{-1}

$$C_{-1} = 2C_b - C_1. \quad (61)$$

This gives the boundary concentration as

$$C_b = \frac{\frac{2\phi s D}{\Delta x} C_1 + v_0 C_0}{\frac{2\phi s D}{\Delta x} + v_0}. \quad (62)$$

From this expression the ghost node concentration is obtained

$$C_{-1} = \frac{\frac{2\phi s D}{\Delta x} C_1 + v_0(2C_0 - C_1)}{\frac{2\phi s D}{\Delta x} + v_0}. \quad (63)$$

The derivative is equal to

$$\frac{\partial C_{-1}}{\partial x} = \left[\frac{\frac{2\phi s D}{\Delta x} - v_0}{\frac{2\phi s D}{\Delta x} + v_0} \right] \frac{\partial C_1}{\partial x}. \quad (64)$$

8.11.97

Reference to [8.1.97] Comparison of Operator Splitting and Implicit Finite Difference Algorithms. A discrepancy was found between the operator splitting and implicit finite difference algorithms applied to the repository scale model for Yucca Mountain. It was determined that the operator splitting algorithm is fundamentally flawed for two-phase flow with variable saturation. This was demonstrated by performing the transport step with the saturation held constant over the time step. The new comparison is shown in Figure 6. While not perfect, it is much closer than the previous result. The remaining differences are presumed due to differences inherent in the operator splitting algorithm, and not due to bugs or programming. It should be noted that the implicit finite difference algorithm also may introduce significant numerical dispersion. The Na^+ profile is not as good as previously obtained which gave identical agreement [not shown].

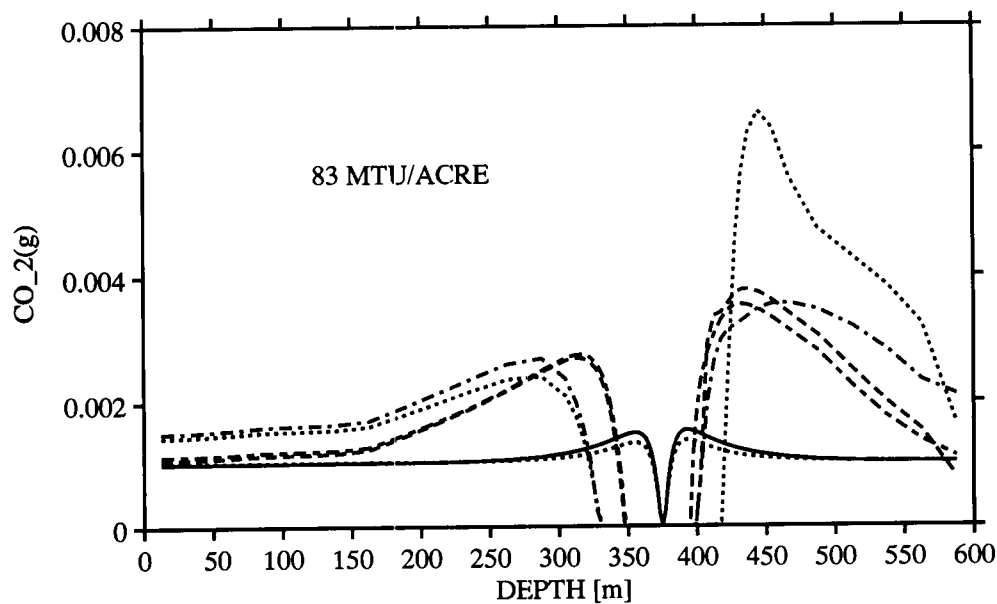


Figure 6: Comparison of $\text{CO}_2(g)$ concentrations for the operator splitting and implicit finite difference algorithms in MULTIFLO. The solid, long-short-dash, and dash-dotted curves refer to the operator splitting algorithm at 10, 50 and 100 years. The dotted curves refer to the implicit finite difference algorithm at the same times.

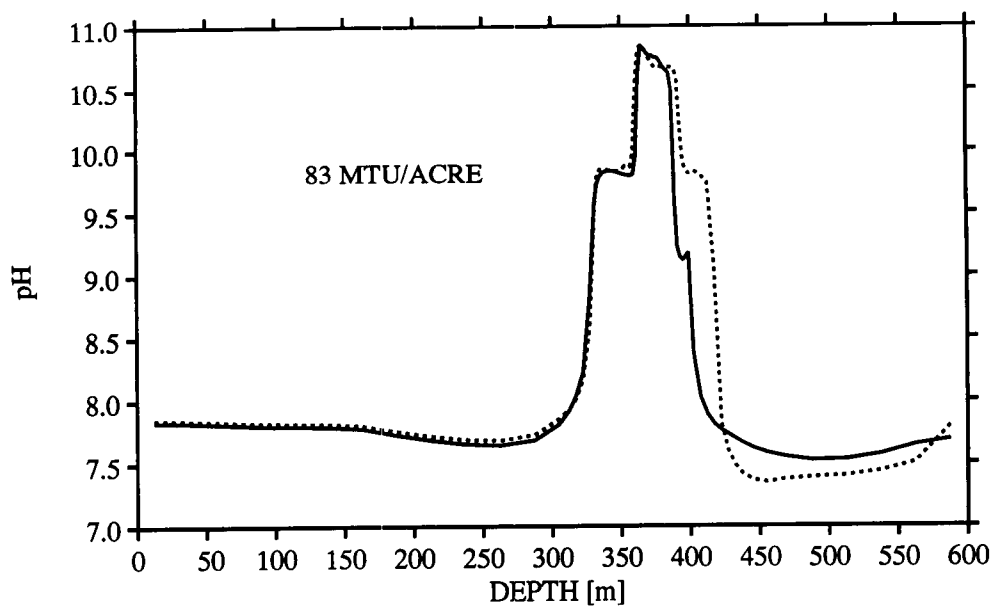


Figure 7: Comparison of the pH at 100 years for the operator splitting and implicit finite difference algorithms in MULTIFLO. The solid curve refers to the operator splitting algorithm and the dotted curve to the implicit finite difference algorithm.

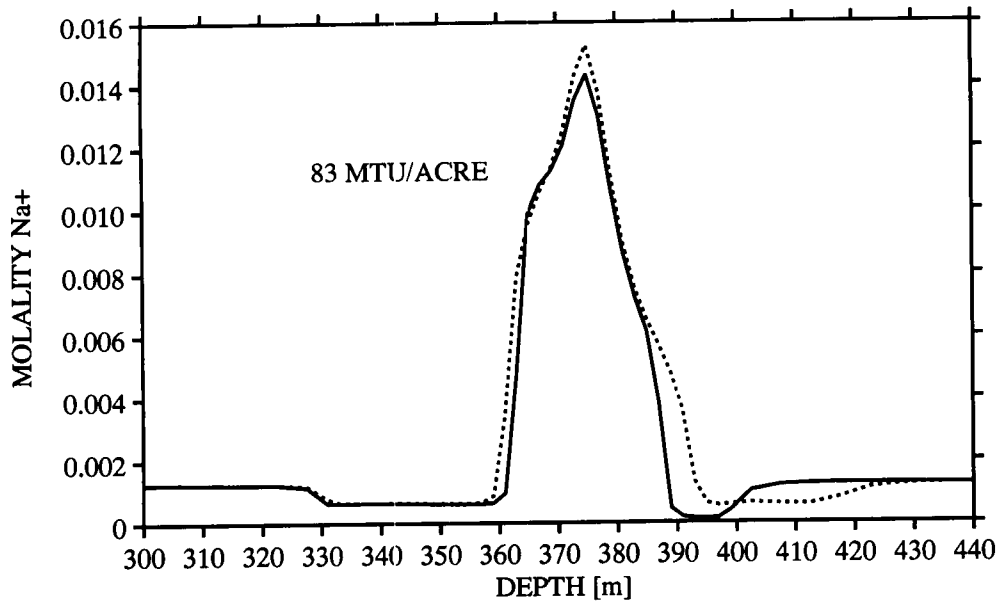


Figure 8: Comparison of the concentration of Na^+ at 100 years for the operator splitting and implicit finite difference algorithms in MULTIFLO. The solid curve refers to the operator splitting algorithm and the dotted curve to the implicit finite difference algorithm.

The difficulties with operator splitting applied to two-phase flow with variable saturation can be seen as follows. The complete transport equations are given by

$$\frac{\partial}{\partial t} [\phi (s_l \Psi_j^l + s_g \Psi_j^g)] + \nabla \cdot (\Omega_j^l + \Omega_j^g) = - \sum_m \nu_{jm} I_m. \quad (65)$$

In operator splitting form this equation is split as

$$\frac{\partial}{\partial t} (\phi s_l \Psi_j^l) + \nabla \cdot \Omega_j^l = 0, \quad (66)$$

and

$$\frac{\partial}{\partial t} (\phi s_g \Psi_j^g) + \nabla \cdot \Omega_j^g = 0, \quad (67)$$

representing independent liquid and gas phase transport steps, and

$$\frac{\partial}{\partial t} [\phi (s_l \Psi_j^l + s_g \Psi_j^g)] = - \sum_m \nu_{jm} I_m, \quad (68)$$

for the reaction step. For the “Gedanken” calculation in which the system is considered to be closed (i.e. zero flux throughout the system) the operator splitting equations become

$$\frac{\partial}{\partial t} (\phi s_l \Psi_j^l) = 0, \quad (69)$$

$$\frac{\partial}{\partial t} (\phi s_g \Psi_j^g) = 0, \quad (70)$$

for the transport step, and

$$\frac{\partial}{\partial t} [\phi (s_l \Psi_j^l + s_g \Psi_j^g)] = 0, \quad (71)$$

for the reaction step. Clearly these equations are incompatible, since only the sum of gaseous plus aqueous concentrations is conserved and not the individual concentrations. One possibility around this is to hold the saturation fixed in the nonreactive transport step. This gives the correct result for the case of zero flux. However, this approach is valid only for a closed system. For the case of a nonvolatile species such as Na^+ , the correct transport step must include variable saturation according to Eqn.(66). There does not appear to be any way to satisfactorily satisfy the transport equations for aqueous-gaseous and aqueous-aqueous interacting species within the operator splitting formulation.

9.10.97 Reference to [8.1.97] Comparison of Operator Splitting and Implicit Finite Difference Algorithms. To further investigate problems encountered with operator splitting and two-phase flow a comparison was made with the implicit formulation for the $\text{CO}_{2(g)}$ concentration with zero flux. The results were found to be identical. The discrepancy is thus assumed to lie in the difference in treatment of the flux terms between the two approaches. For nonvolatile species it follows that

Transport Step:

$$\frac{\partial}{\partial t} (\phi s_l \Psi_j^l) + \nabla \cdot \Omega_j^l = 0 \quad (72)$$

$$\hat{\Psi}_j^l = \left(\frac{s_l}{s_l'} \right) \Psi_j^l - \frac{\Delta t}{\phi s_l'} \Delta \Omega_j^l \quad (73)$$

Reaction Step:

$$\frac{\partial}{\partial t} (\phi s_l \Psi_j^l) = - \sum_m \nu_{jm} I_m \quad (74)$$

$$\begin{aligned} \Psi_j^{l'} &= \hat{\Psi}_j^l - \frac{\Delta t}{\phi s_l'} \sum_m \nu_{jm} I_m \\ &= \left(\frac{s_l}{s_l'} \right) \Psi_j^l - \frac{\Delta t}{\phi s_l'} \left(\Delta \Omega_j^l + \sum_m \nu_{jm} I_m \right) \end{aligned}$$

36/40

This approach appears to correctly handle nonvolatile species also. Thus it remains an open question why the operator splitting algorithm does not give the same result as the implicit finite difference when the flux is nonzero.

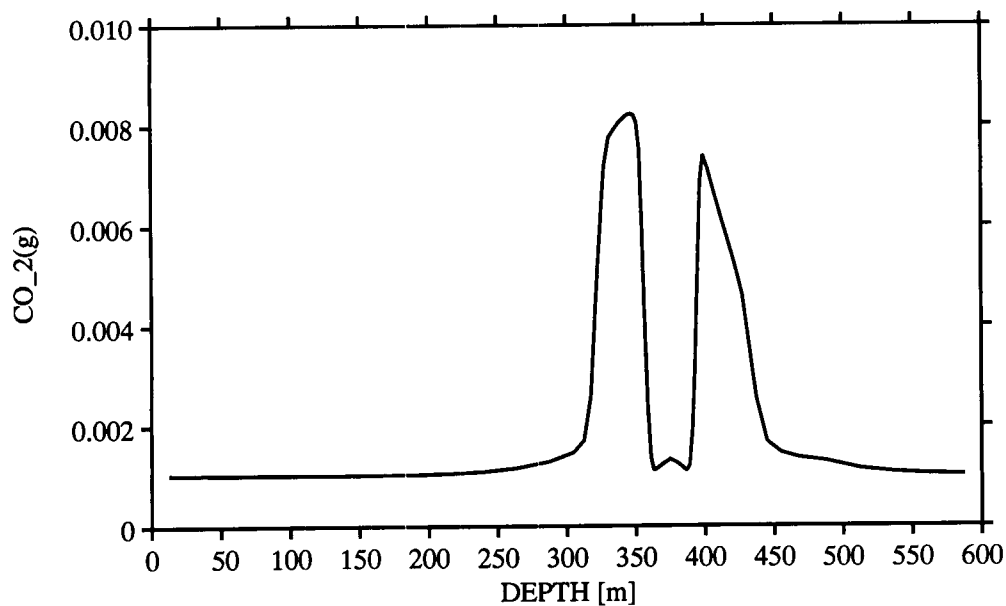


Figure 9: The $\text{CO}_{2(g)}$ concentration for operator splitting and implicit finite difference algorithms in MULTIFLO for the case of zero flux at 100 years.

P. C. Lichtner

SCIENTIFIC NOTEBOOK

INITIALS: SC

TPA-97

Account Number: 20-8519-001

Description: TPA Code Testing

PI: Sitakanta Mohanty

Date Due:

Objective: Carry out tests of the TPA code.

8.15.97 File: /u02/lichtner_u02/TPA/run1/tpa.inp. The output file ebsrel.res contains numbers less than $1.e-99$. For Cm246 the values were found:

nuclide name = Cm246

time step	time	ciperyrinsaintoloweruz
1	0.0000E+00	0.0000E+00
2	2.3102E+01	0.0000E+00
3	4.6744E+01	0.0000E+00
4	7.0940E+01	0.0000E+00
174	5.3077E+04	1.5706E-14
175	5.4343E+04	1.2586E-15
176	5.5638E+04	9.8517E-26
177	5.6964E+04	1.0433E-56
178	5.8321E+04	1.7443E-89
179	5.9709E+04	1.5707-124
180	6.1130E+04	1.5758-157
181	6.2584E+04	9.4956-190
182	6.4073E+04	1.4526-220
183	6.5596E+04	2.5027-252
184	6.7154E+04	1.7648E-17
185	6.8750E+04	2.3755E-16
186	7.0382E+04	1.9829E-16
199	9.5433E+04	2.8188E-16
200	9.7690E+04	3.7857E-16
201	1.0000E+05	3.8428E-16

8.16.97 Run 2:

The parameter ChlorideMultFactor was modified to

```
*loguniform
constant
ChlorideMultFactor
1000.0, 100.0
```


The job did not finish but hanged in uzft. This was probably due to attempting to run the computation to 100,000 years.

```
|skippy:/u02/lichtner_u02/TPA> tpa.e
=====
exec: Welcome to TPA Version 3.1beta3
=====
Specified Global Parameters:

      NumberOfRealizations = 1
      NumberOfSubareas = 1
      MaximumTime[yr] = 100000.
      Volcanism scenario = 0 (yes=1, no=0)
      Faulting scenario = 0 (yes=1, no=0)
      Seismic scenario = 0 (yes=1, no=0)

The specified path for data and codes = $TPA3_1BETA3/

**To modify global parameters or the path, stop code execution using control-C**
.....
      subarea 1 of 1          realization 1 of 1
.....
exec: calling uzflow
exec: calling nfenv
exec: calling ebsfail
      ebsfail: time of WP failure = 3061.6 yr
exec: failed WPs from INITIAL event = 794 at time = 0.0 yr
exec: failed WPs from CORROSION event = 7148 at time = 3061.6 yr
      *** failed WPs: all WPs failed ***
exec: calling ebsrel
Note: the following IEEE floating-point arithmetic exceptions
occurred and were never cleared; see ieee_flags(3M):
Inexact; Underflow;
Sun's implementation of IEEE arithmetic is discussed in
the Numerical Computation Guide.
      Highest release rates from Sub Area 1
      Tc99 4.0317E+01 [Ci/yr/SA] at 4.483E+03 yr
      Am243 1.8595E+01 [Ci/yr/SA] at 1.900E+04 yr
      Ni59 7.7762E+00 [Ci/yr/SA] at 4.483E+03 yr
      Np237 2.6692E+00 [Ci/yr/SA] at 4.483E+03 yr
      C14 2.5523E+00 [Ci/yr/SA] at 4.483E+03 yr
      U234 2.3919E+00 [Ci/yr/SA] at 4.093E+04 yr
exec: calling uzft
```

8.21.97 Run 3: Ran the revised beta 4 version to 60,000 and 100,000 years. Job completed in 3055 seconds for 60,000 years and for 100,000 years the run took 4402.699 seconds. Chloride multiplication factor was set to 1000. A single realization was computed with a single subarea. Slightly different results were obtained depending on whether the final time set was 60,000 (solid curve) or 100,000 years (dashed curve).

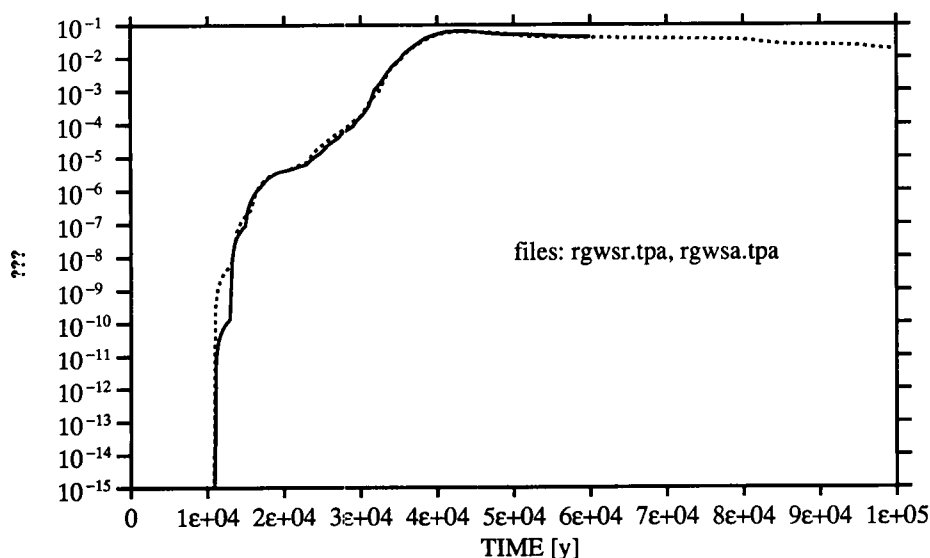


Figure 10: TPA code results for Run 3.

The file `nearfld.res` defining near-field environment variables was compared with more recent preliminary calculations for the chloride concentration using a drift scale model (See Scientific Notebook [7.17.97]). The results are shown in the accompanying Figure (11).

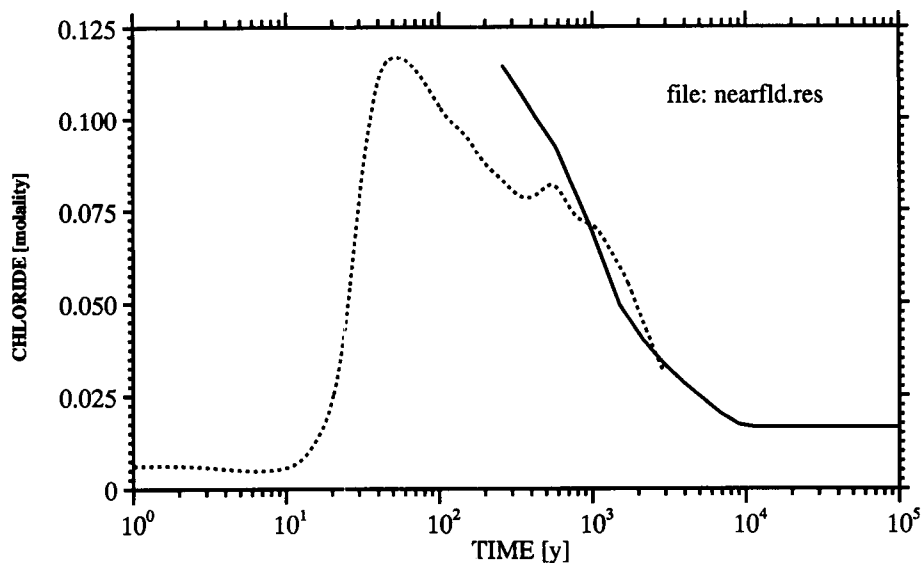


Figure 11: Chloride concentration for a recent drift-scale calculation (dotted curve) and that plotted from the file `nearfld.res` used in the TPA code (solid curve).

40/40

P. C. Lichtner

SCIENTIFIC NOTEBOOK

INITIALS: PC

BHP COPPER PROJECT

Account Number: **20-8519-001**

Description: Modeling In Situ Leaching of Copper

Collaborators: G. Wittmeyer

Date Due: Final Report December 22, 1996

Objective: Application of the computer code MULTIFLO to determine how the BHP Copper Florence pilot leaching facility must be designed and operated in order to maximize copper recovery.

No action.

SCIENTIFIC NOTEBOOK

by

Peter C. Lichtner

Printed: January 4, 1998

P. C. Lichtner

SCIENTIFIC NOTEBOOK

INITIALS:

PC

SCIENTIFIC NOTEBOOK

by

Peter C. Lichtner

**Southwest Research Institute
Center for Nuclear Waste Regulatory Analyses
San Antonio, Texas**

January 4, 1998

P. C. Lichtner

SCIENTIFIC NOTEBOOKINITIALS: PCZ**INITIAL ENTRIES**

Scientific NoteBook: # 095

Issued to: P. C. Lichtner

Issue Date: Tuesday, November 16, 1993

Computerized Initials: PCZ

By agreement with the CNWRA QA this NoteBook is to be printed at approximate quarterly intervals. This computerized Scientific NoteBook is intended to address the criteria of CNWRA QAP-001.

Table 1: Computing Equipment

Machine Name	Type	OS	Location
gravenstein.cnwra.swri.edu	Pentium Workstation	NEXTSTEP	desk Rm A-126
	133 Mhz	Version 3.3	Bldg. 189
	128 MB RAM		
skippy.cnwra.swri.edu	Sun SPARC 20	SOLARIS 5.5	network
	128 MB RAM		

TABLE OF CONTENTS

INITIAL ENTRIES	ii
FIGURES	iv
TABLES	v
NEAR-FIELD ENVIRONMENT: TECHNICAL ASSISTANCE	1
[10.15.97]	1
[12.12.97]	7
NEAR-FIELD ENVIRONMENT: CODE DEVELOPMENT	32
[11.18.97]	32
ChangeLog MULTIFLO	32
TPA-97	35
GAS RESEARCH INSTITUTE	36
[11.5.97]	36
[12.23.97]	49
BHP COPPER PROJECT	61

LIST OF FIGURES

- 1 Dual continuum stationary state solution for the nonreactive case. Fracture concentration is represented by the solid curve and matrix concentration by the thick dashed curve. See text for explanation of parameters used in the calculation. 25
- 2 Dual continuum stationary state solution for the nonreactive case. Fracture concentration is represented by the solid curve and matrix concentration by the thick dashed curve. See text for explanation of parameters used in the calculation. 25
- 3 Dual continuum stationary state solution for the nonreactive case. Fracture concentration is represented by the solid curve and matrix concentration by the thick dashed curve. Single continuum results for matrix and fracture are exhibited by the short- and long-dashed curves, respectively. See text for explanation of parameters used in the calculation. 26
- 4 Dual continuum stationary state solution. Fracture concentration is represented by the solid curve and matrix concentration by the thick dashed curve. Single continuum results for matrix and fracture are exhibited by the short- and long-dashed curves, respectively. See text for explanation of parameters used in the calculation. 28
- 5 Dual continuum stationary state solution. Fracture concentration is represented by the solid curve and matrix concentration by the thick dashed curve. Single continuum results for matrix and fracture are exhibited by the short- and long-dashed curves, respectively. See text for explanation of parameters used in the calculation. 29
- 6 Dual continuum stationary state solution. Fracture concentration is represented by the solid curve and matrix concentration by the thick dashed curve. Single continuum results for matrix and fracture are exhibited by the short- and long-dashed curves, respectively. See text for explanation of parameters used in the calculation. 29
- 7 Grid for DCM showing connections indicated by the double arrows. Even nodes correspond to matrix blocks and odd nodes to fractures. 30

LIST OF TABLES

1	Computing Equipment	ii
2	Parameters used for the analytical stationary state solutions.	27
3	Diffusion coefficients for a selected set of species in an aqueous solution at 25°C and infinite dilution. Values taken from Newman (1991) and Oelkers and Helgeson (1988).	41
4	Parameter Values	51

NEAR-FIELD ENVIRONMENT

Account Number: **20-1402-561**

Description: Near-field Environment Technical Assistance

Collaborators: Dr. R. Pabalan

Collaborators: Dr. C. I. Steefel (Consultant)

Collaborators: Dr. M. Seth (Consultant)

Objective: Application of the computer code MULTIFLO, and submodules **GEM** and **METRA** to the Yucca Mountain HLW Repository.

10.15.97 Microbial Reactions in MULTIFLO. A formulation of incorporating microbial reactions into MULTIFLO was investigated based on a mechanistic approach.

Modeling Biomass Synthesis and Biodegradation Processes

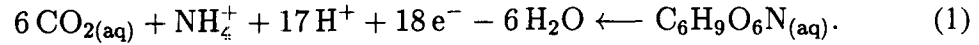
An excellent introduction into the field of microbially induced processes has been given by Rittmann and VanBriesen (1996). They derive overall reactions for biomass synthesis resulting from biodegradation reactions based on H_3NTA as the electron-donor primary substrate. Two different electron-acceptor substrates $\text{O}_{2(aq)}$ and NO_3^- are considered by the authors. In addition to these other important electron-acceptor primary substrates include SO_4^{2-} , $\text{CO}_{2(aq)}$ and Fe^{3+} .

The approach used by Rittmann and VanBriesen (1996) is somewhat cumbersome in that mass- rather than mole-based measures are used to represent organic substances. Their approach complicates the derivation of overall reactions describing biomass synthesis. The discussion presented here provides a unified treatment of organic reactions coupled to the usual aqueous acid-base, complexing, and mineral reactions employing mole-based quantities.

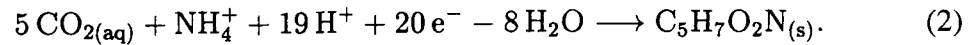
A important feature of many biologically induced reactions is that they are strictly irreversible. As a consequence these reactions do not go to equilibrium. The reactions stop when either all donor or acceptor substrate material or biomass is completely devoured (i.e. completely utilized).

Rittmann and VanBriesen (1996) present a derivation of overall reactions governing biomass synthesis based on considerations of molecular biology at the cell level. Bac-

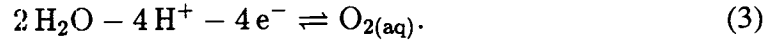
teria oxidize the electron-donor substrate to produce NADH (nicotinamide adenine dinucleotide). With H_3NTA ($\text{C}_6\text{H}_9\text{O}_6\text{N}_{(\text{aq})}$) as primary electron-donor substrate 18 electrons are transferred according to the reaction



Biomass synthesis with biomass represented as $\text{C}_5\text{H}_7\text{O}_2\text{N}_{(\text{s})}$ results in the transfer of 20 electrons

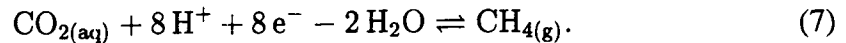
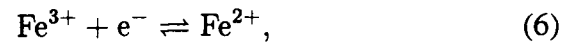
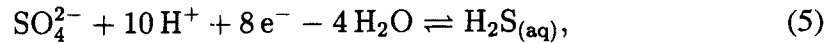
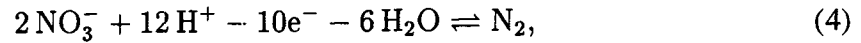


With oxygen as the electron acceptor substrate, 4 electrons are transferred



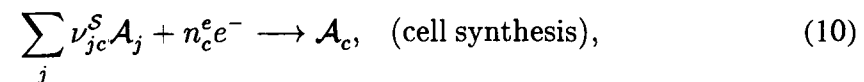
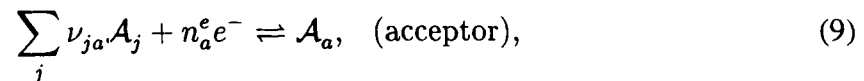
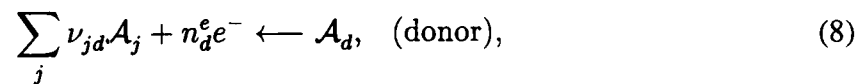
The overall reaction for biomass synthesis is derived by combining these reactions to balance electrons taking into account intra-cell process.

Electron acceptors other than oxygen may be involved in biomass synthesis. For example, reaction (3) may be replaced by any one of the reactions



These reactions may occur simultaneously or individually depending on the nature of geochemical system. Within a flow column they may occur in different, possibly overlapping, regions along the flow path.

In terms of a given set of primary species $\{\mathcal{A}_j\}$ excluding electron donor \mathcal{A}_d and acceptor \mathcal{A}_a species, the reactions for oxidation of the primary electron-donor substrate, reduction of the primary electron-acceptor substrate, and biomass synthesis can be written as half-cell reactions in the general form



where \mathcal{A}_c represents biomass. A fourth reaction describes biomass decay expressed as the overall reaction

$$\nu_{ac}^{\mathcal{D}} \mathcal{A}_a + \sum_j \nu_{jc}^{\mathcal{D}} \mathcal{A}_j \leftarrow \mathcal{A}_c. \quad (11)$$

Note that the electron donor primary substrate does not appear in this reaction as it involves a transfer of electrons to the acceptor substrate.

The transfer of electrons from the electron donor substrate must be conserved by cell processes of synthesis and respiration generating more biomass and energy. If the quantity f_s° represents the fraction of electrons going to biomass synthesis, then the fraction of electrons for respiration providing energy is

$$f_e^\circ = 1 - f_s^\circ. \quad (12)$$

The overall reaction for biomass synthesis is constructed from a linear combination of reactions (8), (9) and (10) with weighting factors f_s° and f_e° . This may be accomplished by first writing these reactions in terms of a single electron

$$\frac{1}{n_d^e} \mathcal{A}_d - \frac{1}{n_d^e} \sum_j \nu_{jd} \mathcal{A}_j \longrightarrow e^-, \quad (13)$$

$$\frac{1}{n_a^e} \mathcal{A}_a - \frac{1}{n_a^e} \sum_j \nu_{ja} \mathcal{A}_j \rightleftharpoons e^-, \quad (14)$$

$$\frac{1}{n_c^e} \mathcal{A}_c - \frac{1}{n_c^e} \sum_j \nu_{jc}^{\mathcal{S}} \mathcal{A}_j \longleftarrow e^-. \quad (15)$$

Combining these reactions with weighting factors f_s° and f_e° according to

$$\mathcal{R}_{13} - f_e^\circ \mathcal{R}_{14} - f_s^\circ \mathcal{R}_{15}, \quad (16)$$

yields the following overall reaction for biomass synthesis

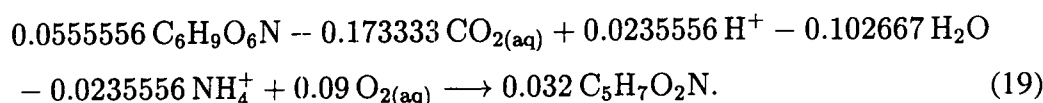
$$\frac{1}{n_d^e} \mathcal{A}_d - \frac{1 - f_s^\circ}{n_a^e} \mathcal{A}_a + \sum_j \left[\frac{f_s^\circ}{n_c^e} \nu_{jc}^{\mathcal{S}} + \frac{1 - f_s^\circ}{n_a^e} \nu_{ja} - \frac{1}{n_d^e} \nu_{jd} \right] \mathcal{A}_j \longrightarrow \frac{f_s^\circ}{n_c^e} \mathcal{A}_c. \quad (17)$$

The true yield \mathcal{Y}_c^d for biomass synthesis is defined as the ratio of the rate of cell production to the rate of donor substrate utilization

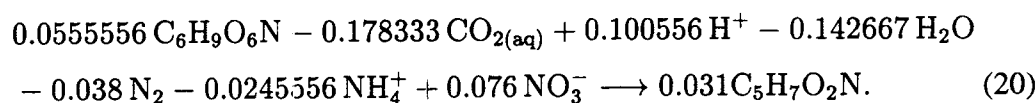
$$\mathcal{Y}_c^d = f_s^\circ \frac{n_d^e}{n_c^e}, \quad (18)$$

proportional to the electron transfer coefficient and the ratio of electrons transferred in the donor and biomass synthesis reactions. The biomass yield is a function of both the biomass synthesis reaction and electron donor substrate as well as the electron synthesis factor f_s° .

With oxygen as the electron acceptor substrate, and taking $f_s^\circ = 0.64$, $n_c^e = 20$, $n_d^e = 18$, and $n_a^e = -4$, this reaction becomes



The yield \mathcal{Y} has the value $\mathcal{Y} = 0.576$. Using as electron acceptor NO_3^- with $f_s^\circ = 0.62$ gives



For this reaction the yield \mathcal{Y} has the value $\mathcal{Y} = 0.558$.

Reactions (19) and (20) are linearly independent provided the intra-cell electron synthesis factor f_s° is different for different electron acceptors. Otherwise the reactions are linearly dependent. Provided local equilibrium prevails within the aqueous phase between different redox couples, not necessarily a good approximation for these systems, reactions based on different electron-acceptor substrates with equal intra-cell electron factors f_s° are linearly dependent and as a consequence their stoichiometry does not play a role in the transport equations, their rates being additive. Only if disequilibrium of redox couples is provided does the stoichiometry of the overall reaction come into play.

Kinetic Rate Law. Introducing the yield, reaction (17) can be written as

$$\frac{1}{\mathcal{Y}_c^d} \mathcal{A}_d - \frac{1 - f_s^\circ}{f_s^\circ} \frac{n_c^e}{n_a^e} \mathcal{A}_a + \sum_j \left[\nu_{jc}^s + \frac{1 - f_s^\circ}{f_s^\circ} \frac{n_c^e}{n_a^e} \nu_{ja} - \frac{1}{\mathcal{Y}_c^d} \nu_{jd} \right] \mathcal{A}_j \longrightarrow \mathcal{A}_c, \quad (21)$$

in which the stoichiometric coefficient multiplying biomass is normalized to unity. The kinetic rate law for biomass synthesis is presumed to be adequately described by the Monod rate law

$$I_c = k_c \chi_c \frac{C_d}{K_d + C_d} \frac{C_a}{K_a + C_a}, \quad (22)$$

for single acceptor and donor substrates with concentrations C_a and C_d , respectively, and where k_c represents the rate constant and χ_c denotes the concentration of cells. Note that an affinity factor, present in mineral precipitation and dissolution reactions, is absent from the rate law. The rate law describing biomass decay is assumed to be first order of the form

$$I_c^D = -\lambda_c \chi_c, \quad (23)$$

where λ_c denotes the decay constant.

Mass Transport Equations. To set up the mass transport equations the first step is to identify an appropriate set of primary and secondary species to represent the reactions taking place in the particular system at hand. The primary electron donor substrate must be chosen as primary species as well as at least one on the primary electron acceptor substrates. If redox reactions are described through kinetic rate laws then all electron acceptors become primary species. On the other hand if redox reactions are represented by local equilibrium constraints, perhaps catalyzed by the presence of bacteria, then only one electron acceptor can be chosen as primary species, with the remaining electron acceptors included as aqueous secondary species. In addition to the biomass synthesis reaction (21) and decay reaction (11), and possibly electron acceptor equilibria, other reactions including homogeneous reactions

$$\nu_{di}^{aq} \mathcal{A}_d + \nu_{ai}^{aq} \mathcal{A}_a + \sum_j \nu_{ji}^{aq} \mathcal{A}_j \rightleftharpoons \mathcal{A}_i, \quad (24)$$

and mineral precipitation and dissolution reactions

$$\nu_{di}^{min} \mathcal{A}_d + \nu_{ai}^{min} \mathcal{A}_a + \sum_j \nu_{jm}^{min} \mathcal{A}_j \rightleftharpoons \mathcal{M}_m, \quad (25)$$

must also be accounted for in a geochemical system. In these reactions allowance is made for participation by both the electron donor and acceptor substrates. For the set of primary species $\{\mathcal{A}_d, \mathcal{A}_a, \mathcal{A}_j\}$, the mass transport equations have the following

form for primary species

$$\hat{\mathcal{L}}C_d = -\frac{1}{\mathcal{Y}_c^d} I_c^{\mathcal{S}} - \sum_i \nu_{di}^{aq} I_i^{aq} - \sum_m \nu_{dm}^{min} I_m^{min}, \quad (26)$$

$$\hat{\mathcal{L}}C_a = \frac{1-f_s^o}{f_s^o} \frac{n_c^e}{n_a^e} I_c^{\mathcal{S}} + \nu_{ac}^{\mathcal{D}} \lambda_c \chi_c - \sum_i \nu_{ai}^{aq} I_i^{aq} - \sum_m \nu_{am}^{min} I_m^{min}, \quad (27)$$

$$\begin{aligned} \hat{\mathcal{L}}C_j = & - \left[\nu_{jc}^{\mathcal{S}} + \frac{1-f_s^o}{f_s^o} \frac{n_c^e}{n_a^e} \nu_{ja} - \frac{1}{\mathcal{Y}_c^d} \nu_{jd} \right] I_c^{\mathcal{S}} + \nu_{jc}^{\mathcal{D}} \lambda_c \chi_c \\ & - \sum_i \nu_{ji}^{aq} I_i^{aq} - \sum_m \nu_{jm}^{min} I_m^{min}, \end{aligned} \quad (28)$$

for secondary species

$$\hat{\mathcal{L}}C_i = I_i^{aq}, \quad (29)$$

for biomass

$$\frac{\partial \chi_c}{\partial t} = I_c^{\mathcal{S}} - \lambda_c \chi_c, \quad (30)$$

and finally for minerals

$$\frac{\partial \phi_m}{\partial t} = \bar{V}_m I_m^{min}. \quad (31)$$

The mineral reaction rates are denoted by I_m^{min} , and the homogeneous aqueous reaction rates by I_i^{aq} .

Reaction rates for homogeneous equilibria I_i^{aq} may be eliminated by replacing the corresponding transport equations with mass action equations. This results in the primary species transport equations

$$\hat{\mathcal{L}}\Psi_d = -\frac{1}{\mathcal{Y}_c^d} I_c^{\mathcal{S}} - \sum_m \nu_{dm}^{min} I_m^{min}, \quad (32)$$

$$\hat{\mathcal{L}}\Psi_a = \frac{1-f_s^o}{f_s^o} \frac{n_c^e}{n_a^e} I_c^{\mathcal{S}} + \nu_{ac}^{\mathcal{D}} \lambda_c \chi_c - \sum_i \nu_{ai}^{aq} I_i^{aq} - \sum_m \nu_{am}^{min} I_m^{min}, \quad (33)$$

$$\hat{\mathcal{L}}\Psi_j = - \left[\nu_{jc}^{\mathcal{S}} + \frac{1-f_s^o}{f_s^o} \frac{n_c^e}{n_a^e} \nu_{ja} - \frac{1}{\mathcal{Y}_c^d} \nu_{jd} \right] I_c^{\mathcal{S}} + \nu_{jc}^{\mathcal{D}} \lambda_c \chi_c - \sum_m \nu_{jm}^{min} I_m^{min}, \quad (34)$$

where

$$\Psi_d = C_d + \sum_i \nu_{di}^{aq} C_i, \quad (35)$$

$$\Psi_a = C_a + \sum_i \nu_{ai}^{aq} C_i, \quad (36)$$

$$\Psi_j = C_j + \sum_i \nu_{ji}^{aq} C_i. \quad (37)$$

Parallel Reactions. So far the discussion has focused on a single electron acceptor being present. However, in natural systems it is common for a number of different electron acceptor substrates to be present at any one time. In such cases several parallel reactions representing biosynthesis may take place simultaneously. These reactions may be written collectively in the general form

$$\sum_j \nu_{jc}^{\beta} \mathcal{A}_j \longrightarrow \mathcal{A}_c, \quad (\beta = 1, \dots, N_a), \quad (38)$$

where the sum over the index j includes electron donor and acceptor substrates in addition to the other primary species, and N_a represents the number of electron acceptor substrates indexed by the superscript β . The reaction rate is given by the Monod rate law

$$I_c^{\beta} = k_c^{\beta} \chi_c \frac{C_{a_{\beta}}}{K_{a_{\beta}} + C_{a_{\beta}}} \frac{C_d}{K_d + C_d}, \quad (39)$$

with electron acceptor concentration $C_{a_{\beta}}$. The total rate for biomass synthesis is given by the sum over all parallel reactions related to different electron acceptors

$$\begin{aligned} I_c &= \sum_{\beta} I_c^{\beta}, \\ &= \chi_c \frac{C_d}{K_d + C_d} \sum_{\beta} \frac{k_c^{\beta} C_{a_{\beta}}}{K_{a_{\beta}} + C_{a_{\beta}}} \end{aligned} \quad (40)$$

For example, for parallel reactions based on $\text{O}_{2(aq)}$ and NO_3^- as electron acceptors the total rate for biomass synthesis is equal to the sum of the individual rates

$$\begin{aligned} I_c &= I_{\text{O}_{2(aq)}} + I_{\text{NO}_3^-}, \\ &= \chi_c \frac{C_d}{K_d + C_d} \left[\frac{k_{\text{O}_{2(aq)}} C_{\text{O}_{2(aq)}}}{K_{\text{O}_{2(aq)}} + C_{\text{O}_{2(aq)}}} + \frac{k_{\text{NO}_3^-} C_{\text{NO}_3^-}}{K_{\text{NO}_3^-} + C_{\text{NO}_3^-}} \right]. \end{aligned} \quad (41)$$

The primary species mass transport equations can be written in the form

$$\hat{\mathcal{L}}\Psi_j = - \sum_{c\beta} \nu_{jc}^{\beta} I_c^{\beta} - \sum_{jm} \nu_{jm} I_m^{\min}, \quad (42)$$

and for biomass synthesis as

$$\frac{\partial \chi_c}{\partial t} = \sum_{\beta} I_c^{\beta} = I_c. \quad (43)$$

The equations may be further generalized to more than one electron donor substrate if desired.

12.12.97 Dual Continuum Model [DCM] Formulation. A SRD was prepared for incorporating the DCM into MULTIFLO. The resulting code version will be designated 1.1. The mathematical details of the DCM are derived and an analytical solution to be used to benchmark the code is developed.

INTRODUCTION

Transport of reacting solute species through fractures plays an important role in many geochemical processes involving natural systems. Fracture dominated flow systems are involved in contaminant migration and ore deposition. Previous work to incorporate fracture and matrix interaction has been confined to an explicit representation of the fracture network (Tang et al., 1981; Steefel and Lichtner, 1997). This work provides an extension of the dual continuum approach for describing flow in fractured rock to transport of reactive solute species. A general nonisothermal, variably saturated porous medium is considered.

At the proposed high-level nuclear waste disposal site at Yucca Mountain, Nevada, different pore (matrix) and fracture water compositions have been observed. In addition, recent observations of ^{36}Cl indicate the existence of fast pathways from the ground surface to the watertable which are presumed related to flow in fractures. To describe such situations it is important to be able to distinguish between fracture and matrix flow systems. Two available approaches, one the dual continuum model (DCM) and the other the multiple interacting continuum (MINC) model (Pruess and Narisimhan, 1980), have been applied to YM. The dual continuum model is applicable to the case where the matrix forms a connected flow region unobstructed by fractures. The MINC model on the other hand applies when matrix blocks are disconnected from one another by the presence of through-going fractures.

BACKGROUND

Several different approaches have been used in the past to model fracture-matrix interaction. The simplest of these is the equivalent continuum model (ECM). In this model it is assumed that the fracture and matrix are able to communicate with each other instantaneously. The liquid saturation in the fracture and matrix is controlled by capillary equilibrium between the two domains. The fractured porous medium is

represented as an equivalent continuum with porosity taken as the average between the fracture and matrix porosities according to the relation

$$\phi_{\text{ecm}} = \phi_f^b + (1 - \phi_f^b)\phi_m, \quad (44)$$

where ϕ_f^b represents the fracture continuum porosity based on a bulk rock REV, and ϕ_m the intrinsic matrix porosity. For most situations of interest the matrix porosity is much larger than the fracture porosity which is much less than one, and as a result the equivalent continuum porosity is approximately equal to the matrix porosity. Liquid saturation in the ECM is obtained as a weighted average between matrix and fracture saturations

$$s_l^{\text{ecm}} = \frac{\phi_f^b s_l^f + (1 - \phi_f^b)\phi_m s_l^m}{\phi_{\text{ecm}}}. \quad (45)$$

The ECM permeability is given by

$$k_{\text{ecm}} = \phi_f^b k_f + (1 - \phi_f^b)k_m, \quad (46)$$

and the relative permeability by

$$k_r^{\text{ecm}} = \frac{\phi_f^b k_f k_r^f + (1 - \phi_f^b)k_m k_r^m}{\phi_{\text{ecm}}}. \quad (47)$$

Central to the ECM approximation is the assumption of capillary equilibrium between fracture and matrix continua

$$p_c^f(s_l^f) = p_c^m(s_l^m). \quad (48)$$

The equations for saturation and capillary equilibrium provide two simultaneous equations to determine the fracture and matrix saturations in terms of the equivalent continuum saturation. The ECM leads to very stringent conditions on the flow properties in the fracture network, requiring almost fully saturated conditions in the matrix before fluid flow in the fracture can commence. This property of the ECM can greatly underestimate fracture flow under transient conditions.

In a similar fashion to permeability it is also possible to define the ECM diffusivity according to the expression

$$D_{\text{ecm}} = \frac{\phi_f^b D_f + (1 - \phi_f^b)\phi_m D_m}{\phi_{\text{ecm}}}, \quad (49)$$

and a similar relation for tortuosity.

MATHEMATICAL FORMULATION

The dual continuum model represents a fractured porous medium as two interacting continua: one continuum represents the fracture network and the other the rock matrix. In the case of solute transport a linear coupling term describes mass transfer between the two continua. For variably saturated systems the coupling is a nonlinear function of the saturation and linear in the pressure difference between matrix and fracture network. The dual continuum model is presumed valid provided the rock mass contains fractures which are connected to form a continuous flow network, typical of rock with a high density of fractures which are closely spaced. The matrix must also form a connected flow regime. For a system with widely spaced continuous fractures which isolate matrix blocks thereby disrupting their continuity, the dual continuum approach is not valid and an explicit representation of each fracture or a multiple interacting continua model (MINC) approach may be necessary.

Dual Continua

The dual continuum model is composed of two distinct continua, referred to as fracture and matrix, represented by the letters f and m . Flow equations for the dual continuum model consist of separate mass conservation equations for the matrix and fracture continua with a coupling term linear in the fluid pressure difference between the domains. For fluid flow the coupling term is proportional to the difference in pressures, and for gaseous diffusion to the difference in mole fractions of water and air in the matrix and fracture network. A representative elemental volume (REV) of the bulk rock consists of contributions from fracture and matrix continua

$$V = V_f + V_m, \quad (50)$$

with bulk REV volume V , and bulk fracture V_f and matrix V_m volumes. The fracture and matrix volumes may be further broken down into pore and solid fractions

$$V_f = V_p^f + V_{\text{solid}}^f, \quad (51a)$$

and

$$V_m = V_p^m + V_{\text{solid}}^m. \quad (51b)$$

The bulk fracture porosity ϕ_f^b is defined relative to the bulk rock volume as

$$\phi_f^b = \frac{V_p^f}{V}, \quad (52)$$

and the intrinsic fracture porosity as

$$\phi_f = \frac{V_p^f}{V_f}. \quad (53)$$

The two porosities are related by the expression

$$\phi_f^b = \sigma_f \phi_f, \quad (54)$$

where σ_f is defined as

$$\sigma_f = \frac{V_f}{V}. \quad (55)$$

Note that σ_f corresponds to the fracture porosity for the case that the fractures are not filled with solid ($V_f^p = V_f$). The intrinsic matrix porosity ϕ_m , defined as

$$\phi_m = \frac{V_p^m}{V_m}, \quad (56)$$

is related to bulk matrix porosity ϕ_m^b by the expression

$$\begin{aligned} \phi_m^b &= \frac{V_p^m}{V}, \\ &= \frac{V_p^m}{V_m} \frac{V_m}{V}, \\ &= \sigma_m \phi_m, \end{aligned} \quad (57)$$

where σ_m is defined as

$$\sigma_m = \frac{V_m}{V}, \quad (58)$$

with

$$\sigma_f + \sigma_m = 1. \quad (59)$$

Mineral concentrations in the fracture are expressed in terms of intrinsic volume fractions as

$$\phi_s^\alpha = \frac{V_s^\alpha}{V_\alpha}, \quad (60)$$

for the s th mineral. The intrinsic matrix and fracture properties satisfy the sum rules

$$\phi_\alpha + \sum_s \phi_s^\alpha = 1. \quad (61)$$

Flux Relations

The total volumetric flow Q [$\text{m}^3 \text{s}^{-1}$] of fluid into a dual continuum porous medium consists of contributions from fracture and matrix

$$Q = Q_f + Q_m. \quad (62)$$

The Darcy velocity q for the medium as a whole is defined as

$$q = \frac{Q}{A} = q_f + q_m, \quad (63)$$

where

$$q_\alpha = \frac{Q_\alpha}{A}, \quad (\alpha = f, m). \quad (64)$$

In these relations A represents the cross-sectional area of the bulk medium. Fluid velocities intrinsic to each continuum may be defined as

$$u_\alpha = \frac{Q_\alpha}{A_\alpha}, \quad (65)$$

where

$$A = A_f + A_m. \quad (66)$$

The velocities u_α correspond to Darcy velocities of the individual continua. It follows that

$$q_\alpha = \frac{Q_\alpha}{A} = \frac{Q_\alpha}{A_\alpha} \frac{A_\alpha}{A} = \sigma_\alpha u_\alpha, \quad (67)$$

where it is assumed that

$$\sigma_\alpha = \frac{A_\alpha}{A} = \frac{V_\alpha}{V}. \quad (68)$$

The total Darcy velocity q is related to the individual continua velocities u_α by the weighted sum

$$q = \sigma_f u_f + \sigma_m u_m. \quad (69)$$

Finally, average pore velocities may be defined for each continuum as

$$v_\alpha = \frac{u_\alpha}{\phi_\alpha}. \quad (70)$$

MASS CONSERVATION EQUATIONS

General Mass Conservation Equations

The DCM mass conservation equations for fracture and matrix continua based on a bulk rock REV can be written for some observable physical property Z in the form

$$\frac{\partial}{\partial t} (\sigma_f Z_f) + \nabla \cdot \sigma_f \mathbf{J}_Z^f = \mathcal{R}_Z^f - \Gamma_Z, \quad (71)$$

for the fracture continuum, and

$$\frac{\partial}{\partial t} (\sigma_m Z_m) + \nabla \cdot \sigma_m \mathbf{J}_Z^m = \mathcal{R}_Z^m + \Gamma_Z, \quad (72)$$

for the matrix continuum. The solute flux is defined by

$$\mathbf{J}_Z^\alpha = -\tau_\alpha \phi_\alpha D_\alpha \nabla C_Z^\alpha + \mathbf{u}_\alpha C_Z^\alpha, \quad (73)$$

with tortuosity τ_α and diffusion coefficient D_α assumed to be the same for all species.

Mass conservation equations involving intrinsic properties are obtained by dividing the bulk-REV based fracture and matrix conservation equations through by the factors σ_f and σ_m , respectively, yielding

$$\frac{\partial Z_f}{\partial t} + \nabla \cdot \mathbf{J}_Z^f = \mathcal{R}_Z^f - \frac{1}{\sigma_f} \Gamma_Z^f, \quad (74)$$

and

$$\frac{\partial Z_m}{\partial t} + \nabla \cdot \mathbf{J}_Z^m = \mathcal{R}_Z^m + \frac{1}{\sigma_m} \Gamma_Z^m. \quad (75)$$

Note that in these equations the fracture-matrix coupling terms are modified by the factor σ_α .

Fluid Flow Conservation Equations

The conservation equations for the H₂O component (w) and the air component (a) are given by

$$\begin{aligned} & \frac{\partial}{\partial t} \left[\phi_f \left(s_l^f n_l^f X_{wl}^f + s_g^f n_g^f X_{wg}^f \right) \right] \\ & + \nabla \cdot \left[\mathbf{u}_l^f n_l^f X_{wl}^f + \mathbf{u}_g^f n_g^f X_{wg}^f - D_g^f n_g^f \nabla X_{wg}^f \right] = Q_w^f - \frac{\Gamma_w}{\sigma_f}, \end{aligned} \quad (76a)$$

and

$$\begin{aligned} & \frac{\partial}{\partial t} \left[\phi_f \left(s_l^f n_l^f X_{al}^f + s_g^f n_g^f X_{ag}^f \right) \right] \\ & + \nabla \cdot \left[\mathbf{u}_l^f n_l^f X_{al}^f + \mathbf{u}_g^f n_g^f X_{ag}^f - D_g^f n_g^f \nabla X_{ag}^f \right] = Q_a^f - \frac{\Gamma_a}{\sigma_f}, \end{aligned} \quad (76b)$$

for the fracture continuum, and

$$\begin{aligned} & \frac{\partial}{\partial t} \left[\phi_m \left(s_l^m n_l^m X_{wl}^m + s_g^m n_g^m X_{wg}^m \right) \right] \\ & + \nabla \cdot \left[\mathbf{u}_l^m n_l^m X_{wl}^m + \mathbf{u}_g^m n_g^m X_{wg}^m - D_g^m n_g^m \nabla X_{wg}^m \right] = Q_w^m + \frac{\Gamma_w}{\sigma_m}, \end{aligned} \quad (77a)$$

and

$$\begin{aligned} & \frac{\partial}{\partial t} \left[\phi_m \left(s_l^m n_l^m X_{al}^m + s_g^m n_g^m X_{ag}^m \right) \right] \\ & + \nabla \cdot \left[\mathbf{u}_l^m n_l^m X_{al}^m + \mathbf{u}_g^m n_g^m X_{ag}^m - D_g^m n_g^m \nabla X_{ag}^m \right] = Q_a^m + \frac{\Gamma_a}{\sigma_m}, \end{aligned} \quad (77b)$$

for the matrix continuum. The superscripts m and f refer to the fracture and matrix continua, respectively. The matrix and fracture saturation states are denoted by s_l^m and s_l^f , respectively. The quantities Q_w and Q_a represent source/sink terms. The Darcy fluxes for liquid and gas, \mathbf{u}_l , \mathbf{u}_g , are defined by

$$\mathbf{u}_l = -\frac{k k_{rl}}{\mu_l} \nabla (p_l - \rho_l g z), \quad (78a)$$

and

$$\mathbf{u}_g = -\frac{k k_{rg}}{\mu_g} \nabla (p_g - \rho_g g z), \quad (78b)$$

for fracture and matrix continua, where k denotes the saturated permeability, p the fluid pressure, $\mu_{l,g}$ the viscosity of the liquid and gas phases with mass densities $\rho_{l,g}$, and g the acceleration due to gravity. The quantities $n_{l,g}$ refer to the density of the liquid and gas phases based on a molar representation. The mole fractions $X_{wl,g}$, $X_{al,g}$ satisfy the relations

$$X_{wl} + X_{al} = 1, \quad X_{wg} + X_{ag} = 1. \quad (79)$$

Diffusion of water in the aqueous phase is neglected. The liquid and gas pressures are related through the capillary pressure:

$$p_l = p_g - p_c. \quad (80)$$

The effective binary gas diffusion coefficient is defined in terms of temperature, pressure and material properties by

$$D_g = \omega \alpha \phi s_g D_g^0 \frac{p_0}{p} \left[\frac{T + T_0}{T_0} \right]^\theta, \quad (81)$$

where T_0 , p_0 denote reference temperature and pressure, θ is an empirical constant, and ω is an enhancement factor (Walton and Lichtner, 1995). The enhancement factor is usually considered to be inversely proportional to the gas saturation s_g which thus cancels from the expression for the effective gas diffusion coefficient.

The coupling term Γ_i , ($i = w, a$) is equal to the sum of liquid and gas phase contributions

$$\Gamma_i = \Gamma_i^l + \Gamma_i^g. \quad (82)$$

The quantity Γ_i^π for phase π involves two terms, the first is proportional to the difference between fracture and matrix pressures resulting in flow between the fracture network and matrix, and the second is proportional to the difference in mole fractions of water and air resulting in diffusive transport between the two continua

$$\Gamma_i^\pi = \gamma_\pi (p_\pi^f - p_\pi^m) + \delta_{\pi g} \gamma'_\pi (X_{il}^f - X_{ig}^m), \quad (\pi = l, g). \quad (83)$$

The coupling strength γ_π is assumed to be directly proportional to the specific surface area of the fracture continuum A_f and the product of the saturated permeability and relative permeability of the matrix, and inversely proportional to the dynamic viscosity and length parameter l_{fm} representing the average distance between matrix blocks and fractures

$$\gamma_\pi = A_f \frac{k_m k_{r\pi}^m}{\mu_\pi l_{fm}}. \quad (84)$$

The coupling strength γ'_π represents the contribution from diffusion and is proportional to the gaseous diffusion coefficient

$$\gamma'_\pi = A_f \frac{D_g}{l_{fm}}. \quad (85)$$

It is assumed that there is no effect of gravity on the coupling terms and hence that the fracture and matrix are at the same elevation locally.

The gaseous diffusive flux can be eliminated from the mass transport equations by adding Eqns.(76a) and (76b) for the fracture continuum, and Eqns.(77a) and (77b) for the matrix continuum to give

$$\begin{aligned} \frac{\partial}{\partial t} [\phi_f (s_l^f n_l^f + s_g^f n_g^f)] \\ + \nabla \cdot (\mathbf{u}_l^f n_l^f + \mathbf{u}_g^f n_g^f) = Q_w^f + Q_a^f - \frac{1}{\sigma_f} (\Gamma_w + \Gamma_a), \end{aligned} \quad (86a)$$

and

$$\begin{aligned} \frac{\partial}{\partial t} [\phi_m (s_l^m n_l^m + s_g^m n_g^m)] \\ + \nabla \cdot (\mathbf{u}_l^m n_l^m + \mathbf{u}_g^m n_g^m) = Q_w^m + Q_a^m + \frac{1}{\sigma_m} (\Gamma_w + \Gamma_a), \end{aligned} \quad (86b)$$

Adding these equations eliminates the fracture-matrix coupling terms providing the total mass balance equation for water and air as:

$$\begin{aligned} \frac{\partial}{\partial t} [\phi_f (s_l^f n_l^f + s_g^f n_g^f) + \phi_m (s_l^m n_l^m + s_g^m n_g^m)] \\ + \nabla \cdot (\mathbf{u}_l^f n_l^f + \mathbf{u}_g^f n_g^f + \mathbf{u}_l^m n_l^m + \mathbf{u}_g^m n_g^m) = Q_w^f + Q_a^f + Q_w^m + Q_a^m. \end{aligned} \quad (87)$$

Energy Balance Equation

Separate energy balance equations apply to the fracture and matrix which may be at different temperatures T_f and T_m , respectively. Assuming thermodynamic equilibrium between rock and fluid, these equations are given by

$$\begin{aligned} \frac{\partial}{\partial t} [\phi_f (s_l^f n_l^f U_l^f + s_g^f n_g^f U_g^f)] + \nabla \cdot (\mathbf{u}_l^f n_l^f H_l^f + \mathbf{u}_g^f n_g^f H_g^f) \\ + \frac{\partial}{\partial t} [(1 - \phi_f) C_p^f \rho_f T_f] - \nabla \cdot \kappa_f \nabla T_f = Q_e^f - \frac{\Gamma_e}{\sigma_f}, \end{aligned} \quad (88a)$$

for the fracture, and

$$\begin{aligned} \frac{\partial}{\partial t} [\phi_m (s_l^m n_l^m U_l^m + s_g^m n_g^m U_g^m)] + \nabla \cdot (\mathbf{u}_l^m n_l^m H_l^m + \mathbf{u}_g^m n_g^m H_g^m) \\ + \frac{\partial}{\partial t} [(1 - \phi_m) C_p^m \rho_m T] - \nabla \cdot \kappa_m \nabla T_m = Q_e^m + \frac{\Gamma_e}{\sigma_m}, \end{aligned} \quad (88b)$$

for the matrix. In these equations T denotes the temperature, U_π the total internal energy and H_π the total enthalpy of the π th fluid phase, C_p the heat capacity, κ the

thermal conductivity, and Q_e a source term. Heat produced by chemical reactions is ignored. The thermal coupling term Γ_e is defined by

$$\Gamma_e = \gamma_e(T_f - T_m) + A_f(\bar{v}_w H_w + \bar{v}_a H_a), \quad (89)$$

where

$$\gamma_e = A_f \frac{\bar{\kappa}}{l_{fm}}, \quad (90)$$

where $\bar{\kappa}$ and \bar{v} are average values for thermal conduction and fluid flow velocity across the fracture–matrix interface.

Together with appropriate initial and boundary conditions, the mass conservation equations for air, Eqns. (76b) and (77b), the total mass balance equation, Eqn. (86a) and (86b), and the heat balance equations Eqns. (88a) and (88b) are solved simultaneously using an implicit finite difference scheme for the fracture and matrix continua.

Reactive Transport Equations

Within the dual continuum formulation separate solute transport equations must be written for fracture and matrix continua. The formulation which follows takes into account homogeneous reactions within the aqueous phase and heterogeneous reactions involving mineral precipitation–dissolution reactions and reactions involving gaseous species. Other reactions including sorption and microbial reactions may be easily included if desired. A common set of chemical reactions are allowed to take place in each continua described by the aqueous complexing reactions

$$\sum_j \nu_{ji} \mathcal{A}_j \rightleftharpoons \mathcal{A}_i, \quad (91)$$

mineral reactions

$$\sum_s \nu_{js} \mathcal{A}_j \rightleftharpoons \mathcal{M}_s. \quad (92)$$

These reactions are written in terms of a common set of basis or primary species denoted by \mathcal{A}_j which are assumed to all belong to the aqueous phase. Reactions written in this form are referred to as canonical reactions.

For a variably saturated porous medium solute mass transport equations for fracture and matrix continua have the form written for combined liquid and gas phases

$$\frac{\partial}{\partial t} \left[\phi_f \left(s_l^f C_{jl}^f + s_g^f C_{jg}^f \right) \right] + \nabla \cdot \left[\mathbf{J}_{jl}^f + \mathbf{J}_{jg}^f \right] = - \sum_i \nu_{ji} I_i^f - \sum_s \nu_{js} I_s^f - \frac{\Gamma_j}{\sigma_f}, \quad (93a)$$

$$\frac{\partial}{\partial t} \left[\phi_f \left(s_l^f C_{il}^f + s_g^f C_{ig}^f \right) \right] + \nabla \cdot \left[\mathbf{J}_{il}^f + \mathbf{J}_{ig}^f \right] = I_i^f - \frac{\Gamma_i}{\sigma_f}, \quad (93b)$$

for the fracture network, and

$$\frac{\partial}{\partial t} \left[\phi_m \left(s_l^m C_{jl}^m + s_g^m C_{jg}^m \right) \right] + \nabla \cdot \left[\mathbf{J}_{jl}^m + \mathbf{J}_{jg}^m \right] = - \sum_i \nu_{ji} I_i^m - \sum_s \nu_{js} I_s^m + \frac{\Gamma_j}{\sigma_m}, \quad (94a)$$

$$\frac{\partial}{\partial t} \left[\phi_m \left(s_l^m C_{il}^m + s_g^m C_{ig}^m \right) \right] + \nabla \cdot \left[\mathbf{J}_{il}^m + \mathbf{J}_{ig}^m \right] = I_i^m + \frac{\Gamma_i}{\sigma_m}, \quad (94b)$$

for the matrix. The fracture-matrix coupling terms Γ_j , Γ_i for primary and secondary species are defined by

$$\Gamma_j = \gamma_l \left(C_{jl}^f - C_{jl}^m \right) + \gamma_g \left(C_{jg}^f - C_{jg}^m \right) + A_f \left[\bar{v}_l \bar{C}_{jl} + \bar{v}_g \bar{C}_{jg} \right], \quad (95a)$$

and

$$\Gamma_i = \gamma_l \left(C_{il}^f - C_{il}^m \right) + \gamma_g \left(C_{ig}^f - C_{ig}^m \right) + A_f \left[\bar{v}_l \bar{C}_{il} + \bar{v}_g \bar{C}_{ig} \right], \quad (95b)$$

where γ is a coupling strength parameter, \bar{v} represents the average flow velocity between fracture and matrix, and $\bar{C}_{j,i}$ denotes the upstream concentration. The coupling strength γ is proportional to the fracture surface area per unit bulk volume of porous medium and inversely proportional to the characteristic length l_{fm} separating the fracture and matrix continua according to the expression

$$\gamma = A_f \frac{\phi_m D_m \phi_f D_f}{\phi_m D_m + \phi_f D_f} \frac{1}{l_{fm}}, \quad (96)$$

The fracture specific surface area may be related to twice the average fracture aperture δ times the fracture porosity by the expression

$$A_f = \phi_f \frac{2}{\delta} = \frac{2}{d_f}, \quad (97)$$

where d_f denotes the fracture spacing. An essential property of the coupling terms Γ_j and Γ_i is that they are linear functions of the solute concentrations. Furthermore, the coupling coefficient γ is the same for all species. If this were not the case the mass transport equations would not conserve charge, for example.

The reaction rate I_s^α is defined by

$$I_s^\alpha = -k_s A_s^\alpha [1 - K_s Q_s^\alpha], \quad (98)$$

where the mineral surface area is defined as

$$A_s^\alpha = \frac{6\phi_s^\alpha}{b_s^\alpha}, \quad (99)$$

with mineral grain size b_s^α .

Mineral mass transfer equations within the fracture and matrix continua have the simple form

$$\frac{\partial \phi_s^f}{\partial t} = \bar{V}_s I_s^f, \quad (100a)$$

for the fracture continuum, and

$$\frac{\partial \phi_s^m}{\partial t} = \bar{V}_s I_s^m, \quad (100b)$$

for the matrix, where ϕ_s^f and ϕ_s^m refer to the mineral volume fractions in the fracture and matrix continua, respectively, with molar volumes \bar{V}_s . The mineral volume fractions and fracture and matrix porosities must sum to unity according to the relation

$$\sum_s (\phi_s^f + \phi_s^m) + \phi_f + \phi_m = 1. \quad (101)$$

Assuming local equilibrium for aqueous complexing reactions, the reaction rates I_i^f and I_i^m may be eliminated from the mass transport equations for the primary species yielding the revised primary species conservation equations

$$\begin{aligned} \frac{\partial}{\partial t} \left[\phi_f \left(s_l^f \Psi_{jl}^f + s_g^f \Psi_{jg}^f \right) \right] + \nabla \cdot \left[\Omega_{jl}^f + \Omega_{jg}^f \right] = \\ - \sum_s \nu_{js} I_s^f - \frac{1}{\sigma_f} \left(\Gamma_j + \sum_i \nu_{ji} \Gamma_i \right), \end{aligned} \quad (102a)$$

for the fracture continuum, and

$$\begin{aligned} \frac{\partial}{\partial t} [\phi_m (s_l^m \Psi_{jl}^m + s_g^m \Psi_{jg}^m)] + \nabla \cdot [\Omega_{jl}^m + \Omega_{jg}^m] = \\ - \sum_s \nu_{js} I_s^m + \frac{1}{\sigma_m} \left(\Gamma_j + \sum_i \nu_{ji} \Gamma_i \right), \end{aligned} \quad (102b)$$

for the matrix continuum. The generalized concentration and flux, Ψ_j and Ω_j , are defined by

$$\Psi_{j\pi} = \delta_{j\pi} C_{j\pi} + \sum_i \nu_{ji} C_{i\pi}, \quad (103)$$

and

$$\Omega_{j\pi} = \delta_{j\pi} \mathbf{J}_{j\pi} + \sum_i \nu_{ji} \mathbf{J}_{i\pi}. \quad (104)$$

The coupling terms become

$$\begin{aligned} \Gamma_j + \sum_i \nu_{ji} \Gamma_i &= \gamma_l \left[(C_{jl}^f - C_{jl}^m) + \sum_i \nu_{ji} (C_{il}^f - C_{il}^m) \right] \\ &+ \gamma_g \left[(C_{jg}^f - C_{jg}^m) + \sum_i \nu_{ji} (C_{ig}^f - C_{ig}^m) \right], \\ &= \gamma_l (\Psi_{jl}^f - \Psi_{jl}^m) + \gamma_g (\Psi_{jg}^f - \Psi_{jg}^m), \end{aligned} \quad (105)$$

and thus because of linearity, can be represented as the difference between the generalized concentrations in the fracture and matrix.

ANALYTICAL STATIONARY STATE SOLUTION

A simple analytical expression exists for the stationary state solution to the mass transport equations for a single component system with linear kinetics. The stationary state solution is important for describing the time evolution of a reacting system (Lichtner, 1988), and may be used to investigate the qualitative properties of the dual continuum model as well as for benchmarking numerical implementations. A single reacting species is considered obeying the reaction



with solid $\mathcal{A}_{(s)}$. The transport equations expressed in terms of intrinsic properties for the solute species in the fracture and matrix are assumed to have the form

$$\frac{\partial}{\partial t} (\tau_f \phi_f C_f) + \nabla \cdot \mathbf{J}_f = -k_f (C_f - C_{eq}) - \frac{\gamma}{\sigma_f} (C_f - C_m), \quad (107a)$$

$$\frac{\partial}{\partial t} (\tau_m \phi_m C_m) + \nabla \cdot \mathbf{J}_m = -k_m (C_m - C_{eq}) + \frac{\gamma}{\sigma_m} (C_f - C_m). \quad (107b)$$

The coupling term is presumed to be linear in the difference in fracture–matrix concentrations at each node. The coupling strength γ has the same units as the kinetic rate constants [s^{-1}]. In a single spatial dimension the solute flux terms have the form

$$J_f = -\tau_f \phi_f D \frac{\partial C_f}{\partial x} + v_f C_f, \quad (108a)$$

and

$$J_m = -\tau_m \phi_m D \frac{\partial C_m}{\partial x} + v_m C_m. \quad (108b)$$

For conditions of a stationary state the mass conservation equations then become in a single spatial dimension

$$-\tau_f \phi_f D_f \frac{d^2 C_f}{dx^2} + v_f \frac{dC_f}{dx} = -k_f (C_f - C_{eq}) - \frac{\gamma}{\sigma_f} (C_f - C_m), \quad (109a)$$

and

$$-\tau_m \phi_m D_m \frac{d^2 C_m}{dx^2} + v_m \frac{dC_m}{dx} = -k_m (C_m - C_{eq}) + \frac{\gamma}{\sigma_m} (C_f - C_m). \quad (109b)$$

The kinetic rate constants k_f and k_m are effective rate constants equal to the product of the intrinsic rate constant times the specific surface area for the fracture and matrix continua, respectively. Thus they may differ greatly in each continua. The transport equations are subject to the following boundary conditions at the entrance to the fractured porous medium

$$C_f(0) = C_f^0, \quad (110a)$$

and

$$C_m(0) = C_m^0. \quad (110b)$$

At large distances from the inlet the concentration must approach the equilibrium concentration for the solid C_{eq} .

Before proceeding it is useful to measure the solute concentration relative to the equilibrium concentration by introducing the relative concentrations

$$C'_f = C_f - C_{eq}, \quad (111a)$$

and

$$C'_m = C_m - C_{eq}. \quad (111b)$$

To solve the stationary state transport equations, first note that the fracture continuum transport equation may be solved for the matrix concentration C'_m to give

$$C'_m = \left(1 + \frac{\sigma_f k_f}{\gamma}\right) C'_f + \frac{\sigma_f v_f}{\gamma} \frac{dC'_f}{dx} - \frac{\sigma_f \tau_f \phi_f D_f}{\gamma} \frac{d^2 C'_f}{dx^2}. \quad (112)$$

If this expression is substituted into the matrix continuum transport equation there results the following fourth order ordinary differential equation with constant coefficients

$$a(\gamma) \frac{d^4 C'_f}{dx^4} - b(\gamma) \frac{d^3 C'_f}{dx^3} + c(\gamma) \frac{d^2 C'_f}{dx^2} + d(\gamma) \frac{dC'_f}{dx} + e(\gamma) C'_f = 0, \quad (113)$$

where the coefficients $a(\gamma)$, $b(\gamma)$, $c(\gamma)$, $d(\gamma)$, and $e(\gamma)$ are defined by

$$a(\gamma) = \frac{\sigma_m \tau_m \phi_m D_m \sigma_f \tau_f \phi_f D_f}{\gamma}, \quad (114a)$$

$$b(\gamma) = \frac{\sigma_m \sigma_f}{\gamma} (v_m \tau_f \phi_f D_f + v_f \tau_m \phi_m D_m), \quad (114b)$$

$$c(\gamma) = \frac{\sigma_f v_f \sigma_m v_m}{\gamma} - \sigma_m \tau_m \phi_m D_m \left(1 + \frac{\sigma_f k_f}{\gamma}\right) - \sigma_f \tau_f \phi_f D_f \left(1 + \frac{\sigma_m k_m}{\gamma}\right), \quad (114c)$$

$$d(\gamma) = \sigma_m v_m \left(1 + \frac{\sigma_f k_f}{\gamma}\right) + \sigma_f v_f \left(1 + \frac{\sigma_m k_m}{\gamma}\right), \quad (114d)$$

$$\begin{aligned} e(\gamma) &= \gamma \left[\left(1 + \frac{\sigma_f k_f}{\gamma}\right) \left(1 + \frac{\sigma_m k_m}{\gamma}\right) - 1 \right] \\ &= \frac{\sigma_f k_f \sigma_m k_m}{\gamma} + \sigma_f k_f + \sigma_m k_m. \end{aligned} \quad (114e)$$

The most general solution to Eqn.(113) for an infinite system subject to the boundary conditions at the inlet and outlet has the form

$$C_f(x; \gamma) = Ae^{-q_1 x} + Be^{-q_2 x} + C_{eq}, \quad (115)$$

where $q_1(\gamma)$ and $q_2(\gamma)$ are the two nonnegative roots of the characteristic fourth order polynomial

$$p(q; \gamma) = a(\gamma)q^4 + b(\gamma)q^3 + c(\gamma)q^2 - d(\gamma)q + e(\gamma) = 0. \quad (116)$$

Note that because the coefficient $e(\gamma)$ is positive, there must always exist an even number of positive roots. Because $d(\gamma) \geq 0$, there can be only two nonnegative roots. The matrix concentration has the form

$$C_m(x) = w_1 A e^{-q_1 x} + w_2 B e^{-q_2 x} + C_{eq}, \quad (117)$$

where

$$w_1 = 1 + \frac{\sigma_f k_f}{\gamma} - \frac{\sigma_f v_f}{\gamma} q_1 - \frac{\sigma_f \tau_f \phi_f D_f}{\gamma} q_1^2, \quad (118a)$$

and

$$w_2 = 1 + \frac{\sigma_f k_f}{\gamma} - \frac{\sigma_f v_f}{\gamma} q_2 - \frac{\sigma_f \tau_f \phi_f D_f}{\gamma} q_2^2. \quad (118b)$$

The coefficients A and B are related to the boundary conditions imposed on the solution by the two simultaneous equations

$$A + B = C_f^0 - C_{eq}, \quad (119a)$$

$$w_1 A + w_2 B = C_m^0 - C_{eq}. \quad (119b)$$

These equations have the solution

$$A = \frac{(C_m^0 - C_{eq}) - w_2(C_f^0 - C_{eq})}{w_1 - w_2}, \quad (120a)$$

and

$$B = \frac{w_1(C_f^0 - C_{eq}) - (C_m^0 - C_{eq})}{w_1 - w_2}. \quad (120b)$$

Nonreactive Transport

Several distinct cases can be considered. A nontrivial stationary state solution exists in the case of nonreactive transport. In this case the coefficient $e(\gamma) = 0$, and as a consequence one of the roots to the characteristic polynomial is zero. The characteristic polynomial reduces to

$$q (a(\gamma)q^3 + b(\gamma)q^2 + c(\gamma)q - d) = 0. \quad (121)$$

This equation has one positive root because $d = v_m + v_f > 0$. The fracture and matrix solutions are given by

$$C_f = A + Be^{-q_2 x}, \quad (122a)$$

and

$$C_m = A + \left(1 - \frac{\sigma_f v_f}{\gamma} - \frac{\sigma_f \tau_f \phi_f D_f}{\gamma}\right) Be^{-q_2 x}. \quad (122b)$$

Both fracture and matrix solutions approach a common asymptote equal to the coefficient A given by

$$A = \frac{C_m^0 - w_2 C_f^0}{1 - w_2}. \quad (123)$$

The coefficient B is equal to

$$B = \frac{C_f^0 - C_m^0}{1 - w_2}. \quad (124)$$

For the special case of zero flow in the matrix ($v_m = 0$) and zero diffusion in the fracture ($D_f = 0$), the coefficient $a = 0$ giving the solution

$$q_2 = \frac{-\gamma c \pm \sqrt{(\gamma c)^2 + 4b'd}}{2b'}, \quad (125)$$

where

$$b' = \sigma_m \sigma_f (v_m \tau_f \phi_f D_f + v_f \tau_m \phi_m D_m) = \sigma_m \sigma_f v_f \tau_m \phi_m D_m. \quad (126)$$

For large γ it follows that

$$q_2 = \frac{\gamma}{\sigma_f v_f}. \quad (127)$$

Thus γ replaces the kinetic rate constant k_f .

It is clear that in the DCM the matrix has an infinite storage capacity. This storage capacity is utilized when the coupling strength γ is large. In this case the fracture concentration approaches the matrix concentration. For weak coupling the fracture concentration dominates with the matrix concentration approaching asymptotically the inlet fracture concentration.

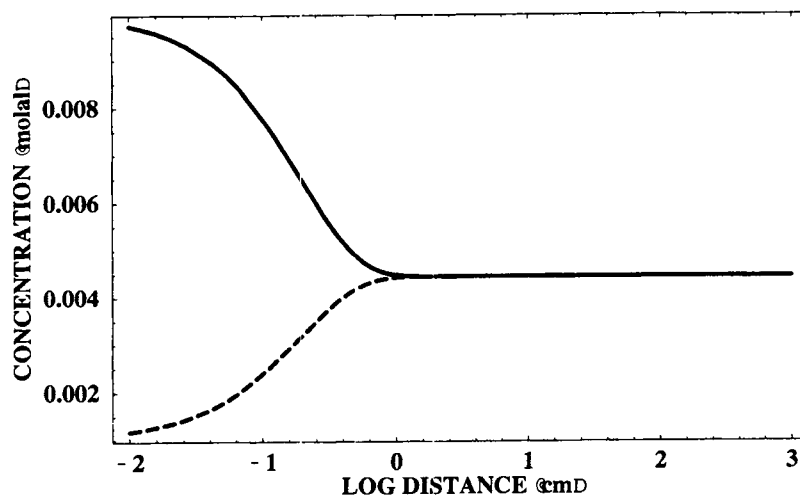


Figure 1: Dual continuum stationary state solution for the nonreactive case. Fracture concentration is represented by the solid curve and matrix concentration by the thick dashed curve. See text for explanation of parameters used in the calculation.

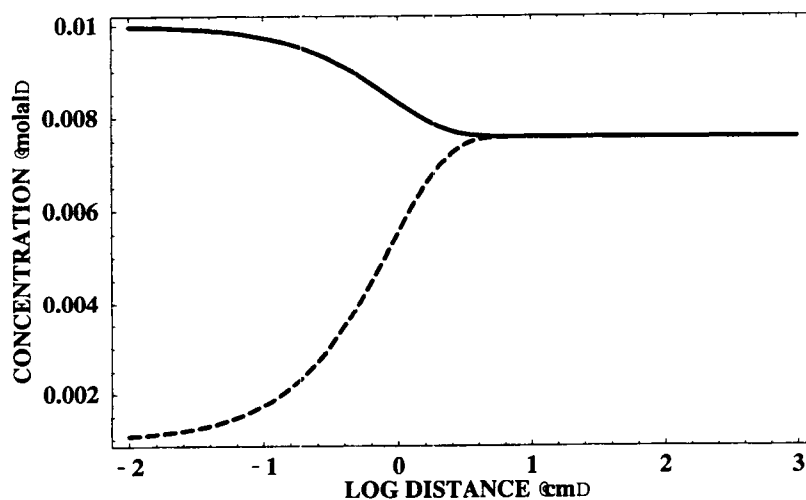


Figure 2: Dual continuum stationary state solution for the nonreactive case. Fracture concentration is represented by the solid curve and matrix concentration by the thick dashed curve. See text for explanation of parameters used in the calculation.

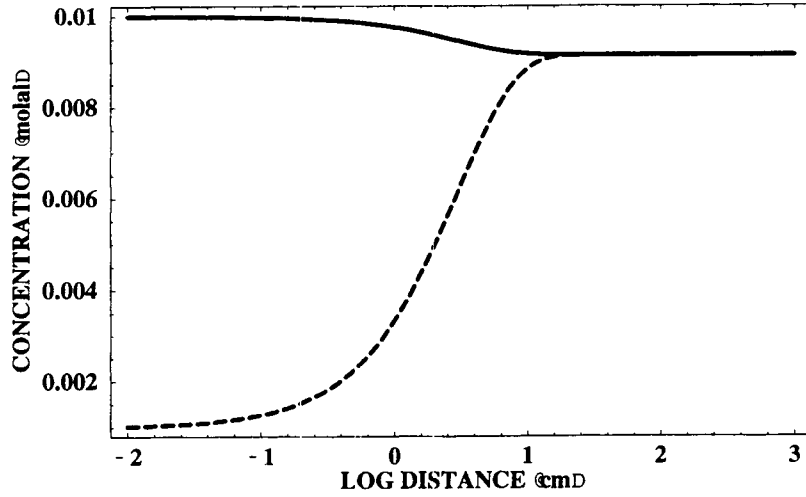


Figure 3: Dual continuum stationary state solution for the nonreactive case. Fracture concentration is represented by the solid curve and matrix concentration by the thick dashed curve. Single continuum results for matrix and fracture are exhibited by the short- and long-dashed curves, respectively. See text for explanation of parameters used in the calculation.

Reactive Transport

For pure diffusion with reaction in both the rock matrix and fractures only even powers are present and the characteristic polynomial reduces to

$$p(q; \gamma) = a(\gamma)q^4 + c(\gamma)q^2 + e(\gamma) = 0. \quad (128)$$

The solution is given explicitly by the expression

$$q^2 = \frac{-c}{2a} \left(1 \pm \sqrt{1 + \frac{4ae}{c}} \right). \quad (129)$$

For the case of pure advection in the fracture and matrix the polynomial reduces to a quadratic expression

$$p(q; \gamma) = c(\gamma)q^2 - d(\gamma)q + e(\gamma) = 0. \quad (130)$$

Finally for the case of pure advective transport in the fractures and pure diffusion in the matrix a third order polynomial is obtained

$$p(q; \gamma) = b(\gamma)q^3 + c(\gamma)q^2 - d(\gamma)q + e(\gamma) = 0. \quad (131)$$

In the limit $\gamma \rightarrow \infty$, the equivalent continuum model is retrieved. The porosity becomes the ecm porosity and the matrix and fracture concentrations are equal.

In the opposite limit, $\gamma \rightarrow 0$, the fracture and matrix concentrations evolved uncoupled from each other with the result

$$C_f^o(x) = (C_f^0 - C_{eq})e^{-q_f x} + C_{eq}, \quad (132a)$$

and

$$C_m^o(x) = (C_m^0 - C_{eq})e^{-q_m x} + C_{eq}, \quad (132b)$$

For the case of pure advection in the fracture network and pure diffusion in the matrix the inverse equilibration lengths q_f and q_m are defined by (Lichtner, 1988)

$$q_f = \frac{k_f}{v_f}, \quad (133a)$$

and

$$q_m = \sqrt{\frac{k_m}{\phi_m D}}. \quad (133b)$$

The general expression for combined advection and diffusion is given in Lichtner (1988).

Table 2: Parameters used for the analytical stationary state solutions.

Variable	Figure 4	Figure 5	Figure 6
γ [s ⁻¹]	10 ⁻⁹	10 ⁻¹⁰	10 ⁻¹¹
ϕ_f	0.001		
v_f [m y ⁻¹]	1		
D_f [cm ² s ⁻¹]	0		
k_f [moles cm ³ s ⁻¹]	0		
C_f^0 [molal]	0.001		
ϕ_m	0.1		
v_m [m y ⁻¹]	0		
D_m [cm ² s ⁻¹]	10 ⁻⁵		
k_m [moles cm ³ s ⁻¹]	10 ⁻¹⁰		
C_m^0 [molal]	0.001		
C_{eq} [molal]	0.1		

Several examples are presented for the parameter values listed in Table 2. To simplify the problem further it is assumed that fluid flow takes place only in the fracture network at a sufficiently rapid rate that diffusion can be neglected. Dispersion in the fracture network is also neglected. In the matrix, transport is assumed to take place by diffusion only. Dissolution of the solid is assumed to take place in the matrix only. The matrix pore water reaches a plateau where it remains undersaturated with respect to the solid until finally both fracture and matrix pore waters come to equilibrium with the solid. For stronger coupling between fracture and matrix continua the fracture water comes to equilibrium with the solid at a shorter distance from the inlet. The matrix pore water requires a greater distance to equilibrate with the solid compared to the case of no interaction with the fracture as indicated by the short-dashed curves.

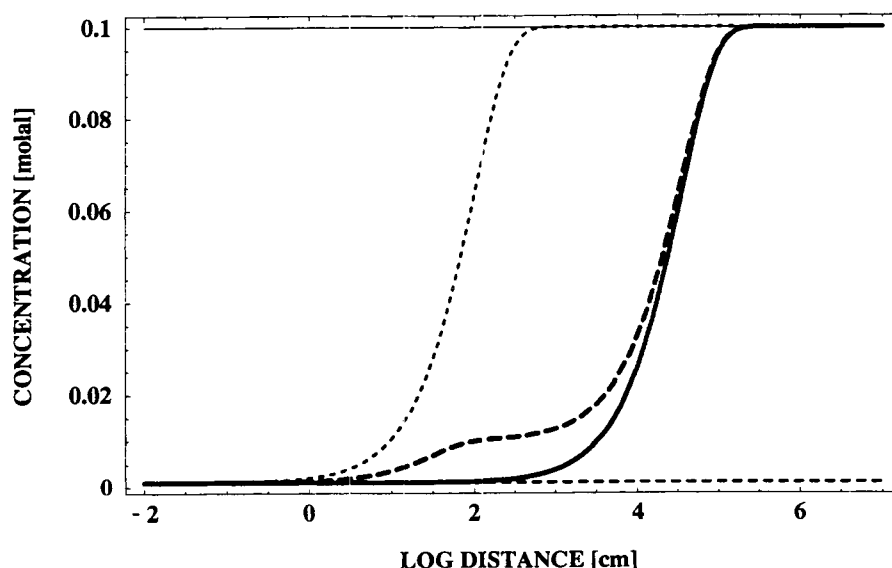


Figure 4: Dual continuum stationary state solution. Fracture concentration is represented by the solid curve and matrix concentration by the thick dashed curve. Single continuum results for matrix and fracture are exhibited by the short- and long-dashed curves, respectively. See text for explanation of parameters used in the calculation.

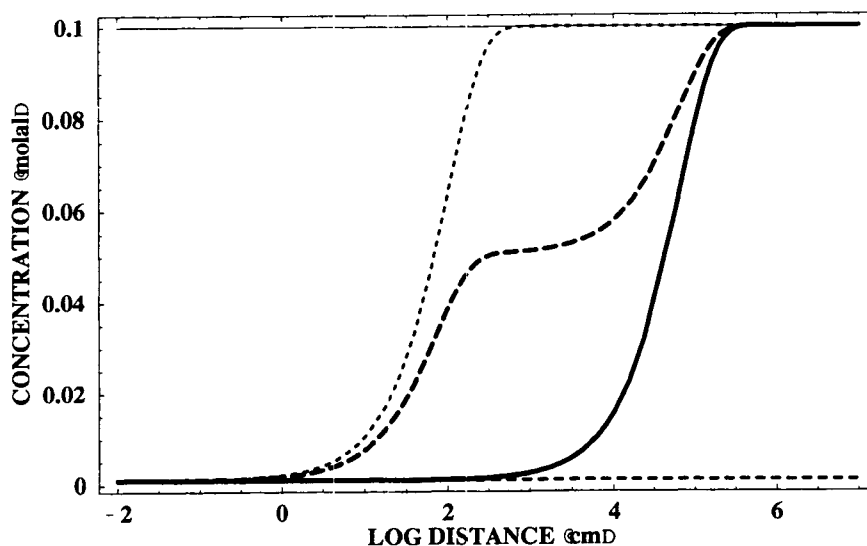


Figure 5: Dual continuum stationary state solution. Fracture concentration is represented by the solid curve and matrix concentration by the thick dashed curve. Single continuum results for matrix and fracture are exhibited by the short- and long-dashed curves, respectively. See text for explanation of parameters used in the calculation.

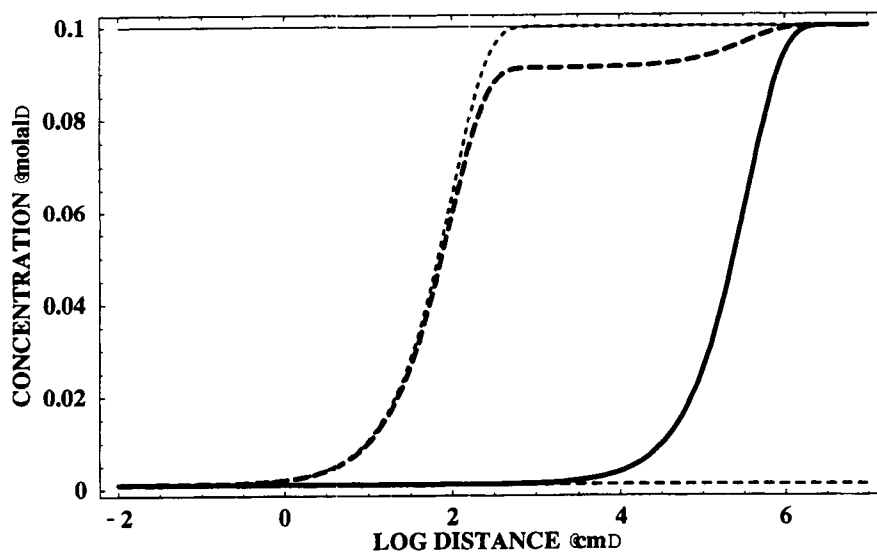


Figure 6: Dual continuum stationary state solution. Fracture concentration is represented by the solid curve and matrix concentration by the thick dashed curve. Single continuum results for matrix and fracture are exhibited by the short- and long-dashed curves, respectively. See text for explanation of parameters used in the calculation.

NUMERICAL SOLUTION TO THE MULTICOMPONENT DUAL CONTINUUM EQUATIONS

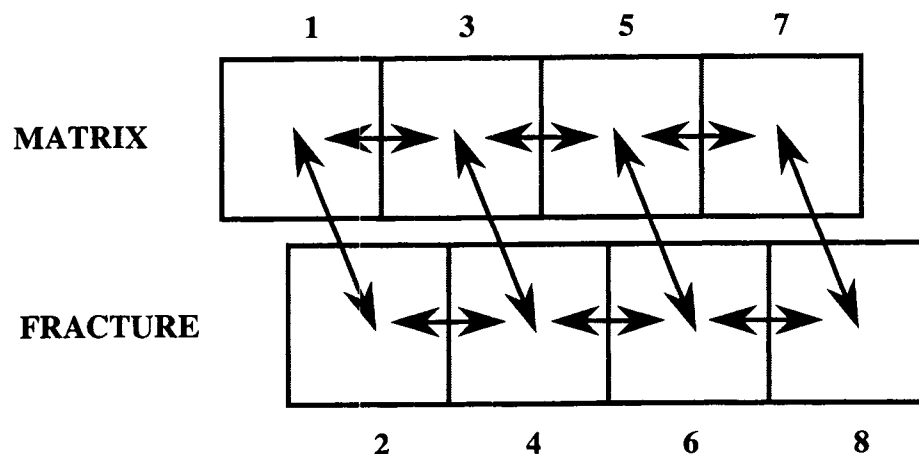


Figure 7: Grid for DCM showing connections indicated by the double arrows. Even nodes correspond to matrix blocks and odd nodes to fractures.

The structure of the Jacobian matrix is shown in Eqn.(134). (Definition of symbols: \bigcirc = matrix, \times = fracture, \otimes = fracture-matrix coupling.)

	1	2	3	4	5	6	7	8
1	\bigcirc	\otimes	\bigcirc					
2	\otimes	\times		\times				
3	\bigcirc		\bigcirc	\otimes	\bigcirc			
4		\times	\otimes	\times		\times		
5			\bigcirc		\bigcirc	\otimes	\bigcirc	
6				\times	\otimes	\times		\times
7					\bigcirc		\bigcirc	\otimes
8						\times	\otimes	\times

(134)

DISCUSSION

The value for the coupling strength must be determined ideally by calibration with field data and experiment. However, it should be noted that the coupling parameter γ , in general, could be time and space dependent. For example, precipitation of fracture coatings could significantly alter the coupling strength. Thus chemical reactions may alter the communication between the fracture network and matrix over time.

CONCLUSION

REFERENCES

- Lichtner, P.C. (1988) The quasi-stationary state approximation to coupled mass transport and fluid-rock interaction in a porous media. *Geochimica et Cosmochimica Acta*, 52:143–165.
- Lichtner, P.C., and Seth, M. S. (1997) User's manual for MULTIFLO: Multicomponent-multiphase reactive transport model. CNWRA, San Antonio, TX.

Account Number: **20-1402-562**

Description: Near-field Environment Code Development – MULTIFLO

Collaborators: Dr. M. Seth (Consultant)

Objective: Development of the computer code MULTIFLO, and submodules **GEM** and **METRA**.

11.18.97 Progress in Version 2.2 of MULTIFLO. Progress in version 2.2 of MULTIFLO has involved coding MINC capability into **METRA**, and unstructured grid into **METRA** and **GEM**. Work remains to incorporate MINC into **GEM**. Work will soon begin to test these implementations in **METRA** against the code TOUGH2 as benchmark. There does not exist a benchmark code for testing **GEM**. In structured grid mode both codes function as in their previous versions with the exception of **GEM** when run in the hybrid finite difference scheme. It was found that for the first few time steps, the old **GEM** version 1.0 gave erroneous results as a result of incorrect incorporation of boundary conditions in the hybrid scheme. It is not planned to correct this bug as the old version of **GEM** will be replaced by the new one.

ChangeLog MULTIFLO

ChangeLog METRA

12.12.97 PCL Revised plots.f to avoid division by zero when computing relative humidity for zero porosity blocks.

9.3.97 PCL Revised plots.f to be compatible with TecPlot.

8.26.97 PCL Minor bug fixes and incorporated TecPlot format for 2D and 3D plot files.

8.13.97 PCL Corrected a bug in plot.f which incorrectly printed the x- and y-velocities at node interfaces.

8.5.97 PCL/MS Variable delpa was not being initialized. Changed code following statement label 100 as follows:

if (inds(m).eq.-1) then

delpa = zero

else

delpa = pak(m)-pa(m)

endif

7.23.97 PCL Added z-coordinate label to 3D velocity plot in plot.f.

7.22.97 PCL Added printout of nodes corresponding to maximum changes in pressure, saturation and temperature to screen dump.

7.21.97 PCL/MS Corrected code for LINEar capillary pressure option in subroutine inpmetra.f.

ChangeLog GEM

10.24.97 PCL Corrected a bug which multiplied the gaseous diffusion coefficient by a factor of 10. The bug occurred in the conversion of pressure to concentration units. A new constant rgasjj was added equal to 10 times the original gas constant rgasj.

10.23.97 PCL Added new keyword DBASe to read the thermodynamic database.

10.22.97 PCL Corrected stdyste.f to properly limit time step for a negative change in solid concentration at an advancing front to prescribed tolerance including zero.

8.14.97 PCL Added option itype = 0 to indicate input as log to base 10.

8.10.97 PCL Operator splitting for liquid and gas transport was revised. During the transport step the saturation is now held fixed to its value at the beginning of the time step. The saturation change is incorporated only into the reaction step in path.f. In addition the mass balance routine massbal.f was corrected to use the saturation at the end of the time step, ssat, rather than at the beginning of the step, sat.

8.8.97 PCL Revised stepgem.f to increase time step if ratio > 1 but less than 2. Previously the time step was increased only if ratio > 2.

8.7.97 PCL A bug was discovered in the operator splitting algorithm in subroutines coslg.f and opslgtl.f which required that the number of gases be equal to or less than the number of primary species. This was corrected by replacing $r(j+(n-1)*nc)$ by $r(n)$ throughout the two subroutines.

8.5.97 PCL Moved data statements in initgem.f to the block data routine blkdtgem.f.

8.4.97 PCL Added flux boundary conditions to GEM (see Scientific Notebook, 3rd Quarter, 1997, entry [8.4.97] Flux boundary conditions).

8.1.97 PCL Changed dimension of xex0, xex, xxex, and dk from ncomp to nex, the number of exchangeable cations.

7.31.97 PCL Replaced the definition of the gas constant by multiplying by 1.d-3, eliminating this factor throughout the code.

7.28.97 PCL Added sort routine indexx.f taken from Numerical Recipes to sort the secondary species concentrations and print in decending magnitude.

7.24.97 PCL Added tecplot headers to graph2d.f and graph3d.f.

7.23.97 PCL Added printout of the cpu time in seconds to time history plot in updtgem.f and initgem.f.

7.23.97 PCL Changed the dimension of cpusub(30) to cpusub(50) and added the cpu time per time step in cpusec.f.

7.23.97 PCL Replaced por(nnn) by por(n) in path.f.

7.23.97 PCL Removed check on negative values of ppsig in subroutine opspltgl.f for two-phase operator splitting.

7.22.97 PCL Made modifications to mode parameter to allow mode=0 to define distribution of species calculation with no transport.

7.22.97 PCL Modified eqlib.f and associated code to improve efficiency of distribution of species of calculation for initial and boundary conditions.

7.21.97 PCL Added source/sink term to cihytwph.f.

P. C. Lichtner

SCIENTIFIC NOTEBOOK

INITIALS:

SCZ

TPA-97

Account Number: **20-8519-001**

Description: TPA Code Testing

PI: Sitakanta Mohanty

Date Due:

Objective: Carry out tests of the TPA code.

No action.

GAS RESEARCH INSTITUTEAccount Number: **20-1136-003**

Description: Modeling Pipe Line Corrosion Under Disbonded Coatings

Collaborators: N. Sridhar PI

Date Due:

Objective: The main objective of this task is to develop the computer code TECTRAN and apply the code to modeling pipe line corrosion under disbonded coatings.

11.5.97 SRD Preparation. The SRD for TECTRAN is currently under preparation. The original approach for incorporating species-dependent diffusion coefficients was abandoned because it did not allow for harmonic averaging of the solute flux across grid boundaries. This is deemed essential especially for circumstances in which the porosity or tortuosity may become close to zero. The original formulation incorporated the quantity Ψ_j^D defined as

$$\Psi_j^D = D_j C_j + \sum_i \nu_{ji} D_i C_i. \quad (135)$$

The flux involved the gradient $\nabla \Psi_j^D$. However, it is necessary to harmonic average the coefficients of the individual gradients ∇C_i rather than $\nabla \Psi_j^D$.

The scope of the implementation is outlined below in a draft of the SRD.

INTRODUCTION

This Software Requirements Description (SRD) document describes proposed enhancements and modifications to the existing computer code **GEM**, a numerical model describing multiphase, multicomponent, reactive transport in fully or partially saturated porous media. The present version of **GEM**, however, does not include electrochemical capabilities. The task outlined in this SRD is the incorporation of electrochemical processes into **GEM**. The resulting software will be referred to as the **TECTRAN** (Transient Electromigration Chemical Transport) code. In addition the capability for modeling concentrated electrolyte solutions will be incorporated into **TECTRAN**. Chemical reactions incorporated in **GEM** code include homogeneous

equilibria, a kinetic formulation of mineral precipitation/dissolution reactions, and ion-exchange based on a local equilibrium description.

The numerical algorithms used in **GEM** and **TECTRAN** are fully implicit and operator splitting time stepping algorithms based on integrated finite difference. The fully implicit approach allows much larger time steps than would be possible for an explicit finite difference algorithm for very small-scale geometries such as crevices.

The code **TECTRAN** will be used to predict the local environment and corrosion rate under a disbonded coating of a steel pipeline for different external conditions (Sridhar et al., 1997).

SOFTWARE REQUIREMENT DESCRIPTION (SRD) for TECTRAN Version 1.0

This SRD briefly outlines the software function, technical basis, and computational approach, that are relevant to the proposed enhancements to the existing code **GEM**, Version 1.1 (Lichtner and Seth, 1997). The enhanced version will be issued as **TECTRAN** Version 1.0. The programming language used in **TECTRAN** is FORTRAN. The code will be developed on a Sun-sparc workstation, and PC's running NEXTSTEP and PC-UNIX. It will be also ported and tested on Windows 95 and/or NT operating systems.

Software Function

Planned additions to the code **GEM** include incorporation of the following items:

- (i) electrochemical migration,
- (ii) corrosion kinetics based on the Butler-Volmer and other kinetic rate laws,
- (iii) kinetic homogeneous reactions,
- (iv) activity coefficients for high ionic strength (to be supplied by OLI),
- (v) species-dependent diffusion coefficients (to be amplified by OLI),
- (vi) surface complexation,
- (vii) microbially induced reactions.

Each of these items is discussed in more detail below. A more detailed description of electrochemical-related processes can be found in the report by Lichtner (1994).

Electrochemical Migration

A description of electrochemical migration involves introducing an electric potential acting on charged ions. The flux density \mathbf{J}_i for a dissolved species in a porous medium with porosity ϕ is assumed to have the form

$$\mathbf{J}_i = -\tau\phi z_i u_i C_i F \nabla \Phi - \tau\phi D_i (\nabla C_i + C_i \nabla \ln \gamma_i) + \mathbf{v} C_i, \quad (136)$$

where the first term refers to electrochemical migration, the second term to aqueous diffusion, and the last term to advective transport. Here z_i , u_i , γ_i , and D_i denote the valence, mobility, activity coefficient, and diffusivity of the i th species, respectively. The quantity τ refers to the tortuosity of the porous medium, Φ represents the electrical potential field, F denotes the Faraday constant, and \mathbf{v} denotes the Darcy fluid velocity. This form for the solute flux will be incorporated into **TECTRAN** with appropriate algorithms to compute the activity coefficients under high ionic strength.

Corrosion Rate Laws

Electrochemical reactions will include corrosion of steel, reduction of dissolved oxygen, and evolution of hydrogen. These reactions may be either kinetically or mass transfer controlled. For surface controlled electrochemical reactions, one possible form for the current density associated with the corroding metal is a Butler-Volmer type equation

$$i_k = i_k^{eq} \left\{ \exp \left[\frac{\alpha_k n_k F}{RT} \eta_k \right] - \exp \left[-\frac{(1 - \alpha_k) n_k F}{RT} \eta_k \right] \right\}, \quad (137)$$

where i_k^{eq} denotes the equilibrium exchange current density. The first term represents the anodic and the second term the cathodic current density. The potential η_k refers to the overpotential defined as the difference between the actual potential and the equilibrium potential

$$\eta_k = \mathcal{E}_k - \mathcal{E}_k^{eq}, \quad (138)$$

where \mathcal{E}_k^{eq} denotes the equilibrium potential determined according to the Nernst equation

$$\mathcal{E}_k^{eq} = \mathcal{E}_k^\ominus + \frac{RT}{n_k F} \sum_j \nu_{jk} \ln a_j, \quad (139)$$

where \mathcal{E}_k^\ominus denotes the standard state potential and ν_{jk} refer to the reaction coefficients. The parameter α_k can be determined from a Tafel plot relating the overpotential to the logarithm of the current density relative to the exchange current density.

When $|\eta| \gg 1$, the Butler-Volmer rate law diverges leading to transport controlled reaction. In this case a modified form of the Butler-Volmer equation must be used. One possibility is to consider diffusion across a thin film of thickness δ . The current density in this case has the form for transport of oxygen

$$i_{O_2(aq)} = -k_{O_2(aq)} C_{O_2(aq)}^{bulk} \frac{\exp \left[-\frac{z_{O_2(aq)} \beta F \eta}{RT} \right]}{1 + \frac{k_{O_2(aq)} \delta}{4F\phi\tau D_{O_2(aq)}} \exp \left[-\frac{z_{O_2(aq)} \beta F \eta}{RT} \right]}, \quad (140)$$

where $k_{O_2(aq)}$ denotes the reaction rate constant for the oxygen reduction reaction [$\text{C m mol}^{-1} \text{ s}^{-1}$], $D_{O_2(aq)}$ denotes the diffusivity of oxygen in the aqueous solution [$\text{m}^2 \text{ s}^{-1}$], and $C_{O_2(aq)}^{bulk}$ the bulk concentration of oxygen in solution [molality].

Kinetic Homogeneous Reactions

Irreversible homogeneous reactions within the aqueous phase are especially important for describing oxidation/reduction reactions in natural environments. In natural waters, redox couples are commonly not in thermodynamic equilibrium and hence a redox potential cannot be defined. In such cases it is imperative to describe such reactions using a kinetic rate law. The reaction rate law of the form of an elementary reaction will be incorporated into **TECTRAN**

$$I_r^{irr} = k_r^f \prod_{\nu_{jr} > 0} (\gamma_j C_j)^{\nu_{jr}} - k_r^b \prod_{\nu_{jr} < 0} (\gamma_j C_j)^{-\nu_{jr}}, \quad (141)$$

where $k_r^{f,b}$ denote the forward and backward rate constants. Other forms of the rate law for reduction of dissolved oxygen which may be mass transfer limited will also be included.

Activity Coefficients for High Ionic Strength

OLI will provide a routine to compute activity coefficients and aqueous speciation for high ionic strength aqueous solutions. The activity coefficient model is based on the Bromley (1972) theory for interactions between cations and anions and the Pitzer (1973) model for ion-molecule and molecule-molecule interactions. In the absence of experimental data, the work of Meissner (1978) will be used to estimate activity coefficient parameters.

Input variables to the activity coefficient routine will consist of temperature, pressure, thermodynamic equilibrium constants, and concentrations of primary species in molality units. Output will provide the solution ionic strength, concentrations of secondary species, and activity coefficients of both primary and secondary species. Primary and secondary species are distinguished by the homogeneous aqueous reactions written in the form



where the species \mathcal{A}_j refer to primary species N_c in number, and the species \mathcal{A}_i are referred to as secondary species. The matrix ν_{ji} denotes the stoichiometric coefficients. The routine supplied by OLI will compute the concentration of secondary species through the mass action equations

$$m_i = \gamma_i^{-1} K_i \prod_{j=1}^{N_c} (\gamma_j m_j)^{\nu_{ji}}. \quad (143)$$

In this equation m_j and m_i denote molalities, γ_j and γ_i activity coefficients, respectively, of primary and secondary species, and $K_i(T, p)$ represents the equilibrium constant for reaction (142), in general a function of temperature T and pressure p .

The I/O structure of the activity coefficient subroutine is:

subroutine activity

input variables: $T, p, N_c, N_{\text{cmplx}}, \nu_{ji}, K_i, m_j$

output variables: $I, m_i, \gamma_i, \gamma_j$

where I represents the ionic strength and N_{cmplx} the number of aqueous complexes. Additional input parameters as supplied by OLI will be needed in the activity coefficient algorithm.

Species-Dependent Aqueous Diffusion Coefficients

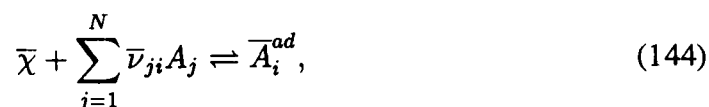
The code **TECTRAN** will incorporate species-dependent aqueous diffusion coefficients. Typical values for aqueous diffusion coefficients of solute species are listed in Table 3. The use of species-dependent diffusion coefficients greatly complicates the multicomponent transport equations and leads to concentration-dependent effective diffusion coefficients.

Table 3: Diffusion coefficients for a selected set of species in an aqueous solution at 25°C and infinite dilution. Values taken from Newman (1991) and Oelkers and Helgeson (1988).

species	diffusion constant	species	diffusion constant	species	diffusion constant	species	diffusion constant
$\text{cm}^2 \text{s}^{-1} \times 10^5$							
Cs ⁺	2.100	F ⁻	2.100	Cu ²⁺	0.800	SO ₄ ²⁻	1.065
Cu ⁺	1.200	Cl ⁻	2.032	Ca ²⁺	0.792		
H ⁺	9.312	HCO ₃ ⁻	1.105	Fe ²⁺	0.800		
K ⁺	1.957	HSO ₄ ⁻	1.330	Mg ²⁺	0.706		
Na ⁺	1.334	I ⁻	2.044	Ni ²⁺	0.800		
NH ₄ ⁺	1.954	OH ⁻	5.260	Sr ²⁺	0.900		
				Zn ²⁺	0.800		

Diffuse Double-Layer Model

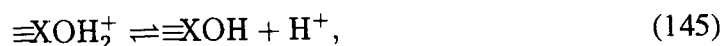
In a later version of **TECTRAN**, the diffuse double-layer model for adsorption will be incorporated into **TECTRAN**. The double-layer model has been shown to apply to sorption on oxides such as iron oxide (Dzombak and Morel, 1990) and should be an important process for modeling pipeline disbonded coatings. The double-layer model may be formulated generally in terms of the following set of surface complexation reactions



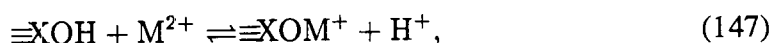
where $\bar{\chi}$ denotes the neutral oxide surface site, $\bar{\nu}_{ji}$ refers to the stoichiometric coefficients involving primary aqueous solute species A_j , and \bar{A}_i^{ad} represents the i th

adsorbed surface species. In what follows an overscore is used to designate quantities referred to the surface of the oxide mineral.

Examples of these reactions for adsorption of a divalent cation M^{2+} on an oxide surface are expressed by



and



where $\equiv\text{XOH}_2^+$ and $\equiv\text{XO}^-$ represent surface hydroxyl groups describing protonation and deprotonation of the surface, $\equiv\text{XOH}$ represents the unoccupied surface sites, and $\equiv\text{XOM}^+$ represents adsorption of the cation M^{2+} .

The mass action equations corresponding to Eqn.(144) have the general form

$$\begin{aligned} \bar{C}_i &= \bar{K}_i \bar{C}_{\bar{x}} \prod_{j=1}^N (\gamma_j C_j P^{z_j})^{\bar{\nu}_{ji}}, \\ &= \bar{K}_i \bar{C}_{\bar{x}} P^{\bar{z}_i} \prod_{j=1}^N (\gamma_j C_j)^{\bar{\nu}_{ji}}, \end{aligned} \quad (148)$$

where C_j denotes the bulk concentration of the j th primary species, and the factor P is given by the Boltzmann distribution

$$P = e^{-F\psi_0/RT}, \quad (149)$$

where ψ_0 the electric double-layer potential evaluated at the surface, R the gas constant, and T the temperature. The latter expression is obtained noting that the valence associated with the i th adsorbed species \bar{z}_i is related to the valencies of the primary species by the equation

$$\bar{z}_i = \sum_j \bar{\nu}_{ji} z_j. \quad (150)$$

Conservation of sites is described by the equation

$$\begin{aligned} \bar{C}_s &= \bar{C}_{\bar{x}} + \sum_i \bar{C}_i, \\ &= \bar{C}_{\bar{x}} \left\{ 1 + \sum_i \bar{K}_i P^{\bar{z}_i} \prod_{j=1}^N (\gamma_j C_j)^{\bar{\nu}_{ji}} \right\}. \end{aligned} \quad (151)$$

From this relation and the mass action equations, Eqn.(148), the sorption isotherms for the concentration of empty sites and adsorbed species are given by

$$\bar{C}_{\bar{x}} = \frac{\bar{C}_s}{1 + \sum \bar{K}_i P^{\bar{z}_i} \prod_{j=1}^N (\gamma_j C_j)^{\bar{\nu}_{ji}}}, \quad (152)$$

and

$$\bar{C}_i = \frac{\bar{C}_s \bar{K}_i P^{\bar{z}_i} \prod_{l=1}^N (\gamma_l C_l)^{\bar{\nu}_{li}}}{1 + \sum_{i'} \bar{K}_{i'} P^{\bar{z}_{i'}} \prod_{j=1}^N (\gamma_j C_j)^{\bar{\nu}_{ji'}}}. \quad (153)$$

The surface charge σ_0 is balanced by the total charge contained within the double-layer according to the expression

$$\begin{aligned} \sigma_0 &= F \sum_i \bar{z}_i \bar{C}_i, \\ &= \sqrt{2\epsilon DRT} \left[\sum_j C_j (e^{-z_j F\psi_0/RT} - 1) + \sum_i C_i (e^{-z_i F\psi_0/RT} - 1) \right]. \end{aligned} \quad (154)$$

For a z:z electrolyte this equation simplifies to

$$\sigma = F \sum_i \bar{z}_i \bar{C}_i = \sqrt{2\epsilon DRT} \sinh \frac{F\psi_0}{RT}. \quad (155)$$

A potential problem with the double-layer model of adsorption is that in its conventional formulation for batch-type systems it does not conserve charge within the aqueous solution when combined with transport (Lichtner, 1996). Although the adsorption reaction given in Eqn.(144), as do all chemical reactions, conserves charge, it does not conserve charge separately within the aqueous and solid phases. By contrast the ion-exchange model does conserve charge separately in both phases. One approach to guaranteeing charge conservation has been given by Borkovec and Westall (1983) and implemented in reactive transport models by Parkhurst (1995). This approach will be considered in the **TECTRAN** code.

Microbially Induced Reactions

Microbial reactions could be important for realistic modeling of corrosion processes in pipeline. Microbial reactions will be incorporated into later versions of **TECTRAN** by using recent techniques developed for modeling microbial reactions in reactive transport models (Rittmann and VanBriesen, 1996). Double Monod kinetic rate

laws will be used to describe biomass synthesis. For the biomass synthesis reaction written in canonical form as



the reaction rate is determined through the Monod kinetic rate law as

$$I_m = k_m \mathcal{X}_m \prod_j \frac{C_j}{K_j + C_j}. \quad (157)$$

The product over the index j includes an electron donor and acceptor. The quantity \mathcal{X}_m refers to the concentration in moles/L of biomass. The transport equations for aqueous species read

$$\frac{\partial}{\partial t} (\phi C_j) + \nabla \cdot \mathbf{J}_j = - \sum_m \nu_{jm} I_m, \quad (158)$$

with concentration C_j and flux \mathbf{J}_j of the j th primary species. Biomass synthesis and decay is described by the mass transfer equation

$$\frac{\partial \mathcal{X}_m}{\partial t} = I_m - \lambda_m \mathcal{X}_m, \quad (159)$$

where λ_m represents the biomass decay constant.

IMPLEMENTATION

The tasks will be prioritized in the order as presented with initial work focused on incorporating electrochemical reactions into **TECTRAN**. Completion of this task will enable initial results on pipeline corrosion to be obtained without waiting for the remaining tasks to be completed. The results obtained in these preliminary studies can then be compared with the addition of high ionic strength activity coefficient corrections, species-dependent diffusion coefficients, sorption, and microbially induced reactions enabling the importance of these effects to be investigated. The tasks involving high ionic strength solutions, species-dependent diffusion coefficients, sorption, and microbially induced reactions will be started after the activities in Task-002 (Sridhar et al., 1997) have been substantially completed.

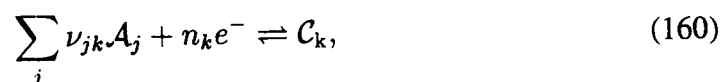
Implementation of these processes into the **TECTRAN** code will require adding new keywords to the input data file. These keywords consist of

- AQIR:** keyword for homogeneous kinetic reactions,
- CORROsion:** keyword for entering various electrochemical kinetic rate laws including the Butler-Volmer rate law and associated parameters,
- ACTivity:** keyword for choosing the activity coefficient algorithm,
- and others as needed.

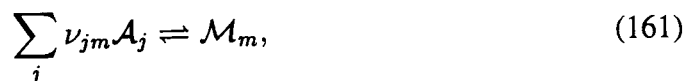
First Phase Implementation

During the first implementation phase several approximations will be made to facilitate developing the code to the point where preliminary results can be obtained. These approximations will involve using equal diffusion coefficients for all aqueous species and neglecting activity coefficient corrections for high ionic strength solutions.

Reactions to be considered are corrosion of steel, secondary mineral reactions, and homogeneous aqueous reactions. These reactions may be written in the canonical form in terms of a set of basis or primary species denoted by $\{\mathcal{A}_j\}$. The remaining species are referred to as secondary species. The primary species are chosen from the set of aqueous species but may otherwise be arbitrary so long as all reactions in the system may be expressed in terms of them. Corrosion reactions have the general form



for solid and aqueous species \mathcal{C}_k . Mineral precipitation and dissolution reactions have the form



for mineral \mathcal{M}_m , and homogeneous aqueous reactions are expressed as



for the aqueous complex \mathcal{A}_i . The corresponding reaction rates are denoted by I_k^{corr} , I_m and I_i , respectively. The matrices ν_{jk} , ν_{jm} , and ν_{ji} refer to the stoichiometric reaction coefficients. The species e^- represents the electron with stoichiometric coefficient n_k .

The mass transport equations for primary species in a fully saturated porous medium with porosity ϕ have the form

$$\frac{\partial}{\partial t}(\phi \Psi_j) + \nabla \cdot \Omega_j = - \sum_k \nu_{jk} I_k^{\text{corr}} - \sum_m \nu_{jm} I_m. \quad (163)$$

In this equation the “total” aqueous concentration Ψ_j is defined by

$$\Psi_j = C_j + \sum_i \nu_{ji} C_i, \quad (164)$$

with individual species concentrations represented by C_j for primary species and C_i for aqueous secondary species. The concentration of aqueous secondary species are related to the concentrations of the primary species by the mass action equations

$$C_i = \gamma_i^{-1} K_i \prod_j (\gamma_j C_j)^{\nu_{ji}}, \quad (165)$$

with equilibrium constant K_i and activity coefficients γ_i . Thus these species are assumed to be in local equilibrium. The “total” flux Ω_j is defined by

$$\Omega_j = J_j + \sum_i \nu_{ji} J_i, \quad (166)$$

where the solute flux J_l consists of contributions from advection, diffusion, and electrochemical migration

$$J_l = v C_l - \tau \phi D \nabla C_l - \tau \phi \frac{\mathcal{F}}{RT} D z_l C_l \nabla \Phi, \quad (167)$$

where v represents the Darcy flow velocity, D refers to the aqueous diffusion coefficient assumed to be the same for all species, z_l refers to the valence of the l th species, \mathcal{F} represents the Faraday constant, Φ denotes the potential, R denotes the gas constant, and T refers to the temperature. With this expression for the solute flux, the “total” flux Ω_j becomes

$$\Omega_j = v \Psi_j - \tau \phi D \nabla \Psi_j - \tau \phi \frac{\mathcal{F}}{RT} D \Psi_j^z \nabla \Phi, \quad (168)$$

where the quantity Ψ_j^z is defined by the expression

$$\Psi_j^z = z_j C_j + \sum_i \nu_{ji} z_i C_i. \quad (169)$$

The electric potential is determined by enforcing local charge balance on the aqueous solution. Charge balance requires that

$$\sum_j z_j \Psi_j = 0. \quad (170)$$

Multiplying the transport equations by the valence z_j , summing over all primary species and making use of the charge balance relation, yields the differential equation for the potential

$$\begin{aligned} \nabla \cdot \mathbf{i} &= - \sum_{jk} z_j \nu_{jk} I_k^{\text{corr}}, \\ &= - \sum_k z_k I_k^{\text{corr}}, \end{aligned} \quad (171)$$

where the electric current density \mathbf{i} is defined by

$$\mathbf{i} = \sum_j z_j \Omega_j, \quad (172)$$

$$= -\tau \phi \frac{\mathcal{F}}{RT} D \nabla \Phi \sum_j z_j \Psi_j^z, \quad (173)$$

$$= -\kappa \nabla \Phi, \quad (174)$$

The quantity κ represents the Debye length and is defined by

$$\kappa = \tau \phi \frac{\mathcal{F}}{RT} D \sum_j z_j \Psi_j^z. \quad (175)$$

Thus the potential and charge conservation is maintained by solving the differential equation

$$\nabla \cdot (\kappa \nabla \Phi) = \sum_k z_k I_k^{\text{corr}}. \quad (176)$$

In one dimension this equation becomes

$$\frac{\partial}{\partial x} \left(\kappa \frac{\partial \Phi}{\partial x} \right) = \sum_k z_k I_k^{\text{corr}}. \quad (177)$$

Integrated over the flow path in a crevice of length L from x to the mouth gives

$$\kappa(x) \frac{\partial \Phi}{\partial x} - \kappa(L) \frac{\partial \Phi}{\partial x} \Big|_L = \sum_k z_k \int_L^x I_k^{\text{corr}}(x') dx'. \quad (178)$$

These equations will be programmed into **GEM** to produce the first version of **TEC-TRAN**.

REFERENCES

- Borkovec, M., and Westall, J. 1983. Solution of the Poisson-Boltzmann equation for surface excesses of ions in the diffuse layer at the oxide-electrolyte interface. *J. Electroanal. Chem.* 150:325-337.
- Bromley, L.A. 1973. *AIChE J.* 19:313.
- Dzombak, D.A. and Morel, F.M. 1990. *Surface Complex Modeling, Hydrous Ferric Oxide*. Wiley-Interscience, New York.
- Lichtner, P.C., and Seth, M.S. 1997. User's manual for MULTIFLO: Multicomponent-multiphase reactive transport model. CNWRA 97-000. San Antonio, Texas: Center for Nuclear Regulatory Analyses. In preparation.
- Lichtner, P.C. 1994. *Engineered Barrier System Performance Assessment Code (EB-SPAC) Progress Report October 1, 1993, through September 25, 1994*. CNWRA 94-026. San Antonio, TX: Center for Nuclear Waste Regulatory Analyses.
- Lichtner, P.C. 1996. Continuum formulation of multicomponent-multiphase reactive transport. In *Reactive Transport in Porous Media*, (eds. Lichtner, P.C., Steefel, C.I., and Oelkers, E.H.), Chapter 1, *Reviews in Mineralogy* 34:1-81.
- Meissner, H.P. 1978. *AIChE Symp. Ser.* 173:74.
- Newman, J.S. 1991. *Electrochemical Systems*, 2ed. Prentice Hall, Englewood cliffs, New Jersey, 560pp.
- Oelkers, E.H. and Helgeson, H.C. 1988. Calculation of the thermodynamic and transport properties of aqueous species at high pressures and temperatures: aqueous tracer diffusion coefficients of ions to 1000°C and 5kb. *Geochimica et Cosmochimica Acta* 52:63-85.
- Parkhurst, D.L. 1995. User's guide to PHREEQC—a computer program for speciation, reaction-path, advective-transport, and inverse geochemical calculations. U.S. Geological Survey, Water-Resources Investigations Report 95-4227.
- Pitzer, K.S. 1973. *J. Phys. Chem.* 77:268.
- Rittmann, B.E., and VanBriesen, J.M. 1996. Microbiological processes in reactive modeling. In *Reactive Transport in Porous Media*, (eds. Lichtner, P.C., Steefel, C.I., and Oelkers, E.H.), Chapter 7, *Reviews in Mineralogy* 34:311-334.
- Sridhar, N., Anderko, A. Dunn, D.S., Lichtner, P.C., Lyle, F.F., and Orazem, M. 1997. Models for mitigating corrosion under disbonded coating on steel pipeline.

Part I — Technical Proposal. SwRI Revised Proposal 20-18639A. San Antonio, TX: Center for Nuclear Waste Regulatory Analyses.

12.23.97 Formulation of Corrosion Rate Laws and Current/Potential Relations

GENERAL FORM OF THE CORROSION RATE LAW

The corrosion rate is defined through the current as

$$i_m(\Phi) = i_m^\circ \left\{ \exp \left[\alpha \frac{n_m F}{RT} (\Phi - \Phi_m) \right] - \exp \left[-\beta \frac{n_m F}{RT} (\Phi - \Phi_m) \right] \right\}, \quad (179)$$

referred to as the Butler-Volmer rate law, where Φ_m is defined by the Nernst equation

$$\Phi_m = \Phi_m^\circ + \frac{RT}{n_m F} \sum_j \nu_{jm} \ln a_j. \quad (180)$$

The standard potential Φ_m° is related to the equilibrium constant K_m by the expression

$$\Phi_m^\circ = \frac{RT}{n_m F} \ln K_m. \quad (181)$$

With this relation the Nernst equation can be written in the concise form

$$\Phi_m = \frac{RT}{n_m F} \ln [K_m Q_m]. \quad (182)$$

The corrosion current i_m is related to the usual reaction rate I_m by multiplying the current by the specific mineral surface area s_m and dividing by the Faraday constant

$$I_m^e(\Phi) = -\frac{1}{F} s_m i_m(\Phi). \quad (183)$$

The negative sign appears because the usual rate is defined as negative for dissolution and positive for precipitation. Defining the rate constant k_m in terms of the exchange current i_m° as

$$k_m = \frac{1}{F} i_m^\circ, \quad (184)$$

the reaction rate $I_m^e(\Phi)$ is equal to

$$\begin{aligned} I_m^e(\Phi) &= -k_m s_m \left\{ \exp \left[\alpha \frac{n_m F}{RT} (\Phi - \Phi_m) \right] - \exp \left[-\beta \frac{n_m F}{RT} (\Phi - \Phi_m) \right] \right\}, \\ &= -k_m s_m \left\{ e^{\alpha(\eta_m(\Phi) - \ln[K_m Q_m])} - e^{-\beta(\eta_m(\Phi) - \ln[K_m Q_m])} \right\}, \end{aligned} \quad (185)$$

where

$$\eta_m(\Phi) = \frac{n_m F}{RT} \Phi. \quad (186)$$

The derivative of the reaction rate can be expressed as

$$\begin{aligned} \frac{\partial I_m^e}{\partial C_l} &= k_m s_m \left\{ \alpha e^{\alpha(\eta_m - \ln[K_m Q_m])} + \beta e^{-\beta(\eta_m - \ln[K_m Q_m])} \right\} \frac{\partial \ln Q_m}{\partial C_l}, \\ &= k_m s_m \frac{\nu_{lm}}{C_l} \left\{ \alpha e^{\alpha(\eta_m - \ln[K_m Q_m])} + \beta e^{-\beta(\eta_m - \ln[K_m Q_m])} \right\} \end{aligned} \quad (187)$$

where

$$\frac{\partial \ln Q_m}{\partial C_l} = \frac{\nu_{lm}}{C_l}. \quad (188)$$

These results can be compared with the usual reaction rate defined by

$$I_m = -k_m s_m [1 - K_m Q_m], \quad (189)$$

with the derivative

$$\begin{aligned} \frac{\partial I_m}{\partial C_l} &= k_m s_m K_m Q_m \frac{\partial \ln Q_m}{\partial C_l}, \\ &= k_m s_m K_m Q_m \frac{\nu_{lm}}{C_l}. \end{aligned} \quad (190)$$

Specific Electrode Reactions

Iron Dissolution

Corrosion of iron is described by the reaction



The current density is expressed in terms of the potential Φ as

$$i_{\text{active}}^{\text{steel}} = i_{0, \text{Fe}/\text{Fe}^{2+}} \exp \left[\frac{\alpha_{\text{Fe}} z_{\text{Fe}} F (\Phi - \Phi_{\text{Fe}/\text{Fe}^{2+}})}{RT} \right], \quad (192)$$

where

$i_{0,\text{Fe}/\text{Fe}^{2+}}$ —exchange current density for the dissolution of iron

α_{Fe} —charge transfer coefficient for the dissolution of iron

z_{Fe} —number of electrons involved in the dissolution of iron

F —Faraday's constant ($96,485 \text{ C mol}^{-1}$)

Φ —potential (V_{SHE})

$\Phi_{\text{Fe}/\text{Fe}^{2+}}^{\circ}$ —equilibrium potential for the dissolution of iron

R —gas constant ($8.314 \text{ J mol}^{-1} \text{ K}^{-1}$)

T —temperature in K

Table 4: Parameter Values

Parameter	Value	Reference
$i_{0,\text{Fe}/\text{Fe}^{2+}}$	10^{-10} A/m^2	Heusler (1976)
	$10^{-1} \text{ to } 10^{-6} \text{ A/m}^2$	Bockris et al. (1961)
	10^{-2} A/m^2	Conway (1952)
z_{Fe}	2	
b_{Fe}	40 mV/decade of current	De Waard and Milliams (1975) Ogundeke and White (1986)
$\Phi_{\text{Fe}/\text{Fe}^{2+}}^{\circ}$	$-0.440 V_{\text{SHE}}$	Bard et al. (1985)

Value of $i_{0,\text{Fe}/\text{Fe}^{2+}}$:

Heusler (1976) 10^{-10} A/m^2 .

Bockris et al. (1961) $10^{-1} \text{ to } 10^{-6} \text{ A/m}^2$ depending on $[\text{Fe}^{2+}]$, pH, and anionic species in solution.

Conway (1952) 10^{-2} A/m^2 typical exchange current densities for dissolution of iron and nickel.

z_{Fe} is equal to 2.

α_{Fe} is calculated according to:

$$\alpha_{\text{Fe}} = 2.303 \frac{RT}{b_{\text{Fe}} z_{\text{Fe}} F}, \quad (193)$$

where

$$b_{\text{Fe}} \text{---Tafel slope for the dissolution of iron.} \quad (194)$$

b_{Fe} measured to be 40 mV/decade of current (De Waard and Milliams, 1975; Ogundele and White, 1986)

The equilibrium potential $\Phi_{\text{Fe}/\text{Fe}^{2+}}$ is given by the Nernst equation

$$\Phi_{\text{Fe}/\text{Fe}^{2+}}(V_{\text{SHE}}) = \Phi_{\text{Fe}/\text{Fe}^{2+}}^{\circ} + 2.303 \frac{RT}{z_{\text{Fe}}F} \log[\text{Fe}^{2+}], \quad (195)$$

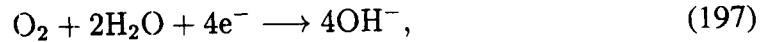
$$= \Phi_{\text{Fe}/\text{Fe}^{2+}}^{\circ} + \frac{RT}{z_{\text{Fe}}F} \ln[\text{Fe}^{2+}], \quad (196)$$

where

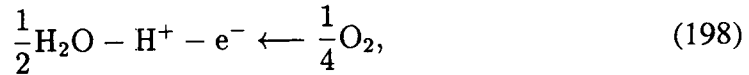
$\Phi_{\text{Fe}/\text{Fe}^{2+}}^{\circ}$ —standard potential for the dissolution of iron is $-0.440 V_{\text{SHE}}$ (Bard et al., 1985)

Oxygen Reduction

Oxygen reduction is described by the reaction



or equivalently



The current density is assumed to have the form

$$i_{\text{O}_2}^{\text{steel}} = i_{0,\text{O}_2}^{\text{steel}} \frac{\exp \left[-\frac{\beta_{\text{O}_2} z_{\text{O}_2} F (\Phi - \Phi_{\text{O}_2})}{RT} \right]}{1 + \left\{ \frac{i_{0,\text{O}_2}^{\text{steel}} \delta}{4FD_{\text{O}_2}C_{\text{O}_2}^{\text{bulk}}} \exp \left[-\frac{\beta_{\text{O}_2} z_{\text{O}_2} F (\Phi - \Phi_{\text{O}_2})}{RT} \right] \right\}}, \quad (199)$$

where

$i_{0,\text{O}_2}^{\text{steel}}$ —exchange current density for the reduction of oxygen on steel

β_{O_2} —charge transfer coefficient for the reduction of oxygen

z_{O_2} —number of electrons involved in the reduction of oxygen

Φ_{O_2} —equilibrium potential for the reduction of oxygen

δ —thickness of the diffusion layer

D_{O_2} —diffusion coefficient for oxygen

$C_{\text{O}_2}^{\text{bulk}}$ —concentration of dissolved oxygen in the bulk solution

$\delta = 5 \times 10^{-4}$ m in a stationary system; 5×10^{-5} m in a well agitated system (Bockris and Reddy, 1977).

Φ_{O_2} is calculated according to the Nernst equation as follows:

$$\Phi_{O_2} = \Phi_{O_2}^{\circ} + \frac{RT}{F} \ln[H^+] + \frac{1}{4} \frac{RT}{F} \ln P_{O_2}, \quad (200)$$

where

$$\Phi_{O_2}^{\circ} \text{—standard potential for the reduction of oxygen (} V_{SHE} \text{)} \quad (201)$$

$$P_{O_2} \text{—partial pressure of oxygen (atm)} \quad (202)$$

The temperature dependence for is based on data published by Macdonald et al. (1972).

$$\Phi_{O_2}^{\circ} = 1.47172 - 8.15 \times 10^{-4} T. \quad (203)$$

The exchange current density for the reduction of oxygen on A516 steel, i_{0,O_2}^{steel} , is calculated as follows:

$$i_{0,O_2}^{\text{steel}} = i_{0,O_2(298)}^{\text{steel}} \exp \left[\frac{\Delta H_{a,O_2}}{R} \left(\frac{1}{298} - \frac{1}{T} \right) \right], \quad (204)$$

where

$$i_{0,O_2(298)}^{\text{steel}} \text{—exchange current density for the reduction of oxygen on steel at 298 K} \quad (205)$$

$$\Delta H_{a,O_2} \text{—activation enthalpy for the reduction of oxygen} \quad (206)$$

On passivated iron $i_{0,O_2(298)}^{\text{steel}} = 1 \times 10^{-6}$ A/m² (Calvo and Schiffrin, 1988). $\Delta H_{a,O_2} = 40$ kJ/mol (Calvo, 1979).

β_{O_2} is calculated according to

$$\beta_{O_2} = 2.303 \frac{RT}{b_{O_2} z_{O_2} F}, \quad (207)$$

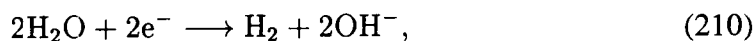
where

$$z_{O_2} = 4, \quad (208)$$

$$b_{O_2} = 120 \text{ mV/decade.} \quad (209)$$

Water Reduction

Hydrogen evolution is described by the reaction



or



The current density is given by

$$i_{\text{H}_2\text{O}}^{\text{steel}} = i_{0,\text{H}_2\text{O}} \exp \left[-\frac{\beta_{\text{H}_2\text{O}} z_{\text{H}_2\text{O}} F (\Phi - \Phi_{\text{H}_2\text{O}})}{RT} \right], \quad (212)$$

where

$$i_{0,\text{H}_2\text{O}} \text{—exchange current density for the reduction of water,} \quad (213)$$

$$\beta_{\text{H}_2\text{O}} \text{—charge transfer coefficient for the reduction of water,} \quad (214)$$

$$z_{\text{H}_2\text{O}} \text{—number of electrons involved in the reduction of water,} \quad (215)$$

$$\Phi_{\text{H}_2\text{O}} \text{—equilibrium potential for the reduction of water.} \quad (216)$$

$\Phi_{\text{H}_2\text{O}}$ is calculated according to the equation

$$\Phi_{\text{H}_2\text{O}} = \Phi_{\text{H}_2\text{O}}^\circ + \frac{RT}{F} \ln[\text{H}^+], \quad (217)$$

where

$$\Phi_{\text{H}_2\text{O}}^\circ \text{—standard potential for the reduction of water (= 0 mV}_{\text{SHE}}) \quad (218)$$

$$(219)$$

The exchange current density for water reduction at 298 K, $i_{0,\text{H}_2\text{O},(298)}$, is calculated as a function of pH according to the equation

$$i_{0,\text{H}_2\text{O},(298)} = 2Fk_1[\text{H}^+]^{\beta_{\text{H}_2\text{O}}}. \quad (220)$$

$k_1 = 5.18 \times 10^{-8} \text{ mol m}^{-2} \text{ s}^{-1}$ (Bockris and Reddy 1977). $i_{0,\text{H}_2\text{O},(298)} = 10^{-2} \text{ A/m}^2$ at pH 0 (Bockris and Reddy 1977).

The exchange current density at any temperature can then be calculated according to the equation

$$i_{0,\text{H}_2\text{O}}^{\text{steel}} = i_{0,\text{H}_2\text{O},(298)}^{\text{steel}} \exp \left[\frac{\Delta H_{a,\text{H}_2\text{O}}}{R} \left(\frac{1}{298} - \frac{1}{T} \right) \right], \quad (221)$$

where

$$\Delta H_{a,H_2O} \text{—activation enthalpy for the reduction of water.} \quad (222)$$

$\Delta H_{a,H_2O} = 20 \text{ kJ/mol}$ (Calvo, 1979). β_{H_2O} is calculated according to

$$\beta_{H_2O} = 2.303 \frac{RT}{b_{H_2O} z_{H_2O} F}, \quad (223)$$

where

$$z_{H_2O} = 2, \quad (224)$$

$$b_{H_2O} = 120 \text{ mV/decade.} \quad (225)$$

SOLUTE TRANSPORT EQUATIONS

The primary species transport equations have the form

$$\frac{\partial}{\partial t} (\phi \Psi_j) + \nabla \cdot \Omega_j = - \sum_k \nu_{jk}^e I_k^e - \sum_m \nu_{jm}^e I_m^e - \sum_m \nu_{jm}^s I_m^s - \sum_r \nu_{jr}^{irr} I_r^{irr}, \quad (226)$$

$$\frac{\partial}{\partial t} (\phi \Psi_k) + \nabla \cdot \Omega_k = I_k^e - \sum_m \nu_{km}^s I_m^s - \sum_r \nu_{kr}^{irr} I_r^{irr}. \quad (227)$$

The solute flux for the i th species consists of contributions from electrochemical migration and the usual advective and diffusive transport terms

$$\mathbf{J}_i = -\tau \phi z_i u_i C_i F \nabla \Phi + \mathbf{J}_i^0, \quad (228)$$

The Fickian diffusion and advective terms are contained in the term \mathbf{J}_i^0

$$\mathbf{J}_i^0 = -\tau \phi D_i \nabla C_i + \mathbf{q} C_i. \quad (229)$$

The generalized concentration Ψ_j and flux Ω_j are defined by

$$\Psi_j = C_j + \sum_i \nu_{ji} C_i, \quad (230)$$

and

$$\Omega_j = \mathbf{J}_j + \sum_i \nu_{ji} \mathbf{J}_i. \quad (231)$$

The generalized flux may be expressed as

$$\Omega_j = -\tau\phi\Psi_j^z \frac{F}{RT} \nabla\Phi + \Omega_j^0, \quad (232)$$

where the quantity Ψ_j^z is defined by

$$\Psi_j^z = z_j D_j C_j + \sum_i \nu_{ji} z_i D_i C_i, \quad (233)$$

and

$$\Omega_j^0 = J_j^0 + \sum_i \nu_{ji} J_i^0, \quad (234)$$

$$= -\tau\phi \left(D_j \nabla C_j + \sum_i \nu_{ji} D_i \nabla C_i \right). \quad (235)$$

Current Density and Potential Relations

The potential Φ is an unknown quantity along with the primary species solute concentrations C_j . Once these quantities are known all other quantities are determined. The additional equation necessary to determine the potential is conservation of charge. To determine the potential it is first necessary to compute the aqueous solution current density. The current density i is defined by the relation

$$i = F \sum_j z_j \Omega_j, \quad (236)$$

$$= -\tau\phi \frac{F^2}{RT} \nabla\Phi \sum_j z_j \Psi_j^z + F \sum_j z_j \Omega_j^0. \quad (237)$$

Defining

$$i_0 = F \sum_j z_j \Omega_j^0, \quad (238)$$

and κ by

$$\kappa = \frac{\tau\phi F^2}{RT} \sum_j z_j \Psi_j^z, \quad (239)$$

the gradient in the potential can be expressed as

$$\nabla\Phi = -\frac{i - i_0}{\kappa}. \quad (240)$$

With this relation the potential can be eliminated from the expression for the generalized flux to give

$$\Omega_j = \frac{\omega_j}{F}(\mathbf{i} - \mathbf{i}_0) + \Omega_j^0, \quad (241)$$

where

$$\omega_j = \frac{\Psi_j^z}{\sum_l z_l \Psi_l^z}. \quad (242)$$

With this result the primary species transport equations have the form

$$\begin{aligned} \frac{\partial}{\partial t}(\phi \Psi_j) + \nabla \cdot \Omega_j^0 + \nabla \cdot \frac{\omega_j}{F}(\mathbf{i} - \mathbf{i}_0) = \\ - \sum_k \nu_{jk}^e I_k^e(\Phi) - \sum_m \nu_{jm}^e I_m^e(\Phi) - \sum_m \nu_{jm}^s I_m^s. \end{aligned} \quad (243)$$

Multiplying by the charge Fz_j and summing over all primary species assuming that

$$\sum_j z_j \Psi_j = 0, \quad (244)$$

yields

$$\nabla \cdot \mathbf{i} = F \left(\sum_m n_m I_m^e(\Phi) + \sum_k n_k I_k^e(\Phi) \right). \quad (245)$$

To obtain this result, note that

$$\sum_j z_j \omega_j = 1, \quad (246)$$

and

$$\sum_j z_j \nu_{jm} = n_m, \quad (247)$$

$$\sum_j z_j \nu_{jk} = n_k, \quad (248)$$

$$\sum_j z_j \nu_{js} = 0. \quad (249)$$

Note that if all diffusion coefficients are the same the current density \mathbf{i}_0 vanishes.

An equation for the potential alone can be derived by taking the divergence of Eqn.(240) and substituting Eqn.(245) to give

$$\nabla^2 \Phi + \nabla \ln \kappa \cdot \nabla \Phi = \frac{1}{\kappa} (j_e + \nabla \cdot \mathbf{i}_0), \quad (250)$$

where

$$j_e(\Phi) = F \left(\sum_m n_m I_m^e(\Phi) + \sum_k n_k I_k^e(\Phi) \right). \quad (251)$$

NUMERICAL SOLUTION

In order to solve the electrochemical transport equations numerically an iterative procedure must be used. The current density i depends on the concentration of the primary species as well as the potential Φ through the Butler-Volmer rate law. Therefore it is necessary to solve Eqns.(245) and (240) simultaneously for given concentrations of the primary species. In this way charge balance is maintained in the aqueous solution.

The residual function is defined by

$$R_{jn} = \phi_n \Delta \Psi_{jn} V_n + \Delta t \{ \Omega_{j,n+1} A_{n+1} - \Omega_{jn} A_n \} + \Delta t V_n \left\{ \sum \nu_{jk}^e I_{kn}^e + \sum \nu_{jm}^e I_{mn}^e + \sum \nu_{jm}^s I_{mn}^s \right\}. \quad (252)$$

Substituting the expression for the flux

$$\Omega_{jn} = \Omega_{jn}^0 + \frac{\omega_{jn}}{F} (i_n - i_{0n}), \quad (253)$$

and collecting terms yields

$$R_{jn} = \phi_n \Delta \Psi_{jn} V_n + \Delta t \{ \Omega_{j,n+1}^0 A_{n+1} - \Omega_{jn}^0 A_n \} + \frac{\Delta t}{F} \{ \omega_{j,n+1} (i_{n+1} - i_{0n+1}) A_{n+1} - \omega_{jn} (i_n - i_{0n}) A_n \} + \Delta t V_n \left\{ \sum \nu_{jk}^e I_{kn}^e + \sum \nu_{jm}^e I_{mn}^e + \sum \nu_{jm}^s I_{mn}^s \right\}. \quad (254)$$

Multiplying by the charge z_j and summing over all primary species yields

$$\sum z_j R_{jn} = \phi_n V_n \sum z_j \Delta \Psi_{jn} + \frac{\Delta t}{F} \{ i_{n+1} A_{n+1} - i_n A_n + j_{en} V_n \}, \quad (255)$$

where

$$j_{en} = F \left(\sum z_j \nu_{jk}^e I_{kn}^e + \sum z_j \nu_{jm}^e I_{mn}^e \right), \\ = F \left(\sum n_k I_{kn}^e + \sum n_m I_{mn}^e \right). \quad (256)$$

Note that the current density i_0 cancels out. Charge conservation is ensured by noting that if the current satisfies the finite difference equation

$$A_{n+1} i_{n+1} = i_n A_n - j_{en} V_n, \quad (257)$$

then it follows that

$$\sum z_j \Delta \Psi_{jn} = 0, \quad (258)$$

and therefore if the aqueous solution is initially electrically neutral it must remain so with time.

Diffusive Flux

The finite difference form of the diffusive flux Ω_j^0 evaluated at interface $\{n; m1, m2\}$ can be written as

$$\Omega_{jn} = -T_j (C_{j,m1} - C_{j,m2}) - \sum_i \nu_{ji} T_i (C_{i,m1} - C_{i,m2}), \quad (259)$$

where

$$T_k = \frac{\overline{\tau \phi s_l D_k}}{d_{m1} + d_{m2}} A_n, \quad (260)$$

The electrochemical contribution to the flux has the form

$$q_{jn} = \omega_{jn} \sum_k z_l \Omega_{ln}. \quad (261)$$

REFERENCES

- Bard, A.J., R. Parsons, and J. Jordan, eds. 1985. *Standard Potentials in Aqueous Solutions*. New York: Marcel Dekker, Inc.
- Bockris, J.O'M., and A.K.N. Reddy. 1977. *Modern Electrochemistry*. New York: Plenum Press.
- Bockris, J.O'M., D. Drazic, and A.R. Despic. 1961. The electrode kinetics of the deposition and dissolution of iron. *Electrochimica Acta* 4: 325–361.
- Calvo, E.J. 1979. Study of the Electroreduction Reaction of Oxygen on Passive Metals in Different Aqueous Media (in Spanish). Ph.D. dissertation, Universidad Nacional de La Plata (Argentina).
- Calvo, E.J., and D.J. Schiffrin. 1988. The electrochemical reduction of oxygen on passive iron in alkaline solutions. *Journal of Electroanalytical Chemistry* 243: 171–185.
- Conway, B.E. 1952. *Electrochemical Data*. Amsterdam, Netherlands: Elsevier.
- De Waard, C., and D.E. Milliams. 1975. Carbonic acid corrosion of steel. *Corrosion* 31: 177–181.
- Heusler, K.E. 1976. Influence of temperature and pressure on the kinetics of electrode processes. *High Temperature, High Pressure Electrochemistry in Aqueous Systems*. D. deG. Jones and R.W. Staehle, eds. Houston, TX: National Association of Corrosion Engineers.
- Macdonald, D.D., G.R. Shierman, and P. Butler. 1972. The Thermodynamics of Metal-water Systems at Elevated Temperatures. Part 2: The Iron-Water System. AECL-4137. Pinawa, Canada: Atomic Energy of Canada Limited.
- Ogundele, G.I., and W.E. White. 1986. Some observations on corrosion of carbon steel in aqueous environments containing carbon dioxide. *Corrosion* 42: 71–78.

P. C. Lichtner

SCIENTIFIC NOTEBOOK

INITIALS: SCZ

BHP COPPER PROJECT

Account Number: **20-8519-001**

Description: Modeling In Situ Leaching of Copper

Collaborators: G. Wittmeyer

Date Due: Final Report December 22, 1996

Objective: Application of the computer code MULTIFLO to determine how the BHP Copper Florence pilot leaching facility must be designed and operated in order to maximize copper recovery.

No action.

308

Q199806260001

108

Electronic Scientific Notebook No.
095E:Development of the Code MULTIFLO to
Describe Multiphase Reactive Transport
(12/18/1995 through 04/17/1997)

SCIENTIFIC NOTEBOOK

Peter C. Lichtner

April 30, 1998

1st Quarter

SCIENTIFIC NOTEBOOK

Peter C. Lichtner

April 30, 1998

1st Quarter

Southwest Research Institute

Center for Nuclear Waste Regulatory Analyses

San Antonio, Texas

INITIAL ENTRIES

Scientific NoteBook: # 095

Issued to: P. C. Lichtner

Issue Date: Tuesday, November 16, 1993

Computerized Initials: SC

By agreement with the CNWRA QA this NoteBook is to be printed at approximate quarterly intervals. This computerized Scientific NoteBook is intended to address the criteria of CNWRA QAP-001.

Table 1: Computing Equipment

Machine Name	Type	OS	Location
gravenstein.cnwra.swri.edu	Pentium Workstation	NEXTSTEP	desk Rm A-126
	133 Mhz	Version 3.3	Bldg. 189
	128 MB RAM		
skippy.cnwra.swri.edu	Sun SPARC 20	SOLARIS 5.5	network
	128 MB RAM		

TABLE OF CONTENTS

INITIAL ENTRIES	ii
FIGURES	iv
TABLES	v
NEAR-FIELD ENVIRONMENT: TECHNICAL ASSISTANCE	1
[2.3.98]	1
[2.9.98]	7
[2.20.98]	10
[3.17.98]	15
NEAR-FIELD ENVIRONMENT: CODE DEVELOPMENT	36
[3.31.98]	36
GAS RESEARCH INSTITUTE	37
[1.8.98]	37

LIST OF FIGURES

1	Kaolinite volume fraction for an elapsed time of 10,000 years.	1
2	Kaolinite reaction rate for an elapsed time of 10,000 years.	2
3	Liquid saturation plotted as a function of depth for different times.	15
4	Liquid saturation plotted as a function of depth.	16

LIST OF TABLES

1	Computing Equipment	ii
---	-------------------------------	----

NEAR-FIELD ENVIRONMENT

Account Number: **20-1402-561**

Description: Near-field Environment Technical Assistance

Collaborators: Dr. R. Pabalan

Collaborators: Dr. C. I. Steefel (Consultant)

Collaborators: Dr. M. Seth (Consultant)

Objective: Application of the computer code MULTIFLO, and submodules **GEM** and **METRA** to the Yucca Mountain HLW Repository.

2.3.98 DCM Convergence. The DCM (Dual Continuum Model) appears slow to converge and can result in spurious results with variable grid spacing. This is shown in Figure 1 where the volume fraction of kaolinite is plotted for different equal grid spacings and for unequal grid spacing (marked by crosses).

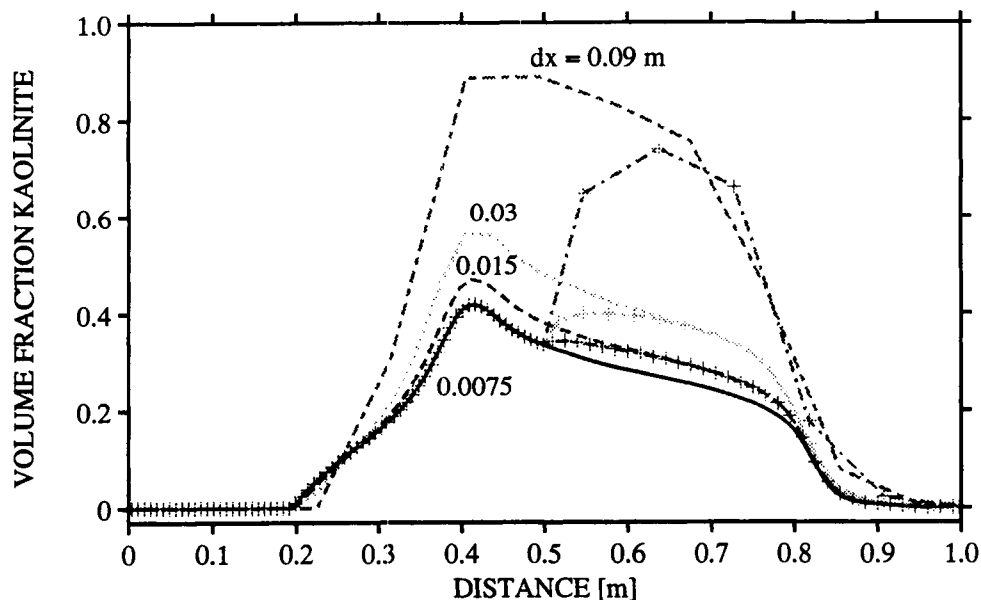


Figure 1: Kaolinite volume fraction for an elapsed time of 10,000 years.

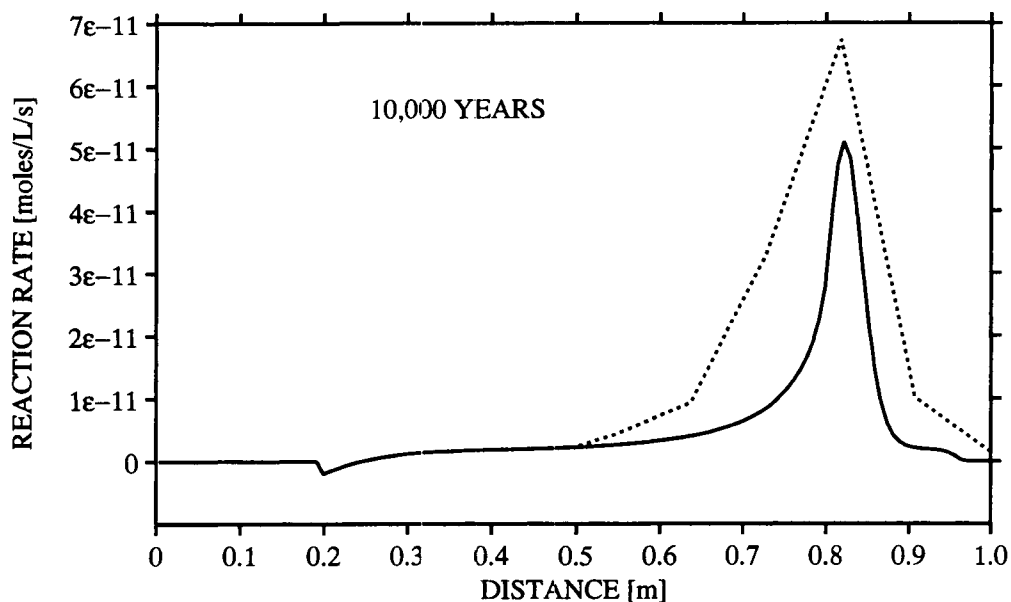


Figure 2: Kaolinite reaction rate for an elapsed time of 10,000 years.

Input file used for the simulations is listed below.

```

k-feldspar dissolution
dcm: Jan. 21, 1997
:      geometry nx ny nz mode iprint idebug iwarn il i2
GRID   DCMXYZ   99  1  1  2    1    0    0   13 20
:
DBASE
/home/skippy/lichtner/bin/database/master25.V8.R5
:
OPTS
:   idata istart imod iexact iscale ihrmc isst
:   0      0     10    0     0     1    -1
:
:   itmax ihalmax ivmax ndamp icntmx
:   16     32     0     0     3
:
:   method iops ifor isurf iact loglin icon  counr tpulse wtup
:   1      0     2     1     1     0     1     5.
:
:   isync ipor iperm permfac porfac
COUPLE  0     0     0     3.     1.
:

```

```

PLTFiles
:iplot  a  s  t  m si sf  v  z  b in  e ex ti  g itex mk err
      1  1  1  1  1  0  0  1  0  0  0  0  0  0  0  0  1
:
:      tol ttol  tolneg tolpos  tolexp  dthalf qkmax tolstdst tol c
TOLR 1.d-13 2.e-2 1.e-8  1.e-2  5.d0    .5      590.  1.e-12  1.e-13
:
:      mcyc  cc  c   flx r  sp  qk  pk  rk  a1  a2  a3
DEBUg    0      1  1   0   1   1   1   1   1
:
DCMPARA                                     ! not used
:i1 i2 j1 j2 k1 k2  xlm  volf  areamodf  pormtx  swmtx  tortfac
  1 99  1  1  1  1  0.1 1.e-3   10.      0.05   1.      1.
0
:      isat isothrm iread  por0  phir  sat  w  lambda toldelt  tolpor
ISYSstem -1    0      0      1.0 1.    1.0 .5   1.    1.e-3   1.e-3
:
:      vx0  vy0  vz0 vgx  vgy  vgz[m/yr]  alphax  alphay  alphaz[m] vmfac
FLOW 1000.0   0.    0.    0.    0.    0.      0.      0.      0.    0.
:
:      d0[cm^2/s]  delhaq[kJ/mol]  dgas[cm^2/s]  dgexp  tortaq  tortg  idif
DIFF  1.d-5      12.6              2.13d-1      1.8   1.d0   1.d0   0
:
:flag 1: T(x)    = d x^3 + a x^2 + b x + c (meters)
:      2: T(x)    = a + (b-a) exp[-((x-x0)/c)^2] + (d - a) * x / xlen
:      3:T(x,t)=a+1/2(b-a)(erf[(x+c-x0)/2sqr(dt)]-erf[(x-c-x0)/2sqr(dt)])
:      p (bars) temp flag  a    b    c    d    x0    xlen
PTINit 1.e5   25.    0   25  300  250  125  1000.  2.d3
:
:master species for controlling time stepping
Master h+
:
Dxyz
67*0.0075 32*0.09
  1.
  1.
:
:  isolv level north nitmax idetail rmaxtol rtwotol smaxtol
SOLV   4    1      3    100      0    1.e-20 1.e-20 1.e-12
:
:initial and boundary conditions: 1-conc., 2-flux, 3-zero gradient
COMP

```

```

:
:i1 i2 j1 j2 k1 k2
  1 99 1 1 1 1
0
:
      fracture
:species itype ctot mineral guess
k+        3 1.e-4 k-feldspar
al+3      3 1.e-9 muscovite
h+        8 8.0 kaolinite
sio2(aq)  3 1.e-4 quartz
cl-       -1 1.e-4
      :blank
:
      matrix
:species itype ctot mineral guess
k+        3 1.e-4 k-feldspar
al+3      3 1.e-9 muscovite
h+        8 8.0 kaolinite
sio2(aq)  3 1.e-4 quartz
cl-       -1 1.e-4
0
:
Bcon
:ibndtyp ifacx tmpbc dist area vell velg por sl porm slm imtx
  1      1      25.    0.    0.    0.    0.    0.    0.    0.    0.    1
:i1 i2 j1 j2 k1 k2
  1 1 1 1 1 1
0
:
      fracture
:species itype ctot mineral guess
k+        1 1.e-6
al+3      1 1.e-8
h+        8 4.0
sio2(aq)  1 1.e-6
cl-       -1 1.e-4
:
      matrix
:species itype ctot mineral guess
k+        3 1.e-4 k-feldspar
al+3      3 1.e-9 muscovite
h+        8 8.0 kaolinite
sio2(aq)  3 1.e-4 quartz
cl-       -1 1.e-4
:

```



```

:ibndtyp
  3  2  25.
:i1 i2 j1 j2 k1 k2
99 99  1  1  1  1
0
:
      fracture
:species  itype  ctot  mineral  guess
k+         3    1.e-4  k-feldspar
al+3       3    1.e-9  muscovite
h+         8    8.0    kaolinite
sio2(aq)   3    1.e-4  quartz
cl-        -1    1.e-4
:
      matrix
:species  itype  ctot  mineral  guess
k+         3    1.e-4  k-feldspar
al+3       3    1.e-9  muscovite
h+         8    8.0    kaolinite
sio2(aq)   3    1.e-4  quartz
cl-        -1    1.e-4
0
:
Stol  1.  1.  1.  1.  1.
:
Aqcx
oh-          5.5e-5
aloh+2       1.0e-5
alo2-
al(oh)2+     1.0e-5
:al(oh)3(aq) 1.0e-5
:al(oh)4-     1.0e-5
h3sio4-      1.0e-5
h2sio4-2     1.0e-5
      :blank
:
Mnrl
quartz
kaolinite
k-feldspar
muscovite
gibbsite
      :blank
Gases

```

```

:blank

:
MNIR
:mineral  npar fkin delh  tau
k-feldspar  0  1.  35.  1.e-3
:itypkin npri  nsec  sig rk
    20    0    0    1.  3.02e-16
:
                                matrix  fracture
:i1 i2 j1 j2 k1 k2  vol  area  vol  area
1 99  1  1  1  1  0.2  24.  0.  24.
0
gibbsite  0  1.  35.  1.e-3
    20    0    0    1.  -14.
1 99  1  1  1  1  0.0  1.  0.0  1.
0
kaolinite  0  1.  35.  1.e-3
:itypkin npri  nsec  sig rk
    20    0    0    1.  -14.
1 99  1  1  1  1  0.0  1.  0.0  1.
0
muscovite  0  1.  35.  1.e-3
:itypkin npri  nsec  sig rk
    20    0    0    1.  -14.
1 99  1  1  1  1  0.0  1.  0.0  1.
0
quartz  0  1.  35.  1.e-3
:itypkin npri  nsec  sig rk
    20    0    0    1.  3.16e-18
1 99  1  1  1  1  0.75  40.  0.  40.
0
:blank

:
:ion-exchange reactions
:Ionx  0  1.0
:
:Brkp  1
:20 1 1
:
Dtstep[y]  1 3.e-6
1.e-6      50.0
:
Time[y] 3 1.e2 1.e3 1.e4 2.5e4 5.e4 7.5e4 1.e5

```

:
ENDS

2.9.98 DCM Benchmark. The DCM was compared with the stationary state analytical solution for a single component system.

Input file used for the DCM benchmark test is listed below.

```

                                test data for 1-d dcm
Sept. 24, 1997
:
:      geometry nx ny nz mode iprint idebug iwarn
GRID   DCMXYZ  200  1  1  2      1      0      0      1  2
:
DBASE
/home/skippy/lichtner/bin/database/master25.V8.R5
:
OPTS
:  idata istart imod iexact iscale ihrmc isst
:    0      0      10  0      0      1    -1
:
:  itmax ihalmax ivmax ndamp
:    24    16     5     0
:
:  method iops ifor isurf iact loglin icon  cournr
:    1      0     0     0     0     0     1     5.
:
:  isync ipor iperm permfac porfac
COUPLE  0     0     0     3.     0.
:
PLTFiles
:iplot a s t m si sf v z b in e ex ti g itex md err
:    1  1  0  0  1  0  0  1  0  0  0  0  0  0  0  0  0  1
:
:  tol  ttol  tolneg tolpos  tolexp dthalf qkmax  tolstdst tolcl
TOLR 1.d-12 1.e-1 1.e-6 1.e-2 4.d0 .5 590. 1.e-6 1.e-12
:
:  mcyc cc c flx r sp qk pk rk a1 a2 a3
DEBUG  0  1  1  0  1  1  1  1  1  1
:
DCMPARA
:il i2 j1 j2 k1 k2 xlm volf areamodf pormtx swmtx tortfac
! not used

```

P. C. Lichtner

SCIENTIFIC NOTEBOOK

INITIALS: PC

```

1 200 1 1 1 1 0.1 1.e-3 8.32528e-4 0.1 1. 1.
0
:      isat isothrm iread porf phir sat w lambda toldelt tolpor
ISYSem -1 0 0 1.e-0 1.e-0 1.0 0.5 1.0 1.e-3 1.e-10
:
:      vx0 vy0 vz0 vgx vgy vgz[m/yr] alphax alphay alphaz[m] vmfac
FLOW 1.e3 0. 0. 0. 0. 0. 0. 0. 0. 0.
:
:      d0[cm^2/s] delhaq[kJ/mol] dgas[cm^2/s] dgexp tortaq tortg idif
DIFF 1.d-5 12.6 2.13d-1 1.8 1.d0 1.d0 0
:
:flag 1: T(x) = d x^3 + a x^2 + b x + c (meters)
:      2: T(x) = a + (b-a) exp[-((x-x0)/c)^2] + (d - a) * x / xlen
:      3:T(x,t)=a+1/2(b-a)(erf[(x+c-x0)/2sqr(dt)]-erf[(x-c-x0)/2sqr(dt)])
:      p(bars) temp flag a b c d x0 xlen
PTINit 1.e5 25. 0 25 300 250 125 1000. 2.d3
:
:master species for controlling time stepping
MASTER ALL
:
DXYZ
20*0.002 10*0.01 10*0.02 10*0.05 10*0.1 10*0.25 10*0.5
10*1. 20*2. 20*5. 20*10. 10*20. 10*50. 30*100.
1*1.
1.
:
:      isolv level north nitmax idetail rmaxtol rtwotol smaxtol
SOLV 3 1 4 100 0 1.e-20 1.e-20 1.e-12
:
:initial and boundary conditions: 1-conc., 2-flux, 3-zero gradient
:
COMP
:i1 i2 j1 j2 k1 k2
1 200 1 1 1 1
0
:      fracture
:species itype ctot mineral guess
sio2(aq) 3 1.e-1 quartz**
:blank
:      matrix
:species itype ctot mineral guess
sio2(aq) 3 1.e-1 quartz**

```

```

0
:
BCON
:ibndtyp ifacx tmpbc dist area vell velg por sl porm slm imtx
  1      1      25.    0.    0.    0.    0.    0.    0.    0.    0
: i1 i2 j1 j2 k1 k2
  1  1  1  1  1  1
0
:
      fracture
:species  itype  ctot  mineral guess
sio2(aq)   1      1.e-3
:
      matrix
:species  itype  ctot  mineral guess
sio2(aq)   1      1.e-3  quartz**
:
:bndtyp  iface  temp
  3       2     25.
:
: i1 i2 j1 j2 k1 k2
200 200  1  1  1  1
0
:
      fracture
:species  itype  ctot  mineral guess
sio2(aq)   3      1.e-1  quartz**
:
      matrix
:species  itype  ctot  mineral guess
sio2(aq)   3      1.e-1  quartz**
0
:
STOL  1.  1.  1.  1.  1.  1.  1.  1.  1.  1.
:
AQCX
      :blank
:
MNRL
quartz**
      :blank
:
GASEs
      :blank
:
MNIR

```

```

:mineral  npar fkin delh  tau
quartz**      0    1.  75.  1.e-3
:itypkin npri  nsec  sig   rk
      20    0    0    1.   -14.d0
:
:          matrix      fracture
:i1  i2  j1  j2  k1  k2  vol  area  vol  area
      1 200  1  1  1  1  0.9  1.0  0.0  1.0
0
      :blank
:
:BRKP      1
:200
:
Dtstep[y] 1 3.e-9
1.e-9      10.
:
Time 4 1. 10. 100. 200.
:
ENDS
-1 0. 0.

```

2.20.98 DCM Verification with 2D Simulation. The DCM was compared with a 2D formulation with 50×2 nodes to test the convergence problems noted in the DCM. Grid spacing used in the calculations were $\Delta x = 0.03$ m and 0.09 m, and $\Delta y_1 = 2\delta$, $\Delta y_2 = \Delta x - 2\delta$, where 2δ represents the fracture aperture. The surface areas in the 2D simulation were set according to the relations:

$$\text{areamf1} = \frac{\epsilon_f}{l_f} \Delta y_1 \Delta z, \quad (1)$$

$$\text{areamf2} = \frac{1 - \epsilon_f}{l_m} \Delta y_2 \Delta z, \quad (2)$$

$$\text{areamf3} = \frac{6}{l_m} (1 - \epsilon_f) \lambda \Delta x \Delta z, \quad (3)$$

where areamf1 corresponds to the fracture-fracture interfacial area, areamf2 the matrix-matrix interfacial area, and areamf3 the fracture-matrix area. The following values were used in the comparison test: $\epsilon_f = 10^{-3}$, $l_m = 0.1$ m, $\lambda = 10$ and the fracture aperture $l_f = 3.3356 \times 10^{-5}$ m. Input file used for the 2D verification problem is listed below. Identical results were obtained with the 2D and the DCM formulations.

k-feldspar dissolution

2D: Jan. 21, 1997

```

:      geometry nx ny nz mode iprint idebug iwarn il i2
GRID      XYZ    50  2  1  2      1      0      0    48 52
:GRID      DCMXYZ  50  2  1  2      1      0      0    13 20
:
DBASE
/home/skippy/lichtner/bin/database/master25.V8.R5
:
OPTS
:  idata istart imod  iexact iscale ihrmc isst
    0      0      10      0      0      1    -1
:
:  itmax ihalmax ivmax ndamp icntmx
    16     32      0      0      3
:
:  method iops  ifor  isurf iact  loglin  icon  cournr  tpulse  wtup
    1      0      2      1      1      0      1      5.
:
:      isync ipor iperm  permfac porfac
COUPle    0      0      0      3.      1.
:
PLTFiles
:iplot  a  s  t  m si sf  v  z  b in  e ex ti  g itex mk err
    1  1  1  1  1  0  0  1  0  0  0  0  0  0  0  0  0  1
:
:      tol ttol  tolneg tolpos  tolexp  dthalf gkmax tolstdst tolc
TOLR 1.d-13 2.e-2 1.e-8  1.e-2  5.d0    .5    590.  1.e-12  1.e-13
:
:      mcyc cc  c  flx r  sp  qk  pk  rk  a1  a2  a3
DEBUg    0      1  1  0  1  1  1  1  1  1
:
:DCMPARA                                     ! not used
:i1 i2 j1 j2 k1 k2  xlm  volf  areamodf  pormtx  swmtx  tortfac
: 1 50  1  1  1  1  0.1  1.e-3   10.    0.05    1.    1.
:0
:      isat isothrm iread  por0  phir  sat  w  lambda toldelt  tolpor
ISYSstem -1    0      0    1.0  1.    1.0  .5  1.    1.e-3  1.e-3
:
:      vx0 vy0 vz0 vgx vgy vgz[m/yr]  alphax  alphay  alphaz[m] vmfac
FLOW 1000.0    0.    0.    0.    0.    0.    0.    0.    0.    0.
:

```

```

:  d0[cm^2/s]  delhaq[kJ/mol]  dgas[cm^2/s]  dgexp  tortaq  tortg  idif
DIFF  1.d-5      12.6              2.13d-1      1.8  1.d0  1.d0  0
:
:flag 1: T(x)   = d x^3 + a x^2 + b x + c (meters)
:      2: T(x)   = a + (b-a) exp[-((x-x0)/c)^2] + (d - a) * x / xlen
:      3:T(x,t)=a+1/2(b-a)(erf[(x+c-x0)/2sqr(dt)]-erf[(x-c-x0)/2sqr(dt)])
:      p (bars) temp flag  a      b      c      d      x0      xlen
PTINit 1.e5  25.  0  25  300  250  125  1000.  2.d3
:
:master species for controlling time stepping
Master h+
:
Dxyz
50*0.03
3.3356d-5 0.0999666
  1.
:
:  isolv level north nitmax idetail rmaxtol rtwotol smaxtol
SOLV   4   1   3   100   0   1.e-20 1.e-20 1.e-12
:
:initial and boundary conditions: 1-conc., 2-flux, 3-zero gradient
COMP
:i1 i2 j1 j2 k1 k2
  1 50  1  2  1  1
0
:
:              fracture
:species  itype  ctot  mineral  guess
k+         3    1.e-4  k-feldspar
al+3       3    1.e-9  muscovite
h+         8    8.0    kaolinite
sio2(aq)   3    1.e-4  quartz
cl-        -1    1.e-4
:blank
0
:
Bcon
:ibndtyp ifacx tmpbc dist area vell velg por sl porm slm imtx
  1      1    25.   0.   0.   0.   0.   0.   0.   0.   0.   0
:i1 i2 j1 j2 k1 k2
  1  1  1  1  1  1
0
:
:              fracture

```



```

:species  itype  ctot  mineral  guess
k+         1     1.e-6
al+3       1     1.e-8
h+         8     4.0
sio2(aq)   1     1.e-6
cl-        -1    1.e-4
:
:ibndtyp  ifacx  tmpbc  dist  area  vell  velg  por  sl  porm  slm  imtx
      3      2      25.
:i1  i2  j1  j2  k1  k2
 50  50   1   1   1   1
0
:
               fracture
:species  itype  ctot  mineral  guess
k+         3     1.e-4  k-feldspar
al+3       3     1.e-9  muscovite
h+         8     8.0    kaolinite
sio2(aq)   3     1.e-4  quartz
cl-        -1    1.e-4
0
:
Stol  1.  1.  1.  1.  1.
:
Aqcx
oh-          5.5e-5
aloh+2       1.0e-5
alo2-
al(oh)2+     1.0e-5
:al(oh)3(aq) 1.0e-5
:al(oh)4-     1.0e-5
h3sio4-      1.0e-5
h2sio4-2     1.0e-5
               :blank
:
Mnrl
quartz
kaolinite
k-feldspar
muscovite
gibbsite
               :blank
Gases

```

```

:blank

:
VOLUME
:i1 i2 j1 j2 k1 k2   vol  porosity
  1 50  1  1  1  1   0.03e-3  1.0
  1 50  2  2  1  1   0.02997  0.05
0
:
MNIR
:mineral  npar fkin delh  tau
k-feldspar  0  1.  35.  1.e-2
:itypkin npri  nsec  sig  rk
  20      0      0    1.   3.02e-16
:
:matrix      fracture
:i1 i2 j1 j2 k1 k2   vol  area  vol  area
1 50  1  1  1  1   0.0  24.   0.   24.
1 50  2  2  1  1   0.2  24.   0.   24.
0
gibbsite    0  1.  35.  1.e-2
  20      0      0    1.   -14.
1 50  1  2  1  1   0.0    1.  0.0    1.
0
kaolinite   0  1.  35.  1.e-2
:itypkin npri  nsec  sig  rk
  20      0      0    1.   -14.
1 50  1  2  1  1   0.0    1.  0.0    1.
0
muscovite   0  1.  35.  1.e-2
:itypkin npri  nsec  sig  rk
  20      0      0    1.   -14.
1 50  1  2  1  1   0.0    1.  0.0    1.
0
quartz       0  1.  35.  1.e-2
:itypkin npri  nsec  sig  rk
  20      0      0    1.   3.16e-18
1 50  1  1  1  1   0.0  40.   0.   40.
1 50  2  2  1  1   0.75 40.   0.   40.
0
:blank

:
:ion-exchange reactions
:Ionx  0      1.0

```

```

:
:Brkp    1
:20 1 1
:
Dtstep[y]    1 3.e-6
1.e-6        50.0
:
Time[y] 3 1.e2 1.e3 1.e4 2.5e4 5.e4 7.5e4 1.e5
:
ENDS
29.9796 9.99 599.4

```

3.17.98 DCM/METRA: Effect of Variable Grid Spacing. It was found that the DCM is highly sensitive to changes in grid spacing. Shown in Figure 3 is a comparison of the liquid saturation for equal grid spacing (solid curves) with variable grid spacing (dotted curves). At changes in grid spacing rabbit ears appear pointing upward and downward depending on whether the grid spacing increases or decreases, respectively.

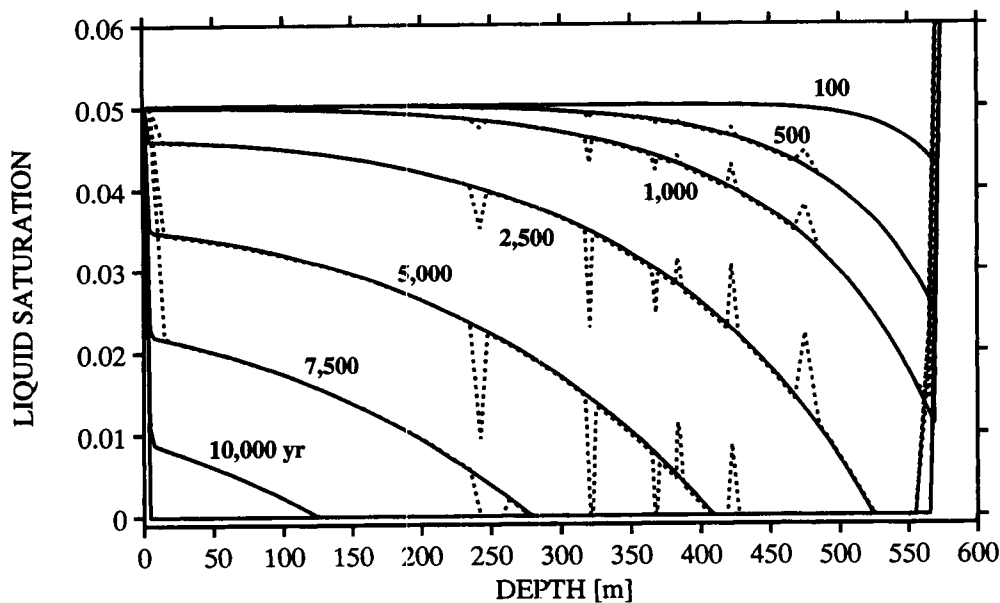


Figure 3: Liquid saturation plotted as a function of depth for different times.

Shown in Figure 4 is a comparison with CTOUGH which shows identical behavior at jumps in grid spacing.

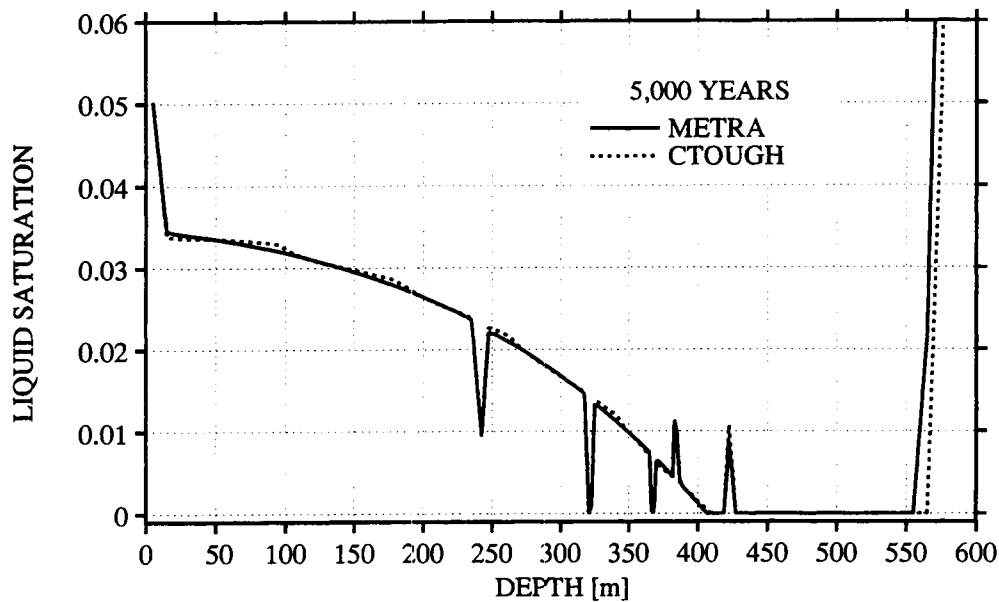


Figure 4: Liquid saturation plotted as a function of depth.

Input files used in the calculations are listed below.

Data for Multiflo simulator (initial data : 2D, 83.4 AML, Yucca Mt.)

Dec. 27, 1996

RSTART 0

:

: XYZ = 1 table look-up, pref = ref. press.

: RADIAL = 0 correlations, tref = ref temp.

: OTHER

:grid geometry nx ny nz ivplwr ipvcal iout gravity pref tref href

:Grid XYZ 1 1 121 1 0 3 0 0 0 0

Grid DCMXYZ 1 1 121 0 0 3 0 0 0 0

:

Pckr :relative perm and pc keyword

: i type-curve swirm rpmm(lamda) alpham swext sgc iecm

: swirf rpmf(lamda) alphaf phim phif permm permf

:Topopah Spring (150-475 m)

1 Van-Gen 0.05 0.7636 1.305e-5 0. 0. 0

2 Van-Gen 0.05 0.4400 5.8e-7 0. 0. 0

:blank line

:

Thermal-prop

: no rho cpr ckdry cksat crp crt tau cdiff cexp enbd

```

1 2.58e3 840. 2.10 2.10 0 0 0.0 2.13e-5 1.8 0.
0
: igrd rw re
DXYZ 0 0. 1.
: (dx(i),i=1,nx)
1.
:
: (dy(j),j=1,ny)
1.
:
: (dz(k),k=1,nz)
10. 10. 10. 10. 10. 10. 10. 10. 10. 10.
10. 10. 10. 10. 10. 10. 10. 10. 10. 10.
10. 10. 10. 10. 5. 5. 5. 5. 5. 5.
5. 5. 5. 5. 5. 5. 5. 5. 5. 5.
2. 2. 2. 2. 2. 2. 2. 2. 2. 2.
2. 2. 2. 2. 2. 2. 2. 2. 2. 2.
2. 2. 2. 1.5 1. 1. 1. 1. 1. 1.
1. 1. 1. 1. 1. 1. 1. 1. 1. 1.5
2. 2. 2. 2. 2. 2. 2. 2. 2. 2.
2. 2. 2. 2. 2. 2. 2. 2. 5. 5.
5. 5. 5. 5. 5. 5. 5. 5. 10. 10.
10. 10. 10. 10. 10. 10. 10. 10. 10. 10.
10.
PhiK
:i1 i2 j1 j2 k1 k2 ist ithr vb por permx permy permz porm prmm istm itm
1 1 1 1 1 121 1 1 0. 1. 1.e-10 1.e-10 1.e-10 .1 1.e-17 2 1
1 1 1 1 1 1 1 1 1.e20 1. 1.e-10 1.e-10 1.e-10 .1 1.e-17 2 1
1 1 1 1 121 121 1 1 1.e20 1. 1.e-10 1.e-10 1.e-10 .1 1.e-17 2 1
0
Init !init
: i1 i2 j1 j2 k1 k2 p t sg xg2 pm tm sgm xgm
:
1 1 1 1 1 121 8.54972E+04 15. 0.95 0.0 8.5497E+04 15. 0.2 0.
1 1 1 1 121 121 9.05002E+04 30. 0. 0. 9.0500E+04 30. 0.0 0.
0
:
DCMPARA
: i1 i2 j1 j2 k1 k2 volf areamodf xlm ylm zlm
1 1 1 1 1 121 .01 1. 0.1 0.1 0.1
0
:

```

```

:EQUIL  587.50 1.e5  30.  0.0255319 0.0  -1
:EQUIL  5.0    1.e5  25.  0. 0.2  1
:EQUIL  595.0  1.065627E+05  25.  0.0 0.0  -1
:
Recurrent-data
-1. 0. 0.
:skip
Bcon  2
:itype iface i1 i2 j1 j2
1      TOP    1  1  1  1
:time qbc pbc      tbc  sgbc  xabc
:matrix
  0.  0.  8.55e4  15.0  0.20  0.
:fracture
  0.  0.  8.55e4  15.0  0.95  0.
0
1      BOTTOM 1  1  1  1
  0.  0.  9.05e4  30.0  0.00  0.
  0.  0.  9.05e4  30.0  0.00  0.
0
:noskip
:
Rstart 1 1 0
Output  A=1  C=1  B=1 S=-1
:Output  C=1 S=-1
:  isolve newtnmn newtnmx north nitmx level
Solve 4      1      7      4      100  1
:
:AUTO-step  DPMXE      DSMXE  DTMPMXE  DP2MXe TACCEL IAUTODT FAC1
AUTO-step  1.e3      0.02    5.0      1.e3  1.e-3  0  0
:
:TOLR TOLP  TOLS  TOLT  TOLP2  TOLM  TOLA  TOLE rtwotol rmxtol smxtol
Tolr  1. 1.e-4  1.e-3  1.e+1 1.e-5 1.e-3 1.e-3 1.e-20 1.e-20 1.e-20
:
:Limit dpmx      dsmx dtmpmx dp2mx dtmn dtmx icutmx
LIMIT 1.e4      .05    10.    1.e4  1.e-10 5.e8 50
Plots 1 3
:Time[y]  1.
:Time[y]  10.
Time[y]  100.
Time[y]  500.
Time[y]  1000.

```

```

Time[y] 2500.
Time[y] 5000.
Time[y] 7500.
Time[y] 1.e4
Noskip
Steady[y] 1.e-8 1.e-6 1.e-1
Ends

```

CTOUGH:

```

1-D two-phase problem multi.dat
ROCKS
:
: mat nad drock por permx permy permz cwet spht
matx 2 2.58E+03 0.3 1.0E-17 1.0E-17 1.0E-17 2.1 840.0
:
: comp expan cdry tortx
0.0 0.0 2.1 0.0
: irp rp(1) rp(2) rp(3) rp(4) rp(5) rp(6) rp(7)
7 0.4400 0.05 1.0 0.0 0.0 0.0 0.0
: icp cp(1) cp(2) cp(3) cp(4) cp(5) cp(6) cp(7)
11 0.4400 0.05 5.8e-7 0.0 1.0 1.0E-1 0.0
:
: mat nad drock por permx permy permz cwet spht
frac 2 2.580E+03 1.0 1.0E-10 1.0E-10 1.0E-10 2.1 840.
:
: comp expan cdry tortx
0.0 0.0 2.1 0.0
: irp rp(1) rp(2) rp(3) rp(4) rp(5) rp(6) rp(7)
7 0.7636 0.05 1.0 0.0 0.0 0.0 0.0
: icp cp(1) cp(2) cp(3) cp(4) cp(5) cp(6) cp(7)
11 0.7636 0.05 1.305e-5 0.0 1.0 1.1E-1 0.0
: reqd blank line
:
:
PARAM
:nt kt mcy msc cyp diffo mop-4 5 6 7 8 9 0 1 2 3 4 5 6 7 8 9 0 1 2 3 4
: 0 2 9999 0 999 2.130E-05 1.8 0 0 6 0 0 0 0 0 0 0 0 0 0 0 0 4 1
0 2 9999 0 999 0.000E-05 1.8 0 0 0 0 0 0 0 0 0 0 0 0 0 0 0 4 1
: tstart timax delten dltnx elst gf redlt scale
0. 1.e4 -1 0. M 1 9.81 0 0
:

```

```

: dlt(1) dlt(2) dlt(3) dlt(4) dlt(5).....
  1.e+03 0.e+00 0.e+00 0.e+00 0.e+00 0.e+00 0.e+00 0.e+00
:
: rel re2 u wup wnr dfac
  0.e+00 0.e+00 0.e+00 0.e+00 0.e+00 1.e-07
: dep(1) dep(2) dep(3)
  1.e5      .2      25.
:
OPTN
: ilimsl idsolc knudsn ipctem ivplow ilopt
  0      0      0      0      1      0
DTSTP
: dpgmax dsgmax dtempmx dxmax
  1.e+04 .05      .5      .0
:
TIMES
: iti ite dealf tintr
  8 8 0.      0.
:
: tis(1) tis(2) tis(3) tis(4) ...
  10. 100. 500. 1000. 2500. 5000. 7500. 10000.
:3.1536e6 3.1536e7 3.1536e8 3.1536e9 3.1536e10 3.1536e11 3.939e12
:
:
START
:
ELEME
:
M      1  0  0 matx      .990E+20
M      2  0  0 matx      .990E+01
M      3  0  0 matx      .990E+01
M      4  0  0 matx      .990E+01
M      5  0  0 matx      .990E+01
M      6  0  0 matx      .990E+01
M      7  0  0 matx      .990E+01
M      8  0  0 matx      .990E+01
M      9  0  0 matx      .990E+01
M     10  0  0 matx      .990E+01
M     11  0  0 matx      .990E+01
M     12  0  0 matx      .990E+01
M     13  0  0 matx      .990E+01
M     14  0  0 matx      .990E+01

```


P. C. Lichtner

SCIENTIFIC NOTEBOOK

INITIALS: PCZ

M	15	0	0	matx	.990E+01
M	16	0	0	matx	.990E+01
M	17	0	0	matx	.990E+01
M	18	0	0	matx	.990E+01
M	19	0	0	matx	.990E+01
M	20	0	0	matx	.990E+01
M	21	0	0	matx	.990E+01
M	22	0	0	matx	.990E+01
M	23	0	0	matx	.990E+01
M	24	0	0	matx	.990E+01
M	25	0	0	matx	.495E+01
M	26	0	0	matx	.495E+01
M	27	0	0	matx	.495E+01
M	28	0	0	matx	.495E+01
M	29	0	0	matx	.495E+01
M	30	0	0	matx	.495E+01
M	31	0	0	matx	.495E+01
M	32	0	0	matx	.495E+01
M	33	0	0	matx	.495E+01
M	34	0	0	matx	.495E+01
M	35	0	0	matx	.495E+01
M	36	0	0	matx	.495E+01
M	37	0	0	matx	.495E+01
M	38	0	0	matx	.495E+01
M	39	0	0	matx	.495E+01
M	40	0	0	matx	.495E+01
M	41	0	0	matx	.198E+01
M	42	0	0	matx	.198E+01
M	43	0	0	matx	.198E+01
M	44	0	0	matx	.198E+01
M	45	0	0	matx	.198E+01
M	46	0	0	matx	.198E+01
M	47	0	0	matx	.198E+01
M	48	0	0	matx	.198E+01
M	49	0	0	matx	.198E+01
M	50	0	0	matx	.198E+01
M	51	0	0	matx	.198E+01
M	52	0	0	matx	.198E+01
M	53	0	0	matx	.198E+01
M	54	0	0	matx	.198E+01
M	55	0	0	matx	.198E+01
M	56	0	0	matx	.198E+01

M	57	0	0	matx	.198E+01
M	58	0	0	matx	.198E+01
M	59	0	0	matx	.198E+01
M	60	0	0	matx	.198E+01
M	61	0	0	matx	.198E+01
M	62	0	0	matx	.198E+01
M	63	0	0	matx	.198E+01
M	64	0	0	matx	.148E+01
M	65	0	0	matx	.990E+00
M	66	0	0	matx	.990E+00
M	67	0	0	matx	.990E+00
M	68	0	0	matx	.990E+00
M	69	0	0	matx	.990E+00
M	70	0	0	matx	.990E+00
M	71	0	0	matx	.990E+00
M	72	0	0	matx	.990E+00
M	73	0	0	matx	.990E+00
M	74	0	0	matx	.990E+00
M	75	0	0	matx	.990E+00
M	76	0	0	matx	.990E+00
M	77	0	0	matx	.990E+00
M	78	0	0	matx	.990E+00
M	79	0	0	matx	.990E+00
M	80	0	0	matx	.148E+01
M	81	0	0	matx	.198E+01
M	82	0	0	matx	.198E+01
M	83	0	0	matx	.198E+01
M	84	0	0	matx	.198E+01
M	85	0	0	matx	.198E+01
M	86	0	0	matx	.198E+01
M	87	0	0	matx	.198E+01
M	88	0	0	matx	.198E+01
M	89	0	0	matx	.198E+01
M	90	0	0	matx	.198E+01
M	91	0	0	matx	.198E+01
M	92	0	0	matx	.198E+01
M	93	0	0	matx	.198E+01
M	94	0	0	matx	.198E+01
M	95	0	0	matx	.198E+01
M	96	0	0	matx	.198E+01
M	97	0	0	matx	.198E+01
M	98	0	0	matx	.198E+01

M	99	0	0	matx	.495E+01
M	100	0	0	matx	.495E+01
M	101	0	0	matx	.495E+01
M	102	0	0	matx	.495E+01
M	103	0	0	matx	.495E+01
M	104	0	0	matx	.495E+01
M	105	0	0	matx	.495E+01
M	106	0	0	matx	.495E+01
M	107	0	0	matx	.495E+01
M	108	0	0	matx	.495E+01
M	109	0	0	matx	.990E+01
M	110	0	0	matx	.990E+01
M	111	0	0	matx	.990E+01
M	112	0	0	matx	.990E+01
M	113	0	0	matx	.990E+01
M	114	0	0	matx	.990E+01
M	115	0	0	matx	.990E+01
M	116	0	0	matx	.990E+01
M	117	0	0	matx	.990E+01
M	118	0	0	matx	.990E+01
M	119	0	0	matx	.990E+01
M	120	0	0	matx	.990E+01
M	121	0	0	matx	.990E+01
M	122	0	0	matx	.990E+20
F	1	0	0	frac	.10E+20
F	2	0	0	frac	.100E+00
F	3	0	0	frac	.100E+00
F	4	0	0	frac	.100E+00
F	5	0	0	frac	.100E+00
F	6	0	0	frac	.100E+00
F	7	0	0	frac	.100E+00
F	8	0	0	frac	.100E+00
F	9	0	0	frac	.100E+00
F	10	0	0	frac	.100E+00
F	11	0	0	frac	.100E+00
F	12	0	0	frac	.100E+00
F	13	0	0	frac	.100E+00
F	14	0	0	frac	.100E+00
F	15	0	0	frac	.100E+00
F	16	0	0	frac	.100E+00
F	17	0	0	frac	.100E+00
F	18	0	0	frac	.100E+00

F	19	0	0	frac	.100E+00
F	20	0	0	frac	.100E+00
F	21	0	0	frac	.100E+00
F	22	0	0	frac	.100E+00
F	23	0	0	frac	.100E+00
F	24	0	0	frac	.100E+00
F	25	0	0	frac	.500E-01
F	26	0	0	frac	.500E-01
F	27	0	0	frac	.500E-01
F	28	0	0	frac	.500E-01
F	29	0	0	frac	.500E-01
F	30	0	0	frac	.500E-01
F	31	0	0	frac	.500E-01
F	32	0	0	frac	.500E-01
F	33	0	0	frac	.500E-01
F	34	0	0	frac	.500E-01
F	35	0	0	frac	.500E-01
F	36	0	0	frac	.500E-01
F	37	0	0	frac	.500E-01
F	38	0	0	frac	.500E-01
F	39	0	0	frac	.500E-01
F	40	0	0	frac	.500E-01
F	41	0	0	frac	.200E-01
F	42	0	0	frac	.200E-01
F	43	0	0	frac	.200E-01
F	44	0	0	frac	.200E-01
F	45	0	0	frac	.200E-01
F	46	0	0	frac	.200E-01
F	47	0	0	frac	.200E-01
F	48	0	0	frac	.200E-01
F	49	0	0	frac	.200E-01
F	50	0	0	frac	.200E-01
F	51	0	0	frac	.200E-01
F	52	0	0	frac	.200E-01
F	53	0	0	frac	.200E-01
F	54	0	0	frac	.200E-01
F	55	0	0	frac	.200E-01
F	56	0	0	frac	.200E-01
F	57	0	0	frac	.200E-01
F	58	0	0	frac	.200E-01
F	59	0	0	frac	.200E-01
F	60	0	0	frac	.200E-01

P. C. Lichtner

SCIENTIFIC NOTEBOOK

INITIALS: PC

F	61	0	0	frac	.200E-01
F	62	0	0	frac	.200E-01
F	63	0	0	frac	.200E-01
F	64	0	0	frac	.150E-01
F	65	0	0	frac	.100E-01
F	66	0	0	frac	.100E-01
F	67	0	0	frac	.100E-01
F	68	0	0	frac	.100E-01
F	69	0	0	frac	.100E-01
F	70	0	0	frac	.100E-01
F	71	0	0	frac	.100E-01
F	72	0	0	frac	.100E-01
F	73	0	0	frac	.100E-01
F	74	0	0	frac	.100E-01
F	75	0	0	frac	.100E-01
F	76	0	0	frac	.100E-01
F	77	0	0	frac	.100E-01
F	78	0	0	frac	.100E-01
F	79	0	0	frac	.100E-01
F	80	0	0	frac	.150E-01
F	81	0	0	frac	.200E-01
F	82	0	0	frac	.200E-01
F	83	0	0	frac	.200E-01
F	84	0	0	frac	.200E-01
F	85	0	0	frac	.200E-01
F	86	0	0	frac	.200E-01
F	87	0	0	frac	.200E-01
F	88	0	0	frac	.200E-01
F	89	0	0	frac	.200E-01
F	90	0	0	frac	.200E-01
F	91	0	0	frac	.200E-01
F	92	0	0	frac	.200E-01
F	93	0	0	frac	.200E-01
F	94	0	0	frac	.200E-01
F	95	0	0	frac	.200E-01
F	96	0	0	frac	.200E-01
F	97	0	0	frac	.200E-01
F	98	0	0	frac	.200E-01
F	99	0	0	frac	.500E-01
F	100	0	0	frac	.500E-01
F	101	0	0	frac	.500E-01
F	102	0	0	frac	.500E-01

P. C. Lichtner

SCIENTIFIC NOTEBOOK

INITIALS: PCZ

```

F 103 0 0 frac .500E-01
F 104 0 0 frac .500E-01
F 105 0 0 frac .500E-01
F 106 0 0 frac .500E-01
F 107 0 0 frac .500E-01
F 108 0 0 frac .500E-01
F 109 0 0 frac .100E+00
F 110 0 0 frac .100E+00
F 111 0 0 frac .100E+00
F 112 0 0 frac .100E+00
F 113 0 0 frac .100E+00
F 114 0 0 frac .100E+00
F 115 0 0 frac .100E+00
F 116 0 0 frac .100E+00
F 117 0 0 frac .100E+00
F 118 0 0 frac .100E+00
F 119 0 0 frac .100E+00
F 120 0 0 frac .100E+00
F 121 0 0 frac .100E+00
F 122 0 0 frac .010E+20

```

:blank

:

CONNE

:

```

M 1 F 1 0 0 0 1 .500E-01 .168E-03 .588E+03 .000E+00
M 2 F 2 0 0 0 1 .500E-01 .168E-03 .588E+03 .000E+00
M 3 F 3 0 0 0 1 .500E-01 .168E-03 .588E+03 .000E+00
M 4 F 4 0 0 0 1 .500E-01 .168E-03 .588E+03 .000E+00
M 5 F 5 0 0 0 1 .500E-01 .168E-03 .588E+03 .000E+00
M 6 F 6 0 0 0 1 .500E-01 .168E-03 .588E+03 .000E+00
M 7 F 7 0 0 0 1 .500E-01 .168E-03 .588E+03 .000E+00
M 8 F 8 0 0 0 1 .500E-01 .168E-03 .588E+03 .000E+00
M 9 F 9 0 0 0 1 .500E-01 .168E-03 .588E+03 .000E+00
M 10 F 10 0 0 0 1 .500E-01 .168E-03 .588E+03 .000E+00
M 11 F 11 0 0 0 1 .500E-01 .168E-03 .588E+03 .000E+00
M 12 F 12 0 0 0 1 .500E-01 .168E-03 .588E+03 .000E+00
M 13 F 13 0 0 0 1 .500E-01 .168E-03 .588E+03 .000E+00
M 14 F 14 0 0 0 1 .500E-01 .168E-03 .588E+03 .000E+00
M 15 F 15 0 0 0 1 .500E-01 .168E-03 .588E+03 .000E+00
M 16 F 16 0 0 0 1 .500E-01 .168E-03 .588E+03 .000E+00
M 17 F 17 0 0 0 1 .500E-01 .168E-03 .588E+03 .000E+00
M 18 F 18 0 0 0 1 .500E-01 .168E-03 .588E+03 .000E+00

```

P. C. Lichtner

SCIENTIFIC NOTEBOOK

INITIALS: PCZ

M	19	F	19	0	0	0	1	.500E-01	.168E-03	.588E+03	.000E+00
M	20	F	20	0	0	0	1	.500E-01	.168E-03	.588E+03	.000E+00
M	21	F	21	0	0	0	1	.500E-01	.168E-03	.588E+03	.000E+00
M	22	F	22	0	0	0	1	.500E-01	.168E-03	.588E+03	.000E+00
M	23	F	23	0	0	0	1	.500E-01	.168E-03	.588E+03	.000E+00
M	24	F	24	0	0	0	1	.500E-01	.168E-03	.588E+03	.000E+00
M	25	F	25	0	0	0	1	.500E-01	.168E-03	.294E+03	.000E+00
M	26	F	26	0	0	0	1	.500E-01	.168E-03	.294E+03	.000E+00
M	27	F	27	0	0	0	1	.500E-01	.168E-03	.294E+03	.000E+00
M	28	F	28	0	0	0	1	.500E-01	.168E-03	.294E+03	.000E+00
M	29	F	29	0	0	0	1	.500E-01	.168E-03	.294E+03	.000E+00
M	30	F	30	0	0	0	1	.500E-01	.168E-03	.294E+03	.000E+00
M	31	F	31	0	0	0	1	.500E-01	.168E-03	.294E+03	.000E+00
M	32	F	32	0	0	0	1	.500E-01	.168E-03	.294E+03	.000E+00
M	33	F	33	0	0	0	1	.500E-01	.168E-03	.294E+03	.000E+00
M	34	F	34	0	0	0	1	.500E-01	.168E-03	.294E+03	.000E+00
M	35	F	35	0	0	0	1	.500E-01	.168E-03	.294E+03	.000E+00
M	36	F	36	0	0	0	1	.500E-01	.168E-03	.294E+03	.000E+00
M	37	F	37	0	0	0	1	.500E-01	.168E-03	.294E+03	.000E+00
M	38	F	38	0	0	0	1	.500E-01	.168E-03	.294E+03	.000E+00
M	39	F	39	0	0	0	1	.500E-01	.168E-03	.294E+03	.000E+00
M	40	F	40	0	0	0	1	.500E-01	.168E-03	.294E+03	.000E+00
M	41	F	41	0	0	0	1	.500E-01	.168E-03	.118E+03	.000E+00
M	42	F	42	0	0	0	1	.500E-01	.168E-03	.118E+03	.000E+00
M	43	F	43	0	0	0	1	.500E-01	.168E-03	.118E+03	.000E+00
M	44	F	44	0	0	0	1	.500E-01	.168E-03	.118E+03	.000E+00
M	45	F	45	0	0	0	1	.500E-01	.168E-03	.118E+03	.000E+00
M	46	F	46	0	0	0	1	.500E-01	.168E-03	.118E+03	.000E+00
M	47	F	47	0	0	0	1	.500E-01	.168E-03	.118E+03	.000E+00
M	48	F	48	0	0	0	1	.500E-01	.168E-03	.118E+03	.000E+00
M	49	F	49	0	0	0	1	.500E-01	.168E-03	.118E+03	.000E+00
M	50	F	50	0	0	0	1	.500E-01	.168E-03	.118E+03	.000E+00
M	51	F	51	0	0	0	1	.500E-01	.168E-03	.118E+03	.000E+00
M	52	F	52	0	0	0	1	.500E-01	.168E-03	.118E+03	.000E+00
M	53	F	53	0	0	0	1	.500E-01	.168E-03	.118E+03	.000E+00
M	54	F	54	0	0	0	1	.500E-01	.168E-03	.118E+03	.000E+00
M	55	F	55	0	0	0	1	.500E-01	.168E-03	.118E+03	.000E+00
M	56	F	56	0	0	0	1	.500E-01	.168E-03	.118E+03	.000E+00
M	57	F	57	0	0	0	1	.500E-01	.168E-03	.118E+03	.000E+00
M	58	F	58	0	0	0	1	.500E-01	.168E-03	.118E+03	.000E+00
M	59	F	59	0	0	0	1	.500E-01	.168E-03	.118E+03	.000E+00
M	60	F	60	0	0	0	1	.500E-01	.168E-03	.118E+03	.000E+00

P. C. Lichtner

SCIENTIFIC NOTEBOOK

INITIALS: PCZ

M	61	F	61	0	0	0	1	.500E-01	.168E-03	.118E+03	.000E+00
M	62	F	62	0	0	0	1	.500E-01	.168E-03	.118E+03	.000E+00
M	63	F	63	0	0	0	1	.500E-01	.168E-03	.118E+03	.000E+00
M	64	F	64	0	0	0	1	.500E-01	.168E-03	.882E+02	.000E+00
M	65	F	65	0	0	0	1	.500E-01	.168E-03	.588E+02	.000E+00
M	66	F	66	0	0	0	1	.500E-01	.168E-03	.588E+02	.000E+00
M	67	F	67	0	0	0	1	.500E-01	.168E-03	.588E+02	.000E+00
M	68	F	68	0	0	0	1	.500E-01	.168E-03	.588E+02	.000E+00
M	69	F	69	0	0	0	1	.500E-01	.168E-03	.588E+02	.000E+00
M	70	F	70	0	0	0	1	.500E-01	.168E-03	.588E+02	.000E+00
M	71	F	71	0	0	0	1	.500E-01	.168E-03	.588E+02	.000E+00
M	72	F	72	0	0	0	1	.500E-01	.168E-03	.588E+02	.000E+00
M	73	F	73	0	0	0	1	.500E-01	.168E-03	.588E+02	.000E+00
M	74	F	74	0	0	0	1	.500E-01	.168E-03	.588E+02	.000E+00
M	75	F	75	0	0	0	1	.500E-01	.168E-03	.588E+02	.000E+00
M	76	F	76	0	0	0	1	.500E-01	.168E-03	.588E+02	.000E+00
M	77	F	77	0	0	0	1	.500E-01	.168E-03	.588E+02	.000E+00
M	78	F	78	0	0	0	1	.500E-01	.168E-03	.588E+02	.000E+00
M	79	F	79	0	0	0	1	.500E-01	.168E-03	.588E+02	.000E+00
M	80	F	80	0	0	0	1	.500E-01	.168E-03	.882E+02	.000E+00
M	81	F	81	0	0	0	1	.500E-01	.168E-03	.118E+03	.000E+00
M	82	F	82	0	0	0	1	.500E-01	.168E-03	.118E+03	.000E+00
M	83	F	83	0	0	0	1	.500E-01	.168E-03	.118E+03	.000E+00
M	84	F	84	0	0	0	1	.500E-01	.168E-03	.118E+03	.000E+00
M	85	F	85	0	0	0	1	.500E-01	.168E-03	.118E+03	.000E+00
M	86	F	86	0	0	0	1	.500E-01	.168E-03	.118E+03	.000E+00
M	87	F	87	0	0	0	1	.500E-01	.168E-03	.118E+03	.000E+00
M	88	F	88	0	0	0	1	.500E-01	.168E-03	.118E+03	.000E+00
M	89	F	89	0	0	0	1	.500E-01	.168E-03	.118E+03	.000E+00
M	90	F	90	0	0	0	1	.500E-01	.168E-03	.118E+03	.000E+00
M	91	F	91	0	0	0	1	.500E-01	.168E-03	.118E+03	.000E+00
M	92	F	92	0	0	0	1	.500E-01	.168E-03	.118E+03	.000E+00
M	93	F	93	0	0	0	1	.500E-01	.168E-03	.118E+03	.000E+00
M	94	F	94	0	0	0	1	.500E-01	.168E-03	.118E+03	.000E+00
M	95	F	95	0	0	0	1	.500E-01	.168E-03	.118E+03	.000E+00
M	96	F	96	0	0	0	1	.500E-01	.168E-03	.118E+03	.000E+00
M	97	F	97	0	0	0	1	.500E-01	.168E-03	.118E+03	.000E+00
M	98	F	98	0	0	0	1	.500E-01	.168E-03	.118E+03	.000E+00
M	99	F	99	0	0	0	1	.500E-01	.168E-03	.294E+03	.000E+00
M	100	F	100	0	0	0	1	.500E-01	.168E-03	.294E+03	.000E+00
M	101	F	101	0	0	0	1	.500E-01	.168E-03	.294E+03	.000E+00
M	102	F	102	0	0	0	1	.500E-01	.168E-03	.294E+03	.000E+00

P. C. Lichtner

SCIENTIFIC NOTEBOOK

INITIALS: PC

M	103	F	103	0	0	0	1	.500E-01	.168E-03	.294E+03	.000E+00
M	104	F	104	0	0	0	1	.500E-01	.168E-03	.294E+03	.000E+00
M	105	F	105	0	0	0	1	.500E-01	.168E-03	.294E+03	.000E+00
M	106	F	106	0	0	0	1	.500E-01	.168E-03	.294E+03	.000E+00
M	107	F	107	0	0	0	1	.500E-01	.168E-03	.294E+03	.000E+00
M	108	F	108	0	0	0	1	.500E-01	.168E-03	.294E+03	.000E+00
M	109	F	109	0	0	0	1	.500E-01	.168E-03	.588E+03	.000E+00
M	110	F	110	0	0	0	1	.500E-01	.168E-03	.588E+03	.000E+00
M	111	F	111	0	0	0	1	.500E-01	.168E-03	.588E+03	.000E+00
M	112	F	112	0	0	0	1	.500E-01	.168E-03	.588E+03	.000E+00
M	113	F	113	0	0	0	1	.500E-01	.168E-03	.588E+03	.000E+00
M	114	F	114	0	0	0	1	.500E-01	.168E-03	.588E+03	.000E+00
M	115	F	115	0	0	0	1	.500E-01	.168E-03	.588E+03	.000E+00
M	116	F	116	0	0	0	1	.500E-01	.168E-03	.588E+03	.000E+00
M	117	F	117	0	0	0	1	.500E-01	.168E-03	.588E+03	.000E+00
M	118	F	118	0	0	0	1	.500E-01	.168E-03	.588E+03	.000E+00
M	119	F	119	0	0	0	1	.500E-01	.168E-03	.588E+03	.000E+00
M	120	F	120	0	0	0	1	.500E-01	.168E-03	.588E+03	.000E+00
M	121	F	121	0	0	0	1	.500E-01	.168E-03	.588E+03	.000E+00
M	122	F	122	0	0	0	1	.500E-01	.168E-03	.588E+03	.000E+00
F	1	F	2	0	0	0	3	.500E+01	.500E+01	.100E-01	.100E+01
F	2	F	3	0	0	0	3	.500E+01	.500E+01	.100E-01	.100E+01
F	3	F	4	0	0	0	3	.500E+01	.500E+01	.100E-01	.100E+01
F	4	F	5	0	0	0	3	.500E+01	.500E+01	.100E-01	.100E+01
F	5	F	6	0	0	0	3	.500E+01	.500E+01	.100E-01	.100E+01
F	6	F	7	0	0	0	3	.500E+01	.500E+01	.100E-01	.100E+01
F	7	F	8	0	0	0	3	.500E+01	.500E+01	.100E-01	.100E+01
F	8	F	9	0	0	0	3	.500E+01	.500E+01	.100E-01	.100E+01
F	9	F	10	0	0	0	3	.500E+01	.500E+01	.100E-01	.100E+01
F	10	F	11	0	0	0	3	.500E+01	.500E+01	.100E-01	.100E+01
F	11	F	12	0	0	0	3	.500E+01	.500E+01	.100E-01	.100E+01
F	12	F	13	0	0	0	3	.500E+01	.500E+01	.100E-01	.100E+01
F	13	F	14	0	0	0	3	.500E+01	.500E+01	.100E-01	.100E+01
F	14	F	15	0	0	0	3	.500E+01	.500E+01	.100E-01	.100E+01
F	15	F	16	0	0	0	3	.500E+01	.500E+01	.100E-01	.100E+01
F	16	F	17	0	0	0	3	.500E+01	.500E+01	.100E-01	.100E+01
F	17	F	18	0	0	0	3	.500E+01	.500E+01	.100E-01	.100E+01
F	18	F	19	0	0	0	3	.500E+01	.500E+01	.100E-01	.100E+01
F	19	F	20	0	0	0	3	.500E+01	.500E+01	.100E-01	.100E+01
F	20	F	21	0	0	0	3	.500E+01	.500E+01	.100E-01	.100E+01
F	21	F	22	0	0	0	3	.500E+01	.500E+01	.100E-01	.100E+01
F	22	F	23	0	0	0	3	.500E+01	.500E+01	.100E-01	.100E+01

P. C. Lichtner

SCIENTIFIC NOTEBOOK

INITIALS: PCZ

F	23	F	24	0	0	0	3	.500E+01	.500E+01	.100E-01	.100E+01
F	24	F	25	0	0	0	3	.500E+01	.250E+01	.100E-01	.100E+01
F	25	F	26	0	0	0	3	.250E+01	.250E+01	.100E-01	.100E+01
F	26	F	27	0	0	0	3	.250E+01	.250E+01	.100E-01	.100E+01
F	27	F	28	0	0	0	3	.250E+01	.250E+01	.100E-01	.100E+01
F	28	F	29	0	0	0	3	.250E+01	.250E+01	.100E-01	.100E+01
F	29	F	30	0	0	0	3	.250E+01	.250E+01	.100E-01	.100E+01
F	30	F	31	0	0	0	3	.250E+01	.250E+01	.100E-01	.100E+01
F	31	F	32	0	0	0	3	.250E+01	.250E+01	.100E-01	.100E+01
F	32	F	33	0	0	0	3	.250E+01	.250E+01	.100E-01	.100E+01
F	33	F	34	0	0	0	3	.250E+01	.250E+01	.100E-01	.100E+01
F	34	F	35	0	0	0	3	.250E+01	.250E+01	.100E-01	.100E+01
F	35	F	36	0	0	0	3	.250E+01	.250E+01	.100E-01	.100E+01
F	36	F	37	0	0	0	3	.250E+01	.250E+01	.100E-01	.100E+01
F	37	F	38	0	0	0	3	.250E+01	.250E+01	.100E-01	.100E+01
F	38	F	39	0	0	0	3	.250E+01	.250E+01	.100E-01	.100E+01
F	39	F	40	0	0	0	3	.250E+01	.250E+01	.100E-01	.100E+01
F	40	F	41	0	0	0	3	.250E+01	.100E+01	.100E-01	.100E+01
F	41	F	42	0	0	0	3	.100E+01	.100E+01	.100E-01	.100E+01
F	42	F	43	0	0	0	3	.100E+01	.100E+01	.100E-01	.100E+01
F	43	F	44	0	0	0	3	.100E+01	.100E+01	.100E-01	.100E+01
F	44	F	45	0	0	0	3	.100E+01	.100E+01	.100E-01	.100E+01
F	45	F	46	0	0	0	3	.100E+01	.100E+01	.100E-01	.100E+01
F	46	F	47	0	0	0	3	.100E+01	.100E+01	.100E-01	.100E+01
F	47	F	48	0	0	0	3	.100E+01	.100E+01	.100E-01	.100E+01
F	48	F	49	0	0	0	3	.100E+01	.100E+01	.100E-01	.100E+01
F	49	F	50	0	0	0	3	.100E+01	.100E+01	.100E-01	.100E+01
F	50	F	51	0	0	0	3	.100E+01	.100E+01	.100E-01	.100E+01
F	51	F	52	0	0	0	3	.100E+01	.100E+01	.100E-01	.100E+01
F	52	F	53	0	0	0	3	.100E+01	.100E+01	.100E-01	.100E+01
F	53	F	54	0	0	0	3	.100E+01	.100E+01	.100E-01	.100E+01
F	54	F	55	0	0	0	3	.100E+01	.100E+01	.100E-01	.100E+01
F	55	F	56	0	0	0	3	.100E+01	.100E+01	.100E-01	.100E+01
F	56	F	57	0	0	0	3	.100E+01	.100E+01	.100E-01	.100E+01
F	57	F	58	0	0	0	3	.100E+01	.100E+01	.100E-01	.100E+01
F	58	F	59	0	0	0	3	.100E+01	.100E+01	.100E-01	.100E+01
F	59	F	60	0	0	0	3	.100E+01	.100E+01	.100E-01	.100E+01
F	60	F	61	0	0	0	3	.100E+01	.100E+01	.100E-01	.100E+01
F	61	F	62	0	0	0	3	.100E+01	.100E+01	.100E-01	.100E+01
F	62	F	63	0	0	0	3	.100E+01	.100E+01	.100E-01	.100E+01
F	63	F	64	0	0	0	3	.100E+01	.750E+00	.100E-01	.100E+01
F	64	F	65	0	0	0	3	.750E+00	.500E+00	.100E-01	.100E+01

P. C. Lichtner

SCIENTIFIC NOTEBOOK

INITIALS: PC

F	65	F	66	0	0	0	3	.500E+00	.500E+00	.100E-01	.100E+01
F	66	F	67	0	0	0	3	.500E+00	.500E+00	.100E-01	.100E+01
F	67	F	68	0	0	0	3	.500E+00	.500E+00	.100E-01	.100E+01
F	68	F	69	0	0	0	3	.500E+00	.500E+00	.100E-01	.100E+01
F	69	F	70	0	0	0	3	.500E+00	.500E+00	.100E-01	.100E+01
F	70	F	71	0	0	0	3	.500E+00	.500E+00	.100E-01	.100E+01
F	71	F	72	0	0	0	3	.500E+00	.500E+00	.100E-01	.100E+01
F	72	F	73	0	0	0	3	.500E+00	.500E+00	.100E-01	.100E+01
F	73	F	74	0	0	0	3	.500E+00	.500E+00	.100E-01	.100E+01
F	74	F	75	0	0	0	3	.500E+00	.500E+00	.100E-01	.100E+01
F	75	F	76	0	0	0	3	.500E+00	.500E+00	.100E-01	.100E+01
F	76	F	77	0	0	0	3	.500E+00	.500E+00	.100E-01	.100E+01
F	77	F	78	0	0	0	3	.500E+00	.500E+00	.100E-01	.100E+01
F	78	F	79	0	0	0	3	.500E+00	.500E+00	.100E-01	.100E+01
F	79	F	80	0	0	0	3	.500E+00	.750E+00	.100E-01	.100E+01
F	80	F	81	0	0	0	3	.750E+00	.100E+01	.100E-01	.100E+01
F	81	F	82	0	0	0	3	.100E+01	.100E+01	.100E-01	.100E+01
F	82	F	83	0	0	0	3	.100E+01	.100E+01	.100E-01	.100E+01
F	83	F	84	0	0	0	3	.100E+01	.100E+01	.100E-01	.100E+01
F	84	F	85	0	0	0	3	.100E+01	.100E+01	.100E-01	.100E+01
F	85	F	86	0	0	0	3	.100E+01	.100E+01	.100E-01	.100E+01
F	86	F	87	0	0	0	3	.100E+01	.100E+01	.100E-01	.100E+01
F	87	F	88	0	0	0	3	.100E+01	.100E+01	.100E-01	.100E+01
F	88	F	89	0	0	0	3	.100E+01	.100E+01	.100E-01	.100E+01
F	89	F	90	0	0	0	3	.100E+01	.100E+01	.100E-01	.100E+01
F	90	F	91	0	0	0	3	.100E+01	.100E+01	.100E-01	.100E+01
F	91	F	92	0	0	0	3	.100E+01	.100E+01	.100E-01	.100E+01
F	92	F	93	0	0	0	3	.100E+01	.100E+01	.100E-01	.100E+01
F	93	F	94	0	0	0	3	.100E+01	.100E+01	.100E-01	.100E+01
F	94	F	95	0	0	0	3	.100E+01	.100E+01	.100E-01	.100E+01
F	95	F	96	0	0	0	3	.100E+01	.100E+01	.100E-01	.100E+01
F	96	F	97	0	0	0	3	.100E+01	.100E+01	.100E-01	.100E+01
F	97	F	98	0	0	0	3	.100E+01	.100E+01	.100E-01	.100E+01
F	98	F	99	0	0	0	3	.100E+01	.250E+01	.100E-01	.100E+01
F	99	F	100	0	0	0	3	.250E+01	.250E+01	.100E-01	.100E+01
F	100	F	101	0	0	0	3	.250E+01	.250E+01	.100E-01	.100E+01
F	101	F	102	0	0	0	3	.250E+01	.250E+01	.100E-01	.100E+01
F	102	F	103	0	0	0	3	.250E+01	.250E+01	.100E-01	.100E+01
F	103	F	104	0	0	0	3	.250E+01	.250E+01	.100E-01	.100E+01
F	104	F	105	0	0	0	3	.250E+01	.250E+01	.100E-01	.100E+01
F	105	F	106	0	0	0	3	.250E+01	.250E+01	.100E-01	.100E+01
F	106	F	107	0	0	0	3	.250E+01	.250E+01	.100E-01	.100E+01

P. C. Lichtner

SCIENTIFIC NOTEBOOK

INITIALS: SC

F 107	F 108	0	0	0	3	.250E+01	.250E+01	.100E-01	.100E+01
F 108	F 109	0	0	0	3	.250E+01	.500E+01	.100E-01	.100E+01
F 109	F 110	0	0	0	3	.500E+01	.500E+01	.100E-01	.100E+01
F 110	F 111	0	0	0	3	.500E+01	.500E+01	.100E-01	.100E+01
F 111	F 112	0	0	0	3	.500E+01	.500E+01	.100E-01	.100E+01
F 112	F 113	0	0	0	3	.500E+01	.500E+01	.100E-01	.100E+01
F 113	F 114	0	0	0	3	.500E+01	.500E+01	.100E-01	.100E+01
F 114	F 115	0	0	0	3	.500E+01	.500E+01	.100E-01	.100E+01
F 115	F 116	0	0	0	3	.500E+01	.500E+01	.100E-01	.100E+01
F 116	F 117	0	0	0	3	.500E+01	.500E+01	.100E-01	.100E+01
F 117	F 118	0	0	0	3	.500E+01	.500E+01	.100E-01	.100E+01
F 118	F 119	0	0	0	3	.500E+01	.500E+01	.100E-01	.100E+01
F 119	F 120	0	0	0	3	.500E+01	.500E+01	.100E-01	.100E+01
F 120	F 121	0	0	0	3	.500E+01	.500E+01	.100E-01	.100E+01
F 121	F 122	0	0	0	3	.500E+01	.500E-30	.100E-01	.100E+01
M 1	M 2	0	0	0	3	.500E+01	.500E+01	.990E+00	.100E+01
M 2	M 3	0	0	0	3	.500E+01	.500E+01	.990E+00	.100E+01
M 3	M 4	0	0	0	3	.500E+01	.500E+01	.990E+00	.100E+01
M 4	M 5	0	0	0	3	.500E+01	.500E+01	.990E+00	.100E+01
M 5	M 6	0	0	0	3	.500E+01	.500E+01	.990E+00	.100E+01
M 6	M 7	0	0	0	3	.500E+01	.500E+01	.990E+00	.100E+01
M 7	M 8	0	0	0	3	.500E+01	.500E+01	.990E+00	.100E+01
M 8	M 9	0	0	0	3	.500E+01	.500E+01	.990E+00	.100E+01
M 9	M 10	0	0	0	3	.500E+01	.500E+01	.990E+00	.100E+01
M 10	M 11	0	0	0	3	.500E+01	.500E+01	.990E+00	.100E+01
M 11	M 12	0	0	0	3	.500E+01	.500E+01	.990E+00	.100E+01
M 12	M 13	0	0	0	3	.500E+01	.500E+01	.990E+00	.100E+01
M 13	M 14	0	0	0	3	.500E+01	.500E+01	.990E+00	.100E+01
M 14	M 15	0	0	0	3	.500E+01	.500E+01	.990E+00	.100E+01
M 15	M 16	0	0	0	3	.500E+01	.500E+01	.990E+00	.100E+01
M 16	M 17	0	0	0	3	.500E+01	.500E+01	.990E+00	.100E+01
M 17	M 18	0	0	0	3	.500E+01	.500E+01	.990E+00	.100E+01
M 18	M 19	0	0	0	3	.500E+01	.500E+01	.990E+00	.100E+01
M 19	M 20	0	0	0	3	.500E+01	.500E+01	.990E+00	.100E+01
M 20	M 21	0	0	0	3	.500E+01	.500E+01	.990E+00	.100E+01
M 21	M 22	0	0	0	3	.500E+01	.500E+01	.990E+00	.100E+01
M 22	M 23	0	0	0	3	.500E+01	.500E+01	.990E+00	.100E+01
M 23	M 24	0	0	0	3	.500E+01	.500E+01	.990E+00	.100E+01
M 24	M 25	0	0	0	3	.500E+01	.250E+01	.990E+00	.100E+01
M 25	M 26	0	0	0	3	.250E+01	.250E+01	.990E+00	.100E+01
M 26	M 27	0	0	0	3	.250E+01	.250E+01	.990E+00	.100E+01
M 27	M 28	0	0	0	3	.250E+01	.250E+01	.990E+00	.100E+01

P. C. Lichtner

SCIENTIFIC NOTEBOOK

INITIALS: PC

M	28	M	29	0	0	0	3	.250E+01	.250E+01	.990E+00	.100E+01
M	29	M	30	0	0	0	3	.250E+01	.250E+01	.990E+00	.100E+01
M	30	M	31	0	0	0	3	.250E+01	.250E+01	.990E+00	.100E+01
M	31	M	32	0	0	0	3	.250E+01	.250E+01	.990E+00	.100E+01
M	32	M	33	0	0	0	3	.250E+01	.250E+01	.990E+00	.100E+01
M	33	M	34	0	0	0	3	.250E+01	.250E+01	.990E+00	.100E+01
M	34	M	35	0	0	0	3	.250E+01	.250E+01	.990E+00	.100E+01
M	35	M	36	0	0	0	3	.250E+01	.250E+01	.990E+00	.100E+01
M	36	M	37	0	0	0	3	.250E+01	.250E+01	.990E+00	.100E+01
M	37	M	38	0	0	0	3	.250E+01	.250E+01	.990E+00	.100E+01
M	38	M	39	0	0	0	3	.250E+01	.250E+01	.990E+00	.100E+01
M	39	M	40	0	0	0	3	.250E+01	.250E+01	.990E+00	.100E+01
M	40	M	41	0	0	0	3	.250E+01	.100E+01	.990E+00	.100E+01
M	41	M	42	0	0	0	3	.100E+01	.100E+01	.990E+00	.100E+01
M	42	M	43	0	0	0	3	.100E+01	.100E+01	.990E+00	.100E+01
M	43	M	44	0	0	0	3	.100E+01	.100E+01	.990E+00	.100E+01
M	44	M	45	0	0	0	3	.100E+01	.100E+01	.990E+00	.100E+01
M	45	M	46	0	0	0	3	.100E+01	.100E+01	.990E+00	.100E+01
M	46	M	47	0	0	0	3	.100E+01	.100E+01	.990E+00	.100E+01
M	47	M	48	0	0	0	3	.100E+01	.100E+01	.990E+00	.100E+01
M	48	M	49	0	0	0	3	.100E+01	.100E+01	.990E+00	.100E+01
M	49	M	50	0	0	0	3	.100E+01	.100E+01	.990E+00	.100E+01
M	50	M	51	0	0	0	3	.100E+01	.100E+01	.990E+00	.100E+01
M	51	M	52	0	0	0	3	.100E+01	.100E+01	.990E+00	.100E+01
M	52	M	53	0	0	0	3	.100E+01	.100E+01	.990E+00	.100E+01
M	53	M	54	0	0	0	3	.100E+01	.100E+01	.990E+00	.100E+01
M	54	M	55	0	0	0	3	.100E+01	.100E+01	.990E+00	.100E+01
M	55	M	56	0	0	0	3	.100E+01	.100E+01	.990E+00	.100E+01
M	56	M	57	0	0	0	3	.100E+01	.100E+01	.990E+00	.100E+01
M	57	M	58	0	0	0	3	.100E+01	.100E+01	.990E+00	.100E+01
M	58	M	59	0	0	0	3	.100E+01	.100E+01	.990E+00	.100E+01
M	59	M	60	0	0	0	3	.100E+01	.100E+01	.990E+00	.100E+01
M	60	M	61	0	0	0	3	.100E+01	.100E+01	.990E+00	.100E+01
M	61	M	62	0	0	0	3	.100E+01	.100E+01	.990E+00	.100E+01
M	62	M	63	0	0	0	3	.100E+01	.100E+01	.990E+00	.100E+01
M	63	M	64	0	0	0	3	.100E+01	.750E+00	.990E+00	.100E+01
M	64	M	65	0	0	0	3	.750E+00	.500E+00	.990E+00	.100E+01
M	65	M	66	0	0	0	3	.500E+00	.500E+00	.990E+00	.100E+01
M	66	M	67	0	0	0	3	.500E+00	.500E+00	.990E+00	.100E+01
M	67	M	68	0	0	0	3	.500E+00	.500E+00	.990E+00	.100E+01
M	68	M	69	0	0	0	3	.500E+00	.500E+00	.990E+00	.100E+01
M	69	M	70	0	0	0	3	.500E+00	.500E+00	.990E+00	.100E+01

P. C. Lichtner

SCIENTIFIC NOTEBOOK

INITIALS: PC

M	70	M	71	0	0	0	3	.500E+00	.500E+00	.990E+00	.100E+01
M	71	M	72	0	0	0	3	.500E+00	.500E+00	.990E+00	.100E+01
M	72	M	73	0	0	0	3	.500E+00	.500E+00	.990E+00	.100E+01
M	73	M	74	0	0	0	3	.500E+00	.500E+00	.990E+00	.100E+01
M	74	M	75	0	0	0	3	.500E+00	.500E+00	.990E+00	.100E+01
M	75	M	76	0	0	0	3	.500E+00	.500E+00	.990E+00	.100E+01
M	76	M	77	0	0	0	3	.500E+00	.500E+00	.990E+00	.100E+01
M	77	M	78	0	0	0	3	.500E+00	.500E+00	.990E+00	.100E+01
M	78	M	79	0	0	0	3	.500E+00	.500E+00	.990E+00	.100E+01
M	79	M	80	0	0	0	3	.500E+00	.750E+00	.990E+00	.100E+01
M	80	M	81	0	0	0	3	.750E+00	.100E+01	.990E+00	.100E+01
M	81	M	82	0	0	0	3	.100E+01	.100E+01	.990E+00	.100E+01
M	82	M	83	0	0	0	3	.100E+01	.100E+01	.990E+00	.100E+01
M	83	M	84	0	0	0	3	.100E+01	.100E+01	.990E+00	.100E+01
M	84	M	85	0	0	0	3	.100E+01	.100E+01	.990E+00	.100E+01
M	85	M	86	0	0	0	3	.100E+01	.100E+01	.990E+00	.100E+01
M	86	M	87	0	0	0	3	.100E+01	.100E+01	.990E+00	.100E+01
M	87	M	88	0	0	0	3	.100E+01	.100E+01	.990E+00	.100E+01
M	88	M	89	0	0	0	3	.100E+01	.100E+01	.990E+00	.100E+01
M	89	M	90	0	0	0	3	.100E+01	.100E+01	.990E+00	.100E+01
M	90	M	91	0	0	0	3	.100E+01	.100E+01	.990E+00	.100E+01
M	91	M	92	0	0	0	3	.100E+01	.100E+01	.990E+00	.100E+01
M	92	M	93	0	0	0	3	.100E+01	.100E+01	.990E+00	.100E+01
M	93	M	94	0	0	0	3	.100E+01	.100E+01	.990E+00	.100E+01
M	94	M	95	0	0	0	3	.100E+01	.100E+01	.990E+00	.100E+01
M	95	M	96	0	0	0	3	.100E+01	.100E+01	.990E+00	.100E+01
M	96	M	97	0	0	0	3	.100E+01	.100E+01	.990E+00	.100E+01
M	97	M	98	0	0	0	3	.100E+01	.100E+01	.990E+00	.100E+01
M	98	M	99	0	0	0	3	.100E+01	.250E+01	.990E+00	.100E+01
M	99	M	100	0	0	0	3	.250E+01	.250E+01	.990E+00	.100E+01
M	100	M	101	0	0	0	3	.250E+01	.250E+01	.990E+00	.100E+01
M	101	M	102	0	0	0	3	.250E+01	.250E+01	.990E+00	.100E+01
M	102	M	103	0	0	0	3	.250E+01	.250E+01	.990E+00	.100E+01
M	103	M	104	0	0	0	3	.250E+01	.250E+01	.990E+00	.100E+01
M	104	M	105	0	0	0	3	.250E+01	.250E+01	.990E+00	.100E+01
M	105	M	106	0	0	0	3	.250E+01	.250E+01	.990E+00	.100E+01
M	106	M	107	0	0	0	3	.250E+01	.250E+01	.990E+00	.100E+01
M	107	M	108	0	0	0	3	.250E+01	.250E+01	.990E+00	.100E+01
M	108	M	109	0	0	0	3	.250E+01	.500E+01	.990E+00	.100E+01
M	109	M	110	0	0	0	3	.500E+01	.500E+01	.990E+00	.100E+01
M	110	M	111	0	0	0	3	.500E+01	.500E+01	.990E+00	.100E+01
M	111	M	112	0	0	0	3	.500E+01	.500E+01	.990E+00	.100E+01

P. C. Lichtner

SCIENTIFIC NOTEBOOK

INITIALS: PC

```

M 112 M 113 0 0 0 3 .500E+01 .500E+01 .990E+00 .100E+01
M 113 M 114 0 0 0 3 .500E+01 .500E+01 .990E+00 .100E+01
M 114 M 115 0 0 0 3 .500E+01 .500E+01 .990E+00 .100E+01
M 115 M 116 0 0 0 3 .500E+01 .500E+01 .990E+00 .100E+01
M 116 M 117 0 0 0 3 .500E+01 .500E+01 .990E+00 .100E+01
M 117 M 118 0 0 0 3 .500E+01 .500E+01 .990E+00 .100E+01
M 118 M 119 0 0 0 3 .500E+01 .500E+01 .990E+00 .100E+01
M 119 M 120 0 0 0 3 .500E+01 .500E+01 .990E+00 .100E+01
M 120 M 121 0 0 0 3 .500E+01 .500E+01 .990E+00 .100E+01
M 121 M 122 0 0 0 3 .500E+01 .500E+01 .990E+00 .100E+01

```

:Blank Line

INCON

```

M 1 121 1 .100E+00
      .854970E+05      .207810E+00      .150000E+02
F 1 121 1 .100E+01
      .854972E+05      .949800E+00      .150000E+02
M 122 0 0 .100E+00
      .90500E+05      .300000E+02      .000
F 122 0 0 .100E+01
      .90500E+05      .300000E+02      .00

```

:Blank Line

SOLVE

: precon accel nz nx

D4 NONE -122 2

:

ENDCY

Account Number: **20-1402-562**

Description: Near-field Environment Code Development – MULTIFLO

Collaborators: Dr. M. Seth (Consultant)

Objective: Development of the computer code MULTIFLO, and submodules **GEM** and **METRA**.

3.31.98 ChangeLog MULTIFLO

ChangeLog METRA 1.2b

3/31/98 PCL pproc.f

A bug in pproc.f (metra) and pprcgem.f. Uncomment the commented line and comment the line below as shown here in both the routines.

```

      if(igeom.eq.0.or.igeom.eq.2) then
        igeomtry = 1
        nconn = (nx-1)*ny*nz+nx*(ny-1)*nz+nx*ny*(nz-1) ! uncomment this
line
c      nconn = nbpor-ny*nz+jl(ny)+kl(nz) ! comment/delete this line

```

3/30/98 PCL pproc.f

```

      avgsigma = (sigmaf(mm1)+sigmaf(mm2))*half
      area(nc1) = area(nc)*avgsigma
c to add the following line
      area(nc) = area(nc)-area(nc1) ! adjust mtx-mtx area <--add line
end do
      nconn = nconn+nconn+nbpor
400 continue

```

3/26/98 PCL outmetra.f

Need to put include frfmt.h where izro is in common.

GAS RESEARCH INSTITUTEAccount Number: **20-1136-003**

Description: Modeling Pipe Line Corrosion Under Disbonded Coatings

Collaborators: N. Sridhar PI

Date Due:

Objective: The main objective of this task is to develop the computer code TECTRAN and apply the code to modeling pipe line corrosion under disbonded coatings.

1.8.98 Direct Computation of Potential

An equation for the direct computation of the potential Φ is given by the Poisson-like equation

$$\nabla \cdot \kappa \nabla \Phi = \nabla \cdot \mathbf{i}_0 - j_e, \quad (4)$$

where

$$j_e(\Phi) = F \left(\sum_m n_m I_m^e(\Phi) + \sum_k n_k I_k^e(\Phi) \right). \quad (5)$$

Future work will attempt to use this equation in 2D simulations in place the present method which iterates between the potential and current.

Electronic Scientific Notebook No.
095E:Development of the Code MULTIFLO to
Describe Multiphase Reactive Transport
(12/18/1995 through 04/17/1997)

SCIENTIFIC NOTEBOOK

Peter C. Lichtner

June 24, 1998

2nd Quarter

SCIENTIFIC NOTEBOOK

Peter C. Lichtner

June 24, 1998

2nd Quarter

Southwest Research Institute

Center for Nuclear Waste Regulatory Analyses

San Antonio, Texas

P. C. Lichtner

SCIENTIFIC NOTEBOOKINITIALS: PCL**INITIAL ENTRIES**

Scientific NoteBook: # 095

Issued to: P. C. Lichtner

Issue Date: Tuesday, November 16, 1993

Close Date: Thursday, June 25, 1998

Computerized Initials: PCL

By agreement with the CNWRA QA this NoteBook is to be printed at approximate quarterly intervals. This computerized Scientific NoteBook is intended to address the criteria of CNWRA QAP-001.

Table 1: Computing Equipment

Machine Name	Type	OS	Location
gravenstein.cnwra.swri.edu	Pentium Workstation	NEXTSTEP	desk Rm A-126
	133 Mhz	Version 3.3	Bldg. 189
	128 MB RAM		
skippy.cnwra.swri.edu	Sun SPARC 20	SOLARIS 5.5	network
	128 MB RAM		

TABLE OF CONTENTS

INITIAL ENTRIES	ii
FIGURES	iv
TABLES	v
NEAR-FIELD ENVIRONMENT: TECHNICAL ASSISTANCE	1
[5.27.98] DCM.	1
[6.1.98] Coupled DCM.	11
NEAR-FIELD ENVIRONMENT: CODE DEVELOPMENT	17
[4.1.98] ChangeLog MULTIFLO	17
GAS RESEARCH INSTITUTE	21
[5.8.98] Benchmark Problems	21
[6.23.98] ChangeLog TECTRAN.	33
[6.25.98] Close of GRI Project.	33

LIST OF FIGURES

1	Matrix and fracture liquid saturation profiles in the absence of infiltration.	2
2	Matrix and fracture liquid saturation profiles for 5 mm/y infiltration.	3
3	Matrix and fracture chloride concentration plotted as a function of time at the repository horizon in the absence of infiltration.	11
4	Comparison of the concentration for numerical (solid curve) and analytical (dotted curves) results for elapsed times of 0.1 and 0.5 hours.	25
5	Comparison of the diffusive current density i_0 for numerical (solid curve) and analytical (dotted curves) results for elapsed times of 0.1 and 0.5 hours.	26
6	Comparison of the potential for numerical (solid curve) and analytical (dotted curves) results for elapsed times of 0.1 and 0.5 hours.	27
7	Stationary state concentration profiles C_1 and C_2 for Fe^{2+} (solid curve) and Cl^- (dotted curve). The tip of the crevice is located at the origin and the mouth at 0.01 m.	30
8	Stationary state profiles for the potential Φ (solid curve), and diffusive (dashed curve) and total current (dotted curve) densities i and i_0	31
9	Transient concentration profiles for C_A and comparison with numerical (solid curves) and analytical (dotted curves) solutions.	33

LIST OF TABLES

1 Computing Equipment ii

NEAR-FIELD ENVIRONMENTAccount Number: **20-1402-561**

Description: Near-field Environment Technical Assistance

Collaborators: Dr. M. Seth (Consultant)

Objective: Application of the computer code MULTIFLO, and submodules **GEM** and **METRA** to the Yucca Mountain HLW Repository.

5.27.98 DCM. The DCM (Dual Continuum Model) is applied to a 1D column with (Figure 2) and without (Figure 1) infiltration. Constant grid spacing of 1 m was used in the calculation. The stratigraphy consists of a number of layers as listed below. Depths of each layer are set according to:

```
tcw11=42 (*25-55*);
tcw12=6;
tcw13=3;
ptn21=3;
ptn23=3;
ptn24=6 (*5-6*);
ptn25=16 (*10-16*);
tsw31=4 (*3-4*);
tsw32=45 (*35-45*);
tsw33=45 (*6-45*);
tsw34=10 (*6-10*);
tsw35=70 (*60-71*);
tsw36=106 (*90-106*);
tsw37=30 (*18-30*);
chlvc=30 (*25-30*);
chlzc=30 (*25-30*);
ch2zc=19 (*13-19*);
ch3zc=52 (*42-52*);
ch4zc=20 (*17-20*);
pp3vp=50 (*25-50*);
pp2zp=10 (*0-10*);
list={tcw11,tcw12,tcw13,ptn21,ptn23,ptn24,ptn25,
tsw31,tsw32,tsw33,tsw34, tsw35,tsw36,tsw37,
chlvc,chlzc,ch2zc,ch3zc,ch4zc,pp3vp,pp2zp};
listwt={tcw11,tcw12,tcw13,ptn21,ptn23,ptn24,ptn25,
tsw31,tsw32,tsw33,tsw34, tsw35,tsw36,tsw37,
chlvc,chlzc,ch2zc,ch3zc,ch4zc}
listr={tcw11,tcw12,tcw13,ptn21,ptn23,ptn24,ptn25,
tsw31,tsw32,tsw33,tsw34, tsw35/2.};
Apply[Plus,list]
Apply[Plus,listwt]
Apply[Plus,listr]
{42,6,3,3,3,6,16,4,45,45,10,70,106,30,30,30,19,52,20}
600
540
218.
```

The repository depth is 218 m. Total height of the column is 540 m. The thickness of each stratigraphic unit is computed as follows:

```
listz={tcw11,
tcw11+tcw12,
tcw11+tcw12+tcw13,
tcw11+tcw12+tcw13+ptn21,
```



```

tcw11+tcw12+tcw13+ptn21+ptn23,
tcw11+tcw12+tcw13+ptn21+ptn23+ptn24,
tcw11+tcw12+tcw13+ptn21+ptn23+ptn24+ptn25,
tcw11+tcw12+tcw13+ptn21+ptn23+ptn24+ptn25+tsw31,
tcw11+tcw12+tcw13+ptn21+ptn23+ptn24+ptn25+tsw31+tsw32,
tcw11+tcw12+tcw13+ptn21+ptn23+ptn24+ptn25+tsw31+tsw32+tsw33,
tcw11+tcw12+tcw13+ptn21+ptn23+ptn24+ptn25+tsw31+tsw32+tsw33+tsw34,
tcw11+tcw12+tcw13+ptn21+ptn23+ptn24+ptn25+tsw31+tsw32+tsw33+tsw34+tsw35,
tcw11+tcw12+tcw13+ptn21+ptn23+ptn24+ptn25+tsw31+tsw32+tsw33+tsw34+tsw35+tsw36,

tcw11+tcw12+tcw13+ptn21+ptn23+ptn24+ptn25+tsw31+tsw32+tsw33+tsw34+tsw35+tsw36+
tsw37,
tcw11+tcw12+tcw13+ptn21+ptn23+ptn24+ptn25+tsw31+tsw32+tsw33+tsw34+tsw35+tsw36+
tsw37+chlvc,
tcw11+tcw12+tcw13+ptn21+ptn23+ptn24+ptn25+tsw31+tsw32+tsw33+tsw34+tsw35+tsw36+
tsw37+chlvc+chlzc,
tcw11+tcw12+tcw13+ptn21+ptn23+ptn24+ptn25+tsw31+tsw32+tsw33+tsw34+tsw35+tsw36+
tsw37+chlvc+chlzc+ch2zc,
tcw11+tcw12+tcw13+ptn21+ptn23+ptn24+ptn25+tsw31+tsw32+tsw33+tsw34+tsw35+tsw36+
tsw37+chlvc+chlzc+ch2zc+ch3zc,
tcw11+tcw12+tcw13+ptn21+ptn23+ptn24+ptn25+tsw31+tsw32+tsw33+tsw34+tsw35+tsw36+
tsw37+chlvc+chlzc+ch2zc+ch3zc+ch4zc,
tcw11+tcw12+tcw13+ptn21+ptn23+ptn24+ptn25+tsw31+tsw32+tsw33+tsw34+tsw35+tsw36+
tsw37+chlvc+chlzc+ch2zc+ch3zc+ch4zc+pp3vp,
tcw11+tcw12+tcw13+ptn21+ptn23+ptn24+ptn25+tsw31+tsw32+tsw33+tsw34+tsw35+tsw36+
tsw37+chlvc+chlzc+ch2zc+ch3zc+ch4zc+pp3vp+pp2zp)
{52,58,61,64,67,73,89,93,138,183,193,263,369,399,429,459,478,530,550,600,610}

```

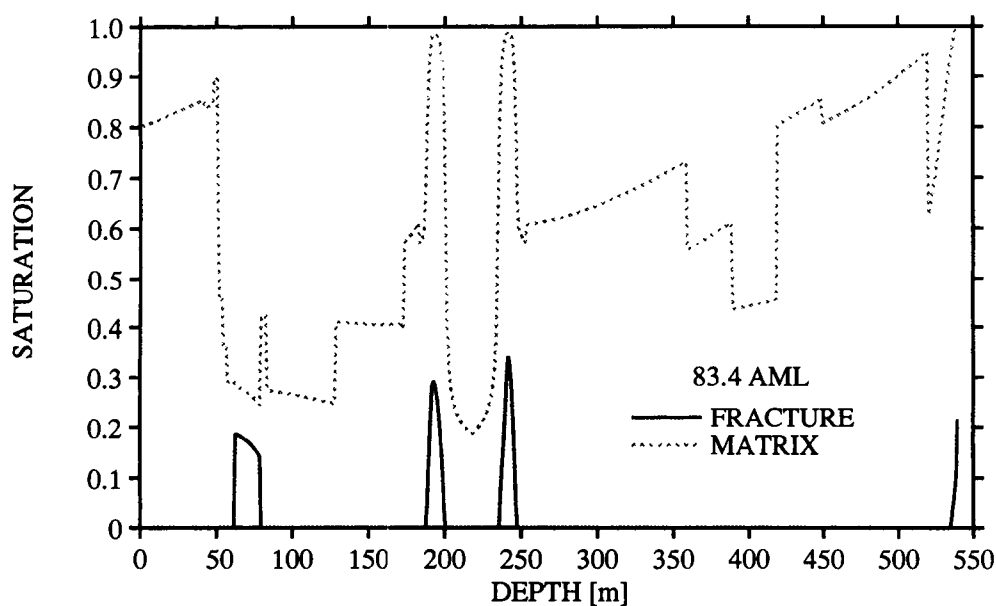


Figure 1: Matrix and fracture liquid saturation profiles in the absence of infiltration.

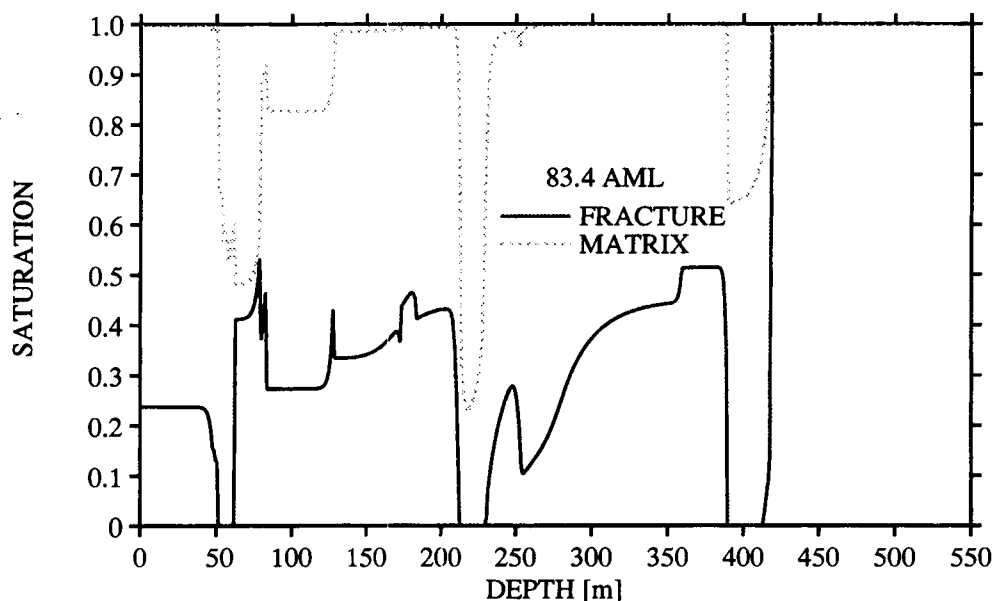


Figure 2: Matrix and fracture liquid saturation profiles for 5 mm/y infiltration.

Input files used in the simulations are listed below for GEM and METRA.

```

k-feldspar dissolution
dcm: Jan. 21, 1997
:      geometry  nx  ny  nz  mode  iprint  idebug  iwarn  il  i2
GRID  DCMXYZ      1  1 600  2      1      0      0      1  5
:
:/usr/mss/multi/database/masterT.V8.R5
:/sparc20/lichtner/bin/database/mastertemp.V8.R5
DBASE
/home/skippy/lichtner/bin/database/mastertemp.V8.R5
:
OPTS
:  idata  istart  imod  iexact  iscale  ihrmc  isst
:    0      0      1      0      0      0     -1
:
:  itmax  ihalmax  ivmax  ndamp  icntmx
:   16     32      0      0      3
:
:  method  iops  ifor  isurf  iact  loglin  icon  counr  tpulse  wtup
:    1      0      2      1      1      0      1  -1.e7
:
:  isync  ipor  iperm  permfac  porfac  icksat  slcutoff
COUPLE  0      0      0      3.      1.      1      5.e-3
:
PLTFiles
:iplot  a  s  t  m  si  sf  v  z  bin  e  ex  ti  g  itex  mk  err
:    1  1  1  1  1  0  0  1  0  2  0  0  0  1  1  0  0  1
:
:  tol  ttol  tolneg  tolpos  tclexp  dthalf  qkmax  tolstdst  tolc
TOLR 1.d-11 2.e-2 1.e-8 1.e-2 5.d0  .5    590.  1.e-12  1.e-16
:
:  mcyc  cc  c  flx  r  sp  ck  pk  rk  al  a2  a3
DEBUG  0      1  1  0  1  1  1  1  1  1
:
DCMPARA
:i1  i2  j1  j2  k1  k2  volf  areamodf  xlm  ylm  zlm  porm  swm
:  1  1  1  1  1  600  1.e-2  1.e-5  .1  .1  .1  0.5  0.5

```

```

0
:      isat isothrm iread por0 phir sat w lambda toldelt tolpor
ISYSstem 0 1 0 0.5 1. 0.5 .5 1. 1.e-3 1.e-3
:
:      vx0 vy0 vz0 vgx vgy vgz[m/yr] alphax alphas alphaz[m] vmfac
FLOW 0. 0. 0. 0. 0. 0. 0. 0. 0. 1.
:
:      d0[cm^2/s] delhaq[kJ/mol] dgas[cm^2/s] dgexp tortaq tortg idif
DIFF 1.d-5 12.6 2.13d-1 1.8 0.5d0 0.5d0 0
:
:flag 1: T(x) = d x^3 + a x^2 + b x + c (meters)
:      2: T(x) = a + (b-a) exp[-((x-x0)/c)^2] + (d - a) * x / xlen
:      3: T(x,t)=a+1/2(b-a)(erf[(x+c-x0)/2sqr(dt)]-erf[(x-c-x0)/2sqr(dt)])
:      p (bars) temp flag a b c d x0 xlen
PTINit 1.e5 25. 0 25 300 250 125 1000. 2.d3
:
:master species for controlling time stepping
Master ALL
:
:5*0.025 20*0.05 25*0.125 25*0.25 15*0.5 10*1.0
Dxyz
1.
1.
600*5.
:
:      isolv level north nitmax ideta:l rmaxtol rtwotol smaxtol
SOLV 3 1 1 100 0 1.e-20 1.e-20 1.e-12
:
:initial and boundary conditions: 1-conc., 2-flux, 3-zero gradient
COMP
:
:i1 i2 j1 j2 k1 k2
1 1 1 1 1 600
0
:
:      fracture
:species itype ctot mineral guess
cl- 1 2.5e-3
:
:      matrix
:species itype ctot mineral guess
cl- 1 2.5e-3
0
:
:skip
Bcon
:ibndtyp ifacx tmpbc dist area vell velg por sl porm slm imtx
1 3 15. 0. 0. 0. 0. 0. 0. 0. 0
:
:i1 i2 j1 j2 k1 k2
1 1 1 1 1 1
0
:
:      fracture
:species itype ctot mineral guess
cl- 1 2.5e-3
:
:      matrix
:species itype ctot mineral guess
cl- 1 2.5e-3
:
:ibndtyp ifacx tmpbc dist area vell velg por sl porm slm imtx
1 4 30.
:
:i1 i2 j1 j2 k1 k2
1 1 1 1 600 600
0
:
:      fracture
:species itype ctot mineral guess
cl- 1 2.5e-3
:
:      matrix
:species itype ctot mineral guess
cl- 1 2.5e-3
0
noskip
:

```

```

Stol 1. 1. 1. 1. 1. 1.
:
skip
AQCX
oh-
hcl(aq)
co2(aq)
co3-2
caco3(aq)
cahco3+
caoh+
cac1+
cac12(aq)
nahco3(aq)
nacl(aq)
naoh(aq)
h3sio4-
h2sio4-2
:blank
:
MNRL
quartz
cristobalite(alpha)
sio2(am)
chalcedony
calcite
tobermorite-14a
:blank
:
GASEs
co2(g)
:blank
:
:skip
MNIR
:mineral npar fkin delh tau
quartz 1 1.e10 87.5 1.e-3
:itypkin npri nsec sig rk
20 0 0 1. 1.2589e-18
:
:matrix fracture
:i1 i2 j1 j2 k1 k2 vol area vol area
1 1 1 1 1 600 0.1 100. 0.0995 100.
0
cristobalite(alpha) 1 1.e10 87.5 1.e-3
20 0 0 1. 3.16e-17
1 1 1 1 1 600 0.23 100. 0.23 100.
0
calcite 1 1. 35. 1.e-3
20 0 0 1. -10.
1 1 1 1 1 600 0.02 1. 0. 1.
0
tobermorite-14a 1 1. 35. 1.e-3
:itypkin npri nsec sig rk
20 0 0 1. -14.
1 1 1 1 1 600 0. 1. 0. 1.
0
sio2(am) 1 1. 62.8 1.e-3
:itypkin npri nsec sig rk
20 0 0 1. 7.944e-17
1 1 1 1 1 600 0. 100. 0. 100.
0
:blank
noskip
:
:ion-exchange reactions
:Ionx 0 1.0
:
Brkp 1
1 1 218
:
Dtstep[y] 3 3.e-6 500. 1.e3

```

```

1.e-6      1.      2. 100.0
:
Time[y] 9 10. 25. 50. 100. 500. 1.e3 5.e3 1.e4 5.e4 1.e5
:
ENDS

METRA-DCM, 83 kW/ac
May 7 , 1998
:
: New stratigraphy. Unit thickness are averages of values presented in
: LBL document:
: 'Site-Scale Unsaturated Zone Model of Yucca Mountain, Nevada', 8/96,
: pg. 437 (LBNL-39315).
: Permeabilities and van Genuchten parameters for units taken from LBL
: document:
: 'The Site-Scale Unsaturated
: Zone Model of Yucca Mountain, Nevada for the Viability Assessment',
: 6/97, pgs
: 6-32 thru 6-34 ( calibrated values, Fm = 0.492 (LBNL-40376)). Residual
: saturations,
: porosities, and thermal properties taken from TSPA-93 and TSPA-95
: (PP values assumed to be same as TSw values).
:
: Infiltration rate = 1.0 mm/yr.
:
: 1-D
:
:
RSTART 0
:
: XYZ          = 1 table look-up;; pref = ref. press.
: RADIAL       = 0 correlations;   tref = ref temp.
: OTHER
:
: geometry nx ny  nz ivplr ipvcal iout gravity pref tref href
Grid DCMXYZ   1 1 550 1      1      1      0      0      0      0
:
Pckr          :relative perm and pc keyword
: 1 type-curv  swirm  rpmm(lamda) alphaswext  sgc  iecm
:
: (TCw11 - matrix)
: 1 Van-Gen    0.021  0.232    1.17e-6    0.0    0.0    0
:
: (TCw11 - fracture)
: 2 Van-Gen    0.04   0.492    2.95e-4    0.0    0.0    0
:
: (TCw12 - matrix)
: 3 Van-Gen    0.021  0.236    1.32e-6    0.0    0.0    0
:
: (TCw12 - fracture)
: 4 Van-Gen    0.04   0.492    2.95e-4    0.0    0.0    0
:
: (TCw13 - matrix)
: 5 Van-Gen    0.021  0.427    6.46e-7    0.0    0.0    0
:
: (TCw13 - fracture)
: 6 Van-Gen    0.04   0.492    9.12e-5    0.0    0.0    0
:
: 1 type-curv  swirm  rpmm(lamda) alphaswext  sgc  iecm
:
: (PTn21 - matrix)
: 7 Van-Gen    0.154  0.231    3.80e-5    0.0    0.0    0
:
: (PTn21 - fracture)
: 8 Van-Gen    0.04   0.492    1.10e-3    0.0    0.0    0
:
: (PTn23 - matrix)
: 9 Van-Gen    0.154  0.287    4.57e-5    0.0    0.0    0
:
: (PTn23 - fracture)
: 10 Van-Gen   0.04   0.492    3.39e-3    0.0    0.0    0

```

```

:
: (PTn24 - matrix)
:   11 Van-Gen    0.154    0.349    4.27e-5    0.0    0.0    0
:
: (PTn24 - fracture)
:   12 Van-Gen    0.04    0.492    9.33e-4    0.0    0.0    0
:
:   i type-curv    swirm    rpmm(lamda)    alpham    swext    sgc    iecm
:
: (PTn25 - matrix)
:   13 Van-Gen    0.154    0.279    1.95e-4    0.0    0.0    0
:
: (PTn25 - fracture)
:   14 Van-Gen    0.04    0.279    1.95e-4    0.0    0.0    0
:
: (TSw31 - matrix)
:   15 Van-Gen    0.045    0.237    1.00e-5    0.0    0.0    0
:
: (TSw31 - fracture)
:   16 Van-Gen    0.04    0.481    3.98e-5    0.0    0.0    0
:
: (TSw32 - matrix)
:   17 Van-Gen    0.045    0.273    2.29e-5    0.0    0.0    0
:
: (TSw32 - fracture)
:   18 Van-Gen    0.04    0.488    9.33e-5    0.0    0.0    0
:
:   i type-curv    swirm    rpmm(lamda)    alpham    swext    sgc    iecm
:
: (TSw33 - matrix)
:   19 Van-Gen    0.045    0.247    6.76e-6    0.0    0.0    0
:
: (TSw33 - fracture)
:   20 Van-Gen    0.04    0.492    1.78e-4    0.0    0.0    0
:
: (TSw34 - matrix)
:   21 Van-Gen    0.045    0.322    1.02e-6    0.0    0.0    0
:
: (TSw34 - fracture)
:   22 Van-Gen    0.04    0.492    9.77e-5    0.0    0.0    0
:
: (TSw35 - matrix: Repository horizon)
:   23 Van-Gen    0.045    0.229    3.31e-6    0.0    0.0    0
:
: (TSw35 - fracture: Repository horizon)
:   24 Van-Gen    0.04    0.492    1.10e-4    0.0    0.0    0
:
:   i type-curv    swirm    rpmm(lamda)    alpham    swext    sgc    iecm
:
: (TSw36 - matrix)
:   25 Van-Gen    0.045    0.414    7.41e-7    0.0    0.0    0
:
: (TSw36 - fracture)
:   26 Van-Gen    0.04    0.492    1.32e-4    0.0    0.0    0
:
: (TSw37 - matrix)
:   27 Van-Gen    0.045    0.387    1.55e-6    0.0    0.0    0
:
: (TSw37 - fracture)
:   28 Van-Gen    0.04    0.492    1.17e-4    0.0    0.0    0
:
: (CH1vc - matrix)
:   29 Van-Gen    0.121    0.190    6.61e-5    0.0    0.0    0
:
: (CH1vc - fracture)
:   30 Van-Gen    0.04    0.492    1.17e-3    0.0    0.0    0
:
:   i type-curv    swirm    rpmm(lamda)    alpham    swext    sgc    iecm
:
: (CH1zc - matrix)
:   31 Van-Gen    0.097    0.366    8.32e-7    0.0    0.0    0

```

```

:
: (CH1zc - fracture)
: 32 Van-Gen      0.04      0.492      1.12e-3      0.0      0.0      0
:
: (CH2zc - matrix) Note: van Gen values assumed to be same as CH3zc
: see pg 437 in 1996 doc mentioned above.
: 33 Van-Gen      0.097      0.220      1.95e-6      0.0      0.0      0
:
: (CH2zc - fracture) Note: van Gen values assumed to be same as CH3zc
: see pg 437 in 1996 doc mentioned above.
: 34 Van-Gen      0.04      0.492      1.23e-3      0.0      0.0      0
:
: (CH3zc - matrix)
: 35 Van-Gen      0.097      0.220      1.95e-6      0.0      0.0      0
:
: (CH3zc - fracture)
: 36 Van-Gen      0.04      0.492      1.23e-3      0.0      0.0      0
:
: i type-curve swirm rpmm(lamda) alpham swext sgc iecm
:
: (CH4zc - matrix)
: 37 Van-Gen      0.097      0.477      7.76e-6      0.0      0.0      0
:
: (CH4zc - fracture)
: 38 Van-Gen      0.04      0.492      1.15e-3      0.0      0.0      0
:
: (PP3vp - matrix)
: 39 Van-Gen      0.045      0.311      1.74e-5      0.0      0.0      0
:
: (PP3vp - fracture)
: 40 Van-Gen      0.04      0.492      1.41e-3      0.0      0.0      0
:
: (PP2zp - matrix)
: 41 Van-Gen      0.045      0.316      1.66e-6      0.0      0.0      0
:
: (PP2zp - fracture)
: 42 Van-Gen      0.04      0.492      3.72e-4      0.0      0.0      0
:
0      : blank line to end pckr data
:
:
:
Thermal-prop
: no rho cpr ckdry cksat crp crt tau cdiff cexp enbd
1 2.580e+03 728. 1.69 1.69 0 0 .5 2.13e-5 1.8 0. :TCw
2 2.580e+03 422. 0.61 0.61 0 0 .5 2.13e-5 1.8 0. :PTn
3 2.580e+03 840. 2.10 2.10 0 0 .5 2.13e-5 1.8 0. :TSw
4 2.580e+03 948. 1.28 1.28 0 0 .5 2.13e-5 1.8 0. :TSv
5 2.580e+03 488. 0.84 0.84 0 0 .5 2.13e-5 1.8 0. :CHnv
5 2.580e+03 526. 1.42 1.42 0 0 .5 2.13e-5 1.8 0. :CHnz
:
0
:
: igrd rw re
DXYZ 0
: (dx(i),i=1,nx)
1.0
: (dy(j),j=1,ny)
1.
: (dz(k),k=1,nz)
1.
PhiK
:il i2 j1 j2 k1 k2 ist itm vb porf permxf permyf permzf pormm permm istm ithrm
1 1 1 1 1 52 2 1 0. 1. 6.0e-12 6.0e-12 6.0e-12 0.087 5.4e-18 1 1 : TCw11
1 1 1 1 53 58 4 1 0. 1. 6.0e-12 6.0e-12 6.0e-12 0.087 5.4e-18 3 1 : TCw12
1 1 1 1 59 61 6 1 0. 1. 2.4e-12 2.4e-12 2.4e-12 0.087 4.9e-17 5 1 : TCw13
1 1 1 1 62 64 8 2 0. 1. 3.0e-13 3.0e-13 3.0e-13 0.421 3.1e-14 7 2 : PTn21
1 1 1 1 65 67 10 2 0. 1. 2.9e-12 2.9e-12 2.9e-12 0.421 8.3e-14 9 2 : PTn23
1 1 1 1 68 73 12 2 0. 1. 1.2e-13 1.2e-13 1.2e-13 0.421 1.1e-13 11 2 : PTn24
1 1 1 1 74 89 14 2 0. 1. 2.5e-13 2.5e-13 2.5e-13 0.421 2.5e-13 13 2 : PTn25
1 1 1 1 90 93 16 3 0. 1. 1.7e-12 1.7e-12 1.7e-12 0.139 4.9e-17 15 3 : TSw31
1 1 1 1 94 138 18 3 0. 1. 1.8e-12 1.8e-12 1.8e-12 0.139 2.8e-16 17 3 : TSw32

```

P. C. Lichtner

SCIENTIFIC NOTEBOOK

INITIALS: SC

```

1 1 1 1 139 183 20 3 0. 1. 8.9e-13 8.9e-13 8.9e-13 0.139 1.1e-17 19 3 : TSw33
1 1 1 1 184 193 22 3 0. 1. 4.5e-13 4.5e-13 4.5e-13 0.139 4.1e-18 21 3 : TSw34
1 1 1 1 194 263 24 3 0. 1. 1.4e-12 1.4e-12 1.4e-12 0.139 1.5e-17 23 3 : TSw35
1 1 1 1 264 369 26 3 0. 1. 1.2e-12 1.2e-12 1.2e-12 0.139 8.9e-17 25 3 : TSw36
1 1 1 1 370 399 28 3 0. 1. 1.2e-12 1.2e-12 1.2e-12 0.139 1.3e-17 27 3 : TSw37
1 1 1 1 400 429 30 4 0. 1. 1.7e-13 1.7e-13 1.7e-13 0.331 1.3e-12 29 4 : CH1vc
1 1 1 1 430 459 32 5 0. 1. 2.4e-14 2.4e-14 2.4e-14 0.306 1.4e-17 31 5 : CH1zc
1 1 1 1 460 478 34 5 0. 1. 1.2e-14 1.2e-14 1.2e-14 0.306 9.1e-18 33 5 : CH2zc
1 1 1 1 479 530 36 5 0. 1. 1.2e-14 1.2e-14 1.2e-14 0.306 9.1e-18 35 5 : CH3zc
1 1 1 1 531 550 38 5 0. 1. 1.5e-14 1.5e-14 1.5e-14 0.306 1.5e-17 37 5 : CH4zc
: 1 1 1 1 551 600 40 3 0. 1. 6.9e-13 6.9e-13 3.9e-13 0.306 2.8e-15 39 3 : PP3vp
: 1 1 1 1 601 610 42 3 0. 1. 6.5e-14 6.5e-14 6.4e-14 0.306 5.8e-17 41 3 : PP2zp
0
:
Init init
:
: i1 i2 j1 j2 k1 k2 p t sg xg2 pm tm sgm xgm
: 1 1 1 1 1 550 1.e5 25. 0.95 0. 1.e5 25. 0.2 0.
:/
:
DCMPARA
: i1 i2 j1 j2 k1 k2 volf areamodf xlm ylm zlm
1 1 1 1 1 550 0.01 1.0 0.1 0.1 0.1
0
:
: depth pdepth tdepth tgrad param iequil
Equil 550. 9.1e4 30. 0.025 0. -1
:
Recurrent-data
:skip
Bcon 2
:itype iface i1 i2 j1 j2
3 TOP 1 1 1 1
:time qbc pbc tbc sgbc xabc
:matrix
0. 5.e-3 8.5e4 15.0 0.2 0.
:fracture
0. 5.e-3 8.5e4 15.0 0.95 0.
0
:itype iface i1 i2 j1 j2
1 BOTTOM 1 1 1 1
0. 0. 9.1e4 30.0 0. 0.
0. 0. 9.1e4 30.0 0. 0.
0
noskip
:
Rstart 1 0
Output A=1 C=1 B=1 S=-1
: isolate newtnmn newtnmx north nitmx level
Solve 3 1 10 4 100 1
:
:AUTO-step DPMXE DSMXE DTMPMXE DP2MXE TACCEL IAUTODT FAC1
AUTO-step 5.e3 0.03 3.0 1.e4 1.e-3 0 0
:
: TOLP TOLS TOLT TOLP2 TOLM TOLA TOLE rtwtol rmxtol smxtol
Tolr 1. 1.e-4 1.e-3 1.e+1 1.e-5 1.e-3 1.e-3 1.e-20 1.e-20 1.e-20
:
:Limit dpmx dsmx dtmpmx dp2mx dtmn dtmx dtfac
LIMIT 1.e5 .1 10. 1.e5 1.e-9 5.e8 .33
: ns fach facm (fach and facm are multipliers to
: read-in values of qht and qmt)
:Plots 1 1
:Steady[y] 1.e-8 1.e-6 1.e-1
:Ends
Source 1 1.0 1. 83.4 AML
: is js ks istyp
1 1 1 1 228 228 31
: timeq(sec) T/qht (C/(J/s)) qmt (kg/s)
0.00000E+00 1.87730E+01
6.30720E+07 1.81217E+01
1.26144E+08 1.75357E+01

```


P. C. Lichtner

SCIENTIFIC NOTEBOOK

INITIALS: SC

```

1.89216E+08 1.68897E+01
2.52288E+08 1.63046E+01
3.15360E+08 1.57715E+01
4.73040E+08 1.45818E+01
6.30720E+08 1.34618E+01
7.88400E+08 1.25071E+01
9.46080E+08 1.16163E+01
1.26144E+09 1.02515E+01
1.57680E+09 8.99586E+00
2.36520E+09 6.82702E+00
3.15360E+09 5.65219E+00
4.73040E+09 4.24896E+00
6.30720E+09 3.53303E+00
9.46080E+09 2.82589E+00
1.26144E+10 2.40733E+00
1.57680E+10 2.08456E+00
1.89216E+10 1.81067E+00
2.52288E+10 1.44680E+00
3.15360E+10 1.20944E+00
3.94200E+10 9.81818E-01
4.73040E+10 8.27487E-01
6.30720E+10 6.33691E-01
7.88400E+10 5.48998E-01
9.46080E+10 4.89297E-01
1.26144E+11 4.38708E-01
1.57680E+11 4.02873E-01
1.89216E+11 3.70297E-01
2.20752E+11 3.44801E-01
2.52288E+11 3.24128E-01
2.83824E+11 3.06917E-01
3.15360E+11 2.92001E-01
3.46896E+11 2.69319E-01
3.78432E+11 2.50151E-01
4.09968E+11 2.33722E-01
4.41504E+11 2.19473E-01
4.73040E+11 2.06987E-01
5.51880E+11 1.81593E-01
6.30720E+11 1.62125E-01
7.88400E+11 1.34131E-01
9.46080E+11 1.14855E-01
1.26144E+12 8.27996E-02
1.57680E+12 6.29212E-02
1.89216E+12 4.90735E-02
2.20752E+12 3.97719E-02
2.52288E+12 3.31523E-02
2.83824E+12 2.82343E-02
3.15360E+12 2.44608E-02
4.73040E+12 1.84539E-02
0
:
Output A=1 C=1
:
:  isolv  newtnmn  newtnmx  north  nitmax  level
Solve 3      2      12      2     100      1
:
: AUTO-step  DPMXE   DSMXE  DTMPMXE  DP2MXe  TACCEL  IAUTODT  FAC1
AUTO-step  5.0E+3  0.03   3.0      5.e3  1.0e-3    0        0
:
: TOLR TOLP TOLS  TOLT  TOLP2  TOLM  TOLA  TOLE  rtwtol  rmxtol  smxtol
Tolr  1. 5.e-4 5.e-3 1.    1.e-3 1.e-3 1.e-3 1.e-12 1.e-12 1.e-12
:
: Limit dpmx  dsmx dtmpmx dp2mx  dtmn  dtmx  icutmx
LIMIT 1.e4   .06  5.    1.e4   1.e-9 1.e4
:
Plots 1 1 1
228
Time[y] 10.
Time[y] 50.
Time[y] 100.
Time[y] 500.
Time[y] 1000.

```

```

Time[y] 2000.
Time[y] 5000.
Time[y] 1.e4
Time[y] 5.e4
Time[y] 1.e5
Ends

```

6.1.98 Coupled DCM. The DCM (Dual Continuum Model) is applied to a 1D column with simple chemistry. The fracture completely dries out. To handle this situation a saturation cutoff factor is introduced when the liquid saturation drops below a specified value given in the GEM input file (see listing below). Liquid and gas flow velocities are set to zero at the interfaces to the node in question. When the system rewets, the flow velocities are turned back on.

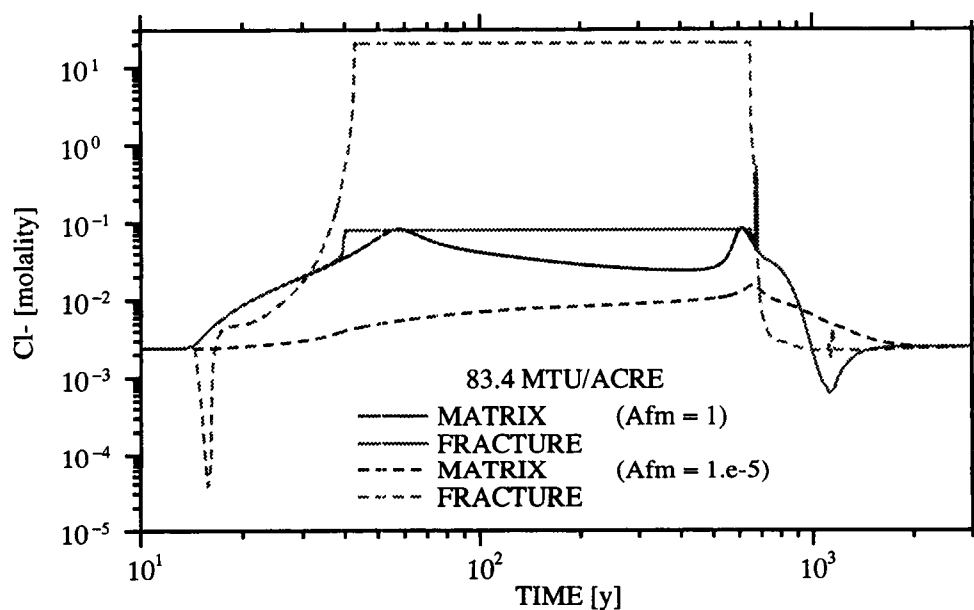


Figure 3: Matrix and fracture chloride concentration plotted as a function of time at the repository horizon in the absence of infiltration.

Input files used in the simulations are listed below for GEM and METRA.

```

k-feldspar dissolution
dcm: Jan. 21, 1997
:
:   geometry  nx  ny  nz  mode  iprint  idebug  iwarn  i1 i2
GRID  DCMXYZ      1   1 600   2      1      0      0      1  5
:
: /usr/mss/multi/database/masterT.V8.R5
: /sparc20/lichtner/bin/database/mastertemp.V8.R5
DBASE
/home/skipky/lichtner/bin/databases/mastertemp.V8.R5
:
OPTS

```

P. C. Lichtner

SCIENTIFIC NOTEBOOK

INITIALS: SCZ

```

:  idata istart imod iexact iscale ihrmc isst
:  0      0      1      0      0      0      -1
:
:  itmax ihalmax ivmax ndamp icntmx
:  16     32     0      0      3
:
:  method iops ifor isurf iact loglin icon cournr tpulse wtup
:  1      0      2      1      1      0      1 -1.e7
:
:  isync ipor iperm permfac porfac icksat slcutoff
COUPLE 0      0      0      3.      1.      1      5.e-3
:
PLTFiles
: iplot a s t m si sf v z b in e ex ti g itex mk err
:  1      1      1      1      0      0      1      0      2      0      0      0      1      1      0      0      1
:
:  tol ttol tolneg tolpos tolexp dthalf gkmax tolstdst tolc
TOLR 1.d-11 2.e-2 1.e-8 1.e-2 5.d0 .5 590. 1.e-12 1.e-12
:
:  mcycc cc c flx r sp qk pk rk a1 a2 a3
DEBUG 0      1      1      0      1      1      1      1      1
:
DCMPARA
: i1 i2 j1 j2 k1 k2 volf areamodf xlm ylm zlm porm swm
:  1  1  1  1  1  1 600 1.e-2 1.e-5 .1 .1 .1 .1 0.5 0.5
0
:  isat isothrm iread por0 phir sat w lambda toldelt tolpor
ISYSem 0      1      0      0.5 1. 0.5 .5 1. 1.e-3 1.e-3
:
:  vx0 vy0 vz0 vgx vgy vgz[m/yr] alphax alphay alphaz[m] vmfac
FLOW 0. 0. 0. 0. 0. 0. 0. 0. 0. 0. 0. 1.
:
:  d0[cm^2/s] delhaq[kJ/mol] dgas[cm^2/s] dgexp tortaq tortg idif
DIFF 1.d-5 12.6 2.13d-1 1.8 0.5d0 0.5d0 0
:
: flag 1: T(x) = d x^3 + a x^2 + b x + c (meters)
: 2: T(x) = a + (b-a) exp[-((x-x0)/c)^2] + (d - a) * x / xlen
: 3: T(x,t)=a+1/2(b-a)(erf[(x+c-x0)/2sqrt(dt)]-erf[(x-c-x0)/2sqrt(dt)])
: p (bars) temp flag a b c d x0 xlen
PTInit 1.e5 25. 0 25 300 250 125 1000. 2.d3
:
: master species for controlling time stepping
Master ALL
:
: 5*0.025 20*0.05 25*0.125 25*0.25 15*0.5 10*1.0
Dxyz
1.
1.
600*5.
:
: isolv level north nitmax idetail rmaxtol rtwotol smaxtol
SOLV 4 1 1 100 0 1.e-20 1.e-20 1.e-12
:
: initial and boundary conditions: 1-conc., 2-flux, 3-zero gradient
COMP
:
: i1 i2 j1 j2 k1 k2
: 1 1 1 1 1 1 600
0
: fracture
: species itype ctot mineral guess
cl- 1 2.5e-3
:
: matrix
: species itype ctot mineral guess
cl- 1 2.5e-3
0
:
: skip
Bcon
: ibndtyp ifacx tmpbc dist area vell velg por s1 porm slm imtx

```

```

      1      3      15.      0.      0.      0.      0.      0.      0.      0
:il i2 j1 j2 k1 k2
      1      1      1      1      1      1
0
:
:fracture
:species itype ctot mineral guess
cl-      1      2.5e-3
:
:matrix
:species itype ctot mineral guess
cl-      1      2.5e-3
:
:ibndtyp ifacx tmpbc dist area vell velg por sl porm slm imtx
      1      4      30.
:il i2 j1 j2 k1 k2
      1      1      1      1      600      600
0
:fracture
:species itype ctot mineral guess
cl-      1      2.5e-3
:
:matrix
:species itype ctot mineral guess
cl-      1      2.5e-3
0
noskip
:
Stol 1. 1. 1. 1. 1. 1.
:
skip
AQCX
oh-
hcl(aq)
co2(aq)
co3-2
caco3(aq)
cahco3+
caoh+
cacl+
cacl2(aq)
nahco3(aq)
nacl(aq)
naoh(aq)
h3sio4-
h2sio4-2
:blank
:
MNRL
quartz
cristobalite(alpha)
sio2(am)
chalcedony
calcite
tobermorite-14a
:blank
:
GASEs
co2(g)
:blank
:
:skip
MNIR
:mineral npar fkin delh tau
quartz 1 1.e10 87.5 1.e-3
:itypkin npri nsec sig rk
      20      0      0      1.      1.2589e-18
:
:matrix fracture
:il i2 j1 j2 k1 k2 vol area vol area
      1      1      1      1      1      600      0.1      100.      0.0995      100.
0
cristobalite(alpha) 1 1.e10 87.5 1.e-3
      20      0      0      1.      3.16e-17
      1      1      1      1      1      600      0.23      100.      0.23      100.

```

P. C. Lichtner

SCIENTIFIC NOTEBOOK

INITIALS: SCZ

```

0
calcite 1 1. 35. 1.e-3
  20 0 0 1. -10.
  1 1 1 1 1 600 0.02 1. 0. 1.
0
tobermorite-14a 1 1. 35. 1.e-3
:itypkin npri nsec sig rk
  20 0 0 1. -14.
  1 1 1 1 1 600 0. 1. 0. 1.
0
sio2(am) 1 1. 62.8 1.e-3
:itypkin npri nsec sig rk
  20 0 0 1. 7.944e-17
  1 1 1 1 1 600 0. 100. 0. 100.
0
:blank
noskip
:
:ion-exchange reactions
:Ionx 0 1.0
:
Brkp 1
1 1 375
:
Dtstep[y] 3 3.e-6 500. 1.e3
1.e-6 1. 2. 100.0
:
Time[y] 9 10. 1.5821E+01 25. 50. 100. 500. 1.e3 5.e3 1.e4 5.e4 1.e5
:
ENDS

Data for Multiflo simulator: DCM run with heat load
May 8, 1998
RSTART 0
:
: XYZ = 1 table look-up, pref = ref. press.
: RADIAL = 0 correlations, tref = ref temp.
: OTHER
:grid geometry nx ny nz ivplwr ipvcal iout gravity pref tref href
:Grid XYZ 1 1 600 1 0 3 0 0 0 0
Grid DCMXYZ 1 1 600 1 1 3 -1 0 0 0 1
:
Pckr :relative perm and pc keyword
: 1 type-curve swirr rpmm(lamda) alpham swext sgc iecm
: swirr rpmm(lamda) alphaf phim phif perm permf
:Topopah Spring (150-475 m)
  1 Van-Gen 0.01 0.7636 1.305e-5 0.06 0. 0
  2 Van-Gen 0.05 0.4400 5.8e-7 0.1 0. 0
:
: (TSw35 - fracture: Repository horizon)
: 1 Van-Gen 0.04 0.492 1.10e-4 0.0 0.0 0
:
: (TSw35 - matrix: Repository horizon)
: 2 Van-Gen 0.045 0.229 3.31e-6 0.0 0.0 0
:blank line
:
Thermal-prop
: no rho cpr ckdry cksat crp crt tau cdiff cexp enbd
  1 2.580e3 840. 2.8 2.8 0 0 0.5 2.13e-5 1.8 0.
0
: igrd rw re
DXYZ 0 0. 1.
: (dx(i),i=1,nx)
1.
:
: (dy(j),j=1,ny)
1.
:
: (dz(k),k=1,nz)
1.
:

```

P. C. Lichtner

SCIENTIFIC NOTEBOOK

INITIALS: PC

```

PhiK
:il i2 j1 j2 k1 k2 ist ithr vb por permx permy permz porm prmm istm itm
:1 1 1 1 1 600 1 1 0. 1. 1.2e-12 1.2e-12 1.2e-12 0.139 8.9e-17 2 1
  1 1 1 1 1 600 1 1 0. 1. 1.0e-11 1.0e-11 1.0e-11 0.11 1.8e-18 2 1
:1 1 1 1 1 1 1 1 1.1e20 1. 1.2e-12 1.2e-12 1.2e-12 0.139 8.9e-17 2 1
:1 1 1 1 600 600 1 1 1.1e20 1. 1.2e-12 1.2e-12 1.2e-12 0.139 8.9e-17 2 1
0
Init init
: il i2 j1 j2 k1 k2 p t sg xg2 pm tm sgm xgm
: 1 1 1 1 1 600 1.e5 25. 0.5 0. 1.e5 25. 0.5 0.
: 0
:
DCMPARA
: il i2 j1 j2 k1 k2 volf areamcdf xlm ylm zlm
: 1 1 1 1 1 1 .01 0.e-5 .1 .1 .1
  1 1 1 1 1 600 .01 1.e-5 .1 .1 .1
: 1 1 1 1 600 600 .01 0.e-5 .1 .1 .1
0
:
:EQUIL 587.50 1.e5 30. 0.0255319 0.02 -1
:EQUIL 5.0 1.e5 25. 0. 0.2 1
:EQUIL 595.0 1.065627E+05 25. 0.0 0.0 -1
:
Recurrent-data
:skip
Bcon 2
:itype iface il i2 j1 j2
1 TOP 1 1 1 1
:time qbc pbc tbc sgbc xabc
:matrix
0. 0.e-1 8.5e4 15.0 0.2 0.
:fracture
0. 0.e-1 8.5e4 15.0 0.95 0.
0
:itype iface il i2 j1 j2
1 BOTTOM 1 1 1 1
0. 0. 9.1e4 30.0 0. 0.
0. 0. 9.1e4 30.0 0. 0.
0
noskip
:
Rstart 1 0
Output A=1 C=1 B=1 S=-1
: isolve newtnmn newtnmx north nitmx level
Solve 3 1 10 4 100 1
:
:AUTO-step DPMXE DSMXE DTPMXE DP2MXE TACCEL IAUTODT FAC1
AUTO-step 5.e3 0.03 3.0 1.e4 1.e-3 0 0
:
: TOLP TOLS TOLT TOLP2 TOLM TOLA TOLE rtwtol rmxtol smxtol
Tolr 1. 1.e-4 1.e-3 1.e+1 1.e-5 1.e-3 1.e-3 1.e-20 1.e-20 1.e-20
:
:Limit dpmx dsmx dtmpmx dp2mx dtmn dtmx dtfac
LIMIT 1.e5 .1 10. 1.e5 1.e-6 5.e8 .33
: ns fach facm (fach and facm are multipliers to
: read-in values of qht and qmt)
:Plots 1 1
:Steady[y] 1.e-8 1.e-6 1.e-1
:Ends
:skip
Source 1 1.0 1. 1 83.4 AML
: is js ks istyp
1 1 1 1 375 375 31
: timeq(sec) T/qht (C/(J/s)) qmt (kg/s)
0.00000E+00 1.87730E+01
6.30720E+07 1.81217E+01
1.26144E+08 1.75357E+01
1.89216E+08 1.68897E+01
2.52288E+08 1.63046E+01
3.15360E+08 1.57715E+01
4.73040E+08 1.45818E+01

```

```

6.30720E+08 1.34618E+01
7.88400E+08 1.25071E+01
9.46080E+08 1.16163E+01
1.26144E+09 1.02515E+01
1.57680E+09 8.99586E+00
2.36520E+09 6.82702E+00
3.15360E+09 5.65219E+00
4.73040E+09 4.24896E+00
6.30720E+09 3.53303E+00
9.46080E+09 2.82589E+00
1.26144E+10 2.40733E+00
1.57680E+10 2.08456E+00
1.89216E+10 1.81067E+00
2.52288E+10 1.44680E+00
3.15360E+10 1.20944E+00
3.94200E+10 9.81818E-01
4.73040E+10 8.27487E-01
6.30720E+10 6.33691E-01
7.88400E+10 5.48998E-01
9.46080E+10 4.89297E-01
1.26144E+11 4.38708E-01
1.57680E+11 4.02873E-01
1.89216E+11 3.70297E-01
2.20752E+11 3.44801E-01
2.52288E+11 3.24128E-01
2.83824E+11 3.06917E-01
3.15360E+11 2.92001E-01
3.46896E+11 2.69319E-01
3.78432E+11 2.50151E-01
4.09968E+11 2.33722E-01
4.41504E+11 2.19473E-01
4.73040E+11 2.06987E-01
5.51880E+11 1.81593E-01
6.30720E+11 1.62125E-01
7.88400E+11 1.34131E-01
9.46080E+11 1.14855E-01
1.26144E+12 8.27996E-02
1.57680E+12 6.29212E-02
1.89216E+12 4.90735E-02
2.20752E+12 3.97719E-02
2.52288E+12 3.31523E-02
2.83824E+12 2.82343E-02
3.15360E+12 2.44608E-02
4.73040E+12 1.84539E-02
0

```

noskip

Plots 1 1 1

375

```

Time[y] 10.
Time[y] 50.
Time[y] 100.
Time[y] 500.
Time[y] 1000.
Time[y] 2000.
Time[y] 5000.
Time[y] 1.e4
Time[y] 5.e4
Time[y] 1.e5

```

Ends

Account Number: **20-1402-562**

Description: Near-field Environment Code Development – MULTIFLO

Collaborators: Dr. M. Seth (Consultant)

Objective: Development of the computer code MULTIFLO, and submodules **GEM** and **METRA**.

4.1.98 **ChangeLog MULTIFLO**

ChangeLog GEM 1.2b

6/17/98 PCL

Corrected calls to distvel.f in read2.f and corrected subroutine distvel.f to be consistent with call arguments for computation of areas in y and z directions.

ChangeLog METRA 1.2b

5/26/98 udtvpk.f and updtpsk.f

Replaced .le. by .lt. to remove oscillations in saturation during rewetting. Replace

```
if(upvk.le.pk(m)-pak(m)) then
```

with

```
if(upvk.lt.pk(m)-pak(m)) then
```

5/22/98 bcond.f

```
cerr yakmm = pbc(IBC)*uupkm
```

```
yakmm = pabc(IBC)*uupkm
```

5/16/98 plots.f

Corrected printing in DCM mode for nz-nx problem:

```
do i2 = 1, n2
```

```
do i1 = 1, n1
```

```
m = i2+(i1-1)*nx
```

```
m = kkk+(m-1)*ndloc1
```

```
call humidty (m,psatkm,rh,rhol,rhog,xla,xair)
```



```

        write(iunit3,'(1pe10.4,100(a1,1pg13.4e3),a1,1pe10.4)')
        .   cord1(i1),tab, cord2(i2),tab,p(m),tab,tmp(r(m),tab,
        .   one-sg(m),tab,sg(m),tab,xla,tab,xair,tab,pcwk(m),tab,rh,tab,
        .   psatkm,tab,rhol,tab,rhog
        .   enddo
        enddo

```

4/6/98 inpmetra.f

Replace the starred segments from the following in inpmetra.f. In here 'nvol' is computed internally and not read by user as before. The manual has to be changed to reflect it.

```

        do i = 1,10
            if(word(i:i).ne.' ') go to 614
        end do
614   write(image,502) (word(j:j),j = i,i+2)
        read (image,618) dim
618   format(a3)

        if(igeom.ge.0)
            *call range (i1,i2,j1,j2,k1,k2,nx,ny,nz,key,ierr)

c*****
        call frfmt (ione,ifour,iten,11,izro,izro,ity)
        ii2 = 10
        if(nminct.lt.ii2) ii2 = nminct
        read (image,622) nminct,(vol(i),i = 1,ii2)
622   format (i4,10f11.0)
c           nminct = nminc+1 (matrix+fracture continua)
        ii1 = 1
632   nvol = ii2
        do i = ii1,ii2
            if(vol(i).le.zero) go to 626
        end do
        go to 628
626   nvol = i-1
        go to 630

628   if(nminct.gt.ii2) then
624       ii1 = ii2+1

```

```

        ii2 = ii2+nvalue
        if (ii2.gt.nminct) ii2 = nminct
        call frfmt (nvalue,12,izro,izro,izro,izro,ityp)
        read (image,570) (vol(i),i= ii1,ii2)
        if(nminct.gt.ii2) go to 632
    endif
630    continue
c*****
        do ltype = 1,3
            if(dim.eq.type(ltype)) goto 606
        end do
        write(iferr,625) dim
625    format(1x,' *** Error: Unknown Proximity Function ID ',a5/)
        stop

4/6/98 in inpmetra.f

        if(iistm.le.zero) iistm = iiecm(iist)
    endif

        if(iistm.eq.0) iistm = iist
        if(iithrm.eq.0) iithrm = iithr <-- change to iithr from ithr
        vb(m)      = uvb
=====
in read.f in inpmtra.f

        do i = i1,i2
            if(a(i).eq.0.) then
                if(igeom.eq.1.or.igeom.eq.3) return <-- replace this line

c... if less than nx non-zero values are read, set all the zero
=====
in tkvp.f in pvtfunc.f

replace call to pvth2o as below.

        dt2dt = term2*(two*kn(8)*term2-one/ul)*utcl
        utsp = upsk*(dtl1dt-dt2dt)          ! = dPs/dT

        call pvth2o (upsk,zero,upsk,utk,udwk,uhwk,udgk,uhgk,utsp,udwp,
        * udwt,uhw,uhwt,udgp,udgt,uhgt,uhgt,-1,1,0,scale,ierr)

```

c u1 = (utk-tfirst)*dtempr+one

4/2/98 PCL mainmetra.f maingem.f mainmlti.f/dcmfrac.f

Add statement: character*4 key.

4/2/98 PCL pvtfunc.f/tkvp.f

Eliminated use of table-lookup when ipvtcal=1.

4/1/98 PCL

The array dx has to be dimensioned as dx(0:*) in radcord.f routines which appear in mainmlti.f, maingem.f, and mainmtra.f.

GAS RESEARCH INSTITUTEAccount Number: **20-1136-003**

Description: Modeling Pipe Line Corrosion Under Disbonded Coatings

Collaborators: N. Sridhar PI

Objective: The main objective of this task is to develop the computer code TECTRAN and apply the code to modeling pipe line corrosion under disbonded coatings.

5.8.98 Benchmark Problems**BENCHMARK PROBLEMS**

The electrochemical reactive transport equations for the case of ionic species without complexing reactions have the simple form

$$\frac{\partial}{\partial t} \phi C_i + \frac{\partial J_i}{\partial x} = -\nu_{ik} I_k^e, \quad (1)$$

with the flux J_i consisting of diffusive and electromigration terms

$$J_i = -\phi D_i \frac{\partial C_i}{\partial x} - \frac{F\phi}{RT} z_i D_i C_i \frac{\partial \Phi}{\partial x}. \quad (2)$$

A single electrochemical reaction of the form



involving the k th aqueous species is considered with reaction rate I_k^e . Thus $\nu_{ik} = \delta_{ik}$.

Charge balance requires the condition

$$\sum_i z_i C_i = 0. \quad (4)$$

The total solution current density i is defined by

$$i = F \sum_i z_i J_i, \quad (5)$$

$$= -F\phi \sum_i z_i D_i \frac{\partial C_i}{\partial x} - \left[\frac{F^2\phi}{RT} \sum_i z_i^2 D_i C_i \right] \frac{\partial \Phi}{\partial x}, \quad (6)$$

$$= i_0 + i_\Phi, \quad (7)$$

where the contribution to the current from electrochemical migration is given by

$$i_{\Phi} = -\kappa \frac{\partial \Phi}{\partial x}, \quad (8)$$

the diffusive current i_0 is given by

$$i_0 = -F\phi \sum_i z_i D_i \frac{\partial C_i}{\partial x}, \quad (9)$$

and where κ is defined by

$$\kappa = \frac{F^2 \phi}{RT} \sum_i z_i^2 D_i C_i. \quad (10)$$

Thus the net current i can be expressed as the sum of the diffusive and the electrochemical migration currents. Defining the quantity ω_i as

$$\omega_i = \frac{F^2 \phi}{RT \kappa} z_i D_i C_i, \quad (11)$$

$$= \frac{z_i D_i C_i}{\sum_l z_l^2 D_l C_l}, \quad (12)$$

with the property

$$\sum_i z_i \omega_i = 1, \quad (13)$$

the flux becomes

$$J_i = -\phi D_i \frac{\partial C_i}{\partial x} + \frac{\omega_i}{F} (i - i_0), \quad (14)$$

$$= J_i^0 - \omega_i \sum_l z_l J_l^0 + \frac{\omega_i}{F} i, \quad (15)$$

where J_i^0 refers to the diffusive contribution to the flux defined by

$$J_i^0 = -\phi D_i \frac{\partial C_i}{\partial x}. \quad (16)$$

Multiplying the transport equations by $F z_i$ and summing over all species gives

$$\frac{\partial}{\partial t} \left(\phi F \sum_i z_i C_i \right) + \frac{\partial}{\partial x} \left(F \sum_i z_i J_i \right) = -F \sum_i z_i \nu_{ik} I_k^e. \quad (17)$$

Making use of charge balance and the definition of the total current density, this equation relates the divergence of the current density to the electrochemical corrosion rate

$$\frac{\partial i}{\partial x} = -F \sum_i z_i \nu_{ik} I_k^e = -F n_e I_k^e. \quad (18)$$

The potential is determined from the differential equation

$$\frac{\partial \Phi}{\partial x} = -\frac{i - i_0}{\kappa}. \quad (19)$$

Nonreacting Binary System

An analytical solution exists for a binary system composed of two species with valencies z_1, z_2 . The transport equations are given by

$$\frac{\partial C_1}{\partial t} - D_1 \frac{\partial^2 C_1}{\partial x^2} - F \frac{z_1 D_1}{RT} \frac{\partial}{\partial x} \left[C_1 \frac{\partial \Phi}{\partial x} \right] = 0, \quad (20)$$

and

$$\frac{\partial C_2}{\partial t} - D_2 \frac{\partial^2 C_2}{\partial x^2} - F \frac{z_2 D_2}{RT} \frac{\partial}{\partial x} \left[C_2 \frac{\partial \Phi}{\partial x} \right] = 0. \quad (21)$$

Charge conservation implies the relation

$$z_1 C_1 + z_2 C_2 = 0, \quad (22)$$

and thus C_1 and C_2 are proportional to one another

$$C_2 = -\frac{z_1}{z_2} C_1. \quad (23)$$

The diffusive current density i_0 defined by

$$i_0 = -F \phi \left(z_1 D_1 \frac{\partial C_1}{\partial x} + z_2 D_2 \frac{\partial C_2}{\partial x} \right), \quad (24)$$

becomes

$$= -F \phi z_1 (D_1 - D_2) \frac{\partial C_1}{\partial x}. \quad (25)$$

The potential and current density are related by the equation

$$\kappa \frac{\partial \Phi}{\partial x} = i_0, \quad (26)$$

where κ is defined by

$$\kappa = \frac{F^2 \phi}{RT} (z_1^2 D_1 C_1 + z_2^2 D_2 C_2), \quad (27)$$

$$= \frac{F^2 \phi}{RT} (z_1 D_1 - z_2 D_2) z_1 C_1. \quad (28)$$

The potential is determined from the integral

$$\Phi(x) = \Phi_0 + \int_0^x \frac{i_0(x')}{\kappa(x')} dx', \quad (29)$$

$$= \Phi_0 - \frac{RT}{F} \frac{D_1 - D_2}{z_1 D_1 - z_2 D_2} \int_0^x \frac{1}{C_1} \frac{\partial C_1}{\partial x'} dx', \quad (30)$$

$$= \Phi_0 - \frac{RT}{F} \frac{D_1 - D_2}{z_1 D_1 - z_2 D_2} [\ln C_1(x) - \ln C_1(0)], \quad (31)$$

with Φ_0 giving the potential at $x = 0$.

Eliminating the potential from the transport equations yields uncoupled equations for C_1 and C_2 given by

$$\frac{\partial C_1}{\partial t} - D_{\text{eff}} \frac{\partial^2 C_1}{\partial x^2} = 0, \quad (32)$$

and

$$\frac{\partial C_2}{\partial t} - D_{\text{eff}} \frac{\partial^2 C_2}{\partial x^2} = 0. \quad (33)$$

Thus both species migrate with time with a common effective diffusion coefficient D_{eff} given by

$$D_{\text{eff}} = D_1 - \omega_1 z_1 (D_1 - D_2), \quad (34)$$

$$= D_2 - \omega_2 z_2 (D_2 - D_1), \quad (35)$$

$$= \frac{(z_1 - z_2) D_1 D_2}{z_1 D_1 - z_2 D_2}. \quad (36)$$

The quantities ω_1 and ω_2 are defined by

$$\omega_1 = \frac{z_1 D_1 C_1}{z_1^2 D_1 C_1 + z_2^2 D_2 C_2}, \quad (37)$$

$$= \frac{D_1}{z_1 D_1 - z_2 D_2}, \quad (38)$$

and

$$\omega_2 = \frac{1}{z_2} (1 - z_1 \omega_1), \quad (39)$$

$$= -\frac{D_2}{z_1 D_1 - z_2 D_2}. \quad (40)$$

For a binary system with $z_1 = -z_2 = 1$, the effective diffusion coefficient is equal to the harmonic mean

$$D_{\text{eff}} = \frac{2D_1 D_2}{D_1 + D_2}. \quad (41)$$

These results are applied to a binary system consisting of the two species Na^+ and Cl^- with equal initial concentrations of 10^{-4} M and inlet concentrations at $x = 0$ of 0.1 M. The potential is fixed at zero at the inlet. Diffusion coefficients of 1.334×10^{-9} and $2.032 \times 10^{-9} \text{ m}^2 \text{ s}^{-1}$ for sodium and chloride ions, respectively, are used in the

calculation. The effective diffusion coefficient has the value $1.68 \times 10^{-9} \text{ m}^2 \text{ s}^{-1}$. The concentration profile is shown in Figure 4, the current density i_0 is shown in Figure 5, and the potential in Figure 6 along with a comparison with the numerical solution.

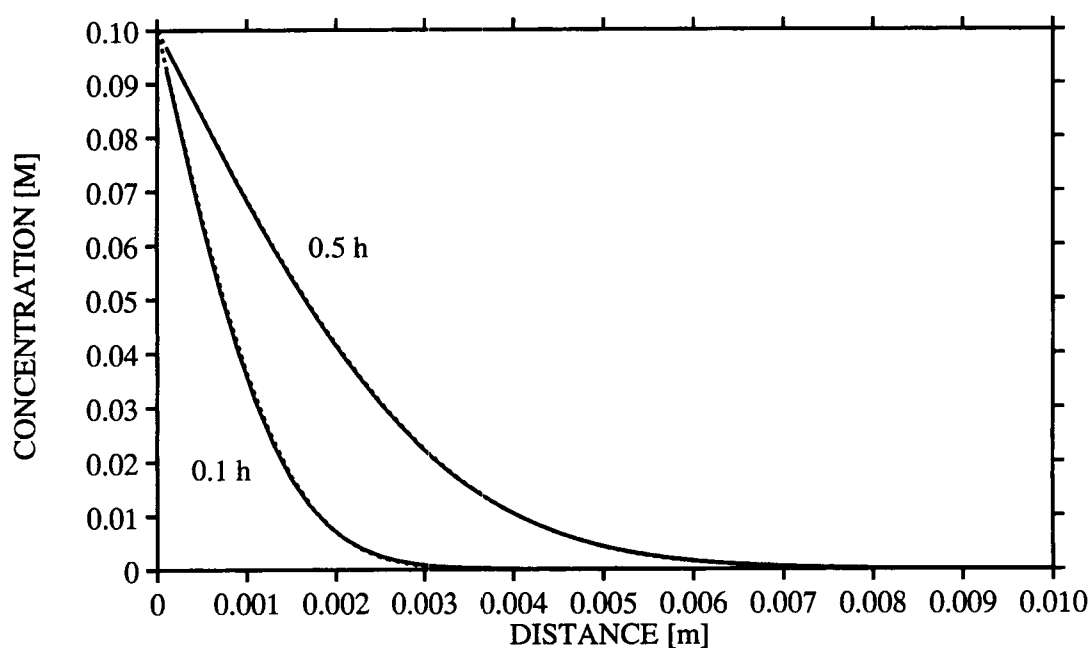


Figure 4: Comparison of the concentration for numerical (solid curve) and analytical (dotted curves) results for elapsed times of 0.1 and 0.5 hours.

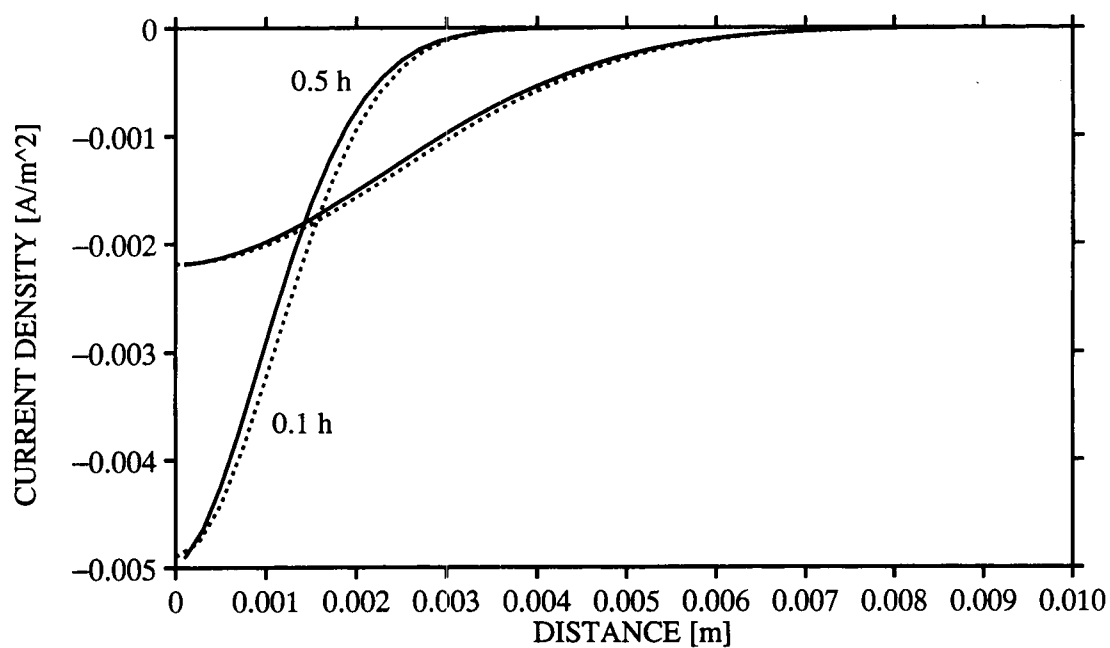


Figure 5: Comparison of the diffusive current density i_0 for numerical (solid curve) and analytical (dotted curves) results for elapsed times of 0.1 and 0.5 hours.

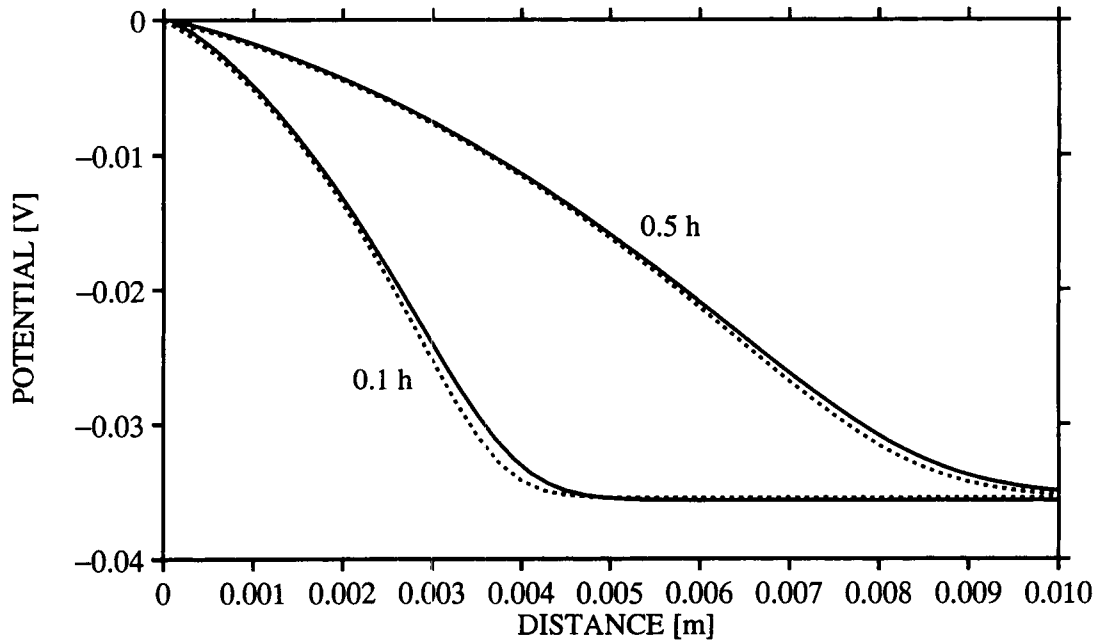


Figure 6: Comparison of the potential for numerical (solid curve) and analytical (dotted curves) results for elapsed times of 0.1 and 0.5 hours.

Reacting Binary System

A single electrochemical reaction is considered of the form



The reaction rate is assumed to be constant throughout the length of the crevice with potential-independent rate denoted by I_e . Denoting the concentration of species \mathcal{A}^{+n_e} with valence $z_1 = n_e$ by C_1 , and the concentration of a counterbalancing species \mathcal{A}_2 of negative valence z_2 by C_2 , the transport equations become

$$\frac{\partial \phi C_1}{\partial t} - \phi D_1 \frac{\partial^2 C_1}{\partial x^2} - F \phi \frac{z_1 D_1}{RT} \frac{\partial}{\partial x} \left[C_1 \frac{\partial \Phi}{\partial x} \right] = -I_e, \quad (43)$$

and

$$\frac{\partial \phi C_2}{\partial t} - \phi D_2 \frac{\partial^2 C_2}{\partial x^2} - F \phi \frac{z_2 D_2}{RT} \frac{\partial}{\partial x} \left[C_2 \frac{\partial \Phi}{\partial x} \right] = 0. \quad (44)$$

The two transport equations are coupled through the potential-dependent term.

Eliminating the potential Φ leads to the transport equations

$$\frac{\partial \phi C_1}{\partial t} - \phi D_{\text{eff}} \frac{\partial^2 C_1}{\partial x^2} + \frac{\omega_1}{F} \frac{\partial i}{\partial x} = -I_e, \quad (45)$$

and

$$\frac{\partial \phi C_2}{\partial t} - \phi D_{\text{eff}} \frac{\partial^2 C_2}{\partial x^2} + \frac{\omega_2}{F} \frac{\partial i}{\partial x} = 0, \quad (46)$$

with D_{eff} given by Eqn.(36).

The current density i satisfies the differential equation

$$\frac{\partial i}{\partial x} = -F n_e I_e. \quad (47)$$

For far from equilibrium conditions a constant dissolution rate prevails and the rate is equal to the product of the kinetic rate constant k times the specific surface area s

$$I_e = -ks. \quad (48)$$

In this case the current density becomes a linear function of distance along the crevice

$$i(x) = F n_e k s x, \quad (49)$$

with crevice tip located at $x = 0$. With these results, for far from equilibrium conditions the transport equations take the form

$$\frac{\partial \phi C_1}{\partial t} - \phi D_{\text{eff}} \frac{\partial^2 C_1}{\partial x^2} = ks(1 - n_e \omega_1), \quad (50)$$

and

$$\frac{\partial \phi C_2}{\partial t} - \phi D_{\text{eff}} \frac{\partial^2 C_2}{\partial x^2} = -ks n_e \omega_2. \quad (51)$$

Charge balance results in a source term for the anion mass transport equation even though this species is not directly involved in the corrosion reaction. A common effective diffusion coefficient appears in both cation and anion transport equations to ensure electroneutrality.

With boundary conditions of fixed concentration at the mouth of the crevice ($x = l$), and zero flux at the tip ($x = 0$), the transport equations admit the stationary state solution

$$C_1(x) = C_1^l - \frac{1}{2} a_1 (x - l)(x + l), \quad (52)$$

and

$$C_2(x) = C_2^l + \frac{1}{2}a_2(x-l)(x+l), \quad (53)$$

with

$$a_1 = \frac{ks}{\phi D_{\text{eff}}} (1 - n_e \omega_1), \quad (54)$$

and

$$a_2 = \frac{ks}{\phi D_{\text{eff}}} n_e \omega_2. \quad (55)$$

Note that the system is electrically neutral because

$$z_1 a_1 = z_2 a_2, \quad (56)$$

and the boundary condition at the inlet is assumed to be electrically neutral

$$z_1 C_1^l + z_2 C_2^l = 0. \quad (57)$$

The diffusive current is given by

$$i_0(x) = -F\phi \left(z_1 D_1 \frac{dC_1}{dx} + z_2 D_2 \frac{dC_2}{dx} \right), \quad (58)$$

$$= -F\phi (-z_1 D_1 a_1 + z_2 D_2 a_2) x, \quad (59)$$

$$= -F\phi z_1 (z_1 D_1 \omega_1 + z_2 D_2 \omega_2 - D_1) x. \quad (60)$$

The potential is determined from the integral

$$\Phi(x) = \Phi_l + \int_x^l \frac{i(x') - i_0(x')}{\kappa(x')} dx', \quad (61)$$

$$= \Phi_l + \alpha \int_x^l \frac{x'}{\kappa(x')} dx', \quad (62)$$

where α is a constant.

As an example, corrosion of iron is considered in a two-component system with species Fe^{2+} and Cl^- . The concentration is fixed at the right-hand end of the column with values of 0.1 M for Fe^{2+} and 0.2 M for Cl^- , and the potential is fixed at zero. Diffusion coefficients of 0.8×10^{-5} and $2.032 \times 10^{-5} \text{ cm}^2 \text{ s}^{-1}$ are used for Fe^{2+} and Cl^- , respectively. Zero flux boundary conditions are imposed at the left-hand

side. The dissolution rate for Fe is fixed at 10^{-9} moles $\text{cm}^{-3} \text{s}^{-1}$. Secondary products are not allowed to form. Results are shown in Figures 7 and 8 for the solute concentrations, potential, and current corresponding to the stationary state solution. The numerical results are in excellent agreement with the analytical solution.

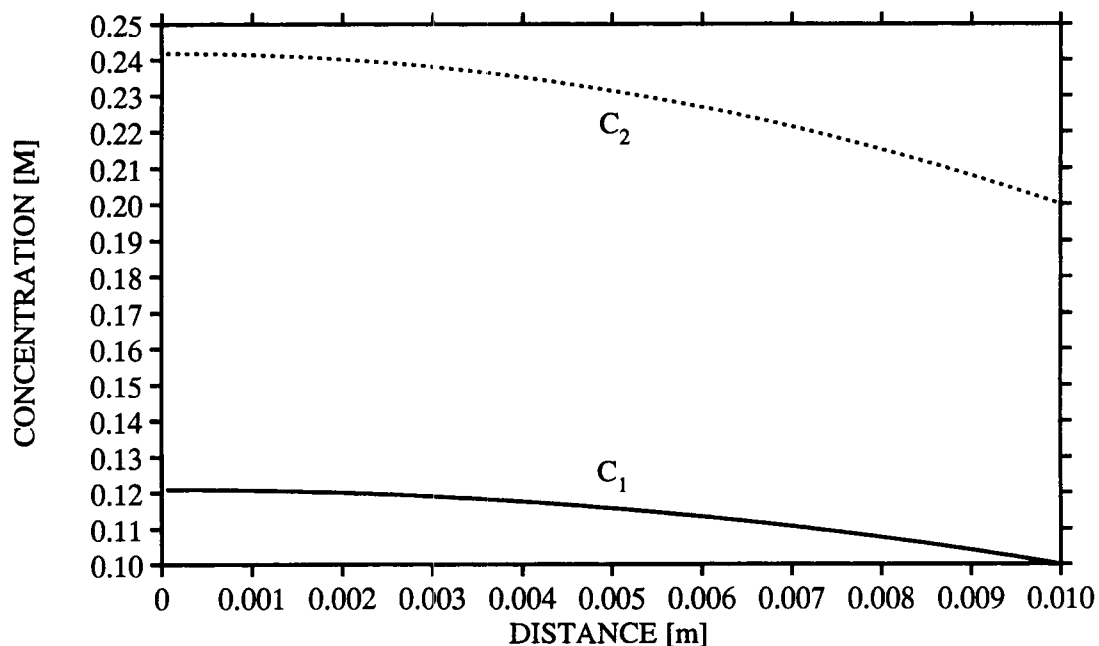


Figure 7: Stationary state concentration profiles C_1 and C_2 for Fe^{2+} (solid curve) and Cl^- (dotted curve). The tip of the crevice is located at the origin and the mouth at 0.01 m.

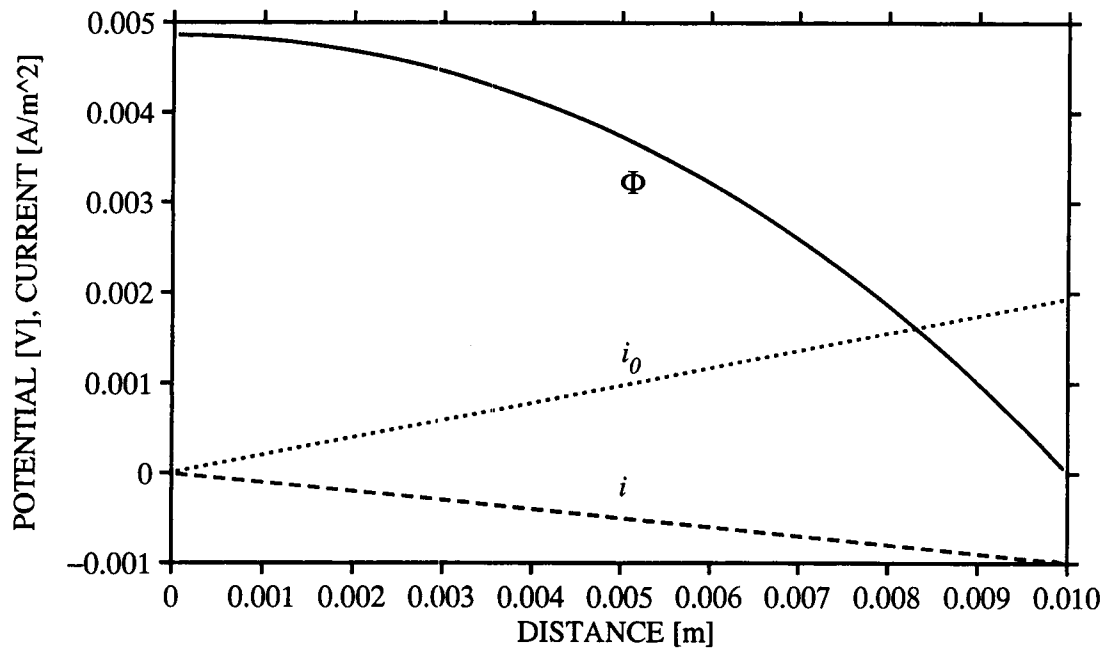


Figure 8: Stationary state profiles for the potential Φ (solid curve), and diffusive (dashed curve) and total current (dotted curve) densities i and i_0 .

Aqueous Kinetic Reactions

An analytical solution exists for the aqueous kinetic reaction



The rate for this reaction can be expressed as

$$I = k_f C_A - k_b C_B, \quad (64)$$

$$= k_f C_A - k_b (C - C_A), \quad (65)$$

$$= (k_f + k_b) C_A - k_b C, \quad (66)$$

$$= -k_b C \left[1 - \frac{k_f + k_b}{k_b C} C_A \right], \quad (67)$$

$$= -k[1 - KC_A], \quad (68)$$

where C denotes the sum of the concentrations of species \mathcal{A} and \mathcal{B}

$$C = C_A + C_B, \quad (69)$$

and

$$K = \frac{k_f + k_b}{k_b C}, \quad (70)$$

$$= \frac{1}{C}(K_{\text{eq}} + 1). \quad (71)$$

The equilibrium constant K_{eq} refers to reaction 63. The transport equations have the form

$$\frac{\partial}{\partial t}(\phi C_A) + \nabla \cdot \mathbf{J}_A = -I, \quad (72)$$

$$\frac{\partial}{\partial t}(\phi C_B) + \nabla \cdot \mathbf{J}_B = I. \quad (73)$$

Adding these two equations yields the non-reaction transport equation for the sum of the concentrations of species A and B

$$\frac{\partial}{\partial t}[\phi(C_A + C_B)] + \nabla \cdot (\mathbf{J}_A + \mathbf{J}_B) = 0. \quad (74)$$

Thus according to this result, if the initial and boundary conditions for $C = C_A + C_B$ are the same and equal to a constant, C will remain constant with time. For the special case that C is constant, an analytical solution exists given by

$$C_A(x, t) = C_{\text{eq}} - \frac{(C_{\text{eq}} - C_0)}{2} \left(\exp \left[(1 - \lambda) \frac{vx}{2D} \right] \operatorname{erfc} \left[\frac{x - \lambda vt}{2\sqrt{Dt}} \right] \right. \\ \left. + \exp \left[(1 + \lambda) \frac{vx}{2D} \right] \operatorname{erfc} \left[\frac{x + \lambda vt}{2\sqrt{Dt}} \right] \right), \quad (75)$$

where

$$\lambda = \sqrt{1 + 4 \frac{ksD}{\phi v^2}}. \quad (76)$$

As an example, inlet and initial conditions of

$$C_A^0 = 0.9, C_B^0 = 0.1, \quad (77)$$

and

$$C_A^{(i)} = 0.1, C_B^{(i)} = 0.9, \quad (78)$$

are considered. For this choice $C = 1$, $K_{\text{eq}} = 9$, and $K = 10$. For $ks = 10^{-12}$ moles $\text{cm}^{-3} \text{ s}^{-1}$, $D = 10^{-5} \text{ cm}^2 \text{ s}^{-1}$, $v = 1 \text{ m y}^{-1}$, and $\phi = 1$, the results for species A are shown in Figure 9 for times of 0.05, 0.125, 0.25, 0.375, and 0.5 years.

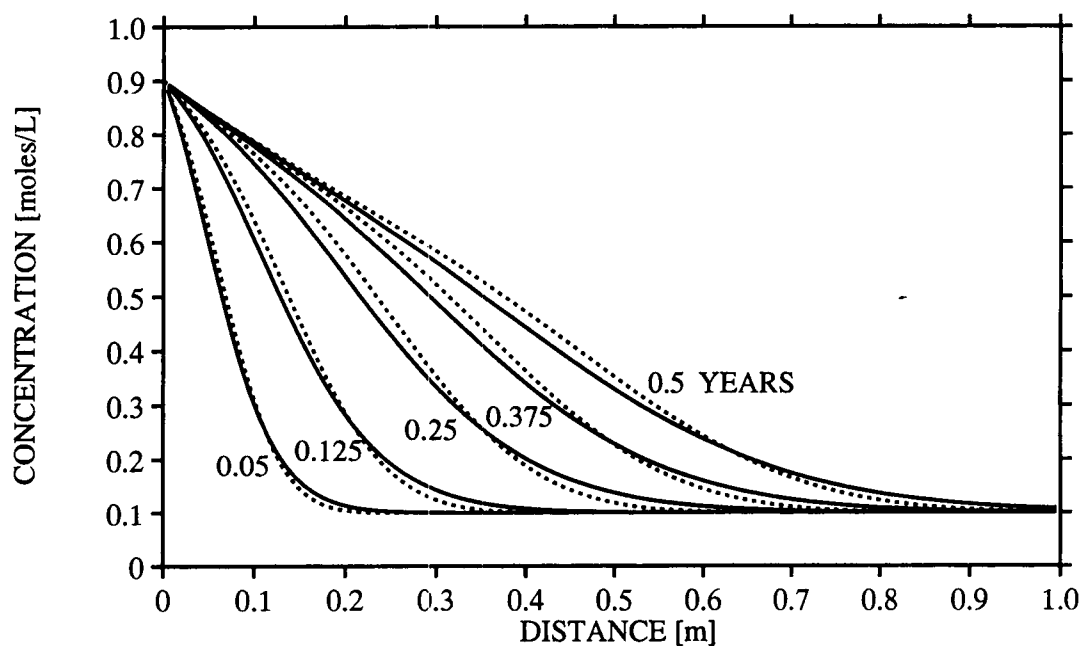


Figure 9: Transient concentration profiles for C_A and comparison with numerical (solid curves) and analytical (dotted curves) solutions.

6.23.98 **ChangeLog TECTRAN.**

ChangeLog TECTRAN 1.0

6/23/98 PCL read2.f

Keyword AQIR read zero for area and then set area = 1.

Fixed in unformatted read.

6.25.98 **Close of GRI Project.**

As of this date work on TECTRAN by PCL was concluded.